University of Pavia

Department of Electrical, Computer and Biomedical Engineering

Doctoral dissertation

Data-driven Nonlinear Model Predictive Control: Stability, Robustness and Offset-free Tracking

Candidate: Irene Schimperna

Supervisor: Prof. Lalo Magni
Co-supervisor: Prof. Chiara Toffanin

A.Y. 2024/2025
Cycle XXXVIII

Abstract

The use of data-driven and learning-based models in model predictive control (MPC) has gained an increasing popularity in recent years thanks to the growing availability of data collected in industrial plants and on the development of powerful deep learning techniques. In this framework, the aim of this thesis is to design nonlinear MPC algorithms with guaranteed stability and robustness properties based on data-driven models of the system under control. A particular attention is devoted to the development of strategies that take into account modeling errors and uncertainties, and that guarantee offset-free tracking.

The first part of the thesis explores the design of MPC algorithms for incrementally input-to-state stable (δISS) nonlinear systems modeled by recurrent neural networks (RNN). This class of models can be trained using input-output data, and stability properties of the model can be enforced during the training procedure. Considering different RNN architectures, the thesis develops output-feedback MPC algorithms that ensure closed-loop stability, satisfaction of input and incremental input constraints, robust satisfaction of output constraints in presence of uncertainties and offset-free tracking. Moreover, considering a general δISS system, it is presented how it is possible to guarantee stability considering a positive semi-definite stage cost in the MPC optimization problem (e.g. for output weighting), and how it is possible to enlarge the feasibility region employing an artificial reference.

The second part of the thesis considers data-driven models in the Koopman framework, and studies how convergence to the origin can be guaranteed in presence of modeling errors. First, an offset-free MPC algorithm is designed for systems modeled using extended dynamic mode decomposition (EDMD). Then, considering kernel based EDMD models, it is shown how asymptotic stability of MPC without terminal ingredients can be achieved provided that there exist suitable bounds on the modeling error.

The last part of the thesis presents the application of MPC to the current control in synchronous reluctance motors, showing performance improvement in presence of model uncertainties compared to the baseline control approaches.

All the control algorithms developed in the thesis have been theoretically analyzed, and their validity is assessed in simulation examples.

Contents

Acronyms

δISS	Incremental Input-to-State Stability
BPTT	Back-Propagation Through Time
CSS-MPC	Continuous Control Set Model Predictive Control
DTC	Direct Torque Control
EDMD	Extended Dynamic Mode Decomposition
EDMDc	Extended Dynamic Mode Decomposition with Control
ESN	Echo State Network
FCS-MPC	Finite Control Set Model Predictive Control
FEM	Finite-Element Method
FFNN	Feed-Forward Neural Network
FHOCP	Finite Horizon Optimal Control Problem
FOC	Field Oriented Control
GRU	Gated Recurrent Unit
IOSS	Input-Output-to-State Stability
ISpS	Input-to-State Practical Stability
ISS	Input-to-State Stability
kEDMD	Kernel Extended Dynamic Mode Decomposition
LMI	Linear Matrix Inequality
LPV	Linear Parameter-Varying
LSTM	Long Short-Term Memory
LTI	Linear Time-Invariant
LUT	Look-Up Table
MIMO	Multiple Input Multiple Output
MLP	Multi-Layer Perceptron
MOAS	Maximal Output Admissible Set
MPC	Model Predictive Control
MSE	Mean Squared Error
MTPA	Maximum Torque Per Ampere
MTPV	Maximum Torque Per Volt

NARX	Nonlinear AutoRegressive-eXogenous
NMPC	Nonlinear Model Predictive Control
NN	Neural Network
NNARX	Neural Nonlinear AutoRegressive-eXogenous
ODE	Ordinary Differential Equation
PAS	Practical Asymptotic Stability
PI	Proportional Integral
PI-RNN	Physics-Informed Recurrent Neural Network
PMSM	Permanent Magnet Synchronous Motor
QP	Quadratic Program
RBF	Radial Basis Function
ReLU	Rectified Linear Unit
REN	Recurrent Equilibrium Network
RH	Receding Horizon
RKHS	Reproducing Kernel Hilbert Space
RNN	Recurrent Neural Network
SafEDMD	Stability- and certificate-oriented EDMD
SISO	Single Input Single Output
SynchRel	Synchronous Reluctance motor
UBIBS	Uniformly Bounded Input Bounded State

List of Figures

List of Tables

Chapter 1

Introduction

Model predictive control (MPC) is a successful optimization-based control technique, with a well-established theoretical framework, and a strong industrial impact [197]. It is based on a simple, yet effective idea. At each sampling time instant, MPC solves an optimization problem over a finite horizon to determine the best future input sequence to fed to the system according to a given cost function. Then, only the first element of the optimal input sequence is applied to the plant, the new state is measured and the optimization is solved again starting from the new state and on a shifted window. Since the optimization is formulated over a finite horizon, its solution can be computed online, and thus nonlinear systems and explicit constraints can be easily taken into account.

MPC relies on a system model to perform predictions of the future evolution of the system. The model can be obtained by first principles, using data-driven methods, or by a combination of the two. The derivation of first principle models can be time consuming, and is not trivial when the system is complex and there is a lack of knowledge of the physical laws that govern it. Moreover, there are often some parts of the system dynamics that are difficult to model accurately, such as frictions or uncertainties due to the manufacturing process. Even when a physical description of the system is available, the identification of all the parameters of the model can be a hard task. For these reasons, the use of data-driven models has a long history in MPC, that starts from the very first formulations. In fact, some of the first MPC algorithms relied on simple impulse response models identified from plant data. In recent years, thanks to the growing availability of data and to the development of powerful method, increasingly sophisticated data-driven identification and control methods have been developed. Many industrial processes generate and store huge amounts of process data at every time instant of every day, containing all the information of process operations and equipments, that can be exploited for model identification, control design, fault detection and state and disturbance observations. The use of data-

driven control strategies allows to alleviate the need for human knowledge in the loop, since it provides some standardized procedures for the controller design that can be applied starting from the plant data, without requiring an accurate knowledge of the physical laws of the system [106]. Moreover, there have been a fruitful interchange of ideas between the deep learning and the control community, allowing the development of new effective learning-based methodologies.

Data-driven control methods can be classified in *direct* and *indirect* approaches. In direct data-driven control, the system data are directly used for the derivation of a controller, completely avoiding the model identification step. In this category find, e.g., iterative feedback tuning [102], virtual reference feedback tuning [39] and methods based on Willems' fundamental lemma [62]. In indirect data-driven control, instead, a data-driven model is identified first, and then is used to synthesize a model-based control. In the literature, many data-driven MPC algorithms have been proposed. For linear systems, a popular data-driven approach [13] is based on the use of Willems' fundamental lemma [241] avoiding the model identification step and directly using input-output data [71, 163]. This direct method has been shown to be equivalent to a (relaxed) indirect approach, where a linear model is identified first, and then is used in the MPC predictions [167]. For nonlinear systems, a common indirect method consists in the use of data-driven surrogate models. Such models can be obtained, e.g., by means of nonlinear ARX models [61], neural networks [199], Bayesian identification [190], Koopman operator-based system identification [137] and Gaussian process regression [100, 135].

Both when using first principle models and data-driven ones, model uncertainties and errors are unavoidable. MPC guarantees and performances are strongly related to the model quality. Hence, the study of MPC algorithms in presence of disturbances and uncertainties is a field of active research. A part of the literature studies inherent robustness of MPC, i.e. under which assumptions the MPC control law designed using the nominal model asymptotically stabilizes also the uncertain system [160, 87, 253]. Another widely studied field is the formulation of robust MPC algorithms, that are explicitly designed to cope with uncertainties [169]. Many different methods have been developed in the literature, that differ for the considered framework (e.g. deterministic or stochastic), the objective, and the assumptions on the uncertainty.

The aim of this thesis is to study methods to guarantee stability, robustness and offset-free tracking of MPC using data-driven models in the prediction and optimization step. This is done considering different classes of data-driven models, based on recently proposed powerful learning techniques. In the first part of the thesis, we provide a general introduction on stability and on MPC. Then, we focus on the design of MPC for incrementally input-to-state stable (δISS) systems [210], using recurrent neural

network (RNN) models. For this class of systems, we design different output-feedback MPC algorithms with guaranteed stability [211] to solve a variety of control problems, that include robust satisfaction of output constraints in presence of model uncertainties [212, 213], offset-free tracking [215, 213, 77], constraints on the input variation [209, 77] and the use of a positive semi-definite stage cost [77]. The algorithms are designed for different RNN classes, and it is shown how to generalize the requirements to any δISS system, without considering the specific model equations but only assuming the knowledge of a δISS-Lyapunov function [77]. The third part of the thesis considers data-driven models in the Koopman operator framework, and is focused on the design of algorithms that guarantee convergence to the desired equilibrium point. To this end, we exploit offset-free MPC algorithms [208] or the bounds on the modeling error that are available for kernel-based Koopman models [23, 216]. In the last part of the thesis we deal with a real world application, that is the control on current in synchronous reluctance motors, and we show how MPC can improve performances in presence of uncertainties in comparison to standard baseline control strategies [214].

1.1 Thesis structure

The thesis is divided in four parts and is structured as follows.

Part I – Introduction to MPC and stability In the first part of the thesis we introduce the concept of stability, and we give a general overview of the aspects of MPC that are studied in the thesis. This part of the thesis is composed by two chapters.

Chapter 2 introduces the stability notions that are used along the thesis, considering both autonomous systems and systems with input. In the second part of the chapter, a new result about incremental input-to-state stability of interconnected discrete-time systems is presented.

Chapter 3 provides a general overview on MPC. First, we introduce the MPC algorithm, and we describe the most common techniques to guarantee closed-loop stability. Then, we describe the more complex control problems that can be managed with MPC, and we summarize the techniques used in the thesis to deal with them.

Part II – MPC for δISS systems using RNN models This part of the thesis is devoted to the design of MPC algorithms for incrementally input-to-state stable (δISS) systems. Most of the proposed MPC schemes are based on data-driven models belonging to the class of recurrent neural networks (RNN). Since the system under control is δISS, the considered

RNN models are trained in a way that guarantees that they are also δISS. This part of the thesis is structured as follows.

Chapter 4 After a brief review of the methods to model dynamical systems using neural networks, this chapter introduces RNNs, and describes the architectures that are considered in the thesis. For each architecture we report the sufficient conditions for δISS, and we explain how to train the model to guarantee the satisfaction of the stability conditions.

Chapter 5 introduces the main ideas behind the design of observers and MPC algorithms for δISS systems. These methods are then exploited for the design of an MPC based on a recurrent equilibrium network model of the system under control. The algorithm is tested in simulation on a pH neutralization process.

Chapter 6 designs a robust MPC scheme based on a gated recurrent unit model of the system. In particular, we guarantee satisfaction of input and output constraints, recursive feasibility and stability in presence of bounded uncertainties of the model. The algorithm is tested in simulation on a four-tanks system.

Chapter 7 presents an MPC algorithm for long short-term memory network models, that guarantees robust constraint satisfaction and offset-free tracking of asymptotically constant set-points. To do so, the control algorithm includes an enlarged observer, a reference calculator, and a robust MPC that exploits a constraint tightening technique to guarantee constraint satisfaction in presence of model uncertainties and disturbances. The pH neutralization process is consider as benchmark example to test the proposed control approach.

Chapter 8 studies the issue of constraints on the input variation in RNN-based MPC. In particular, we propose a stabilizing MPC formulation that can be applied to any δISS RNN model, under the knowledge of a δISS-Lyapunov function and of an observer with a suitable structure. The design of MPC ingredients is exemplified in the case of a long short-term memory network model, and is tested on the four-tanks process.

Chapter 9 proposes an offset-free, output-feedback, tracking MPC algorithm for generic δISS systems subject to input and input rate constraints. The algorithm allows to use of a positive semi-definite stage cost (e.g. for output weighting), and includes an artificial reference to enlarge the feasibility region. The algorithm is tested on the pH neutralization process, considering a recurrent equilibrium network model of the system.

Part III – Data-driven MPC in the Koopman operator framework In this part of the thesis we present some MPC design methodologies using data-driven surrogate models based on the Koopman operator. A particular focus is placed on the derivation of algorithms guaranteeing convergence to the origin, exploiting offset-free MPC algorithms or bounds on the error of the surrogate models.

Chapter 10 introduces the Koopman operator framework and extended dynamic mode decomposition (EDMD), that is a data-driven method to obtain approximations of the Koopman operator. In particular, we present different approaches to derive surrogate models for autonomous and actuated systems.

Chapter 11 presents an offset-free MPC algorithm using nonlinear Koopman-based models. Two formulations of the algorithm are provided, considering both the case in which the target equilibrium of the system is fully known and the case in which only a partial information about the set-point is available. The algorithm is tested in simulation on the van-der-Pol oscillator and on the four-tanks process.

Chapter 12 is devoted to the derivation of conditions on the error of the surrogate model under which data-driven MPC asymptotically stabilizes the system. The derived requirements are then verified for data-driven models in the Koopman framework based on kernel EDMD, exploiting the availability of point-wise bounds on the approximation error. Our findings are demonstrated considering the van-der-Pol oscillator and the four-tanks process as simulation examples.

Part IV – Applications In this part of the thesis we focus on the use of MPC in a real world application, consisting in the control of currents in synchronous reluctance motors.

Chapter 13 presents stabilizing velocity form MPC algorithm for the control of currents in synchronous reluctance motors. From a theoretical point of view, the main advantages with respect to the literature about the use of MPC for the control of electric motors is the guaranteed stability. In the simulations, the proposed method achieves similar performances of the state of the art control based on PIs and decoupling in the nominal case, but it is more robust to model uncertainties and does not require a precise knowledge of the function that relates inductances to currents, that is typically difficult to obtain.

Chapter 14 draws the conclusions of the thesis.

1.2 List of peer-reviewed scientific publications

In the following we report the list of the publications derived from the work described in this thesis.

Journal

- [216] **Schimperna, I.**, Worthmann, K., Schaller, M., Bold, L. and Magni L. (2025). *Data-driven Model Predictive Control: Asymptotic Stability despite Approximation Errors exemplified in the Koopman framework.* Submitted, available at `https://arxiv.org/abs/2505.05951`.

- [77] Galuppini, G., **Schimperna, I.** and Magni L. (2025). *Offset-free Output Feedback Tracking MPC for δISS Nonlinear Systems Subject to Input and Input Rate Constraints.* IEEE Transactions on Automatic Control.

- [210] **Schimperna, I.**, Magni, L. (2025). *On Incremental Input-to-State Stability of interconnected discrete-time systems.* Automatica, 179, 112406.

- [214] **Schimperna, I.**, Rubino, A. and Magni, L. (2025). *Velocity Form MPC for Current Control in Synchronous Reluctance Motors.* IEEE Transactions on Control Systems Technology, 33(6), 2463-2469.

- [209] **Schimperna, I.**, Galuppini, G., Magni, L. (2024). *Recurrent Neural Network Based MPC for Systems With Input and Incremental Input Constraints.* IEEE Control Systems Letters, 8, 814-819.

- [213] **Schimperna, I.**, and Magni, L. (2024). *Robust offset-free constrained model predictive control with long short-term memory networks.* IEEE Transactions on Automatic Control 69(12), 8172-8187.

- [212] **Schimperna, I.**, and Magni, L. (2024). *Robust constrained nonlinear model predictive control with gated recurrent unit model.* Automatica, 161, 111472.

Conference proceeding

- [208] **Schimperna, I.**, Bold, L. and Worthmann, K. (2025). *Offset-free Nonlinear MPC with Koopman-based Surrogate Models.* IFAC-PapersOnLine, 59(19), 466-471. Presented at the 13th IFAC Symposium on Nonlinear Control Systems.

- [23] Bold, L., Schaller, M., **Schimperna, I.**, and Worthmann, K. (2025). *Kernel EDMD for data-driven nonlinear Koopman MPC with*

stability guarantees. IFAC-PapersOnLine, 59(19), 478-483. Presented at the 13th IFAC Symposium on Nonlinear Control Systems.

- [211] **Schimperna, I.**, and Magni, L. (2024). *Recurrent equilibrium network models for nonlinear model predictive control.* IFAC-PapersOnLine, 58(18), 226-231. Presented at the 8th IFAC Conference on Nonlinear Model Predictive Control NMPC.

- [215] **Schimperna, I.**, Toffanin, C., and Magni, L. (2023). *On offset-free model predictive control with long short-term memory networks.* IFAC-PapersOnLine, 56(1), 156-161. Presented at 12th IFAC Symposium on Nonlinear Control Systems.

1.3 Notation

Given two numbers $a, b \in \mathbb{Z}$, we use the abbreviation $[a : b] := \mathbb{Z} \cap [a, b]$.

Considering a vector v, $v_{(j)}$ is its j-th component, $v^\top$ is its transpose, $\|v\|_2$ is its 2-norm, $\|v\|_\infty$ is its infinity-norm and $\|v\|_A^2 = v^\top A v$ is the squared norm weighted with matrix A. $|v|$ is the vector containing the absolute values of the elements of v. $\|v\|$ is used when the relation hold independently on the choice of the norm. Inequalities between vectors are considered element by element. Given two vectors v and w, $v \otimes w$ is their Hadamard product (element-wise product).

Considering a matrix M, $M_{(ij)}$ is its element in position ij, $M_{(i*)}$ is its i-th row, $M_{(*j)}$ is its j-th column, $\rho(M)$ is its spectral radius, i.e. the maximum absolute value of its eigenvalues, $\|M\|_2$ and $\|M\|_\infty$ are its induced 2-norm and ∞-norm, while $\|M\|_F$ is its Frobenius norm. $M^\dagger$ is the pseudo-inverse of matrix M. With $\lambda_{max}(M)$ and $\lambda_{min}(M)$ we denote the maximum and minimum eigenvalues of the symmetric matrix M. Positive definite and positive semi-definite matrices are denoted respectively by $M \succ 0$ and $M \succeq 0$. Given a matrix $A \succ 0$, $A^{1/2}$ is the unique positive definite matrix B such that $BB = A$.

$\mathbf{0}_{m,n}$ is the $m \times n$ null matrix, $\mathbf{I}_n$ is the $n \times n$ identity matrix and $\mathbf{1}_n$ and $\mathbf{0}_n$ are respectively the vectors of ones and of zeros of n elements. We use 0 instead of $\mathbf{0}_{m,n}$ when the dimensions are clear from the context. $\text{diag}(d_1, \ldots, d_n)$ is the diagonal matrix with elements $d_1, \ldots, d_n$ on the diagonal.

We denote the ball of center x_0 and radius $r \geq 0$ as $\mathcal{B}_r(x_0) := \{x \in \mathbb{R}^n : \|x - x_0\|_2 \leq r\}$. The symbols $\oplus$ and $\ominus$ represent the Pontryagin set sum and difference, respectively.

The inverse of the function α is α^{-1}. id is the identity function from $\mathbb{R}$ to $\mathbb{R}$. The composition of the scalar functions $\gamma_1(r)$ and $\gamma_2(r)$ is denoted by $\gamma_1 \circ \gamma_2(r) := \gamma_1(\gamma_2(r))$, while their sum is $(\gamma_1 + \gamma_2)(r) := \gamma_1(r) + \gamma_2(r)$. By $\mathcal{C}_b(\Omega; \mathbb{R}^n)$, we denote the space of bounded continuous functions on a set Ω

with codomain $\mathbb{R}^n$, and $\mathcal{C}_b(\Omega) := \mathcal{C}_b(\Omega; \mathbb{R})$. The sigmoid activation function is

$$\sigma(z) := \frac{1}{1 + e^{-z}}.$$

Activation functions $\sigma(\cdot)$ and $\tanh(\cdot)$ are applied to vectors element by element.

We use the bold style to denote time sequences, i.e.

$$\mathbf{u}_{k_1,k_2} := \{u_{k_1}, u_{k_1+1}, \ldots, u_{k_2-1}\}.$$

The norm of the sequence $\mathbf{u}_{k_1,k_2}$ is

$$\|\mathbf{u}_{k_1,k_2}\| := \begin{cases} \sup\{\|u_h\| : k_1 \leq h < k_2\} & \text{if } k_1 < k_2 \\ 0 & \text{if } k_1 = k_2 \end{cases}$$

The subscripts indicating the initial and final time instants of sequences are omitted when clear from the contest.

To indicate the discrete time instant, we typically use the subscript k, i.e. x_k denotes the value of the variable x at time k. In some parts of the thesis, to improve clarity, the time dependency is expressed between parenthesis together with the information about the initial state and the input sequence, i.e. we use $x(k; x_0, \mathbf{u})$ to denote the value of the variable x at time k obtained starting from the initial state x_0 and applying the input sequence $\mathbf{u}$.

The mathrm style is used in the subscripts and superscripts that are not variables.

Part I

Introduction to MPC and stability

Chapter 2

Stability notions

In this chapter we formally present the stability notions used in the thesis. We first consider stability definitions for autonomous systems, and then we define different types of stability for systems with input. The stability notions are presented for discrete-time systems, but they all have a continuous-time counterpart defined in similar way. The last part of the chapter is devoted to the study of the stability properties of the interconnection of incrementally input-to-state stabile (δISS) discrete-time systems. In particular, we derive two different formulations of the small gain theorem for δISS systems.

Section 2.4 about the interconnection of δISS systems is based on:

- [210] **Schimperna, I.**, Magni, L. (2025). *On Incremental Input-to-State Stability of interconnected discrete-time systems.* Automatica, 179, 112406.

2.1 Comparison functions

The stability definitions make use of comparison functions [124], defined as follows.

Definition 2.1 ($\mathcal{K}$-function)**.** *A continuous function $\alpha : \mathbb{R}_{\geq 0} \to \mathbb{R}_{\geq 0}$ is of class $\mathcal{K}$ if $\alpha(r) > 0$ for all $r > 0$, it is strictly increasing and $\alpha(0) = 0$.*

Definition 2.2 ($\mathcal{K}_\infty$-function)**.** *A continuous function $\gamma : \mathbb{R}_{\geq 0} \to \mathbb{R}_{\geq 0}$ is of class $\mathcal{K}_\infty$ if it is a class $\mathcal{K}$ function and $\gamma(r) \to \infty$ for $r \to \infty$.*

Definition 2.3 ($\mathcal{KL}$-function)**.** *A continuous function $\beta : \mathbb{R}_{\geq 0} \times \mathbb{Z}_{\geq 0} \to \mathbb{R}_{\geq 0}$ is of class $\mathcal{KL}$ if $\beta(r, k)$ is a class $\mathcal{K}$ function with respect to r for all k, it is strictly decreasing in k for all $r > 0$, and $\beta(r, k) \to 0$ as $k \to \infty$ for all $r > 0$.*

We report here a useful property of comparison functions that will be employed in the proofs.

Property 2.1 (Weak triangle inequality, [124])**.** *Given $\alpha \in \mathcal{K}$ and any function $\rho \in \mathcal{K}_\infty$, for any $r_1, r_2 \in \mathbb{R}_{\geq 0}$ it holds that*

$$\alpha(r_1 + r_2) \leq \alpha \circ (\rho + \mathrm{id})(r_1) + \alpha \circ (\rho^{-1} + \mathrm{id})(r_2). \tag{2.1}$$

A useful particular case of the previous property is obtained considering $\rho = \mathrm{id}$. In this case we get

$$\alpha(r_1 + r_2) \leq \alpha(2r_1) + \alpha(2r_2). \tag{2.2}$$

2.2 Stability of autonomous systems

In this section we consider the stability properties of an autonomous discrete-time system

$$x_{k+1} = f(x_k) \tag{2.3}$$

with state $x \in \mathbb{R}^n$. System (2.3) can represent both an autonomous system or the feedback connection of a system with a controller. Before stating the stability definitions, we must introduce the concept of equilibrium point and of positive invariant set of the autonomous system (2.3).

Definition 2.4 (Equilibrium point)**.** *A point $\bar{x} \in \mathbb{R}^n$ is an equilibrium point of the system* (2.3) *if*

$$\bar{x} = f(\bar{x}).$$

Definition 2.5 (Positive invariant set)**.** *A closed set $\mathcal{X} \subseteq \mathbb{R}^n$ is positive invariant for the system* (2.3) *if $x \in \mathcal{X}$ implies $f(x) \in \mathcal{X}$.*

2.2.1 Asymptotic stability

In this section we introduce the definitions of Lyapunov stability for the system (2.3). Moreover, we introduce the concept of Lyapunov function, and we state the Lyapunov theorem for asymptotic stability. For a more detailed description of the topic, see [197, Appendix B]. Without loss of generality, the stability definitions are referred to an equilibrium point in the origin of system (2.3).

Definition 2.6. *The equilibrium point $x = 0$ of the system* (2.3) *is:*

1. *Locally stable if, for each $\varepsilon > 0$, there exists $\delta = \delta(\varepsilon) > 0$ such that*

$$\|x_0\| < \delta \implies \|x_k\| < \varepsilon, \quad \forall\, k \in \mathbb{Z}_{\geq 0}.$$

2. *Unstable if it is not stable.*

3. *Locally asymptotically stable if it is stable and δ can be chosen such that*

$$\|x_0\| < \delta \implies \lim_{k \to \infty} x_k = 0.$$

4. *Asymptotically stable in the closed positive invariant set $\mathcal{X}$ including the origin if it is stable and, for all $x_0 \in \mathcal{X}$,*

$$\lim_{k\to\infty} x_k = 0.$$

5. *Globally asymptotically stable if it is asymptotically stable in the set $\mathcal{X} = \mathbb{R}^n$.*

An alternative equivalent definition of asymptotic stability can be given by means of comparison functions.

Definition 2.7. *Suppose that the closed set $\mathcal{X}$ including the origin is a positive invariant set for the system* (2.3)*. The equilibrium point $x = 0$ of the system* (2.3) *is asymptotically stable in $\mathcal{X}$ if there exists a function $\beta \in \mathcal{KL}$ such that for all $x_0 \in \mathcal{X}$ and for all $k \in \mathbb{Z}_{\geq 0}$*

$$\|x_k\| \leq \beta(\|x_0\|, k).$$

Proposition 2.1 (Proposition B.9 in [197])**.** *Suppose that f is continuous. Then, 4. in Definition 2.6 and Definition 2.7 are equivalent.*

The verification of asymptotic stability using the definition is typically a hard task. A common and often more straightforward method to study stability is by means of Lyapunov functions.

Definition 2.8 (Lyapunov function)**.** *A continuous function $V : \mathcal{X} \to \mathbb{R}_{\geq 0}$ is a Lyapunov function for the system* (2.3) *if there exist functions $\alpha_1, \alpha_2, \alpha_3 \in \mathcal{K}_\infty$ such that for all $x \in \mathcal{X}$*

$$\alpha_1(\|x\|) \leq V(x) \leq \alpha_2(\|x\|), \tag{2.4a}$$
$$V(f(x)) - V(x) \leq -\alpha_3(\|x\|). \tag{2.4b}$$

Theorem 2.1 (Lyapunov theorem)**.** *Suppose that the set $\mathcal{X}$ is closed and positive invariant for the system* (2.3)*. If the system* (2.3) *admits a Lyapunov function, then the equilibrium point $x = 0$ is asymptotically stable in the set $\mathcal{X}$.*

2.2.2 Practical asymptotic stability

In this section we define practical asymptotic stability. In standard asymptotic stability, the system trajectories converges to the origin (or to the considered equilibrium). If the origin of the system is practically asymptotically stable, the state trajectories goes towards the origin in a first phase, and then stagnates in a neighborhood of the origin of fixed size. This behavior can be found in closed-loop systems where there is a mismatch between the model used for controller design and the real plant under control.

Definition 2.9 (Practical asymptotic stability)**.** *The origin of the system* (2.3) *is said practically asymptotically stable (PAS) in the set* $\mathcal{X}$ *if there exist* $\beta \in \mathcal{KL}$ *and* $r \geq 0$ *such that for all* $x_0 \in \mathcal{X}$ *and for all* $k \in \mathbb{Z}_{\geq 0}$

$$\|x_k\| \leq \beta(\|x_0\|, k) + r. \tag{2.5}$$

Remark 2.1. *An alternative formulation of PAS requires the existence of a function* $\tilde{\beta} \in \mathcal{KL}$ *and a constant* $\tilde{r} \geq 0$ *such that*

$$\|x_k\| \leq \max\{\tilde{\beta}(\|x_0\|, k), \tilde{r}\}. \tag{2.6}$$

The two formulations of the definition are equivalent. In fact we can exploit that given $a, b \geq 0$*, it holds that* $\max\{a, b\} \leq a + b \leq \max\{2a, 2b\}$ *to show that, given* β *and* r *satisfying* (2.5)*, there exist* $\tilde{\beta}$ *and* $\tilde{r}$ *satisfying* (2.6)*, and vice versa.*

2.3 Stability of systems with input

In this section we consider the stability properties of a discrete-time system with input described by

$$x_{k+1} = f(x_k, u_k), \tag{2.7}$$

where $x \in \mathbb{R}^n$ is the state and $u \in \mathbb{R}^m$ is the input. The input u_k in system (2.7) can represent both the controlled input of the system or an external disturbance. The system can be both an open-loop system or the system obtained by the feedback connection of a controlled system and a controller, where the input represents the exogenous signals that influence the closed-loop. As in the autonomous system case, we first introduce the definitions of equilibrium point and positive invariant set for the system (2.7).

Definition 2.10 (Equilibrium point)**.** *A point* $(\bar{x}, \bar{u})$ *is an equilibrium point of the system* (2.7) *if*

$$\bar{x} = f(\bar{x}, \bar{u}).$$

Definition 2.11 (Positive invariant set)**.** *A closed set* $\mathcal{X} \subseteq \mathbb{R}^n$ *is positive invariant for the system* (2.3) *with inputs* $u \in \mathcal{U}$ *if* $x \in \mathcal{X}$ *implies* $f(x, u) \in \mathcal{X}$ *for all* $u \in \mathcal{U}$*.*

There exist several extensions of the concept of asymptotic stability for systems with input. In this thesis we consider Input-to-State Stability (ISS), that relates the behavior of state trajectories to the magnitude of the initial state and of the input signal, Input-to-State practical Stability (ISpS), that can be seen as en extension of PAS to systems with inputs, and Incremental Input-to-State Stability (δISS), that concerns the difference between couples of state trajectories.

In the following, the stability definitions are stated with respects to the sets $\mathcal{X}$ and $\mathcal{U}$, where the set $\mathcal{X}$ is assumed to be positive invariant with inputs $u \in \mathcal{U}$. If we have that $\mathcal{X} = \mathbb{R}^n$ and $\mathcal{U} = \mathbb{R}^m$, the stability properties are said to be *global*.

2.3.1 Input-to-State Stability

In this section we provide the definitions of ISS and of ISS-Lyapunov function. ISS means that the magnitude of the system trajectory is bounded by a vanishing term that depends on the magnitude of the initial state, and by a term that is related to the magnitude of the input signal. These definitions for discrete-time systems were first introduced in [114]. For convenience, the definitions are given for an equilibrium point in the origin of the system (2.7).

Definition 2.12. *The system $x_{k+1} = f(x_k, u_k)$ is Input-to-State Stable (ISS) in the sets $\mathcal{X}$ and $\mathcal{U}$ if there exist functions $\beta \in \mathcal{KL}$ and $\gamma \in \mathcal{K}$ such that for any $k \geq 0$, any initial condition $x_0 \in \mathcal{X}$ and any input sequence $\mathbf{u}_{0,k} := \{u_0, u_1, ..., u_{k-1}\}$ with $u_h \in \mathcal{U}$ for all $h \in [0 : k-1]$, it holds that*

$$\|x_k\| \leq \beta(\|x_0\|, k) + \gamma\left(\|\mathbf{u}_{0,k}\|\right). \tag{2.8}$$

Definition 2.13 (ISS-Lyapunov function)**.** *A continuous function $V : \mathcal{X} \to \mathbb{R}_{\geq 0}$ is an ISS-Lyapunov function for the system $x_{k+1} = f(x_k, u_k)$ if there exist functions $\alpha_1, \alpha_2, \alpha_3 \in \mathcal{K}_\infty$ and $\gamma \in \mathcal{K}$ such that for all $x \in \mathcal{X}$, $u \in \mathcal{U}$*

$$\alpha_1(\|x\|) \leq V(x) \leq \alpha_2(\|x\|), \tag{2.9a}$$
$$V(f(x,u)) - V(x) \leq -\alpha_3(\|x\|) + \gamma(\|u\|). \tag{2.9b}$$

The following theorem is taken from [90], and is a generalization of [114, Lemma 3.5] that does not require continuity of the Lyapunov function.

Theorem 2.2 (Lyapunov theorem for ISS)**.** *If the system $x_{k+1} = f(x_k, u_k)$ admits a ISS-Lyapunov function in the sets $\mathcal{X}$ and $\mathcal{U}$, then it is ISS in $\mathcal{X}$ and $\mathcal{U}$.*

Definition 2.13 of ISS-Lyapunov function is given in the so called *dissipation form*. In the literature there exists also an alternative formulation, called *implication form* ISS-Lyapunov function. For its definition and its relation to the dissipation-form ISS-Lyapunov function, in particular for systems with discontinuous dynamics, we refer the interested reader to [90].

2.3.2 Input-to-State practical Stability

ISpS is a similar property to ISS, but it does not require the system state to asymptotically reach the origin when the input is null. Instead, it is sufficient that the trajectory reaches asymptotically a neighborhood of the origin of fixed size. An overview of ISpS can be found in [194].

Definition 2.14 (Input-to-State practical Stability)**.** *The system* (2.7) *is Input-to-State Practically Stable (ISpS) in the sets $\mathcal{X}$ and $\mathcal{U}$ if there exist functions $\beta \in \mathcal{KL}$ and $\gamma \in \mathcal{K}$, and a constant $r \geq 0$, such that for any*

$k \in \mathbb{Z}_{\geq 0}$, any initial condition $x_0 \in \mathcal{X}$ and any input sequence $\mathbf{u}_{0,k} := \{u_0, u_1, ..., u_{k-1}\}$ with $u_h \in \mathcal{U}$ for all $h \in [0 : k-1]$, it holds that

$$\|x_k\| \leq \beta(\|x_0\|, k) + \gamma\left(\|\mathbf{u}_{0,k}\|\right) + r.$$

Definition 2.15 (ISpS-Lyapunov function)**.** *A function $V : \mathcal{X} \to \mathbb{R}_{\geq 0}$ is an ISpS Lyapunov function for the system* (2.7) *if there exist functions $\alpha_1, \alpha_2, \alpha_3 \in \mathcal{K}_\infty$, $\gamma \in \mathcal{K}$, and two constants $c_1, c_2 \geq 0$, such that, for any $x \in \mathcal{X}$, $u \in \mathcal{U}$, it holds that*

$$\begin{aligned} &\alpha_1(\|x\|) \leq V(x) \leq \alpha_2(\|x\|) + c_1, \\ &V(f(x,u)) - V(x) \leq -\alpha_3(\|x\|) + \gamma(\|u\|) + c_2. \end{aligned}$$

Theorem 2.3 (Lyapunov theorem for ISpS, [194])**.** *If the system* (2.7) *admits an ISpS-Lyapunov function, then it is ISpS in the sets $\mathcal{X}$ and $\mathcal{U}$.*

2.3.3 Incremental Input-to-State Stability

δISS is a property that describes the stability of state trajectories of a dynamical system with respect to each other. In particular, in a δISS system, the contribution of the initial state vanishes asymptotically, and the difference between state trajectories is bounded by the difference between the corresponding input sequences.

Incremental stability properties of nonlinear continuous-time systems are extensively studied in [7]. The interest in δISS for discrete-time systems was mainly stimulated by the design of robust MPC, where a crucial point to prove recursive feasibility is the analysis of perturbed trajectories. In this perspective, the notions of Incremental Global Asymptotic Stability, δISS and δISS-Lyapunov functions are first introduced for discrete-time systems in [11]. In [232], the main results of [7] regarding the Lyapunov characterization of δISS systems are extended to the discrete-time framework.

Definition 2.16 (Incremental Input-to-State Stability)**.** *The system* (2.7) *is Incrementally Input-to-State Stable (δISS) in the sets $\mathcal{X}$ and $\mathcal{U}$ if there exist functions $\beta \in \mathcal{KL}$ and $\gamma \in \mathcal{K}$ such that for any $k \in \mathbb{Z}_{\geq 0}$, any pair of initial conditions $x_0^{\mathrm{a}}, x_0^{\mathrm{b}} \in \mathcal{X}$, any pair of input sequences $\mathbf{u}_{0,k}^{\mathrm{a}}$ and $\mathbf{u}_{0,k}^{\mathrm{b}}$ with $u_h^{\mathrm{a}}, u_h^{\mathrm{b}} \in \mathcal{U}$ for all $h \in [0 : k-1]$, it holds that*

$$\|x_k^{\mathrm{a}} - x_k^{\mathrm{b}}\| \leq \beta(\|x_0^{\mathrm{a}} - x_0^{\mathrm{b}}\|, k) + \gamma\left(\|\mathbf{u}_{0,k}^{\mathrm{a}} - \mathbf{u}_{0,k}^{\mathrm{b}}\|\right). \tag{2.10}$$

Definition 2.17 (Exponential δISS)**.** *The system* (2.7) *is exponentially δISS in the sets $\mathcal{X}$ and $\mathcal{U}$ if it is δISS in $\mathcal{X}$ and $\mathcal{U}$ and the function β is exponential in the second argument, i.e. there exist $\mu > 0$ and $\lambda \in (0, 1)$ such that*

$$\beta(r, k) \leq \mu r \lambda^k.$$

Definition 2.18 (δISS-Lyapunov function)**.** *A continuous function $V : \mathcal{X} \times \mathcal{X} \to \mathbb{R}_{\geq 0}$ is a δISS-Lyapunov function for the system (2.7) if there exist functions $\alpha_1, \alpha_2, \alpha_3 \in \mathcal{K}_\infty$ and $\gamma \in \mathcal{K}$ such that for any $x^{\mathrm{a}}, x^{\mathrm{b}} \in \mathcal{X}$ and $u^{\mathrm{a}}, u^{\mathrm{b}} \in \mathcal{U}$ it holds that*

$$\alpha_1(\|x^{\mathrm{a}} - x^{\mathrm{b}}\|) \leq V(x^{\mathrm{a}}, x^{\mathrm{b}}) \leq \alpha_2(\|x^{\mathrm{a}} - x^{\mathrm{b}}\|), \tag{2.11a}$$

$$V(f(x^{\mathrm{a}}, u^{\mathrm{a}}), f(x^{\mathrm{b}}, u^{\mathrm{b}})) - V(x^{\mathrm{a}}, x^{\mathrm{b}}) \leq -\alpha_3(\|x^{\mathrm{a}} - x^{\mathrm{b}}\|) + \gamma(\|u^{\mathrm{a}} - u^{\mathrm{b}}\|). \tag{2.11b}$$

Theorem 2.4 (Lyapunov theorem for δISS, [232])**.** *If the system (2.7) admits a δISS-Lyapunov function, then it is δISS in the sets $\mathcal{X}$ and $\mathcal{U}$.*

2.3.4 Contraction

Contraction is a property similar to exponential δISS, but that considers couples of trajectories associated to the same input sequence. In this thesis, we consider contraction as defined in [155] and [201, Definition 2], and reported in the following definition.

Definition 2.19. *The system (2.7) is contracting with rate $\alpha \in (0, 1)$ if, for any two initial conditions $x_0^{\mathrm{a}}, x_0^{\mathrm{b}}$ and any input sequence $\mathbf{u}_{0,k}$, there exists $\mu > 0$ such that*

$$\|x_k^{\mathrm{a}} - x_k^{\mathrm{b}}\| \leq \mu\alpha^k \|x_0^{\mathrm{a}} - x_0^{\mathrm{b}}\|.$$

2.4 Interconnection of incrementally input-to-state stable systems

In this section we study the properties of the interconnection of δISS systems. The study of the stability of interconnected systems is very useful to deal with complex systems, such as network systems [122], and can be exploited in the control design. In this framework a common instrument are small gain theorems. Different formulations of the small gain theorem exist in the literature, depending on the considered stability property and on the class of systems. For instance, small gain theorems were derived for ISS systems both for continuous-time systems [109, 112] and discrete-time systems [114], and for δISS for continuous-time systems [7]. Small gain theorems are also often exploited for control design [110, 111]. However, in the literature there are not many results concerning the interconnection of discrete-time δISS systems, and the only available results are derived for systems with a particular structure. For instance, in [30] and [28], the δISS property of multi-layer RNN is studied with reference to the particular equations of the systems in exam, showing that if all the composing subsystems (i.e. the RNN layers) are δISS, then the overall system is δISS. This is a particular case of a more general result derived in [37] for the cascade connection of

δISS systems. The aim of this section is to study the more general feedback connection of discrete-time δISS systems, deriving conditions under which the overall system enjoys the δISS property. In particular, two different small gain theorems are derived, one based on the definition of δISS and one based on δISS-Lyapunov functions. Notably, the result for the cascade connection of δISS systems of [37] is a particular case of the result derived here.

For sake of simplicity, in this section all the stability properties are considered global. To improve clarity, we will explicitly state the dependence of state trajectories from the initial condition and the input sequence. In particular $x(k, x_0, \mathbf{u})$ denotes the state of the system (2.7) at time step k, emanating from the initial state x_0 and applying the input sequence $\mathbf{u}$.

To derive the results of this section, some additional definitions related to δISS are required.

Definition 2.20 (Incremental asymptotic gain, [232])**.** *The system* (2.7) *has an incremental asymptotic gain if there exists $\tilde{\gamma} \in \mathcal{K}$ such that*

$$\limsup_{k\to\infty} \|x(k; x_0^{\mathrm{a}}, \mathbf{u}_{0,k}^{\mathrm{a}}) - x(k; x_0^{\mathrm{b}}, \mathbf{u}_{0,k}^{\mathrm{b}})\| \leq \tilde{\gamma}\left(\limsup_{k\to\infty} \|u_k^{\mathrm{a}} - u_k^{\mathrm{b}}\|\right).$$

Definition 2.21 (Incremental UBIBS, [232])**.** *The system* (2.7) *is incrementally Uniformly Bounded Input Bounded State (incrementally UBIBS) if there exist $\sigma, \gamma \in \mathcal{K}$ such that*

$$\|\mathbf{x}_{0,\infty}^{\mathrm{a}} - \mathbf{x}_{0,\infty}^{\mathrm{b}}\| \leq \sigma(\|x_0^{\mathrm{a}} - x_0^{\mathrm{b}}\|) + \gamma\left(\|\mathbf{u}_{0,\infty}^{\mathrm{a}} - \mathbf{u}_{0,\infty}^{\mathrm{b}}\|\right),$$

where $\mathbf{x}_{0,\infty}^{\mathrm{a}}$ and $\mathbf{x}_{0,\infty}^{\mathrm{b}}$ are the state sequences obtained with initial states x_0^{a} and x_0^{b} and input sequences $\mathbf{u}_{0,\infty}^{\mathrm{a}}$ and $\mathbf{u}_{0,\infty}^{\mathrm{b}}$.

Theorem 2.5 ([232])**.** *Consider the system* (2.7) *and assume that f is continuous. The following statements are equivalent:*

1. *The system* (2.7) *is δISS.*
2. *The system* (2.7) *has an incremental asymptotic gain and is incrementally UBIBS.*
3. *The system* (2.7) *admits a δISS-Lyapunov function.*

In the following, we consider the interconnected system

$$\begin{cases} x_{k+1} = f(x_k, y_k, u_k) \\ y_{k+1} = g(x_k, y_k, u_k) \end{cases} \tag{2.12}$$

with $x \in \mathbb{R}^{n_x}$, $y \in \mathbb{R}^{n_y}$ and $u \in \mathbb{R}^m$, and where f and g are continuous. The δISS property of the system (2.12) is studied by considering the difference between two trajectories with initial states $[x_0^{\mathrm{a}\top}\ y_0^{\mathrm{a}\top}]^\top$ and $[x_0^{\mathrm{b}\top}\ y_0^{\mathrm{b}\top}]^\top$, and input sequences $\mathbf{u}_{0,\infty}^{\mathrm{a}}$ and $\mathbf{u}_{0,\infty}^{\mathrm{b}}$, respectively.

2.4.1 Small gain theorem for δISS

In order to derive a small gain theorem for the system (2.12), the following technical lemma is introduced first.

Lemma 2.1. *Let $h_x : \mathbb{R}^{n_x} \times \mathbb{R}^{n_x} \to \mathbb{R}^{p_x}$ and $h_y : \mathbb{R}^{n_y} \times \mathbb{R}^{n_y} \to \mathbb{R}^{p_y}$ be two continuous mappings. Assume that h_x is such that if $\limsup_{k\to\infty} \|h_x(x_k^{\mathrm{a}}, x_k^{\mathrm{b}})\|$ is finite then $\limsup_{k\to\infty} \|x_k^{\mathrm{a}} - x_k^{\mathrm{b}}\|$ is finite, and that h_y is such that if $\limsup_{k\to\infty} \|h_y(y_k^{\mathrm{a}}, y_k^{\mathrm{b}})\|$ is finite then $\limsup_{k\to\infty} \|y_k^{\mathrm{a}} - y_k^{\mathrm{b}}\|$ is finite. Assume that the following δISS-like properties hold for the subsystems in* (2.12)

$$\begin{aligned}\|h_x(x_k^{\mathrm{a}}, x_k^{\mathrm{b}})\| \leq \beta_x(\|x_0^{\mathrm{a}} - x_0^{\mathrm{b}}\|, k) + \gamma_u\left(\|\mathbf{u}_{0,k}^{\mathrm{a}} - \mathbf{u}_{0,k}^{\mathrm{b}}\|\right) \\ + \gamma_y\left(\|h_y(\mathbf{y}_{0,k}^{\mathrm{a}}, \mathbf{y}_{0,k}^{\mathrm{b}})\|\right),\end{aligned} \tag{2.13a}$$

$$\begin{aligned}\|h_y(y_k^{\mathrm{a}}, y_k^{\mathrm{b}})\| \leq \beta_y(\|y_0^{\mathrm{a}} - y_0^{\mathrm{b}}\|, k) + \tilde{\gamma}_u\left(\|\mathbf{u}_{0,k}^{\mathrm{a}} - \mathbf{u}_{0,k}^{\mathrm{b}}\|\right) \\ + \gamma_x\left(\|h_x(\mathbf{x}_{0,k}^{\mathrm{a}}, \mathbf{x}_{0,k}^{\mathrm{b}})\|\right).\end{aligned} \tag{2.13b}$$

If there exist $\rho_1, \rho_2 \in \mathcal{K}_\infty$ such that for all $r \geq 0$

$$(\mathrm{id} + \rho_1) \circ \gamma_y \circ (\mathrm{id} + \rho_2) \circ \gamma_x(r) \leq r \tag{2.14}$$

then the following properties hold for the interconnected system:

(P1) There exist $\sigma, \gamma \in \mathcal{K}$ such that

$$\left\| \begin{bmatrix} h_x(\mathbf{x}_{0,k}^{\mathrm{a}}, \mathbf{x}_{0,k}^{\mathrm{b}}) \\ h_y(\mathbf{y}_{0,k}^{\mathrm{a}}, \mathbf{y}_{0,k}^{\mathrm{b}}) \end{bmatrix} \right\| \leq \sigma\left(\left\| \begin{bmatrix} x_0^{\mathrm{a}} - x_0^{\mathrm{b}} \\ y_0^{\mathrm{a}} - y_0^{\mathrm{b}} \end{bmatrix} \right\|\right) + \gamma\left(\|\mathbf{u}_{0,k}^{\mathrm{a}} - \mathbf{u}_{0,k}^{\mathrm{b}}\|\right). \tag{2.15}$$

(P2) There exists $\tilde{\gamma} \in \mathcal{K}$ such that

$$\limsup_{k\to\infty} \left\| \begin{bmatrix} h_x(x_k^{\mathrm{a}}, x_k^{\mathrm{b}}) \\ h_y(y_k^{\mathrm{a}}, y_k^{\mathrm{b}}) \end{bmatrix} \right\| \leq \tilde{\gamma}\left(\limsup_{k\to\infty} \|u_k^{\mathrm{a}} - u_k^{\mathrm{b}}\|\right). \tag{2.16}$$

Proof. The proof is reported in Section 2.6.1.

Remark 2.2. *Given functions γ_x and γ_y, functions $\rho_1, \rho_2 \in \mathcal{K}_\infty$, satisfying* (2.14)*, can be chosen as $\rho_1(r) = \varepsilon_1 r$ and $\rho_2(r) = \varepsilon_2 r$ with $\varepsilon_1, \varepsilon_2 > 0$.*

It is now possible to state the small gain theorem for δISS discrete-time systems.

Theorem 2.6 (Small gain theorem for δISS)**.** *Consider the interconnected system* (2.12)*, and assume that each subsystem is δISS with respect to u and the state of the other subsystem, i.e.*

$$\|x_k^{\mathrm{a}} - x_k^{\mathrm{b}}\| \leq \beta_x(\|x_0^{\mathrm{a}} - x_0^{\mathrm{b}}\|, k) + \gamma_u\left(\|\mathbf{u}_{0,k}^{\mathrm{a}} - \mathbf{u}_{0,k}^{\mathrm{b}}\|\right) + \gamma_y\left(\|\mathbf{y}_{0,k}^{\mathrm{a}} - \mathbf{y}_{0,k}^{\mathrm{b}}\|\right), \tag{2.17a}$$

$$\|y_k^{\mathrm{a}} - y_k^{\mathrm{b}}\| \leq \beta_y(\|y_0^{\mathrm{a}} - y_0^{\mathrm{b}}\|, k) + \tilde{\gamma}_u\left(\|\mathbf{u}_{0,k}^{\mathrm{a}} - \mathbf{u}_{0,k}^{\mathrm{b}}\|\right) + \gamma_x\left(\|\mathbf{x}_{0,k}^{\mathrm{a}} - \mathbf{x}_{0,k}^{\mathrm{b}}\|\right). \tag{2.17b}$$

If there exist $\rho_1, \rho_2 \in \mathcal{K}_\infty$ *such that for all* $r \geq 0$

$$(\mathrm{id} + \rho_1) \circ \gamma_y \circ (\mathrm{id} + \rho_2) \circ \gamma_x(r) \leq r \tag{2.18}$$

then the interconnected system (2.12) *is δISS with respect to* u.

Proof. By applying Lemma 2.1 considering $h_x(x^{\mathrm{a}}, x^{\mathrm{b}}) := x^{\mathrm{a}} - x^{\mathrm{b}}$ and $h_y(y^{\mathrm{a}}, y^{\mathrm{b}}) := y^{\mathrm{a}} - y^{\mathrm{b}}$, it follows that the interconnected system (2.12) is incrementally UBIBS and has an incremental asymptotic gain. Then, the δISS property follows from Theorem 2.5. □

Remark 2.3. *The small gain condition* (2.18) *is equivalent to*

$$(\mathrm{id} + \rho_2) \circ \gamma_x \circ (\mathrm{id} + \rho_1) \circ \gamma_y(r) \leq r$$

for [124, Lemma 27].

2.4.2 Small gain theorem for δISS-Lyapunov functions

In many applications the δISS property is proven by means of δISS-Lyapunov function. Hence, a formulation of the small gain theorem directly based on δISS-Lyapunov functions is derived in the following theorem.

Theorem 2.7. *Assume that the subsystems in* (2.12) *admit δISS-Lyapunov functions* V_x *and* V_y *such that*

$$\alpha_1(\|x^{\mathrm{a}} - x^{\mathrm{b}}\|) \leq V_x(x^{\mathrm{a}}, x^{\mathrm{b}}) \leq \alpha_2(\|x^{\mathrm{a}} - x^{\mathrm{b}}\|) \tag{2.19a}$$

$$\begin{aligned} &V_x(f(x^{\mathrm{a}}, y^{\mathrm{a}}, u^{\mathrm{a}}), f(x^{\mathrm{b}}, y^{\mathrm{b}}, u^{\mathrm{b}})) - V_x(x^{\mathrm{a}}, x^{\mathrm{b}}) \leq \\ &- \alpha_3(V_x(x^{\mathrm{a}}, x^{\mathrm{b}})) + \gamma(V_y(y^{\mathrm{a}}, y^{\mathrm{b}})) + \gamma_u(\|u^{\mathrm{a}} - u^{\mathrm{b}}\|) \end{aligned} \tag{2.19b}$$

and

$$\bar{\alpha}_1(\|y^{\mathrm{a}} - y^{\mathrm{b}}\|) \leq V_y(y^{\mathrm{a}}, y^{\mathrm{b}}) \leq \bar{\alpha}_2(\|y^{\mathrm{a}} - y^{\mathrm{b}}\|) \tag{2.20a}$$

$$\begin{aligned} &V_y(g(x^{\mathrm{a}}, y^{\mathrm{a}}, u^{\mathrm{a}}), g(x^{\mathrm{b}}, y^{\mathrm{b}}, u^{\mathrm{b}})) - V_y(y^{\mathrm{a}}, y^{\mathrm{b}}) \leq \\ &- \bar{\alpha}_3(V_y(y^{\mathrm{a}}, y^{\mathrm{b}})) + \bar{\gamma}(V_x(x^{\mathrm{a}}, x^{\mathrm{b}})) + \bar{\gamma}_u(\|u^{\mathrm{a}} - u^{\mathrm{b}}\|) \end{aligned} \tag{2.20b}$$

where $\alpha_1, \alpha_2, \alpha_3, \bar{\alpha}_1, \bar{\alpha}_2, \bar{\alpha}_3 \in \mathcal{K}_\infty$ *and are such that* $\mathrm{id} - \alpha_3 \in \mathcal{K}$, $\mathrm{id} - \bar{\alpha}_3 \in \mathcal{K}$, *and* $\gamma, \gamma_u, \bar{\gamma}, \bar{\gamma}_u \in \mathcal{K}$. *If there exist functions* $\rho_1, \rho_2, \mu_1, \mu_2 \in \mathcal{K}_\infty$ *such that for all* $r \geq 0$

$$(\mathrm{id} + \rho_1) \circ \alpha_3^{-1} \circ (\mathrm{id} + \mu_1) \circ \gamma \circ (\mathrm{id} + \rho_2) \circ \bar{\alpha}_3^{-1} \circ (\mathrm{id} + \mu_2) \circ \bar{\gamma}(r) \leq r, \tag{2.21}$$

then the interconnected system (2.12) *is δISS with respect to* u.

Proof. The proof is reported in Section 2.6.2.

Remark 2.4. *Two different small gain conditions,* (2.18) *and* (2.21)*, have been derived. These conditions depend on* γ_x, γ_y *and on* $\alpha_3, \gamma, \bar{\alpha}_3, \bar{\gamma}$*, respectively, that are not uniquely defined given the considered system.* γ_x, γ_y *and* $\alpha_3, \gamma, \bar{\alpha}_3, \bar{\gamma}$ *are conceptually related, but the derivation of one set of functions from the other is not straightforward, and is typically based on possibly conservative inequalities. Hence, the derivation of two independent conditions is very useful.*

2.4.3 Cascade connection

An useful particular case of the interconnection of two systems is the cascade connection, i.e. when the system (2.12) is reduced to

$$\begin{cases} x_{k+1} = f(x_k, y_k, u_k) \\ y_{k+1} = g(y_k, u_k) \end{cases} \tag{2.22}$$

In this case, if the two subsystems are δISS, it is always possible to apply the results of Theorem 2.6 with $\gamma_x = 0$. In particular, the following result holds.

Corollary 2.1. *Consider the interconnected system* (2.22)*. If the* x*-subsystem is* δ*ISS with respect to* u *and* y*, and the* y*-subsystem is* δ*ISS with respect to* u*, then the overall system* (2.22) *is* δ*ISS with respect to* u*.*

2.5 Conclusions

In this chapter we have introduced the stability notions used in the thesis, and the corresponding formulations of the Lyapunov theorem. These notions will be used in the reminder of the thesis to characterize both the system under control in open-loop and the behavior of the closed-loop system controlled by MPC. Moreover, we derived two different formulations of the small gain theorem for the interconnection of discrete-time δISS systems. In particular, the formulation of Theorem 2.7 is useful when the stability analysis of the subsystems is carried out by means of Lyapunov functions. Notably, the result for the cascade connection of δISS systems of [37] is a particular case of the generic feedback interconnection studied in this thesis.

2.6 Proofs

2.6.1 Proof of Lemma 2.1

The proof is divided in the proof of the incremental UBIBS-like property (P1) and in the proof of the incremental asymptotic gain-like property (P2).

Property (P1): From (2.13a)

$$
\begin{aligned}
&\|h_x(\mathbf{x}^{\mathrm{a}}_{0,k}, \mathbf{x}^{\mathrm{b}}_{0,k})\| \\
&\overset{(2.13a)}{\leq} \beta_x(\|x^{\mathrm{a}}_0 - x^{\mathrm{b}}_0\|, 0) + \gamma_u\left(\|\mathbf{u}^{\mathrm{a}}_{0,k} - \mathbf{u}^{\mathrm{b}}_{0,k}\|\right) + \gamma_y\left(\|h_y(\mathbf{y}^{\mathrm{a}}_{0,k}, \mathbf{y}^{\mathrm{b}}_{0,k})\|\right) \\
&\overset{(2.13b)}{\leq} \beta_x(\|x^{\mathrm{a}}_0 - x^{\mathrm{b}}_0\|, 0) + \gamma_u\left(\|\mathbf{u}^{\mathrm{a}}_{0,k} - \mathbf{u}^{\mathrm{b}}_{0,k}\|\right) \\
&\quad + \gamma_y\Big(\beta_y(\|y^{\mathrm{a}}_0 - y^{\mathrm{b}}_0\|, 0) + \tilde{\gamma}_u\left(\|\mathbf{u}^{\mathrm{a}}_{0,k} - \mathbf{u}^{\mathrm{b}}_{0,k}\|\right) + \gamma_x\left(\|h_x(\mathbf{x}^{\mathrm{a}}_{0,k}, \mathbf{x}^{\mathrm{b}}_{0,k})\|\right)\Big) \\
&\overset{(2.1)}{\leq} \beta_x(\|x^{\mathrm{a}}_0 - x^{\mathrm{b}}_0\|, 0) + \gamma_u\left(\|\mathbf{u}^{\mathrm{a}}_{0,k} - \mathbf{u}^{\mathrm{b}}_{0,k}\|\right) \\
&\quad + \gamma_y \circ (\mathrm{id} + \rho_2) \circ \gamma_x\left(\|h_x(\mathbf{x}^{\mathrm{a}}_{0,k}, \mathbf{x}^{\mathrm{b}}_{0,k})\|\right) \\
&\quad + \gamma_y \circ (\mathrm{id} + \rho_2^{-1})\left(\beta_y(\|y^{\mathrm{a}}_0 - y^{\mathrm{b}}_0\|, 0) + \tilde{\gamma}_u\left(\|\mathbf{u}^{\mathrm{a}}_{0,k} - \mathbf{u}^{\mathrm{b}}_{0,k}\|\right)\right)
\end{aligned}
$$

for any $\rho_2 \in \mathcal{K}_\infty$. By rearranging the previous inequality, one has that

$$
\begin{aligned}
&(\mathrm{id} - (\gamma_y \circ (\mathrm{id} + \rho_2) \circ \gamma_x))\,(\|h_x(\mathbf{x}^{\mathrm{a}}_{0,k}, \mathbf{x}^{\mathrm{b}}_{0,k})\|) \\
&\leq \beta_x(\|x^{\mathrm{a}}_0 - x^{\mathrm{b}}_0\|, 0) + \gamma_u\left(\|\mathbf{u}^{\mathrm{a}}_{0,k} - \mathbf{u}^{\mathrm{b}}_{0,k}\|\right) \\
&\quad + \gamma_y \circ (\mathrm{id} + \rho_2^{-1})\left(\beta_y(\|y^{\mathrm{a}}_0 - y^{\mathrm{b}}_0\|, 0) + \tilde{\gamma}_u\left(\|\mathbf{u}^{\mathrm{a}}_{0,k} - \mathbf{u}^{\mathrm{b}}_{0,k}\|\right)\right).
\end{aligned}
$$

From (2.14), there exists a function $\rho_1 \in \mathcal{K}_\infty$ such that

$$
(\mathrm{id} - (\gamma_y \circ (\mathrm{id} + \rho_2) \circ \gamma_x))\,(r) \geq \rho_1 \circ \gamma_y \circ (\mathrm{id} + \rho_2) \circ \gamma_x(r).
$$

Hence

$$
\begin{aligned}
&\rho_1 \circ \gamma_y \circ (\mathrm{id} + \rho_2) \circ \gamma_x(\|h_x(\mathbf{x}^{\mathrm{a}}_{0,k}, \mathbf{x}^{\mathrm{b}}_{0,k})\|) \\
&\leq \beta_x(\|x^{\mathrm{a}}_0 - x^{\mathrm{b}}_0\|, 0) + \gamma_u\left(\|\mathbf{u}^{\mathrm{a}}_{0,k} - \mathbf{u}^{\mathrm{b}}_{0,k}\|\right) \\
&\quad + \gamma_y \circ (\mathrm{id} + \rho_2^{-1})\left(\beta_y(\|y^{\mathrm{a}}_0 - y^{\mathrm{b}}_0\|, 0) + \tilde{\gamma}_u\left(\|\mathbf{u}^{\mathrm{a}}_{0,k} - \mathbf{u}^{\mathrm{b}}_{0,k}\|\right)\right).
\end{aligned}
$$

Note that $\rho_3 := \rho_1 \circ \gamma_y \circ (\mathrm{id} + \rho_2) \circ \gamma_x$ is the composition of functions of classes $\mathcal{K}$ and $\mathcal{K}_\infty$, hence it is a $\mathcal{K}_\infty$ function and is invertible. By using the weak triangle inequality on the last term of the right hand side and applying ρ_3^{-1} to both sides, it is possible to obtain that there exist functions $\sigma_1, \gamma_1 \in \mathcal{K}$ such that

$$
\|h_x(\mathbf{x}^{\mathrm{a}}_{0,k}, \mathbf{x}^{\mathrm{b}}_{0,k})\| \leq \sigma_1\left(\left\|\begin{bmatrix} x^{\mathrm{a}}_0 - x^{\mathrm{b}}_0 \\ y^{\mathrm{a}}_0 - y^{\mathrm{b}}_0 \end{bmatrix}\right\|\right) + \gamma_1\left(\|\mathbf{u}^{\mathrm{a}}_{0,k} - \mathbf{u}^{\mathrm{a}}_{0,k}\|\right). \tag{2.23}
$$

In a similar way it is possible to obtain that there exist functions $\sigma_2, \gamma_2 \in \mathcal{K}$ such that

$$
\|h_y(\mathbf{y}^{\mathrm{a}}_{0,k}, \mathbf{y}^{\mathrm{b}}_{0,k})\| \leq \sigma_2\left(\left\|\begin{bmatrix} x^{\mathrm{a}}_0 - x^{\mathrm{b}}_0 \\ y^{\mathrm{a}}_0 - y^{\mathrm{b}}_0 \end{bmatrix}\right\|\right) + \gamma_2\left(\|\mathbf{u}^{\mathrm{a}}_{0,k} - \mathbf{u}^{\mathrm{b}}_{0,k}\|\right). \tag{2.24}
$$

The incremental UBIBS-like property (2.15) follows from (2.23) and (2.24) by taking $\sigma = \sqrt{\sigma_1^2 + \sigma_2^2}$ and $\gamma = \sqrt{\gamma_1^2 + \gamma_2^2}$.

Property (P2): From (2.23) and (2.24) it follows that if $\limsup_{k\to\infty} \left\|u_k^{\mathrm{a}} - u_k^{\mathrm{b}}\right\|$ is finite, then there exists some $c > 0$ (depending on $\|x_0^{\mathrm{a}} - x_0^{\mathrm{b}}\|$, $\|y_0^{\mathrm{a}} - y_0^{\mathrm{b}}\|$ and $\|\mathbf{u}_{0,\infty}^{\mathrm{a}} - \mathbf{u}_{0,\infty}^{\mathrm{b}}\|$) such that $\|h_x(x_k^{\mathrm{a}}, x_k^{\mathrm{b}})\| \leq c$ and $\|h_y(y_k^{\mathrm{a}}, y_k^{\mathrm{b}})\| \leq c$ for all $k \in \mathbb{Z}_{\geq 0}$. Hence, the limits $\limsup_{k\to\infty} \|h_x(x_k^{\mathrm{a}}, x_k^{\mathrm{b}})\|$ and $\limsup_{k\to\infty} \|h_y(y_k^{\mathrm{a}}, y_k^{\mathrm{b}})\|$ are finite. Then, by assumption, also $\limsup_{k\to\infty} \|x_k^{\mathrm{a}} - x_k^{\mathrm{b}}\|$ and $\limsup_{k\to\infty} \|y_k^{\mathrm{a}} - y_k^{\mathrm{b}}\|$ are finite.

Define $\bar{k} := \lceil \frac{k}{2} \rceil$. Then

$$\begin{aligned}
\|h_x(x_k^{\mathrm{a}}, x_k^{\mathrm{b}})\| &\overset{(2.13a)}{\leq} \beta_x(\|x_{\bar{k}}^{\mathrm{a}} - x_{\bar{k}}^{\mathrm{b}}\|, k - \bar{k}) + \gamma_u\left(\|\mathbf{u}_{\bar{k},k}^{\mathrm{a}} - \mathbf{u}_{\bar{k},k}^{\mathrm{b}}\|\right) \\
&\quad + \gamma_y\left(\|h_y(\mathbf{y}_{\bar{k},k}^{\mathrm{a}}, \mathbf{y}_{\bar{k},k}^{\mathrm{b}})\|\right) \\
&\leq \beta_x(\bar{c}, k - \bar{k}) + \gamma_u\left(\|\mathbf{u}_{\bar{k},k}^{\mathrm{a}} - \mathbf{u}_{\bar{k},k}^{\mathrm{b}}\|\right) + \gamma_y\left(\|h_y(\mathbf{y}_{\bar{k},k}^{\mathrm{a}}, \mathbf{y}_{\bar{k},k}^{\mathrm{b}})\|\right)
\end{aligned}$$

for some $\bar{c} > 0$. Take the limit superior and exploit its subadditivity property

$$\begin{aligned}
\limsup_{k\to\infty} \|h_x(x_k^{\mathrm{a}}, x_k^{\mathrm{b}})\| &\leq \limsup_{k\to\infty} \beta_x(\bar{c}, k - \bar{k}) + \limsup_{k\to\infty} \gamma_u\left(\|\mathbf{u}_{\bar{k},k}^{\mathrm{a}} - \mathbf{u}_{\bar{k},k}^{\mathrm{b}}\|\right) \\
&\quad + \limsup_{k\to\infty} \gamma_y\left(\|h_y(\mathbf{y}_{\bar{k},k}^{\mathrm{a}}, \mathbf{y}_{\bar{k},k}^{\mathrm{b}})\|\right) \\
&\leq \gamma_u\left(\limsup_{k\to\infty} \|u_k^{\mathrm{a}} - u_k^{\mathrm{b}}\|\right) + \gamma_y\left(\limsup_{k\to\infty} \|h_y(y_k^{\mathrm{a}}, y_k^{\mathrm{b}})\|\right).
\end{aligned} \tag{2.25}$$

Similarly

$$\limsup_{k\to\infty} \|h_y(y_k^{\mathrm{a}}, y_k^{\mathrm{b}})\| \leq \tilde{\gamma}_u\left(\limsup_{k\to\infty} \|u_k^{\mathrm{a}} - u_k^{\mathrm{b}}\|\right) + \gamma_x\left(\limsup_{k\to\infty} \|h_x(x_k^{\mathrm{a}}, x_k^{\mathrm{b}})\|\right). \tag{2.26}$$

Substitute (2.26) in (2.25)

$$\begin{aligned}
&\limsup_{k\to\infty} \|h_x(x_k^{\mathrm{a}}, x_k^{\mathrm{b}})\| \\
&\leq \gamma_y\left(\gamma_x\left(\limsup_{k\to\infty} \|h_x(x_k^{\mathrm{a}}, x_k^{\mathrm{b}})\|\right) + \tilde{\gamma}_u\left(\limsup_{k\to\infty} \|u_k^{\mathrm{a}} - u_k^{\mathrm{b}}\|\right)\right) \\
&\quad + \gamma_u\left(\limsup_{k\to\infty} \|u_k^{\mathrm{a}} - u_k^{\mathrm{b}}\|\right) \\
&\overset{(2.1)}{\leq} \gamma_y \circ (\mathrm{id} + \rho_2) \circ \gamma_x\left(\limsup_{k\to\infty} \|h_x(x_k^{\mathrm{a}}, x_k^{\mathrm{b}})\|\right) \\
&\quad + \gamma_y \circ (\mathrm{id} + \rho_2^{-1}) \circ \tilde{\gamma}_u\left(\limsup_{k\to\infty} \|u_k^{\mathrm{a}} - u_k^{\mathrm{b}}\|\right) + \gamma_u\left(\limsup_{k\to\infty} \|u_k^{\mathrm{a}} - u_k^{\mathrm{b}}\|\right)
\end{aligned}$$

for any $\rho_2 \in \mathcal{K}_\infty$. Rearranging the previous inequality

$$\begin{aligned}&(\mathrm{id} - (\gamma_y \circ (\mathrm{id} + \rho_2) \circ \gamma_x)) \left(\limsup_{k\to\infty} \|h_x(x_k^{\mathrm{a}}, x_k^{\mathrm{b}})\| \right) \\ &\leq \gamma_y \circ (\mathrm{id} + \rho_2^{-1}) \circ \tilde{\gamma}_u \left(\limsup_{k\to\infty} \|u_k^{\mathrm{a}} - u_k^{\mathrm{b}}\| \right) + \gamma_u \left(\limsup_{k\to\infty} \|u_k^{\mathrm{a}} - u_k^{\mathrm{b}}\| \right).\end{aligned}$$

From (2.14), with steps similar to the first part of the proof, it follows that there exists a function $\rho_1 \in \mathcal{K}_\infty$ such that

$$\begin{aligned}&\rho_1 \circ \gamma_y \circ (\mathrm{id} + \rho_2) \circ \gamma_x \left(\limsup_{k\to\infty} \|h_x(x_k^{\mathrm{a}}, x_k^{\mathrm{b}})\| \right) \\ &\leq \gamma_y \circ (\mathrm{id} + \rho_2^{-1}) \circ \tilde{\gamma}_u \left(\limsup_{k\to\infty} \|u_k^{\mathrm{a}} - u_k^{\mathrm{b}}\| \right) + \gamma_u \left(\limsup_{k\to\infty} \|u_k^{\mathrm{a}} - u_k^{\mathrm{b}}\| \right).\end{aligned}$$

Then the incremental asymptotic gain-like property (P2) can be proven by applying ρ_3^{-1} to both sides of the inequality, and repeating the same reasoning for $\limsup_{k\to\infty} \|h_y(y_k^{\mathrm{a}}, y_k^{\mathrm{b}})\|$. □

2.6.2 Proof of Theorem 2.7

The proof of Theorem 2.7 makes use of the following auxiliary Lemma.

Lemma 2.2. *If system* (2.7) *has a δISS-Lyapunov function V such that*

$$\begin{aligned}&V(f(x^{\mathrm{a}}, u^{\mathrm{a}}), f(x^{\mathrm{b}}, u^{\mathrm{b}})) - V(x^{\mathrm{a}}, x^{\mathrm{b}}) \\ &\leq -\alpha_3(V(x^{\mathrm{a}}, x^{\mathrm{b}})) + \gamma(\|u^{\mathrm{a}} - u^{\mathrm{b}}\|)\end{aligned}$$

with $\alpha_3 \in \mathcal{K}_\infty$ such that $\mathrm{id} - \alpha_3 \in \mathcal{K}$ *and $\gamma \in \mathcal{K}$, then there exist $\beta \in \mathcal{KL}$ and $\tilde{\gamma} \in \mathcal{K}$ such that*

$$\begin{aligned}&V(x(k, x_0^{\mathrm{a}}, \mathbf{u}_{0,k}^{\mathrm{a}}), x(k, x_0^{\mathrm{b}}, \mathbf{u}_{0,k}^{\mathrm{b}})) \\ &\leq \beta \left(V(x_0^{\mathrm{a}}, x_0^{\mathrm{b}}), k \right) + \tilde{\gamma}(\|\mathbf{u}_{0,k}^{\mathrm{a}} - \mathbf{u}_{0,k}^{\mathrm{b}}\|)\end{aligned}$$

where $\tilde{\gamma} = \alpha_3^{-1} \circ \rho^{-1} \circ \gamma$ for any function $\rho \in \mathcal{K}_\infty$ such that $\mathrm{id} - \rho \in \mathcal{K}_\infty$.

Proof. Consider any function $\rho \in \mathcal{K}_\infty$ such that $\mathrm{id} - \rho \in \mathcal{K}_\infty$, and define the sets $\mathcal{S}(k) := \{(x^{\mathrm{a}}, x^{\mathrm{b}}) \in \mathbb{R}^n \times \mathbb{R}^n : V(x^{\mathrm{a}}, x^{\mathrm{b}}) \leq b(k)\}$, where $b(k) := \alpha_3^{-1} \circ \rho^{-1} \circ \gamma(\|\mathbf{u}_{0,k+1}^{\mathrm{a}} - \mathbf{u}_{0,k+1}^{\mathrm{b}}\|)$. Distinguish two cases:

(C1) $(x_k^{\mathrm{a}}, x_k^{\mathrm{b}}) \in \mathcal{S}(k)$;

(C2) $(x_k^{\mathrm{a}}, x_k^{\mathrm{b}}) \notin \mathcal{S}(k)$.

Case (C1): One has that

$$\begin{aligned} V(x^{\mathrm{a}}_{k+1}, x^{\mathrm{b}}_{k+1}) &\leq (\mathrm{id} - \alpha_3)(V(x^{\mathrm{a}}_k, x^{\mathrm{b}}_k)) + \gamma(\|u^{\mathrm{a}}_k - u^{\mathrm{b}}_k\|) \\ &\leq (\mathrm{id} - \alpha_3)(V(x^{\mathrm{a}}_k, x^{\mathrm{b}}_k)) + \gamma(\|\mathbf{u}^{\mathrm{a}}_{0,k+1} - \mathbf{u}^{\mathrm{b}}_{0,k+1}\|). \end{aligned}$$

Since $\mathrm{id} - \alpha_3 \in \mathcal{K}$,

$$\begin{aligned} V(x^{\mathrm{a}}_{k+1}, x^{\mathrm{b}}_{k+1}) &\leq (\mathrm{id} - \alpha_3)(b(k)) + \gamma(\|\mathbf{u}^{\mathrm{a}}_{0,k+1} - \mathbf{u}^{\mathrm{b}}_{0,k+1}\|) \\ &= -(\mathrm{id} - \rho) \circ \alpha_3(b(k)) + b(k) - \rho \circ \alpha_3(b(k)) \\ &\quad + \gamma(\|\mathbf{u}^{\mathrm{a}}_{0,k+1} - \mathbf{u}^{\mathrm{b}}_{0,k+1}\|) \\ &= -(\mathrm{id} - \rho) \circ \alpha_3(b(k)) + b(k) \\ &\leq b(k) = \alpha_3^{-1} \circ \rho^{-1} \circ \gamma(\|\mathbf{u}^{\mathrm{a}}_{0,k+1} - \mathbf{u}^{\mathrm{b}}_{0,k+1}\|) \\ &= \tilde{\gamma}(\|\mathbf{u}^{\mathrm{a}}_{0,k+1} - \mathbf{u}^{\mathrm{b}}_{0,k+1}\|) \end{aligned}$$

i.e. $(x^{\mathrm{a}}_{k+1}, x^{\mathrm{b}}_{k+1}) \in \mathcal{S}(k)$. Moreover, note that $\mathcal{S}(k+1) \supseteq \mathcal{S}(k)$ because $b(k+1) = \tilde{\gamma}(\|\mathbf{u}^{\mathrm{a}}_{0,k+2} - \mathbf{u}^{\mathrm{b}}_{0,k+2}\|) \geq \tilde{\gamma}(\|\mathbf{u}^{\mathrm{a}}_{0,k+1} - \mathbf{u}^{\mathrm{b}}_{0,k+1}\|) = b(k)$. Hence, if the system is in Case (C1) at time step k, it remains in Case (C1) for all the subsequent time steps.
Case (C2): One has that

$$\begin{aligned} V(x^{\mathrm{a}}_{k+1}, x^{\mathrm{b}}_{k+1}) - V(x^{\mathrm{a}}_k, x^{\mathrm{b}}_k) &\leq -\alpha_3(V(x^{\mathrm{a}}_k, x^{\mathrm{b}}_k)) + \gamma(\|u^{\mathrm{a}}_k - u^{\mathrm{b}}_k\|) \\ &= -(\mathrm{id} - \rho) \circ \alpha_3(V(x^{\mathrm{a}}_k, x^{\mathrm{b}}_k)) \\ &\quad - \rho \circ \alpha_3(V(x^{\mathrm{a}}_k, x^{\mathrm{b}}_k)) + \gamma(\|u^{\mathrm{a}}_k - u^{\mathrm{b}}_k\|) \\ &\leq -(\mathrm{id} - \rho) \circ \alpha_3(V(x^{\mathrm{a}}_k, x^{\mathrm{b}}_k)). \end{aligned}$$

Since the system can be in Case (C2) only in the initial time steps, it is possible to use [113, Lemma 4.3] to show that there exists a function $\beta \in \mathcal{KL}$ such that

$$V(x^{\mathrm{a}}_k, x^{\mathrm{b}}_k) \leq \beta(V(x^{\mathrm{a}}_0, x^{\mathrm{b}}_0), k).$$

Finally, the Lemma is proven combining Cases (C1) and (C2). □

Proof of Theorem 2.7. In view of Lemma 2.2, it is possible to rewrite (2.19b) and (2.20b) as

$$\begin{aligned} V_x(x^{\mathrm{a}}_k, x^{\mathrm{b}}_k) &\leq \beta_x\left(V_x(x^{\mathrm{a}}_0, x^{\mathrm{b}}_0), k\right) \\ &\quad + \alpha_3^{-1} \circ \rho_x^{-1}\left(\gamma(\|V_y(\mathbf{y}^{\mathrm{a}}_{0,k}, \mathbf{y}^{\mathrm{b}}_{0,k})\|) + \gamma_u(\|\mathbf{u}^{\mathrm{a}}_{0,k} - \mathbf{u}^{\mathrm{b}}_{0,k}\|)\right), \\ V_y(y^{\mathrm{a}}_k, y^{\mathrm{b}}_k) &\leq \beta_y\left(V_y(y^{\mathrm{a}}_0, y^{\mathrm{b}}_0), k\right) \\ &\quad + \bar{\alpha}_3^{-1} \circ \rho_y^{-1}\left(\bar{\gamma}(\|V_x(\mathbf{x}^{\mathrm{a}}_{0,k}, \mathbf{x}^{\mathrm{b}}_{0,k})\|) + \bar{\gamma}_u(\|\mathbf{u}^{\mathrm{a}}_{0,k} - \mathbf{u}^{\mathrm{b}}_{0,k}\|)\right), \end{aligned}$$

for any couple of functions $\rho_x, \rho_y \in \mathcal{K}_\infty$ such that $\mathrm{id} - \rho_x \in \mathcal{K}_\infty$ and $\mathrm{id} - \rho_y \in \mathcal{K}_\infty$ and for some functions $\beta_x, \beta_y \in \mathcal{KL}$. Applying the weak triangle inequality (2.1) and using (2.19a) and (2.20a), one obtains that for any $\mu_x, \mu_y \in \mathcal{K}_\infty$

$$\begin{aligned} V_x(x_k^{\mathrm{a}}, x_k^{\mathrm{b}}) \leq \hat{\beta}_x \left(\|x_0^{\mathrm{a}} - x_0^{\mathrm{b}}\|, k \right) \\ + \alpha_3^{-1} \circ \rho_x^{-1} \circ (\mathrm{id} + \mu_x) \circ \gamma(\|V_y(\mathbf{y}_{0,k}^{\mathrm{a}}, \mathbf{y}_{0,k}^{\mathrm{b}})\|) \\ + \alpha_3^{-1} \circ \rho_x^{-1} \circ (\mathrm{id} + \mu_x^{-1}) \circ \gamma_u(\|\mathbf{u}_{0,k}^{\mathrm{a}} - \mathbf{u}_{0,k}^{\mathrm{b}}\|) \end{aligned}$$

and

$$\begin{aligned} V_y(y_k^{\mathrm{a}}, y_k^{\mathrm{b}}) \leq \hat{\beta}_y \left(\|y_0^{\mathrm{a}} - y_0^{\mathrm{b}}\|, k \right) \\ + \bar{\alpha}_3^{-1} \circ \rho_y^{-1} \circ (\mathrm{id} + \mu_y) \circ \bar{\gamma}(\|V_x(\mathbf{x}_{0,k}^{\mathrm{a}}, \mathbf{x}_{0,k}^{\mathrm{b}})\|) \\ + \bar{\alpha}_3^{-1} \circ \rho_y^{-1} \circ (\mathrm{id} + \mu_y^{-1}) \circ \bar{\gamma}_u(\|\mathbf{u}_{0,k}^{\mathrm{a}} - \mathbf{u}_{0,k}^{\mathrm{b}}\|) \end{aligned}$$

where $\hat{\beta}_x(r,k) := \beta_x(\alpha_2(r), k)$ and $\hat{\beta}_y(r,k) := \beta_y(\bar{\alpha}_2(r), k)$.

Pick $\hat{\mu}_x, \mu_x \in \mathcal{K}_\infty$ such that $(\mathrm{id} + \hat{\mu}_x) \circ (\mathrm{id} + \mu_x)(r) = (\mathrm{id} + \mu_1)(r)$ for all $r \geq 0$ (this is always possible in view of [124, Lemma 23]), and ρ_x such that $\rho_x^{-1} = \mathrm{id} + \hat{\mu}_x$. Similarly, pick $\hat{\mu}_y, \mu_y \in \mathcal{K}_\infty$ such that $(\mathrm{id} + \hat{\mu}_y) \circ (\mathrm{id} + \mu_y)(r) = (\mathrm{id} + \mu_2)(r)$ for all $r \geq 0$, and ρ_y such that $\rho_y^{-1} = \mathrm{id} + \hat{\mu}_x$. Then, in view of (2.21), it is possible to apply Lemma 2.1 with $h_x = V_x$, $h_y = V_y$, $\gamma_y = \alpha_3^{-1} \circ (\mathrm{id} + \mu_1) \circ \gamma$ and $\gamma_x = \bar{\alpha}_3^{-1} \circ (\mathrm{id} + \mu_2) \circ \bar{\gamma}$ to obtain that there exist $\sigma, \hat{\gamma}, \tilde{\gamma} \in \mathcal{K}$ such that

$$\left\| \begin{bmatrix} V_x(\mathbf{x}_{0,k}^{\mathrm{a}}, \mathbf{x}_{0,k}^{\mathrm{b}}) \\ V_y(\mathbf{y}_{0,k}^{\mathrm{a}}, \mathbf{y}_{0,k}^{\mathrm{b}}) \end{bmatrix} \right\| \leq \sigma \left(\left\| \begin{bmatrix} x_0^{\mathrm{a}} - x_0^{\mathrm{b}} \\ y_0^{\mathrm{a}} - y_0^{\mathrm{b}} \end{bmatrix} \right\| \right) + \hat{\gamma} \left(\|\mathbf{u}_{0,k}^{\mathrm{a}} - \mathbf{u}_{0,k}^{\mathrm{b}}\| \right) \tag{2.27a}$$

and

$$\limsup_{k \to \infty} \left\| \begin{bmatrix} V_x(x_k^{\mathrm{a}}, x_k^{\mathrm{b}}) \\ V_y(y_k^{\mathrm{a}}, y_k^{\mathrm{b}}) \end{bmatrix} \right\| \leq \tilde{\gamma} \left(\limsup_{k \to \infty} \|u_k^{\mathrm{a}} - u_k^{\mathrm{b}}\| \right). \tag{2.27b}$$

Inequalities (2.27a) and (2.27b) can be combined with (2.19a) and (2.20a) to obtain that the system is incrementally UBIBS and has an incremental asymptotic gain. Then, δISS follows from Theorem 2.5. □

Chapter 3

Introduction to Model Predictive Control

In this chapter, we introduce the basics of MPC and the main control problems that are analyzed in the thesis. First, we introduce the MPC algorithm in the simplest case, that is the regulation to a constant set-point, and we present the two main methods to achieve closed-loop stability, that are the design of terminal ingredients and the use of a long enough prediction horizon in combination with a cost controllability property of the system. Then, we analyze the more complex control problems that will be studied in the remaining parts of the thesis in combination with data-driven models. In particular, output-feedback MPC schemes are introduced in Section 3.3. In Section 3.4 we deal with the issue of state constraints in presence of model uncertainty, and we give a general overview of robust MPC algorithms. In Section 3.5 we introduce some algorithms for offset-free tracking MPC in presence of disturbances and model-plant mismatch. A modified MPC scheme to deal with incremental input constraints is shown in Section 3.6. Finally, the use of artificial reference and of semi-definite stage cost in the MPC algorithm are analyzed respectively in Sections 3.7 and 3.8.

The presentation of this chapter is done in a general way, and we introduce all the main ideas while neglecting some of the technical details, that will instead be treated in an exhaustive way in the following chapters for each one of the specific MPC algorithms.

3.1 MPC algorithm

Consider a discrete-time system

$$x_{k+1} = f(x_k, u_k) \tag{3.1}$$

with state $x \in \mathbb{R}^n$ and input $u \in \mathbb{R}^m$. In the simplest formulation of the MPC, the control objective is to perform regulation to a reference equilib-

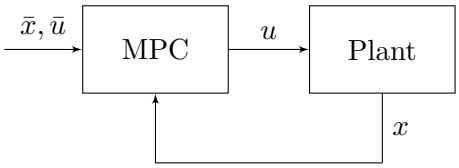

Figure 3.1: Block diagram of the MPC algorithm.

rium $(\bar{x}, \bar{u})$ of the system. The control problem may include input constraints $u \in \mathcal{U} \subseteq \mathbb{R}^m$ and state constraints $x \in \mathcal{X} \subseteq \mathbb{R}^n$.

In the MPC algorithm, we solve a finite horizon optimal control problem (FHOCP) at each time step, and then we apply to the plant only the first element of the optimal input sequence, according to the so-called receding horizon (RH) principle. Since the FHOCP solved at each time step is initialized using the current value of the system state, the MPC algorithm implicitly defines a state-feedback control law.

The cost function in the optimization problem is given by the sum of the stage cost over N steps in the future, where N is called *prediction horizon*. The stage cost is a function $\ell : \mathbb{R}^n \times \mathbb{R}^m \to \mathbb{R}$. A typical choice is the use of quadratic positive definite stage cost functions, i.e. cost functions in the form

$$\ell(x, u) = \|x - \bar{x}\|_Q^2 + \|u - \bar{u}\|_R^2 \tag{3.2}$$

where $Q = Q^\top \in \mathbb{R}^{n \times n}$ and $R = R^\top \in \mathbb{R}^{m \times m}$ are positive definite matrices, while $(\bar{x}, \bar{u})$ is the reference equilibrium of the system under control. The final state in the optimization problem may be penalized more according to a terminal cost $V_\mathrm{f} : \mathbb{R}^n \to \mathbb{R}$. The terminal cost is often designed to take into account the cost on the infinite horizon, and can be used to enforce stability of the closed-loop. It is also possible to include a terminal constraint on the last predicted state, that is given by the set $\mathcal{X}_\mathrm{f}$. The terminal set is used to ensure constraint satisfaction on the infinite horizon. The MPC algorithm is reported in Algorithm 3.1. The algorithm considers the ideal case (also called *nominal* case), in which the future predictions of the system used to compute the cost and constraints are obtained using the system dynamics (3.1). When the exact description of the system is not available, a surrogate model can be used in (3.3c). A common method is the use of first principle models or gray box models. In this thesis we explore the use of data-driven models. Through the thesis, we use k to denote the current time step of the system, while i is used as an index in the FHOCP predictions.

The block diagram that schematically represents the components of the closed-loop with MPC is reported in Figure 3.1, where we can see the state-feedback nature of the MPC control law. This schema will be modified with additional blocks in the next sections to consider more complex control problems.

In order for the MPC algorithm to be well defined, it is required that the

Algorithm 3.1 Model Predictive Control

Input: Horizon $N \in \mathbb{N}$, input constraints $\mathcal{U}$, state constraints $\mathcal{X}$, stage cost $\ell(\cdot,\cdot)$, terminal cost $V_{\mathrm{f}}(\cdot)$, terminal set $\mathcal{X}_{\mathrm{f}}$

For each $k = 0, 1, ...$

(1) Measure current state x_k.

(2) Let $\mathbf{u} := \{u_{i|k}\}_{i=0}^{N-1}$. Solve the finite horizon optimal control problem

$$\begin{aligned}
\min_{\mathbf{u}} \quad & \sum_{i=0}^{N-1} \ell(x_{i|k}, u_{i|k}) + V_{\mathrm{f}}(x_{N|k}) && \text{(3.3a)}\\
\text{s.t.} \quad & x_{i|k} = x_k && \text{(3.3b)}\\
& x_{i+1|k} = f(x_{i|k}, u_{i|k}), \quad \text{for } i \in [0 : N-1] && \text{(3.3c)}\\
& u_{i|k} \in \mathcal{U}, \quad \text{for } i \in [0 : N-1] && \text{(3.3d)}\\
& x_{i|k} \in \mathcal{X}, \quad \text{for } i \in [0 : N-1] && \text{(3.3e)}\\
& x_{N|k} \in \mathcal{X}_{\mathrm{f}} && \text{(3.3f)}
\end{aligned}$$

to obtain the optimal control sequence $\mathbf{u}^\star = \{u^\star_{0|k}, \ldots, u^\star_{N-1|k}\}$.

(3) Apply the MPC feedback law

$$u_k = \mu^{\mathrm{MPC}}(x_k) = u^\star_{0|k}. \tag{3.4}$$

optimal control problem (3.3) is feasible for all k. This property is not always guaranteed when state constraints are present in the optimization problem. Therefore, one of the key properties that must be guaranteed when designing an MPC control law is *recursive feasibility*. The MPC control law is said to be recursively feasible if the existence of a solution of the FHOCP at time step $k = 0$ implies that the FHOCP is feasible $\forall\, k \in \mathbb{Z}_{\geq 0}$.

We introduce now some useful notation. We denote the MPC cost function as

$$J(x, \mathbf{u}) := \sum_{i=0}^{N-1} \ell(x_{i|k}, u_{i|k}) + V_{\mathrm{f}}(x_{N|k})$$

where $\mathbf{u} := \{u_{0|k}, \ldots, u_{N-1|k}\}$, $x_{0|k} := x$ and $x_{i|k}$ are defined according to (3.3c). We also define $V(x) := J(x, \mathbf{u}^\star)$ as the optimal cost of (3.3). $V(x)$ is also called *(optimal) value function*. In some parts of the thesis, the dependence of the cost function and of the value function from the prediction horizon will be explicitly stated, and it will be indicated as a subscript, i.e. by using $J_N(x, \mathbf{u})$ and $V_N(x)$.

3.2 MPC stability

In general it is not guaranteed that the MPC Algorithm 3.1 stabilizes the system (3.1). In fact, there are several examples in which the application of the MPC control law renders unstable systems that are open-loop stable and even linear, see, e.g., the chain of mass-spring-dampers example in Section VII-A in [133]. For this reason, the study of stabilizing MPC algorithms is very important. There are two main methods in the literature to design stabilizing MPC algorithms. The first one relies on the design of the terminal cost and terminal constraint. The second uses a sufficiently long prediction horizon in combination with a cost controllability property of the system under control.

In the simplest version, the stabilizing MPC algorithms require the use of a positive definite stage cost ℓ. This means that the stage cost must satisfy the following assumption.

Assumption 3.1. *There exists a function $\alpha_\ell \in \mathcal{K}_\infty$ such that*

$$\ell(x, u) \geq \alpha_\ell(\|x - \bar{x}\|) \tag{3.5}$$

for all $x \in \mathcal{X}$ and $u \in \mathcal{U}$.

The most common choice is a quadratic stage cost as in (3.2), with positive definite matrices Q and R. The use of a stage cost that is only positive semi-definite is further discussed in Section 3.8.

3.2.1 Stability based on terminal ingredients

This method [169, 197] is based on the knowledge of a locally stabilizing auxiliary control law μ_a for the system, that is used for the design of the terminal cost V_f and the terminal set $\mathcal{X}_\mathrm{f}$.

Assumption 3.2. *The terminal set $\mathcal{X}_\mathrm{f}$ and the terminal cost V_f are such that, for an auxiliary control law $\mu_\mathrm{a} : \mathcal{X}_\mathrm{f} \to \mathbb{R}^m$, it holds that:*

1. *$\mathcal{X}_\mathrm{f} \subseteq \mathcal{X}$ and contains the target equilibrium $\bar{x}$ in its interior;*
2. *$\mathcal{X}_\mathrm{f}$ is a positive invariant set for the system under the auxiliary control law, i.e. $f(x, \mu_\mathrm{a}(x)) \in \mathcal{X}_\mathrm{f}$ for all $x \in \mathcal{X}_\mathrm{f}$;*
3. *$\mu_\mathrm{a}(x) \in \mathcal{U}$ for all $x \in \mathcal{X}_\mathrm{f}$;*
4. *The terminal cost $V_\mathrm{f} : \mathcal{X}_\mathrm{f} \to \mathbb{R}_{\geq 0}$ is such that*

$$V_\mathrm{f}(f(x, \mu_\mathrm{a}(x))) - V_\mathrm{f}(x) \leq -\ell(x, \mu_\mathrm{a}(x)) \tag{3.6}$$

for all $x \in \mathcal{X}_\mathrm{f}$. Moreover, there exists $\alpha_\mathrm{f} \in \mathcal{K}_\infty$ such that

$$V_\mathrm{f}(x) \leq \alpha_\mathrm{f}(\|x - \bar{x}\|) \quad \forall x \in \mathcal{X}_\mathrm{f}. \tag{3.7}$$

In the following, we state the main result about asymptotic stability of MPC with terminal ingredients. The proof is reported for tutorial reasons, and to introduce some of the notation that will be employed in the stability proofs along the thesis.

Theorem 3.1. *Let Assumptions 3.1 and 3.2 hold and assume that $\mathcal{U}$ is bounded. Let $\mathcal{X}_N$ be the set of states from which there exists a solution of the FHOCP. Then, the MPC Algorithm 3.1 is recursively feasible and $x = \bar{x}$ is an asymptotically stable equilibrium point of the closed-loop system in the set $\mathcal{X}_N$.*

Proof. The proof is composed by the proof of recursive feasibility and the proof of asymptotic stability.

Recursive feasibility. Assume that the FHOCP (3.3) is feasible at time step k, and denote the optimal input sequence by $\mathbf{u}_k^\star := \{u_{0|k}^\star, \dots, u_{N-1|k}^\star\}$. Moreover, denote by $\mathbf{x}_k^\star := \{x_{0|k}^\star, \dots, x_{N|k}^\star\}$ the associated optimal state sequence, defined by $x_{0|k}^\star := x_k$ and $x_{i+1|k}^\star := f(x_{i|k}^\star, u_{i|k}^\star)$. Then, it is possible to define a feasible input sequence $\tilde{\mathbf{u}}_{k+1}$ at the subsequent time step as

$$\tilde{\mathbf{u}}_{k+1} := \{u_{1|k}^\star, \dots, u_{N-1|k}^\star, \mu_{\mathrm{a}}(x_{N|k}^\star)\}. \tag{3.8}$$

Note that the state trajectory associated to $\tilde{\mathbf{u}}_{k+1}$ is given by

$$\tilde{\mathbf{x}}_{k+1} := \{x_{1|k}^\star, \dots, x_{N|k}^\star, f(x_{N|k}^\star, \mu_{\mathrm{a}}(x_{N|k}^\star))\}.$$

The sequence $\tilde{\mathbf{u}}_{k+1}$ respects the constraint (3.3d) in view of Point 3. of Assumption 3.2. Moreover, the state trajectory $\tilde{\mathbf{x}}_{k+1}$ respect constraints (3.3e)-(3.3f) in view of Points 1. and 2. of Assumption 3.2. Hence, we have shown the existence of a feasible sequence at time $k+1$, which implies recursive feasibility of the optimization problem.

Asymptotic stability. In this part of the proof we show that the optimal MPC cost $V(x)$ is a Lyapunov function for the closed-loop system in $\mathcal{X}_N$, by showing that it respects the conditions in (2.4). Using Assumption 3.1, we can derive the lower bound

$$V(x) \geq \ell(x_{0|k}^\star, u_{0|k}^\star) \overset{(3.3b)}{=} \ell(x, u_{0|k}^\star) \overset{(3.5)}{\geq} \alpha_\ell(\|x - \bar{x}\|).$$

To derive an upper bound for $V(x)$, we first define the input sequence $\tilde{\mathbf{u}}_k$ obtained by applying iteratively the auxiliary control law μ_{a} to the system (3.1) starting from x. In view of Points 2. and 3. in Assumption 3.2, the sequence $\tilde{\mathbf{u}}_k$ is feasible for all $x \in \mathcal{X}_{\mathrm{f}}$. Denote by $\tilde{\mathbf{x}}_k := \{\tilde{x}_{i|k}\}_{i=0}^N$ the associated state trajectory. By MPC optimality, for all $x \in \mathcal{X}_{\mathrm{f}}$ we have that

$$V(x) \leq J(x, \tilde{\mathbf{u}}_k) = \sum_{i=0}^{N-1} \ell(\tilde{x}_{i|k}, \mu_{\mathrm{a}}(\tilde{x}_{i|k})) + V_{\mathrm{f}}(\tilde{x}_{N|k}) \leq V_{\mathrm{f}}(x)$$

where the last inequality is obtained by applying (3.6) iteratively in a telescopic sum. Then, in view of (3.7), we have that for all $x \in \mathcal{X}_\mathrm{f}$

$$V(x) \leq \alpha_\mathrm{f}(\|x - \bar{x}\|).$$

Then, the upper bound can be extended to all $x \in \mathcal{X}_N$ using [197, Proposition 2.16].

To show the decrease of $V(x)$, we make use of the feasible control sequence $\tilde{\mathbf{u}}_{k+1}$ defined in (3.8). In view of the MPC optimality, we have that

$$\begin{aligned} V(f(x_k, \mu^\mathrm{MPC}(x_k))) - V(x_k) &\leq J(f(x_k, \mu^\mathrm{MPC}(x_k)), \tilde{\mathbf{u}}_{k+1}) - V(x_k) \\ &= \ell(x^\star_{N|k}, \mu_\mathrm{a}(x^\star_{N|k})) + V_\mathrm{f}(f(x^\star_{N|k}, \mu_\mathrm{a}(x^\star_{N|k}))) \\ &\quad - V_\mathrm{f}(x^\star_{N|k}) - \ell(x_k, \mu^\mathrm{MPC}(x_k)) \\ &\overset{(3.6)}{\leq} -\ell(x_k, \mu^\mathrm{MPC}(x_k)) \overset{(3.5)}{\leq} -\alpha_\ell(\|x_k - \bar{x}\|). \end{aligned}$$

We have shown that V is a Lyapunov function on $\mathcal{X}_N$. Then the MPC closed-loop is asymptotically stable in view of Theorem 2.1. □

When the control problem is more complex, the proof of Theorem 3.1 can be modified in order to take into account all the possible differences with respect to the nominal case. In particular, a main concern in the thesis is the presence of differences between the model used in the MPC optimization in (3.3c) and the system under control, so that the initialization of the MPC at time step $k+1$ is different from $x^\star_{1|k}$. This is the typical case when data-driven models are used, or when the state is not directly measurable and a state observer is introduced in the closed-loop.

There exist several algorithms that exploit this method to guarantee closed-loop stability [169]. The simpler method consists in the use of a terminal equality constraint, firstly introduced in [123]. This algorithm considers $V_\mathrm{f} = 0$ and $\mathcal{X}_\mathrm{f} = \{\bar{x}\}$, which trivially satisfy Assumption 3.2 with the control law $\mu_\mathrm{a}(x) = \bar{u}$. In this MPC algorithm, the state predictions must arrive at the equilibrium at the end of the horizon. This method is easy to design, but it often suffers of bad performances and of a limited feasibility region, in particular when the prediction horizon is short. The decrease of performances is related to the fact that the solution of the optimization is strongly influenced by the terminal constraint and may not reflect the objective required by the cost.

For linear systems with a quadratic stage cost, the design of terminal ingredients is typically based on the use of the auxiliary control law $\mu_\mathrm{a}(x) = Kx$, where the gain $K \in \mathbb{R}^{m \times n}$ and the associated Lyapunov function $V_\mathrm{f}(x) = \|x\|^2_P$ can be derived, e.g., from the solution of the discrete time Riccati equation associated to the infinite horizon linear quadratic control. Then, the terminal constraint set can be chosen as a suitable sublevel set of the terminal cost $V_\mathrm{f}(x)$, or as the maximal output admissible set (MOAS,

[81]) of the closed-loop system associated with the feedback law $u = Kx$. The use of the MOAS has the advantage of providing a polytopic terminal set. This method to obtain a stabilizing MPC algorithm can be extended to nonlinear systems by using a linearization of the system under control in the reference equilibrium, see [41, 161].

3.2.2 Stability based on cost controllability

The design of terminal ingredients may be a demanding task for nonlinear systems, because it relies on the explicit knowledge of an auxiliary control law, a Lyapunov function and a control invariant set. For this reason, MPC algorithms that guarantee stability without the use of terminal conditions have been developed both for discrete-time systems [20] and for continuous-time ones [198]. The typical approach to achieve asymptotic stability without terminal conditions relies on cost controllability, a controllability condition originally proposed in [86, 233], in combination with a sufficiently long prediction horizon [92, 51], see [244] for a unifying comparison. In this case Algorithm 3.1 is implemented using $V_\mathrm{f} = 0$ and $\mathcal{X}_\mathrm{f} = \mathcal{X}$.

The following (standard) definition is taken from [20, Definition 1].

Definition 3.1 (Admissible control sequence)**.** *A sequence of control values* $\mathbf{u} = \{u_{0|k}, \dots, u_{N-1|k}\}$ *is called* admissible *for* $x_k \in \mathcal{X}$ *and* $N \in \mathbb{N} \cup \{\infty\}$ *if*

$$f(x_{i|k}, u_{i|k}) \in \mathcal{X} \quad \textit{and} \quad u_{i|k} \in \mathcal{U}$$

for all $i \in \{0, 1, \dots, N-1\}$*. The set of admissible control sequences of length* $N \in \mathbb{N} \cup \{\infty\}$ *is denoted by* $\mathcal{U}_N(x_k)$*.*

We can now introduce the cost controllability assumption required to prove closed-loop stability.

Assumption 3.3 (Cost controllability)**.** *The system* (3.1) *with stage cost* $\ell(x, u)$ *is cost controllable, i.e. there exists a monotonically increasing and bounded sequence* $(B_N)_{N \in \mathbb{N}}$ *such that, for every state* x*, there exists a control sequence* $\mathbf{u} \in \mathcal{U}_\infty(x)$ *satisfying the growth bound*

$$V_N(x) \leq J_N(x, \mathbf{u}) \leq B_N \ell^\star(x) \quad \forall N \in \mathbb{N}, \tag{3.9}$$

where $\ell^\star := \min_{u \in \mathcal{U}} \ell(x, u)$*.*

If the stage cost ℓ is positive definite, i.e. it respects Assumption 3.1, the cost controllability assumption implies the existence of a control sequence that drives the system state to $\bar{x}$ asymptotically. Note that in (3.9) the first inequality directly follows from the definition of the value function.

Then, the following stability theorem holds.

Theorem 3.2. *Let Assumptions 3.1 and 3.3 hold. Let the prediction horizon N be chosen such that*

$$\alpha_N := 1 - \frac{(B_2 - 1)(B_N - 1)\prod_{i=3}^{N}(B_i - 1)}{\prod_{i=2}^{N} B_i - (B_2 - 1)\prod_{i=3}^{N}(B_i - 1)} \in (0, 1). \tag{3.10}$$

Then, $x = \bar{x}$ is an asymptotically stable equilibrium point of the closed-loop system in each sublevel set

$$V_c^{-1} := \{x \in \mathcal{X} : V_N(x) \leq c\} \subset \text{int}(\mathcal{X}).$$

The proof of Theorem 3.2 shows that the value function $V_N(x)$ is a Lyapunov function of the closed-loop system satisfying

$$V_N(f(x, \mu^{\text{MPC}}(x))) - V_N(x) \leq -\alpha_N \ell(x, \mu^{\text{MPC}}(x)).$$

Condition (3.10) on the value of α_N is satisfied when the prediction horizon is sufficiently long, i.e. there exists $\bar{N} \in \mathbb{N}$ such that $\alpha_N \in (0, 1)$ for all $N \geq \bar{N}$. However, it is in general difficult to find the minimum value of $\bar{N}$ guaranteeing asymptotic stability, and its estimates can be rather conservative [133]. For linear systems, there exist approaches based on the Riccati equation to derive the minimum horizon that guarantees stability, see [179] and [245, Section 5.5].

3.3 Output-feedback

The classic MPC algorithm defines a state-feedback control law. However, the state of the system under control is not always directly measurable. In output-feedback MPC the only measurable quantity is the system output $y \in \mathbb{R}^p$, that typically is also the quantity of interest of the control. We consider the output as a static function of the system state and input, i.e.

$$y_k = g(x_k, u_k). \tag{3.11}$$

A common method to manage this situation is the introduction of a state observer in the closed-loop. A state observer is a dynamical system that takes as inputs the input u and output y of the system, and produces as output $\hat{x} \in \mathbb{R}^n$, that is an estimation of the system state x. Its general equation can be written as

$$\hat{x}_{k+1} = \hat{f}(\hat{x}_k, u_k, y_k). \tag{3.12}$$

There exists a vast literature about the design of state observers [14]. Some common methods include Luenberger observers [157], Kalman filters and extended Kalman filters [238], high gain observers [126], moving horizon estimators [197] and sliding mode observers [223].

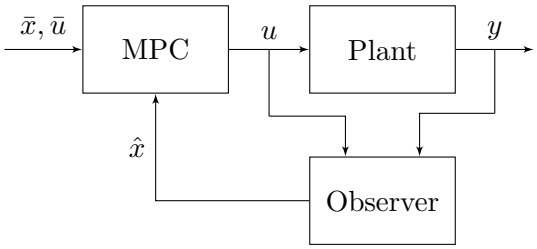

Figure 3.2: Block diagram of the output feedback MPC algorithm.

The schematic layout of the output-feedback MPC algorithm is reported in Figure 3.2. With respect to the standard MPC closed-loop in Figure 3.1, we have an additional block inserted between the plant and the MPC. Then, in the FHOCP initialization (3.3b), the observer state estimation $\hat{x}$ is used instead of the real state value, which is not available. More specifically, the initialization constraint (3.3b) is substituted by $x_{0|k} = \hat{x}_k$.

To study asymptotic stability of the output-feedback MPC closed-loop composed by (3.1)-(3.11)-(3.12)-(3.4) it is possible to use similar techniques to the state-feedback case. The main difference is that now the closed-loop system has two states: the system state x and the observer state $\hat{x}$. Moreover, the MPC feedback law μ^{MPC} is a function of the observer state $\hat{x}$ and not of the system state. To study stability, the effect of the two states can be separated by performing a change of variables. Instead of considering $[x^\top \ \hat{x}^\top]^\top$, we study the system with states $[e^\top \ \hat{x}^\top]^\top$, where $e := x - \hat{x}$ is the observer estimation error. Then, in a first step, we study the observer estimation error dynamics. Typically, it is possible to infer stability of the observer estimation error independently on the value of the system input. Then, the closed-loop system can be seen as the cascade connection of two systems: the one describing the observer estimation error, and a system

$$\hat{x}_{k+1} = f(\hat{x}_k, \mu^{\text{MPC}}(\hat{x}_k)) + e_{k+1}.$$

The stability of this second subsystem can be studied by modifying the standard MPC stability proofs to consider e_{k+1} as an external perturbing term.

The final stability result that can be derived depends on how the behavior of the observer estimation error e is characterized in the first step of the proof. If there are no uncertainties and disturbances affecting the system, and the observer is properly designed, it is possible to show that the observer estimation error converges to 0. In this case it is possible to show asymptotic stability of the closed-loop system following the arguments of the proof of Theorem 3 in [219]. Instead, when there are disturbances affecting the system, the estimation error e does not converge to zero, but decreases until it reaches a neighborhood of the origin whose size depends on the magnitude

of the disturbance. In this case, it is typically possible to prove that the closed-loop is ISS or ISpS with respect to the disturbance term.

3.4 State constraints and robust MPC

One of the main features of MPC is the possibility to explicitly include hard constraints on the system state in the control problem formulation. The stabilizing MPC algorithms described in the previous section are capable to guarantee recursive feasibility. When the system under control behaves exactly as its model, the satisfaction of constraint (3.3e) by the optimal solution guarantees that also the system state respects the constraints. In fact one has that $x_{k+1} = f(x_k, \mu^{\text{MPC}}(x_k)) = x^\star_{1|k}$.

However, in most of the practical cases, the model used in the MPC does not exactly describes the behavior of the system under control. In presence of model-plant mismatch or disturbances and state or output constraints, it is necessary to rely on robust MPC techniques to guarantee robust feasibility and constraint satisfaction despite the uncertainties [169].

There exist many different approaches to robust MPC, and they are distinguished by how the uncertainty is characterized. In the deterministic approaches, the uncertainty is described by a disturbance bounded in a deterministic set. Alternatively, the uncertainty can be characterized in a probabilistic framework. In this case, we have a *stochastic MPC*. The design of the algorithm depends also on how the uncertainty is assumed to affect the system. The simpler case is the one of additive uncertainty, where the uncertainty effect is assumed to behave as an disturbance that is added to the state equation. Another widely studied case is the one of parametric uncertainty, that is an uncertainty affecting the parameters of the system model.

In case of linear systems with deterministic additive uncertainty, the most common solution is tube MPC [145]. For nonlinear systems in a deterministic setting, the most common approaches for the design of robust MPC are constraint tightening methods, for example based on the Lipschitz constant of the system under control [164, 191] or on an incremental controllability property [132], and min-max approaches [194]. In a stochastic framework, some possible approaches can be found in [100, 69, 96]. Stochastic MPC must also consider the issue of feasibility, that cannot be guaranteed by the standard MPC algorithms in presence of unbounded disturbances. Possible methods to solve this issue are the use of indirect feedback [101] or of back-up controllers [188].

When a state observer is present, its estimation error is an additional source of uncertainty that must be taken into account by the MPC. In most of the literature about output MPC the observer estimation error is regarded as a generic disturbance [204]. Few exceptions can be found in [130], that

proposes a constraint tightening technique based on the evolution of the maximum observer estimation error, and in [50], that uses a min-max optimization problem to simultaneously compute a moving horizon estimation and a robust MPC.

In this thesis, we consider deterministically bounded additive disturbances, and the presence of an observer estimation error. The proposed robust MPC algorithms are based on the constraint tightening approach proposed in [130], that exploits an incremental controllability property of the system and an incremental stability property of the observer estimation error. In particular, robust MPC algorithms considering recurrent neural networks models will be designed and analyzed in Chapters 6 and 7.

3.5 Offset-free tracking

In presence of model-plant mismatch and disturbances, the MPC algorithm does not guarantee zero-error regulation, and typically the closed-loop system presents a static tracking error at steady state. A common method to solve this issue is the use of the so-called *offset-free MPC*. This approach was first introduced for linear systems in [186], and was further developed in [159, 184]. The extension of offset-free MPC to nonlinear systems was first proposed in [173]. Tutorial reviews and comparisons of different formulations can be found in [183, 185].

More formally, the objective of offset-free MPC is to guarantee that

$$\lim_{k\to\infty} y_k = y^0 \tag{3.13}$$

where $y^0 \in \mathbb{R}^p$ is the MPC output reference. In this algorithm, the model used for the MPC predictions is enlarged with an artificial disturbance $d \in \mathbb{R}^{n_d}$, obtaining an augmented model in the form

$$x_{k+1} = f_{\mathrm{d}}(x_k, u_k, d_k) \tag{3.14a}$$
$$d_{k+1} = d_k + w_k \tag{3.14b}$$
$$y_k = g_{\mathrm{d}}(x_k, u_k, d_k) \tag{3.14c}$$

where f_{d} and g_{d} are such that

$$f_{\mathrm{d}}(x, u, 0) = f(x, u), \quad g_{\mathrm{d}}(x, u, 0) = g(x, u).$$

The term $w \in \mathbb{R}^{n_d}$ represents the variation of the disturbance term between consecutive time steps and, depending on the MPC formulation, it can be considered equal to zero at all time steps or as an exogenous unknown vanishing input of the closed-loop, such that $\lim_{k\to\infty} w_k = 0$. We point out that the disturbance model (3.14b) is not directly employed in the MPC algorithm, but it is only used in the analysis of the closed-loop properties.

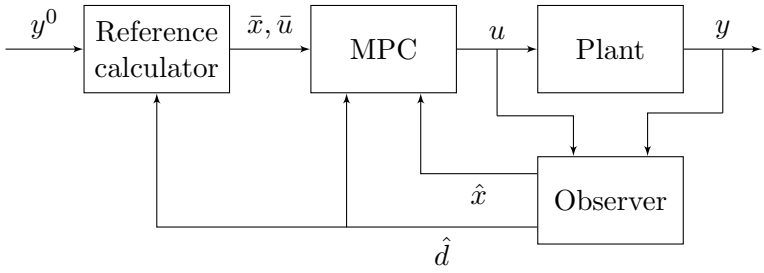

Figure 3.3: Block diagram of the offset-free MPC algorithm.

The schematic layout of the offset-free MPC is reported in Figure 3.3, and is composed by three main blocks. The first block is an observer. Differently from the case considered in Section 3.3, the observer is based on the augmented system (3.14), and estimates both the system state and the disturbance term. If the system state is measurable, a deadbeat observer can be employed to estimate the disturbance only, see [185, Theorem 15]. The observer outputs are the state estimation $\hat{x} \in \mathbb{R}^n$ and the disturbance estimation $\hat{d} \in \mathbb{R}^{n_d}$. The second block of the schema is the *reference calculator*, that computes the MPC references $\bar{x}, \bar{u}$ starting from the output reference y^0 and from the current value of the observer disturbance estimation $\hat{d}$. In the more general version, the reference calculator solves the following optimization problem

$$\min_{\bar{x},\bar{u}} \quad \ell_{\mathrm{r}}(\bar{x}, \bar{u}) \tag{3.15a}$$

$$\text{s.t.} \quad \bar{x} = f_{\mathrm{d}}(\bar{x}, \bar{u}, \hat{d}) \tag{3.15b}$$

$$y^0 = g_{\mathrm{d}}(\bar{x}, \bar{u}, \hat{d}) \tag{3.15c}$$

$$\bar{u} \in \mathcal{U}, \quad \bar{x} \in \mathcal{X}. \tag{3.15d}$$

The function $\ell_{\mathrm{r}} : \mathbb{R}^n \times \mathbb{R}^m \to \mathbb{R}$ is a steady state cost function, and it is employed to choose between all the possible equilibrium points satisfying (3.15b)-(3.15c). The optimization problem is assumed to be feasible and to have a unique solution. If (3.15b)-(3.15c) have a unique solution, it is not necessary to implement the reference calculator as an optimization problem, but it is sufficient to compute the unique solution of the system of equations. The output of the reference calculator are the MPC state and input references $\bar{x}, \bar{u}$. Note that since the disturbance estimation $\hat{d}$ may change at every time step, also the MPC references may vary. The last block of the control schema is the MPC. The MPC employs the dynamics (3.14a) of the augmented model to make the predictions, with the disturbance set at the current value of the observer estimation $\hat{d}$ and maintained constant along the horizon. The MPC predictions are initialized by the observer state estimate $\hat{x}$. Moreover, in the MPC cost we penalize the difference of the state

and input to the current value of the references $\bar{x}, \bar{u}$ computed by the reference calculator. If the observer and the MPC are properly designed, this algorithm is able to guarantee the offset-free tracking property (3.13) also in presence of model-plant mismatch and asymptotically constant disturbances.

In this thesis, different offset-free MPC algorithms are developed. In Chapter 7, a robust offset-free MPC algorithm is designed for long short-term memory neural network models. The control algorithm proposed in Chapter 9 for δISS systems guarantees the offset-free tracking property. Finally, an offset-free MPC algorithm is developed in Chapter 11 for Koopman operator-based surrogate models.

For linear systems with measurable state, a convenient alternative to offset-free MPC to achieve zero tracking error is the use of the *velocity form MPC* [237, 16, 15], that does not require the introduction of an observer. This method consists in considering in the MPC model the state increment and the output error as an enlarged state, and the control increment as manipulated variable. The velocity form MPC algorithm is described in detail in Chapter 13, and is applied to the current control in synchronous reluctance motors. A possible extension of velocity form MPC exists for nonlinear systems [49], that requires a velocity-based linearization of the model. In [185] it is shown that the velocity form MPC can be seen as a particular case of offset-free MPC.

3.6 Incremental input constraints

With incremental input constraints (or input rate constraints), we indicate constraints on the variation of the input between subsequent time steps, i.e. on $\Delta u_k := u_k - u_{k-1}$. While input, state and output constraints are commonly considered, the control input *variation* is often just penalized in the cost, and is not included in the hard constraints. As a matter of fact, the satisfaction of incremental input constraints can be very important to guarantee the safety of the system. For example, in hydraulic networks, the speed of control valves is usually limited. Fast valve operations results in strong hydraulic transients, which could stress and eventually damage the structure of the network [75]. Similarly, in mechanical systems, it is desirable to avoid large accelerations and jerks that could wear out the system [147]. In the control of assisted an driverless vehicles, accelerations and jerks are limited to improve passengers comfort [156]. In [56], incremental input constraints are introduced in the control of a mobile robot, in the consideration of the safety and comfort needs in real life.

A common way to take into account constraints on the input variation is to consider Δu as an optimization variable in the MPC, and then employ a discrete time integrator to obtain the control variable u. A discrete time

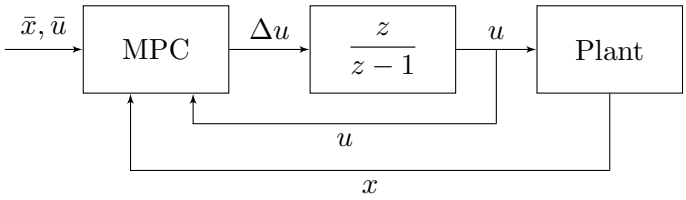

Figure 3.4: Block diagram of the MPC algorithm with incremental input constraints.

integrator can be represented in the Z-transform by the transfer function $\frac{z}{z-1}$, or as the state-space system

$$\begin{aligned} v_{k+1} &= v_k + \Delta u_k \\ u_k &= v_k + \Delta u_k \end{aligned}$$

with input Δu, state v and output u. We point out that the state of the discrete-time integrator at time k is equal to its output at time $k-1$. Hence, in the following chapters, u_{k-1} is considered as state of the discrete-time integrator at time k, without introducing the additional notation v to indicate the integrator state.

The resulting closed-loop is schematically represented in the block diagram in Figure 3.4. We note that the system under control considered by the MPC is composed by the discrete time integrator and the plant. Then, when studying the stability properties of the closed-loop system in Figure 3.4, we have to consider that the state of the closed-loop system is composed by the union of the plant state and the state of the discrete-time integrator. Hence, if stability is enforced by means of terminal ingredients, both those components must be considered in their design. This aspect is further studied in Chapters 8 and 9, considering the particular class of open-loop δISS plants, in combination with recurrent neural network models.

3.7 MPC for tracking and the use of artificial references

In the standard MPC algorithm, given the reference output $y_{\mathrm{t}} \in \mathbb{R}^p$, the state and input references $(\bar{x}, \bar{u})$ to be used in the MPC cost (3.2)-(3.3a) can be computed as the equilibrium state and input associated to the output y_{t}. Instead, in MPC for tracking, we consider the MPC reference as an additional variable of the optimization problem, called *artificial reference*. The artificial reference is given by the triplet $(x_{\mathrm{s}}, u_{\mathrm{s}}, y_{\mathrm{s}})$, and it is constrained

to be an equilibrium of the system under control, i.e.

$$x_\mathrm{s} = f(x_\mathrm{s}, u_\mathrm{s})$$
$$y_\mathrm{s} = g(x_\mathrm{s}, u_\mathrm{s}).$$

The MPC stage cost penalizes the difference of the state and input from the artificial reference, instead of penalizing the difference from $(\bar{x}, \bar{u})$ as in (3.2). To ensure that the system is driven to the desired equilibrium, an additional term $V_\mathrm{O}(y_\mathrm{s} - y_\mathrm{t})$ is summed to the cost function. The function V_O is called *offset cost*, and must satisfy some technical convexity assumptions, see [151, Assumption 2]. A common choice of the offset cost is the use of a quadratic positive definite function $V_\mathrm{O}(y_\mathrm{s} - y_\mathrm{t}) = \|y_\mathrm{s} - y_\mathrm{t}\|_T^2$, with $T = T^\top \succ 0$.

Let $\mathcal{Y}_\mathrm{t} \subseteq \mathbb{R}^p$ be a convex set of equilibrium outputs whose associated equilibrium state and input respect the constraints. If all the elements of the tracking MPC algorithm are properly designed, it is possible to prove that the closed-loop is stable, fulfills the constraints throughout time and converges to an equilibrium point such that

1. If $y_\mathrm{t} \in \mathcal{Y}_\mathrm{t}$, then $\lim_{k\to\infty} \|y_k - y_\mathrm{t}\| = 0$;
2. If $y_\mathrm{t} \notin \mathcal{Y}_\mathrm{t}$, then $\lim_{k\to\infty} \|y_k - y_\mathrm{s}^\star\| = 0$, where

$$y_\mathrm{s}^\star := \arg\min_{y_\mathrm{s} \in \mathcal{Y}_\mathrm{t}} V_\mathrm{O}(y_\mathrm{s} - y_\mathrm{t}).$$

This means that the system output reaches its reference y_t if it is feasible. If the reference is not feasible, then the output will reach the closest possible value according to the offset cost, that is $y_\mathrm{s}^\star$.

The use of artificial references in MPC allows to enlarge the feasibility region with respect to the standard MPC algorithm. In fact, one of the possible issues of MPC is the limited size of the feasibility region in presence of constraints on the system state. This can be particularly critical when a terminal set is introduced in the algorithm, that may reduce the feasibility region and may deteriorate the performances with respect to the unconstrained case. Moreover, the MPC for tracking allows to maintain feasibility in presence of variations of the reference y_t and when the y_t cannot be reached respecting the constraints. The introduction of the artificial reference can be particularly beneficial when a terminal equality constraint MPC algorithm is employed.

The MPC algorithm with artificial reference for linear systems is described and analyzed in [150], and for nonlinear systems in [151]. The basic approach is further extended to solve more complex control problems, e.g. the tracking of dynamic target signals [131] and the use of semi-definite stage costs [76], or to consider the use of harmonic artificial references, which allows to further enlarge the domain of attraction [141]. For a comprehensive review of MPC algorithms using an artificial reference we refer to [142].

In this thesis, the use of artificial references is considered in the MPC algorithm developed in Chapter 9 for δISS systems, and in the velocity form MPC schema designed for the current control in synchronous reluctance motors in Chapter 13.

3.8 Semi-definite stage cost

In the classical MPC formulations described in the previous sections, a key point to guarantee stability of the closed-loop is the use of a positive definite stage cost ℓ, see Assumption 3.1. However, in many practical cases, the penalization of the system output is more meaningful than the penalization of the full system state. This is in particular true when high order and/or black-box models [153] are used in the MPC predictions. Due to the high model dimensionality, the tuning of a state-based cost function may be cumbersome and lead to suboptimal results. In all these cases, the use of a semi-definite stage cost may be a solution. Stability results for NMPC with positive semi-definite stage cost have been derived in [86]. This approach is also studied in [133], where an analysis of the minimum prediction horizon to guarantee stability is carried out, and in [76], where the use of semi-definite stage costs is combined with the use of artificial references.

In this framework, the standard MPC stability proofs have to be suitably modified. In particular, it is not possible to use the MPC optimal cost only as Lyapunov function. Instead, the candidate Lyapunov function is composed by the sum of the MPC optimal cost and of a cost detectability function $\Psi : \mathbb{R}^n \to \mathbb{R}_{\geq 0}$. The cost detectability function satisfies the following properties for all $u \in \mathcal{U}$ and $x \in \mathcal{X}$

$$\Psi(x) \leq \gamma_0 \mu(\|x - \bar{x}\|) \tag{3.16a}$$

$$\Psi(f(x,u)) - \Psi(x) \leq -\varepsilon_0 \mu(\|x - \bar{x}\|) + \ell(x,u) \tag{3.16b}$$

for some constants $\gamma_0, \varepsilon_0 > 0$ and a $\mathcal{K}_\infty$ function μ. The key element in the proof is inequality (3.16b), that requires that whenever the stage cost $\ell(x,u)$ is equal to zero, the cost detectability function decreases with a rate related to the distance of the current state to the desired set-point. Cost detectability functions can be obtained by relying on input-output-to-state stability (IOSS) [38, 3] or on strict dissipativity methodologies [89, 104]. For nonlinear autoregressive-exogenous (NARX) models, and in case of quadratic input-output stage cost, a suitable cost detectability function can be obtained by relying on the knowledge of the lag/observability index (NARX models are final-state observable) [133]. For linear systems and quadratic cost, a quadratic cost detectability function can be computed by solving an LMI problem, as discussed in [89].

Another class of MPC algorithms that do not consider a positive definite stage cost is the one of *economic MPC* [68, 196], that is outside of the scope

of the thesis. In economic MPC there are no restrictions on the structure of the cost, allowing also for negative stage costs. Typically, the cost in economic MPC is related to some measurable physical quantity to minimize or to some economic criterion. The stability proofs use different arguments to the ones described in this section.

Part II

MPC for δISS systems using RNN models

Chapter 4

Incrementally Input-to-State Stable Recurrent Neural Networks

The following chapters of the thesis are devoted to the design of MPC algorithms for open-loop nonlinear δISS systems, using surrogate models based on recurrent neural networks (RNN).

The choice of considering δISS systems is motivated by different reasons. The first one is safety. δISS systems have the property that similar input sequences produce to similar output sequences. This is a desirable property when using black-box identification. In fact, if small perturbations of the input could lead to large output variations, it is hard to predict how the model will behave with unseen values of the inputs. Moreover, since the system state will be considered not measurable and we will use only input-output data, it is desirable that the effect of the initial state vanishes asymptotically. The second reason is that limiting the class of systems simplifies the control design with respect to the general case of nonlinear systems. In the next chapters, the δISS property of the system will be extensively exploited for the design of the MPC algorithms. Finally, a lot of real world systems are δISS. For linear time-invariant (LTI) systems, asymptotic stability implies δISS. For general globally Lipschitz continuous systems, a Lipschitz constant in the interval $(0, 1)$ implies δISS [11]. The δISS property of the system under control can be checked either by a direct computation of a δISS-Lyapunov function, or by relying on recent results related to convergent dynamics or contraction-metric analysis, see e.g. [79, 231]. Moreover, for non δISS systems, an inner closed-loop can be introduced to pre-stabilize the system. This is a common method in complex control systems, where a hierarchical control structure is often used.

RNNs are chosen for their flexibility, and for the possibility of being trained by means of input-output data only. Moreover, we exploit the wide

literature about RNN models that are open-loop δISS, see the results in [27] and in the derived articles. This allows to have a model that provides the same stability properties of the system under control.

After a general overview of the use of neural networks (NN) for system identification, in this chapter we introduce the RNN architectures that will be employed in the control schemes developed in the following chapters of the thesis, that are long short-term memory (LSTM), gated recurrent units (GRU) and recurrent equilibrium networks (REN). For each of these architectures, we state sufficient δISS conditions, and we explain how these conditions can be enforced in the training. Finally, we give a brief summary of other δISS RNN structures available in the literature.

The derivation of the δISS property of the REN model in Section 4.4.1 is taken from:

- [211] **Schimperna, I.**, and Magni, L. (2024). *Recurrent equilibrium network models for nonlinear model predictive control*. IFAC-PapersOnLine, 58(18), 226-231. Presented at the 8th IFAC Conference on Nonlinear Model Predictive Control NMPC 2024, Kyoto, Japan.

4.1 Neural network models of dynamical systems

Neural networks (NN) are a powerful class of flexible and modular mathematical models, that can be learned with data-driven methods. In view of their universal approximation capability [55, 105] and of their performances, NNs have been extensively employed in control design from the early days [107]. A very common application of NNs in the control field is their use for the identification nonlinear systems models to be employed for the design of model-based control algorithms, such as MPC [199]. Other possible applications of NNs in control are detailed in [33], and include the approximation of computationally intensive control laws [99, 67], the synthesis of controllers directly from data [118, 58], the learning of model uncertainties [248, 74] and their use as part of reinforcement learning algorithms [148].

There exists a variety of different methods for the use of NNs for system identification, spanning from purely black-box models to physics-informed ones. When using a black-box approach, the choice of the NN architecture depends on the available data. The simpler case is when the system state is known and measurable. Then, it is possible to learn is the static map $f : \mathbb{R}^n \times \mathbb{R}^m \to \mathbb{R}^n$. Since this function is static and does not have a time dependence, it is possible to use feed-forward neural networks (FFNN), such as multi-layer perceptrons (MLP) to approximate it. This class of models are sometimes called neural state-space models, and have been applied, e.g., in [154, 73]. Instead, when only input-output data are available, a different approach is required to correctly describe the dynamic relation between these

two quantities. Many works consider an autoregressive approach, in which sequences of past inputs and outputs of the system are used to predict the next system output [189, 220]. This can be done with NNs with different architectures, including autoencoder structures [165]. Another successful method is the use of recurrent neural networks (RNN), a family of NN specialized to deal with sequential data. RNNs have the same mathematical structure of a dynamical system, with an internal state that can memorize the information contained in the past inputs of the network [84]. Reviews of different approaches for the use of RNN models in MPC can be found in [117, 146].

The alternative to purely black-box models is the use of physics-informed approaches, in which the data-driven learning is combined with the available knowledge about the physics of the system [240, 121, 54]. One of the possible methods involve the use of a physics-informed loss function in the training phase, enforcing relevant physical relations [66]. Another strategy consists in embedding the physical knowledge directly in the NN architecture. This latter approach include cases in which some physical constraint, e.g. the positivity of some quantity, is hard coded in the network architecture [59], and the case in which the NN is designed with a structure that matches the topology of the physical system. For example, in [82, 83], the authors design a physics-informed RNN (PI-RNN) composed by different RNN modules, whose connection reflects the network structure of the underlying system. Finally, another possible approach consists in models that combines a physics-based part with a black-box part, as done, e.g., in [25].

4.1.1 Recurrent Neural Networks

RNNs, firstly introduced in [206], are a particular class of NNs able to deal with sequential data and temporal dependencies, due to the presence of an internal state. In the machine learning field, this architecture is mainly used to process sequential data in applications like time series prediction, natural language processing, translation and handwriting recognition. In this thesis, RNNs are used to model dynamical systems from input output data. This task corresponds to a sequence-to-sequence prediction considering sequences of the same length, meaning that for each value of the input sequence the RNN produces one value of the predicted output sequence. Mathematically, RNNs are discrete-time dynamical systems in the form

$$\begin{aligned} x_{k+1} &= f(x_k, u_k) \\ y_k &= g(x_k, u_k), \end{aligned}$$

with input $u \in \mathbb{R}^m$, state $x \in \mathbb{R}^n$ and output $y \in \mathbb{R}^p$. Functions f and g have a predefined structure that depends on the considered architecture, and depend on trainable parameters called *weights*. This notation will be

used throughout the thesis for all the different RNN architectures. In most RNNs architectures, the state x is an artificial quantity used to store the information about the previous inputs, and it has no physical meaning. The output y corresponds to the prediction of the RNN, and the objective of the training is to obtain a model whose output matches the real output of the system under control. We follow the most common approach and we define RNNs in discrete-time, but in the literature there exist also continuous time RNN structures [249].

In this thesis we consider different RNN architectures. The first ones are Long Short-Term Memory (LSTM) and Gated Recurrent Unit (GRU), that are the most popular RNN architectures in the machine learning field. In addition, we consider Recurrent Equilibrium Networks (REN), an architecture recently proposed in the control field [201] with interesting stability properties. Since we assume that the system under control is δISS, we require that its model has the same property. This choice is often taken for the design of RNN-based controllers for δISS systems [27]. The δISS property of the model allows to guarantee that the effect of the state initialization vanishes, and that a small input variation does not lead to a large state variation. This is a desirable property that is in general not satisfied by NNs. In fact, it has been observed that NNs can be very sensitive to small changes in inputs [229]. Moreover, since the state of the RNN models has no physical meaning, it is desirable that its initialization does not affect the output predictions in the long term.

4.2 Long Short-Term Memory

Long Short-Term Memory (LSTM) neural networks have been first introduced in [103]. Their popularity is due to the fact that they solved the vanishing gradient problem that affects the training of simpler RNN architectures. LSTM neural networks have been successfully employed in a variety of tasks in different fields, including to model dynamical processes considered in automatic control, see [146] for a detailed list.

The LSTM module is composed by two states: the cell state $c \in \mathbb{R}^{n_c}$ and the hidden state $h \in \mathbb{R}^{n_c}$, where n_c is also called number of neurons. Then, the LSTM state is $x := [c^\top \ h^\top]^\top \in \mathbb{R}^{2n_c}$. At each time-step k, the LSTM network receives an input $u \in \mathbb{R}^m$ and produces an output prediction $y \in \mathbb{R}^p$. Cell state and hidden state are modified through structures called gates. The equations that describe the LSTM network are the following

$$\begin{aligned} c_{k+1} = {} & \sigma(W_{\mathrm{f}} u_k + U_{\mathrm{f}} h_k + b_{\mathrm{f}}) \otimes c_k \\ & + \sigma(W_{\mathrm{i}} u_k + U_{\mathrm{i}} h_k + b_{\mathrm{i}}) \otimes \tanh(W_{\mathrm{c}} u_k + U_{\mathrm{c}} h_k + b_{\mathrm{c}}) \end{aligned} \tag{4.1a}$$

$$h_{k+1} = \sigma(W_{\mathrm{o}} u_k + U_{\mathrm{o}} h_k + b_{\mathrm{o}}) \otimes \tanh(c_{k+1}) \tag{4.1b}$$

$$y_k = W_{\mathrm{y}} h_k + b_{\mathrm{y}} \tag{4.1c}$$

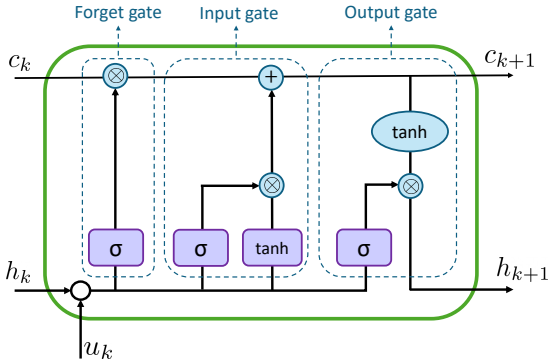

Figure 4.1: Schematic representation of the LSTM cell.

where both $\tanh(\cdot)$ and $\sigma(\cdot)$ activation functions are applied to vectors element by element. Note that $\tanh(\cdot)$ and $\sigma(\cdot)$ are Lipschitz continuous functions, with Lipschitz constants respectively of 1 and $\frac{1}{4}$. Matrices $W_{\mathrm{f}}, W_{\mathrm{i}}, W_{\mathrm{c}}, W_{\mathrm{o}} \in \mathbb{R}^{n_c \times m}$, $U_{\mathrm{f}}, U_{\mathrm{i}}, U_{\mathrm{c}}, U_{\mathrm{o}} \in \mathbb{R}^{n_c \times n_c}$, $W_{\mathrm{y}} \in \mathbb{R}^{p \times n_c}$ and vectors $b_{\mathrm{f}}, b_{\mathrm{i}}, b_{\mathrm{c}}, b_{\mathrm{o}} \in \mathbb{R}^{n_c}$, $b_{\mathrm{y}} \in \mathbb{R}^{p}$ contain the trainable weights of the network. The LSTM cell, described by the state equations (4.1a)-(4.1b), is schematically represented in Figure 4.1.

4.2.1 Stability of LSTM networks

Stability conditions for LSTM models have been extensively studied in the literature. The first results [225, 63] consist in conditions for asymptotic stability of the autonomous LSTM model, and are based on linearization approaches. Instead, in [172], the authors derived a sufficient condition for the contraction of the LSTM model without biases for any value of the input. The first stability result that takes into account the effect of the input is the ISS condition proposed in [31]. Later, a different condition for ISS and a condition for δISS have been derived by the same authors in [230]. More recently, a new and less conservative condition for ISS of LSTM networks based on infinity norms have been proposed in [60].

In this thesis, we consider LSTM neural networks satisfying the sufficient condition for δISS proposed in [230]. This condition is valid for inputs bounded in the set

$$\mathcal{U} := \{u \in \mathbb{R}^m : \|u\|_\infty \leq u_{\max}\}. \tag{4.2}$$

Assumption 4.1. *The weights of the LSTM network* (4.1) *respect the condition* $\rho(A_\delta) < 1$*, where*

$$A_\delta := \begin{bmatrix} \bar{\sigma}_{\mathrm{f}} & \alpha \\ \bar{\sigma}_{\mathrm{o}}\bar{\sigma}_{\mathrm{f}} & \alpha\bar{\sigma}_{\mathrm{o}} + \frac{1}{4}\bar{\sigma}_{\mathrm{x}}\|U_{\mathrm{o}}\|_2 \end{bmatrix}$$

and

$$\bar{\sigma}_{\mathrm{f}} := \sigma(\|[W_{\mathrm{f}} u_{\max}\ U_{\mathrm{f}}\ b_{\mathrm{f}}]\|_\infty),$$
$$\bar{\sigma}_{\mathrm{i}} := \sigma(\|[W_{\mathrm{i}} u_{\max}\ U_{\mathrm{i}}\ b_{\mathrm{i}}]\|_\infty),$$
$$\bar{\sigma}_{\mathrm{o}} := \sigma(\|[W_{\mathrm{o}} u_{\max}\ U_{\mathrm{o}}\ b_{\mathrm{o}}]\|_\infty),$$
$$\bar{\sigma}_{\mathrm{c}} := \tanh(\|[W_{\mathrm{c}} u_{\max}\ U_{\mathrm{c}}\ b_{\mathrm{c}}]\|_\infty),$$
$$\bar{\sigma}_{\mathrm{x}} := \tanh\left(\frac{\bar{\sigma}_{\mathrm{i}}\bar{\sigma}_{\mathrm{c}}}{1-\bar{\sigma}_{\mathrm{f}}}\right),$$
$$\alpha := \frac{1}{4}\|U_{\mathrm{f}}\|_2 \frac{\bar{\sigma}_{\mathrm{i}}\bar{\sigma}_{\mathrm{c}}}{1-\bar{\sigma}_{\mathrm{f}}} + \bar{\sigma}_{\mathrm{i}}\|U_{\mathrm{c}}\|_2 + \frac{1}{4}\|U_{\mathrm{c}}\|_2\bar{\sigma}_{\mathrm{c}}.$$

Theorem 4.1 ([230])**.** *Let Assumption 4.1 hold. Then it is possible to upper bound the difference between any couple of system trajectories* $x^{\mathrm{a}} = [(c^{\mathrm{a}})^\top\ (h^{\mathrm{a}})^\top]^\top$ *and* $x^{\mathrm{b}} = [(c^{\mathrm{b}})^\top\ (h^{\mathrm{b}})^\top]^\top$ *with the following inequality*

$$\begin{bmatrix} \|c^{\mathrm{a}}_{k+1} - c^{\mathrm{b}}_{k+1}\|_2 \\ \|h^{\mathrm{a}}_{k+1} - h^{\mathrm{b}}_{k+1}\|_2 \end{bmatrix} \leq A_\delta \begin{bmatrix} \|c^{\mathrm{a}}_{k} - c^{\mathrm{b}}_{k}\|_2 \\ \|h^{\mathrm{a}}_{k} - h^{\mathrm{b}}_{k}\|_2 \end{bmatrix} + B_\delta \|u^{\mathrm{a}}_k - u^{\mathrm{b}}_k\|_2$$

where

$$B_\delta := \begin{bmatrix} \beta \\ \beta\bar{\sigma}_{\mathrm{o}} + \frac{1}{4}\bar{\sigma}_{\mathrm{x}}\|W_{\mathrm{o}}\|_2 \end{bmatrix}$$
$$\beta := \frac{1}{4}\|W_{\mathrm{f}}\|_2 \frac{\bar{\sigma}_{\mathrm{i}}\bar{\sigma}_{\mathrm{c}}}{1-\bar{\sigma}_{\mathrm{f}}} + \bar{\sigma}_{\mathrm{i}}\|W_{\mathrm{c}}\|_2 + \frac{1}{4}\|W_{\mathrm{i}}\|_2\bar{\sigma}_{\mathrm{c}}$$

and the LSTM system (4.1) *is exponentially δISS in the sets* $\mathcal{X}$ *and* $\mathcal{U}$*, where* $\mathcal{X} := \mathcal{C} \times \mathcal{H}$*, with*

$$\mathcal{C} := \left\{ c \in \mathbb{R}^n : \|c\|_\infty \leq \frac{\bar{\sigma}_{\mathrm{i}}\bar{\sigma}_{\mathrm{c}}}{1-\bar{\sigma}_{\mathrm{f}}} \right\}, \tag{4.3a}$$

$$\mathcal{H} := \{ h \in \mathbb{R}^n : \|h\|_\infty \leq 1 \}. \tag{4.3b}$$

4.2.2 Training of δISS LSTM networks

In this thesis, RNNs are trained using datasets composed by input-output sequences from the system that we want to model, and the data are divided in standard way in training, validation and test datasets. The procedure for the training of RNNs is based on gradient descent algorithms, such as ADAM [127] and RMSProp [85], combined with a back-propagation through time (BPTT) method for the automatic computation of the gradient of the network with respect to its weights [84]. As loss function we consider the mean squared error (MSE), which is defined as

$$\mathrm{MSE} := \frac{1}{p}\frac{1}{T}\sum_{k=0}^{T} \|y_{\mathrm{real},k} - y_k\|_2^2,$$

where T is the length of the sequence, y_{real} are the real system output and y are the RNN predictions. A key element to speed-up the training and obtain a high prediction accuracy is the normalization of the model inputs and outputs. This step is also useful to obtain inputs in a set in the form specified in (4.2) and required by the stability conditions. After the training, we use the FIT index to assess the quality of the final model, which is defined as

$$\text{FIT} := 100 \left(1 - \frac{\|\mathbf{y}_{\text{real}} - \mathbf{y}\|_2}{\|\mathbf{y}_{\text{real}} - y_{\text{avg}}\|_2} \right) \%,$$

where $\mathbf{y}_{\text{real}}$ is the vector containing the sequence of real outputs, $\mathbf{y}$ is the vector of the predictions and y_{avg} is the average of $\mathbf{y}_{\text{real}}$. The FIT index takes values in $(-\infty, 100]\%$, with a FIT of 100% corresponding to a perfect model, and a FIT equal to 0% corresponding to a model giving the same prediction error as the trivial model predicting the average of the real output.

To train RNN networks satisfying a sufficient condition for stability, we follow the procedure proposed and detailed in [33]. In particular, this method allows to obtain a RNN model that satisfies any condition expressed in the form

$$\nu < 0,$$

where ν is a scalar function of the system weights. This method consists in adding a regularization term in the loss function that penalizes set of weights that do not respect the stability condition, weighted by an hyperparameter λ^+. It is also possible to include an additional term in the loss to penalize ν also when it already satisfies the stability condition, weighted by an hyperparameter λ^-. This is particularly useful in situations in which it is desirable that the stability condition is satisfied with some margin, and it helps to improve the smoothness of the training procedure avoiding continuous jumps between sets of weights that respect and do not respect the stability condition. Then, the loss function employed in the training is

$$\text{MSE} + \lambda^+ \max\{0, \nu\} + \lambda^- \min\{0, \nu\}. \tag{4.4}$$

Typically λ^+ is chosen larger than λ^-, that can also be set to zero without compromising the stability of the final model. To ensure that the final model satisfies the stability condition, a condition on the termination of the training can be added. In particular the training is terminated after a predefined number of epochs only if the stability condition is satisfied, otherwise it was left running for a larger number of epochs.

To use this method for the training of δISS LSTMs, the condition of Assumption 4.1 has to be first rewritten in the form $\nu < 0$. This was done in [230] using the Jury criterion, where it is shown that the condition $\rho(A_\delta) < 1$ is equivalent to require that

$$-1 + \bar{\sigma}_{\text{f}} + \alpha \bar{\sigma}_{\text{o}} + \frac{1}{4} \bar{\sigma}_{\text{x}} \|U_{\text{o}}\|_2 < \frac{1}{4} \bar{\sigma}_{\text{f}} \bar{\sigma}_{\text{x}} \|U_{\text{o}}\|_2 < 1.$$

Recent results using both simulated [28] and real data [30] have shown that the imposition of stability conditions in the training of RNNs may slightly increase the number of epochs required for the convergence of the training, but it does not affect the prediction capabilities of the model, even if the space of admissible weights is reduced with respect to the unconstrained case.

4.3 Gated Recurrent Units

Gated Recurrent Unit (GRU) neural networks have been firstly introduced in [44] as a simplification of the LSTM structure, with a lower number of trainable parameters for the same number of units. As LSTMs, GRU networks are in the family of the gated RNN. In fact, also in this class of networks, the state is updated through gate structures. The performances of LSTM and GRU are comparable, and the choice of the best model depend on the application [46]. As LSTMs, also GRUs have been exploited in a variety of applications, both related and not related with automatic control [146].

The GRU model has a state $x \in \mathbb{R}^n$, and, given the input $u \in \mathbb{R}^m$ of the plant, it produces an output prediction $y \in \mathbb{R}^p$. The model equations are the following

$$x_{k+1} = z_k \otimes x_k + (1 - z_k) \otimes h_k \tag{4.5a}$$
$$z_k = \sigma(W_{\mathrm{z}} u_k + U_{\mathrm{z}} x_k + b_{\mathrm{z}}) \tag{4.5b}$$
$$r_k = \sigma(W_{\mathrm{r}} u_k + U_{\mathrm{r}} x_k + b_{\mathrm{r}}) \tag{4.5c}$$
$$h_k = \tanh(W_{\mathrm{h}} u_k + U_{\mathrm{h}}(r_k \otimes x_k) + b_{\mathrm{h}}) \tag{4.5d}$$
$$y_k = U_{\mathrm{o}} x_k + b_{\mathrm{o}}. \tag{4.5e}$$

where matrices $W_{\mathrm{h}}, W_{\mathrm{z}}, W_{\mathrm{r}} \in \mathbb{R}^{n \times m}$, $U_{\mathrm{h}}, U_{\mathrm{z}}, U_{\mathrm{r}} \in \mathbb{R}^{n \times n}$, $U_{\mathrm{o}} \in \mathbb{R}^{p \times n}$ and vectors $b_{\mathrm{h}}, b_{\mathrm{z}}, b_{\mathrm{r}} \in \mathbb{R}^n$, $b_{\mathrm{o}} \in \mathbb{R}^p$ contain the trainable weights of the network. $z_k = z(x_k, u_k)$ is called update gate, while $r_k = r(x_k, u_k)$ is called forget gate or reset gate and $h_k = h(x_k, u_k)$ is the candidate activation. The state equation (4.5a) is schematically represented in Figure 4.2.

4.3.1 Stability of GRU networks

The literature about conditions for stability of GRU networks is less broad than the one for LSTMs. The local stability properties of the autonomous GRU network are studied in [224], while the stability of the GRU model with input is studied in [28], where conditions for its ISS and δISS are derived. In this thesis, we consider GRU networks that satisfy the sufficient condition for δISS derived in [28] and reported in the following theorem. The stability result is valid under the assumption that the input of the GRU is bounded in the set

$$\mathcal{U} := \{u \in \mathbb{R}^m : \|u\|_\infty \leq 1\}.$$

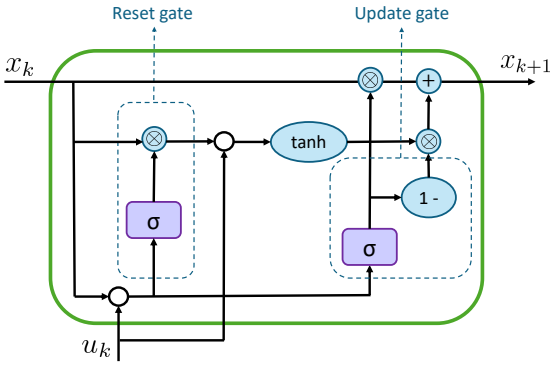

Figure 4.2: Schematic representation of the GRU cell.

This condition can be satisfied by a proper normalization of the input signals, provided that the input is bounded.

Theorem 4.2 ([28]). *If the GRU model* (4.5) *is such that*

$$\nu := \|U_{\mathrm{h}}\|_\infty \left(\frac{1}{4}\|U_{\mathrm{r}}\|_\infty + \bar{\sigma}_{\mathrm{r}}\right) + \frac{1}{4}\frac{1+\bar{\phi}_{\mathrm{h}}}{1-\bar{\sigma}_{\mathrm{z}}}\|U_{\mathrm{z}}\|_\infty < 1 \tag{4.6}$$

where

$$\begin{aligned}
\bar{\sigma}_{\mathrm{z}} &:= \sigma(\|[W_{\mathrm{z}} \quad U_{\mathrm{z}} \quad b_{\mathrm{z}}]\|_\infty) \\
\bar{\sigma}_{\mathrm{r}} &:= \sigma(\|[W_{\mathrm{r}} \quad U_{\mathrm{r}} \quad b_{\mathrm{r}}]\|_\infty) \\
\bar{\phi}_{\mathrm{h}} &:= \tanh(\|[W_{\mathrm{h}} \quad U_{\mathrm{h}} \quad b_{\mathrm{h}}]\|_\infty)
\end{aligned}$$

then it is δISS in the sets $\mathcal{X}$ *and* $\mathcal{U}$*, where*

$$\mathcal{X} := \{x \in \mathbb{R}^n : \|x\|_\infty \leq 1\}. \tag{4.7}$$

To train a GRU network respecting the δISS condition (4.6) it is possible to use the same approach described in Section 4.2.2 for the training of δISS LSTM models.

4.4 Recurrent Equilibrium Networks

Recurrent Equilibrium Networks (REN) are a recently proposed RNN architecture [201], designed as the recurrent counterparts of the feed-forward deep equilibrium model proposed in [10]. One of the characterizing properties of this architecture is that it is possible to parametrize it in a way that guarantees the model contraction property while performing the training in an unconstrained way, without the need of adding regularization terms in

the training loss. RENs are state-space models that include a nonlinear part given by an equilibrium network [10], and have the following structure

$$x_{k+1} = Ax_k + B_1 w_k + B_2 u_k + b_{\mathrm{x}} \tag{4.8a}$$
$$y_k = C_2 x_k + D_{21} w_k + D_{22} u_k + b_{\mathrm{y}} \tag{4.8b}$$

where w_k is the solution of the equilibrium network

$$w_k = \phi(D_{11} w_k + C_1 x_k + D_{12} u_k + b_{\mathrm{v}}) \tag{4.8c}$$

where $x \in \mathbb{R}^n$, $w \in \mathbb{R}^q$, $u \in \mathbb{R}^m$ and $y \in \mathbb{R}^p$. Note that (4.8c) defines w implicitly as the solution of an equilibrium problem. $\phi(\cdot)$ is a nonlinear activation function that is applied to vectors element by element and respects the following assumption.

Assumption 4.2. *The activation function $\phi(\cdot)$ is piecewise differentiable and slope-restricted in $[0, 1]$, i.e.*

$$0 \leq \frac{\phi(a) - \phi(b)}{a - b} \leq 1, \quad \forall a, b \in \mathbb{R}, a \neq b.$$

Assumption 4.2 is satisfied by many commonly used activation functions, such as the sigmoid, the hyperbolic tangent and the Rectified Linear Unit (ReLU). The equilibrium network (4.8c) is said to be *well-posed* if for all x and u there exists a unique solution w of the equation that defines the equilibrium network. Sufficient conditions for the well-posedness of feed-forward equilibrium networks have been found in [200], and are exploited in [201] to extend the analysis to the recurrent counterpart.

4.4.1 Stability of the REN model

In this subsection, the stability and robustness properties of REN models are analysed. In particular, a δISS condition is derived following the method proposed in [201] to analyse contraction.

Theorem 4.3. *Consider the REN model (4.8) satisfying Assumption 4.2. Given $\bar{\alpha} \in (0, 1)$, if there exist $P = P^\top \succ 0$ and $\Lambda \in \mathbb{D}^+$ such that*

$$\tilde{Q} := \begin{bmatrix} \bar{\alpha}^2 P & -C_1^\top \Lambda \\ -\Lambda C_1 & W \end{bmatrix} - \begin{bmatrix} A^\top \\ B_1^\top \end{bmatrix} P \begin{bmatrix} A^\top \\ B_1^\top \end{bmatrix}^\top \succ 0 \tag{4.9}$$

where $W := 2\Lambda - \Lambda D_{11} - D_{11}^\top \Lambda$ and $\mathbb{D}^+$ denotes the set of the diagonal positive definite matrices, then the REN model is well-posed and exponentially δISS.

Proof. The proof is reported in Section 4.6.1.

Remark 4.1. *Condition* (4.9) *is the condition derived in [201] for the contraction of the REN. In Theorem 4.3 we have shown that this condition also implies exponential δISS of the model. Exponential δISS is a stronger property than contraction. In fact contraction only characterizes the behavior of couples of trajectories obtained applying the same input sequence, while δISS provides also guarantees for the behavior of state trajectories obtained by applying different input sequences.*

4.4.2 Training of REN models

When implementing a REN model, we have to consider that the equilibrium layer (4.8c) is defined implicitly, and the computation of the value w_k requires the solution of an equilibrium problem if D_{11} is a full matrix. To do so, it is necessary to use an iterative algorithm to solve the system of equations. When training RENs using gradient descent, the Jacobian of the equilibrium network (4.8c) with respect to the model weights must be computed. The Jacobian expression can be found using the implicit function theorem, as shown in [10], so that it is not necessary to backpropagate the gradient through the solving algorithm used in the forward pass. A possible method to simplify the REN implementation is to consider the subclass of acyclic RENs, in which the matrix D_{11} is strictly lower triangular, and the solution of (4.8c) can be written in explicit form. In [201] it is shown that this is not a limitation, as acyclic REN achieve similar performances to the general REN. For the training of the REN models used in the simulation examples of this thesis, the Anderson acceleration algorithm [5] has been employed for the solution of the equilibrium problems.

To obtain a REN model satisfying condition (4.9), we use the direct parametrization proposed in [201]. In particular, the REN model written in the direct parametrization satisfies (4.9) for all the possible values of the parameters. Hence, it is possible to use unconstrained optimization methods for the training, without introducing regularization terms in the loss function. This is an advantage because it does not require the tuning of the hyperparameters λ^+ and λ^- weighting the regularization term in the loss (4.4), which is typically done in a trial-and-error way.

4.5 Other δISS RNN structures

4.5.1 Multi-layer RNN

The LSTM and GRU structures described in Sections 4.2 and 4.3 are *shallow*, i.e. consisting of a single layer. In complex applications, one may benefit from the use of RNNs composed by several layers, also called *deep* RNN. In multi-layer RNNs, the state of the LSTM layer (4.1a)-(4.1b) or of the GRU layer (4.5a) is not directly fed into an affine output transformation, but it

is considered as input of the subsequent layer. The number of layers in the RNN is a tuning parameter, that is chosen to improve performances.

In the literature, there exist sufficient conditions for δISS also for these more complex structures. In particular, sufficient conditions for the δISS of multi-layer GRU are derived in [28], and of multi-layer LSTM in [30]. Those results show that if all the layers composing the deep GRU or the deep LSTM satisfy the sufficient condition for δISS of the shallow network, then the deep network is δISS. These results can be seen as a particular case of the more general properties derived in Section 2.4 for the interconnection of δISS systems. In fact, as reported in Corollary 2.1, the cascade connection of δISS systems is δISS.

4.5.2 Other classes of δISS RNN

In the literature, there exist many other RNN classes whose stability properties have been characterized. One of the first networks to be characterized in terms of δISS are echo state networks (ESN) in [8], where the network is also used as surrogate model in MPC. Another class of NNs analyzed from the stability point of view is the one of neural nonlinear autoregressive exogenous (NNARX) models, i.e. NARX models in which FFNNs are used as regressor functions to predict the future output value based on past values of the system input and output. In [29], these models are written in the form of a RNN, considering as state the concatenation of the previous inputs and outputs used for regression. Then, sufficient conditions for ISS and δISS of the model are derived. In [57], a sufficient condition for δISS is derived for a general class of RNN that includes ESN and NNARX models. This condition is also exploited in the derivation of an LMI-based method for control design. Finally, in [162], the authors study the ISS and δISS property of gated graph neural networks, a RNN architecture particularly suited for distributed tasks.

All the stability conditions considered so far are global, i.e. are valid either for $x \in \mathbb{R}^n$, or in a positive invariant subset of $\mathbb{R}^n$ where it is reasonable that the RNN state lies at all time steps. This may a limitation in some applications, for example when considering systems that are not globally δISS. To overcome this issue, in [143], some regional stability conditions for a particular class of RNNs are derived.

4.6 Proofs

4.6.1 Proof of Theorem 4.3

In the proof, the REN equations (4.8) are denoted in compact way by

$$\begin{aligned} x_{k+1} &= f(x_k, u_k) \\ y_k &= g(x_k, u_k). \end{aligned}$$

Moreover, we denote the difference between trajectories using $\Delta x = x^{\mathrm{a}} - x^{\mathrm{b}}$, and similarly for the other variables. Finally,

$$v := D_{11} w + C_1 x + D_{12} u + b_{\mathrm{v}}.$$

The proof of well-posedness follows from Theorem 1 of [201].

The proof of δISS is based on the study of

$$V(x^{\mathrm{a}}, x^{\mathrm{b}}) = \|\Delta x\|_P^2$$

as a δISS-Lyapunov function. We first note that (2.11a) is trivially satisfied in view of the quadratic nature of $V(x^{\mathrm{a}}, x^{\mathrm{b}})$.

Condition (2.11b) is now proven. To do so, we first derive some relations between Δw, Δx and Δu. Assumption 4.2 implies that

$$(\phi(a) - \phi(b))(a - b) \geq (\phi(a) - \phi(b))^2 \quad \forall a, b \in \mathbb{R}. \tag{4.10}$$

Then, for any diagonal matrix $\Lambda \succ 0$ we have that

$$\Delta w^\top \Lambda \Delta v \geq \Delta w^\top \Lambda \Delta w \tag{4.11}$$

where

$$\Delta v = C_1 \Delta x + D_{11} \Delta w + D_{12} \Delta u. \tag{4.12}$$

By substituting (4.12) in (4.11) we obtain

$$-\frac{1}{2} \Delta w^\top W \Delta w + \Delta w^\top \Lambda C_1 \Delta x + \Delta w^\top \Lambda D_{12} \Delta u \geq 0. \tag{4.13}$$

It is now possible to analyze the evolution of the δISS-Lyapunov function between consecutive time steps.

$$\begin{aligned} &\left\| f(x^{\mathrm{a}}, u^{\mathrm{a}}) - f(x^{\mathrm{b}}, u^{\mathrm{b}}) \right\|_P^2 - \|\Delta x\|_P^2 \\ &= \|A \Delta x + B_1 \Delta w + B_2 \Delta u\|_P^2 - \|\Delta x\|_P^2 \\ &\overset{(4.13)}{\leq} \Delta x^\top A^\top P A \Delta x + \Delta w^\top B_1^\top P B_1 \Delta w \\ &+ \Delta u^\top B_2^\top P B_2 \Delta u + 2 \Delta x^\top A^\top P B_1 \Delta w \\ &+ 2 \Delta x^\top A^\top P B_2 \Delta u + 2 \Delta w^\top B_1^\top P B_2 \Delta u \\ &- \Delta x^\top P \Delta x - \bar{\alpha}^2 \Delta x^\top P \Delta x + \bar{\alpha}^2 \Delta x^\top P \Delta x \\ &- \Delta w^\top W \Delta w + 2 \Delta w^\top \Lambda C_1 \Delta x + 2 \Delta w^\top \Lambda D_{12} \Delta u \end{aligned}$$

$$
\begin{aligned}
&\overset{(4.9)}{=} -\begin{bmatrix}\Delta x\\ \Delta w\end{bmatrix}^\top \tilde{Q}\begin{bmatrix}\Delta x\\ \Delta w\end{bmatrix}\\
&+\Delta u^\top B_2^\top P B_2 \Delta u + 2\Delta x^\top A^\top P B_2 \Delta u\\
&+2\Delta w^\top (B_1^\top P B_2 + \Lambda D_{12})\Delta u + (\bar{\alpha}^2 - 1)\Delta x^\top P \Delta x.
\end{aligned}
$$

Since $\tilde{Q} \succ 0$,

$$
\begin{aligned}
-\begin{bmatrix}\Delta x\\ \Delta w\end{bmatrix}^\top \tilde{Q}\begin{bmatrix}\Delta x\\ \Delta w\end{bmatrix} &\leq -\lambda_{min}(\tilde{Q})\left\|\begin{bmatrix}\Delta x\\ \Delta w\end{bmatrix}\right\|_2^2\\
&\leq -\lambda_{min}(\tilde{Q})\left\|\Delta w\right\|_2^2.
\end{aligned}
$$

Then

$$
\begin{aligned}
&\left\|f(x^{\mathrm{a}},u^{\mathrm{a}}) - f(x^{\mathrm{b}},u^{\mathrm{b}})\right\|_P^2 - \|\Delta x\|_P^2\\
&\leq -\lambda_{min}(\tilde{Q})\Delta w^\top \Delta w + \Delta u^\top B_2^\top P B_2 \Delta u\\
&+2\Delta x^\top A^\top P B_2 \Delta u + 2\Delta w^\top (B_1^\top P B_2 + \Lambda D_{12})\Delta u\\
&-(1-\bar{\alpha}^2)\Delta x^\top P \Delta x.
\end{aligned}
$$

Given $\tau \in (0,1)$, by completing the squares, we obtain that

$$
\begin{aligned}
&\left\|f(x^{\mathrm{a}},u^{\mathrm{a}}) - f(x^{\mathrm{b}},u^{\mathrm{b}})\right\|_P^2 - \|\Delta x\|_P^2\\
&\leq -\tau(1-\bar{\alpha}^2)\Delta x^\top P \Delta x + \Delta u^\top B_2^\top P B_2 \Delta u\\
&+\frac{1}{\lambda_{min}(\tilde{Q})}\Delta u^\top (B_1^\top P B_2 + \Lambda D_{12})^\top (B_1^\top P B_2 + \Lambda D_{12})\Delta u\\
&+\frac{1}{(1-\tau)(1-\bar{\alpha}^2)}\Delta u^\top B_2^\top P^\top A P^{-1} A^\top P B_2 \Delta u,
\end{aligned}
\tag{4.14}
$$

i.e. $V(x^{\mathrm{a}},x^{\mathrm{b}})$ respects condition (2.11b). Then, in view of Theorem 2.4 and on the existence of a δISS Lyapunov function respecting (2.11a) and (2.11b), the REN model is δISS. □

Chapter 5

MPC design for δISS systems and application to REN models

In this chapter, we introduce some of the main ideas that can be used for the design of MPC algorithms for δISS systems, and that will be exploited also in the following chapters. In particular, we provide some guidelines for the design of the MPC terminal ingredients and for the design of the observer, exploiting the δISS property of the system under control. These general ideas are then applied to the design of an MPC algorithm based on REN models. The REN-based MPC is tested in simulation on a pH neutralization process.

The REN-based MPC algorithm is taken from:

- [211] **Schimperna, I.**, and Magni, L. (2024). *Recurrent equilibrium network models for nonlinear model predictive control*. IFAC-PapersOnLine, 58(18), 226-231. Presented at the 8th IFAC Conference on Nonlinear Model Predictive Control NMPC 2024, Kyoto, Japan.

5.1 Design of MPC algorithms for δISS systems

In this section, we consider the problem of designing a stabilizing MPC algorithm for a globally δISS nonlinear system. In the formulation of this chapter we only consider input constraints, with the input constraint set $\mathcal{U}$ containing the input reference $\bar{u}$ in its interior. We also consider the observer design problem in case of output-feedback. This is the typical case when using RNN models, in which the state does not have a physical meaning but is an artificial quantity that is used to memorize the past history of the system.

5.1.1 MPC for δISS systems

The δISS property of the system facilitates the design of stabilizing MPC algorithms based on terminal ingredients. In fact, it is possible to use as auxiliary control law to satisfy Assumption 3.2 the constant control law $\mu_a(x) = \bar{u}$ for all $x \in \mathbb{R}^n$. In view of the δISS property of the system, the state trajectory associated to the constant input $\bar{u}$ converges to the equilibrium state $\bar{x}$. Then, an open-loop δISS Lyapunov function can be used as terminal cost of the MPC. Since the δISS property is assumed to hold globally, if there are no state constraints it is not necessary to introduce a terminal constraint in the optimization. This is an advantage because it allows to always have feasibility of the optimization problem.

In presence of constraints on the system state, it is necessary to introduce a terminal set that respects Points 1. and 2. of Assumption 3.2. The simpler design of the terminal set consists in the use of a sublevel set of a terminal cost included in the state constraint set $\mathcal{X}$. This aspect will be further analyzed in the MPC design in Chapters 6 and 7.

5.1.2 Observer for δISS systems

If the state of the system is not measurable, an observer must be introduced in the closed-loop, as explained in Section 3.3. The δISS property is very useful for the design of observers [7]. In fact, it can be seen as an "open-loop observability" property, meaning that for δISS systems the trivial open-loop observer is guaranteed to provide a converging state estimation. This property immediately follows from the definition (2.10) of δISS, where we can see that if we provide the same input sequence to the system, the state trajectories starting from any initial state converge asymptotically.

Typically, the open-loop observer does not provide the best performances in terms of convergence speed of the state estimation. However, it can serve as baseline for the design of more complex observers, and it ensures the existence of an observer structure with guaranteed convergence properties.

5.2 MPC design for REN models

In this section, we show the procedure for the design of an observer and a stabilizing MPC for a system modeled by a REN, following the ideas presented in the previous section. The control design and the stability analysis are carried out under the assumption that the REN model (4.8) exactly represents the dynamics of the system under control.

5.2.1 Observer for the REN model

The state x of the REN model has no physical meaning, but it encodes the memory of the past inputs of the plant. So, when the REN model is used to

provide the predictions for the MPC, it is important to initialize the state in a meaningful way, that is consistent with the past history of the plant. In order to do so, an observer is introduced in the control loop, and is used to provide an estimate $\hat{x}$ of the state x of the REN model.

The observer for the REN model is designed with a structure similar to the one of the REN model (4.8), but including in the state equation an additional term to penalize the difference between the output predicted by the observer and the real output. The equations of the REN observer are the following

$$\hat{x}_{k+1} = A\hat{x}_k + B_1\hat{w}_k + B_2u_k + b_{\mathrm{x}} + L(y_k - \hat{y}_k) \tag{5.1a}$$
$$\hat{w}_k = \phi(D_{11}\hat{w}_k + C_1\hat{x}_k + D_{12}u_k + b_{\mathrm{v}}) \tag{5.1b}$$
$$\hat{y}_k = C_2\hat{x}_k + D_{21}\hat{w}_k + D_{22}u_k + b_{\mathrm{y}} \tag{5.1c}$$

where $L \in \mathbb{R}^{n\times p}$ is the observer gain, that has to be properly tuned in order to guarantee convergence, as reported in the next Theorem.

Theorem 5.1. *If the plant behaves according to* (4.8)*, with $\phi(\cdot)$ satisfying Assumption 4.2, and respects the δISS condition* (4.9)*, and the observer gain L is selected so that there exist $P_{\mathrm{o}} = P_{\mathrm{o}}^\top \succ 0$, $\Lambda \in \mathbb{D}^+$ and $\bar{\alpha}_{\mathrm{o}} \in (0, 1]$ such that*

$$\tilde{Q}_{\mathrm{o}} \succ 0, \tag{5.2}$$

where

$$\tilde{Q}_{\mathrm{o}} := \begin{bmatrix} \bar{\alpha}_{\mathrm{o}}^2 P_{\mathrm{o}} & -C_1^\top\Lambda \\ -\Lambda C_1 & W \end{bmatrix} - \begin{bmatrix} (A - LC_2)^\top \\ (B_1 - LD_{21})^\top \end{bmatrix} P_{\mathrm{o}} \begin{bmatrix} (A - LC_2)^\top \\ (B_1 - LD_{21})^\top \end{bmatrix}^\top$$

and $W := 2\Lambda - \Lambda D_{11} - D_{11}^\top\Lambda$, then the observer provides an exponentially converging and bounded state estimation, i.e. $x_k - \hat{x}_k \to 0$ for $k \to \infty$ and there exist $M > 0$ and $\mu \in (0, 1)$ such that

$$\|x_k - \hat{x}_k\|_2 \leq M\mu^k \|x_0 - \hat{x}_0\|_2 . \tag{5.3}$$

Proof. The proof is reported in Section 5.5.1.

Remark 5.1. *A possible suboptimal choice of the observer gain is the open-loop observer with $L = \mathbf{0}_{n,p}$. In fact, with this choice,* (5.2) *is trivially satisfied for $P_{\mathrm{o}} = P$ and $\bar{\alpha}_{\mathrm{o}} = \bar{\alpha}$.*

5.2.2 MPC design

The objective of the MPC is to stabilize the system at an equilibrium point $(\bar{x}, \bar{u}, \bar{y})$ of the REN model, while respecting an input constraint $u \in \mathcal{U}$. To

do so, the following FHOCP is solved at every time instant k:

$$\min_{u_{\cdot|k}} \sum_{i=0}^{N-1} \left(\left\| x_{i|k} - \bar{x} \right\|_Q^2 + \left\| u_{i|k} - \bar{u} \right\|_R^2 \right) + s \left\| x_{N|k} - \bar{x} \right\|_P^2 \tag{5.4a}$$

$$\text{s.t.} \quad x_{0|k} = \hat{x}_k \tag{5.4b}$$

$$x_{i+1|k} = f(x_{i|k}, u_{i|k}) \tag{5.4c}$$

$$u_{i|k} \in \mathcal{U} \tag{5.4d}$$

where $\bar{u}$ is such that $\bar{u} \in \mathcal{U}$, and the cost matrices are such that $Q = Q^\top \succ 0$, $R = R^\top \succ 0$, P satisfies (4.9) and

$$s = \frac{\lambda_{max}(Q)}{(1 - \bar{\alpha}^2)\lambda_{min}(P)}. \tag{5.5}$$

In (5.4c), the function f represents the REN state equation (4.8a)-(4.8c).

Then, denoting by $\mathbf{u}_k^\star := \{u_{0|k}^\star, ..., u_{N-1|k}^\star\}$ the optimal input sequence at time step k, the MPC control law is selected according to the receding horizon principle, i.e.

$$u_k = \mu^{\text{MPC}}(\hat{x}_k) = u_{0|k}^\star. \tag{5.6}$$

5.2.3 Convergence properties

In the following theorem the main result about the stabilizing properties of the proposed control schema is derived.

Theorem 5.2. *If the REN model respects Assumption 4.2 and the δISS condition* (4.9)*, the observer is tuned in order to satisfy* (5.2)*, and the input constraint set $\mathcal{U}$ is bounded, then the equilibrium point $x = \bar{x}$, $\hat{x} = \bar{x}$ of the closed loop composed by the plant* (4.8)*, the observer* (5.1) *and the MPC* (5.6) *is asymptotically stable.*

Proof. The proof is reported in Section 5.5.2.

5.3 Illustrative example

5.3.1 pH neutralization process

To test the proposed algorithm, we considered the control of the pH neutralization process proposed in [97]. This system is a simplification of the process proposed in [95], that was specifically designed to test advanced control strategies. This is a SISO system, with nonmeasurable state, and is open-loop δISS. The system is highly nonlinear, and its gain varies several order of magnitude over a modest range of pH values. A schematic layout of the process is reported in Figure 5.1. The process consists in a tank where three flows of substances are mixed: an acid flow q_1, a buffer flow q_2, and

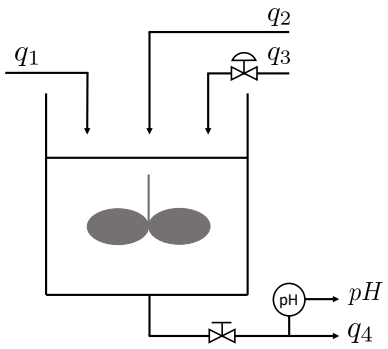

Figure 5.1: Schematic layout of the pH neutralization process.

a basic flow q_3. The basic flow q_3 is considered as controlled variable. The acid flow q_1 is considered constant at the nominal operating point. The buffer flow q_2 is an unmeasurable disturbance. The output of the system is the pH on the output flow q_4. The physical model of the plant is based on conservation equations and equilibrium relations. Defining the state, input and output of the system as

$$x := [W_{a4},\ W_{b4},\ h_1]^\top, \quad u := q_3, \quad y := pH,$$

where W_{a4} is a charge related quantity in the output flow, W_{b4} is the concentration of CO_3^{2-} ions in the output flow, h is the tank level and the acid flow q_1 is assumed to be a constant parameter, the process model can be written in the form

$$\begin{aligned} \dot{x} &= f(x) + g(x)u + p(x)q_2, \\ c(x,y) &= 0, \end{aligned} \tag{5.7}$$

where

$$f(x) = \begin{bmatrix} \frac{q_1}{A_1 x_{(3)}}(W_{a1} - x_{(1)}) \\ \frac{q_1}{A_1 x_{(3)}}(W_{b1} - x_{(2)}) \\ \frac{1}{A_1}(q_1 - C_{v4}(x_{(3)} + z)^n) \end{bmatrix},$$

$$g(x) = \begin{bmatrix} \frac{1}{A_1 x_{(3)}}(W_{a3} - x_{(1)}) \\ \frac{1}{A_1 x_{(3)}}(W_{b3} - x_{(2)}) \\ \frac{1}{A_1} \end{bmatrix},$$

$$p(x) = \begin{bmatrix} \frac{1}{A_1 x_{(3)}}(W_{a2} - x_{(1)}) \\ \frac{1}{A_1 x_{(3)}}(W_{b2} - x_{(2)}) \\ \frac{1}{A_1} \end{bmatrix},$$

$$c(x,y) = x_{(1)} + 10^{y-14} - 10^{-y} + x_{(2)} \frac{1 + 2 \times 10^{y - pK_2}}{1 + 10^{pK_1 - y} + 10^{y - pK_2}}.$$

$z = 11.5cm$	$W_{a1} = 3.00 \cdot 10^{-3}M$	$q_1 = 16.6mL/s$
$C_{v4} = 4.59$	$W_{b1} = 0.00M$	$q_2 = 0.55mL/s$
$n = 0.607$	$W_{a2} = -0.03M$	$q_3 = 15.6mL/s$
$pK_1 = 6.35$	$W_{b2} = 0.03M$	$q_4 = 32.8mL/s$
$pK_2 = 10.25$	$W_{a3} = 3.05 \cdot 10^{-3}M$	$A_1 = 207cm^2$
$h_1 = 14cm$	$W_{b3} = 5.00 \cdot 10^{-5}M$	$W_{a4} = -4.32 \cdot 10^{-4}M$
$pH = 7.0$	$W_{b4} = 5.28 \cdot 10^{-4}M$	

Table 5.1: Nominal operating conditions of the pH system.

The output equation (5.7) can be rewritten in explicit form as

$$\dot{y} = -c_y^{-1}(x, y)c_x(y)\dot{x},$$

where

$$c_x(y) = \left[1,\ \frac{1 + 2 \times 10^{y-pK_2}}{1 + 10^{pK_1-y} + 10^{y-pK_2}},\ 0\right]^\top,$$

$$c_y(x, y) = \ln(10)\Bigg(10^{y-14} + 10^{-y} + x_{(2)}\frac{10^{pK_1-y} + 10^{y-pK_2} + 4(10^{pK_1-y})(10^{y-pK_2})}{(1 + 10^{pK_1-y} + 10^{y-pK_2})^2}\Bigg).$$

The nominal values of the model parameters are reported in Table 5.1.

5.3.2 Simulation results

For the MPC simulations of this section, the buffer flow q_2 is considered constant at its nominal value, and the system input $q_3 = u$ is considered saturated in

$$u \in \mathcal{U} := [12.5, 17]\ mL/s.$$

To derive a REN model of the plant, a dataset is collected by forcing a simulator of the system with multilevel pseudo-random inputs, and the output response is sampled with a sampling time $T_s = 10s$. A sequence of 20000 time steps is collected, and is divided into 15000 time steps for training, 2500 time steps for validation and 2500 time steps for testing. Then, the training data is divided into shortest subsequences of 100 time steps each, and the training was performed with a batch size of 25.

To simplify the implementation we considered an acyclic REN, where D_{11} is strictly lower triangular, that has shown to provide models of similar quality of the general REN. The training code is implemented in Python, using PyTorch library. In particular, a model with $n = 5$, $q = 8$, hyperbolic tangent as activation function and with guaranteed contraction property is

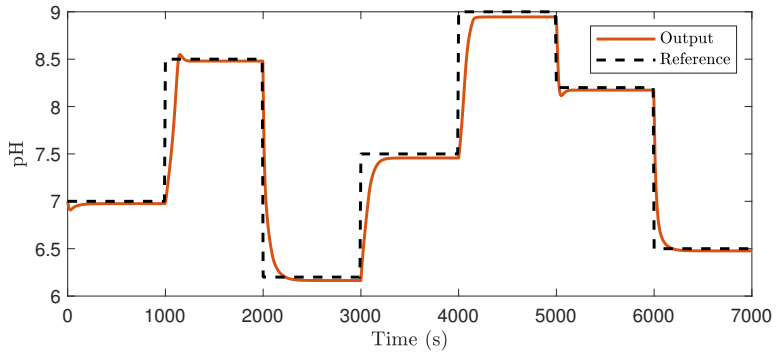

Figure 5.2: Simulation results: output (pH).

trained using ADAM optimizer for 200 epochs. The final model used for the MPC implementation obtains a satisfactory FIT of 86.8% on the test dataset.

To select the observer gain L we solve the following optimization problem

$$\max_{L} \quad \lambda_{min}(\tilde{Q}_{\mathrm{o}}) \tag{5.8}$$

where $\tilde{Q}_{\mathrm{o}}$ is computed fixing $P_{\mathrm{o}} = P$ and $\bar{\alpha}_{\mathrm{o}} = \bar{\alpha}$, and P is obtained according to the formulas reported in [201]. This is a nonlinear optimization problem, and is solved using Matlab *fmincon* function, initializing the solver in the feasible point $L = \mathbf{0}_{n,p}$. The idea behind the optimization (5.8) is that large eigenvalues of $\tilde{Q}_{\mathrm{o}}$ are related to a fast convergence of the observer estimation error in view of Equation (5.12) in the proofs. In the FHOCP, the cost matrices are set to $Q = 100 I_n$, $R = 1$, and s is chosen according to (5.5). The prediction horizon is set to $N = 10$. The simulation is carried out in Matlab, and the FHOCP is solved using CasADi [6]. In the simulation, step-wise variations of the output reference $\bar{y}$ has been applied to the controller. The resulting closed-loop trajectory is reported in Figure 5.2, while the control variable evolution is reported in Figure 5.3, showing that the controller is able to manage the plant in a satisfactory way and to respect the saturation constraints on the input. A small static gain mismatch is present, that is due to modeling errors.

5.4 Conclusions

In this chapter, an observer and a stabilizing MPC are proposed for the REN model, following general design ideas that can be adapted to any δISS model. The observer is based on the REN model equations, and a condition for its convergence is derived. In the MPC formulation, a terminal cost is introduced in order to guarantee closed-loop stability. Since no state or

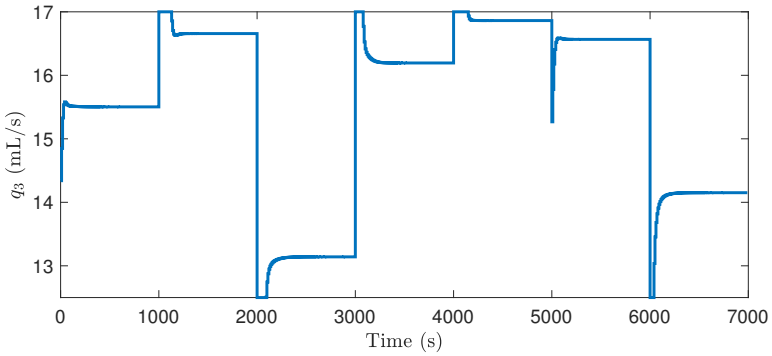

Figure 5.3: Simulation results: input (q_3).

output constraints are considered, in view of the δISS property of the model, it is not necessary to include a terminal constraint.

5.5 Proofs

5.5.1 Proof of Theorem 5.1

In this proof, we study the evolution of the observer estimation error $x - \hat{x}$. By subtracting (5.1a) from (4.8a) and substituting the expressions (4.8b) for y and (5.1c) for $\hat{y}$, we obtain that

$$x_{k+1} - \hat{x}_{k+1} = (A - LC_2)(x_k - \hat{x}_k) + (B_1 - LD_{21})(w_k - \hat{w}_k). \tag{5.9}$$

Let's now denote

$$\begin{aligned} v_k &:= D_{11}w_k + C_1 x_k + D_{12}u_k + b_{\mathrm{v}} \\ \hat{v}_k &:= D_{11}\hat{w}_k + C_1 \hat{x}_k + D_{12}u_k + b_{\mathrm{v}} \end{aligned}$$

so that $w_k = \phi(v_k)$ and $\hat{w}_k = \phi(\hat{v}_k)$. We have that

$$v_k - \hat{v}_k = C_1(x_k - \hat{x}_k) + D_{11}(w_k - \hat{w}_k). \tag{5.10}$$

In view of (4.10), for any diagonal matrix $\Lambda \succ 0$ we have that

$$(w_k - \hat{w}_k)^\top \Lambda (v_k - \hat{v}_k) \geq (w_k - \hat{w}_k)^\top \Lambda (w_k - \hat{w}_k).$$

Substituting (5.10) we obtain

$$\frac{1}{2}(w_k - \hat{w}_k)^\top W (w_k - \hat{w}_k) - (x_k - \hat{x}_k)^\top C_1^\top \Lambda (w_k - \hat{w}_k) \leq 0. \tag{5.11}$$

Let's now consider

$$\begin{bmatrix} x_k - \hat{x}_k \\ w_k - \hat{w}_k \end{bmatrix}^\top \tilde{Q}_{\mathrm{o}} \begin{bmatrix} x_k - \hat{x}_k \\ w_k - \hat{w}_k \end{bmatrix}.$$

In view of (5.9) and positive definiteness of $\tilde{Q}_{\mathrm{o}}$, if $x_k \neq \hat{x}_k$

$$\begin{aligned} &\|x_{k+1} - \hat{x}_{k+1}\|^2_{P_{\mathrm{o}}} < \bar{\alpha}_{\mathrm{o}}^2 \|x_k - \hat{x}_k\|^2_{P_{\mathrm{o}}} \\ &- 2(x_k - \hat{x}_k)^\top C_1^\top \Lambda (w_k - \hat{w}_k) + (w_k - \hat{w}_k)^\top W (w_k - \hat{w}_k) \\ &\overset{(5.11)}{\leq} \bar{\alpha}_{\mathrm{o}}^2 \|x_k - \hat{x}_k\|^2_{P_{\mathrm{o}}} \end{aligned} \tag{5.12}$$

Then the bound (5.3) and convergence can be proven by iterating the previous equation over k. □

5.5.2 Proof of Theorem 5.2

To study the stability of the closed loop system in presence of perturbation terms due to the observer estimation error $x - \hat{x}$, we consider as Lyapunov function the optimal cost of the MPC, i.e.

$$V(\hat{x}_k) = \sum_{i=0}^{N-1} \left(\left\| x^\star_{i|k} - \bar{x} \right\|^2_Q + \left\| u^\star_{i|k} - \bar{u} \right\|^2_R \right) + s \left\| x^\star_{N|k} - \bar{x} \right\|^2_P$$

where $\mathbf{x}^\star_k = \{x^\star_{0|k}, ..., x^\star_{N|k}\}$ denote the optimal state sequence at time k, defined by $x^\star_{i+1|k} := f(x^\star_{i|k}, u^\star_{i|k})$ with $x^\star_{0|k} := \hat{x}_k$.

Firstly, we note that

$$V(\hat{x}_k) \geq a \|\hat{x}_k - \bar{x}\|_2^2 ,$$

where $a = \lambda_{min}(Q)$.

To derive an upper bound for $V(\hat{x}_k)$, we consider the suboptimal control sequence $\tilde{\mathbf{u}}_k = \{\tilde{u}_{0|k}, ..., \tilde{u}_{N-1|k}\}$ defined by $\tilde{u}_{i|k} := \bar{u}$ for all $i = 0, ..., N-1$. We denote with $\tilde{\mathbf{x}}_k = \{\tilde{x}_{0|k}, ..., \tilde{x}_{N|k}\}$ the associated state trajectory defined by $\tilde{x}_{i+1|k} := f(\tilde{x}_{i|k}, \tilde{u}_{i|k})$ with $\tilde{x}_{0|k} := \hat{x}_k$. We have that

$$V(\hat{x}_k) \leq \sum_{i=0}^{N-1} \left\| \tilde{x}_{i|k} - \bar{x} \right\|^2_Q + s \left\| \tilde{x}_{N|k} - \bar{x} \right\|^2_P .$$

Then, in view of the δISS property of the REN model, noting that $\bar{x}$ is the state evolution with initial state $\bar{x}$ and input $\bar{u}$, there exists $b > 0$ such that

$$V(\hat{x}_k) \leq b \|\hat{x}_k - \bar{x}\|_2^2 .$$

Let's now study the variation of the Lyapunov function between subsequent time steps. At time $k+1$ we have that

$$V(\hat{x}_{k+1}) = \sum_{i=0}^{N-1} \left(\left\| x^\star_{i|k+1} - \bar{x} \right\|^2_Q + \left\| u^\star_{i|k+1} - \bar{u} \right\|^2_R \right) + s \left\| x^\star_{N|k+1} - \bar{x} \right\|^2_P$$

where $\mathbf{u}^\star_{k+1} = \{u^\star_{0|k+1}, ..., u^\star_{N-1|k+1}\}$ is the optimal input sequence at time $k+1$, and $\mathbf{x}^\star_{k+1} = \{x^\star_{0|k+1}, ..., x^\star_{N|k+1}\}$ is the associated state trajectory, defined by $x^\star_{i+1|k+1} := f(x^\star_{i|k+1}, u^\star_{i|k+1})$ with $x^\star_{0|k+1} := \hat{x}_{k+1}$. Note that, in view of the presence of the observer, $\hat{x}_{k+1}$ can be different from $x^\star_{1|k}$.

To prove the decreasing property of the Lyapunov function, we introduce the suboptimal input sequence $\tilde{\mathbf{u}}_{k+1} = \{\tilde{u}_{0|k+1}, ..., \tilde{u}_{N-1|k+1}\}$ defined by $\tilde{u}_{i|k+1} := u^\star_{i+1|k}$ for $i = 0, ..., N-2$ and $\tilde{u}_{N-1|k+1} := \bar{u}$. We denote by $\tilde{\mathbf{x}}_{k+1} = \{\tilde{x}_{0|k+1}, ..., \tilde{x}_{N|k+1}\}$ the associate state trajectory, defined by $\tilde{x}_{i+1|k+1} := f(\tilde{x}_{i|k+1}, \tilde{u}_{i|k+1})$ with $\tilde{x}_{0|k+1} := \hat{x}_{k+1}$.

To take into account the different initialization of the FHOCP at each time step we introduce the following error terms for $i = 1, ..., N+1$

$$\varepsilon_{k+i} := \tilde{x}_{i-1|k+1} - x^\star_{i|k}$$

where $x^\star_{N+1|k} := f(x^\star_{N|k}, \bar{u})$.

In view of optimality, we have that

$$\begin{aligned}
V(\hat{x}_{k+1}) &\leq \sum_{i=0}^{N-1} \left(\left\|\tilde{x}_{i|k+1} - \bar{x}\right\|_Q^2 + \left\|\tilde{u}_{i|k+1} - \bar{u}\right\|_R^2 \right) + s \left\|\tilde{x}_{N|k+1} - \bar{x}\right\|_P^2 \\
&= \sum_{i=0}^{N-1} \left(\left\|x^\star_{i+1|k} - \bar{x}\right\|_Q^2 + \|\varepsilon_{k+i+1}\|_Q^2 + 2(x^\star_{i+1|k} - \bar{x})^\top Q \varepsilon_{k+i+1} \right) \\
&+ \sum_{i=0}^{N-2} \left\|u^\star_{i+1|k} - \bar{u}\right\|_R^2 + s \left\|x^\star_{N+1|k} - \bar{x}\right\|_P^2 \\
&+ s \|\varepsilon_{k+N+1}\|_P^2 + 2s(x^\star_{N+1|k} - \bar{x})^\top P \varepsilon_{k+N+1}.
\end{aligned}$$

Then

$$\begin{aligned}
V(\hat{x}_{k+1}) - V(\hat{x}_k) \leq &- \left\|x^\star_{0|k} - \bar{x}\right\|_Q^2 - \left\|u^\star_{0|k} - \bar{u}\right\|_R^2 \\
&+ \left\|x^\star_{N|k} - \bar{x}\right\|_Q^2 + s \left\|x^\star_{N+1|k} - \bar{x}\right\|_P^2 - s \left\|x^\star_{N|k} - \bar{x}\right\|_P^2 \\
&+ \sum_{i=0}^{N-1} \left(\|\varepsilon_{k+i+1}\|_Q^2 + 2(x^\star_{i+1|k} - \bar{x})^\top Q \varepsilon_{k+i+1} \right) \\
&+ s \|\varepsilon_{k+N+1}\|_P^2 + 2s(x^\star_{N+1|k} - \bar{x})^\top P \varepsilon_{k+N+1}.
\end{aligned}$$

Let's consider now the terms related to the states at time steps $k+N$ and $k+N+1$, and let's use the δISS property of the REN. In particular, since $\bar{x} = f(\bar{x}, \bar{u})$, the Lyapunov inequality (4.14) can be applied with $\Delta u = 0$

and $\tau = 1$:

$$\begin{aligned}
&\left\|x^\star_{N|k} - \bar{x}\right\|_Q^2 + s\left\|x^\star_{N+1|k} - \bar{x}\right\|_P^2 - s\left\|x^\star_{N|k} - \bar{x}\right\|_P^2 \\
&\leq \lambda_{max}(Q)\left\|x^\star_{N|k} - \bar{x}\right\|_2^2 + s\Big(\left\|x^\star_{N+1|k} - \bar{x}\right\|_P^2 - \left\|x^\star_{N|k} - \bar{x}\right\|_P^2\Big) \\
&\overset{(4.14)}{\leq} \lambda_{max}(Q)\left\|x^\star_{N|k} - \bar{x}\right\|_2^2 + s(\bar{\alpha}^2 - 1)\left\|x^\star_{N|k} - \bar{x}\right\|_P^2 \\
&\leq \big(\lambda_{max}(Q) - s(1-\bar{\alpha}^2)\lambda_{min}(P)\big)\left\|x^\star_{N|k} - \bar{x}\right\|_2^2 \overset{(5.5)}{=} 0
\end{aligned}$$

Then

$$V(\hat{x}_{k+1}) - V(\hat{x}_k) \leq -\left\|x^\star_{0|k} - \bar{x}\right\|_Q^2 - \left\|u^\star_{0|k} - \bar{u}\right\|_R^2 + p_k$$

where

$$\begin{aligned}
p_k = \sum_{i=0}^{N-1} &\Big(\|\varepsilon_{k+i+1}\|_Q^2 + 2(x^\star_{i+1|k} - \bar{x})^\top Q\varepsilon_{k+i+1}\Big) \\
&+ s\,\|\varepsilon_{k+N+1}\|_P^2 + 2s(x^\star_{N+1|k} - \bar{x})^\top P\varepsilon_{k+N+1}.
\end{aligned}$$

In view of the boundedness and convergence of the observer estimation error, there exist $M_1 > 0$ such that $\|\varepsilon_{k+i+1}\|_2 \leq M_1\|x_k - \hat{x}_k\|_2$, and $\varepsilon_{k+i+1} \to 0$ for $k \to \infty$, for all $i = 0, ..., N$. Moreover, for the δISS property of the model and the boundedness of $\mathcal{U}$, the system state x_k is guaranteed to be bounded for any k. In view of (5.3) and of the boundedness of x_k and of $\|x_0 - \hat{x}_0\|_2$, there exist $M_2, M_3 > 0$ such that $\left\|x^\star_{i+1|k} - \bar{x}\right\|_2 \leq M_2\left\|x^\star_{0|k} - \bar{x}\right\|_2 = M_2\|\hat{x}_k - \bar{x}\|_2 \leq M_3$, for $i = 0, ..., N$. Then the Lyapunov function $V(\hat{x}_k)$ is such that

$$\begin{aligned}
a\,\|\hat{x}_k - \bar{x}\|_2^2 \leq V(\hat{x}_k) \leq b\,\|\hat{x}_k - \bar{x}\|_2^2 \\
V(\hat{x}_{k+1}) - V(\hat{x}_k) \leq -c\,\|\hat{x}_k - \bar{x}\|_2^2 + p_k
\end{aligned}$$

for some $a, b, c > 0$, where p_k is bounded by a quantity that depends only on $\|x_k - \hat{x}_k\|_2$, and $p_k \to 0$ for $k \to \infty$.

In view of the properties of $V(\hat{x}_k)$, stability of the equilibrium point of the closed loop system can be proven following the proof of Theorem 3 in [219]. □

Chapter 6

Robust MPC with GRU networks

In this chapter, we consider the design of MPC for a δISS GRU model in presence of output constraints. The proposed control algorithm includes a state observer designed as in [32], and a constraint tightening method is used in the design of the robust MPC algorithm to take into account the presence f modeling errors and of the observer estimation error. In particular, we model the uncertainty as an additive disturbance acting on the output of the GRU model, and we design the constraint tightening inspired by [130] on the base of an incremental Lyapunov function of the model and of a Lyapunov function for the observer estimation error. The model Lyapunov function is also used to derive the terminal ingredients for the MPC, following the ideas already detailed in Section 5.1.1. Compared to the MPC formulation for δISS GRU models proposed in [32], our algorithm does not require a large prediction horizon, allowing to keep the computational cost low, and considers the presence of output constraints.

The content of this chapter is based on:

- [212] **Schimperna, I.**, and Magni, L. (2024). *Robust constrained nonlinear model predictive control with gated recurrent unit model.* Automatica, 161, 111472.

6.1 Problem formulation and control algorithm

The objective of the GRU-based MPC designed in this chapter is to perform regulation at a set point $\bar{y}$, while respecting input saturation constraints

$$u \in \mathcal{U} = \{u \in \mathbb{R}^m : \|u\|_\infty \leq 1\} \tag{6.1}$$

and compact polytopic constraints on the output

$$y \in \mathcal{Y} = \{y \in \mathbb{R}^p : Ly \leq h\} \tag{6.2}$$

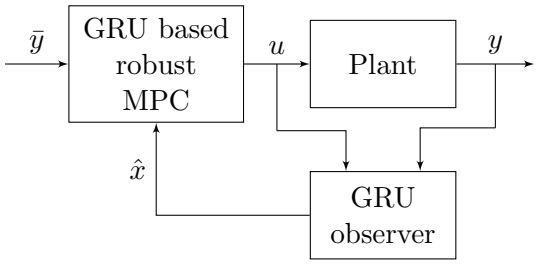

Figure 6.1: Block diagram of the control scheme.

where $L \in \mathbb{R}^{q \times p}$ and $h \in \mathbb{R}^q$. The formulation of the input saturation constraint as unity boundedness of u is very general, since it can be obtained by applying a proper normalization to the input of the model. The schematic layout of the proposed control algorithm is reported in Figure 6.1, and is composed by two main blocks. The first block is an observer, that provides an estimation of the state of the GRU model on the basis of the input and the output of the plant. The second block is the robust MPC, that solves a FHOCP and gives in output the first element of the optimal input sequence. In the FHOCP, the evolution of the plant is predicted by the GRU model, and the constraints are tightened to guarantee their robust satisfaction despite the presence of model-plant mismatch and of the observer estimation error. Moreover, the terminal ingredients of the FHOCP are designed to guarantee stability.

6.2 Gated Recurrent Unit model and observer

6.2.1 Model properties and uncertainty description

We consider a GRU NN as model of the system under control, described by equation (4.5). In this chapter we take into account the presence of modeling errors. Hence, we denote the output of the GRU model produced by equation (4.5e) by $\xi \in \mathbb{R}^p$ instead than by y, to distinguish it from the real system output y. The GRU model is also denoted in a more compact way by

$$x_{k+1} = f(x_k, u_k) \tag{6.3a}$$

$$\xi_k = g(x_k). \tag{6.3b}$$

We consider a GRU model satisfying the sufficient condition for δISS of Theorem 4.2, with the state $x \in \mathcal{X}$, where $\mathcal{X}$ is defined in (4.7). Under this condition, it is possible to define an incremental Lyapunov function for the GRU model, that is used to define the terminal ingredients for the MPC and the parameters for the constraint tightening.

Lemma 6.1. *If the GRU model respects condition* (4.6)*, then*

$$V_{\mathrm{s}}(x^{\mathrm{a}}, x^{\mathrm{b}}) = \|x^{\mathrm{a}} - x^{\mathrm{b}}\|_\infty$$

is an incremental Lyapunov function for the system (6.3)*, such that*

$$V_{\mathrm{s}}((x^{\mathrm{a}})^+, (x^{\mathrm{b}})^+) \leq \rho_{\mathrm{s}} V_{\mathrm{s}}(x^{\mathrm{a}}, x^{\mathrm{b}}) \tag{6.4a}$$

$$LU_{\mathrm{o}}(x^{\mathrm{a}} - x^{\mathrm{b}}) \leq c_{\mathrm{s}} V_{\mathrm{s}}(x^{\mathrm{a}}, x^{\mathrm{b}}) \tag{6.4b}$$

where $(x^{\mathrm{a}})^+ := f(x^{\mathrm{a}}, u)$*,* $(x^{\mathrm{b}})^+ := f(x^{\mathrm{b}}, u)$*,* $\rho_{\mathrm{s}} := \bar{\sigma}_{\mathrm{z}} + (1 - \bar{\sigma}_{\mathrm{z}})\nu$ *and* $c_{\mathrm{s}} \in \mathbb{R}^q$ *with* $c_{\mathrm{s}(j)} := \|(LU_{\mathrm{o}})_{(j*)}\|_\infty$*.*

Proof. The proof is reported in Section 6.6.1.

Note that if $\nu < 1$, then $\rho_s < 1$. In fact ρ_s is the average between 1 and ν weighted by $\bar{\sigma}_{\mathrm{z}} \in (0, 1)$. Hence, $\rho_s \in (\nu, 1)$.

Because of model-plant mismatch, the GRU model is not an exact representation of the dynamics of the system under control. We assume that the real plant with input u and output y behaves as a perturbed version of its GRU model, described by the following equations

$$x_{k+1} = f(x_k, u_k) \tag{6.5a}$$

$$y_k = g(x_k) + w_{\mathrm{y},k} \tag{6.5b}$$

where w_{y} is bounded in the set

$$w_{\mathrm{y}} \in \mathcal{W}_{\mathrm{y}} := \{w_{\mathrm{y}} \in \mathbb{R}^p : \|w_{\mathrm{y}}\|_\infty \leq \bar{w}_{\mathrm{y}}\}$$

and $\bar{w}_{\mathrm{y}} \in \mathbb{R}$ can be estimated as the maximum output error of the model.

6.2.2 Observer

The state x of the GRU model has no physical meaning, hence it cannot be directly measured from the system, but it needs to be estimated by means of an observer. In particular, we use the observer for the GRU proposed in [32], that is described by the following equations

$$\hat{x}_{k+1} = \hat{z}_k \otimes \hat{x}_k + (1 - \hat{z}_k) \otimes \hat{h}_k \tag{6.6a}$$

$$\hat{z}_k = \sigma(W_{\mathrm{z}} u_k + U_{\mathrm{z}} \hat{x}_k + b_{\mathrm{z}} + L_{\mathrm{z}}(y_k - \hat{y}_k)) \tag{6.6b}$$

$$\hat{r}_k = \sigma(W_{\mathrm{r}} u_k + U_{\mathrm{r}} \hat{x}_k + b_{\mathrm{r}} + L_{\mathrm{r}}(y_k - \hat{y}_k)) \tag{6.6c}$$

$$\hat{h}_k = \tanh(W_{\mathrm{h}} u_k + U_{\mathrm{h}}(\hat{r}_k \otimes \hat{x}_k) + b_{\mathrm{h}}) \tag{6.6d}$$

$$\hat{y}_k = U_{\mathrm{o}} \hat{x}_k + b_{\mathrm{o}} \tag{6.6e}$$

where $L_{\mathrm{z}}, L_{\mathrm{r}} \in \mathbb{R}^{n \times p}$ are observer gains that must be properly selected, $\hat{z}_k = \hat{z}(\hat{x}_k, u_k, y_k)$, $\hat{r}_k = \hat{r}(\hat{x}_k, u_k, y_k)$ and $\hat{h}_k = \hat{h}(\hat{x}_k, u_k, y_k)$. In presence of perturbations, it is not possible to guarantee that the observer estimation error converges to zero. However it is possible to prove that it is ISS with respect to the perturbation term w_{y}.

Lemma 6.2. *If the plant behaves according to* (6.5) *and respects the δISS condition* (4.6)*, $x \in \mathcal{X}$, $\hat{x} \in \mathcal{X}$, $u \in \mathcal{U}$ and the observer gains L_z and L_r are selected so that*

$$\nu_o < 1 \tag{6.7}$$

where

$$\nu_o := \|U_h\|_\infty \left(\frac{1}{4} \|U_r - L_r U_o\|_\infty + \bar{\sigma}_r \right) + \frac{1}{4} \frac{1 + \bar{\phi}_h}{1 - \bar{\sigma}_z} \|U_z - L_z U_o\|_\infty$$

then the function

$$V_o(x - \hat{x}) := \|x - \hat{x}\|_\infty$$

is an ISS-Lyapunov function for the system describing the observer estimation error $\hat{x} - x$ with respect to the input w_y, such that

$$V_o(x^+ - \hat{x}^+) \leq \rho_o V_o(x - \hat{x}) + \kappa \|w_y\|_\infty \tag{6.8a}$$

$$LU_o(x - \hat{x}) \leq c_o V_o(x - \hat{x}) \tag{6.8b}$$

$$\left\| \hat{x}^+ - f(\hat{x}, u) \right\|_\infty \leq L_{max} V_o(x - \hat{x}) + \kappa \|w_y\|_\infty \tag{6.8c}$$

where $x^+ = f(x, u)$, $\hat{x}^+$ is the next state computed by the observer (6.6)*, $\rho_o := \bar{\sigma}_z + (1 - \bar{\sigma}_z)\nu_o$, $c_o \in \mathbb{R}^q$ with $c_{o(j)} := \|(LU_o)_{(j*)}\|_\infty$, and*

$$\kappa = \frac{1}{4}(1 + \bar{\phi}_h)\|L_z\|_\infty + \frac{1}{4}\bar{\sigma}_z \|U_h\|_\infty \|L_r\|_\infty$$

$$L_{max} = \frac{1}{4}(1 + \bar{\phi}_h) \|L_z U_o\|_\infty + \frac{1}{4}\bar{\sigma}_z \|U_h\|_\infty \|L_r U_o\|_\infty .$$

Proof. The proof is reported in Section 6.6.2.

Remark 6.1. *A possible suboptimal choice of the gains of the observer that satisfies the condition $\nu_o < 1$ is the open loop observer with $L_z = L_r = \mathbf{0}_{n,p}$. In fact with this choice $\nu_o = \nu$, that is smaller than 1 by assumption.*

Theorem 6.1. *If the plant behaves according to* (6.5) *and respects the δISS condition* (4.6)*, $x \in \mathcal{X}$, $\hat{x} \in \mathcal{X}$, $u \in \mathcal{U}$, $w_y \in \mathcal{W}_y$ and $\nu_o < 1$, then the system that describes the observer estimation error $x - \hat{x}$ is ISS with respect to the input w_y.*

Proof. The proof follows from Theorem 2.2, in view of the existence of an ISS-Lyapunov function $V_o(x - \hat{x})$. □

6.3 MPC design

6.3.1 Tightened constraint design

On the base of the derived Lyapunov functions for the model and for the observer estimation error, it is possible to introduce the coefficients $a_i, b_i \in$

$\mathbb{R}^q$ for the constraint tightening that will be employed in the robust MPC. Such coefficients are designed as follows [130]

$$a_0 := c_{\mathrm{o}}, \quad b_0 := \mathbf{0}_{q,1}, \tag{6.9a}$$

$$a_{i+1} := \rho_{\mathrm{o}} a_i + \rho_{\mathrm{s}}^i L_{max} c_{\mathrm{s}}, \tag{6.9b}$$

$$b_{i+1} := b_i + a_i \bar{w} + c_{\mathrm{s}} \rho_{\mathrm{s}}^i \bar{w}, \tag{6.9c}$$

where $\bar{w}$ is such that

$$\kappa \left\| w_{\mathrm{y}} \right\|_\infty \leq \bar{w} \tag{6.10}$$

for all $w_{\mathrm{y}} \in \mathcal{W}_{\mathrm{y}}$.

For the constraint tightening the MPC uses also a time variant term $\hat{e}_{\mathrm{o}} \in \mathbb{R}$ related to the uncertainty of the observer. The evolution in time of this term corresponds to the worst case evolution of the observer ISS-Lyapunov function $V_{\mathrm{o}}(x - \hat{x})$:

$$\hat{e}_{\mathrm{o},k+1} = \rho_{\mathrm{o}} \hat{e}_{\mathrm{o},k} + \bar{w}. \tag{6.11}$$

Note that depending on the values of $\hat{e}_{\mathrm{o},0}$, ρ_{o} and $\bar{w}$, $\hat{e}_{\mathrm{o}}$ can increase or decrease, but its behavior is always monotonic with

$$\lim_{k \to \infty} \hat{e}_{\mathrm{o},k} = \bar{e}_\infty := \frac{\bar{w}}{1 - \rho_{\mathrm{o}}}.$$

6.3.2 Robust MPC formulation

It is now introduced the Finite Horizon Optimal Control Problem (FHOCP) solved by the MPC. In the FHOCP the deviation of states and inputs from the reference values $\bar{x}$ and $\bar{u}$ is penalized. These references values are computed from the GRU model (6.3) as the equilibrium state and input corresponding to the output $\xi = \bar{y}$.

Definition 6.1 (FHOCP)**.** *Given the prediction horizon N, the FHOCP for the robust MPC is the following:*

$$\min_{u_{\cdot|k}} \sum_{i=0}^{N-1} \left(\left\| x_{i|k} - \bar{x} \right\|_Q^2 + \left\| u_{i|k} - \bar{u} \right\|_R^2 \right) + s \left\| x_{N|k} - \bar{x} \right\|_\infty^2 \tag{6.12a}$$

$$s.t. \quad x_{0|k} = \hat{x}_k \tag{6.12b}$$

$$x_{i+1|k} = f(x_{i|k}, u_{i|k}) \tag{6.12c}$$

$$L(U_{\mathrm{o}} x_{i|k} + b_{\mathrm{o}}) + w_L \leq h - a_i \hat{e}_{\mathrm{o},k} - b_i \tag{6.12d}$$

$$u_{i|k} \in \mathcal{U} \tag{6.12e}$$

$$for\ i = 0, ..., N-1$$

$$x_{N|k} \in \mathcal{X}_f \tag{6.12f}$$

where Q and R are positive definite matrices and are design choices, while

$$s \geq \frac{n\lambda_{max}(Q)}{1-\rho_{\mathrm{s}}^2}. \tag{6.13}$$

The term $w_L \in \mathbb{R}^q$ for the constraint tightening is defined element by element as

$$w_{L(j)} = \sum_{k=1}^{p} |L_{(jk)}| \bar{w}_{\mathrm{y}} \tag{6.14}$$

for $j = 1, ..., q$.

$\mathcal{X}_f$ is a terminal set chosen as a level line of the terminal cost

$$\mathcal{X}_f := \{x \in \mathbb{R}^n : \|x - \bar{x}\|_\infty \leq \alpha\} \tag{6.15}$$

with

$$\alpha := \min_{j=1,...,q} \frac{-L_{(j*)}\bar{y} + h_{(j)} - \tilde{e}_{\mathrm{o}} a_{N(j)} - b_{N(j)} - w_{L(j)}}{\left\|(LU_{\mathrm{o}})_{(j*)}\right\|_\infty} \tag{6.16a}$$

where

$$\tilde{e}_{\mathrm{o}} := \max\{\hat{e}_{\mathrm{o},0}, \bar{e}_\infty\}. \tag{6.16b}$$

At each time step k the solution of the FHOCP is denoted by $\mathbf{u}_k^\star = \{u_{0|k}^\star, ..., u_{N-1|k}^\star\}$. According to the Receding Horizon principle, the MPC control law is obtained applying only the first element of the optimal input sequence, i.e.

$$u_k = \mu^{\mathrm{MPC}}(\hat{x}_k, \hat{e}_{\mathrm{o},k}) = u_{0|k}^\star. \tag{6.17}$$

6.3.3 Recursive feasibility and stability analysis

In this section we analyze the recursive feasibility and stability of the proposed control schema. First, note that in order to have a solution of the FHOCP, it is necessary that $\alpha > 0$. To guarantee this condition we introduce the following assumption on the set-point.

Assumption 6.1. *The set-point $\bar{y}$ is such that*

$$L\bar{y} < h - \tilde{e}_{\mathrm{o}} a_N - b_N - w_L.$$

Let's define the state of the closed-loop system, shifted with respect to the nominal equilibrium, as $\psi = [(x - \bar{x})^\top \ (\hat{x} - \bar{x})^\top \ (\hat{e}_{\mathrm{o}} - \bar{e}_\infty)]^\top$ and the feasible set of states

$$\begin{aligned}\mathcal{X}^{\mathrm{MPC}} := \{&\psi : x, \hat{x} \in \mathcal{X}, \hat{e}_{\mathrm{o}} \text{ is such that } V_{\mathrm{o}}(x - \hat{x}) \leq \hat{e}_{\mathrm{o}} \\ &\text{and } \exists \text{ a solution of the FHOCP}\}.\end{aligned} \tag{6.18}$$

Then, it is possible to state the following theorem concerning the properties of the closed-loop system.

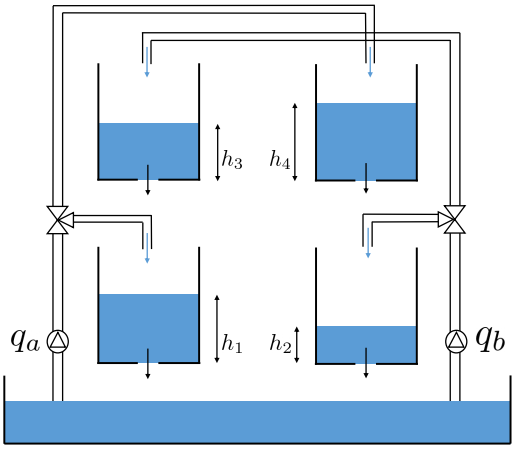

Figure 6.2: Schematic layout of the four-tanks plant.

Theorem 6.2. *If the plant behaves according to* (6.5)*, the GRU model respects the δISS condition* (4.6)*, the observer gains are selected to satisfy condition* (6.7)*, Assumption 6.1 is satisfied and the following inequality holds*

$$\rho_{\mathrm{s}}^{N}\left(L_{max}\hat{e}_{\mathrm{o},k}+\bar{w}\right)\leq\alpha(1-\rho_{\mathrm{s}}) \tag{6.19}$$

for all $k\geq 0$, then the FHOCP is recursively feasible, the constraints (6.1) *and* (6.2) *are satisfied $\forall\psi\in\mathcal{X}^{\mathrm{MPC}}$ and the closed loop system is ISS with respect to the input w_{y}, for $\psi\in\mathcal{X}^{\mathrm{MPC}}$ and $w_{\mathrm{y}}\in\mathcal{W}_{\mathrm{y}}$.*

Proof. The proof is reported in Section 6.6.3.

Remark 6.2. *The satisfaction of inequality* (6.19) *depends on the values of N, L_{max} and $\bar{w}$. The value of L_{max} is related to the observer gains L_{z} and L_{r}, that can be selected as small as needed, as noted in Remark 6.1. The term N can be enlarged to satisfy the condition for recursive feasibility. However, with large values of N, the requirement of Assumption 6.1 may become more conservative, and the computation effort needed to solve the optimization increases. Lastly, $\bar{w}$ is related to the maximum of the perturbation term w_{y}, that represents the modeling error. Hence, recursive feasibility can be obtained for any value of the prediction horizon N when the modeling error w_{y} is small enough, by using a proper tuning of the observer gains.*

6.4 Illustrative example

6.4.1 Four-tanks process

As numerical example to test the proposed control algorithm we consider the four tank benchmark described in [4]. The schematic layout of the plant

Symbol	Value	Unit	Description
a_1	1.31e-4	m^2	Discharge constant of tank 1
a_2	1.51e-4	m^2	Discharge constant of tank 2
a_3	9.27e-5	m^2	Discharge constant of tank 3
a_4	8.82e-5	m^2	Discharge constant of tank 4
S	0.06	m^2	Cross-section of the tanks
γ_a	0.3	-	Parameter of the 3-way valve
γ_b	0.4	-	Parameter of the 3-way valve
$q_{a_{max}}$	3.26	m^3/h	Maximum flow of q_a
$q_{b_{max}}$	4	m^3/h	Maximum flow of q_b
q_{min}	0	m^3/h	Minimum flow of q_a and q_b
$\bar{q}_a$	1.63	m^3/h	Equilibrium of q_a
$\bar{q}_b$	2	m^3/h	Equilibrium of q_b
h_1^0	0.65	m	Nominal level of tank 1
h_2^0	0.66	m	Nominal level of tank 2
h_3^0	0.65	m	Nominal level of tank 3
h_4^0	0.66	m	Nominal level of tank 4
q_a^0	1.63	m^3/h	Nominal flow of q_a
q_b^0	2.00	m^3/h	Nominal flow of q_b

Table 6.1: Numerical values of the parameters of the four tanks system.

is reported in Figure 6.2. The system is characterized by the following differential equations:

$$\begin{aligned}
\dot{h}_1 &= -\frac{a_1}{S}\sqrt{2gh_1} + \frac{a_3}{S}\sqrt{2gh_3} + \frac{\gamma_a}{S}q_a \\
\dot{h}_2 &= -\frac{a_2}{S}\sqrt{2gh_2} + \frac{a_4}{S}\sqrt{2gh_4} + \frac{\gamma_b}{S}q_b \\
\dot{h}_3 &= -\frac{a_3}{S}\sqrt{2gh_3} + \frac{1-\gamma_b}{S}q_b \\
\dot{h}_4 &= -\frac{a_4}{S}\sqrt{2gh_4} + \frac{1-\gamma_a}{S}q_a
\end{aligned} \tag{6.20}$$

where the states h_1, h_2, h_3, h_4 are the water level in the four different tanks, while the inputs are q_a and q_b and represent the inlet flows in the two valves. The numerical values of the system parameters and their descriptions can be found in Table 6.1.

6.4.2 Simulation results

The objective of the developed control algorithm is to control the water level in the two bottom tanks, h_1 and h_2, while respecting the following constraints:

$$q_a \in [0.0, 9.05] \times 10^{-4} m^3/s, \qquad h_1 \in [0.0, 2.0] m,$$
$$q_b \in [0.0, 11.1] \times 10^{-4} m^3/s, \qquad h_2 \in [0.0, 2.0] m.$$

To obtain the dataset for the training of the GRU network, a simulator of the plant is forced with a multilevel pseudo-random signal, and the output response is sampled with a sampling time $T_\mathrm{s} = 25s$. In particular, q_a and q_b in the dataset are two piecewise constant signals, with random values within the saturation constraints and a random changing step time. A sequence of input-output data of 20000 time steps is collected, and it is split in 15000 time steps for training, 2500 for validation and 2500 for testing. Then, the training data is divided into shortest subsequences of length 500 time steps each, and the training is performed using a batch size of 5. To enforce the δISS property in the final network, we use the procedure detailed in Section 4.2.2. The training is performed in Python, using TensorFlow library. The final network has $n = 20$ neurons, respects the δISS condition (4.6), and has a FIT on the test dataset of 92.7% for h_1 and of 89.7% for h_2. For the simulation, the observer gains L_r and L_z are selected to minimize ν_o, that is equivalent to minimize $\|U_\mathrm{r} - L_\mathrm{r} U_\mathrm{o}\|_\infty$ and $\|U_\mathrm{z} - L_\mathrm{z} U_\mathrm{o}\|_\infty$. The resulting gains are such that $\|L_\mathrm{r}\|_\infty = 0.002$ and $\|L_\mathrm{z}\|_\infty = 0.003$. The cost matrices for the MPC are set to $Q = \mathbf{I}_n$ and $R = 0.01\mathbf{I}_m$, and we select a prediction horizon of $N = 15$. $\bar{w}_\mathrm{y}$ is estimated as the maximum absolute value of the prediction error on the test dataset in the normalized variables, obtaining $\bar{w}_\mathrm{y} = 0.12$. To try to keep as low as possible the initial observer estimation error, the initial output of the plant is measured and $\hat{x}_0$ is set to the equilibrium point of the GRU network corresponding to that output. The initial value of $\hat{e}_\mathrm{o}$ is assumed to be 0.02, and it monotonically decreases to $\bar{e}_\infty \approx 0.01$. The simulation is performed by applying step-wise variations of the reference $\bar{y}$, where all the values of the reference respect Assumption 6.1. When $\bar{y}$ changes, the value of α that defines the terminal set is updated. The simulation parameters are such that condition (6.19) is satisfied for all $k \geq 0$. The closed-loop simulation is performed in Matlab, and the FHOCP is solved with *fmincon* function of Matlab optimization toolbox. The resulting closed-loop trajectories are reported in Figure 6.3, showing that the controller is able to manage the plant in a robust satisfactory way in spite of uncertainties due to modeling errors. Only a small static gain mismatch is present.

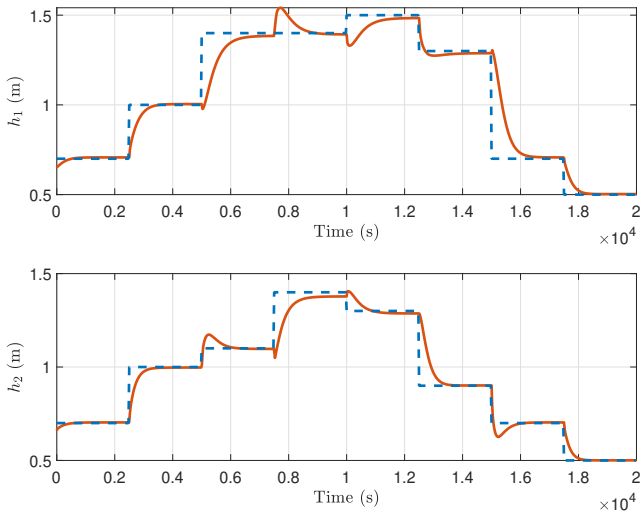

Figure 6.3: Closed loop performances: output (solid red line) and references (dashed blue line).

6.5 Conclusions

This chapter develops and analyses a robust MPC algorithm with input and output constraints, based on the use of a GRU model. Robustness and recursive feasibility are achieved using a constraint tightening approach, based on Lyapunov functions for the model and for the observer estimation error. The MPC formulation includes terminal ingredients that allow to guarantee ISS of the closed-loop system with respect to the perturbation terms without having requirements on the length of the prediction horizon, allowing to maintain the computational effort tractable.

As also verified in the simulations, this control algorithm only guarantees ISS of the closed-loop, and a static error may be present at steady state. To solve this issue, in the next chapter we propose a robust MPC algorithm that also includes offset-free tracking capabilities.

6.6 Proofs

For sake of readability, in some of the proofs the time index k is omitted, and the quantities at the subsequent time step are denoted by the superscript $^+$.

The following property is used in the proofs.

Lemma 6.3. *Given two vectors* $x, y \in \mathbb{R}^n$

$$\|x + y\|_\infty^2 \leq \|x\|_\infty^2 + \|y\|_\infty^2 + 2\,\|x \otimes y\|_\infty \tag{6.21}$$

Proof.

$$\begin{aligned}
\|x+y\|_\infty^2 &= \left(\max_i |x_{(i)}+y_{(i)}|\right)^2 = \max_i (x_{(i)}+y_{(i)})^2 \\
&= \max_i (x_{(i)}^2 + y_{(i)}^2 + 2x_{(i)}y_{(i)}) \\
&= \max_i |x_{(i)}^2 + y_{(i)}^2 + 2x_{(i)}y_{(i)}| \\
&\leq \max_i |x_{(i)}^2| + \max_i |y_{(i)}^2| + 2\max_i |x_{(i)}y_{(i)}| \\
&= \|x\|_\infty^2 + \|y\|_\infty^2 + 2\|x \otimes y\|_\infty
\end{aligned}$$

□

6.6.1 Proof of Lemma 6.1

Preliminarily, note that if $x \in \mathcal{X}$ and $u \in \mathcal{U}$, then $\bar{\sigma}_\mathrm{z}$, $\bar{\sigma}_\mathrm{r}$ and $\bar{\phi}_\mathrm{h}$ are bounds for z, r and h, as shown in [28]. In particular we have that

$$|z_{(j)}| \leq \|z\|_\infty \leq \bar{\sigma}_\mathrm{z}, \tag{6.22a}$$
$$|r_{(j)}| \leq \|r\|_\infty \leq \bar{\sigma}_\mathrm{r}, \tag{6.22b}$$
$$|h_{(j)}| \leq \|h\|_\infty \leq \bar{\phi}_\mathrm{h}. \tag{6.22c}$$

Moreover, in view of the symmetry of the sigmoid activation function $\sigma(\cdot)$, we have that for $j = 1, ..., n$

$$0 < 1 - \bar{\sigma}_\mathrm{z} \leq z_{(j)} \leq \bar{\sigma}_\mathrm{z} < 1, \tag{6.23a}$$
$$0 < 1 - \bar{\sigma}_\mathrm{z} \leq 1 - z_{(j)} \leq \bar{\sigma}_\mathrm{z} < 1. \tag{6.23b}$$

Condition (6.4a). Let's start by denoting $z^\mathrm{a} = z(x^\mathrm{a}, u)$, $r^\mathrm{a} = r(x^\mathrm{a}, u)$, $h^\mathrm{a} = h(x^\mathrm{a}, u)$, and let's adopt the same notation for $z^\mathrm{b}, r^\mathrm{b}, h^\mathrm{b}$. Moreover, let $\Delta x = x^\mathrm{a} - x^\mathrm{b}$. Let's now consider the time evolution of the j-th component of Δx:

$$\begin{aligned}
\Delta x_{(j)}^+ &= z_{(j)}^\mathrm{a} x_{(j)}^\mathrm{a} + (1 - z_{(j)}^\mathrm{a}) h_{(j)}^\mathrm{a} - z_{(j)}^\mathrm{b} x_{(j)}^\mathrm{b} - (1 - z_{(j)}^\mathrm{b}) h_{(j)}^\mathrm{b} \\
&= z_{(j)}^\mathrm{a}(x_{(j)}^\mathrm{a} - x_{(j)}^\mathrm{b}) + (z_{(j)}^\mathrm{a} - z_{(j)}^\mathrm{b}) x_{(j)}^\mathrm{b} \\
&\quad + (1 - z_{(j)}^\mathrm{a})(h_{(j)}^\mathrm{a} - h_{(j)}^\mathrm{b}) + (z_{(j)}^\mathrm{b} - z_{(j)}^\mathrm{a}) h_{(j)}^\mathrm{b}.
\end{aligned}$$

It is possible to take the absolute value of both sides, and to study the different terms separately. Firstly note that we have that $|x_{(j)}^\mathrm{b}| \leq \|x^\mathrm{b}\|_\infty \leq 1$ in $\mathcal{X}$, and that the bounds (6.22) hold.

Exploiting the lipschitzianity of $\sigma(\cdot)$ we can derive that

$$|z_{(j)}^\mathrm{a} - z_{(j)}^\mathrm{b}| \leq \left\| z^\mathrm{a} - z^\mathrm{b} \right\|_\infty \leq \frac{1}{4} \|U_\mathrm{z}\|_\infty \|\Delta x\|_\infty .$$

In a similar way, we have that

$$|r^{\mathrm{a}}_{(j)} - r^{\mathrm{b}}_{(j)}| \leq \left\| r^{\mathrm{a}} - r^{\mathrm{b}} \right\|_\infty \leq \frac{1}{4} \|U_{\mathrm{r}}\|_\infty \|\Delta x\|_\infty .$$

Finally, exploiting the lipschitzianity of $\tanh(\cdot)$, we have that

$$\begin{aligned}
|h^{\mathrm{a}}_{(j)} - h^{\mathrm{b}}_{(j)}| &\leq \left\| h^{\mathrm{a}} - h^{\mathrm{b}} \right\|_\infty \\
&\leq \|U_{\mathrm{h}}\|_\infty \left\| r^{\mathrm{a}} \otimes x^{\mathrm{a}} - r^{\mathrm{b}} \otimes x^{\mathrm{b}} \right\|_\infty \\
&= \|U_{\mathrm{h}}\|_\infty \left\| r^{\mathrm{a}} \otimes (x^{\mathrm{a}} - x^{\mathrm{b}}) + (r^{\mathrm{a}} - r^{\mathrm{b}}) \otimes x^{\mathrm{b}} \right\|_\infty \\
&\leq \|U_{\mathrm{h}}\|_\infty \left(\bar{\sigma}_{\mathrm{r}} \left\| x^{\mathrm{a}} - x^{\mathrm{b}} \right\|_\infty + \left\| r^{\mathrm{a}} - r^{\mathrm{b}} \right\|_\infty \right) \\
&\leq \|U_{\mathrm{h}}\|_\infty \left(\frac{1}{4} \|U_{\mathrm{r}}\|_\infty + \bar{\sigma}_{\mathrm{r}} \right) \left\| x^{\mathrm{a}} - x^{\mathrm{b}} \right\|_\infty .
\end{aligned}$$

Combining the previous inequalities we have that for all $j = 1, ..., n$

$$|\Delta x^+_{(j)}| \leq \kappa_{\mathrm{x},j} \|\Delta x\|_\infty$$

where

$$\kappa_{\mathrm{x},j} := z^{\mathrm{a}}_{(j)} + \frac{1}{4}(1 + \bar{\phi}_{\mathrm{h}}) \|U_{\mathrm{z}}\|_\infty + (1 - z^{\mathrm{a}}_{(j)}) \|U_{\mathrm{h}}\|_\infty \left(\frac{1}{4} \|U_{\mathrm{r}}\|_\infty + \bar{\sigma}_{\mathrm{r}} \right).$$

In view of the definition of infinity norm, to prove (6.4a), i.e. $\|\Delta x^+\|_\infty \leq \rho_s \|\Delta x\|_\infty$, it is sufficient to show that $\kappa_{\mathrm{x},j} \leq \rho_s$ for all j. In this regard we have that

$$\frac{\kappa_{\mathrm{x},j} - z^{\mathrm{a}}_{(j)}}{1 - z^{\mathrm{a}}_{(j)}} = \frac{1}{4} \frac{1 + \bar{\phi}_{\mathrm{h}}}{1 - z^{\mathrm{a}}_{(j)}} \|U_{\mathrm{z}}\|_\infty + \|U_{\mathrm{h}}\|_\infty \left(\frac{1}{4} \|U_{\mathrm{r}}\|_\infty + \bar{\sigma}_{\mathrm{r}} \right) \overset{(6.23\mathrm{b})}{\leq} \nu.$$

Then for all $j = 1, ..., n$

$$\begin{aligned}
\kappa_{\mathrm{x},j} &\leq \nu(1 - z^{\mathrm{a}}_{(j)}) + z^{\mathrm{a}}_{(j)} = z^{\mathrm{a}}_{(j)}(1 - \nu) + \nu \\
&\overset{(6.23\mathrm{a})}{\leq} \bar{\sigma}_{\mathrm{z}}(1 - \nu) + \nu = \nu(1 - \bar{\sigma}_{\mathrm{z}}) + \bar{\sigma}_{\mathrm{z}} = \rho_s.
\end{aligned}$$

This concludes the proof of (6.4a).

Condition (6.4b). Consider the j-th row of $LU_{\mathrm{o}}(x^{\mathrm{a}} - x^{\mathrm{b}})$ for $j = 1, ..., q$:

$$\begin{aligned}
&(LU_{\mathrm{o}})_{(j*)}(x^{\mathrm{a}} - x^{\mathrm{b}}) \leq \|(LU_{\mathrm{o}})_{(j*)}(x^{\mathrm{a}} - x^{\mathrm{b}})\|_\infty \\
&\leq \|(LU_{\mathrm{o}})_{(j*)}\|_\infty \|x^{\mathrm{a}} - x^{\mathrm{b}}\|_\infty = \|(LU_{\mathrm{o}})_{(j*)}\|_\infty V_{\mathrm{s}}(x^{\mathrm{a}}, x^{\mathrm{b}}).
\end{aligned}$$

□

6.6.2 Proof of Lemma 6.2

Condition (6.8a). Let's study the time evolution of the j-th component of the observer estimation error, for all $j = 1, ..., n$:

$$\begin{aligned} x^+_{(j)} - \hat{x}^+_{(j)} &= z_{(j)}x_{(j)} + (1 - z_{(j)})h_{(j)} - \hat{z}_{(j)}\hat{x}_{(j)} - (1 - \hat{z}_{(j)})\hat{h}_{(j)} \\ &= z_{(j)}(x_{(j)} - \hat{x}_{(j)}) + (z_{(j)} - \hat{z}_{(j)})\hat{x}_{(j)} \\ &\quad + (1 - z_{(j)})(h_{(j)} - \hat{h}_{(j)}) + (\hat{z}_{(j)} - z_{(j)})\hat{h}_{(j)}. \end{aligned}$$

We can now take the absolute value of both sides, and study the different terms separately. First, we note that $\mathcal{X}$ is a positive invariant set for $\hat{x}$, since $\hat{x}^+_{(j)}$ is computed as the convex combination of $\hat{x}_{(j)}$ and $\hat{h}_{(j)} \in (-1, 1)$. Then $|\hat{x}_{(j)}| \leq \|\hat{x}\|_\infty \leq 1$ and $|\hat{h}_{(j)}| \leq \|\hat{h}\|_\infty \leq \bar{\phi}_{\mathrm{h}}$.

Exploiting the lipschitzianity of $\sigma(\cdot)$ we can derive that

$$\begin{aligned} |z_{(j)} - \hat{z}_{(j)}| \leq \|z - \hat{z}\|_\infty &\leq \frac{1}{4}\|U_{\mathrm{z}}(x - \hat{x}) - L_{\mathrm{z}}(y - \hat{y})\|_\infty \\ &\leq \frac{1}{4}\|U_{\mathrm{z}} - L_{\mathrm{z}}U_{\mathrm{o}}\|_\infty \|x - \hat{x}\|_\infty + \frac{1}{4}\|L_{\mathrm{z}}\|_\infty \|w_{\mathrm{y}}\|_\infty . \end{aligned}$$

In the same way, we have that

$$\begin{aligned} |r_{(j)} - \hat{r}_{(j)}| &\leq \|r - \hat{r}\|_\infty \\ &\leq \frac{1}{4}\|U_{\mathrm{r}} - L_{\mathrm{r}}U_{\mathrm{o}}\|_\infty \|x - \hat{x}\|_\infty + \frac{1}{4}\|L_{\mathrm{r}}\|_\infty \|w_{\mathrm{y}}\|_\infty . \end{aligned}$$

Finally, exploiting the lipschitzianity of $\tanh(\cdot)$, we have that

$$\begin{aligned} |h_{(j)} - \hat{h}_{(j)}| \leq \left\|h - \hat{h}\right\|_\infty &\leq \|U_{\mathrm{h}}\|_\infty \|r \otimes x - \hat{r} \otimes \hat{x}\|_\infty \\ &= \|U_{\mathrm{h}}\|_\infty \|r \otimes (x - \hat{x}) + (r - \hat{r}) \otimes \hat{x}\|_\infty \\ &\leq \|U_{\mathrm{h}}\|_\infty (\bar{\sigma}_{\mathrm{r}} \|x - \hat{x}\|_\infty + \|r - \hat{r}\|_\infty) \\ &\leq \|U_{\mathrm{h}}\|_\infty \left(\frac{1}{4}\|U_{\mathrm{r}} - L_{\mathrm{r}}U_{\mathrm{o}}\|_\infty + \bar{\sigma}_{\mathrm{r}}\right) \|x - \hat{x}\|_\infty \\ &\quad + \frac{1}{4}\|U_{\mathrm{h}}\|_\infty \|L_{\mathrm{r}}\|_\infty \|w_{\mathrm{y}}\|_\infty . \end{aligned}$$

Combining the previous computations we have that for all $j = 1, ..., n$

$$|x^+_{(j)} - \hat{x}^+_{(j)}| \leq \kappa_{\mathrm{o},j} \|x - \hat{x}\|_\infty + \kappa_{\mathrm{w},j}\|w_{\mathrm{y}}\|_\infty$$

where

$$\begin{aligned} \kappa_{\mathrm{o},j} := z_{(j)} &+ \frac{1}{4}(1 + \bar{\phi}_{\mathrm{h}}) \|U_{\mathrm{z}} - L_{\mathrm{z}}U_{\mathrm{o}}\|_\infty \\ &+ (1 - z_{(j)}) \|U_{\mathrm{h}}\|_\infty \left(\frac{1}{4}\|U_{\mathrm{r}} - L_{\mathrm{r}}U_{\mathrm{o}}\|_\infty + \bar{\sigma}_{\mathrm{r}}\right), \end{aligned}$$

$$\kappa_{\mathrm{w},j} := \frac{1}{4}(1+\phi_{\mathrm{h}})\|L_{\mathrm{z}}\|_\infty + (1-z_{(j)})\frac{1}{4}\|U_{\mathrm{h}}\|_\infty\|L_{\mathrm{r}}\|_\infty.$$

It is now sufficient to show that $\kappa_{\mathrm{o},j} \leq \rho_{\mathrm{o}}$ for all j and $\kappa_{\mathrm{w},j} \leq \kappa$ for all j to prove condition (6.8a). The inequality for $\kappa_{\mathrm{w},j}$ follows immediately considering that $1 - z_{(j)} \leq \bar{\sigma}_{\mathrm{z}}$, as already noted in (6.23b). Considering $\kappa_{\mathrm{o},j}$, we have that

$$\begin{aligned}\frac{\kappa_{\mathrm{o},j} - z_{(j)}}{1 - z_{(j)}} &= \|U_{\mathrm{h}}\|_\infty \left(\frac{1}{4}\|U_{\mathrm{r}} - L_{\mathrm{r}}U_{\mathrm{o}}\|_\infty + \bar{\sigma}_{\mathrm{r}}\right) + \frac{1}{4}\frac{1+\bar{\phi}_{\mathrm{h}}}{1-z_{(j)}}\|U_{\mathrm{z}} - L_{\mathrm{z}}U_{\mathrm{o}}\|_\infty \\ &\overset{(6.23b)}{\leq} \nu_{\mathrm{o}}.\end{aligned}$$

Then

$$\begin{aligned}\kappa_{\mathrm{o},j} &\leq \nu_{\mathrm{o}}(1 - z_{(j)}) + z_{(j)} = z_{(j)}(1-\nu_{\mathrm{o}}) + \nu_{\mathrm{o}} \\ &\overset{(6.23a)}{\leq} \bar{\sigma}_{\mathrm{z}}(1-\nu_{\mathrm{o}}) + \nu_{\mathrm{o}} = \nu_{\mathrm{o}}(1-\bar{\sigma}_{\mathrm{z}}) + \bar{\sigma}_{\mathrm{z}} = \rho_{\mathrm{o}}.\end{aligned}$$

Condition (6.8b). The proof is similar to the proof of condition (6.4b) in Lemma 6.1.

Condition (6.8c). Let's study $\hat{x}^+ - f(\hat{x}, u)$

$$\begin{aligned}\hat{x}^+ - f(\hat{x},u) &= \hat{z}(\hat{x},u,y)\otimes\hat{x} + (1-\hat{z}(\hat{x},u,y))\otimes\hat{h}(\hat{x},u,y) \\ &\quad - z(\hat{x},u)\otimes\hat{x} - (1-z(\hat{x},u))\otimes h(\hat{x},u) \\ &= (\hat{z}(\hat{x},u,y) - z(\hat{x},u))\otimes\hat{x} \\ &\quad + (1-z(\hat{x},u))\otimes(\hat{h}(\hat{x},u,y) - h(\hat{x},u)) \\ &\quad + (z(\hat{x},u) - \hat{z}(\hat{x},u,y))\otimes\hat{h}(\hat{x},u,y) \\ &= (\hat{z}(\hat{x},u,y) - z(\hat{x},u))\otimes(\hat{x} - \hat{h}(\hat{x},u,y)) \\ &\quad + (1-z(\hat{x},u))\otimes(\hat{h}(\hat{x},u,y) - h(\hat{x},u)).\end{aligned}$$

Let's now take the infinity norm of both sides of this expression, and consider separately the different terms of this sum. In view of lipschitzianity of $\sigma(\cdot)$ and of the fact that $\left\|\hat{h}(\hat{x},u,y)\right\|_\infty \leq \bar{\phi}_{\mathrm{h}}$, we have that

$$\begin{aligned}&\left\|(\hat{z}(\hat{x},u,y) - z(\hat{x},u))\otimes(\hat{x} - \hat{h}(\hat{x},u,y))\right\|_\infty \\ &\leq \frac{1}{4}\|L_{\mathrm{z}}(y-\hat{y})\|_\infty \left\|\hat{x} - \hat{h}(\hat{x},u,y)\right\|_\infty \\ &\leq \frac{1}{4}(1+\bar{\phi}_{\mathrm{h}})\left(\|L_{\mathrm{z}}U_{\mathrm{o}}\|_\infty\|x-\hat{x}\|_\infty + \|L_{\mathrm{z}}\|_\infty\|w_{\mathrm{y}}\|_\infty\right).\end{aligned}$$

Note now that

$$\begin{aligned}\|\hat{r}(\hat{x},u,y) - r(\hat{x},u)\|_\infty &\leq \frac{1}{4}\|L_{\mathrm{r}}(y-\hat{y})\|_\infty \\ &\leq \frac{1}{4}\|L_{\mathrm{r}}U_{\mathrm{o}}\|_\infty\|x-\hat{x}\|_\infty + \frac{1}{4}\|L_{\mathrm{r}}\|_\infty\|w_{\mathrm{y}}\|_\infty.\end{aligned}$$

Then, in view of lipschitzianity of $\tanh(\cdot)$ and of (6.23b)

$$\begin{aligned}&\left\|(1-z(\hat{x},u))\otimes(\hat{h}(\hat{x},u,y)-h(\hat{x},u))\right\|_\infty\\&\leq\|(1-z(\hat{x},u))\|_\infty\|U_{\mathrm{h}}(\hat{x}\otimes\hat{r}(\hat{x},u,y)-\hat{x}\otimes r(\hat{x},u))\|\\&\leq\frac{1}{4}\bar{\sigma}_{\mathrm{z}}\|U_{\mathrm{h}}\|_\infty\left(\|L_{\mathrm{r}}U_{\mathrm{o}}\|_\infty\|x-\hat{x}\|_\infty+\|L_{\mathrm{r}}\|_\infty\|w_{\mathrm{y}}\|_\infty\right)\end{aligned}$$

Combining the previous computation we obtain that

$$\left\|\hat{x}^+-f(\hat{x},u)\right\|_\infty\leq L_{max}\|x-\hat{x}\|_\infty+\kappa\|w_{\mathrm{y}}\|_\infty,$$

so that (6.8c) is proven. □

6.6.3 Proof of Theorem 6.2

Proof of the satisfaction of constraints (6.1) *and* (6.2) *for* $\psi\in\mathcal{X}^{\mathrm{MPC}}$. Satisfaction of (6.1) is obtained thanks to the constraint (6.12e) in the FHOCP. To prove satisfaction of (6.2), first note that for $j=1,...,q$

$$w_{L(j)}=\max_{w_{\mathrm{y}}\in\mathcal{W}_{\mathrm{y}}}L_{(j*)}w_{\mathrm{y}}. \tag{6.24}$$

Then

$$\begin{aligned}Ly_k&\overset{(6.5b)}{=}L(U_{\mathrm{o}}x_k+b_{\mathrm{o}}+w_{\mathrm{y},k})\overset{(6.8b)}{\leq}L(U_{\mathrm{o}}\hat{x}_k+b_{\mathrm{o}}+w_{\mathrm{y},k})+c_{\mathrm{o}}V_{\mathrm{o}}(x_k-\hat{x}_k)\\&\overset{(6.12b)(6.18)}{\leq}L(U_{\mathrm{o}}x_{0|k}+b_{\mathrm{o}})+Lw_{\mathrm{y},k}+c_{\mathrm{o}}\hat{e}_{\mathrm{o},k}\\&\overset{(6.24)}{\leq}L(U_{\mathrm{o}}x_{0|k}+b_{\mathrm{o}})+w_L+c_{\mathrm{o}}\hat{e}_{\mathrm{o},k}\overset{(6.9a)(6.12d)}{\leq}h-a_0\hat{e}_{\mathrm{o},k}+a_0\hat{e}_{\mathrm{o},k}=h.\end{aligned}$$

Definition and study of the candidate solution. We define now a candidate solution for the FHOCP that will be exploited both in the proof of recursive feasibility and in the proof of stability. Firstly, given the optimal solution $\mathbf{u}_k^\star$ of the optimization problem at time step k, let's denote with $\mathbf{x}_k^\star=\{x_{0|k}^\star,...,x_{N-1|k}^\star\}$ the associate state trajectory defined by $x_{i+1|k}^\star:=f(x_{i|k}^\star,u_{i|k}^\star)$ with $x_{0|k}^\star:=\hat{x}_k$. Let's also define $x_{N+1|k}^\star:=f(x_{N|k}^\star,\bar{u})$. Then, let's define $\tilde{\mathbf{u}}_{k+1}=\{\tilde{u}_{i|k+1}\}_{i=0}^{N-1}$ the candidate solution at time step $k+1$, where $\tilde{u}_{i|k+1}:=u_{i+1|k}^\star$ for $i=0,...,N-2$ and $\tilde{u}_{N-1|k+1}:=\bar{u}$. Consider also the associate trajectory $\tilde{\mathbf{x}}_{k+1}=\{\tilde{x}_{0|k+1},...,\tilde{x}_{N|k+1}\}$ defined by $\tilde{x}_{i+1|k+1}:=f(\tilde{x}_{i|k+1},\tilde{u}_{i|k+1})$ with $\tilde{x}_{0|k+1}:=\hat{x}_{k+1}$.

Note that, in view of the presence of the term w_{y} and of the observer, $\hat{x}_{k+1}$ can be different from $x_{1|k}^\star$, and this difference propagates along the prediction horizon so that $\tilde{x}_{i-1|k+1}\neq x_{i|k}^\star$. In the following, we derive bounds on the difference between the optimal state trajectory at time step k and the candidate solution at time step $k+1$. In this regard, let's define for $i=1,...,N+1$

$$\varepsilon_{k+i}:=\tilde{x}_{i-1|k+1}-x_{i|k}^\star.$$

For $i = 1$ we have that $\varepsilon_{k+1} = \tilde{x}_{0|k+1} - x^\star_{1|k} = \hat{x}_{k+1} - f(\hat{x}_k, u^\star_{0|k})$. In view of (6.8c)

$$\begin{aligned}\|\varepsilon_{k+1}\|_\infty &\overset{(6.8c)}{\leq} L_{max}\|x_k - \hat{x}_k\|_\infty + \kappa\|w_{\mathrm{y},k}\|_\infty \\ &\overset{(6.18)(6.10)}{\leq} L_{max}\hat{e}_{\mathrm{o},k} + \bar{w}.\end{aligned}$$

Then, for $i = 2, ..., N+1$, in view of (6.4a), we have that

$$\begin{aligned}\|\varepsilon_{k+i}\|_\infty &\leq \rho_{\mathrm{s}}^{i-1}\|\varepsilon_{k+1}\|_\infty \\ &\leq \rho_{\mathrm{s}}^{i-1}L_{max}\|x_k - \hat{x}_k\|_\infty + \rho_{\mathrm{s}}^{i-1}\kappa\|w_{\mathrm{y},k}\|_\infty \\ &\leq \rho_{\mathrm{s}}^{i-1}(L_{max}\hat{e}_{\mathrm{o},k} + \bar{w}).\end{aligned} \tag{6.25}$$

Proof of recursive feasibility. We first verify that the terminal set is designed so that $x \in \mathcal{X}_f \implies L(U_{\mathrm{o}}x + b_{\mathrm{o}}) + w_L \leq h - a_N\hat{e}_{\mathrm{o}} - b_N$. We first note that

$$U_{\mathrm{o}}x + b_{\mathrm{o}} = U_{\mathrm{o}}(x - \bar{x}) + U_{\mathrm{o}}\bar{x} + b_{\mathrm{o}} = U_{\mathrm{o}}(x - \bar{x}) + \bar{y}.$$

Consider now the j-th row of $L(U_{\mathrm{o}}x + b_{\mathrm{o}}) + w_L$, for $j = 1, ..., q$ and for $x \in \mathcal{X}_{\mathrm{f}}$:

$$\begin{aligned}(L(U_{\mathrm{o}}x + b_{\mathrm{o}}) + w_L)_{(j)} &= (L(U_{\mathrm{o}}(x - \bar{x}) + \bar{y}) + w_L)_{(j)} \\ &= (LU_{\mathrm{o}})_{(j*)}(x - \bar{x}) + \bar{y}) + L_{(j*)}\bar{y} + w_{L(j)} \\ &\leq \left\|(LU_{\mathrm{o}})_{(j*)}(x - \bar{x})\right\|_\infty + L_{(j*)}\bar{y} + w_{L(j)} \\ &\leq \left\|(LU_{\mathrm{o}})_{(j*)}\right\|_\infty\|x - \bar{x}\|_\infty + L_{(j*)}\bar{y} + w_{L(j)} \\ &\overset{(6.15)}{\leq} \left\|(LU_{\mathrm{o}})_{(j*)}\right\|_\infty\alpha + L_{(j*)}\bar{y} + w_{L(j)} \\ &\overset{(6.16)}{\leq} h_{(j)} - \tilde{e}_{\mathrm{o}}a_{N(j)} - b_{N(j)} \\ &\leq h_{(j)} - \hat{e}_{\mathrm{o}}a_{N(j)} - b_{N(j)}\end{aligned}$$

i.e. $x \in \mathcal{X}_f \implies L(U_{\mathrm{o}}x + b_{\mathrm{o}}) \leq h - a_N\hat{e}_{\mathrm{o}} - b_N$.

Then, using the candidate sequence introduced in the previous part of the proof and in view of the fact that $x \in \mathcal{X}_f \implies L(U_{\mathrm{o}}x + b_{\mathrm{o}}) + w_L \leq h - a_N\hat{e}_{\mathrm{o},k} - b_N$, recursive feasibility with respect to (6.12d) can be proven as follows:

$$\begin{aligned}&L(U_{\mathrm{o}}\tilde{x}_{i|k+1} + b_{\mathrm{o}}) + w_L \\ &\overset{(6.4b)}{\leq} L(U_{\mathrm{o}}x^\star_{i+1|k} + b_{\mathrm{o}}) + w_L + c_{\mathrm{s}}V_{\mathrm{s}}(\tilde{x}_{i|k+1}, x^\star_{i+1|k}) \\ &\overset{(6.12d)}{\leq} h - a_{i+1}\hat{e}_{\mathrm{o},k} - b_{i+1} + c_{\mathrm{s}}\|\varepsilon_{k+i+1}\|_\infty \\ &\overset{(6.9)(6.25)}{\leq} h - \rho_{\mathrm{o}}a_i\hat{e}_{\mathrm{o},k} - \rho_{\mathrm{s}}^i L_{max}c_{\mathrm{s}}\hat{e}_{\mathrm{o},k} \\ &\quad - b_i - a_i\bar{w} - c_{\mathrm{s}}\rho_{\mathrm{s}}^i\bar{w} + c_{\mathrm{s}}\rho_{\mathrm{s}}^i(L_{max}\hat{e}_{\mathrm{o},k} + \bar{w}) \\ &\overset{(6.11)}{=} h - a_i\hat{e}_{\mathrm{o},k+1} - b_i.\end{aligned}$$

Finally, we can prove recursive feasibility with respect to the terminal constraint (6.12f), i.e. prove that $\left\|\tilde{x}_{N|k+1} - \bar{x}\right\|_\infty \leq \alpha$ given that $\|x^\star_{N|k} - \bar{x}\|_\infty \leq \alpha$:

$$\begin{aligned}\left\|\tilde{x}_{N|k+1} - \bar{x}\right\|_\infty &\leq \left\|\tilde{x}_{N|k+1} - x^\star_{N+1|k}\right\|_\infty + \left\|x^\star_{N+1|k} - \bar{x}\right\|_\infty \\ &\overset{(6.4a)}{\leq} \left\|\varepsilon_{k+N+1}\right\|_\infty + \rho_{\mathrm{s}} \left\|x^\star_{N|k} - \bar{x}\right\|_\infty \\ &\overset{(6.25)}{\leq} \rho_{\mathrm{s}}^N (L_{max}\hat{e}_{\mathrm{o},k} + \bar{w}) + \rho_{\mathrm{s}}\alpha \overset{(6.19)}{\leq} \alpha.\end{aligned}$$

Proof of stability. First, note that the evolution of the state $\hat{e}_{\mathrm{o}}$ does not depend on w_{y}, and that $\hat{e}_{\mathrm{o},k} \to \bar{e}_\infty$ for $k \to \infty$.

Then, instead of studying directly the evolution of the closed loop states $\begin{bmatrix} x - \bar{x} \\ \hat{x} - \bar{x} \end{bmatrix}$, it is possible to make a change of variables and study the equivalent system with state $\begin{bmatrix} x - \hat{x} \\ \hat{x} - \bar{x} \end{bmatrix}$. The advantage is that in Theorem 6.1 we have already derived the ISS property for the subsystem that describes the evolution of $x - \hat{x}$. Hence it is now sufficient to study the subsystem that describes the evolution of $\hat{x} - \bar{x}$, considering $x - \hat{x}$ as an additional input. To do so, we consider as candidate ISS-Lyapunov function the optimal cost of the MPC optimization, i.e.

$$V(\hat{x}_k - \bar{x}) = \sum_{i=0}^{N-1} \left(\|x^\star_{i|k} - \bar{x}\|_Q^2 + \|u^\star_{i|k} - \bar{u}\|_R^2 \right) + s \left\|x^\star_{N|k} - \bar{x}\right\|_\infty^2.$$

We start by proving that our candidate Lyapunov function respects (2.9a). We have that

$$V(\hat{x}_k - \bar{x}) \geq \|x^\star_{0|k} - \bar{x}\|_Q^2 \geq \lambda_{min}(Q)\|\hat{x}_k - \bar{x}\|_2^2.$$

Consider now the input sequence $\tilde{u}_{i|k} = \bar{u}$ for $i = 0, ..., N-1$, and the corresponding state trajectory $\tilde{x}_{i|k}$. This input sequence is feasible at least for $\hat{x}_k$ close to $\bar{x}$, i.e. for $\|\hat{x}_k - \bar{x}\|_2 \leq \delta$ for some $\delta > 0$. Hence, for $\hat{x}_k$ such that $\|\hat{x}_k - \bar{x}\|_2 \leq \delta$, we have that

$$V(\hat{x}_k - \bar{x}) \leq \sum_{i=0}^{N-1} \|\tilde{x}_{i|k} - \bar{x}\|_Q^2 + s \left\|\tilde{x}_{N|k} - \bar{x}\right\|_\infty^2.$$

In view of the δISS property of the GRU model there exist $\mu \geq 0$ and $\lambda \in (0, 1)$ such that

$$\|\tilde{x}_{i|k} - \bar{x}\|_2 \leq \mu\lambda^i \|\tilde{x}_{0|k} - \bar{x}\|_2 = \mu\lambda^i \|\hat{x}_k - \bar{x}\|_2.$$

Therefore there exist a constant $\tilde{b} > 0$ such that if $\|\hat{x}_k - \bar{x}\| \leq \delta$ then

$$V(\hat{x}_k - \bar{x}) \leq \tilde{b}\|\hat{x}_k - \bar{x}\|_2^2.$$

Consider now $\hat{x}_k$ such that $\|\hat{x}_k - \bar{x}\| > \delta$. Note that there exists $V_{max} > 0$ such that $V(\hat{x}_k - \bar{x}) \leq V_{max}$ in $\mathcal{X}^{\text{MPC}}$. Then

$$V(\hat{x}_k - \bar{x}) \leq \frac{V_{max}}{\delta^2} \|\hat{x}_k - \bar{x}\|_2^2.$$

Hence we have that

$$V(\hat{x}_k - \bar{x}) \leq b\|\hat{x}_k - \bar{x}\|_2^2$$

with $b = \max\{\tilde{b}, \frac{V_{max}}{\delta^2}\}$, so that (2.9a) is verified.

We consider now the variation of the Lyapunov function between subsequent time steps, to prove that (2.9b) is verified:

$$\begin{aligned}
&V(\hat{x}_{k+1} - \bar{x}) - V(\hat{x}_k - \bar{x}) \\
&= \sum_{i=0}^{N-1} \left(\|x^\star_{i|k+1} - \bar{x}\|_Q^2 + \|u^\star_{i|k+1} - \bar{u}\|_R^2 \right) + s \left\| x^\star_{N|k+1} - \bar{x} \right\|_\infty^2 \\
&- \left(\sum_{i=0}^{N-1} \left(\|x^\star_{i|k} - \bar{x}\|_Q^2 + \|u^\star_{i|k} - \bar{u}\|_R^2 \right) + s \left\| x^\star_{N|k} - \bar{x} \right\|_\infty^2 \right).
\end{aligned}$$

Considering the feasible solution $\tilde{u}_{i|k+1}$, we have that the corresponding cost is larger or equal than the optimal cost at timestep $k+1$. Then

$$\begin{aligned}
&V(\hat{x}_{k+1} - \bar{x}) - V(\hat{x}_k - \bar{x}) \\
&\leq \sum_{i=0}^{N-1} \left(\|\tilde{x}_{i|k+1} - \bar{x}\|_Q^2 + \|\tilde{u}_{i|k+1} - \bar{u}\|_R^2 \right) + s \left\| \tilde{x}_{N|k+1} - \bar{x} \right\|_\infty^2 \\
&\quad - \left(\sum_{i=0}^{N-1} \left(\|x^\star_{i|k} - \bar{x}\|_Q^2 + \|u^\star_{i|k} - \bar{u}\|_R^2 \right) + s \left\| x^\star_{N|k} - \bar{x} \right\|_\infty^2 \right) \\
&= -\|x^\star_{0|k} - \bar{x}\|_Q^2 - \|u^\star_{0|k} - \bar{u}\|_R^2 \\
&\quad + \sum_{i=1}^{N-1} \left(\|\tilde{x}_{i-1|k+1} - \bar{x}\|_Q^2 - \|x^\star_{i|k} - \bar{x}\|_Q^2 \right) \\
&\quad + \sum_{i=1}^{N-1} \left(\|\tilde{u}_{i-1|k+1} - \bar{u}\|_R^2 - \|u^\star_{i|k} - \bar{u}\|_R^2 \right) + \|\tilde{x}_{N-1|k+1} - \bar{x}\|_Q^2 \\
&\quad + \|\tilde{u}_{N-1|k+1} - \bar{u}\|_R^2 + s \left\| \tilde{x}_{N|k+1} - \bar{x} \right\|_\infty^2 - s \left\| x^\star_{N|k} - \bar{x} \right\|_\infty^2.
\end{aligned}$$

In this expression, all the terms related to the input cancels out in view of how the candidate input sequence was selected, except for $-\|u^\star_{0|k} - \bar{u}\|_R^2$.

Considering now the state terms between time steps $k+1$ and $k+N-1$,

we have that

$$\begin{aligned}
&\sum_{i=1}^{N-1} \left(\|\tilde{x}_{i-1|k+1} - \bar{x}\|_Q^2 - \|x^\star_{i|k} - \bar{x}\|_Q^2 \right) \\
&= \sum_{i=1}^{N-1} \left(\|\varepsilon_{k+i} + x^\star_{i|k} - \bar{x}\|_Q^2 - \|x^\star_{i|k} - \bar{x}\|_Q^2 \right) \\
&= \sum_{i=1}^{N-1} \left(\|\varepsilon_{k+i}\|_Q^2 + (x^\star_{i|k} - \bar{x})^\top Q \varepsilon_{k+i} \right).
\end{aligned}$$

Consider now the state terms at time steps $k+N$ and $k+N+1$, i.e.

$$\|\tilde{x}_{N-1|k+1} - \bar{x}\|_Q^2 - s \left\| x^\star_{N|k} - \bar{x} \right\|_\infty^2 + s \left\| \tilde{x}_{N|k+1} - \bar{x} \right\|_\infty^2.$$

We have that

$$\begin{aligned}
&\|\tilde{x}_{N-1|k+1} - \bar{x}_{k+1}\|_Q^2 = \|x^\star_{N|k} - \bar{x} + \varepsilon_{k+N}\|_Q^2 \\
&= \|x^\star_{N|k} - \bar{x}\|_Q^2 + \|\varepsilon_{k+N}\|_Q^2 + (x^\star_{N|k} - \bar{x})^\top Q \varepsilon_{k+N}.
\end{aligned}$$

Moreover, recalling that $\tilde{x}_{N|k+1} = f(\tilde{x}_{N-1|k+1}, \bar{u})$, in view of the δISS property of the GRU network, one has

$$\begin{aligned}
&s \left\| \tilde{x}_{N|k+1} - \bar{x} \right\|_\infty^2 \overset{(6.4a)}{\leq} s\rho_{\mathrm{s}}^2 \left\| \tilde{x}_{N-1|k+1} - \bar{x} \right\|_\infty^2 \\
&= s\rho_{\mathrm{s}}^2 \left\| x^\star_{N|k} - \bar{x} + \varepsilon_{k+N} \right\|_\infty^2 \\
&\overset{(6.21)}{\leq} s\rho_{\mathrm{s}}^2 \left\| x^\star_{N|k} - \bar{x} \right\|_\infty^2 + s\rho_{\mathrm{s}}^2 \left\| \varepsilon_{k+N} \right\|_\infty^2 + 2s\rho_{\mathrm{s}}^2 \left\| x^\star_{N|k} - \bar{x} \right\|_\infty \left\| \varepsilon_{k+N} \right\|_\infty.
\end{aligned}$$

Then the following inequality holds:

$$\begin{aligned}
&\|\tilde{x}_{N-1|k+1} - \bar{x}\|_Q^2 - s \left\| x^\star_{N|k} - \bar{x} \right\|_\infty^2 + s \left\| \tilde{x}_{N|k+1} - \bar{x} \right\|_\infty^2 \\
&\leq \left\| x^\star_{N|k} - \bar{x} \right\|_Q^2 + s\rho_{\mathrm{s}}^2 \left\| x^\star_{N|k} - \bar{x} \right\|_\infty^2 - s \left\| x^\star_{N|k} - \bar{x} \right\|_\infty^2 \\
&\quad + \|\varepsilon_{k+N}\|_Q^2 + (x^\star_{N|k} - \bar{x})^\top Q \varepsilon_{k+N} \\
&\quad + s\rho_{\mathrm{s}}^2 \left\| \varepsilon_{k+N} \right\|_\infty^2 + 2s\rho_{\mathrm{s}}^2 \left\| x^\star_{N|k} - \bar{x} \right\|_\infty \left\| \varepsilon_{k+N} \right\|_\infty.
\end{aligned}$$

Using the fact that for a vector $v \in \mathbb{R}^n$ it holds $\|v\|_Q^2 \leq \lambda_{max}(Q) \|v\|_2^2$ and that $\|v\|_\infty \leq \sqrt{n} \|v\|_2$, we have that

$$\begin{aligned}
&\left\| x^\star_{N|k} - \bar{x} \right\|_Q^2 + s\rho_{\mathrm{s}}^2 \left\| x^\star_{N|k} - \bar{x} \right\|_\infty^2 - s \left\| x^\star_{N|k} - \bar{x} \right\|_\infty^2 \\
&\leq \left(n\lambda_{max}(Q) - (1 + \rho_{\mathrm{s}}^2)s \right) \left\| x^\star_{N|k} - \bar{x} \right\|_\infty^2 \overset{(6.13)}{\leq} 0.
\end{aligned}$$

Finally, we have that

$$-\|x^\star_{0|k}-\bar{x}\|^2_Q-\|u^\star_{0|k}-\bar{u}\|^2_R\leq-\lambda_{min}(Q)\|\hat{x}_k-\bar{x}\|^2_2.$$

Combining all the computations we obtain that

$$V(\hat{x}_{k+1}-\bar{x})-V(\hat{x}_k-\bar{x})\leq-c\|\hat{x}_k-\bar{x}\|^2_2+\gamma(k)$$

where $c=\lambda_{min}(Q)$ and

$$\begin{aligned}\gamma(k)=\sum_{i=1}^{N-1}\left(\|\varepsilon_{k+i}\|^2_Q+(x^\star_{i|k}-\bar{x})^\top Q\varepsilon_{k+i}\right)+\|\varepsilon_{k+N}\|^2_Q+(x^\star_{N|k}-\bar{x})^\top Q\varepsilon_{k+N}\\+s\rho_{\mathrm{s}}^2\|\varepsilon_{k+N}\|^2_\infty+2s\rho_{\mathrm{s}}^2\left\|x^\star_{N|k}-\bar{x}\right\|_\infty\|\varepsilon_{k+N}\|_\infty.\end{aligned}$$

In view of the bounds for ε_{k+i} derived in (6.25) and on the boundedness of the states of the GRU, there exist functions $\gamma_1,\gamma_2\in\mathcal{K}$ such that

$$V(\hat{x}_{k+1}-\bar{x})-V(\hat{x}_k-\bar{x})\leq-c\|\hat{x}_k-\bar{x}\|^2_2+\gamma_1(\|x_k-\hat{x}_k\|)+\gamma_2(\|w_{\mathrm{y},k}\|)$$

i.e. $V(\hat{x}_k-\bar{x})$ is an ISS-Lyapunov function for the subsystem describing the evolution of $\hat{x}-\bar{x}$, considering as inputs $x-\hat{x}$ and w_{y}.

To sum up, we have shown that the closed loop system can be described by two connected subsystems. The subsystem that describes the evolution of $x-\hat{x}$ is ISS with respect to the input w_{y}, and is independent by the subsystem describing the evolution of $\hat{x}-\bar{x}$. The subsystem that describes the evolution of $\hat{x}-\bar{x}$ is ISS considering as inputs $x-\hat{x}$ and w_{y}. Then, in view of [114, Theorem 2], the overall system composed by the cascade connection of the two subsystems is ISS with respect to the input w_{y}. □

Chapter 7

Robust offset-free MPC with LSTM networks

In this chapter, we design an MPC algorithm for δISS LSTM models that takes into account constraints on the system output and guarantees offset-free tracking of slow time variant references. In particular, the algorithm proposed in [230] has been modified to cope with time variant set-points and disturbances, output constraints and to guarantee zero-error regulation for asymptotically constant set-points and disturbances. Robust satisfaction of the output constraints is obtained with a constraint tightening method inspired by [130] and similar to the one proposed in the previous chapter. The control algorithm proposed in this chapter includes also an augmented observer and a Reference Calculator to guarantee offset-free tracking in presence of model uncertainties and external disturbances [173]. The design of the observer and of the MPC terminal ingredients for the LSTM model are inspired by [230], but are modified to solve a more complex control problem.

The material in this chapter is taken from:

- [213] **Schimperna, I.**, and Magni, L. (2024). *Robust offset-free constrained model predictive control with long short-term memory networks.* IEEE Transactions on Automatic Control 69(12), 8172-8187.

A preliminary version of the work, that does not consider output constraints, is published in:

- [215] **Schimperna, I.**, Toffanin, C., and Magni, L. (2023). *On offset-free model predictive control with long short-term memory networks.* IFAC-PapersOnLine, 56(1), 156-161. Presented at 12th IFAC Symposium on Nonlinear Control Systems.

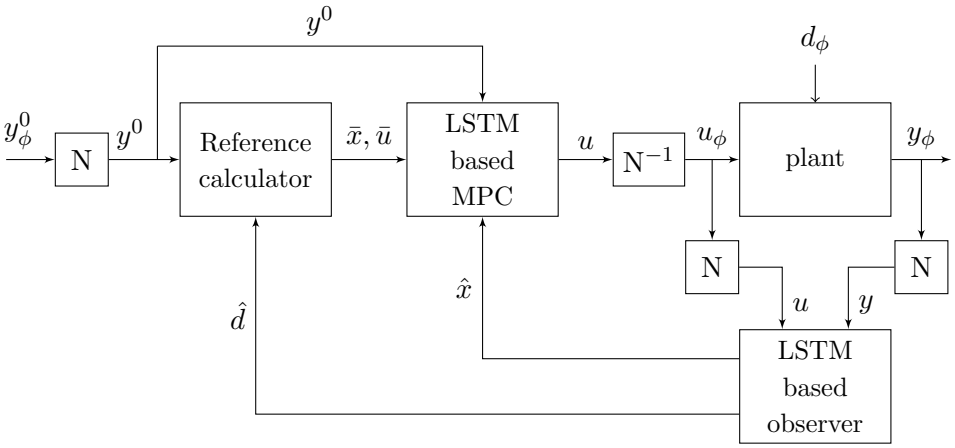

Figure 7.1: Block diagram of the control scheme.

7.1 Problem formulation and control algorithm

In this chapter, we consider as system under control a nonlinear plant with unknown dynamics, input $u_\phi \in \mathbb{R}^m$, output $y_\phi \in \mathbb{R}^p$ and a possible unknown bounded asymptotically constant disturbance d_ϕ. The plant input is saturated, i.e.

$$u_\phi \in \mathcal{U}_\phi = \{u_\phi \in \mathbb{R}^m : u_{\phi,min} \leq u_\phi \leq u_{\phi,max}\} \tag{7.1}$$

with $u_{\phi,min}, u_{\phi,max} \in \mathbb{R}^m$, and the output has to be limited in

$$y_\phi \in \mathcal{Y}_\phi = \{y_\phi \in \mathbb{R}^p : y_{\phi,min} \leq y_\phi \leq y_{\phi,max}\} \tag{7.2}$$

with $y_{\phi,min}, y_{\phi,max} \in \mathbb{R}^p$. For sake of simplicity in this chapter we only consider box constraints on the output, but all the derivations can be extended to polytopic constraints following the methods presented in Chapter 6.

Assumption 7.1. *The plant has the same number of inputs and outputs, i.e.* $m = p$.

Remark 7.1. *Assumption 7.1 is typical of offset-free MPC schemes [173] for nonlinear systems, and is required to have a unique input combination associated to each output at equilibrium. However, if* $m > p$ *the proposed algorithm can still be applied by selecting a subset of* p *inputs to be used for control and leaving the other* $m - p$ *inputs constant.*

The objective of the control is to achieve null error at steady state for an asymptotically constant reference y^0_ϕ also in presence of model-plant mismatch and of bounded asymptotically constant plant disturbances d_ϕ, and to respect input and output constraints. The proposed control algorithm,

whose block diagram is reported in Figure 7.1, is based on an LSTM nominal model of the plant. A key element to obtain a well tuned LSTM model is the normalization of input and output signals, that is represented in the scheme with the blocks "N" and that consists in an affine transformation that scales the variables in a predefined range (typically [-1,1]). The normalized input is denoted with u and the normalized output with y. For the normalized variables constraints (7.1)-(7.2) become

$$u \in \mathcal{U} = \{u \in \mathbb{R}^m : \|u\|_\infty \leq u_{max}\} \tag{7.3}$$

where $u_{max} \in \mathbb{R}$ and is typically equal to 1, and

$$y \in \mathcal{Y} = \{y \in \mathbb{R}^p : y_{min} \leq y \leq y_{max}\} \tag{7.4}$$

where $y_{min}, y_{max} \in \mathbb{R}^p$.

To achieve null error at steady state, the LSTM model is augmented with an asymptotically constant disturbance term d. Then an observer based on the equations of the LSTM model provides an estimation $\hat{x}$ of the state x of the LSTM and an estimation $\hat{d}$ of the disturbance d. At each sampling instant the current values of the normalized set-point y^0 and of the disturbance estimation $\hat{d}$ are used by a Reference Calculator to compute the current values of input and state set-points $\bar{u}$ and $\bar{x}$ for the MPC. The last block is the MPC, that solves a FHOCP and gives in output the first element of the achieved optimal control sequence. Since in the control problem formulation output constraints are considered, to ensure recursive feasibility in presence of the observer estimation error and time variant set-points, it is necessary to rely on a robust MPC algorithm.

As usually done for the analysis of offset-free control schemes, closed-loop stability and constraint satisfaction will be proven in Section 7.2.1 under the assumption that the plant behaves according to its LSTM model with an asymptotically constant additive disturbance d, as reported in Figure 7.2, while offset-free will be shown in Section 7.2.2 for the real closed-loop system (Figure 7.1) under the assumption that closed-loop convergence is not lost.

In the next subsections the different components of the control scheme are presented in detail.

7.1.1 LSTM model

We consider a LSTM model of the system under control, described by (4.1). We denote the model prediction produced by (4.1c) by $\xi \in \mathbb{R}^p$ instead of y, to distinguish it from the real output of the plant. The LSTM model is indicated in a more compact way by

$$x_{k+1} = f(x_k, u_k) \tag{7.5a}$$

$$\xi_k = g(x_k) \tag{7.5b}$$

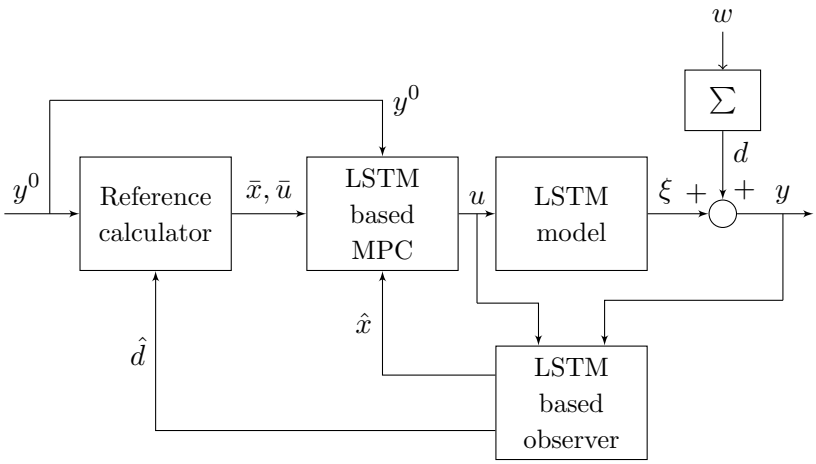

Figure 7.2: Block diagram of the nominal closed-loop control scheme, where the real plant is replaced by its LSTM model augmented with a disturbance term.

where $x = [c^\top \ h^\top]^\top \in \mathbb{R}^{2n_c}$. In the following, we assume that the model respects the δISS condition of Assumption 4.1. Then, it is possible to compute an incremental Lyapunov function for the model. Such Lyapunov function will be used to define the terminal cost, the terminal constraint and the constraint tightening for the MPC.

Lemma 7.1. *Let the LSTM model respect Assumption 4.1, and denote* $x^{\mathrm{a}} = [(c^{\mathrm{a}})^\top \ (h^{\mathrm{a}})^\top]^\top$, $x^{\mathrm{b}} = [(c^{\mathrm{b}})^\top \ (h^{\mathrm{b}})^\top]^\top$ *with* $x^{\mathrm{a}}, x^{\mathrm{b}} \in \mathcal{X}$ *(defined in Theorem 4.1), and* P_{s} *the solution of the Lyapunov equation* $A_\delta^\top P_{\mathrm{s}} A_\delta - P_{\mathrm{s}} = -Q_{\mathrm{s}}$ *for some symmetric positive definite matrix* Q_{s}*. Then the function*

$$V_{\mathrm{s}}(x^{\mathrm{a}}, x^{\mathrm{b}}) = \left\| \begin{bmatrix} \|c^{\mathrm{a}} - c^{\mathrm{b}}\|_2 \\ \|h^{\mathrm{a}} - h^{\mathrm{b}}\|_2 \end{bmatrix} \right\|_{P_{\mathrm{s}}}$$

is an incremental Lyapunov function for the system (7.5)*, such that for all* $u \in \mathcal{U}$

$$c_{\mathrm{s,l}} \|x^{\mathrm{a}} - x^{\mathrm{b}}\|_2 \leq V_{\mathrm{s}}(x^{\mathrm{a}}, x^{\mathrm{b}}) \leq c_{\mathrm{s,u}} \|x^{\mathrm{a}} - x^{\mathrm{b}}\|_2 \tag{7.6a}$$

$$V_{\mathrm{s}}((x^{\mathrm{a}})^+, (x^{\mathrm{b}})^+) \leq \rho_{\mathrm{s}} V_{\mathrm{s}}(x^{\mathrm{a}}, x^{\mathrm{b}}) \tag{7.6b}$$

$$|W_{\mathrm{y}}(h^{\mathrm{a}} - h^{\mathrm{b}})| \leq c_{\mathrm{s}} V_{\mathrm{s}}(x^{\mathrm{a}}, x^{\mathrm{b}}) \tag{7.6c}$$

where $(x^{\mathrm{a}})^+ := f(x^{\mathrm{a}}, u)$, $(x^{\mathrm{b}})^+ := f(x^{\mathrm{b}}, u)$, $c_{\mathrm{s,l}} := \sqrt{\lambda_{min}(P_{\mathrm{s}})}$, $c_{\mathrm{s,u}} := \sqrt{\lambda_{max}(P_{\mathrm{s}})}$, $\rho_{\mathrm{s}} := \sqrt{1 - \frac{\lambda_{min}(Q_{\mathrm{s}})}{\lambda_{max}(P_{\mathrm{s}})}}$ *and* $c_{\mathrm{s}} \in \mathbb{R}^p$ *with*
$c_{\mathrm{s}(j)} := \left\| \begin{bmatrix} 0 & \|W_{\mathrm{y}(j*)}\|_2 \end{bmatrix} P_{\mathrm{s}}^{-1/2} \right\|_2$.

Proof. The proof is reported in Section 7.5.1.

7.1.2 State and disturbance observer

We introduce now a disturbance model to take into account the inaccuracy of the model and the effect of the possible disturbance d_ϕ. The disturbance is denoted by $d \in \mathbb{R}^p$, and is modelled as the integral of a bounded unknown input $w \in \mathbb{R}^p$, that represents its variation. This representation is motivated by the fact that one of the goals of the chapter is to guarantee zero error at steady state when y^0 and d_ϕ are constant, and therefore w is null. The equations of the LSTM model augmented with the disturbance are

$$\begin{aligned} c_{k+1} &= \sigma(W_\mathrm{f} u_k + U_\mathrm{f} h_k + b_\mathrm{f}) \otimes c_k \\ &\quad + \sigma(W_\mathrm{i} u_k + U_\mathrm{i} h_k + b_\mathrm{i}) \otimes \tanh(W_\mathrm{c} u_k + U_\mathrm{c} h_k + b_\mathrm{c}) \end{aligned} \tag{7.7a}$$

$$h_{k+1} = \sigma(W_\mathrm{o} u_k + U_\mathrm{o} h_k + b_\mathrm{o}) \otimes \tanh(c_{k+1}) \tag{7.7b}$$

$$d_{k+1} = d_k + w_k \tag{7.7c}$$

$$y_k = W_\mathrm{y} h_k + b_\mathrm{y} + d_k \tag{7.7d}$$

and are also denoted by

$$\chi_{k+1} = f_{aug}(\chi_k, u_k) + E w_k \tag{7.8a}$$

$$y_k = g_{aug}(\chi_k) \tag{7.8b}$$

where $\chi := [x^\top \; d^\top]^\top$ and matrix E can be obtained from (7.7). Observer convergence, robust constraint satisfaction and offset-free tracking can be achieved only for bounded disturbances. For this reason in the following d and w are assumed to be bounded, i.e. $d \in \mathcal{D} := \{d \in \mathbb{R}^p : \|d\|_\infty \leq d_{max}\}$ and $w \in \mathcal{W} := \{w \in \mathbb{R}^p : \|w\| \leq w_{max}\}$.

To achieve offset-free tracking it is necessary that for the model augmented with the constant disturbance there exists an equilibrium associated to any possible pair (u, y), and that this equilibrium is unique, see [173, Assumption 2]. In the following lemma and corollary it is shown that in view of the δISS property of the LSTM model it is sufficient to add the disturbance only on the output transformation to satisfy this property. Hence, the disturbance is not included also in the state equations.

Lemma 7.2. *If the dynamical system $x_{k+1} = f(x_k, u_k)$ is exponentially δISS in the sets $\mathcal{X}$ and $\mathcal{U}$, then, given a constant input $u \in \mathcal{U}$, there exists a unique corresponding equilibrium state $x^* \in \mathcal{X}$, such that*

$$x^* = f(x^*, u). \tag{7.9}$$

Corollary 7.1. *For the augmented system (7.7), given (u, y) with $u \in \mathcal{U}$, there exist unique values (x^*, d^*) with $x^* \in \mathcal{X}$ such that*

$$x^* = f(x^*, u) \tag{7.10a}$$

$$y = g(x^*) + d^*. \tag{7.10b}$$

Proofs. The proofs of Lemma 7.2 and of Corollary 7.1 are reported in Section 7.5.2.

We design now an observer to obtain an estimation $\hat{\chi} = [\hat{x}^\top \ \hat{d}^\top]^\top$, with $\hat{x} = [\hat{c}^\top \ \hat{h}^\top]^\top$, of the state χ of the augmented LSTM model (7.7). The structure of the observer is based on the LSTM observer proposed in [230], but it has an additional equation for the estimation of the disturbance d. The equations of the observer are the following

$$\begin{aligned}\hat{c}_{k+1} &= \sigma(W_{\mathrm{f}}u_k + U_{\mathrm{f}}\hat{h}_k + b_{\mathrm{f}} + L_{\mathrm{f}}(y_k - \hat{y}_k)) \otimes \hat{c}_k \\ &\quad + \sigma(W_{\mathrm{i}}u_k + U_{\mathrm{i}}\hat{h}_k + b_{\mathrm{i}} + L_{\mathrm{i}}(y_k - \hat{y}_k)) \otimes \tanh(W_{\mathrm{c}}u_k + U_{\mathrm{c}}\hat{h}_k + b_{\mathrm{c}}) \qquad (7.11a)\\ \hat{h}_{k+1} &= \sigma(W_{\mathrm{o}}u_k + U_{\mathrm{o}}\hat{h}_k + b_{\mathrm{o}} + L_{\mathrm{o}}(y_k - \hat{y}_k)) \otimes \tanh(\hat{c}_{k+1}) \qquad (7.11b)\\ \hat{d}_{k+1} &= \mathrm{sat}(\hat{d}_k + L_{\mathrm{d}}(y_k - \hat{y}_k), d_{max}) \qquad (7.11c)\\ \hat{y}_k &= W_{\mathrm{y}}\hat{h}_k + b_{\mathrm{y}} + \hat{d}_k \qquad (7.11d)\end{aligned}$$

where $\mathrm{sat}(v, v_{max})$ denotes the saturation operator between $-v_{max}$ and v_{max}, that is applied element by element when v is a vector. The observer gains $L_{\mathrm{f}}, L_{\mathrm{i}}, L_{\mathrm{o}} \in \mathbb{R}^{n_c \times p}$ and $L_{\mathrm{d}} \in \mathbb{R}^{p \times p}$ are selected according to the following assumption.

Assumption 7.2. *Denoting*

$$\hat{\bar{\sigma}}_{\mathrm{f}} := \sigma(\|[W_{\mathrm{f}}u_{max},\, U_{\mathrm{f}} - L_{\mathrm{f}}W_{\mathrm{y}},\, b_{\mathrm{f}},\, L_{\mathrm{f}}W_{\mathrm{y}},\, 2L_{\mathrm{f}}d_{max}]\|_\infty),$$

$$\hat{\bar{\sigma}}_{\mathrm{i}} := \sigma(\|[W_{\mathrm{i}}u_{max},\, U_{\mathrm{i}} - L_{\mathrm{i}}W_{y},\, b_{\mathrm{i}},\, L_{\mathrm{i}}W_{\mathrm{y}},\, 2L_{\mathrm{i}}d_{max}]\|_\infty),$$

$$\hat{\bar{\sigma}}_{\mathrm{o}} := \sigma(\|[W_{\mathrm{o}}u_{max},\, U_{\mathrm{o}} - L_{\mathrm{o}}W_{\mathrm{y}},\, b_{\mathrm{o}},\, L_{\mathrm{o}}W_{\mathrm{y}},\, 2L_{\mathrm{o}}d_{max}]\|_\infty),$$

$$\hat{\alpha} := \frac{1}{4}\frac{\bar{\sigma}_{\mathrm{i}}\bar{\sigma}_{\mathrm{c}}}{1-\bar{\sigma}_{\mathrm{f}}}\|U_{\mathrm{f}} - L_{\mathrm{f}}W_{\mathrm{y}}\|_2 + \bar{\sigma}_{\mathrm{i}}\|U_{\mathrm{c}}\|_2 + \frac{1}{4}\bar{\sigma}_{\mathrm{c}}\|U_{\mathrm{i}} - L_{\mathrm{i}}W_{\mathrm{y}}\|_2,$$

$$\hat{\beta} := \frac{1}{4}\frac{\bar{\sigma}_{\mathrm{i}}\bar{\sigma}_{\mathrm{c}}}{1-\bar{\sigma}_{\mathrm{f}}}\|L_{\mathrm{f}}\|_2 + \frac{1}{4}\bar{\sigma}_{\mathrm{c}}\|L_{\mathrm{i}}\|_2,$$

$$\hat{\gamma} := \hat{\bar{\sigma}}_{\mathrm{o}}\hat{\alpha} + \frac{1}{4}\bar{\sigma}_{\mathrm{x}}\|U_{\mathrm{o}} - L_{\mathrm{o}}W_{\mathrm{y}}\|_2,$$

$$A_{\mathrm{d}} := \begin{bmatrix} \hat{\bar{\sigma}}_{\mathrm{f}} & \hat{\alpha} & \hat{\beta} \\ \hat{\bar{\sigma}}_{\mathrm{o}}\hat{\bar{\sigma}}_{\mathrm{f}} & \hat{\gamma} & \hat{\bar{\sigma}}_{\mathrm{o}}\hat{\beta} + \frac{1}{4}\bar{\sigma}_{\mathrm{x}}\|L_{\mathrm{o}}\|_2 \\ 0 & \|L_{\mathrm{d}}W_{\mathrm{y}}\|_2 & \|\mathbf{I}_p - L_{\mathrm{d}}\|_2 \end{bmatrix}, \qquad (7.12)$$

the observer gains $L_{\mathrm{f}}, L_{\mathrm{i}}, L_{\mathrm{o}}, L_{\mathrm{d}}$ are selected so that $\rho(A_{\mathrm{d}}) < 1$.

Remark 7.2. *In Theorem 7.1 it is shown that A_{d} is the matrix dynamic for an upper bound of the estimation error dynamic.*

Remark 7.3. *A possible suboptimal choice for the gains of the observer that satisfies Assumption 7.2 is* $L_\mathrm{f} = L_\mathrm{i} = L_\mathrm{o} = \mathbf{0}_{n_c,p}$ *and* $L_\mathrm{d} = \ell_\mathrm{d}\mathbf{I}_p$ *with* $0 < \ell_\mathrm{d} < 2$*. With this choice the matrix* A_d *becomes*

$$A_\mathrm{d} = \left[\begin{array}{c|c} A_\delta & \mathbf{0}_{2,1} \\ \hline 0 \quad \|L_\mathrm{d}W_\mathrm{y}\|_2 & |\ell_\mathrm{d} - 1| \end{array}\right]$$

and therefore the eigenvalues of A_d *are the eigenvalues of* A_δ *and an eigenvalue in* $|\ell_\mathrm{d} - 1| \in [0, 1)$*. Hence, because the LSTM is tuned with the constraint that* $\rho(A_\delta) < 1$*,* $\rho(A_\mathrm{d}) < 1$*.*

The following lemma defines a positive invariant set for the state $\hat{\chi}$ of the observer, in which it is possible to prove the convergence of the observer estimation.

Lemma 7.3. *If* $h_k \in \mathcal{H}$ *and* $d_k \in \mathcal{D}$*,* $\forall k \in \mathbb{Z}_{\geq 0}$*, then the set* $\hat{\mathcal{I}} := \hat{\mathcal{C}} \times \mathcal{H} \times \mathcal{D}$*, with*

$$\hat{\mathcal{C}} := \left\{ \hat{c} \in \mathbb{R}^n : \|\hat{c}\|_\infty \leq \frac{\hat{\bar{\sigma}}_\mathrm{i}\bar{\sigma}_\mathrm{c}}{1 - \hat{\bar{\sigma}}_\mathrm{f}} \right\}$$

is a positive invariant set for the observer (7.11)*.*

Proof. The proof is reported in Section 7.5.3.

We can now derive the main results related to the observer convergence.

Theorem 7.1. *If the plant behaves according to* (7.7) *with* $x \in \mathcal{X}$*,* $d \in \mathcal{D}$ *and* $w \in \mathcal{W}$*, Assumption 4.1 holds, the observer parameters are selected according to Assumption 7.2 and* $\hat{\chi} \in \hat{\mathcal{I}}$*, then the function*

$$V_\mathrm{o}(\hat{\chi}, \chi) = \left\| \begin{bmatrix} \|\hat{c} - c\|_2 \\ \|\hat{h} - h\|_2 \\ \|\hat{d} - d\|_2 \end{bmatrix} \right\|_{P_\mathrm{o}}, \tag{7.13}$$

where P_o *is the solution of the Lyapunov equation* $A_\mathrm{d}^\top P_\mathrm{o} A_\mathrm{d} - P_\mathrm{o} = -Q_\mathrm{o}$ *for a matrix* $Q_\mathrm{o} = Q_\mathrm{o}^\top \succ 0$*, is an incremental Lyapunov function for the observer estimation error, such that*

$$c_{\mathrm{o,l}} \|\hat{\chi} - \chi\|_2 \leq V_\mathrm{o}(\hat{\chi}, \chi) \leq c_{\mathrm{o,u}} \|\hat{\chi} - \chi\|_2 \tag{7.14a}$$
$$V_\mathrm{o}(\hat{\chi}^+, \chi^+) \leq \rho_\mathrm{o} V_\mathrm{o}(\hat{\chi}, \chi) + \bar{w} \tag{7.14b}$$
$$|W_\mathrm{y}(h - \hat{h}) + (d - \hat{d})| \leq c_\mathrm{o} V_\mathrm{d}(\hat{\chi}, \chi) \tag{7.14c}$$
$$\left\|\hat{\chi}^+ - f_{aug}(\hat{\chi}, u)\right\|_2 \leq L_{max} V_\mathrm{o}(\hat{\chi}, \chi) \tag{7.14d}$$

where $\chi^+ := f_{aug}(\chi, u) + Ew$*,* $\hat{\chi}^+$ *is the next state computed by the observer* (7.11)*,* $c_{\mathrm{o,l}} := \sqrt{\lambda_{min}(P_\mathrm{o})}$*,* $c_{\mathrm{o,u}} := \sqrt{\lambda_{max}(P_\mathrm{o})}$*,* $\rho_\mathrm{o} := \sqrt{1 - \frac{\lambda_{min}(Q_\mathrm{o})}{\lambda_{max}(P_\mathrm{o})}} \in (0, 1)$*,* $\bar{w} := \sqrt{P_{\mathrm{o}(3,3)}} w_{max}$*,* $L_{max} > 0$*, and* $c_\mathrm{o} \in \mathbb{R}^p$ *with* $c_{\mathrm{o}(j)} := \left\| \begin{bmatrix} 0 & \|W_{\mathrm{y}(j*)}\|_2 & 1 \end{bmatrix} P_\mathrm{o}^{-1/2} \right\|_2$.

Moreover, if $w_k \to 0$ *for* $k \to \infty$*, then the observer provides a converging state estimation, i.e.* $\|\chi_k - \hat{\chi}_k\| \to 0$ *for* $k \to \infty$*.*

Proof. The proof is reported in Section 7.5.4.

Remark 7.4. *In view of the properties of the Lyapunov function $V_o(\hat{\chi}, \chi)$, the observer estimation error is also ISS with respect to the disturbance w.*

7.1.3 Reference Calculator

One of the most important characteristics of the proposed algorithm is the possibility to be applied with time variant set-point and disturbances unknown in advance. In order to do so the MPC assumes a constant set-point along the prediction horizon but it is designed to preserve, under suitable assumptions, recursive feasibility even if the exogenous signals change at any time instant. To manage possible variations of the set-point y^0 and/or of the disturbance estimation $\hat{d}$, a Reference Calculator is introduced in the control loop. The goal of the Reference Calculator is to provide the state and input references $\bar{x} = [\bar{c}^\top \ \bar{h}^\top]^\top$ and $\bar{u}$ for the MPC, that are computed by solving the following system of equations:

$$\bar{x} = f(\bar{x}, \bar{u}) \tag{7.15a}$$

$$y^0 = g(\bar{x}) + \hat{d}. \tag{7.15b}$$

To guarantee offset-free of the closed-loop system, we introduce the following assumption on the set-point y^0 and on the LSTM model. An additional assumption on the set-point y^0 will be introduced in the next section.

Assumption 7.3. *The set-point y^0 and the LSTM model* (7.5) *respect the following conditions:*

1. *there exists a bounded set $\mathcal{Y}^0 \subset \mathbb{R}^p$ such that $y^0_k \in \mathcal{Y}^0 \ \forall k \in \mathbb{Z}_{\geq 0}$;*
2. *the set-point is asymptotically constant, i.e. $y^0_k \to y^0_\infty$ for $k \to \infty$;*
3. *$\forall y^0 \in \mathcal{Y}^0$, $\forall \hat{d} \in \mathcal{D}$, there exists $(\bar{x}, \bar{u})$ with $\bar{u} \in \mathcal{U}$ solving* (7.15)*, and the Jacobian matrix*

$$\begin{bmatrix} \frac{\partial}{\partial x}(f(\bar{x}, \bar{u}) - \bar{x}) & \frac{\partial}{\partial u}(f(\bar{x}, \bar{u}) - \bar{x}) \\ \frac{\partial}{\partial x}(g(\bar{x}) + \hat{d} - y^0) & \frac{\partial}{\partial u}(g(\bar{x}) + \hat{d} - y^0) \end{bmatrix} \tag{7.16}$$

is invertible.

Remark 7.5. *The assumption that the Jacobian matrix* (7.16) *is invertible implies that there exists a neighborhood of $(y^0, \hat{d})$ where the solution of the Reference Calculator* (7.15) *is unique.*

Moreover, since a large variation of the set-points $\bar{x}, \bar{u}$ is critical for the MPC recursive feasibility, in the following lemma an upper bound for the variation of the state set-point $\bar{x}$ between consecutive time-steps is derived. This upper bound depends on the variation of the set-point y^0 and on the observer parameters.

Lemma 7.4. *Under Assumption 7.3, given the maximum output estimation error* $\bar{e}_y = \max_{k\in\mathbb{Z}_{\geq 0}} \|y_k - \hat{y}_k\|_2$*, there exists a finite constant* $\bar{K}$ *such that*

$$\|\bar{x}_{k+1} - \bar{x}_k\|_2 \leq \bar{K} \|L_\mathrm{d}\|_2 \bar{e}_y + \bar{K} \left\|y^0_{k+1} - y^0_k\right\|_2 . \tag{7.17}$$

Proof. The proof is reported in Section 7.5.5.

Remark 7.6. *In general* $\bar{K}$ *cannot be computed explicitly, but it can be estimated numerically by gridding.*

7.1.4 Robust MPC formulation

The robust MPC solves at every time-step a FHOCP where the evolution of the states of the system is predicted with the LSTM model and is initialized with the observer state estimation. The cost function penalizes the deviation from the state and the input set-points computed at the current time instant by the Reference Calculator, that are assumed constant along the prediction horizon. The terminal cost and the terminal set are designed to stabilize the closed-loop system. To ensure satisfaction of the output constraints despite the observer estimation error, the disturbance and the set-point variation, a constraint tightening approach similar to the one proposed in [130] and also used in Chapter 6, and a time variant terminal set are employed. For the constraint tightening, we use a time variant term $\hat{e}_\mathrm{o} \in \mathbb{R}$ related to the uncertainty of the observer, whose evolution is described by

$$\hat{e}_{\mathrm{o},k+1} = \rho_\mathrm{o} \hat{e}_{\mathrm{o},k} + \bar{w}. \tag{7.18}$$

Depending on the values of $\hat{e}_{\mathrm{o},0}$, of ρ_o and of $\bar{w}$, $\hat{e}_\mathrm{o}$ can increase or decrease, but its behavior is always monotonic with

$$\lim_{k\to\infty} \hat{e}_{\mathrm{o},k} = \bar{e}_\infty = \frac{\bar{w}}{1-\rho_\mathrm{o}}. \tag{7.19}$$

Definition 7.1 (FHOCP)**.** *Given the prediction horizon* N*, the FHOCP for the robust MPC is the following*

$$\min_{u_{\cdot|k}} \sum_{i=0}^{N-1} \left(\left\|x_{i|k} - \bar{x}_k\right\|^2_Q + \left\|u_{i|k} - \bar{u}_k\right\|^2_R \right) + \left\| \begin{bmatrix} \|c_{N|k} - \bar{c}_k\| \\ \|h_{N|k} - \bar{h}_k\| \end{bmatrix} \right\|^2_{P_\mathrm{f}} \tag{7.20a}$$

$$s.t. \quad x_{0|k} = \hat{x}_k \tag{7.20b}$$

$$x_{i+1|k} = f(x_{i|k}, u_{i|k}) \tag{7.20c}$$

$$W_\mathrm{y} h_{i|k} + b_\mathrm{y} + d_{max}\mathbf{1}_p \leq y_{max} - a_i \hat{e}_{\mathrm{o},k} - b_i \tag{7.20d}$$

$$W_\mathrm{y} h_{i|k} + b_\mathrm{y} - d_{max}\mathbf{1}_p \geq y_{min} + a_i \hat{e}_{\mathrm{o},k} + b_i \tag{7.20e}$$

$$u_{i|k} \in \mathcal{U} \tag{7.20f}$$

$$for\ i = 0, ..., N-1$$

$$x_{N|k} \in \mathcal{X}_f(k) \tag{7.20g}$$

where $Q \succ 0$ and $R \succ 0$ are design choices, while $P_\mathrm{f} \succ 0$ satisfies the Lyapunov condition $A_\delta^\top P_\mathrm{f} A_\delta - P_\mathrm{f} \prec -q\mathbf{I}_2$, where $q = \lambda_{max}(Q)$. Coefficients $a_i \in \mathbb{R}^p$ and $b_i \in \mathbb{R}^p$ for the constraint tightening are defined as

$$a_0 := c_\mathrm{o}, \quad b_0 := \mathbf{0}_{p,1} \tag{7.21a}$$

$$a_{i+1} := \rho_\mathrm{o} a_i + \rho_\mathrm{s}^i c_{\mathrm{s,u}} L_{max} c_{\mathrm{o,s}} \tag{7.21b}$$

$$b_{i+1} := b_i + a_i \bar{w} \tag{7.21c}$$

$\mathcal{X}_f(k)$ is a time variant terminal set, chosen as a sublevel set of the terminal cost:

$$\mathcal{X}_f(k) := \left\{ \begin{bmatrix} c \\ h \end{bmatrix} \in \mathbb{R}^{2n_c} : \left\| \begin{bmatrix} \|c - \bar{c}_k\|_2 \\ \|h - \bar{h}_k\|_2 \end{bmatrix} \right\|_{P_f} \leq \alpha_k \right\} \tag{7.22}$$

with

$$\alpha_k := \min_{j \in [1:p]} \min \left\{ \alpha_{j,k}^{max}, \alpha_{j,k}^{min} \right\} \tag{7.23a}$$

where

$$\alpha_{j,k}^{max} := \left\| [0 \ \ \|W_{\mathrm{y}(j*)}\|_2] P_\mathrm{f}^{-1/2} \right\|_2^{-1} (y_{max(j)} - y_{k(j)}^0 - 2d_{max} - a_{N(j)} \tilde{e}_{\mathrm{o},k} - b_{N(j)}) \tag{7.23b}$$

$$\alpha_{j,k}^{min} := \left\| [0 \ \ \|W_{\mathrm{y}(j*)}\|_2] P_\mathrm{f}^{-1/2} \right\|_2^{-1} (y_{k(j)}^0 - y_{min(j)} - 2d_{max} - a_{N(j)} \tilde{e}_{\mathrm{o},k} - b_{N(j)}) \tag{7.23c}$$

$$\tilde{e}_{\mathrm{o},k} = \max \left\{ \hat{e}_{\mathrm{o},k}, \bar{e}_\infty \right\}. \tag{7.23d}$$

Remark 7.7. *The coefficients for the constraint tightening defined in* (7.21) *are defined analogously to Chapter 6. However, the constraint tightening formulation in* (7.20d)-(7.20e) *is different from the one in* (6.12d)*, because it takes into account also the upper bound of the disturbance d_{max}.*

At each time-step k the solution of the FHOCP is denoted by $\mathbf{u}_k^\star = \{u_{0|k}^\star, ..., u_{N-1|k}^\star\}$. According to the Receding Horizon principle, the MPC control law is obtained applying only the first element of the optimal input sequence, i.e.

$$u_k = \mu^{\mathrm{MPC}}(\hat{x}_k, \hat{e}_{\mathrm{o},k}, \bar{x}_k, \bar{u}_k, y_k^0) = u_{0|k}^\star. \tag{7.24}$$

7.2 Stability and offset-free results

In this section we analyze the properties of the closed-loop. To guarantee offset-free results, in Section 7.2.2 we have to introduce a mild assumption on the convergence of the closed-loop of Figure 7.1. However, we first have to prove recursive feasibility and stability for the nominal closed-loop system reported in Figure 7.2, where the plant is substituted by the LSTM with an additive disturbance on the output (7.7).

7.2.1 Recursive feasibility and stability analysis

In this subsection recursive feasibility and stability of the nominal closed-loop system reported in Figure 7.2 are analyzed. First note that in order to have a solution of the FHOCP, it is necessary that $\alpha_k > 0$ for all $k \in \mathbb{Z}_{\geq 0}$. To guarantee this condition, the following assumption on the set-point is introduced.

Assumption 7.4. *The set-point y^0 is such that*

$$y^0_{k(j)} < y_{max(j)} - 2d_{max} - a_{N(j)}\tilde{e}_{\mathrm{o},k} - b_{N(j)} \tag{7.25a}$$

$$y^0_{k(j)} > y_{min(j)} + 2d_{max} + a_{N(j)}\tilde{e}_{\mathrm{o},k} + b_{N(j)} \tag{7.25b}$$

for all $j = 1, ..., p$, for all $k \in \mathbb{Z}_{\geq 0}$.

Consider the closed-loop system composed by the augmented LSTM (7.8), the observer (7.11), the Reference Calculator (7.15) and the MPC (7.24). This system has state

$$\psi := [c^\top \; h^\top \; \hat{c}^\top \; \hat{h}^\top \; \hat{d}^\top \; \hat{e}_{\mathrm{o}}]^\top$$

and inputs d and y^0. Let's now define the feasible set of states and inputs

$$\begin{aligned}\mathcal{X}^{\mathrm{MPC}} := \{(\psi, d, y^0) : x \in \mathcal{X}, \hat{\chi} \in \hat{\mathcal{I}}, d \in \mathcal{D}, y^0 \in \mathcal{Y}^0,\\ \hat{e}_{\mathrm{o}} \text{ is such that } V_{\mathrm{o}}(\hat{\chi}, \chi) \leq \hat{e}_{\mathrm{o}}\\ \text{and } \exists \text{ a solution of the FHOCP}\}.\end{aligned}$$

Remark 7.8. *In the feasible set $\mathcal{X}^{\mathrm{MPC}}$ it is required that $\hat{e}_{\mathrm{o}}$ is an upper bound for $V_{\mathrm{o}}(\hat{\chi}, \chi)$. This condition is similar to require that $\hat{e}_{\mathrm{o}}$ is an upper bound of the observer estimation error. In fact, using Equation* (7.14a) *and $V_{\mathrm{o}}(\hat{\chi}, \chi) \leq \hat{e}_{\mathrm{o}}$, the following inequality relating $\hat{e}_{\mathrm{o}}$ and $\|\chi - \hat{\chi}\|_2$ can be derived:*

$$\|\chi - \hat{\chi}\|_2 \leq \frac{\hat{e}_{\mathrm{o}}}{c_{\mathrm{o,l}}}.$$

In the following theorem the main result for the nominal closed-loop schema described in Figure 7.2 is derived.

Theorem 7.2. *Let the LSTM model respect Assumption 4.1, and let Assumptions 7.1, 7.2, 7.3, 7.4 hold. Then there exist $\bar{L}_{max} > 0$, $\bar{L}_{\mathrm{d}} > 0$ and $\Delta y^0_{max} > 0$ such that for $L_{max} \leq \bar{L}_{max}$, $\|L\|_{\mathrm{d}} \leq \bar{L}_{\mathrm{d}}$ and y^0 such that $\left\|y^0_{k+1} - y^0_k\right\| \leq \Delta y^0_{max}$ for all $k \in \mathbb{Z}_{\geq 0}$, for the closed-loop system composed by the augmented LSTM* (7.8)*, the observer* (7.11)*, the Reference Calculator* (7.15) *and the MPC* (7.24) *the following properties hold:*

- *constraints* (7.3) *and* (7.4) *are satisfied $\forall (\psi, d, y^0) \in \mathcal{X}^{\mathrm{MPC}}$;*

- *the FHOCP is recursively feasible, i.e.* $(\psi_k, d_k, y_k^0) \in \mathcal{X}^{\text{MPC}} \implies (\psi_{k+1}, d_{k+1}, y_{k+1}^0) \in \mathcal{X}^{\text{MPC}}$*;*

- *the closed-loop system* (7.8)-(7.15)-(7.24) *is ISpS with respect to the observer estimation error* $\chi - \hat{\chi}$ *in* $\mathcal{X}^{\text{MPC}}$*;*

- *if* $d_k \to \bar{d}_\infty$ *for* $k \to \infty$*, then*

$$\lim_{k\to\infty} \|\psi_k - \psi_\infty\| = 0$$

where

$$\psi_\infty = [\bar{c}_\infty^\top \; \bar{h}_\infty^\top \; \bar{c}_\infty^\top \; \bar{h}_\infty^\top \; \bar{d}_\infty^\top \; \bar{e}_\infty]^\top$$

and $\bar{x}_\infty = [\bar{c}_\infty^\top \; \bar{h}_\infty^\top]^\top$ *and* $\bar{u}_\infty$ *are the solution of* (7.15) *when* $y^0 = y_\infty^0$ *and* $\hat{d} = \bar{d}_\infty$*.*

Proof. The proof is reported in Section 7.5.6.

Remark 7.9. *To satisfy the condition on the rate of change of* y^0 *it is sufficient to pass the set-point through a rate limiter.*

7.2.2 Offset-free result

It is now possible to follow the results in [173] to show that the proposed scheme based on the model augmented with the disturbance and on the Reference Calculator guarantees offset-free at steady state also when applied to the real plant (see Figure 7.1), provided that the uncertainty on the model is sufficiently small to preserve convergence and constraints satisfaction, as assumed in the following assumption.

Assumption 7.5. *The plant disturbance* d_ϕ *is bounded and asymptotically constant, and the closed-loop system composed by the plant, the observer* (7.11)*, the Reference Calculator* (7.15) *and the MPC* (7.24) *respects the constraints and converges to constant values strictly in the interior of the feasible set.*

Theorem 7.3. *If Assumptions 7.1, 7.2, 7.3, 7.4, 7.5 are satisfied and the LSTM model respect Assumption 4.1, then the closed-loop system composed by the plant, the observer* (7.11)*, the Reference Calculator* (7.15) *and the MPC* (7.24) *is offset-free at steady state, i.e.* $y_{\phi,k} \to y_{\phi,\infty}^0$ *for* $k \to \infty$*, where* $y_{\phi,\infty}^0 = \lim_{k\to\infty} y_\phi^0$*.*

Proof. The proof is reported in Section 7.5.7.

7.3 Illustrative example

As benchmark example to test the proposed control algorithm we consider the pH neutralization process described in Section 5.3.1. The objective is to control the pH (that is the output y_ϕ) by acting on the alkaline flow $q_3 =: u_\phi$, respecting the input saturation constraint

$$u_\phi \in \mathcal{U}_\phi = [12.5, 17]\ mL/s.$$

In this chapter, the buffer flow q_2 is considered as an unmeasurable time variant disturbance. As output constraint we consider the set $\mathcal{Y}_\phi = [6.0, 9.0]$.

7.3.1 LSTM model identification

To extract the dataset for the training of the LSTM model, a simulator of the plant is forced with multilevel pseudo-random signals, and the input-output response is sampled with a sampling period of $T_\mathrm{s} = 10s$, as done in [230]. In particular, the input signals for the plant simulator are piecewise constant signals with random values in $\mathcal{U}_\phi$, where each constant value is applied for a random time between $10T_\mathrm{s}$ and $100T_\mathrm{s}$. 15 sequences of $N_t = 1500$ time-steps each are extracted, and are split in 10 sequences for training, 3 for validation and 2 for testing. All the sequences are generated considering the disturbance constant at its nominal value $q_2 = 0.55mL/s$. Before the training, inputs and outputs are normalized using their maximum and minimum values present in the training dataset, so that $-1 \leq u \leq 1$ and $-1 \leq y \leq 1$.

The LSTM neural network is developed in Python 3.9, using Tensorflow 2.8. To obtain a final network respecting the δISS condition of Assumption 4.1, the training loss and the stopping rule for the training are modified as detailed in Section 4.2.2. In this case, the tuning of hyperparameter λ^- in the loss function (4.4) is important to obtain a a model that satisfies the δISS condition by a larger margin, providing a model with smaller values of ρ_s. In fact, a small value of ρ_s, together with a small value of ρ_o, implies that coefficients a_i defined in (7.21) are smaller, leading to a less conservative constraint tightening for the MPC.

For the MPC simulations we use an LSTM model with $n = 5$ neurons and with a FIT on the test set of 94.0%. The network is trained using ADAM optimizer for 1000 epochs, with a learning rate of 0.001 and hyperparameters $\lambda^+ = 0.03$ and $\lambda^- = 0.02$. The final model respects the δISS condition of Assumption 4.1, and has $\rho_\mathrm{s} = 0.92$ when the incremental Lyapunov function V_s is computed using $Q_\mathrm{s} = 1000\mathbf{I}_2$.

7.3.2 Control implementation

To tune the controller we assume $d_{max} = 0.1$, that corresponds to the 5% of the range of variation of the output in the training dataset, since the output

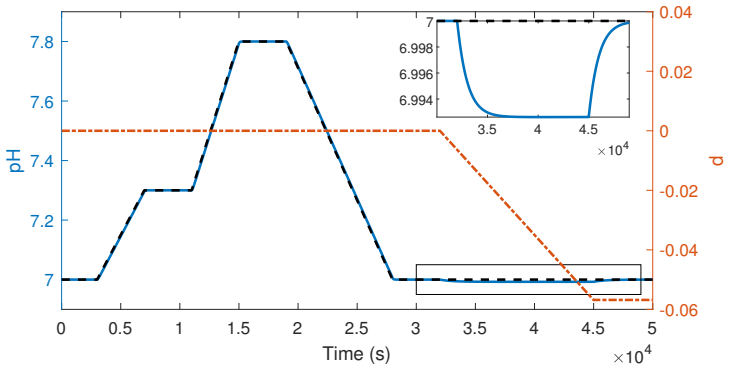

Figure 7.3: Evolution of the output of the LSTM model (blue line) compared with reference y^0 (black dashed line), and evolution of the disturbance d (orange dash-dotted line). y^0 and d are selected to respect the sufficient conditions for recursive feasibility of Theorem 7.2.

is normalized in $[-1, 1]$, and $\bar{w} = 0.01$. Under this assumption, the following parameters are used. The cost matrices are set to $Q = \mathbf{I}_{2n}$ and $R = 1$, and the prediction horizon to $N = 5$. The observer gains $L_{\mathrm{f}}, L_{\mathrm{i}}, L_{\mathrm{o}}$ are chosen by solving the optimization proposed in [230, Proposition 3], while L_{d} is set to 0.01. The matrix P_{o} is obtained by solving the Lyapunov equation with $Q_{\mathrm{o}} = 1000\mathbf{I}_3$, leading to $\rho_{\mathrm{o}} = 0.99$, $L_{max} = 8.4{\times}10^{-4}$, $w_{max} = 4.3{\times}10^{-5}$ and $\bar{e}_{\infty} = 1.04$. Concerning the parameters related to the recursive feasibility condition, $\bar{K} = 2.67$ is estimated by gridding, while $\bar{e}_y$ is set to 0.03. This value is clearly affected by the quality of the initialization of the observer. In the considered simulations this bound is always largely respected. The initial value for the observer state is set to the state equilibrium of the LSTM model associated with the initial output of the system under control and $\hat{d}_0 = 0$. With the considered parameters, the time variant interval for y^0 needed to satisfy Assumption 7.4 converges to [6.49, 8.51] after an initial transient.

7.3.3 Simulation results

First, the conservatism of the feasibility/stability conditions is tested by performing some simulations where the controller is applied on a perturbed version of the LSTM model. In the first simulation, reported in Figure 7.3, slow variations of the set-point y^0 and of the disturbance d are applied, in order to respect all the sufficient conditions required by Theorem 7.2. As predicted by the theory, recursive feasibility, stability and zero error are fulfilled. Then, considering that all the bounds have been derived using a sequence of possibly conservative inequalities, we carried out an analysis to verify the applicability of the control in presence of larger variations of the set-point y^0 and of the disturbance d, that do not satisfy the sufficient

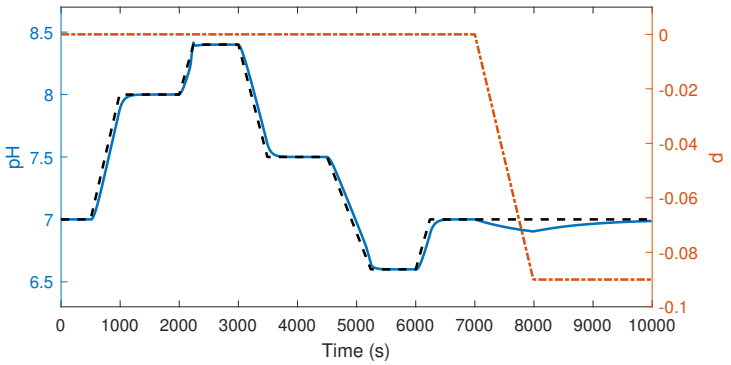

Figure 7.4: Evolution of the output of the LSTM model (blue line) compared with reference y^0 (black dashed line), and evolution of the disturbance d (orange dash-dotted line). The sufficient conditions for recursive feasibility of Theorem 7.2 are not respected, but recursive feasibility is maintained in the practice.

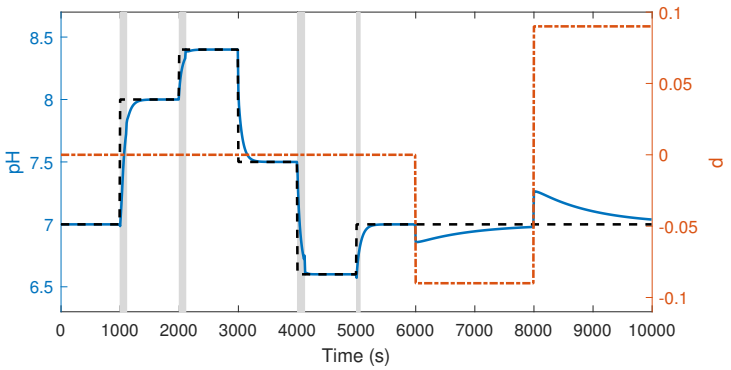

Figure 7.5: Evolution of the output of the LSTM model (blue line) compared with reference y^0 (black dashed line), and evolution of the disturbance d (orange dash-dotted line). In the time instants highlighted in gray the optimization problem (7.20) is not feasible and the control law is selected by solving (7.20) without constraints (7.20d)-(7.20e)-(7.20g).

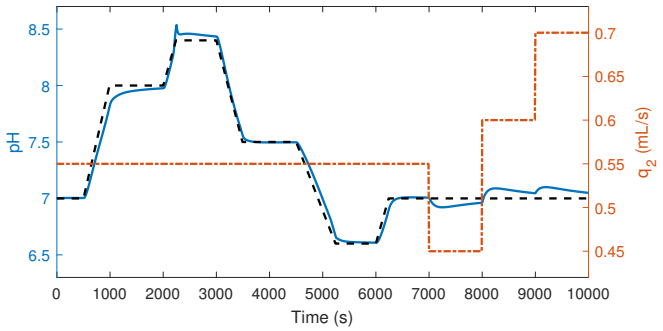

Figure 7.6: Evolution of the output of the real plant (blue line) compared with reference y_ϕ^0 (black dashed line), and evolution of the plant disturbance d_ϕ (orange dash-dotted line), when $L_\mathrm{d} = 0.01$.

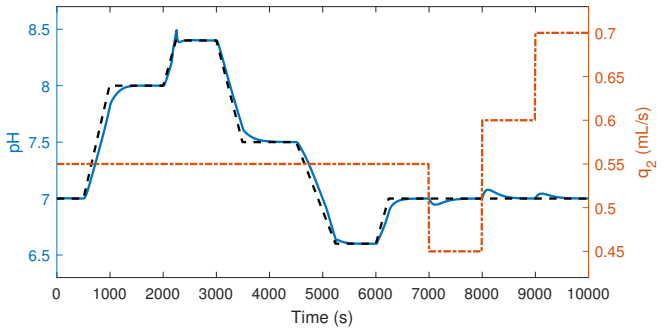

Figure 7.7: Evolution of the output of the real plant (blue line) compared with reference y_ϕ^0 (black dashed line), and evolution of the plant disturbance d_ϕ (orange dash-dotted line), when $L_\mathrm{d} = 0.1$.

conditions required by Theorem 7.2. In particular, in Figures 7.4 and 7.5, simulations with increasingly larger set-point and disturbance variations are reported. In the simulation reported in Figure 7.4 feasibility is never lost, while in Figure 7.5 in the time instants highlighted in gray the FHOCP is not feasible because of the large variations of y^0. Notably, feasibility is maintained also with large step variations of the disturbance d.

Then, the controller is applied to the real plant (represented by the physical equations describing the system). Since model uncertainty is not estimated, the bounds d_{max} and $\bar{w}$ are considered as tuning parameters of the control. Also $\hat{e}_\mathrm{o}$ is considered as an additional tuning parameter of the control, since the states of the plant do not coincide with the states of the LSTM. The first simulation is carried out using the same parameters of the simulations performed using the LSTM model, and is reported in Figure 7.6. It can be noticed that the response of the plant to the disturbances is very slow, and null error is reached only after a very long transient. Hence, in a second simulation, L_d is increased to 0.1 to make the disturbance estimation

in the observer faster. With this tuning of the observer $\rho_o = 0.97$, $L_{max} = 8.5 \times 10^{-3}$ and $\bar{e}_\infty = 0.38$. In this case, the asymptotic interval for y^0 needed to satisfy Assumption 7.4 is $[6.57, 8.43]$. The resulting trajectory is reported in Figure 7.7, and it can be seen that the control is able to correctly manage the plant, maintain the recursive feasibility and achieve null tracking error also in presence of disturbances.

7.4 Conclusions

In chapter we proposed an MPC control scheme based on an LSTM model of the plant under control. The MPC algorithm is able to take into account input and output constraints and to guarantee null error at steady state also in presence of modelling errors and of asymptotically constant bounded disturbances. Offset-free is obtained by introducing the estimation of a disturbance term in the observer, that is used to update at every time-step the reference values for the MPC cost. The satisfaction of output constraints in presence of the observer estimation error and time variant set-point is obtained using a constraint tightening technique, based on an upper bound of the norm of the observer estimation error. The key element for the design of the constraint tightening is the derivation of incremental Lyapunov functions for the LSTM model and for the observer, whose parameters are employed in the definition of the coefficients for the constraint tightening. In the FHOCP formulation for the MPC a time variant terminal constraint is also introduced, that guarantees recursive feasibility in presence of variations of the reference values. Then, ISpS and convergence are proven by means of a Lyapunov function, different from the optimal cost because considers the deviation from the asymptotic values of state and input set-points that are a-priori unknown.

The main limitation of the proposed approach is the conservatism of the robust constrained MPC algorithm that must cope with both the disturbances and the set-point variations. In order to partially reduce this limitation an artificial reference approach could be adopted, avoiding the restriction on the tightened constraints introduced by the set-point variation. Further improvement could be achieved by deriving less conservative bounds along all the proofs. However most of the conservatism is inherent in the worst case deterministic approach. As shown in the simulation example it is possible to find a compromise between a-priori feasibility guarantee and performance by adapting some of the algorithm parameters.

7.5 Proofs

The following lemmas will be used for the proofs.

Lemma 7.5 (Property 3 in [230])**.** *Given two vectors $a, b \in \mathbb{R}^n$ and a positive definite matrix M, for any $\varphi \neq 0$ it holds that*

$$\|a+b\|_M^2 \leq (1+\varphi^2)\|a\|_M^2 + \left(1+\frac{1}{\varphi^2}\right)\|b\|_M^2. \tag{7.26}$$

Lemma 7.6. *Given two sets of n numbers each, $\{a_1, ..., a_n\}$ and $\{b_1, ..., b_n\}$, one has that*

$$\min_{i\in[1:n]} a_i - \min_{i\in[1:n]} b_i \geq \min_{i\in[1:n]}(a_i - b_i). \tag{7.27}$$

Proof. Equation (7.27) can be rearranged as

$$\min_{i\in[1:n]} a_i \geq \min_{i\in[1:n]} b_i + \min_{i\in[1:n]}(a_i - b_i).$$

Let's now denote $c_i = a_i - b_i$ for $i \in [1:n]$. Then

$$\begin{aligned}\min_{i\in[1:n]} a_i &= \min_{i\in[1:n]}(b_i + c_i) \geq \min_{i,j\in[1:n]}(b_i + c_j) = \min_{i\in[1:n]} b_i + \min_{j\in[1:n]} c_j \\ &= \min_{i\in[1:n]} b_i + \min_{i\in[1:n]} c_i = \min_{i\in[1:n]} b_i + \min_{i\in[1:n]}(a_i - b_i).\end{aligned}$$

□

7.5.1 Proof of Lemma 7.1

Condition (7.6a) is easily verified for the definition of V_s.

Condition (7.6b) can be verified as follows:

$$\begin{aligned}V_\mathrm{s}((x^\mathrm{a})^+, (x^\mathrm{b})^+) &= \sqrt{\begin{bmatrix}\|(c^\mathrm{a})^+ - (c^\mathrm{b})^+\|_2 \\ \|(h^\mathrm{a})^+ - (h^\mathrm{b})^+\|_2\end{bmatrix}^\top P_\mathrm{s} \begin{bmatrix}\|(c^\mathrm{a})^+ - (c^\mathrm{b})^+\|_2 \\ \|(h^\mathrm{a})^+ - (h^\mathrm{b})^+\|_2\end{bmatrix}} \\ &\overset{(4.1)}{\leq} \sqrt{\begin{bmatrix}\|c^\mathrm{a} - c^\mathrm{b}\|_2 \\ \|h^\mathrm{a} - h^\mathrm{b}\|_2\end{bmatrix}^\top A_\delta^\top P_\mathrm{s} A_\delta \begin{bmatrix}\|c^\mathrm{a} - c^\mathrm{b}\|_2 \\ \|h^\mathrm{a} - h^\mathrm{b}\|_2\end{bmatrix}} \\ &= \sqrt{\begin{bmatrix}\|c^\mathrm{a} - c^\mathrm{b}\|_2 \\ \|h^\mathrm{a} - h^\mathrm{b}\|_2\end{bmatrix}^\top (P_\mathrm{s} - Q_\mathrm{s}) \begin{bmatrix}\|c^\mathrm{a} - c^\mathrm{b}\|_2 \\ \|h^\mathrm{a} - h^\mathrm{b}\|_2\end{bmatrix}} \\ &\leq \sqrt{\left\|\begin{bmatrix}\|c^\mathrm{a} - c^\mathrm{b}\|_2 \\ \|h^\mathrm{a} - h^\mathrm{b}\|_2\end{bmatrix}\right\|_{P_\mathrm{s}}^2 - \lambda_{min}(Q_\mathrm{s})\left\|\begin{bmatrix}\|c^\mathrm{a} - c^\mathrm{b}\|_2 \\ \|h^\mathrm{a} - h^\mathrm{b}\|_2\end{bmatrix}\right\|^2} \\ &\leq \sqrt{\left(1 - \frac{\lambda_{min}(Q_\mathrm{s})}{\lambda_{max}(P_\mathrm{s})}\right)\left\|\begin{bmatrix}\|c^\mathrm{a} - c^\mathrm{b}\|_2 \\ \|h^\mathrm{a} - h^\mathrm{b}\|_2\end{bmatrix}\right\|_{P_\mathrm{s}}^2} = \rho_\mathrm{s} V_\mathrm{s}(x_\mathrm{a}, x_\mathrm{b}).\end{aligned}$$

Finally, to verify condition (7.6c), consider the j-th row of $|W_\mathrm{y}(h^\mathrm{a} - h^\mathrm{b})|$

for $j = 1, ..., p$:

$$
\begin{aligned}
|W_{\mathrm{y}(j*)}(h^{\mathrm{a}} - h^{\mathrm{b}})| &= \left| [\mathbf{0}_{1,n} \; W_{\mathrm{y}(j*)}] \begin{bmatrix} c^{\mathrm{a}} - c^{\mathrm{b}} \\ h^{\mathrm{a}} - h^{\mathrm{b}} \end{bmatrix} \right| \\
&\leq \left| \left[\|\mathbf{0}_{n,1}\| \;\; \left\|W_{\mathrm{y}(j*)}\right\| \right] \begin{bmatrix} \|c^{\mathrm{a}} - c^{\mathrm{b}}\|_2 \\ \|h^{\mathrm{a}} - h^{\mathrm{b}}\|_2 \end{bmatrix} \right| \\
&= \left| \left[0 \;\; \left\|W_{\mathrm{y}(j*)}\right\| \right] P_{\mathrm{s}}^{-1/2} P_{\mathrm{s}}^{1/2} \begin{bmatrix} \|c^{\mathrm{a}} - c^{\mathrm{b}}\|_2 \\ \|h^{\mathrm{a}} - h^{\mathrm{b}}\|_2 \end{bmatrix} \right| \\
&\leq \left\| \left[0 \;\; \left\|W_{\mathrm{y}(j*)}\right\| \right] P_{\mathrm{s}}^{-1/2} \right\| \cdot \left\| P_{\mathrm{s}}^{1/2} \begin{bmatrix} \|c^{\mathrm{a}} - c^{\mathrm{b}}\|_2 \\ \|h^{\mathrm{a}} - h^{\mathrm{b}}\|_2 \end{bmatrix} \right\| \\
&= c_{\mathrm{s}(j)} V_{\mathrm{s}}(x^{\mathrm{a}}, x^{\mathrm{b}}).
\end{aligned}
$$

□

7.5.2 Proofs of Lemma 7.2 and of Corollary 7.1

Proof of Lemma 7.2

Existence of x^*: We first prove that if a constant input u is applied to a δISS system, then the resulting state trajectory is asymptotically constant. Considering any possible initial state x_0, and applying the definition of δISS (2.10) with $x_0^{\mathrm{b}} = x_0$, $x_0^{\mathrm{a}} = x_1 = f(x_0, u)$ and $u_h^{\mathrm{a}} = u_h^{\mathrm{b}} = u$ for all $h = 0, ..., k-1$, it follows that

$$\|x_{k+1} - x_k\| \leq \beta(\|x_1 - x_0\|, k).$$

Hence the difference between x_{k+1} and x_k becomes small when k increases. By summing up the previous inequality one has that $\lim_{T\to\infty} \|x_T - x_0\| \leq \sum_{k=0}^{\infty} \beta(\|x_1 - x_0\|, k)$, that is finite in view of the exponential nature of the function β. Then, the resulting trajectory is asymptotically constant. Moreover, given any u there exists x^* solving (7.9), that corresponds to the asymptotic value of the trajectories associated to the constant input u. Finally, $x^* \in \mathcal{X}$ in view of the positive invariance of $\mathcal{X}$.

Uniqueness of x^*: Consider the definition of δISS (2.10), and assume that there exist two different equilibrium states x_{a}^* and x_{b}^* corresponding to the same input u. Under this assumption it is possible to study the evolution of the system with $x_0^{\mathrm{a}} = x_{\mathrm{a}}^*$, $x_0^{\mathrm{b}} = x_{\mathrm{b}}^*$ and $u_h^{\mathrm{a}} = u_h^{\mathrm{b}} = u$ for all $h = 0, ..., k-1$. Then, for the δISS assumption, it follows that $\|x_k^{\mathrm{a}} - x_k^{\mathrm{b}}\| \to 0$ for $k \to \infty$. This is a contradiction with the fact that x_{a}^* and x_{b}^* are two different equilibrium states. Then the equilibrium state x^* is unique. □

Proof of Corollary 7.1

The existence and uniqueness of x^* follows from Lemma 7.2. Then there exists a unique value d^* satisfying (7.10b), that is $d^* = y - g(x^*)$. □

7.5.3 Proof of Lemma 7.3

First, we recall from [230] that $\bar{\sigma}_\mathrm{f}$, $\bar{\sigma}_\mathrm{i}$, $\bar{\sigma}_\mathrm{o}$ and $\bar{\sigma}_\mathrm{c}$ are bounds on the values of the gates of the LSTM. In particular, if $h \in \mathcal{H}$ and $u \in \mathcal{U}$, then for $j = 1, ..., n_c$

$$|\sigma(W_\mathrm{f} u + U_\mathrm{f} h + b_\mathrm{f})_{(j)}| \leq \bar{\sigma}_\mathrm{f}, \tag{7.28a}$$

$$|\sigma(W_\mathrm{i} u + U_\mathrm{i} h + b_\mathrm{i})_{(j)}| \leq \bar{\sigma}_\mathrm{i}, \tag{7.28b}$$

$$|\sigma(W_\mathrm{o} u + U_\mathrm{o} h + b_\mathrm{o})_{(j)}| \leq \bar{\sigma}_\mathrm{o}, \tag{7.28c}$$

$$|\tanh(W_\mathrm{c} u + U_\mathrm{c} h + b_\mathrm{c})_{(j)}| \leq \bar{\sigma}_\mathrm{c}. \tag{7.28d}$$

Consider Equation (7.11b) for $\hat{h}$. $\mathcal{H}$ is an invariant set for $\hat{h}$ because each component of $\hat{h}_{k+1}$ is computed as the product between a sigmoid function, whose output lies in $(0, 1)$, and an hyperbolic tangent, whose output lies in $(-1, 1)$.

Moreover, $\mathcal{D}$ is an invariant set for $\hat{d}$ in view of the saturation in Equation (7.11c).

It is now proved that $\hat{\mathcal{C}}$ is a positive invariant set for $\hat{c}$. First note that if $u \in \mathcal{U}$, $h, \hat{h} \in \mathcal{H}$, $d, \hat{d} \in \mathcal{D}$, in view of (7.7d), one has that

$$\begin{aligned}
&|\sigma(W_\mathrm{f} u + U_\mathrm{f} \hat{h} + b_\mathrm{f} + L_\mathrm{f}(y - \hat{y}))_{(j)}| \\
&= \sigma\left((W_\mathrm{f} u + U_\mathrm{f} \hat{h} + b_\mathrm{f} + L_\mathrm{f}(y - \hat{y}))_{(j)}\right) \\
&\leq \sigma\left(\left|(W_\mathrm{f} u + U_\mathrm{f} \hat{h} + b_\mathrm{f} + L_\mathrm{f}(y - \hat{y}))_{(j)}\right|\right) \\
&\leq \sigma\left(\max_{u,h,\hat{h},d,\hat{d}} \max_{j} \left|(W_\mathrm{f} u + U_\mathrm{f} \hat{h} + b_\mathrm{f} + L_\mathrm{f}(y - \hat{y}))_{(j)}\right|\right) \\
&= \sigma\left(\max_{u,h,\hat{h},d,\hat{d}} \|W_\mathrm{f} u + U_\mathrm{f} \hat{h} + b_\mathrm{f} + L_\mathrm{f}(y - \hat{y})\|_\infty\right) \\
&\leq \sigma(\|[W_\mathrm{f} u_{max},\ U_\mathrm{f} - L_\mathrm{f} W_\mathrm{y},\ b_\mathrm{f},\ L_\mathrm{f} W_\mathrm{y},\ 2L_\mathrm{f} d_{max}]\|_\infty) = \hat{\bar{\sigma}}_\mathrm{f}
\end{aligned} \tag{7.29}$$

and that

$$|\sigma(W_\mathrm{i} u + U_\mathrm{i} \hat{h} + b_\mathrm{i} + L_\mathrm{i}(y - \hat{y}))_{(j)}| \leq \hat{\bar{\sigma}}_\mathrm{i}. \tag{7.30}$$

Consider now the j-th component of $\hat{c}$, and assume $\hat{c}_k \in \hat{\mathcal{C}}$, $h_k, \hat{h}_k \in \mathcal{H}$ and $d_k, \hat{d}_k \in \mathcal{D}$. By taking the absolute value of the j-th component of (7.11a) one gets

$$\begin{aligned}
|\hat{c}_{k+1(j)}| &\leq |\sigma(W_\mathrm{f} u_k + U_\mathrm{f} \hat{h}_k + b_\mathrm{f} + L_\mathrm{f}(y - \hat{y}))_{(j)}| \cdot |\hat{c}_{k(j)}| \\
&+ |\sigma(W_\mathrm{i} u_k + U_\mathrm{i} \hat{h}_k + b_\mathrm{i} + L_\mathrm{i}(y - \hat{y}))_{(j)}| \cdot |\tanh(W_\mathrm{c} u_k + U_\mathrm{c} \hat{h}_k + b_\mathrm{c})_{(j)}| \\
&\overset{(7.28\mathrm{d})(7.29)(7.30)}{\leq} \hat{\bar{\sigma}}_\mathrm{f} |\hat{c}_{k(j)}| + \hat{\bar{\sigma}}_\mathrm{i} \bar{\sigma}_\mathrm{c} \leq \frac{\hat{\bar{\sigma}}_\mathrm{i} \bar{\sigma}_\mathrm{c}}{1 - \hat{\bar{\sigma}}_\mathrm{f}}
\end{aligned}$$

i.e. $\hat{\mathcal{C}}$ is a positive invariant set for state $\hat{c}$. □

7.5.4 Proof of Theorem 7.1

The proof is divided in three parts:

1. Derivation of an upper bound for the evolution of the observer estimation error;
2. Proof of the properties (7.14) of the observer Lyapunov function V_{o};
3. Proof of convergence, under the assumption that $w_k \to 0$ for $k \to \infty$.

Part 1: First note that, in a similar way to (7.29), it is possible to show that

$$|\sigma(W_{\mathrm{o}}u + U_{\mathrm{o}}\hat{h} + b_{\mathrm{o}} + L_{\mathrm{o}}(y - \hat{y}))_{(j)}| \leq \hat{\bar{\sigma}}_{\mathrm{o}}. \tag{7.31}$$

Let's now define the error variables $e_{\mathrm{c}} := c - \hat{c}$, $e_{\mathrm{h}} := h - \hat{h}$ and $e_{\mathrm{d}} := d - \hat{d}$, and let's study their evolution in time.

Consider the time evolution of e_c:

$$\begin{aligned}
e_{\mathrm{c}}^{+} &= c^{+} - \hat{c}^{+} \\
&= \sigma(W_{\mathrm{f}}u + U_{\mathrm{f}}h + b_{\mathrm{f}}) \otimes c + \sigma(W_{\mathrm{i}}u + U_{\mathrm{i}}h + b_{\mathrm{i}}) \otimes \tanh(W_{\mathrm{c}}u + U_{\mathrm{c}}h + b_{\mathrm{c}}) \\
&\quad - \Big(\sigma(W_{\mathrm{f}}u + U_{\mathrm{f}}\hat{h} + b_{\mathrm{f}} + L_{\mathrm{f}}(y - \hat{y})) \otimes \hat{c} \\
&\quad + \sigma(W_{\mathrm{i}}u + U_{\mathrm{i}}\hat{h} + b_{\mathrm{i}} + L_{\mathrm{i}}(y - \hat{y})) \otimes \tanh(W_{\mathrm{c}}u + U_{\mathrm{c}}\hat{h} + b_{\mathrm{c}})\Big) \\
&= \sigma(W_{\mathrm{f}}u + U_{\mathrm{f}}\hat{h} + b_{\mathrm{f}} + L_{\mathrm{f}}(y - \hat{y})) \otimes (c - \hat{c}) \\
&\quad + c \otimes \Big(\sigma(W_{\mathrm{f}}u + U_{\mathrm{f}}h + b_{\mathrm{f}}) - \sigma(W_{\mathrm{f}}u + U_{\mathrm{f}}\hat{h} + b_{\mathrm{f}} + L_{\mathrm{f}}(y - \hat{y}))\Big) \\
&\quad + \sigma(W_{\mathrm{i}}u + U_{\mathrm{i}}h + b_{\mathrm{i}}) \otimes \\
&\quad \Big(\tanh(W_{\mathrm{c}}u + U_{\mathrm{c}}h + b_{\mathrm{c}}) - \tanh(W_{\mathrm{c}}u + U_{\mathrm{c}}\hat{h} + b_{\mathrm{c}})\Big) \\
&\quad + \tanh(W_{\mathrm{c}}u + U_{\mathrm{c}}\hat{h} + b_{\mathrm{c}}) \otimes \\
&\quad \Big(\sigma(W_{\mathrm{i}}u + U_{\mathrm{i}}h + b_{\mathrm{i}}) - \sigma(W_{\mathrm{i}}u + U_{\mathrm{i}}\hat{h} + b_{\mathrm{i}} + L_{\mathrm{i}}(y - \hat{y}))\Big).
\end{aligned}$$

Taking the norm of both sides, exploiting $c \in \mathcal{C}$, (4.1c), (7.28), (7.29), (7.31), the definition of $\bar{\sigma}_{\mathrm{x}}$, and the fact that $\sigma(\cdot)$ and $\tanh(\cdot)$ are Lipschitz continuous functions with Lipschitz constants respectively of $\frac{1}{4}$ and 1, one has that

$$\begin{aligned}
\|e_{\mathrm{c}}^{+}\|_2 &\leq \hat{\bar{\sigma}}_{\mathrm{f}}\|e_{\mathrm{c}}\|_2 + \frac{\bar{\sigma}_{\mathrm{i}}\bar{\sigma}_{\mathrm{c}}}{1 - \bar{\sigma}_{\mathrm{f}}}\frac{1}{4}\|U_{\mathrm{f}}h - U_{\mathrm{f}}\hat{h} - L_{\mathrm{f}}W_{\mathrm{y}}(h - \hat{h}) - L_{\mathrm{f}}(d - \hat{d})\|_2 \\
&\quad + \bar{\sigma}_{\mathrm{i}}\|U_{\mathrm{c}}(h - \hat{h})\|_2 + \bar{\sigma}_{\mathrm{c}}\frac{1}{4}\|U_{\mathrm{i}}h - U_{\mathrm{i}}\hat{h} - L_{\mathrm{i}}W_{\mathrm{y}}(h - \hat{h}) - L_{\mathrm{i}}(d - \hat{d})\|_2 \\
&\leq \hat{\bar{\sigma}}_{\mathrm{f}}\|e_{\mathrm{c}}\|_2 + \frac{\bar{\sigma}_{\mathrm{i}}\bar{\sigma}_{\mathrm{c}}}{1 - \bar{\sigma}_{\mathrm{f}}}\frac{1}{4}(\|U_{\mathrm{f}} - L_{\mathrm{f}}W_{\mathrm{y}}\|_2\|e_{\mathrm{h}}\|_2 + \|L_{\mathrm{f}}\|_2\|e_{\mathrm{d}}\|_2) \\
&\quad + \bar{\sigma}_{\mathrm{i}}\|U_{\mathrm{c}}\|_2\|e_{\mathrm{h}}\|_2 + \frac{1}{4}\bar{\sigma}_{\mathrm{c}}(\|U_{\mathrm{i}} - L_{\mathrm{i}}W_{\mathrm{y}}\|_2\|e_{\mathrm{h}}\|_2 + \|L_{\mathrm{i}}\|_2\|e_{\mathrm{d}}\|_2).
\end{aligned}$$

Ordering all terms one has

$$\begin{aligned}\|e_{\mathrm{c}}^{+}\|_2 \leq\ & \hat{\bar{\sigma}}_{\mathrm{f}}\|e_{\mathrm{c}}\|_2 \\ & + \left(\frac{1}{4}\frac{\bar{\sigma}_{\mathrm{i}}\bar{\sigma}_{\mathrm{c}}}{1-\bar{\sigma}_{\mathrm{f}}}\|U_{\mathrm{f}}-L_{\mathrm{f}}W_{\mathrm{y}}\|_2 + \bar{\sigma}_{\mathrm{i}}\|U_{\mathrm{c}}\|_2 + \frac{1}{4}\bar{\sigma}_{\mathrm{c}}\|U_{\mathrm{i}}-L_{\mathrm{i}}W_{\mathrm{y}}\|_2\right)\|e_{\mathrm{h}}\|_2 \\ & + \left(\frac{1}{4}\frac{\bar{\sigma}_{\mathrm{i}}\bar{\sigma}_{\mathrm{c}}}{1-\bar{\sigma}_{\mathrm{f}}}\|L_{\mathrm{f}}\|_2 + \frac{1}{4}\bar{\sigma}_{\mathrm{c}}\|L_{\mathrm{i}}\|_2\right)\|e_{\mathrm{d}}\|_2 \\ =\ & \hat{\bar{\sigma}}_{\mathrm{f}}\|e_{\mathrm{c}}\|_2 + \hat{\alpha}\|e_{\mathrm{h}}\|_2 + \hat{\beta}\|e_{\mathrm{d}}\|_2.\end{aligned} \tag{7.32}$$

Consider the time evolution of e_{h}:

$$\begin{aligned}e_{\mathrm{h}}^{+} &= h^{+} - \hat{h}^{+} \\ &= \sigma(W_{\mathrm{o}}u + U_{\mathrm{o}}h + b_{\mathrm{o}}) \otimes \tanh(c^{+}) \\ &\quad - \sigma(W_{\mathrm{o}}u + U_{\mathrm{o}}\hat{h} + b_{\mathrm{o}} + L_{\mathrm{o}}(y-\hat{y})) \otimes \tanh(\hat{c}^{+}) \\ &= \sigma(W_{\mathrm{o}}u + U_{\mathrm{o}}\hat{h} + b_{\mathrm{o}} + L_{\mathrm{o}}(y-\hat{y})) \otimes (\tanh(c^{+}) - \tanh(\hat{c}^{+})) \\ &\quad + \tanh(c^{+}) \otimes \Big(\sigma(W_{\mathrm{o}}u + U_{\mathrm{o}}h + b_{\mathrm{o}}) - \sigma(W_{\mathrm{o}}u + U_{\mathrm{o}}\hat{h} + b_{\mathrm{o}} + L_{\mathrm{o}}(y-\hat{y}))\Big).\end{aligned}$$

Taking the norm of both sides, exploiting (7.28), (7.29), (7.31), the definition of $\bar{\sigma}_{\mathrm{x}}$, lipschitzianity of $\sigma(\cdot)$ and $\tanh(\cdot)$, one has that

$$\begin{aligned}\|e_{\mathrm{h}}^{+}\|_2 &\leq \hat{\bar{\sigma}}_{\mathrm{o}}\|c^{+} - \hat{c}^{+}\|_2 + \bar{\sigma}_{\mathrm{x}}\frac{1}{4}\|U_{\mathrm{o}}h - U_{\mathrm{o}}\hat{h} - L_{\mathrm{o}}W_{\mathrm{y}}(h-\hat{h}) - L_{\mathrm{o}}(d-\hat{d})\|_2 \\ &\leq \hat{\bar{\sigma}}_{\mathrm{o}}\|e_{\mathrm{c}}^{+}\|_2 + \frac{1}{4}\bar{\sigma}_{\mathrm{x}}\|U_{\mathrm{o}} - L_{\mathrm{o}}W_{\mathrm{y}}\|_2\|e_{\mathrm{h}}\|_2 + \frac{1}{4}\bar{\sigma}_{\mathrm{x}}\|L_{\mathrm{o}}\|_2\|e_{\mathrm{d}}\|_2.\end{aligned}$$

By substituting $\|e_{\mathrm{c}}^{+}\|_2$ with its upper bound (7.32) and ordering all terms one has

$$\|e_{\mathrm{h}}^{+}\|_2 \leq \hat{\bar{\sigma}}_{\mathrm{o}}\hat{\bar{\sigma}}_{\mathrm{f}}\|e_{\mathrm{c}}\|_2 + \hat{\gamma}\|e_{\mathrm{h}}\|_2 + (\hat{\bar{\sigma}}_{\mathrm{o}}\hat{\beta} + \frac{1}{4}\bar{\sigma}_{\mathrm{x}}\|L_{\mathrm{o}}\|_2)\|e_{\mathrm{d}}\|_2. \tag{7.33}$$

Consider the evolution in time of e_{d}. First define $\hat{d}_{ns}^{+} := \hat{d} + L_{\mathrm{d}}(y-\hat{y})$, that is (7.11c) without the saturation operator. Then

$$\begin{aligned}e_{\mathrm{d},ns}^{+} &= d^{+} - \hat{d}_{ns}^{+} = d + w - \hat{d} - L_{\mathrm{d}}W_{\mathrm{y}}(h-\hat{h}) - L_{\mathrm{d}}(d-\hat{d}) \\ &= (I_p - L_{\mathrm{d}})e_{\mathrm{d}} - L_{\mathrm{d}}W_{\mathrm{y}}e_{\mathrm{h}} + w.\end{aligned}$$

By taking the norm of both sides one has that

$$\|e_{\mathrm{d},ns}^{+}\|_2 \leq \|L_{\mathrm{d}}W_{\mathrm{y}}\|_2\|e_{\mathrm{h}}\|_2 + \|I_p - L_{\mathrm{d}}\|_2\|e_{\mathrm{d}}\|_2 + \|w\|_2. \tag{7.34}$$

Moreover, noting that $\|e_{\mathrm{d}}^{+}\|_2 \leq \|e_{\mathrm{d},ns}^{+}\|_2$, it is possible to write in matrix form (7.32), (7.33) and (7.34), obtaining

$$\begin{bmatrix}\|e_{\mathrm{c}}^{+}\|_2 \\ \|e_{\mathrm{h}}^{+}\|_2 \\ \|e_{\mathrm{d}}^{+}\|_2\end{bmatrix} \leq A_{\mathrm{d}}\begin{bmatrix}\|e_{\mathrm{c}}\|_2 \\ \|e_{\mathrm{h}}\|_2 \\ \|e_{\mathrm{d}}\|_2\end{bmatrix} + \begin{bmatrix}0 \\ 0 \\ 1\end{bmatrix}\|w\|_2 \tag{7.35}$$

where A_d is defined in (7.12).

Part 2: Condition (7.14a) is easily verified for the definition of V_o.

Proof of (7.14b) is shown in the following:

$$V_\mathrm{o}(\hat{\chi}^+,\chi^+) = \left\| \begin{bmatrix} \|\hat{c}^+ - c^+\|_2 \\ \|\hat{h}^+ - h^+\|_2 \\ \|\hat{d}^+ - d^+\|_2 \end{bmatrix} \right\|_{P_\mathrm{o}} \overset{(7.35)}{\leq} \left\| A_\mathrm{d} \begin{bmatrix} \|\hat{c} - c\|_2 \\ \|\hat{h} - h\|_2 \\ \|\hat{d} - d\|_2 \end{bmatrix} + \begin{bmatrix} 0 \\ 0 \\ 1 \end{bmatrix} \|w\|_2 \right\|_{P_\mathrm{o}}$$
$$\leq \left\| A_\mathrm{d} \begin{bmatrix} \|\hat{c} - c\|_2 \\ \|\hat{h} - h\|_2 \\ \|\hat{d} - d\|_2 \end{bmatrix} \right\|_{P_\mathrm{o}} + \left\| \begin{bmatrix} 0 \\ 0 \\ 1 \end{bmatrix} \|w\|_2 \right\|_{P_\mathrm{o}}.$$

The two terms of this sum are now considered separately.

For the first term we have that

$$\left\| A_\mathrm{d} \begin{bmatrix} \|\hat{c} - c\|_2 \\ \|\hat{h} - h\|_2 \\ \|\hat{d} - d\|_2 \end{bmatrix} \right\|_{P_\mathrm{o}} = \sqrt{\begin{bmatrix} \|\hat{c} - c\|_2 \\ \|\hat{h} - h\|_2 \\ \|\hat{d} - d\|_2 \end{bmatrix}^\top A_\mathrm{d}^\top P_\mathrm{o} A_\mathrm{d} \begin{bmatrix} \|\hat{c} - c\|_2 \\ \|\hat{h} - h\|_2 \\ \|\hat{d} - d\|_2 \end{bmatrix}}$$
$$= \sqrt{\begin{bmatrix} \|\hat{c} - c\|_2 \\ \|\hat{h} - h\|_2 \\ \|\hat{d} - d\|_2 \end{bmatrix}^\top (P_\mathrm{o} - Q_\mathrm{o}) \begin{bmatrix} \|\hat{c} - c\|_2 \\ \|\hat{h} - h\|_2 \\ \|\hat{d} - d\|_2 \end{bmatrix}}$$
$$\leq \sqrt{\left\| \begin{bmatrix} \|\hat{c} - c\|_2 \\ \|\hat{h} - h\|_2 \\ \|\hat{d} - d\|_2 \end{bmatrix} \right\|_{P_\mathrm{o}}^2 - \lambda_{min}(Q_\mathrm{o}) \left\| \begin{bmatrix} \|\hat{c} - c\|_2 \\ \|\hat{h} - h\|_2 \\ \|\hat{d} - d\|_2 \end{bmatrix} \right\|_2^2}$$
$$\leq \sqrt{\left(1 - \frac{\lambda_{min}(Q_\mathrm{o})}{\lambda_{max}(P_\mathrm{o})}\right) \left\| \begin{bmatrix} \|\hat{c} - c\|_2 \\ \|\hat{h} - h\|_2 \\ \|\hat{d} - d\|_2 \end{bmatrix} \right\|_{P_\mathrm{o}}^2}$$
$$= \sqrt{1 - \frac{\lambda_{min}(Q_\mathrm{o})}{\lambda_{max}(P_\mathrm{o})}} V_\mathrm{o}(\hat{\chi},\chi) = \rho_\mathrm{o} V_\mathrm{o}(\hat{\chi},\chi).$$

For the second term, in view of boundedness of set $\mathcal{W}$, we have that there exists a finite constant $\bar{w}$ such that for all $w \in \mathcal{W}$

$$\left\| \begin{bmatrix} 0 \\ 0 \\ 1 \end{bmatrix} \|w\|_2 \right\|_{P_\mathrm{o}} \leq \sqrt{P_{\mathrm{o}(3,3)}} w_{max} =: \bar{w}.$$

It follows that $V_\mathrm{o}(\hat{\chi}^+,\chi^+) \leq \rho_\mathrm{o} V_\mathrm{o}(\hat{\chi},\chi) + \bar{w}$.

Condition (7.14c) is now verified. Consider the j-th row of $|W_\mathrm{y}(h - \hat{h}) +$

$(d - \hat{d})|$:

$$
\begin{aligned}
&|W_{\mathrm{y}(j*)}(h - \hat{h}) + (d_{(j)} - \hat{d}_{(j)})| \\
&= \left| [\mathbf{0}_{1,n} \; W_{\mathrm{y}(j*)} \; I_{p(j*)}] \begin{bmatrix} c - \hat{c} \\ h - \hat{h} \\ d - \hat{d} \end{bmatrix} \right| \\
&\leq \left| \begin{bmatrix} 0 & \left\| W_{\mathrm{y}(j*)} \right\|_2 & 1 \end{bmatrix} \begin{bmatrix} \|c - \hat{c}\|_2 \\ \|h - \hat{h}\|_2 \\ \|d - \hat{d}\|_2 \end{bmatrix} \right| \\
&= \left| \begin{bmatrix} 0 & \left\| W_{\mathrm{y}(j*)} \right\|_2 & 1 \end{bmatrix} P_{\mathrm{o}}^{-1/2} P_{\mathrm{o}}^{1/2} \begin{bmatrix} \|c - \hat{c}\|_2 \\ \|h - \hat{h}\|_2 \\ \|d - \hat{d}\|_2 \end{bmatrix} \right| \\
&\leq \left\| \begin{bmatrix} 0 & \left\| W_{\mathrm{y}(j*)} \right\|_2 & 1 \end{bmatrix} P_{\mathrm{o}}^{-1/2} \right\|_2 \cdot \left\| P_{\mathrm{o}}^{1/2} \begin{bmatrix} \|c - \hat{c}\|_2 \\ \|h - \hat{h}\|_2 \\ \|d - \hat{d}\|_2 \end{bmatrix} \right\|_2 = c_{\mathrm{o}(j)} V_{\mathrm{o}}(\hat{\chi}, \chi).
\end{aligned}
$$

Finally, to study condition (7.14d), first note that

$$
\left\| \hat{\chi}^+ - f_{aug}(\hat{\chi}, u) \right\|_2 = \left\| \begin{bmatrix} \|\hat{c}^+ - f_{\mathrm{c}}(\hat{\chi}, u)\|_2 \\ \|\hat{h}^+ - f_{\mathrm{h}}(\hat{\chi}, u)\|_2 \\ \|\hat{d}^+ - f_{\mathrm{d}}(\hat{\chi}, u)\|_2 \end{bmatrix} \right\|_2
$$

where f_{c} and f_{h} represent Equations (7.7a) and (7.7b) respectively, and f_{d} represents Equation (7.7c) without the term w_k.

Consider $\hat{c}^+ - f_{\mathrm{c}}(\hat{\chi}, u)$:

$$
\begin{aligned}
\hat{c}^+ - f_{\mathrm{c}}(\hat{\chi}, u) = \; & \sigma(W_{\mathrm{f}} u + U_{\mathrm{f}} \hat{h} + b_{\mathrm{f}} + L_{\mathrm{f}}(y - \hat{y})) \otimes \hat{c} \\
& + \sigma(W_{\mathrm{i}} u + U_{\mathrm{i}} \hat{h} + b_{\mathrm{i}} + L_{\mathrm{i}}(y - \hat{y})) \otimes \tanh(W_{\mathrm{c}} u + U_{\mathrm{c}} \hat{h} + b_{\mathrm{c}}) \\
& - \Big(\sigma(W_{\mathrm{f}} u + U_{\mathrm{f}} \hat{h} + b_{\mathrm{f}}) \otimes \hat{c} \\
& + \sigma(W_{\mathrm{i}} u + U_{\mathrm{i}} \hat{h} + b_{\mathrm{i}}) \otimes \tanh(W_{\mathrm{c}} u + U_{\mathrm{c}} \hat{h} + b_{\mathrm{c}}) \Big) \\
= \; & \Big(\sigma(W_{\mathrm{f}} u + U_{\mathrm{f}} \hat{h} + b_{\mathrm{f}} + L_{\mathrm{f}}(y - \hat{y})) - \sigma(W_{\mathrm{f}} u + U_{\mathrm{f}} \hat{h} + b_{\mathrm{f}}) \Big) \otimes \hat{c} \\
& + \Big(\sigma(W_{\mathrm{i}} u + U_{\mathrm{i}} \hat{h} + b_{\mathrm{i}} + L_{\mathrm{i}}(y - \hat{y})) \\
& - \sigma(W_{\mathrm{i}} u + U_{\mathrm{i}} \hat{h} + b_{\mathrm{i}}) \Big) \otimes \tanh(W_{\mathrm{c}} u + U_{\mathrm{c}} \hat{h} + b_{\mathrm{c}}).
\end{aligned}
$$

Taking the norm of both sides, exploiting the positive invariance of the set $\hat{\mathcal{I}}$, the upper bound (7.28d), and lipschitzianity of $\sigma(\cdot)$ and $\tanh(\cdot)$ we have

that

$$\begin{aligned}\left\|\hat{c}^+ - f_{\mathrm{c}}(\hat{\chi}, u)\right\|_2 &\leq \frac{1}{4}\left\|L_{\mathrm{f}}(y-\hat{y})\right\|_2 \left\|\hat{c}\right\|_2 \\ &\quad + \frac{1}{4}\left\|L_{\mathrm{i}}(y-\hat{y})\right\|_2 \left\|\tanh(W_{\mathrm{c}}u + U_{\mathrm{c}}\hat{h} + b_{\mathrm{c}})\right\|_2 \\ &\leq \frac{1}{4}\frac{\hat{\bar{\sigma}}_{\mathrm{i}}\bar{\sigma}_{\mathrm{c}}}{1-\hat{\bar{\sigma}}_{\mathrm{f}}}\left\|L_{\mathrm{f}}W_{\mathrm{y}}\right\|_2 \left\|h-\hat{h}\right\|_2 + \frac{1}{4}\left\|L_{\mathrm{f}}\right\|_2 \frac{\hat{\bar{\sigma}}_{\mathrm{i}}\bar{\sigma}_{\mathrm{c}}}{1-\hat{\bar{\sigma}}_{\mathrm{f}}}\left\|d-\hat{d}\right\|_2 \\ &\quad + \frac{1}{4}\bar{\sigma}_{\mathrm{c}}\left\|L_{\mathrm{i}}W_{\mathrm{y}}\right\|_2 \left\|h-\hat{h}\right\|_2 + \frac{1}{4}\bar{\sigma}_{\mathrm{c}}\left\|L_{\mathrm{i}}\right\|_2 \left\|d-\hat{d}\right\|_2 \qquad (7.36) \\ &= \left(\frac{1}{4}\frac{\hat{\bar{\sigma}}_{\mathrm{i}}\bar{\sigma}_{\mathrm{c}}}{1-\hat{\bar{\sigma}}_{\mathrm{f}}}\left\|L_{\mathrm{f}}W_{\mathrm{y}}\right\|_2 + \frac{1}{4}\bar{\sigma}_{\mathrm{c}}\left\|L_{\mathrm{i}}W_{\mathrm{y}}\right\|_2\right)\left\|h-\hat{h}\right\|_2 \\ &\quad + \left(\frac{1}{4}\left\|L_{\mathrm{f}}\right\|_2 \frac{\hat{\bar{\sigma}}_{\mathrm{i}}\bar{\sigma}_{\mathrm{c}}}{1-\hat{\bar{\sigma}}_{\mathrm{f}}} + \frac{1}{4}\bar{\sigma}_{\mathrm{c}}\left\|L_{\mathrm{i}}\right\|_2\right)\left\|d-\hat{d}\right\|_2.\end{aligned}$$

Consider $\hat{h}^+ - f_h(\hat{\chi}, u)$:

$$\begin{aligned}\hat{h}^+ - f_{\mathrm{h}}(\hat{\chi}, u) &= \sigma(W_{\mathrm{o}}u + U_{\mathrm{o}}\hat{h} + b_{\mathrm{o}} + L_{\mathrm{o}}(y-\hat{y})) \otimes \tanh(\hat{c}^+) \\ &\quad - \Big(\sigma(W_{\mathrm{o}}u + U_{\mathrm{o}}\hat{h} + b_{\mathrm{o}}) \otimes \tanh(f_{\mathrm{c}}(\hat{\chi}, u))\Big) \\ &= \Big(\sigma(W_{\mathrm{o}}u + U_{\mathrm{o}}\hat{h} + b_{\mathrm{o}} + L_{\mathrm{o}}(y-\hat{y})) \\ &\quad - \sigma(W_{\mathrm{o}}u + U_{\mathrm{o}}\hat{h} + b_{\mathrm{o}})\Big) \otimes \tanh(\hat{c}^+) \\ &\quad + \big(\tanh(\hat{c}^+) - \tanh(f_{\mathrm{c}}(\hat{\chi}, u))\big) \otimes \sigma(W_{\mathrm{o}}u + U_{\mathrm{o}}\hat{h} + b_{\mathrm{o}}).\end{aligned}$$

Taking the norm of both sizes, exploiting the positive invariance of the set $\hat{\mathcal{I}}$, the upper bound (7.28c), lipschitzianity of $\sigma(\cdot)$ and $\tanh(\cdot)$, and by substituting (7.36) we have that

$$\begin{aligned}\left\|\hat{h}^+ - f_{\mathrm{h}}(\hat{\chi}, u)\right\|_2 &\leq \frac{1}{4}\left\|L_{\mathrm{o}}(y-\hat{y})\right\|_2 \tanh\left(\frac{\hat{\bar{\sigma}}_{\mathrm{i}}\bar{\sigma}_{\mathrm{c}}}{1-\hat{\bar{\sigma}}_{\mathrm{f}}}\right) + \left\|\hat{c}^+ - f_{\mathrm{c}}(\hat{\chi}, u)\right\|_2 \bar{\sigma}_{\mathrm{o}} \\ &\leq \frac{1}{4}\tanh\left(\frac{\hat{\bar{\sigma}}_{\mathrm{i}}\bar{\sigma}_{\mathrm{c}}}{1-\hat{\bar{\sigma}}_{\mathrm{f}}}\right)\left\|L_{\mathrm{o}}W_{\mathrm{y}}\right\|_2 \left\|h-\hat{h}\right\|_2 \\ &\quad + \frac{1}{4}\tanh\left(\frac{\hat{\bar{\sigma}}_{\mathrm{i}}\bar{\sigma}_{\mathrm{c}}}{1-\hat{\bar{\sigma}}_{\mathrm{f}}}\right)\left\|L_{\mathrm{o}}\right\|_2 \left\|d-\hat{d}\right\|_2 \\ &\quad + \bar{\sigma}_{\mathrm{o}}\left(\frac{1}{4}\frac{\hat{\bar{\sigma}}_{\mathrm{i}}\bar{\sigma}_{\mathrm{c}}}{1-\hat{\bar{\sigma}}_{\mathrm{f}}}\left\|L_{\mathrm{f}}W_{\mathrm{y}}\right\|_2 + \frac{1}{4}\bar{\sigma}_{\mathrm{c}}\left\|L_{\mathrm{i}}W_{\mathrm{y}}\right\|_2\right)\left\|h-\hat{h}\right\|_2 \\ &\quad + \bar{\sigma}_{\mathrm{o}}\left(\frac{1}{4}\left\|L_{\mathrm{f}}\right\|_2 \frac{\hat{\bar{\sigma}}_{\mathrm{f}}\bar{\sigma}_{\mathrm{c}}}{1-\hat{\bar{\sigma}}_{\mathrm{f}}} + \frac{1}{4}\bar{\sigma}_{\mathrm{c}}\left\|L_{\mathrm{i}}\right\|_2\right)\left\|d-\hat{d}\right\|_2.\end{aligned} \qquad (7.37)$$

Consider $\hat{d}^+ - f_{\mathrm{d}}(\hat{\chi}, u)$:

$$\begin{aligned}\left\|\hat{d}^+ - f_{\mathrm{d}}(\hat{\chi}, u)\right\|_2 &= \left\|\mathrm{sat}(\hat{d} + L_{\mathrm{d}}(y - \hat{y}), d_{max}) - \hat{d}\right\|_2 \\ &\leq \left\|\hat{d} + L_{\mathrm{d}}(y - \hat{y}) - \hat{d}\right\|_2 = \|L_{\mathrm{d}}(y - \hat{y})\|_2 \\ &\leq \|L_{\mathrm{d}} W_{\mathrm{y}}\|_2 \left\|h - \hat{h}\right\|_2 + \|L_{\mathrm{d}}\|_2 \left\|d - \hat{d}\right\|_2 .\end{aligned} \tag{7.38}$$

Combining (7.36), (7.37) and (7.38), we have that

$$\begin{bmatrix}\|\hat{c}^+ - f_{\mathrm{c}}(\hat{\chi}, u)\|_2 \\ \|\hat{h}^+ - f_{\mathrm{h}}(\hat{\chi}, u)\|_2 \\ \|\hat{d}^+ - f_{\mathrm{d}}(\hat{\chi}, u)\|_2\end{bmatrix} \leq L \begin{bmatrix}\|c - \hat{c}\|_2 \\ \|h - \hat{h}\|_2 \\ \|d - \hat{d}\|_2\end{bmatrix} \tag{7.39}$$

where L is a matrix that can be obtained from (7.36)-(7.37)-(7.38). In particular

$$L := \begin{bmatrix}0 & \bar{\alpha} & \bar{\beta} \\ 0 & \bar{\gamma}\|L_{\mathrm{o}} W_{\mathrm{y}}\|_2 + \bar{\sigma}_{\mathrm{o}}\bar{\alpha} & \bar{\gamma}\|L_{\mathrm{o}}\|_2 + \bar{\sigma}_{\mathrm{o}}\bar{\beta} \\ 0 & \|L_{\mathrm{d}} W_{\mathrm{y}}\|_2 & \|L_{\mathrm{d}}\|_2\end{bmatrix}$$

with

$$\bar{\alpha} := \frac{1}{4}\frac{\hat{\bar{\sigma}}_{\mathrm{i}}\bar{\sigma}_{\mathrm{c}}}{1 - \hat{\bar{\sigma}}_{\mathrm{f}}}\|L_{\mathrm{f}} W_{\mathrm{y}}\|_2 + \frac{1}{4}\bar{\sigma}_{\mathrm{c}}\|L_{\mathrm{i}} W_{\mathrm{y}}\|_2$$

$$\bar{\beta} := \frac{1}{4}\|L_{\mathrm{f}}\|_2 \frac{\hat{\bar{\sigma}}_{\mathrm{i}}\bar{\sigma}_{\mathrm{c}}}{1 - \hat{\bar{\sigma}}_{\mathrm{f}}} + \frac{1}{4}\bar{\sigma}_{\mathrm{c}}\|L_{\mathrm{i}}\|_2$$

$$\bar{\gamma} := \frac{1}{4}\tanh\left(\frac{\hat{\bar{\sigma}}_{\mathrm{i}}\bar{\sigma}_{\mathrm{c}}}{1 - \hat{\bar{\sigma}}_{\mathrm{f}}}\right).$$

Taking the norm of both sides of (7.39), we have

$$\begin{aligned}\left\|\hat{\chi}^+ - f_{aug}(\hat{\chi}, u)\right\|_2 &\leq \left\|L \begin{bmatrix}\|c - \hat{c}\|_2 \\ \|h - \hat{h}\|_2 \\ \|d - \hat{d}\|_2\end{bmatrix}\right\|_2 = \left\|L P_{\mathrm{o}}^{-1/2} P_{\mathrm{o}}^{1/2} \begin{bmatrix}\|c - \hat{c}\|_2 \\ \|h - \hat{h}\|_2 \\ \|d - \hat{d}\|_2\end{bmatrix}\right\|_2 \\ &\leq \left\|L P_{\mathrm{o}}^{-1/2}\right\|_2 V_{\mathrm{o}}(\hat{\chi}, \chi)\end{aligned}$$

so that Equation (7.14d) is verified with $L_{max} := \left\|L P_{\mathrm{o}}^{-1/2}\right\|_2$.

Part 3: If $w_k \to 0$ for $k \to \infty$, then observer convergence immediately follows from (7.35). □

7.5.5 Proof of Lemma 7.4

Let's define $\hat{y}^0 := \hat{d} - y^0$ and $\zeta := [\bar{x}^\top \ \bar{u}^\top]^\top$. Then the equilibrium problem (7.15) can be rewritten as the problem of finding the solution of $F(\hat{y}^0, \zeta) = 0$, with

$$F(\hat{y}^0, \zeta) := \begin{bmatrix}f(\bar{x}, \bar{u}) - \bar{x} \\ g(\bar{x}) + \hat{y}^0\end{bmatrix}.$$

In this proof the function $\zeta = \gamma(\hat{y}^0)$ such that $F(\hat{y}^0, \gamma(\hat{y}^0)) = 0$ is studied. Let's define the following Jacobian matrices of F in the point $(\hat{y}^0, \gamma(\hat{y}^0))$:

$$J_\zeta(\hat{y}^0, \gamma(\hat{y}^0)) := \begin{bmatrix} \frac{\partial}{\partial x}(f(\bar{x}, \bar{u}) - \bar{x}) & \frac{\partial}{\partial u}(f(\bar{x}, \bar{u}) - \bar{x}) \\ \frac{\partial}{\partial x}(g(\bar{x}) + \hat{y}^0) & \frac{\partial}{\partial u}(g(\bar{x}) + \hat{y}^0) \end{bmatrix},$$

$$J_{\hat{y}^0}(\hat{y}^0, \gamma(\hat{y}^0)) := \begin{bmatrix} \frac{\partial}{\partial \hat{y}^0}(f(\bar{x}, \bar{u}) - \bar{x}) \\ \frac{\partial}{\partial \hat{y}^0}(g(\bar{x}) + \hat{y}^0) \end{bmatrix} = \begin{bmatrix} \mathbf{0}_{2n_c, p} \\ I_p \end{bmatrix}.$$

Under Assumption 7.3, the implicit function theorem states that

$$\frac{\partial \gamma}{\partial \hat{y}^0}(\hat{y}^0) = -[J_\zeta(\hat{y}^0, \gamma(\hat{y}^0))]^{-1} J_{\hat{y}^0}(\hat{y}^0, \gamma(\hat{y}^0)) = K(\hat{y}^0).$$

Let's denote $K(\hat{y}^0) = [K_{\bar{x}}(\hat{y}^0)^\top \; K_{\bar{u}}(\hat{y}^0)^\top]^\top$, where $K_{\bar{x}}(\hat{y}^0)$ are the first $2n_c$ rows of $K(\hat{y}^0)$ and $K_{\bar{u}}(\hat{y}^0)$ are the remaining m rows. Then, denoting

$$\bar{K} := \max_{\hat{y}^0 : y^0 \in \mathcal{Y}^0, \hat{d} \in \mathcal{D}} \left\| K_{\bar{x}}(\hat{y}^0) \right\|_2$$

it is possible to obtain a relationship between the maximum variation of $\bar{x}$ and the variation of $\hat{y}^0$:

$$\|\bar{x}_{k+1} - \bar{x}_k\|_2 \leq \bar{K} \left\| \hat{y}^0_{k+1} - \hat{y}^0_k \right\|_2.$$

Note that the maximum that defines $\bar{K}$ is always finite in view of the boundedness of the sets $\mathcal{Y}^0$ and $\mathcal{D}$.

The variation of $\hat{y}^0 = \hat{d} - y^0$ can be given by a variation of the disturbance estimation $\hat{d}$ and/or by a variation of the set-point y^0. This two contributions can be separated, obtaining

$$\|\bar{x}_{k+1} - \bar{x}_k\|_2 \leq \bar{K} \left\| \hat{d}_{k+1} - \hat{d}_k \right\|_2 + \bar{K} \left\| y^0_{k+1} - y^0_k \right\|_2. \tag{7.40}$$

The maximum variation of the disturbance estimation $\hat{d}$ depends on the maximum estimation error $\bar{e}_y$ and on the observer gain L_d. In particular it holds that

$$\left\| \hat{d}_{k+1} - \hat{d}_k \right\|_2 \overset{(7.11c)}{\leq} \|L_\mathrm{d}(y_k - \hat{y}_k)\|_2 \leq \|L_\mathrm{d}\|_2 \, \bar{e}_y \tag{7.41}$$

Then, combining (7.40) and (7.41), (7.17) is proven. □

7.5.6 Proof of Theorem 7.2

The proof is divided in 3 parts:

1. Proof of satisfaction of constraints (7.3) and (7.4), given that $(\psi, d, y^0) \in \mathcal{X}^{\mathrm{MPC}}$.

2. Proof of recursive feasibility, that is divided in:

   (a) Show that if $[c^\top\ h^\top]^\top \in \mathcal{X}_f(k)$ then $W_\mathrm{y} h + b_\mathrm{y} + d_{max}\mathbf{1}_p \leq y_{max} - a_N \hat{e}_{\mathrm{o},k} - b_N$ and $W_\mathrm{y} h + b_\mathrm{y} - d_{max}\mathbf{1}_p \geq y_{min} + a_N \hat{e}_{\mathrm{o},k} + b_N$;

   (b) Show that the candidate solution satisfies (7.20d) and (7.20e);

   (c) Show that the candidate solution satisfies the terminal constraint (7.20g).

3. Proof of ISpS and convergence, that is divided in:

   (a) Proof of ISpS;

   (b) Proof of convergence.

Part 1: If $\psi \in \mathcal{X}^{\mathrm{MPC}}$, the satisfaction of the input saturation (7.3) follows from constraint (7.20f) of the FHOCP formulation. Also the satisfaction of the output constraint (7.4) is guaranteed by the control design. In particular $y_k \leq y_{max}$ follows from

$$\begin{aligned} y_k &= W_\mathrm{y} h_k + b_\mathrm{y} + d_k \overset{(7.14c)}{\leq} W_\mathrm{y} \hat{h}_k + b_\mathrm{y} + \hat{d}_k + c_\mathrm{o} V_\mathrm{o}(\hat{\chi}_k, \chi_k) \\ &\leq W_\mathrm{y} h_{0|k} + b_\mathrm{y} + d_{max}\mathbf{1}_p + c_\mathrm{o}\hat{e}_{\mathrm{o},k} \\ &\overset{(7.21a)(7.20d)}{\leq} y_{max} - a_0 \hat{e}_{\mathrm{o},k} + a_0 \hat{e}_{\mathrm{o},k} = y_{max}. \end{aligned}$$

The fact that $y_k \geq y_{min}$ can be proven in a similar way:

$$\begin{aligned} y_k &= W_\mathrm{y} h_k + b_\mathrm{y} + d_k \overset{(7.14c)}{\geq} W_\mathrm{y} \hat{h}_k + b_\mathrm{y} + \hat{d}_k - c_\mathrm{o} V_\mathrm{o}(\hat{\chi}_k, \chi_k) \\ &\geq W_\mathrm{y} h_{0|k} + b_\mathrm{y} - d_{max}\mathbf{1}_p - c_\mathrm{o}\hat{e}_{\mathrm{o},k} \\ &\overset{(7.21a)(7.20e)}{\geq} y_{min} + a_0 \hat{e}_{\mathrm{o},k} - a_0 \hat{e}_{\mathrm{o},k} = y_{min}. \end{aligned}$$

Part 2a: To verify that if $x \in \mathcal{X}_f(k)$ then the tightened output constraints are satisfied, first note that if $x \in \mathcal{X}_f(k)$ then

$$\begin{aligned} \left|W_{\mathrm{y}(j*)}(h - \bar{h}_k)\right| &= \left|[\mathbf{0}_{1,n}\ W_{\mathrm{y}(j*)}] \begin{bmatrix} c - \bar{c}_k \\ h - \bar{h}_k \end{bmatrix}\right| \leq \left|[0\ \left\|W_{\mathrm{y}(j*)}\right\|_2] \begin{bmatrix} \|c - \bar{c}_k\|_2 \\ \left\|h - \bar{h}_k\right\|_2 \end{bmatrix}\right| \\ &= \left|[0\ \left\|W_{\mathrm{y}(j*)}\right\|_2] P_\mathrm{f}^{-1/2} P_\mathrm{f}^{1/2} \begin{bmatrix} \|c - \bar{c}_k\|_2 \\ \left\|h - \bar{h}_k\right\|_2 \end{bmatrix}\right| \\ &\leq \left\|[0\ \left\|W_{\mathrm{y}(j*)}\right\|_2] P_\mathrm{f}^{-1/2}\right\|_2 \cdot \left\|\begin{bmatrix} \|c - \bar{c}_k\|_2 \\ \left\|h - \bar{h}_k\right\|_2 \end{bmatrix}\right\|_{P_\mathrm{f}} \\ &\overset{(7.22)}{\leq} \left\|[0\ \left\|W_{\mathrm{y}(j*)}\right\|_2] P_\mathrm{f}^{-1/2}\right\|_2 \alpha_k. \end{aligned} \tag{7.42}$$

Considering now the j-th row of $W_{\mathrm{y}}h + b_{\mathrm{y}} + d_{max}\mathbf{1}_p$, we have that

$$\begin{aligned}
&W_{\mathrm{y}(j*)}h + b_{\mathrm{y}(j)} + d_{max} \\
&= W_{\mathrm{y}(j*)}(h - \bar{h}_k) + W_{\mathrm{y}(j*)}\bar{h}_k + b_{\mathrm{y}(j)} + \hat{d}_{k(j)} - \hat{d}_{k(j)} + d_{max} \\
&\overset{(7.15b)}{=} W_{\mathrm{y}(j*)}(h - \bar{h}_k) + y^0_{k(j)} - \hat{d}_{k(j)} + d_{max} \\
&\leq \left|W_{\mathrm{y}(j*)}(h - \bar{h}_k)\right| + y^0_{k(j)} + 2d_{max} \\
&\overset{(7.42)}{\leq} \left\| [0 \ \left\|W_{\mathrm{y}(j*)}\right\|_2] P_{\mathrm{f}}^{-1/2} \right\|_2 \alpha_k + y^0_{k(j)} + 2d_{max} \\
&\overset{(7.23a)}{\leq} y_{max(j)} - a_{N(j)}\tilde{e}_{\mathrm{o},k} - b_{N(j)} \overset{(7.23d)}{\leq} y_{max(j)} - a_{N(j)}\hat{e}_{\mathrm{o},k} - b_{N(j)}.
\end{aligned}$$

In a similar way it is possible to prove that $W_{\mathrm{y}}h + b_{\mathrm{y}} - d_{max}\mathbf{1}_p \geq y_{min} + a_N\hat{e}_{\mathrm{o},k} + b_N$. In fact, considering the j-th row of $-W_{\mathrm{y}}h - b_{\mathrm{y}} + d_{max}\mathbf{1}_p$, we obtain that

$$\begin{aligned}
&- W_{\mathrm{y}(j*)}h - b_{\mathrm{y}(j)} + d_{max} \\
&= -W_{\mathrm{y}(j*)}(h - \bar{h}_k) - W_{\mathrm{y}(j*)}\bar{h}_k - b_{\mathrm{y}(j)} - \hat{d}_{k(j)} + \hat{d}_{k(j)} + d_{max} \\
&\overset{(7.15b)}{=} -W_{\mathrm{y}(j*)}(h - \bar{h}_k) - y^0_{(j)} - \hat{d}_{k(j)} + d_{max} \\
&\leq \left|W_{\mathrm{y}(j*)}(h - \bar{h}_k)\right| - y^0_{(j)} + 2d_{max} \\
&\overset{(7.42)}{\leq} \left\| [0 \ \left\|W_{\mathrm{y}(j*)}\right\|_2] P_{\mathrm{f}}^{-1/2} \right\|_2 \alpha_k - y^0_{(j)} + 2d_{max} \\
&\overset{(7.23a)}{\leq} -y_{min(j)} - a_{N(j)}\tilde{e}_{\mathrm{o},k} - b_{N(j)} \overset{(7.23d)}{\leq} -y_{min(j)} - a_{N(j)}\hat{e}_{\mathrm{o},k} - b_{N(j)}.
\end{aligned}$$

Part 2b: Given the optimal solution $\mathbf{u}_k^\star$ of the optimization problem at time-step k, let's denote with $\mathbf{x}_k^\star = \{x^\star_{0|k}, ..., x^\star_{N-1|k}\}$ the associate state trajectory defined by $x^\star_{i+1|k} := f(x^\star_{i|k}, u^\star_{i|k})$ with $x^\star_{0|k} := \hat{x}_k$. Let's also define $x^\star_{N+1|k} := f(x^\star_{N|k}, \bar{u}_{k+1})$.

Let's define $\tilde{\mathbf{u}}_{k+1} = \{\tilde{u}_{i|k+1}\}_{i=0}^{N-1}$ the candidate solution at time-step $k+1$, where $\tilde{u}_{i|k+1} := u^\star_{i+1|k}$ for $i = 0, ..., N-2$ and $\tilde{u}_{N-1|k+1} := \bar{u}_{k+1}$. Note that $\bar{u}_{k+1} \in \mathcal{U}$ for Assumption 7.3. Consider also the associate trajectory $\tilde{\mathbf{x}}_{k+1} = \{\tilde{x}_{0|k+1}, ..., \tilde{x}_{N|k+1}\}$ defined by $\tilde{x}_{i+1|k+1} := f(\tilde{x}_{i|k+1}, \tilde{u}_{i|k+1})$ with $\tilde{x}_{0|k+1} := \hat{x}_{k+1}$.

Preliminarily, note that thanks to Lemma 7.1 and Theorem 7.1 we have that

$$\begin{aligned}
V_{\mathrm{s}}(\tilde{x}_{0|k+1}, x^\star_{1|k}) &\overset{(7.6a)}{\leq} c_{\mathrm{s,u}} \left\|\tilde{x}_{0|k+1} - x^\star_{1|k}\right\|_2 \leq c_{\mathrm{s,u}} \left\| \begin{bmatrix} \tilde{x}_{0|k+1} \\ \hat{d}_{k+1} \end{bmatrix} - \begin{bmatrix} x^\star_{1|k} \\ \hat{d}_k \end{bmatrix} \right\|_2 \\
&\overset{(7.14d)}{\leq} c_{\mathrm{s,u}} L_{max} V_{\mathrm{o}}(\hat{\chi}_k, \chi_k) \leq c_{\mathrm{s,u}} L_{max} \hat{e}_{\mathrm{o},k}
\end{aligned}$$

and that using Lemma 7.1 and inequality (7.6b) recursively it follows that

$$V_{\mathrm{s}}(\tilde{x}_{i|k+1}, x^\star_{i+1|k}) \leq c_{\mathrm{s,u}} \rho_{\mathrm{s}}^i L_{max} \hat{e}_{\mathrm{o},k} \tag{7.43}$$

for $i = 0, ..., N$. Moreover, as shown in Part 2a of the proof, since $x^\star_{N|k} \in \mathcal{X}_f(k)$

$$W_\mathrm{y} h^\star_{N|k} + b_\mathrm{y} + d_{max}\mathbf{1}_p \leq y_{max} - a_N \hat{e}_{\mathrm{o},k} - b_N$$
$$W_\mathrm{y} h^\star_{N|k} + b_\mathrm{y} - d_{max}\mathbf{1}_p \geq y_{min} + a_N \hat{e}_{\mathrm{o},k} + b_N.$$

Hence, $\tilde{x}_{i|k+1}$ satisfies (7.20d) for $i = 0, ..., N-1$ as shown in the following

$$\begin{aligned}
&W_\mathrm{y}\tilde{h}_{i|k+1} + b_\mathrm{y} + d_{max}\mathbf{1}_p \\
&\overset{(7.6c)}{\leq} W_\mathrm{y} h^\star_{i+1|k} + c_\mathrm{s} V_\mathrm{s}(\tilde{x}_{i|k+1}, x^\star_{i+1|k}) + b_\mathrm{y} + d_{max}\mathbf{1}_p \\
&\overset{(7.20e)(7.43)}{\leq} y_{max} - a_{i+1}\hat{e}_{\mathrm{o},k} - b_{i+1} + c_{\mathrm{s,u}}\rho_\mathrm{s}^i L_{max}\hat{e}_{\mathrm{o},k}c_\mathrm{s} \\
&\overset{(7.21)}{=} y_{max} - \rho_\mathrm{o} a_i \hat{e}_{\mathrm{o},k} - c_{\mathrm{s,u}}\rho_\mathrm{s}^i L_{max}\hat{e}_{\mathrm{o},k}c_\mathrm{s} - b_i - a_i\bar{w} + c_{\mathrm{s,u}}\rho_\mathrm{s}^i L_{max}\hat{e}_{\mathrm{o},k}c_\mathrm{s} \\
&\overset{(7.18)}{=} y_{max} - a_i\hat{e}_{\mathrm{o},k+1} - b_i.
\end{aligned}$$

In a similar way it follows that $\tilde{x}_{i|k+1}$ also satisfies (7.20e) for $i = 0, ..., N-1$:

$$\begin{aligned}
&- W_\mathrm{y}\tilde{h}_{i|k+1} - b_\mathrm{y} + d_{max}\mathbf{1}_p \\
&\overset{(7.6c)}{\leq} -W_\mathrm{y} h^\star_{i+1|k} + c_\mathrm{s} V_\mathrm{s}(\tilde{x}_{i|k+1}, x^\star_{i+1|k}) - b_\mathrm{y} + d_{max}\mathbf{1}_p \\
&\overset{(7.20e)(7.43)}{\leq} -y_{min} - a_{i+1}\hat{e}_{\mathrm{o},k} - b_{i+1} + c_{\mathrm{s,u}}\rho_\mathrm{s}^i L_{max}\hat{e}_{\mathrm{o},k}c_\mathrm{s} \\
&\overset{(7.21)}{=} -y_{min} - \rho_\mathrm{o} a_i \hat{e}_{\mathrm{o},k} - c_{\mathrm{s,u}}\rho_\mathrm{s}^i L_{max}\hat{e}_{\mathrm{o},k}c_\mathrm{s} - b_i - a_i\bar{w} + c_{\mathrm{s,u}}\rho_\mathrm{s}^i L_{max}\hat{e}_{\mathrm{o},k}c_\mathrm{s} \\
&\overset{(7.18)}{=} -y_{min} - a_i\hat{e}_{\mathrm{o},k+1} - b_i.
\end{aligned}$$

Part 2c: In this part we prove that $\tilde{x}_{N|k+1} \in \mathcal{X}_f(k+1)$, i.e.

$$\left\| \begin{bmatrix} \|\tilde{c}_{N|k+1} - \bar{c}_{k+1}\|_2 \\ \|\tilde{h}_{N|k+1} - \bar{h}_{k+1}\|_2 \end{bmatrix} \right\|_{P_\mathrm{f}} \leq \alpha_{k+1} \tag{7.44}$$

starting from the fact that $x^\star_{N|k} \in \mathcal{X}_f(k)$, i.e.

$$\left\| \begin{bmatrix} \|c^\star_{N|k} - \bar{c}_k\|_2 \\ \|h^\star_{N|k} - \bar{h}_k\|_2 \end{bmatrix} \right\|_{P_\mathrm{f}} \leq \alpha_k. \tag{7.45}$$

Comparing (7.44) and (7.45) it is apparent that both the sides of the inequalities change. Hence, an upper bound for the left hand side of (7.44) and a lower bound for the variation of the right hand side are computed in the following.

Before deriving the upper bound for the left hand side, we derive the following preliminary inequalities:

$$\left\|\tilde{x}_{N|k+1} - x^\star_{N+1|k}\right\|_2 \overset{(7.6a)}{\leq} \frac{1}{c_{\mathrm{s,l}}} V_\mathrm{s}(\tilde{x}_{N|k+1}, x^\star_{N+1|k}) \overset{(7.43)}{\leq} \frac{c_{\mathrm{s,u}}}{c_{\mathrm{s,l}}}\rho_\mathrm{s}^N L_{max}\hat{e}_{\mathrm{o},k} \tag{7.46}$$

and

$$\left\| \begin{bmatrix} \|c^\star_{N+1|k} - \bar{c}_{k+1}\|_2 \\ \|h^\star_{N+1|k} - \bar{h}_{k+1}\|_2 \end{bmatrix} \right\|_{P_f} \leq \rho_\mathrm{f} \left\| \begin{bmatrix} \|c^\star_{N|k} - \bar{c}_{k+1}\|_2 \\ \|h^\star_{N|k} - \bar{h}_{k+1}\|_2 \end{bmatrix} \right\|_{P_\mathrm{f}} \tag{7.47}$$

with $\rho_\mathrm{f} := \sqrt{1 - \frac{q}{\lambda_{max}(P_\mathrm{f})}}$. The proof of this inequality is similar to the proof of Equation (7.6b) in Lemma 7.1, using $Q_\mathrm{s} = qI_2$.

Then, the upper bound for the left hand side of (7.44) is

$$\begin{aligned}
&\left\| \begin{bmatrix} \|\tilde{c}_{N|k+1} - \bar{c}_{k+1}\|_2 \\ \|\tilde{h}_{N|k+1} - \bar{h}_{k+1}\|_2 \end{bmatrix} \right\|_{P_\mathrm{f}} \\
&\leq \left\| \begin{bmatrix} \|\tilde{c}_{N|k+1} - c^\star_{N+1|k}\|_2 \\ \|\tilde{h}_{N|k+1} - h^\star_{N+1|k}\|_2 \end{bmatrix} \right\|_{P_\mathrm{f}} + \left\| \begin{bmatrix} \|c^\star_{N+1|k} - \bar{c}_{k+1}\|_2 \\ \|h^\star_{N+1|k} - \bar{h}_{k+1}\|_2 \end{bmatrix} \right\|_{P_\mathrm{f}} \\
&\overset{(7.47)}{\leq} \sqrt{\lambda_{max}(P_\mathrm{f})} \left\| \begin{bmatrix} \|\tilde{c}_{N|k+1} - c^\star_{N+1|k}\|_2 \\ \|\tilde{h}_{N|k+1} - h^\star_{N+1|k}\|_2 \end{bmatrix} \right\|_2 + \rho_\mathrm{f} \left\| \begin{bmatrix} \|c^\star_{N|k} - \bar{c}_{k+1}\|_2 \\ \|h^\star_{N|k} - \bar{h}_{k+1}\|_2 \end{bmatrix} \right\|_{P_\mathrm{f}} \\
&\leq \sqrt{\lambda_{max}(P_\mathrm{f})} \left\| \tilde{x}_{N|k+1} - x^\star_{N+1|k} \right\|_2 \\
&\quad + \rho_\mathrm{f} \left\| \begin{bmatrix} \|c^\star_{N|k} - \bar{c}_k\|_2 \\ \|h^\star_{N|k} - \bar{h}_k\|_2 \end{bmatrix} \right\|_{P_\mathrm{f}} + \rho_f \left\| \begin{bmatrix} \|\bar{c}_k - \bar{c}_{k+1}\|_2 \\ \|\bar{h}_k - \bar{h}_{k+1}\|_2 \end{bmatrix} \right\|_{P_\mathrm{f}} \\
&\overset{(7.45)(7.46)}{\leq} \sqrt{\lambda_{max}(P_\mathrm{f})} \left(\frac{c_{\mathrm{s,u}}}{c_{\mathrm{s,l}}} \rho_\mathrm{s}^N L_{max} \hat{e}_{\mathrm{o},k} + \rho_\mathrm{f} \left\| \bar{x}_{k+1} - \bar{x}_k \right\|_2 \right) + \rho_\mathrm{f} \alpha_k \\
&\overset{(7.17)}{\leq} \sqrt{\lambda_{max}(P_\mathrm{f})} \left(\frac{c_{\mathrm{s,u}}}{c_{\mathrm{s,l}}} \rho_\mathrm{s}^N L_{max} \hat{e}_{\mathrm{o},k} + \rho_\mathrm{f} \bar{K} \left\| L_\mathrm{d} \right\|_2 \bar{e}_y + \rho_\mathrm{f} \bar{K} \left\| y^0_{k+1} - y^0_k \right\|_2 \right) \\
&\quad + \rho_\mathrm{f} \alpha_k.
\end{aligned} \tag{7.48}$$

Let's now compute a lower bound for the possible variation of α (right hand side of (7.44) and (7.45)):

$$\begin{aligned}
\alpha_{k+1} - \alpha_k &\overset{(7.23a)}{=} \min_{j \in [1:p]} \min \left\{ \alpha^{max}_{j,k+1}, \alpha^{min}_{j,k+1} \right\} - \min_{j \in [1:p]} \min \left\{ \alpha^{max}_{j,k}, \alpha^{min}_{j,k} \right\} \\
&\overset{(7.27)}{\geq} \min_{j \in [1:p]} \min \left\{ \alpha^{max}_{j,k+1} - \alpha^{max}_{j,k}, \alpha^{min}_{j,k+1} - \alpha^{min}_{j,k} \right\}.
\end{aligned}$$

Noting that

$$\begin{aligned}
&\min\left\{\alpha^{max}_{j,k+1}-\alpha^{max}_{j,k},\alpha^{min}_{j,k+1}-\alpha^{min}_{j,k}\right\}\\
&\overset{(7.23)}{=}\min\Bigg\{-\left\|[0\ \left\|W_{\mathrm{y}(j*)}\right\|_2]P_{\mathrm{f}}^{-1/2}\right\|_2^{-1}\left(y^0_{k+1(j)}-y^0_{k(j)}\right)\\
&-\left\|[0\ \left\|W_{\mathrm{y}(j*)}\right\|_2]P_{\mathrm{f}}^{-1/2}\right\|_2^{-1}a_{N(j)}(\tilde{e}_{\mathrm{o},k+1}-\tilde{e}_{\mathrm{o},k}),\\
&\left\|[0\ \left\|W_{\mathrm{y}(j*)}\right\|_2]P_{\mathrm{f}}^{-1/2}\right\|_2^{-1}\left(y^0_{k+1(j)}-y^0_{k(j)}\right)\\
&-\left\|[0\ \left\|W_{\mathrm{y}(j*)}\right\|_2]P_{\mathrm{f}}^{-1/2}\right\|_2^{-1}a_{N(j)}(\tilde{e}_{\mathrm{o},k+1}-\tilde{e}_{\mathrm{o},k})\Bigg\}\\
&=-\left\|[0\ \left\|W_{\mathrm{y}(j*)}\right\|_2]P_{\mathrm{f}}^{-1/2}\right\|_2^{-1}\left|y^0_{k+1(j)}-y^0_{k(j)}\right|\\
&+\left\|[0\ \left\|W_{\mathrm{y}(j*)}\right\|_2]P_{\mathrm{f}}^{-1/2}\right\|_2^{-1}a_{N(j)}(\tilde{e}_{\mathrm{o},k}-\tilde{e}_{\mathrm{o},k+1})
\end{aligned}$$

it is possible to derive that

$$\begin{aligned}
\alpha_k&\le\alpha_{k+1}+\max_{j\in[1:p]}\left\{\left\|[0\ \left\|W_{\mathrm{y}(j*)}\right\|_2]P_{\mathrm{f}}^{-1/2}\right\|_2^{-1}\left|y^0_{k+1(j)}-y^0_{k(j)}\right|\right\}\\
&\quad-\min_{j\in[1:p]}\left\{\left\|[0\ \left\|W_{\mathrm{y}(j*)}\right\|_2]P_{\mathrm{f}}^{-1/2}\right\|_2^{-1}a_{N(j)}(\tilde{e}_{\mathrm{o},k}-\tilde{e}_{\mathrm{o},k+1})\right\}\\
&\le\alpha_{k+1}+\max_{j\in[1:p]}\left\{\left\|[0\ \left\|W_{\mathrm{y}(j*)}\right\|_2]P_{\mathrm{f}}^{-1/2}\right\|_2^{-1}\left|y^0_{k+1(j)}-y^0_{k(j)}\right|\right\}.
\end{aligned}\tag{7.49}$$

From (7.48) and (7.49) it is possible to obtain

$$\begin{aligned}
&\left\|\begin{bmatrix}\|\tilde{c}_{N|k+1}-\bar{c}_{k+1}\|_2\\ \|\tilde{h}_{N|k+1}-\bar{h}_{k+1}\|_2\end{bmatrix}\right\|_{P_{\mathrm{f}}}\\
&\overset{(7.48)}{\le}\sqrt{\lambda_{max}(P_{\mathrm{f}})}\left(\frac{c_{\mathrm{s,u}}}{c_{\mathrm{s,l}}}\rho_{\mathrm{s}}^N L_{max}\hat{e}_{\mathrm{o},k}+\rho_{\mathrm{f}}\bar{K}\left\|L_{\mathrm{d}}\right\|_2\bar{e}_y+\rho_{\mathrm{f}}\bar{K}\left\|y^0_{k+1}-y^0_k\right\|_2\right)\\
&\quad+\rho_{\mathrm{f}}\alpha_k\\
&\overset{(7.49)}{\le}\sqrt{\lambda_{max}(P_{\mathrm{f}})}\left(\frac{c_{\mathrm{s,u}}}{c_{\mathrm{s,l}}}\rho_{\mathrm{s}}^N L_{max}\hat{e}_{\mathrm{o},k}+\rho_{\mathrm{f}}\bar{K}\left\|L_{\mathrm{d}}\right\|_2\bar{e}_y+\rho_{\mathrm{f}}\bar{K}\left\|y^0_{k+1}-y^0_k\right\|_2\right)\\
&\quad+(\rho_{\mathrm{f}}-1)\alpha_{k+1}\\
&\quad+\rho_{\mathrm{f}}\max_{j=1,\dots,p}\left\{\left\|[0\ \left\|W_{\mathrm{y}(j*)}\right\|_2]P_{\mathrm{f}}^{-1/2}\right\|_2^{-1}\left|y^0_{k+1(j)}-y^0_{k(j)}\right|\right\}+\alpha_{k+1}.
\end{aligned}$$

Finally, note that $\rho_{\mathrm{f}}<1$ by definition and $\alpha_{k+1}>0$ for all k in view of Assumption 7.4. Then there exist $\bar{L}_{max}>0$, $\bar{L}_{\mathrm{d}}>0$ and $\Delta y^0_{max}>0$ such that for $L_{max}\le\bar{L}_{max}$, $\|L_{\mathrm{d}}\|_2\le\bar{L}_{\mathrm{d}}$ and y^0 such that $\left\|y^0_{k+1}-y^0_k\right\|_2\le\Delta y^0_{max}$

$$\left\|\begin{bmatrix}\|\tilde{c}_{N|k+1}-\bar{c}_{k+1}\|_2\\ \|\tilde{h}_{N|k+1}-\bar{h}_{k+1}\|_2\end{bmatrix}\right\|_{P_{\mathrm{f}}}\le\alpha_{k+1}.$$

Part 3: To prove the ISpS and convergence properties of the closed-loop system we introduce a candidate Lyapunov function with a structure similar to the optimal cost of the MPC where the asymptotic values of the state and input set-points are used, instead of their values at time-step k. Note that these values cannot be used in the MPC cost function because they are unknown. The candidate Lyapunov function is defined as

$$W_k := \sum_{i=0}^{N-1} \left(\|x^\star_{i|k} - \bar{x}_\infty\|_Q^2 + \|u^\star_{i|k} - \bar{u}_\infty\|_R^2 \right) + \left\| \begin{bmatrix} \|c^\star_{N|k} - \bar{c}_\infty\|_2 \\ \|h^\star_{N|k} - \bar{h}_\infty\|_2 \end{bmatrix} \right\|_{P_\mathrm{f}}^2$$

where $u^\star_{0|k}, ..., u^\star_{N-1|k}$ and $x^\star_{0|k}, ..., x^\star_{N|k}$ are defined as in Part 2b of this proof, and $x^\star_{N|k} = \left[(c^\star_{N|k})^\top \ (h^\star_{N|k})^\top \right]^\top$. Note that W_k is a function of $x = \hat{x}_k$, $\hat{e}_{\mathrm{o},k}$, $\bar{x}_k$ and $\bar{u}_k$, because all these values are needed to compute the optimal input sequence $\mathbf{u}^\star_k$.

In Part 3a, a lower bound and an upper bound for W_k and a bound on the variation of W_k between subsequent time-steps are derived to prove ISpS. In Part 3b, convergence is shown by studying the asymptotic values of the bounds, under the assumption that $y^0_k \to y^0_\infty$ and $d_k \to \bar{d}_\infty$ for $k \to \infty$.

Part 3a: The lower bound for W_k follows from

$$W_k \geq \|x^\star_{0|k} - \bar{x}_\infty\|_Q^2 = \|\hat{x}_k - \bar{x}_\infty\|_Q^2 \geq \lambda_{min}(Q) \|\hat{x}_k - \bar{x}_\infty\|_2^2. \tag{7.50}$$

The upper bound for W_k is now proven.

Consider the possibly suboptimal control input $\tilde{\mathbf{u}}_k = \{\tilde{u}_{i|k}\}_{i=0}^{N-1}$ with $\tilde{u}_{i|k} := \bar{u}_k$ for all i, and denote by $\tilde{\mathbf{x}}_k = \{\tilde{x}_{0|k}, ..., \tilde{x}_{N|k}\}$ the correspondent state trajectory with initial condition $\tilde{x}_{0|k} := \hat{x}_k$. Note that there exists $\mu > 0$ such that this control input is feasible at time-step k for all $\hat{x}_k$ such that $\|\hat{x}_k - \bar{x}_k\|_2 \leq \mu$.

Three different cases are considered:

1. $\|\hat{x}_k - \bar{x}_\infty\|_2 \leq \frac{\mu}{2}$ and $\|\bar{x}_k - \bar{x}_\infty\|_2 \leq \frac{\mu}{2}$;
2. $\|\hat{x}_k - \bar{x}_\infty\|_2 > \frac{\mu}{2}$;
3. $\|\hat{x}_k - \bar{x}_\infty\|_2 \leq \frac{\mu}{2}$ and $\|\bar{x}_k - \bar{x}_\infty\|_2 > \frac{\mu}{2}$.

Case 1: $\|\hat{x}_k - \bar{x}_\infty\|_2 \leq \frac{\mu}{2}$ and $\|\bar{x}_k - \bar{x}_\infty\|_2 \leq \frac{\mu}{2}$.
In this case the sequence $\tilde{\mathbf{u}}_k$ is feasible. In fact

$$\|\hat{x}_k - \bar{x}_k\|_2 \leq \|\hat{x}_k - \bar{x}_\infty\|_2 + \|\bar{x}_k - \bar{x}_\infty\|_2 \leq \frac{\mu}{2} + \frac{\mu}{2} = \mu.$$

Let's introduce new variables for the difference between the set-point at step k and the set-point for $k \to \infty$

$$\delta\bar{x}_k := \bar{x}_k - \bar{x}_\infty, \quad \delta\bar{u}_k := \bar{u}_k - \bar{u}_\infty,$$
$$\delta\bar{c}_k := \bar{c}_k - \bar{c}_\infty, \quad \delta\bar{h}_k := \bar{h}_k - \bar{h}_\infty.$$

Terms $\delta\bar{x}_k$, $\delta\bar{u}_k$, $\delta\bar{c}_k$, $\delta\bar{h}_k$ can be related to $\hat{d}_k - \bar{d}_\infty$ and $y_k^0 - y_\infty^0$ with a reasoning similar to the proof of Lemma 7.4. In particular, under Assumption 7.3, there exist finite constants $\bar{K}_x$ and $\bar{K}_u$ such that

$$\|\delta\bar{x}_k\|_2 \leq \bar{K}_x \left\|\hat{d}_k - \bar{d}_\infty\right\|_2 + \bar{K}_x \left\|y_k^0 - y_\infty^0\right\|_2 \tag{7.51a}$$

$$\|\delta\bar{u}_k\|_2 \leq \bar{K}_u \left\|\hat{d}_k - \bar{d}_\infty\right\|_2 + \bar{K}_u \left\|y_k^0 - y_\infty^0\right\|_2 . \tag{7.51b}$$

Considering W_k, we have that

$$\begin{aligned} W_k \leq & \sum_{i=0}^{N-1} \left(\|x_{i|k}^\star - \bar{x}_k\|_Q^2 + \|u_{i|k}^\star - \bar{u}_k\|_R^2 \right) + \left\| \begin{bmatrix} \|c_{N|k}^\star - \bar{c}_k\|_2 \\ \|h_{N|k}^\star - \bar{h}_k\|_2 \end{bmatrix} \right\|_{P_\mathrm{f}}^2 \\ & + \sum_{i=0}^{N-1} \left(\|\delta\bar{x}_k\|_Q^2 + \|\delta\bar{u}_k\|_R^2 + 2(x_{i|k}^\star - \bar{x}_k)^\top Q\delta\bar{x}_k + 2(u_{i|k}^\star - \bar{u}_k)^\top R\delta\bar{u}_k \right) \\ & + \left\| \begin{bmatrix} \|\delta\bar{c}_k\|_2 \\ \|\delta\bar{h}_k\|_2 \end{bmatrix} \right\|_{P_\mathrm{f}}^2 + 2 \begin{bmatrix} \|c_{N|k}^\star - \bar{c}_k\|_2 \\ \|h_{N|k}^\star - \bar{h}_k\|_2 \end{bmatrix}^\top P_\mathrm{f} \begin{bmatrix} \|\delta\bar{c}_k\|_2 \\ \|\delta\bar{h}_k\|_2 \end{bmatrix} . \end{aligned}$$

This expression contains the optimal cost of the MPC optimization at step k, that is

$$V_k := \sum_{i=0}^{N-1} \left(\|x_{i|k}^\star - \bar{x}_k\|_Q^2 + \|u_{i|k}^\star - \bar{u}_k\|_R^2 \right) + \left\| \begin{bmatrix} \|c_{N|k}^\star - \bar{c}_k\|_2 \\ \|h_{N|k}^\star - \bar{h}_k\|_2 \end{bmatrix} \right\|_{P_\mathrm{f}}^2 .$$

Consider now the cost associate to the suboptimal control input $\tilde{u}_{i|k}$, and note that it is greater or equal than the optimal cost, i.e.

$$V_k \leq \sum_{i=0}^{N-1} \|\tilde{x}_{i|k} - \bar{x}_k\|_Q^2 + \left\| \begin{bmatrix} \|\tilde{c}_{N|k} - \bar{c}_k\|_2 \\ \|\tilde{h}_{N|k} - \bar{h}_k\|_2 \end{bmatrix} \right\|_{P_\mathrm{f}}^2 .$$

Now we use that

$$\begin{aligned} \left\| \begin{bmatrix} \|\tilde{c}_{N|k} - \bar{c}_k\|_2 \\ \|\tilde{h}_{N|k} - \bar{h}_k\|_2 \end{bmatrix} \right\|_{P_\mathrm{f}}^2 &\leq \lambda_{max}(P_\mathrm{f}) \left\| \begin{bmatrix} \|\tilde{c}_{N|k} - \bar{c}_k\|_2 \\ \|\tilde{h}_{N|k} - \bar{h}_k\|_2 \end{bmatrix} \right\|_2^2 \\ &= \lambda_{max}(P_\mathrm{f}) \|\tilde{x}_{N|k} - \bar{x}_k\|_2^2 \end{aligned}$$

and that, in view of Assumption 4.1 and Theorem 4.1, there exist $\bar{\mu} \geq 0$ and $\lambda \in (0, 1)$ such that $\forall i \geq 0$

$$\|\tilde{x}_{i|k} - \bar{x}_k\|_2 \leq \bar{\mu}\lambda^i \|\tilde{x}_{0|k} - \bar{x}_k\|_2 = \bar{\mu}\lambda^i \|\hat{x}_k - \bar{x}_k\|_2$$

to obtain that there exists a constant $\tilde{b} \geq 0$ such that

$$\begin{aligned} V_k &\leq \tilde{b}\|\hat{x}_k - \bar{x}_k\|_2^2 = \tilde{b}\|\hat{x}_k - \bar{x}_\infty - \delta\bar{x}_k\|_2^2 \\ &= \tilde{b}\|\hat{x}_k - \bar{x}_\infty\|_2^2 + \tilde{b}\|\delta\bar{x}_k\|_2^2 - 2\tilde{b}(\hat{x}_k - \bar{x}_\infty)^\top \delta\bar{x}_k. \end{aligned}$$

Therefore

$$W_k \leq \tilde{b}\|\hat{x}_k - \bar{x}_\infty\|_2^2 + \beta(k) \tag{7.52}$$

where

$$\begin{aligned}\beta(k) := \sum_{i=0}^{N-1} \Big(\|\delta\bar{x}_k\|_Q^2 + \|\delta\bar{u}_k\|_R^2 + 2(x^\star_{i|k} - \bar{x}_k)^\top Q\delta\bar{x}_k + 2(u^\star_{i|k} - \bar{u}_k)^\top R\delta\bar{u}_k \Big) \\ + \left\| \begin{bmatrix} \|\delta\bar{c}_k\|_2 \\ \|\delta\bar{h}_k\|_2 \end{bmatrix} \right\|_{P_\mathrm{f}}^2 + 2 \begin{bmatrix} \|c^\star_{N|k} - \bar{c}_k\|_2 \\ \|h^\star_{N|k} - \bar{h}_k\|_2 \end{bmatrix}^\top P_\mathrm{f} \begin{bmatrix} \|\delta\bar{c}_k\|_2 \\ \|\delta\bar{h}_k\|_2 \end{bmatrix} \\ + \tilde{b}\|\delta\bar{x}_k\|_2^2 - 2\tilde{b}(\hat{x}_k - \bar{x}_\infty)^\top \delta\bar{x}_k.\end{aligned}$$

In view of (7.51) and boundedness of $\mathcal{D}$ and $\mathcal{Y}^0$, terms $\delta\bar{x}_k$, $\delta\bar{u}_k$, $\delta\bar{c}_k$ and $\delta\bar{h}_k$ are bounded for all $k \in \mathbb{Z}_{\geq 0}$. In addition, inputs are limited in $\mathcal{U}$ and states are limited in $\hat{\mathcal{C}} \times \mathcal{H}$. Then there exists a constant $\tilde{c}_1 \geq 0$ such that $\beta(k) \leq \tilde{c}_1$ for all $k \in \mathbb{Z}_{\geq 0}$.

Case 2: $\|\hat{x}_k - \bar{x}_\infty\|_2 > \frac{\mu}{2}$.

There exists $W_{max} > 0$ such that $W_k \leq W_{max}$ in $\mathcal{X}^{\mathrm{MPC}}$. Then

$$W_k \leq \frac{4W_{max}}{\mu^2} \|\hat{x}_k - \bar{x}_\infty\|_2^2. \tag{7.53}$$

Case 3: $\|\hat{x}_k - \bar{x}_\infty\|_2 \leq \frac{\mu}{2}$ and $\|\bar{x}_k - \bar{x}_\infty\|_2 > \frac{\mu}{2}$.

We have that

$$W_k \leq 0\, \|\hat{x}_k - \bar{x}_\infty\|_2^2 + \tilde{\beta}(k) \tag{7.54}$$

with $\tilde{\beta}(k) = W_k \leq W_{max}$.

Hence, in view of (7.52), (7.53) and (7.54),

$$W_k \leq b\|\hat{x}_k - \bar{x}_\infty\|_2^2 + c_1 \tag{7.55}$$

with $b = \max\left\{\tilde{b}, \frac{4W_{max}}{\mu^2}\right\}$ and $c_1 = \max\{\tilde{c}_1, W_{max}\}$.

Let's now study the variation of W_k between subsequent time-steps.

Consider the Lyapunov function at time-step $k+1$:

$$W_{k+1} = \sum_{i=0}^{N-1} \left(\|x^\star_{i|k+1} - \bar{x}_\infty\|_Q^2 + \|u^\star_{i|k+1} - \bar{u}_\infty\|_R^2 \right) + \left\| \begin{bmatrix} \|c^\star_{N|k+1} - \bar{c}_\infty\|_2 \\ \|h^\star_{N|k+1} - \bar{h}_\infty\|_2 \end{bmatrix} \right\|_{P_\mathrm{f}}^2$$

where $\mathbf{u}^\star_{k+1} = \{u^\star_{0|k+1}, ..., u^\star_{N|k+1}\}$ is the optimal sequence given by the MPC at step $k+1$ and $x^\star_{i+1|k+1} := f(x^\star_{i|k+1}, u^\star_{i|k+1})$ with $x^\star_{0|k+1} := \hat{x}_{k+1}$. Note that $\hat{x}_{k+1}$ can be different from $x^\star_{1|k}$. It is possible to derive the following

upper bound for W_{k+1}:

$$
\begin{aligned}
W_{k+1} \leq & \sum_{i=0}^{N-1} \left(\|x^\star_{i|k+1} - \bar{x}_{k+1}\|_Q^2 + \|u^\star_{i|k+1} - \bar{u}_{k+1}\|_R^2 \right) \\
& + \left\| \begin{bmatrix} \|c^\star_{N|k+1} - \bar{c}_{k+1}\|_2 \\ \|h^\star_{N|k+1} - \bar{h}_{k+1}\|_2 \end{bmatrix} \right\|_{P_\mathrm{f}}^2 + \sum_{i=0}^{N-1} \Big(\|\delta\bar{x}_{k+1}\|_Q^2 + \|\delta\bar{u}_{k+1}\|_R^2 \\
& + 2(x^\star_{i|k+1} - \bar{x}_{k+1})^\top Q \delta\bar{x}_{k+1} + 2(u^\star_{i|k+1} - \bar{u}_{k+1})^\top R \delta\bar{u}_{k+1} \Big) \\
& + \left\| \begin{bmatrix} \|\delta\bar{c}_{k+1}\|_2 \\ \|\delta\bar{h}_{k+1}\|_2 \end{bmatrix} \right\|_{P_\mathrm{f}}^2 + 2 \begin{bmatrix} \|c^\star_{N|k+1} - \bar{c}_{k+1}\|_2 \\ \|h^\star_{N|k+1} - \bar{h}_{k+1}\|_2 \end{bmatrix}^\top P_\mathrm{f} \begin{bmatrix} \|\delta\bar{c}_{k+1}\|_2 \\ \|\delta\bar{h}_{k+1}\|_2 \end{bmatrix}.
\end{aligned}
$$

This expression contains the optimal cost of the MPC optimization at step $k+1$, that is

$$
\begin{aligned}
V_{k+1} = & \sum_{i=0}^{N-1} \left(\|x^\star_{i|k+1} - \bar{x}_{k+1}\|_Q^2 + \|u^\star_{i|k+1} - \bar{u}_{k+1}\|_R^2 \right) \\
& + \left\| \begin{bmatrix} \|c^\star_{N|k+1} - \bar{c}_{k+1}\|_2 \\ \|h^\star_{N|k+1} - \bar{h}_{k+1}\|_2 \end{bmatrix} \right\|_{P_\mathrm{f}}^2 .
\end{aligned}
$$

Consider now the feasible trajectory $\tilde{u}_{i|k+1}$ for $i = 0, ..., N-1$ used in Part 2b of this proof. Noting that the cost associated to the feasible trajectory is greater or equal than V_{k+1}, we have

$$
\begin{aligned}
W_{k+1} \leq & \sum_{i=0}^{N-2} \left(\|\tilde{x}_{i|k+1} - \bar{x}_{k+1}\|_Q^2 + \|u^\star_{i+1|k} - \bar{u}_{k+1}\|_R^2 \right) \\
& + \|\tilde{x}_{N-1|k+1} - \bar{x}_{k+1}\|_Q^2 + \|\bar{u}_{k+1} - \bar{u}_{k+1}\|_R^2 \\
& + \left\| \begin{bmatrix} \|\tilde{c}_{N|k+1} - \bar{c}_{k+1}\|_2 \\ \|\tilde{h}_{N|k+1} - \bar{h}_{k+1}\|_2 \end{bmatrix} \right\|_{P_\mathrm{f}}^2 + N\|\delta\bar{x}_{k+1}\|_Q^2 + N\|\delta\bar{u}_{k+1}\|_R^2 \\
& + \sum_{i=0}^{N-1} \left(2(x^\star_{i|k+1} - \bar{x}_{k+1})^\top Q \delta\bar{x}_{k+1} + 2(u^\star_{i|k+1} - \bar{u}_{k+1})^\top R \delta\bar{u}_{k+1} \right) \\
& + \left\| \begin{bmatrix} \|\delta\bar{c}_{k+1}\|_2 \\ \|\delta\bar{h}_{k+1}\|_2 \end{bmatrix} \right\|_{P_\mathrm{f}}^2 + 2 \begin{bmatrix} \|c^\star_{N|k+1} - \bar{c}_{k+1}\|_2 \\ \|h^\star_{N|k+1} - \bar{h}_{k+1}\|_2 \end{bmatrix}^\top P_\mathrm{f} \begin{bmatrix} \|\delta\bar{c}_{k+1}\|_2 \\ \|\delta\bar{h}_{k+1}\|_2 \end{bmatrix}.
\end{aligned}
$$

Therefore, the variation of the Lyapunov function is bounded by

$$
\begin{aligned}
W_{k+1} - W_k \leq & \sum_{i=0}^{N-2} \left(\|\tilde{x}_{i|k+1} - \bar{x}_{k+1}\|_Q^2 + \|u^\star_{i+1|k} - \bar{u}_{k+1}\|_R^2 \right) \\
& + \|\tilde{x}_{N-1|k} - \bar{x}_{k+1}\|_Q^2 + \left\| \begin{bmatrix} \|\tilde{c}_{N|k+1} - \bar{c}_{k+1}\|_2 \\ \|\tilde{h}_{N|k+1} - \bar{h}_{k+1}\|_2 \end{bmatrix} \right\|_{P_f}^2 \\
& + N\|\delta\bar{x}_{k+1}\|_Q^2 + N\|\delta\bar{u}_{k+1}\|_R^2 \\
& + \sum_{i=0}^{N-1} \left(2(x^\star_{i|k+1} - \bar{x}_{k+1})^\top Q \delta\bar{x}_{k+1} + 2(u^\star_{i|k+1} - \bar{u}_{k+1})^\top R \delta\bar{u}_{k+1} \right) \\
& + \left\| \begin{bmatrix} \|\delta\bar{c}_{k+1}\|_2 \\ \|\delta\bar{h}_{k+1}\|_2 \end{bmatrix} \right\|_{P_\mathrm{f}}^2 + 2 \begin{bmatrix} \|c^\star_{N|k+1} - \bar{c}_{k+1}\|_2 \\ \|h^\star_{N|k+1} - \bar{h}_{k+1}\|_2 \end{bmatrix}^\top P_\mathrm{f} \begin{bmatrix} \|\delta\bar{c}_{k+1}\|_2 \\ \|\delta\bar{h}_{k+1}\|_2 \end{bmatrix} \\
& - \sum_{i=0}^{N-1} \left(\|x^\star_{i|k} - \bar{x}_\infty\|_Q^2 + \|u^\star_{i|k} - \bar{u}_\infty\|_R^2 \right) - \left\| \begin{bmatrix} \|c^\star_{N|k} - \bar{c}_\infty\|_2 \\ \|h^\star_{N|k} - \bar{h}_\infty\|_2 \end{bmatrix} \right\|_{P_f}^2 \\
= & - \|x^\star_{0|k} - \bar{x}_\infty\|_Q^2 - \|u^\star_{0|k} - \bar{u}_\infty\|_R^2 \\
& + \sum_{i=1}^{N-1} \left(\|\tilde{x}_{i-1|k+1} - \bar{x}_{k+1}\|_Q^2 - \|x^\star_{i|k} - \bar{x}_\infty\|_Q^2 \right) \\
& + \sum_{i=1}^{N-1} \left(\|u^\star_{i|k} - \bar{u}_{k+1}\|_R^2 - \|u^\star_{i|k} - \bar{u}_\infty\|_R^2 \right) + \|\tilde{x}_{N-1|k+1} - \bar{x}_{k+1}\|_Q^2 \\
& - \left\| \begin{bmatrix} \|c^\star_{N|k} - \bar{c}_\infty\|_2 \\ \|h^\star_{N|k} - \bar{h}_\infty\|_2 \end{bmatrix} \right\|_{P_\mathrm{f}}^2 + \left\| \begin{bmatrix} \|\tilde{c}_{N|k+1} - \bar{c}_{k+1}\|_2 \\ \|\tilde{h}_{N|k+1} - \bar{h}_{k+1}\|_2 \end{bmatrix} \right\|_{P_\mathrm{f}}^2 \\
& + \sum_{i=0}^{N-1} \left(2(x^\star_{i|k+1} - \bar{x}_{k+1})^\top Q \delta\bar{x}_{k+1} + 2(u^\star_{i|k+1} - \bar{u}_{k+1})^\top R \delta\bar{u}_{k+1} \right) \\
& + 2 \begin{bmatrix} \|c^\star_{N|k+1} - \bar{c}_{k+1}\|_2 \\ \|h^\star_{N|k+1} - \bar{h}_{k+1}\|_2 \end{bmatrix}^\top P_\mathrm{f} \begin{bmatrix} \|\delta\bar{c}_{k+1}\|_2 \\ \|\delta\bar{h}_{k+1}\|_2 \end{bmatrix} \\
& + N\|\delta\bar{x}_{k+1}\|_Q^2 + N\|\delta\bar{u}_{k+1}\|_R^2 + \left\| \begin{bmatrix} \|\delta\bar{c}_{k+1}\|_2 \\ \|\delta\bar{h}_{k+1}\|_2 \end{bmatrix} \right\|_{P_\mathrm{f}}^2 .
\end{aligned}
$$

We introduce now the error terms related to the fact that $\tilde{x}_{0|k+1} = \hat{x}_{k+1} \neq x^\star_{1|k}$ because of the presence of the observer in the control loop:

$$\varepsilon_{k+i+1} := \tilde{x}_{i|k+1} - x^\star_{i+1|k},$$

$$\varepsilon_{c,k+N} := \tilde{c}_{N-1|k+1} - c^\star_{N|k},$$

$$\varepsilon_{h,k+N} := \tilde{h}_{N-1|k+1} - h^\star_{N|k}.$$

The different terms of the upper bound of $W_{k+1} - W_k$ are now considered separately.

Consider the state terms at time-steps between $k+1$ and $k+N-1$:

$$\begin{aligned}
&\sum_{i=1}^{N-1} \left(\|\tilde{x}_{i-1|k+1} - \bar{x}_{k+1}\|_Q^2 - \|x^\star_{i|k} - \bar{x}_\infty\|_Q^2 \right) \\
&= \sum_{i=1}^{N-1} \left(\|x^\star_{i|k} - \bar{x}_\infty + \varepsilon_{k+i} - \delta\bar{x}_{k+1}\|_Q^2 - \|x^\star_{i|k} - \bar{x}_\infty\|_Q^2 \right) \\
&= \sum_{i=1}^{N-1} \left(2(x^\star_{i|k} - \bar{x}_\infty)^\top Q(\varepsilon_{k+i} - \delta\bar{x}_{k+1}) + \|\varepsilon_{k+i} - \delta\bar{x}_{k+1}\|_Q^2 \right).
\end{aligned}$$

Consider the input terms at time-steps between $k+1$ and $k+N-1$:

$$\begin{aligned}
&\sum_{i=1}^{N-1} \left(\|u^\star_{i|k} - \bar{u}_{k+1}\|_R^2 - \|u^\star_{i|k} - \bar{u}_\infty\|_R^2 \right) \\
&= \sum_{i=1}^{N-1} \left(\|u^\star_{i|k} - \bar{u}_\infty - \delta\bar{u}_{k+1}\|_R^2 - \|u^\star_{i|k} - \bar{u}_\infty\|_R^2 \right) \\
&= \sum_{i=1}^{N-1} \left(-2(u^\star_{i|k} - \bar{u}_\infty)^\top R\delta\bar{u}_{k+1} \right) + (N-1)\|\delta\bar{u}_{k+1}\|_R^2.
\end{aligned}$$

Finally, consider the state terms at time-steps $k+N$ and $k+N+1$. In view of Lemma 7.5 we have that, for any $\varphi \neq 0$,

$$\begin{aligned}
&\|\tilde{x}_{N-1|k+1} - \bar{x}_{k+1}\|_Q^2 = \|x^\star_{N|k} - \bar{x}_\infty + \varepsilon_{k+N} - \delta\bar{x}_{k+1}\|_Q^2 \\
&\overset{(7.26)}{\leq} (1+\varphi^2)\|x^\star_{N|k} - \bar{x}_\infty\|_Q^2 + \left(1 + \frac{1}{\varphi^2}\right)\|\varepsilon_{k+N} - \delta\bar{x}_{k+1}\|_Q^2 \\
&\leq q(1+\varphi^2)\|x^\star_{N|k} - \bar{x}_\infty\|_2^2 + \left(1 + \frac{1}{\varphi^2}\right)\|\varepsilon_{k+N} - \delta\bar{x}_{k+1}\|_Q^2 \\
&= q(1+\varphi^2)\left\| \begin{bmatrix} \|c^\star_{N|k} - \bar{c}_\infty\|_2 \\ \|h^\star_{N|k} - \bar{h}_\infty\|_2 \end{bmatrix} \right\|_2^2 + \left(1 + \frac{1}{\varphi^2}\right)\|\varepsilon_{k+N} - \delta\bar{x}_{k+1}\|_Q^2.
\end{aligned}$$

Moreover, for any $\varphi \neq 0$,

$$\begin{aligned}
&\left\| \begin{bmatrix} \|\tilde{c}_{N|k+1} - \bar{c}_{k+1}\|_2 \\ \|\tilde{h}_{N|k+1} - \bar{h}_{k+1}\|_2 \end{bmatrix} \right\|_{P_\mathrm{f}}^2 \overset{(4.1)}{\leq} \left\| A_\delta \begin{bmatrix} \|\tilde{c}_{N-1|k+1} - \bar{c}_{k+1}\|_2 \\ \|\tilde{h}_{N-1|k+1} - \bar{h}_{k+1}\|_2 \end{bmatrix} \right\|_{P_\mathrm{f}}^2 \\
&\leq \left\| \begin{bmatrix} \|c^\star_{N|k} - \bar{c}_\infty + \varepsilon_{c,k+N} - \delta\bar{c}_{k+1}\|_2 \\ \|h^\star_{N|k} - \bar{h}_\infty + \varepsilon_{h,k+N} - \delta\bar{h}_{k+1}\|_2 \end{bmatrix} \right\|_{A_\delta^\top P_\mathrm{f} A_\delta}^2
\end{aligned}$$

$$\overset{(7.26)}{\leq} (1+\varphi^2)\left\|\begin{bmatrix}\|c^\star_{N|k}-\bar{c}_\infty\|_2\\ \|h^\star_{N|k}-\bar{h}_\infty\|_2\end{bmatrix}\right\|^2_{A_\delta^\top P_\mathrm{f} A_\delta} + \left(1+\frac{1}{\varphi^2}\right)\left\|\begin{bmatrix}\|\varepsilon_{c,k+N}-\delta\bar{c}_{k+1}\|_2\\ \|\varepsilon_{h,k+N}-\delta\bar{h}_{k+1}\|_2\end{bmatrix}\right\|^2_{A_\delta^\top P_\mathrm{f} A_\delta}.$$

Then the following inequality holds:

$$\begin{aligned}
&-\left\|\begin{bmatrix}\|c^\star_{N|k}-\bar{c}_\infty\|_2\\ \|h^\star_{N|k}-\bar{h}_\infty\|_2\end{bmatrix}\right\|^2_{P_\mathrm{f}} + \|\tilde{x}_{N-1|k+1}-\bar{x}_{k+1}\|^2_Q + \left\|\begin{bmatrix}\|\tilde{c}_{N|k+1}-\bar{c}_{k+1}\|_2\\ \|\tilde{h}_{N|k+1}-\bar{h}_{k+1}\|_2\end{bmatrix}\right\|^2_{P_\mathrm{f}}\\
&\leq \left\|\begin{bmatrix}\|c^\star_{N|k}-\bar{c}_\infty\|_2\\ \|h^\star_{N|k}-\bar{h}_\infty\|_2\end{bmatrix}\right\|^2_{-P_\mathrm{f}+(1+\varphi^2)qI_2+(1+\varphi^2)A_\delta^\top P_\mathrm{f} A_\delta}\\
&+\left(1+\frac{1}{\varphi^2}\right)\|\varepsilon_{k+N}-\delta\bar{x}_{k+1}\|^2_Q + \left(1+\frac{1}{\varphi^2}\right)\left\|\begin{bmatrix}\|\varepsilon_{c,k+N}-\delta\bar{c}_{k+1}\|_2\\ \|\varepsilon_{h,k+N}-\delta\bar{h}_{k+1}\|_2\end{bmatrix}\right\|^2_{A_\delta^\top P_\mathrm{f} A_\delta}.
\end{aligned}$$

By construction P_f is selected such that $A_\delta^\top P_\mathrm{f} A_\delta - P_\mathrm{f} < -qI_2$. Therefore there exists a value of φ small enough to have $-P_\mathrm{f} + (1+\varphi^2)qI_2 + (1+\varphi^2)A_\delta^\top P_\mathrm{f} A_\delta < 0$.

Combining all the computations, we obtain that

$$W_{k+1} - W_k \leq -\|x^\star_{0|k}-\bar{x}_\infty\|^2_Q - \|u^\star_{0|k}-\bar{u}_\infty\|^2_R + \gamma(k) \tag{7.56}$$

where

$$\begin{aligned}
\gamma(k) := &\sum_{i=1}^{N-1}\left(2(x^\star_{i|k}-\bar{x}_\infty)^\top Q(\varepsilon_{k+i}-\delta\bar{x}_{k+1}) + \|\varepsilon_{k+i}-\delta\bar{x}_{k+1}\|^2_Q\right)\\
&+\sum_{i=1}^{N-1}\left(-2(u^\star_{i|k}-\bar{u}_\infty)^\top R\delta\bar{u}_{k+1}\right) + (N-1)\|\delta\bar{u}_{k+1}\|^2_R\\
&+\left(1+\frac{1}{\varphi^2}\right)\|\varepsilon_{k+N}-\delta\bar{x}_{k+1}\|^2_Q\\
&+\left(1+\frac{1}{\varphi^2}\right)\left\|\begin{bmatrix}\|\varepsilon_{c,k+N}-\delta\bar{c}_{k+1}\|_2\\ \|\varepsilon_{h,k+N}-\delta\bar{h}_{k+1}\|_2\end{bmatrix}\right\|^2_{A_\delta^\top P_\mathrm{f} A_\delta}\\
&+\sum_{i=0}^{N-1}\left(2(x^\star_{i|k+1}-\bar{x}_{k+1})^\top Q\delta\bar{x}_{k+1} + 2(u^\star_{i|k+1}-\bar{u}_{k+1})^\top R\delta\bar{u}_{k+1}\right)\\
&+2\begin{bmatrix}\|c^\star_{N|k+1}-\bar{c}_{k+1}\|_2\\ \|h^\star_{N|k+1}-\bar{h}_{k+1}\|_2\end{bmatrix}^\top P_\mathrm{f}\begin{bmatrix}\|\delta\bar{c}_{k+1}\|_2\\ \|\delta\bar{h}_{k+1}\|_2\end{bmatrix} + \left\|\begin{bmatrix}\|\delta\bar{c}_{k+1}\|_2\\ \|\delta\bar{h}_{k+1}\|_2\end{bmatrix}\right\|^2_{P_\mathrm{f}}\\
&+N\|\delta\bar{u}_{k+1}\|^2_R + N\|\delta\bar{x}_{k+1}\|^2_Q.
\end{aligned}$$

In this expression:

- Terms ε_{k+i}, $\varepsilon_{c,k+N}$, $\varepsilon_{h,k+N}$ are present because $\hat{x}_{k+1} \neq x^\star_{1|k}$. These terms have bounds related to the observer estimation error $\chi_k - \hat{\chi}_k$. In particular

$$\|\varepsilon_{k+1}\|_2 \overset{(7.14c)}{\leq} L_{max} V_{\mathrm{o}}(\hat{\chi}_k, \chi_k) \overset{(7.14a)}{\leq} c_{\mathrm{o,u}} L_{max} \|\chi_k - \hat{\chi}_k\|_2 ,$$

$$\|\varepsilon_{k+i}\|_2 \overset{(7.6a)}{\leq} \frac{1}{c_{\mathrm{s,l}}} V_{\mathrm{s}}(\tilde{x}_{i-1|k+1}, x^\star_{i|k}) \overset{(7.6b)}{\leq} \frac{\rho_{\mathrm{s}}^{i-1}}{c_{\mathrm{s,l}}} V_{\mathrm{s}}(\tilde{x}_{0|k+1}, x^\star_{1|k})$$
$$\overset{(7.6a)}{\leq} \frac{c_{\mathrm{s,u}} \rho_{\mathrm{s}}^{i-1}}{c_{\mathrm{s,l}}} \|\varepsilon_{k+1}\|_2 \leq \frac{c_{\mathrm{s,u}} \rho_{\mathrm{s}}^{i-1}}{c_{\mathrm{s,l}}} c_{\mathrm{o,u}} L_{max} \|\chi_k - \hat{\chi}_k\|_2 .$$

- Terms $\delta\bar{x}_{k+1}$, $\delta\bar{u}_{k+1}$, $\delta\bar{c}_{k+1}$, $\delta\bar{h}_{k+1}$ are present because the reference values $\bar{x}$ and $\bar{u}$ change at each time-step with the variation of the disturbance estimation $\hat{d}_k$. As already noted in (7.51), these terms are bounded.

- Inputs are limited thanks to MPC constraint (7.20f).

- States are limited in the set $\mathcal{X}^{\mathrm{MPC}}$.

Moreover, since

$$\|x^\star_{0|k} - \bar{x}_\infty\|_Q^2 + \|u^\star_{0|k} - \bar{u}_\infty\|_R^2 \geq \lambda_{min}(Q) \|\hat{x}_k - \bar{x}_\infty\|_2^2,$$

there exist constants $c = \lambda_{min}(Q)$ and $c_2 \geq 0$ and a $\mathcal{K}$-function $\tilde{\gamma}$ such that

$$W_{k+1} - W_k \leq -c\|\hat{x}_k - \bar{x}_\infty\|_2^2 + \tilde{\gamma}(\|\chi_k - \hat{\chi}_k\|_2) + c_2. \tag{7.57}$$

In view of (7.50)-(7.55)-(7.57), W_k is an ISpS-Lyapunov function. Then, the closed-loop system (7.8)-(7.15)-(7.24) is ISpS with respect to the observer estimation error $\chi - \hat{\chi}$.

Part 3b: To prove convergence, first note that if $d_k \to \bar{d}_\infty$ for $k \to \infty$, the observer estimation error $\chi - \hat{\chi}$ converges to 0 in view of Theorem 7.1. Then, in view of (7.51), terms $\delta\bar{x}_k$, $\delta\bar{u}_k$, $\delta\bar{c}_k$ and $\delta\bar{h}_k$ converge to 0 for $k \to \infty$.

The bounds on W_k and on $W_{k+1} - W_k$ are now studied for $k \to \infty$.

Consider the upper bound of W_k. If $d_k \to \bar{d}_\infty$ and $y^0_k \to y^0_\infty$ for $k \to \infty$, in view of observer convergence, $\|\bar{x}_k - \bar{x}_\infty\| \to 0$ for $k \to \infty$. Then there exists $\bar{k} \in \mathbb{Z}_{\geq 0}$ such that $\|\bar{x}_k - \bar{x}_\infty\|_2 \leq \frac{\mu}{2}$ for all $k \geq \bar{k}$. Hence, for $k \geq \bar{k}$, only Cases 1 and 2 of the upper bound can appear. Then

$$W_k \leq b \|\hat{x}_k - \bar{x}_\infty\|_2^2 + \beta(k) \tag{7.58}$$

where $\beta(k) \to 0$ for $k \to \infty$ for the convergence of $\delta\bar{x}_k$, $\delta\bar{u}_k$, $\delta\bar{c}_k$ and $\delta\bar{h}_k$.

Consider the bound on $W_{k+1} - W_k$ of Equation (7.56). We have that $\gamma(k) \to 0$ for $k \to \infty$ in view of the convergence of the observer estimation error and of $\delta\bar{x}_k$, $\delta\bar{u}_k$, $\delta\bar{c}_k$ and $\delta\bar{h}_k$.

Then for $k \geq \bar{k}$ the Lyapunov function W_k is such that

$$a \left\| \hat{x}_k - \bar{x}_\infty \right\|_2^2 \leq W_k \leq b \left\| \hat{x}_k - \bar{x}_\infty \right\|_2^2 + \beta(k) \tag{7.59a}$$

$$W_{k+1} - W_k \leq -c \left\| \hat{x}_k - \bar{x}_\infty \right\|_2^2 + \gamma(k) \tag{7.59b}$$

for some $a, b, c > 0$, with $\beta(k) \to 0$ and $\gamma(k) \to 0$ for $k \to \infty$.

The fact that $\lim_{k\to\infty} \|\psi_k - \psi_\infty\| = 0$ follows from (7.59), observer convergence proven in Theorem 7.1 and (7.19). □

7.5.7 Proof of Theorem 7.3

The proof follows the proof of Theorem 4 in [173].

In view of Assumption 7.5 the output of the plant converges to a constant value $y_{\phi,\infty}$. Then it is sufficient to prove that $y_{\phi,\infty} = y^0_{\phi,\infty}$.

In view of Assumption 7.5, the observer states $\hat{x}$ and $\hat{d}$ converge to asymptotic values, denoted by $\hat{x}_\infty$ and $\hat{d}_\infty$. By Corollary 7.1 and Theorem 7.1, the observer is nominally error free (i.e. it reaches steady state only if $y = \hat{y}$), and at steady state satisfies

$$\hat{x}_\infty = f(\hat{x}_\infty, u_\infty) \tag{7.60a}$$

$$y_{\phi,\infty} = g(\hat{x}_\infty) + \hat{d}_\infty \tag{7.60b}$$

where u_∞ is the input generated by the controller (Reference Calculator + MPC), and is a function of $\hat{x}_\infty, \hat{d}_\infty, y^0_{\phi,\infty}$. From (7.60a), Assumption 7.3 and Theorem 7.2 it follows that

$$y^0_{\phi,\infty} = g(\hat{x}_\infty) + \hat{d}_\infty. \tag{7.61}$$

Hence, from a comparison of (7.60b) and (7.61), it follows that $y_{\phi,\infty} = y^0_{\phi,\infty}$.

□

Chapter 8

RNN-based MPC for systems with input and input rate constraints

In this chapter, we propose an MPC algorithm based on a generic δISS RNN model for systems with input and incremental input constraints (also called input rate constraints). To take into account the incremental constraint on the input, the input variation is considered as control input, and an integrator is introduced to obtain the actual system input. Closed-loop stability is guaranteed by means of a suitable terminal cost and a terminal equality constraint only on the state of the integrator, that is the input of the system. Since state/output constraints are not considered, and in view of the stability property of the RNN model, no terminal constraint on the model state is required. This is a significant advance because it is not necessary to introduce conservative contracting constraints to cope with the observer estimation and modeling errors. In fact the equality constraint on the state of the integrator is not affected by uncertainties. The proposed algorithm is then applied to control a four-tanks process modeled with an LSTM network. To satisfy all the assumptions introduced in the general algorithm, the input constraint is tightened with respect to the set considered for stability.

The content of this chapter is taken from:

- [209] **Schimperna, I.**, Galuppini, G., and Magni, L. (2024). *Recurrent Neural Network Based MPC for Systems With Input and Incremental Input Constraints*. IEEE Control Systems Letters 8, 814–819.

8.1 Problem formulation

The objective of this chapter is to design an MPC algorithm for a nonlinear system, given its RNN model. In particular, the problem of regulation to

a set point $\bar{y}$ is considered, while respecting constraint on the input and on the maximum input variation, i.e.

$$u \in \mathcal{U}, \quad \Delta u \in \Delta\mathcal{U}, \tag{8.1}$$

where $\Delta u_k = u_k - u_{k-1}$, $\mathcal{U} \subset \mathbb{R}^m$ is a bounded closed set and $\Delta\mathcal{U} \subset \mathbb{R}^m$ includes the origin in its interior. In the following, the RNN model will be denoted in compact form as

$$x_{k+1} = f(x_k, u_k) \tag{8.2a}$$

$$y_k = g(x_k) \tag{8.2b}$$

where $u \in \mathbb{R}^m$ is the input of the model, $y \in \mathbb{R}^p$ is the predicted output, $x \in \mathbb{R}^n$ is the RNN state, and the pedix k denotes the time dependence. As in previous chapters, we consider RNN models that are δISS. The model properties are formalized in the following assumption.

Assumption 8.1. *The model* (8.2) *is δISS in the sets $\mathcal{X}^{\text{ISS}}$ and $\mathcal{U}^{\text{ISS}} \supseteq \mathcal{U}$, and there exists an incremental Lyapunov function $V_{\text{f}}(x^{\text{a}}, x^{\text{b}})$ such that for any $x^{\text{a}}, x^{\text{b}} \in \mathcal{X}^{\text{ISS}}$, $u \in \mathcal{U}^{\text{ISS}}$*

$$a\|x^{\text{a}} - x^{\text{b}}\|_2^2 \leq V_{\text{f}}(x^{\text{a}}, x^{\text{b}}) \leq b\|x^{\text{a}} - x^{\text{b}}\|_2^2 \tag{8.3a}$$

$$V_{\text{f}}(f(x^{\text{a}}, u), f(x^{\text{b}}, u)) - V_{\text{f}}(x^{\text{a}}, x^{\text{b}}) \leq -c\|x^{\text{a}} - x^{\text{b}}\|_2^2 \tag{8.3b}$$

for some $a, b, c > 0$. Moreover, $V_{\text{f}}(x^{\text{a}}, x^{\text{b}})$ is locally Lipschitz continuous in any bounded set, i.e. given any bounded set $\bar{\mathcal{X}} \subseteq \mathcal{X}^{\text{ISS}}$, if $x^{\text{a}}, \tilde{x}^{\text{a}}, x^{\text{b}} \in \bar{\mathcal{X}}$ then there exist a finite constant $\bar{L}_V$ such that

$$\left|V_{\text{f}}(x^{\text{a}}, x^{\text{b}}) - V_{\text{f}}(\tilde{x}^{\text{a}}, x^{\text{b}})\right| \leq \bar{L}_V \left\|x^{\text{a}} - \tilde{x}^{\text{a}}\right\|_2 .$$

δISS conditions and incremental Lyapunov functions that satisfy (8.3) have been presented in the previous chapters for LSTMs, GRUs and RENs, and can be found also for other particular classes of RNNs [57]. Moreover, the property of local Lipschitzianity is satisfied by quadratic functions, that are the most common types of Lyapunov functions used to study RNN stability.

8.2 Control algorithm

In Figure 8.1, we report the scheme of the proposed control algorithm. It is composed by three main blocks. The first one is the observer, that is needed to properly initialize the predictions in the MPC. As already mentioned in the previous chapters, the observer is necessary because in general the state x of the RNN model is not measurable and has no physical meaning. The second block is the MPC. To take into account the constraint on the input variation, the MPC considers Δu as optimization variable. The value of the control variable u is obtained from Δu by means of a discrete time integrator.

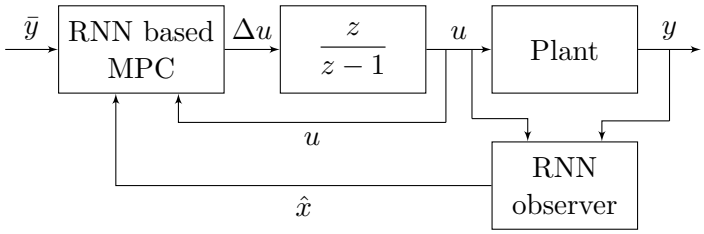

Figure 8.1: Block diagram of the control scheme.

8.2.1 Observer

In view of the δISS property of the model, it is always possible to design a converging observer, see Section 5.1.2. In particular, we consider an observer satisfying the following assumption.

Assumption 8.2. *There exists an observer for the RNN model that can be written in the form*

$$\hat{x}_{k+1} = f(\hat{x}_k, u_k) + \delta x(\hat{x}_k, u_k, y_k) \tag{8.4}$$

where

$$\|\delta x(\hat{x}_k, u_k, y_k)\|_2 \leq L_{max} \|x_k - \hat{x}_k\|_2 \tag{8.5}$$

for some $L_{max} \geq 0$. The observer satisfies the following properties:

1. *there exist a finite $\bar{k} \geq 0$ and a set $\hat{\mathcal{X}}$ such that for any $\hat{x}_0 \in \hat{\mathcal{X}}$, and for any input sequence in $\mathcal{U}$, $\hat{x}_k \in \mathcal{X}^{\text{ISS}}$ $\forall k \geq \bar{k}$;*

2. *the observer estimation error converges to 0, i.e. for any input sequence in $\mathcal{U}$, $\|x_k - \hat{x}_k\| \to 0$ for $k \to \infty$.*

Observers respecting Assumption 8.2 have been designed for LSTMs in [230], for GRUs in [32] (see also Chapter 6), for RENs in Chapter 5 and for other particular classes of RNNs in [57].

8.2.2 MPC design

The MPC solves at every sample time instant a FHOCP, where the deviations from the state and input reference values $\bar{x}$ and $\bar{u}$ are penalized. The references values are computed from the RNN model (8.2) as the equilibrium state and input corresponding to the output $\bar{y}$. It is assumed that $\bar{u} \in \mathcal{U}$ and $\bar{x} \in \mathcal{X}^{\text{ISS}}$. Let $\mathbf{\Delta u}_k := \{\Delta u_{0|k}, \dots, \Delta u_{N-1|k}\}$. Then, the FHOCP is

given by

$$\min_{\mathbf{\Delta u}_k} \sum_{i=0}^{N-1} \left(\left\| x_{i|k} - \bar{x} \right\|_Q^2 + \left\| u_{i|k} - \bar{u} \right\|_R^2 + \left\| \Delta u_{i|k} \right\|_{R_\Delta}^2 \right) + sV_{\mathrm{f}}(x_{N|k}, \bar{x}) \quad (8.6a)$$

$$\text{s.t.} \quad x_{0|k} = \hat{x}_k, \quad u_{0|k} = u_{k-1} \quad (8.6b)$$

$$u_{N|k} = \bar{u} \quad (8.6c)$$

$$\text{for } i = 0, ..., N-1$$

$$x_{i+1|k} = f(x_{i|k}, u_{i+1|k}) \quad (8.6d)$$

$$u_{i+1|k} = u_{i|k} + \Delta u_{i|k} \quad (8.6e)$$

$$u_{i|k} \in \mathcal{U} \quad (8.6f)$$

$$\Delta u_{i|k} \in \Delta\mathcal{U}. \quad (8.6g)$$

In the cost function (8.6a), the matrices $Q = Q^\top \succ 0$, $R = R^\top \succ 0$, $R_\Delta = R_\Delta^\top \succ 0$ and

$$s \geq \frac{\lambda_{max}(Q)}{c} \quad (8.7)$$

are design choices. In order to guarantee closed-loop stability, the terminal equality constraint (8.6c) is introduced on the last element of the input sequence, while no terminal constraints are introduced on the system state. Denote by $\mathbf{\Delta u}_k^\star = \{\Delta u_{0|k}^\star, ..., \Delta u_{N-1|k}^\star\}$ the optimal solution of the FHOCP. According to the receding horizon principle, the MPC control law is

$$\Delta u_k = \mu^{\mathrm{MPC}}(\hat{x}_k, u_{k-1}) = \Delta u_{0|k}^\star.$$

Then, the system input is

$$u_k = u_{k-1} + \mu^{\mathrm{MPC}}(\hat{x}_k, u_{k-1}). \quad (8.8)$$

8.2.3 Stability analysis

In this section, the stability properties of the closed-loop system are analyzed, under the assumption that the system behaves according to its RNN model.

Firstly, note that the feasibility of the FHOCP depends only on the value of u_{k-1} and not on the initial state, since there are no state constraints. Hence, define

$$\mathcal{U}^{\mathrm{MPC}}(\bar{u}) := \{u \in \mathcal{U} : \exists \text{ a sequence } \Delta u_{0|k}, ..., \Delta u_{N-1|k} \\ \text{respecting (8.6c)-(8.6e)-(8.6f)-(8.6g) with } u_{0|k} = u\}.$$

The size of $\mathcal{U}^{\mathrm{MPC}}$ depends on the incremental constraint set $\Delta\mathcal{U}$ and of the prediction horizon N. In presence of a small set $\Delta\mathcal{U}$ it may be necessary to enlarge N to obtain a sufficiently large feasibility set $\mathcal{U}^{\mathrm{MPC}}(\bar{u})$.

Theorem 8.1. *Let Assumptions 8.1-8.2 hold. Then, for the closed-loop system composed by the RNN model* (8.2)*, the observer* (8.4) *and the MPC* (8.8)*, the FHOCP is recursively feasible and the closed-loop system converges to* $x = \bar{x}$*,* $u = \bar{u}$*,* $\hat{x} = \bar{x}$ *with domain of attraction* $x \in \mathcal{X}^{\text{ISS}}$*,* $u \in \mathcal{U}^{\text{MPC}}(\bar{u})$*,* $\hat{x} \in \hat{\mathcal{X}}$*.*

Proof. The proof is reported in Section 8.5.1.

8.3 Illustrative example with LSTM models

This section discusses how the control algorithm proposed in Section 8.2 for the generic RNN model can be applied to the particular case of LSTM networks, considering as system under control the four-tanks process described in Section 6.4.1.

8.3.1 Algorithm for the LSTM model

Consider the LSTM model (4.1) satisfying Assumption 4.1. Then, the LSTM model is δISS in the sets $\mathcal{X}^{\text{ISS}} := \mathcal{C} \times \mathcal{H}$ and $\mathcal{U}^{\text{ISS}}$, where $\mathcal{C}$ and $\mathcal{H}$ are defined in (4.3) and

$$\mathcal{U}^{\text{ISS}} = \{u \in \mathbb{R}^m : \|u\|_\infty \leq u_{max}\}.$$

Under the δISS condition, the function

$$V_{\text{f}}(x^{\text{a}}, x^{\text{b}}) = \left\| \begin{bmatrix} \|c^{\text{a}} - c^{\text{b}}\|_2 \\ \|h^{\text{a}} - h^{\text{b}}\|_2 \end{bmatrix} \right\|_P^2 \tag{8.9}$$

is an incremental Lyapunov function for the LSTM model, where $P \in \mathbb{R}^{2\times 2}$ is the solution of the Lyapunov equation[1]

$$A_\delta^\top P A_\delta - P = -\mathbf{I}_2,$$

$x^{\text{a}} = [(c^{\text{a}})^\top \ (h^{\text{a}})^\top]^\top$ and $x^{\text{b}} = [(c^{\text{b}})^\top \ (h^{\text{b}})^\top]^\top$. Note that condition (8.3) is fulfilled with $a = \lambda_{min}(P)$, $b = \lambda_{max}(P)$ and $c = 1$. Therefore, $V_{\text{f}}(x^{\text{a}}, x^{\text{b}})$ can be used to define the terminal cost for the MPC.

We consider the observer for the LSTM model proposed in [230], that is described by

$$\begin{aligned} \hat{c}_{k+1} = {} & \sigma(W_{\text{f}} u_k + U_{\text{f}} \hat{h}_k + b_{\text{f}} + L_{\text{f}}(y_k - \hat{y}_k)) \otimes \hat{c}_k \\ & + \sigma(W_{\text{i}} u_k + U_{\text{i}} \hat{h}_k + b_{\text{i}} + L_{\text{i}}(y_k - \hat{y}_k)) \otimes \tanh(W_{\text{c}} u_k + U_{\text{c}} \hat{h}_k + b_{\text{c}}) \end{aligned} \tag{8.10a}$$

$$\hat{h}_{k+1} = \sigma(W_{\text{o}} u_k + U_{\text{o}} \hat{h}_k + b_{\text{o}} + L_{\text{o}}(y_k - \hat{y}_k)) \otimes \tanh(\hat{c}_{k+1}) \tag{8.10b}$$

$$\hat{y}_k = W_{\text{y}} \hat{h}_k + b_{\text{y}} \tag{8.10c}$$

[1]The Schur matrix A_δ is defined in Assumption 4.1.

The state of the observer is $\hat{x} = [\hat{c}^\top \ \hat{h}^\top]^\top \in \mathbb{R}^{2n_c}$, and $L_\mathrm{f}, L_\mathrm{i}, L_\mathrm{o} \in \mathbb{R}^{n_c \times p}$ are the observer gains. Under a proper selection of L_f, L_i and L_o, the LSTM observer (8.10) provides a converging state estimation, i.e. $\|\hat{x}_k - x_k\| \to 0$ for $k \to \infty$, for any $\hat{x}_0 \in \mathbb{R}^{2n_c}$.

The observer structure satisfies (8.4)-(8.5). In particular, it is possible to prove (8.5) by following the proof of Theorem 7.1 with $d = \hat{d} = 0$. However, it is not guaranteed that $\mathcal{X}^{\mathrm{ISS}}$ is an invariant set for the observer state $\hat{x}$, as required by Assumption 8.2. To circumvent this issue, a tightened input constraint set $\mathcal{U}$ such that $\mathcal{U} \subset \mathrm{int}(\mathcal{U}^{\mathrm{ISS}})$ can be considered in the MPC formulation. In fact, if $\mathcal{U} \subset \mathrm{int}(\mathcal{U}^{\mathrm{ISS}})$, then there exists a positive invariant set $\mathcal{X} \subset \mathrm{int}(\mathcal{X}^{\mathrm{ISS}})$ for the LSTM state. The observer convergence implies that for any $\varepsilon > 0$ there exists a finite $\bar{k}$ such that $\|\hat{x}_k - x_k\| \leq \varepsilon$ for all $k \geq \bar{k}$. Hence, there exists $\bar{k}$ such that $\hat{x}_{\bar{k}}$ is sufficiently close to $x_{\bar{k}}$ to guarantee that $\hat{x}_{\bar{k}} \in \mathcal{X}^{\mathrm{ISS}}$, in view of the fact that $x_k \in \mathcal{X}$.

In conclusion, in view of the existence of an incremental Lyapunov (8.9) for the LSTM model that satisfies Assumption 8.1, and of an observer that satisfies Assumption 8.2, the proposed control algorithm can be applied using an LSTM model, provided that the input constraint set is such that $\mathcal{U} \subset \mathrm{int}(\mathcal{U}^{\mathrm{ISS}})$.

8.3.2 Simulation results

For the simulation example, we consider the four-tanks process described in Section 6.4.1. We consider the operational and safety constraints $q_a \in [0.0, 9.05]\times10^{-4}m^3/s$, $q_b \in [0.0, 11.1]\times10^{-4}m^3/s$ and $\Delta q_a, \Delta q_b \in [-1.0, 1.0]\times 10^{-4}m^3/s$, where Δq_a and Δq_b are the maximum input variations between subsequent sampling instants. The need for incremental input constraint is motivated by the fact that the system is actuated by pumps, whose acceleration is related to wear and electrical consumption [53].

To derive the LSTM model of the plant, a sampling time of $T_s = 25s$ is considered. The model is trained using an input-output dataset composed of 20000 time steps, that is split in a training set of 15000 time steps, a validation set of 2500 time steps, and a test set of 2500 time steps. The training set is then divided into subsequences of 1000 time steps each, and a training of 1000 epochs is performed using a learning rate of 0.001 and Adam optimizer [127]. The loss function is the sum of the mean squared error and of a regularization term used to enforce the δISS property, see Section 4.2.2. The model inputs and outputs are normalized within the range [-1,1], using the maximum and minimum values of the input constraints to normalize the inputs, and the maximum and minimum values in the training dataset to normalize the outputs. The resulting network has $n_c = 10$ neurons, achieves a FIT on the test dataset of 93.4% for h_1 and of 87.9% for h_2, and fulfills the δISS condition considering $u_{max} = 1.05$, that is larger that the range of feasible inputs in the normalized variables.

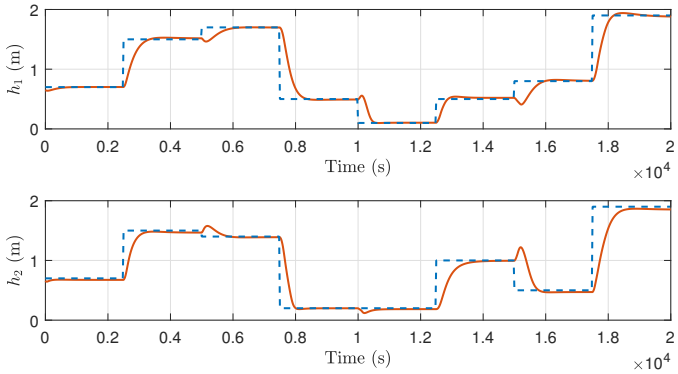

Figure 8.2: Closed-loop trajectories: output (orange solid line) and reference (blue dashed line).

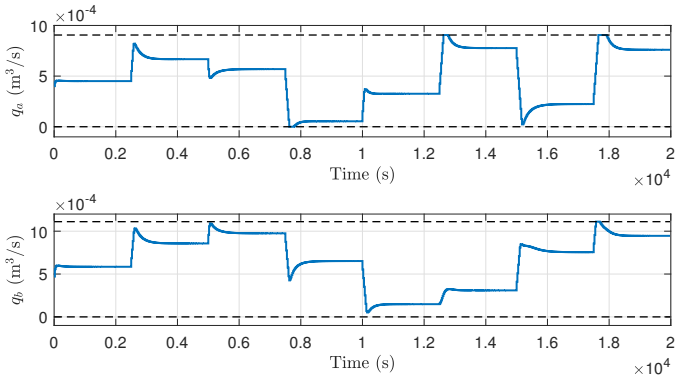

Figure 8.3: Closed-loop trajectories: input (blue solid line) and constraints (black dashed lines).

For the design of the control algorithm, the observer is tuned according to the optimization proposed in [230], whereas the cost matrices for the MPC are set to $Q = \mathbf{I}_{2n_c}$, $R = \mathbf{I}_m$, $R_\Delta = \mathbf{I}_m$ and s is selected according to (8.7) with the equality. The considered prediction horizon is $N = 10$. The closed-loop simulations are performed in Matlab, and the optimization problem is solved numerically using CasADi [6].

The output, input and input variation of the closed-loop trajectories for the four-tanks process are reported respectively in Figures 8.2, 8.3 and 8.4. It can be seen that the control system is capable of correctly managing the plant and respecting the constraints on the input and on the input variation. Moreover, the simulation shows that the proposed algorithm is able to handle also step-wise variations of the reference, and not only constant references as proven in Theorem 8.1. In fact, the feasibility of the FHOCP only depends on the input, so it is maintained provided that the new reference $\bar{u}$ is such that the current value of the input is in $\mathcal{U}^{\text{MPC}}(\bar{u})$.

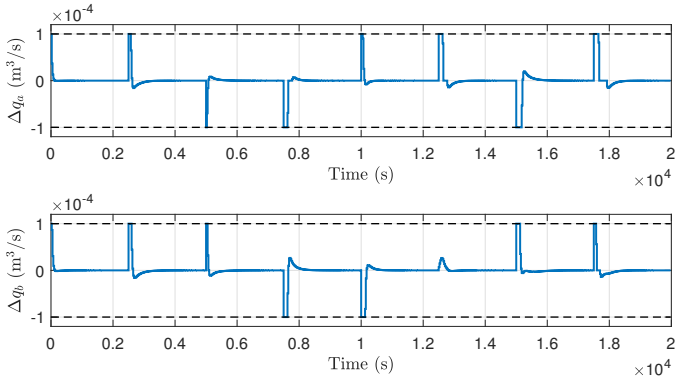

Figure 8.4: Closed-loop trajectories: variation of the input (blue solid line) and constraints (black dashed lines).

8.4 Conclusions

In this chapter, an MPC algorithm based on a δISS RNN model is proposed for systems with hard constraints on the input and on the input incremental variation. Closed-loop convergence is guaranteed by introducing a general formulation for the terminal cost, while a terminal equality constraint on the optimal input sequence takes into account the presence of the integrator. Remarkably, the proposed approach can be easily applied to different δISS RNN architectures. In the application to LSTM models it is shown how it is possible to manage the case where the δISS property is valid only in an invariant set.

8.5 Proofs

8.5.1 Proof of Theorem 8.1

Denote the optimal input sequence and state trajectory computed by the MPC at time step k respectively by $\mathbf{u}_k^\star = \{u_{i|k}^\star\}_{i=0}^N$ and $\mathbf{x}_k^\star = \{x_{i|k}^\star\}_{i=0}^N$, where $x_{0|k}^\star = \hat{x}_k$ and $u_{0|k}^\star = u_{k-1}$.

To prove recursive feasibility, assuming that the FHOCP is feasible at time step k, it is sufficient to consider as candidate solution at time step $k+1$ the sequence $\boldsymbol{\Delta}\tilde{\mathbf{u}}_{k+1} = \{\Delta\tilde{u}_{0|k+1}, ..., \Delta\tilde{u}_{N-1|k+1}\}$, defined by $\Delta\tilde{u}_{i|k+1} := \Delta u_{i+1|k}^\star$ for $i = 1, ..., N-2$ and $\Delta\tilde{u}_{N-1|k+1} := 0$, that trivially satisfies constraints (8.6c)-(8.6f)-(8.6g).

In view of Assumption 8.2, there exists a finite value $\bar{k} \geq 0$ such that $\hat{x}_k \in \mathcal{X}^{\text{ISS}}$ for all $k \geq \bar{k}$. Moreover, for Assumption 8.1, the set $\mathcal{X}^{\text{ISS}}$ is positive invariant for the model state x. Hence, along the proof of convergence, it is assumed that $\hat{x} \in \mathcal{X}^{\text{ISS}}$ and $x \in \mathcal{X}^{\text{ISS}}$, which is true for all $k \geq \bar{k}$. In addition, in view of Assumption 8.2, $\|x_k - \hat{x}_k\|$ is bounded and converges to

zero. Hence, the observer innovation δx is considered as a disturbance term, and it is shown that the closed-loop system is ISS with respect to it. Then, convergence follows in view of (8.5) and of the convergence of the observer estimation error.

In order to prove ISS, consider the optimal cost of the MPC $V(x,u)$ as candidate ISS-Lyapunov function, i.e.

$$V(x,u) = \sum_{i=0}^{N-1} \left(\|x^\star_{i|k} - \bar{x}\|^2_Q + \|u^\star_{i|k} - \bar{u}\|^2_R + \|\Delta u^\star_{i|k}\|^2_{R_\Delta} \right) + sV_{\mathrm{f}}(x^\star_{N|k}, \bar{x})$$

where $x = x^\star_{0|k}$ and $u = u^\star_{0|k}$. Note that V is also a function of u, that is the state of the discrete time integrator at time step k.

Firstly, derive a lower bound for $V(x,u)$

$$\begin{aligned} V(x,u) &\geq \|x^\star_{0|k} - \bar{x}\|^2_Q + \|u^\star_{0|k} - \bar{u}\|^2_R \\ &\geq \lambda_{min}(Q)\,\|x - \bar{x}\|_2^2 + \lambda_{min}(R)\,\|u - \bar{u}\|_2^2 . \end{aligned} \tag{8.11}$$

To derive an upper bound for $V(x,u)$, consider as candidate solution at time k the sequence $\boldsymbol{\Delta}\tilde{\mathbf{u}}_k = \{\Delta\tilde{u}_{0|k}, ..., \Delta\tilde{u}_{N-1|k}\}$, where $\Delta\tilde{u}_{0|k} = \bar{u} - u$ and $\Delta\tilde{u}_{i|k} = 0$ for $i = 1, ..., N-1$. This solution is feasible for u in a neighborhood of $\bar{u}$. Denote by $\tilde{\mathbf{x}}_k = \{\tilde{x}_{i|k}\}_{i=0}^N$ the associate state trajectory. One has that

$$V(x,u) \leq \sum_{i=0}^{N-1} \left\|\tilde{x}_{i|k} - \bar{x}\right\|^2_Q + \|u - \bar{u}\|^2_R + \|\bar{u} - u\|^2_{R_\Delta} + sV_f(\tilde{x}_{N|k}, \bar{x}).$$

In view of the δISS property of the model and of (8.3a), there exists $b_x > 0$ such that, for u in a neighborhood of $\bar{u}$,

$$V(x,u) \leq b_x\,\|x - \bar{x}\|_2^2 + (\lambda_{max}(R) + \lambda_{max}(R_\Delta))\,\|u - \bar{u}\|_2^2 . \tag{8.12}$$

Given this local upper bound, the existence of an upper bound for any $u \in \mathcal{U}^{\mathrm{MPC}}(\bar{u})$ follows from [149, Lemma 4].

To prove the decreasing property of $V(x,u)$, denote $u^+ := u + \mu^{\mathrm{MPC}}(x,u)$ and $x^+ := f(x,u^+) + \delta x$. The term δx due to the observer presence is regarded as an external disturbance. Consider now the candidate solution $\boldsymbol{\Delta}\tilde{\mathbf{u}}_{k+1}$ introduced to prove recursive feasibility. Denote by $\tilde{\mathbf{u}}_{k+1} = \{\tilde{u}_{0|k+1}, ..., \tilde{u}_{N|k+1}\}$ the associate input sequence, defined by $\tilde{u}_{0|k+1} := u^+$ and $\tilde{u}_{i+1|k+1} := \tilde{u}_{i|k+1} + \Delta\tilde{u}_{i|k+1}$ for $i \in [0 : N-1]$, and by $\tilde{\mathbf{x}}_{k+1} = \{\tilde{x}_{0|k+1}, ..., \tilde{x}_{N|k+1}\}$ the associate state trajectory, defined by $\tilde{x}_{0|k+1} := x^+$ and $\tilde{x}_{i+1|k+1} := f(\tilde{x}_{i|k+1}, \tilde{u}_{i+1|k+1})$ for $i \in [0 : N-1]$.

Define $x^\star_{N+1|k} := f(x^\star_{N|k}, \bar{u})$, and denote $\varepsilon_{k+i} := \tilde{x}_{i-1|k+1} - x^\star_{i|k}$ for $i \in$

$[1:N]$. Then

$$
\begin{aligned}
V(x^+,u^+)-V(x,u)\leq\\
&\sum_{i=0}^{N-1}\Big(\left\|\tilde{x}_{i|k+1}-\bar{x}\right\|_Q^2+\left\|\tilde{u}_{i|k+1}-\bar{u}\right\|_R^2\\
&+\left\|\Delta\tilde{u}_{i|k+1}\right\|_{R_\Delta}^2\Big)+sV_f(\tilde{x}_{N|k+1},\bar{x})\\
&-\sum_{i=0}^{N-1}\left(\left\|x^\star_{i|k}-\bar{x}\right\|_Q^2+\left\|u^\star_{i|k}-\bar{u}\right\|_R^2+\left\|\Delta u^\star_{i|k}\right\|_{R_\Delta}^2\right)\\
&-sV_f(x^\star_{N|k},\bar{x})\\
\leq&-\|x-\bar{x}\|_Q^2-\|u-\bar{u}\|_R^2-\left\|\Delta u^\star_{0|k}\right\|_{R_\Delta}^2\\
&+\sum_{i=1}^{N-1}\left(\|\varepsilon_{k+i}\|_Q^2+\varepsilon_{k+i}^\top Q(x^\star_{i|k}-\bar{x})\right)\\
&+sV_f(\tilde{x}_{N|k+1},\bar{x})+\left\|\tilde{x}_{N-1|k+1}-\bar{x}\right\|_Q^2-sV_f(x^\star_{N|k},\bar{x}).
\end{aligned}
$$

Consider now the terms related to the terminal cost. First, note that $\tilde{x}_{N|k+1}$, $x^\star_{N+1|k}$ and $\bar{x}$ are bounded in view of the boundedness of $\mathcal{U}$ and of the δISS property of the system. Then, in view of Assumption 8.1, there exists a Lipschitz constant $\bar{L}_V$ such that

$$
|V_f(\tilde{x}_{N|k+1},\bar{x})-V_f(x^\star_{N+1|k},\bar{x})|\leq\bar{L}_V\left\|\varepsilon_{k+N+1}\right\|_2.
$$

Then

$$
\begin{aligned}
&sV_f(\tilde{x}_{N|k+1},\bar{x})+\left\|\tilde{x}_{N-1|k+1}-\bar{x}\right\|_Q^2-sV_f(x^\star_{N|k},\bar{x})\\
&\leq sV_f(x^\star_{N+1|k},\bar{x})+\|x^\star_{N|k}-\bar{x}\|_Q^2-sV_f(x^\star_{N|k},\bar{x})\\
&\quad+s\bar{L}_V\left\|\varepsilon_{k+N+1}\right\|_2+\|\varepsilon_{k+N}\|_Q^2+\varepsilon_{k+N}^\top Q(x^\star_{N|k}-\bar{x})\\
&\leq sV_f(f(x^\star_{N|k},\bar{u}),f(\bar{x},\bar{u}))-sV_f(x^\star_{N|k},\bar{x})+\lambda_{max}(Q)\|x^\star_{N|k}-\bar{x}\|_2^2\\
&\quad+s\bar{L}_V\left\|\varepsilon_{k+N+1}\right\|_2+\|\varepsilon_{k+N}\|_Q^2+\varepsilon_{k+N}^\top Q(x^\star_{N|k}-\bar{x})\\
&\overset{(8.3b)}{\leq}-sc\|x^\star_{N|k}-\bar{x}\|_2^2+\lambda_{max}(Q)\|x^\star_{N|k}-\bar{x}\|_2^2\\
&\quad+s\bar{L}_V\left\|\varepsilon_{k+N+1}\right\|_2+\|\varepsilon_{k+N}\|_Q^2+\varepsilon_{k+N}^\top Q(x^\star_{N|k}-\bar{x})\\
&\overset{(8.7)}{\leq}s\bar{L}_V\left\|\varepsilon_{k+N+1}\right\|_2+\|\varepsilon_{k+N}\|_Q^2+\varepsilon_{k+N}^\top Q(x^\star_{N|k}-\bar{x}).
\end{aligned}
$$

Combining the computation, one has that

$$\begin{aligned} &V(x^+,u^+)-V(x,u)\leq \\ &-\|x-\bar{x}\|_Q^2-\|u-\bar{u}\|_R^2-\left\|\Delta u_{0|k}^\star\right\|_{R_\Delta}^2 \\ &+\sum_{i=1}^{N-1}\left(\|\varepsilon_{k+i}\|_Q^2+\varepsilon_{k+i}^\top Q(x_{i|k}^\star-\bar{x})\right) \\ &+s\bar{L}_V\|\varepsilon_{k+N+1}\|_2+\|\varepsilon_{k+N}\|_Q^2+\varepsilon_{k+N}^\top Q(x_{N|k}^\star-\bar{x}). \end{aligned}$$

In view of the boundedness of $\mathcal{U}$ and of the δISS property of the system, the values of $x_{i|k}^\star$ are bounded for $i=1,...,N$. Moreover, $\varepsilon_{k+1}=\delta x$ and, for the δISS property of the model, $\|\varepsilon_{k+i+1}\|_2\leq\beta(\|\delta x\|_2,i)$ for a $\mathcal{KL}$-function β. Then, there exists a $\mathcal{K}$-function γ such that

$$V(x^+,u^+)-V(x,u)\leq-\|x-\bar{x}\|_Q^2-\|u-\bar{u}\|_R^2+\gamma(\|\delta x\|_2). \tag{8.13}$$

In view of (8.11)-(8.12)-(8.13), the closed-loop system is ISS with respect to the disturbance δx. Convergence follows from the fact that $\delta x\to 0$ for $k\to\infty$. □

Chapter 9

Offset-free tracking MPC for δISS systems with input rate constraints

In this chapter we propose a stabilizing MPC formulation for δISS systems that considers simultaneously

1. output feedback,
2. artificial reference-based tracking,
3. offset-free tracking of asymptotically constant references,
4. input rate constraints and penalty,
5. use of a positive semi-definite stage cost (e.g. for output weighting).

The proposed MPC algorithm is highly modular, with each aspect taken care of with few specific ingredients, and it joins in a unique framework different aspects that have already been analyzed separately in the previous chapters. For the proposed control algorithm, we prove recursive feasibility and stability by relying on terminal ingredients, and on a cost detectability function. The size of the feasible region depends on input and input rate constraint, and on the length of the horizon, and can greatly benefit from the use of artificial reference variables. The MPC formulation is tested in simulation on the pH neutralization process, whose dynamics is modeled by means of a REN model. In the example it is also shown how to design and tune an observer to estimate both the state and the disturbance, starting from an observer for the state only, using the small gain theorem.

The content of this chapter has been published in:

- [77] Galuppini, G., **Schimperna, I.** and Magni L. (2025). *Offset-free Output Feedback Tracking MPC for δISS Nonlinear Systems Subject to*

Input and Input Rate Constraints. IEEE Transactions on Automatic Control.

9.1 Preliminary notation and definition

In this chapter, given a set $\mathcal{A} \subset \mathbb{R}^n$, we use the notation

$$\mathcal{S}(\mathcal{A}) := \max_{a_1, a_2 \in \mathcal{A}} \|a_1 - a_2\|_2.$$

We also introduce the following definition.

Definition 9.1 (Uniformly strongly convex function, [221])**.** *A function $V : \mathbb{R}^n \to \mathbb{R}$ is uniformly strongly convex if there exists a constant $\sigma > 0$ such that for all $x_1, x_2 \in \mathbb{R}^n$ and $\lambda \in (0, 1)$*

$$V((1-\lambda)x_1 + \lambda x_2) \leq (1-\lambda)V(x_1) + \lambda V(x_2) - \frac{1}{2}\sigma\lambda(1-\lambda)\|x_1 - x_2\|_2^2.$$

9.2 Problem statement

In this chapter, we consider as system under control a disturbed discrete-time system given by

$$x_{k+1} = f(x_k, u_k) \tag{9.1a}$$
$$d_{k+1} = d_k + w_k \tag{9.1b}$$
$$y_{\mathrm{d},k} = h(x_k, u_k) + d_k, \tag{9.1c}$$

with state $x \in \mathbb{R}^n$, input $u \in \mathbb{R}^m$, and output $y_\mathrm{d} \in \mathbb{R}^p$, with $p \leq m$. Functions $f : \mathbb{R}^n \times \mathbb{R}^m \to \mathbb{R}^n$ and $g : \mathbb{R}^n \times \mathbb{R}^m \to \mathbb{R}^p$ are assumed continuous. $d_k \in \mathcal{D} \subset \mathbb{R}^p$ and $w_k \in \mathcal{W} \subset \mathbb{R}^p$ represent respectively an output disturbance term and its variation, and the sets $\mathcal{D}$ and $\mathcal{W}$ are assumed closed and bounded. In the following, we will indicate the disturbed system (9.1) by Σ_d, and we will use $x_\mathrm{d} := [x^\top \ d^\top]^\top$ to denote its state, and $f_\mathrm{d}(x, u, d, w)$ and $h_\mathrm{d}(x, u, d)$ to denote its dynamic equation and output transformation functions, respectively.

The objective of the chapter is to design an output-feedback tracking MPC based on the nominal model Σ of the system, given by

$$x_{k+1} = f(x_k, u_k) \tag{9.2a}$$
$$y_k = h(x_k, u_k), \tag{9.2b}$$

where $y \in \mathbb{R}^p$. The system is subject to hard constraints on the control input and the control input rate: $u_k \in \mathcal{U}$, $\Delta u_k \in \Delta\mathcal{U}$ for all $k \in \mathbb{Z}_{\geq 0}$, with $\Delta u_k := u_k - u_{k-1}$, and with $\mathcal{U} \subset \mathbb{R}^m$ and $\Delta\mathcal{U} \subset \mathbb{R}^m$ compact sets with non empty interior, and $\Delta\mathcal{U}$ containing the origin in its interior. We define y_k^0 as

the exogenous setpoint signal to be tracked at time instant k, and assume $y_k^0 \in \mathcal{Y}^0$ for all $k \in \mathbb{Z}_{\geq 0}$, with $\mathcal{Y}^0 \subset \mathbb{R}^p$ a closed and bounded set.

The nominal model Σ is assumed to be δISS, as formalized in the following assumption.

Assumption 9.1 (δISS property of the model)**.** *The model* (9.2) *is δISS, and there exists a δISS-Lyapunov function $V(x^{\mathrm{a}} - x^{\mathrm{b}})$ such that for any $x^{\mathrm{a}}, x^{\mathrm{b}} \in \mathbb{R}^n$, $u^{\mathrm{a}}, u^{\mathrm{b}} \in \mathbb{R}^m$*

$$\alpha_1(\|x^{\mathrm{a}} - x^{\mathrm{b}}\|_2) \leq V(x^{\mathrm{a}} - x^{\mathrm{b}}) \leq \alpha_2(\|x^{\mathrm{a}} - x^{\mathrm{b}}\|_2), \tag{9.3a}$$

$$V(f(x^{\mathrm{a}}, u^{\mathrm{a}}) - f(x^{\mathrm{b}}, u^{\mathrm{b}})) - V(x^{\mathrm{a}} - x^{\mathrm{b}}) \leq -\alpha_3(\|x^{\mathrm{a}} - x^{\mathrm{b}}\|_2) + \gamma_1(\|x^{\mathrm{a}} - x^{\mathrm{b}}\|_2) \tag{9.3b}$$

with $\alpha_1, \alpha_2, \alpha_3 \in \mathcal{K}_\infty$ and $\gamma_1 \in \mathcal{K}$.

Let an equilibrium state, input, and output of the system Σ be denoted by $(x_{\mathrm{s}}, u_{\mathrm{s}}, y_{\mathrm{s}})$. Then, by introducing an arbitrarily small constant $\varepsilon_{\mathrm{u}} > 0$, define the set of admissible equilibrium states, inputs and outputs such that the constraints are not active as

$$\begin{aligned}
\hat{\mathcal{U}} &:= \{u : u + e_{\mathrm{u}} \in \mathcal{U}, \forall\ \|e_{\mathrm{u}}\|_2 \leq \varepsilon_{\mathrm{u}}\},\\
\mathcal{Z}_{\mathrm{s}} &:= \{(x, u) \in \mathbb{R}^{m+n} : u \in \hat{\mathcal{U}},\ x = f(x, u)\},\\
\mathcal{Y}_{\mathrm{s}} &:= \{y = h(x, u) : (x, u) \in \mathcal{Z}_{\mathrm{s}}\}.
\end{aligned}$$

Assume $\mathcal{Z}_{\mathrm{s}}$ is non empty, and define $\mathcal{Y}_{\mathrm{t}}$ as a non empty convex subset of $\mathcal{Y}_{\mathrm{s}}$. Note that, since $\hat{\mathcal{U}}$ is bounded and Σ is δISS, then $\mathcal{Y}_{\mathrm{s}}$ and $\mathcal{Y}_{\mathrm{t}}$ are bounded.

Assumption 9.2 (Uniqueness of the equilibrium)**.** *For any equilibrium output $y_{\mathrm{s}} \in \mathcal{Y}_{\mathrm{t}}$ there exists a unique equilibrium $(x_{\mathrm{s}}, u_{\mathrm{s}}, y_{\mathrm{s}})$. Moreover, there exist Lipschitz continuous functions $g_{\mathrm{x}} : \mathcal{Y}_{\mathrm{t}} \to \mathbb{R}^n$ and $g_{\mathrm{u}} : \mathcal{Y}_{\mathrm{t}} \to \mathbb{R}^m$ such that $x_{\mathrm{s}} = g_{\mathrm{x}}(y_{\mathrm{s}})$ and $u_{\mathrm{s}} = g_{\mathrm{u}}(y_{\mathrm{s}})$, i.e. $f(g_{\mathrm{x}}(y_{\mathrm{s}}), g_{\mathrm{u}}(y_{\mathrm{s}})) = g_{\mathrm{x}}(y_{\mathrm{s}})$ and $h(g_{\mathrm{x}}(y_{\mathrm{s}}), g_{\mathrm{u}}(y_{\mathrm{s}})) = y_{\mathrm{s}}$.*

Define then a function $g : \mathcal{Y}_{\mathrm{t}} \to \mathbb{R}^{n+m}$ such that $[x_{\mathrm{s}}^\top\ u_{\mathrm{s}}^\top]^\top = g(y_{\mathrm{s}}) = [g_{\mathrm{x}}(y_{\mathrm{s}})^\top\ g_{\mathrm{u}}(y_{\mathrm{s}})^\top]^\top$, and let L_g be its Lipschitz constant. The dependence of $x_{\mathrm{s}}(y_{\mathrm{s}})$ and $u_{\mathrm{s}}(y_{\mathrm{s}})$ on y_{s} may be omitted in the reminder of the chapter for sake of compactness.

Remark 9.1. *Assumption 9.2 is frequently introduced in the design of MPC for tracking as well as offset-free MPC (see e.g., [151, 76, 142, 173]) to ensure convergence of the closed-loop to the desired steady-state. Moreover, if the equilibrium $(x_{\mathrm{s}}, u_{\mathrm{s}}, y_{\mathrm{s}})$ is univocally determined by y_{s}, and f and h are continuously differentiable, a straightforward way to verify g is (locally) Lipschitz is checking that the Jacobian*

$$\begin{bmatrix} \left(\left.\frac{\partial f(x,u)}{\partial x}\right|_{\substack{x=x_{\mathrm{s}}\\u=u_{\mathrm{s}}}} - \mathbf{I}_n\right) & \left.\frac{\partial f(x,u)}{\partial u}\right|_{\substack{x=x_{\mathrm{s}}\\u=u_{\mathrm{s}}}} \\ \left.\frac{\partial h(x,u)}{\partial x}\right|_{\substack{x=x_{\mathrm{s}}\\u=u_{\mathrm{s}}}} & \left.\frac{\partial h(x,u)}{\partial u}\right|_{\substack{x=x_{\mathrm{s}}\\u=u_{\mathrm{s}}}} \end{bmatrix} \tag{9.4}$$

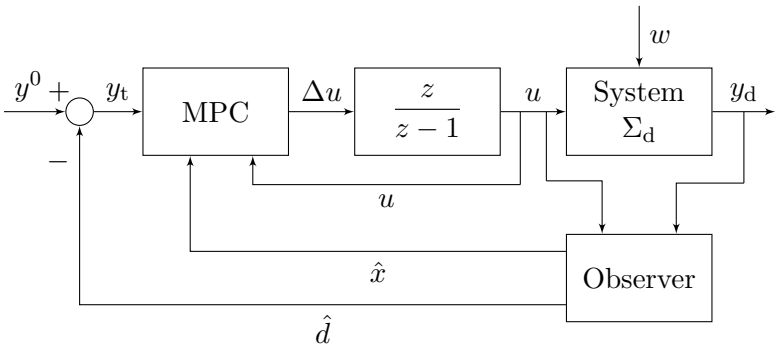

Figure 9.1: Block scheme of the control algorithm.

is nonsingular for all $(x_\mathrm{s}, u_\mathrm{s}) \in \mathcal{Z}_\mathrm{s}$*. Moreover, when uniqueness of the couple* $(x_\mathrm{s}, u_\mathrm{s}) \in \mathcal{Z}_\mathrm{s}$ *corresponding to any* $y_\mathrm{s} \in \mathcal{Y}_\mathrm{t}$ *does not directly follow from* f *and* h*, it can be restored by properly restricting* $\mathcal{Z}_\mathrm{s}$ *to exclude multiple choices.*

9.3 Control design

This section is devoted to the description of the proposed control methodology. The block scheme of the control algorithm is reported in Figure 9.1, and includes a state observer, an MPC, and an integral action acting on the plant input. At each time instant k, the observer provides estimates for both plant state and output disturbance ($\hat{x}_k$ and $\hat{d}_k$). The MPC is in charge of forcing the plant output $y_{\mathrm{d},k}$ to track the setpoint y^0_k. To do so, the MPC is designed based on the knowledge of the nominal δISS system Σ only, and the unmodeled output disturbance d_k is considered by modifying the setpoint provided to the MPC with the disturbance estimation obtained with the observer. Therefore, the MPC setpoint is given by

$$y_{\mathrm{t},k} = y^0_k - \hat{d}_k.$$

Moreover, the integral action allows constraining and penalizing in the MPC both the plant control input u_k, and the control input rate, Δu_k. Each element of the control scheme is discussed in detail in the reminder of this section.

9.3.1 State Observer

Consider a generic time invariant observer for the system Σ_d, with structure

$$\begin{aligned}\hat{x}_{\mathrm{d},k+1} &= f_\mathrm{d}(\hat{x}_k, u_k, \hat{d}_k, 0) + \delta x_\mathrm{d}(\hat{x}_k, u_k, \hat{d}_k, y_{\mathrm{d},k}) \\ &= \begin{bmatrix} f(\hat{x}_k, u_k) \\ \hat{d}_k \end{bmatrix} + \begin{bmatrix} \delta x(\hat{x}_k, u_k, \hat{d}_k, y_{\mathrm{d},k}) \\ \delta d(\hat{x}_k, u_k, \hat{d}_k, y_{\mathrm{d},k}) \end{bmatrix}\end{aligned} \tag{9.5}$$

where $\hat{x}_\mathrm{d} = [\hat{x}^\top \ \hat{d}^\top]^\top \in \mathbb{R}^{n+p}$ is the estimate of the state of Σ_d, and $\delta x_\mathrm{d}(\hat{x}_k, u_k, \hat{d}_k, y_{\mathrm{d},k})$ is the observer innovation[1]. Note that any time invariant observer $\hat{x}_{\mathrm{d},k+1} = \hat{f}_\mathrm{d}(\hat{x}_k, u_k, \hat{d}_k, y_{\mathrm{d},k})$ can be written in this form with $\delta x_\mathrm{d}(\hat{x}_k, u_k, \hat{d}_k, y_{\mathrm{d},k}) = \hat{f}_\mathrm{d}(\hat{x}_k, u_k, \hat{d}_k, y_{\mathrm{d},k}) - f_\mathrm{d}(\hat{x}_k, u_k, \hat{d}_k, 0)$. The state estimation error is given by

$$e_{\mathrm{d},k} := x_{\mathrm{d},k} - \hat{x}_{\mathrm{d},k}. \tag{9.6}$$

Note that the disturbance w affecting the plant is not measurable, and its dynamics not available. This motivates the choice of setting $w_k = 0$ in the design of the observer, thus resulting in a constant output disturbance.

Assumption 9.3 (Bound on the observer innovation term)**.** *There exists a function $\alpha_\mathrm{OI} \in \mathcal{K}$ such that $\|\delta x\|_2 \leq \alpha_\mathrm{OI}(\|e_\mathrm{d}\|_2)$.*

Assumption 9.3 ensures that for $e_\mathrm{d} = 0$ the observer state evolves without any correction based on the system output $y_{\mathrm{d},k}$. Now, let Σ_O be the system that describes the dynamic relation between the system inputs, and the observer estimation error, i.e. the system with state e_d and inputs u and w.

Assumption 9.4 (ISS of the observer estimation error)**.** *The system Σ_O is ISS with respect to the disturbance w, for any input sequence in $\mathcal{U}$.*

Assumption 9.5 (Boundedness of initial conditions)**.** *There exist bounded sets $\mathcal{X}_{\mathrm{d},0} \subset \mathbb{R}^{n+p}$ and $\hat{\mathcal{X}}_{\mathrm{d},0} \subset \mathbb{R}^{n+p}$ such that $x_{\mathrm{d},0} \in \mathcal{X}_{\mathrm{d},0}$ and $\hat{x}_{\mathrm{d},0} \in \hat{\mathcal{X}}_{\mathrm{d},0}$.*

Note that since $\hat{x}_{\mathrm{d},0}$ is a design choice, its boundedness required by Assumption 9.5 can be directly enforced in the algorithm design.

Lemma 9.1 (Boundedness of system and observer states)**.** *Under Assumption 9.1, 9.4 and 9.5, if $u_h \in \mathcal{U}$ for all $h = 0, ..., k-1$, then there exist bounded sets $\mathcal{X} \subset \mathbb{R}^n$ and $\hat{\mathcal{X}}_\mathrm{d} \subset \mathbb{R}^{n+p}$, such that $x_k \in \mathcal{X}$ and $\hat{x}_{\mathrm{d},k} \in \hat{\mathcal{X}}_\mathrm{d}$, for all $k \in \mathbb{Z}_{\geq 0}$.*

Proof. The fact that x_k is bounded $\forall k \in \mathbb{Z}_{\geq 0}$ follows from Assumption 9.1, and boundedness of u. Then, since $\hat{x}_{\mathrm{d},k} = e_{\mathrm{d},k} - x_{\mathrm{d},k}$, the fact that $\hat{x}_{\mathrm{d},k}$ is bounded follows from the ISS property of the observer and from boundedness of w, d, x, $x_{\mathrm{d},0}$ and $\hat{x}_{\mathrm{d},0}$. □

9.3.2 MPC Formulation

As in Chapter 8, to constrain and penalize the control input variation, the MPC considers a system Σ_u given by the model Σ extended by an integral

[1] $\delta x_\mathrm{d}(\hat{x}_k, u_k, \hat{d}_k, y_{\mathrm{d},k})$ will be also denoted as $\delta x_{\mathrm{d},k}$ in the reminder of the chapter, for sake of compactness.

action, as follows

$$x_{k+1} = f(x_k, u_k) \tag{9.7a}$$
$$u_k = u_{k-1} + \Delta u_k \tag{9.7b}$$
$$y_k = h(x_k, u_k). \tag{9.7c}$$

We denote by $\chi_k = [x_k^\top \ u_{k-1}^\top]^\top$ and y_k the state and output of the extended system (9.7). The steady state of Σ_u is given by $[x_\mathrm{s}^\top \ u_\mathrm{s}^\top]^\top = [g_\mathrm{x}(y_\mathrm{s})^\top \ g_\mathrm{u}(y_\mathrm{s})^\top]^\top$, that we will denote in a compact way by χ_s.

For a given state estimation $\hat{x}_k$, a given input u_{k-1}, and a given setpoint $y_{\mathrm{t},k}$[2], the cost function of the proposed MPC is

$$\begin{aligned} J_N(\hat{x}_k, u_{k-1}, y_{\mathrm{t},k}; \mathbf{\Delta u}_k, y_{\mathrm{s},k}) = &\sum_{i=0}^{N-1} \ell(x_{i|k} - x_{\mathrm{s},k}, u_{i|k} - u_{\mathrm{s},k}, \Delta u_{i|k}) \\ &+ V_\mathrm{f}(x_{N|k} - x_{\mathrm{s},k}, y_{\mathrm{s},k}) + V_\mathrm{O}(y_{\mathrm{s},k} - y_{\mathrm{t},k}) \\ &+ \Psi(\hat{x}_k - x_{\mathrm{s},k}, u_{k-1} - u_{\mathrm{s},k}) \end{aligned} \tag{9.8}$$

where $\mathbf{\Delta u}_k = \{\Delta u_{i|k}\}_{i=0}^{N-1}$ is the sequence of control input variations, $y_{\mathrm{s},k}$ is the artificial reference at time k, and N is the control horizon. $x_{i|k}$ and $u_{i|k}$ are respectively the predicted states of the system and of the discrete time integrator, obtained by applying $\mathbf{\Delta u}_k$ to the system Σ_u with initial state $[\hat{x}_k^\top \ u_{k-1}^\top]^\top$. The function $\ell : \mathbb{R}^{n+m+m} \to \mathbb{R}_{\geq 0}$ is the stage cost function, the function $V_\mathrm{f} : \mathbb{R}^n \to \mathbb{R}_{\geq 0}$ is the terminal cost function, the function $V_\mathrm{O} : \mathbb{R}^p \to \mathbb{R}_{\geq 0}$ is the offset cost function, and the function $\Psi : \mathbb{R}^{n+m} \to \mathbb{R}_{\geq 0}$ is the cost detectability function. Specifically, V_O is necessary to regularize the choice of the artificial output reference $y_{\mathrm{s},k}$ with respect to the actual output reference $y_{\mathrm{t},k}$, see [151]. If the stage cost is positive semi-definite (i.e. it does not satisfy Assumption 3.1 on positive definiteness), the cost detectability function Ψ is necessary to regularize the choice of the artificial steady-state $x_{\mathrm{s},k}$ with respect to the current estimated state $\hat{x}_k$, see [76].

The MPC for tracking control law at time step k is derived from the

[2]Recall that the actual MPC setpoint is $y_{\mathrm{t},k} = y_k^0 - \hat{d}_k$, to account for the current disturbance estimation available at time instant k.

solution of the FHOCP

$$\begin{aligned}
\min_{\boldsymbol{\Delta u}_k, y_{\mathrm{s},k}} \quad & J_N(\hat{x}_k, u_{k-1}, y_{\mathrm{t},k}; \boldsymbol{\Delta u}_k, y_{\mathrm{s},k}) && \text{(9.9a)}\\
\text{s.t.} \quad & x_{0|k} = \hat{x}_k, \quad u_{0|k} = u_{k-1} && \text{(9.9b)}\\
& x_{i+1|k} = f(x_{i|k}, u_{i+1|k}), \quad \text{for } i \in [0:N-1] && \text{(9.9c)}\\
& u_{i+1|k} = u_{i|k} + \Delta u_{i|k}, \quad \text{for } i \in [0:N-1] && \text{(9.9d)}\\
& u_{i|k} \in \mathcal{U}, \quad \text{for } i \in [0:N-1] && \text{(9.9e)}\\
& \Delta u_{i|k} \in \Delta\mathcal{U}, \quad \text{for } i \in [0:N-1] && \text{(9.9f)}\\
& x_{\mathrm{s},k} = f(x_{\mathrm{s},k}, u_{\mathrm{s},k}) && \text{(9.9g)}\\
& (x_{\mathrm{s},k}, u_{\mathrm{s},k}) \in \mathcal{Z}_{\mathrm{s}} && \text{(9.9h)}\\
& y_{\mathrm{s},k} = h(x_{\mathrm{s},k}, u_{\mathrm{s},k}) && \text{(9.9i)}\\
& y_{\mathrm{s},k} \in \mathcal{Y}_{\mathrm{t}} && \text{(9.9j)}\\
& u_{N|k} = u_{\mathrm{s},k}. && \text{(9.9k)}
\end{aligned}$$

Denote the optimal input sequence and output reference respectively by $\boldsymbol{\Delta u}_k^\star(\hat{x}_k, u_{k-1}, y_{\mathrm{t},k}) = \{\Delta u_{i|k}^\star\}_{i=0}^{N-1}$ and $y_{\mathrm{s},k}^\star(\hat{x}_k, u_{k-1}, y_{\mathrm{t},k})$, and the corresponding optimal cost by $V_N(\hat{x}_k, u_{k-1}, y_{\mathrm{t},k})$. Moreover, let $x_{\mathrm{s},k}^\star := g_{\mathrm{x}}(y_{\mathrm{s},k}^\star)$ and $u_{\mathrm{s},k}^\star := g_{\mathrm{u}}(y_{\mathrm{s},k}^\star)$. According to the receding horizon policy, the closed-loop control law $\mu_N(\hat{x}_k, u_{k-1}, y_{\mathrm{t},k})$ is

$$\mu_N(\hat{x}_k, u_{k-1}, y_{\mathrm{t},k}) = \Delta u_{0|k}^\star.$$

Then, the system input is

$$u_k = u_{k-1} + \mu_N(\hat{x}_k, u_{k-1}, y_{\mathrm{t},k}).$$

Remark 9.2. *The feasibility of the FHOCP does not depend on the initial system state, since there are no state constraints, but only depends on the value of u_{k-1}, given the input rate constraint set $\Delta\mathcal{U}$, the prediction horizon N, and on the auxiliary reference constraint set $\mathcal{Y}_{\mathrm{t}}$. In particular, if $\mathcal{Y}_{\mathrm{t}} = \mathcal{Y}_{\mathrm{s}}$, then the FHOCP can be made feasible for all $u_{k-1} = u_{0|k} \in \mathcal{U}$ by selecting a sufficiently small value of ε_{u}. In fact, for δISS systems, given a constant input $\bar{u} \in \hat{\mathcal{U}}$, there always exist (unique) associated equilibrium state $\bar{x}$ and equilibrium output $\bar{y}$ (see Lemma 7.2), and therefore $(\bar{x}, \bar{u}) \in \mathcal{Z}_{\mathrm{s}}$ and $\bar{y} \in \mathcal{Y}_{\mathrm{t}}$. Since $\Delta\mathcal{U}$ contains the origin, it is possible to choose ε_{u} sufficiently small to guarantee that, even if $u_{k-1} \in \mathcal{U} \setminus \hat{\mathcal{U}}$, the closest $\bar{u} \in \hat{\mathcal{U}}$ is a feasible auxiliary input reference, while $\overline{\Delta u}_{0|k} = \bar{u} - u_{k-1}$ and $\overline{\Delta u}_{i|k} = 0$ for $i = 1, ..., N-1$ is a feasible control sequence. If instead $\mathcal{Y}_{\mathrm{t}} \subset \mathcal{Y}_{\mathrm{s}}$, the FHOCP is feasible at least for all $u_{k-1} = u_{0|k} \in \hat{\mathcal{U}}$ such that $y_{\mathrm{s},k} = h(x_{\mathrm{s},k}, u_{0|k}) \in \mathcal{Y}_{\mathrm{t}}$, where $x_{\mathrm{s},k} = f(x_{\mathrm{s},k}, u_{0|k})$. In fact, under these assumptions, the control sequence $\overline{\Delta u}_{i|k} = 0$ for $i = 0, ..., N-1$ satisfies all the constraints in the FHOCP. For all the other values of u_{k-1}, feasibility can be achieved if the*

prediction horizon N is sufficiently long. Hence, the introduction of an artificial reference allows to enlarge the feasibility region of the FHOCP with respect to standard MPC, where the feasibility cannot be guaranteed for short horizons N if u_{k-1} is far from the input reference associated to $y_{\mathrm{t},k}$ (compare, e.g., with Chapter 8).

To provide stability guarantees, the stage cost function, the offset cost function and the cost detectability function must fulfill the following assumptions.

Assumption 9.6 (Local Lipschitz continuity)**.** *Let $\hat{\mathcal{X}} := \{\hat{x} \in \mathbb{R}^n \ : \ \exists\, \hat{d} \in \mathbb{R}^p \ : \ \hat{x}_{\mathrm{d}} \in \hat{\mathcal{X}}_{\mathrm{d}}\} \subset \mathbb{R}^n$ and $\hat{\mathcal{D}} := \{\hat{d} \in \mathbb{R}^p \ : \ \exists\, \hat{x} \in \mathbb{R}^n \ : \ \hat{x}_{\mathrm{d}} \in \hat{\mathcal{X}}_{\mathrm{d}}\} \subset \mathbb{R}^p$, and assume that the stage cost function, the terminal cost function, the offset cost function, and the cost detectability function are Lipschitz continuous for $x \in \mathcal{X}$, $u \in \mathcal{U}$, $\Delta u \in \Delta\mathcal{U}$, $d \in \mathcal{D}$, $\hat{x}_k \in \hat{\mathcal{X}}$, $\hat{d} \in \hat{\mathcal{D}}$, $(x_{\mathrm{s}}, u_{\mathrm{s}}) \in \mathcal{Z}_{\mathrm{s}}$, $y_{\mathrm{s}} \in \mathcal{Y}_{\mathrm{t}}$, $y^0 \in \mathcal{Y}^0$. Let their Lipschitz constants be L_ℓ, $L_{V_{\mathrm{f}}}$, $L_{V_{\mathrm{O}}}$, L_Ψ, respectively.*

Note that all sets considered in Assumption 9.6 are bounded by definition or in view of Lemma 9.1.

Assumption 9.7 (Stage cost polynomial upper bound)**.** *Given the stage cost $\ell(x - x_{\mathrm{s}}, u - u_{\mathrm{s}}, \Delta u)$, there exist constants $\lambda_1, \lambda_2 > 0$ and $\eta_1, \eta_2 > 1$ so that*

$$\ell(x - x_{\mathrm{s}}, u - u_{\mathrm{s}}, \Delta u) - \ell(x - x_{\mathrm{s}}, 0, 0) \leq \lambda_1 \|u - u_{\mathrm{s}}\|_2^{\eta_1} + \lambda_2 \|\Delta u\|_2^{\eta_2} \tag{9.10}$$

for (x, u) in a neighborhood of $(x_{\mathrm{s}}, u_{\mathrm{s}})$, $u \in \mathcal{U}$, $\Delta u \in \Delta\mathcal{U}$ and $(x_{\mathrm{s}}, u_{\mathrm{s}}) \in \mathcal{Z}_{\mathrm{s}}$.

Assumption 9.8 (Cost detectability function)**.** *There exists constants γ_0, ε_0, $c > 0$ and $\xi > 1$, and a $\mathcal{K}_\infty$ function μ such that*

$$\Psi(x - x_{\mathrm{s}}, u - u_{\mathrm{s}}) \leq \gamma_0 \mu(\|\chi - \chi_{\mathrm{s}}\|_2) \leq c\|\chi - \chi_{\mathrm{s}}\|_2^{\xi}, \tag{9.11a}$$

$$\begin{aligned} &\Psi(x_{k+1} - x_{\mathrm{s}}, u_k - u_{\mathrm{s}}) - \Psi(x_k - x_{\mathrm{s}}, u_{k-1} - u_{\mathrm{s}}) \\ &\leq -\varepsilon_0 \mu(\|\chi_k - \chi_{\mathrm{s}}\|_2) + \ell(x_k - x_{\mathrm{s}}, u_{k-1} - u_{\mathrm{s}}, \Delta u_k), \end{aligned} \tag{9.11b}$$

for any $x_k \in \mathbb{R}^n$, any $u_{k-1} \in \mathcal{U}$, any $\Delta u_k \in \Delta\mathcal{U}$ and any $(x_{\mathrm{s}}, u_{\mathrm{s}}) \in \mathcal{Z}_{\mathrm{s}}$.

For a discussion of different methods for the design of cost detectability functions satisfying Assumption 9.8, see Section 3.8. Moreover, in Section 9.5 we will explore how to design cost detectability functions for δISS systems if the parts of the cost associated to the input and the input rate are positive definite.

Assumption 9.9 (Offset cost function)**.** *For all $y_{\mathrm{s}} \in \mathcal{Y}_{\mathrm{t}}$ and all $y_{\mathrm{t}} \in \mathbb{R}^p$, the offset cost function $V_{\mathrm{O}} : \mathbb{R}^p \to \mathbb{R}$ is a uniformly strongly convex positive definite function of class $\mathcal{C}^1$ with locally Lipschitz continuous gradient such that the minimizer*

$$y_{\mathrm{s}}^{\diamond} = \arg\min_{y_{\mathrm{s}} \in \mathcal{Y}_{\mathrm{t}}} V_{\mathrm{O}}(y_{\mathrm{s}} - y_{\mathrm{t}})$$

is unique. Moreover, there exists a $\mathcal{K}_\infty$ function α_{O} such that

$$V_{\mathrm{O}}(y_{\mathrm{s}} - y_{\mathrm{t}}) - V_{\mathrm{O}}(y_{\mathrm{s}}^{\diamond} - y_{\mathrm{t}}) \geq \alpha_{\mathrm{O}}(\|y_{\mathrm{s}} - y_{\mathrm{s}}^{\diamond}\|_2).$$

Assumption 9.9 can be satisfied, e.g., using a quadratic offset cost function [151].

Assumption 9.10 (Terminal cost)**.** *Let $V_{\mathrm{f}}(x - x_{\mathrm{s}}, y_{\mathrm{s}})$ be a Lyapunov function such that for all $x \in \mathbb{R}^n, y_{\mathrm{s}} \in \mathcal{Y}_{\mathrm{t}}$, and $x_{\mathrm{s}} = g_{\mathrm{x}}(y_{\mathrm{s}})$, there exist constants $b > 0$ and $\sigma > 1$ which verify*

$$V_{\mathrm{f}}(x - x_{\mathrm{s}}, y_{\mathrm{s}}) \leq b\|x - x_{\mathrm{s}}\|_2^{\sigma} \tag{9.12}$$

and

$$V_{\mathrm{f}}(f(x, u_{\mathrm{s}}) - x_{\mathrm{s}}, y_{\mathrm{s}}) - V_{\mathrm{f}}(x - x_{\mathrm{s}}, y_{\mathrm{s}}) \leq -\ell(x - x_{\mathrm{s}}, 0, 0). \tag{9.13}$$

Remark 9.3. *Assumption 9.10 requires a decrease bounded by an open-loop stage cost (i.e. $u = u_{\mathrm{s}}$ and $\Delta u = 0$). Therefore, following the approach discussed in Section 5.1.1, if the δISS Lyapunov function V defined in Assumption 9.1 is locally Lipschitz continuous in any bounded set, and can be upper bounded as in* (9.12)*, then Assumption 9.10 can be (conservatively) verified by multiplying V with a positive constant s, so that $V_{\mathrm{f}}(x - x_{\mathrm{s}}, y_{\mathrm{s}}) = sV(x - x_{\mathrm{s}})$, and the following inequality holds*

$$-s\alpha_3(\|x - x_{\mathrm{s}}\|_2) \leq -\ell(x - x_{\mathrm{s}}, 0, 0).$$

This idea was followed in Chapter 8 for the design of the terminal cost function, where a lower bound for s is also provided in Equation (8.7)*.*

Remark 9.4. *The proposed control design is highly modular, since each requirement (output feedback, artificial-reference tracking, offset-free, positive semi-definite stage cost, input rate constraints and penalty) is taken care of with few, specific ingredients introducing design overhead. Each ingredient can be straightforwardly removed from the design if the associated requirement does not need to be satisfied.*

9.4 Stability Analysis

In the following theorem we report the main result of this chapter concerning the stability and convergence properties of the proposed control scheme.

Theorem 9.1. *Suppose that Assumptions from 9.1 to 9.10 hold. Then, for any feasible u_{-1},[3] the closed-loop system Σ_{C} composed by the plant Σ_{d}, the MPC controller, the discrete-time integrator, and the observer, fulfills the*

[3] See Remark 9.2.

constraints and is ISpS with respect to the bounded disturbance w. Moreover, consider asymptotically constant setpoint y^0 and output disturbance d (i.e. asymptotically vanishing disturbance w), and denote their asymptotic values by $y^0_\infty := \lim_{k\to\infty} y^0_k$ and $d_\infty := \lim_{k\to\infty} d_k$. Then, for any feasible u_{-1}, the closed-loop system Σ_{C} converges to an equilibrium point such that

1. *If $y_{\mathrm{t},\infty} \in \mathcal{Y}_{\mathrm{t}}$, then $\lim_{k\to\infty} \|y_k - y_{\mathrm{t},\infty}\| = 0$ and $\lim_{k\to\infty} \|y_{\mathrm{d},k} - y^0_\infty\| = 0$.*
2. *If $y_{\mathrm{t},\infty} \notin \mathcal{Y}_{\mathrm{t}}$, then $\lim_{k\to\infty} \|y_k - y^\diamond_{\mathrm{s},\infty}\| = 0$ and $\lim_{k\to\infty} \|y_{\mathrm{d},k} - (y^\diamond_{\mathrm{s},\infty} + d_\infty)\| = 0$*

where

$$\begin{aligned} y^\diamond_{\mathrm{s},\infty} &:= \arg\min_{y_{\mathrm{s}}\in\mathcal{Y}_{\mathrm{t}}} V_{\mathrm{O}}(y_{\mathrm{s}} - y_{\mathrm{t},\infty}), \\ y_{\mathrm{t},\infty} &:= y^0_\infty - \hat{d}_\infty, \\ \hat{d}_\infty &:= \lim_{k\to\infty} \hat{d}_k = d_\infty. \end{aligned}$$

Proof. The proof is reported in Section 9.8.2.

9.5 Input and Input-Rate Regularization

The control design introduced in this chapter allows to use a generic positive semi-definite stage cost in the FHOCP. This section specializes the design to the case of a stage cost that is positive definite with respect to input rate and input, while being positive semi-definite with respect to the system state. Specifically, the section discusses how to exploit the knowledge of a δISS-Lyapunov function for the original system Σ to derive a cost detectability function Ψ satisfying Assumption 9.8 for the extended system Σ_{u}. Note that this result can be useful in many situations, including the case of output weighting. In fact, with output weighting, the stage cost is typically positive definite with respect to the system output, but only positive semi-definite with respect to the system state.

Assumption 9.11. *Consider a δISS-Lyapunov function V for the nominal system Σ defined in Assumption 9.1. Assume that it is Lipschitz continuous, and that there exist constants $c > 0$ and $\xi > 1$, so that, for any $x \in \mathcal{X}$, and any $(x_{\mathrm{s}}, u_{\mathrm{s}}) \in \mathcal{Z}_{\mathrm{s}}$*

$$V(x - x_{\mathrm{s}}) \leq c\|x - x_{\mathrm{s}}\|_2^\xi. \tag{9.14}$$

Moreover, there exist constants $a_\ell, \varepsilon_\ell > 0$ such that

$$\ell(x - x_{\mathrm{s}}, u - u_{\mathrm{s}}, \Delta u) \geq (a_\ell + \varepsilon_\ell)\gamma_1(2\|u - u_{\mathrm{s}}\|_2) + a_\ell\gamma_1(2\|\Delta u\|_2) \tag{9.15}$$

for any $x \in \mathcal{X}$, $(x_{\mathrm{s}}, u_{\mathrm{s}}) \in \mathcal{Z}_{\mathrm{s}}$, $u \in \mathcal{U}$, $\Delta u \in \Delta\mathcal{U}$, and γ_1 as defined in Assumption 9.1.

Then, the following Lemma shows how to exploit Assumption 9.11 to compute a suitable cost detectability function Ψ by directly scaling the δISS Lyapunov function V of the nominal system Σ.

Lemma 9.2. *Consider the δISS system Σ, and suppose Assumption 9.11 holds. Then, Assumption 9.8 holds with $\Psi(x - x_\mathrm{s}, u - u_\mathrm{s}) = a_\ell V(x - x_\mathrm{s})$.*

Proof. The proof is reported in Section 9.8.3.

Note that Assumption 9.11 requires a sufficient penalization of *both* input and input rate in the stage cost. Assumption 9.11 is not required to hold if Ψ is directly derived for the extended system Σ_u, as discussed e.g. in [197, 133].

9.6 Illustrative example

This section showcases the application of the proposed control scheme on the the pH neutralization process described in Section 5.3.1 using a REN model, and it also illustrates a possible approach to design an observer satisfying Assumption 9.4 based on the small gain theorem [114].

In particular, the pH neutralization process is considered with the buffer flow q_2 constant at its nominal value, with a sampling time $T_\mathrm{s} = 10s$ and subject to the following constraints on the input and input rate:

$$u \in [12.5, 17] mL/s, \quad |\Delta u| \leq 0.2 mL/s.$$

9.6.1 REN model

For the MPC implementation a REN model of the system under control is considered, similarly to the numerical example of Chapter 5. In particular, we consider the same model dimension (i.e. $n = 5$, $q = 8$), training data and training parameters except for the number of epochs, increased to 250, and the learning rate, that is initially set to 5×10^{-3} and decreased to 1×10^{-3} after 50 epochs. To simplify the design, we use a simplified version of the REN, removing the contribution of u_k and z_k in the output transformation, obtaining a model with equations

$$x_{k+1} = Ax_k + B_1 z_k + B_2 u_k + b_x \tag{9.16a}$$
$$z_k = \tanh(D_{11} z_k + C_1 x_k + D_{12} u_k + b_v) \tag{9.16b}$$
$$y_k = C_2 x_k + b_y, \tag{9.16c}$$

where $u \in \mathbb{R}$, $y \in \mathbb{R}$, $x \in \mathbb{R}^5$ and $z \in \mathbb{R}^8$. Also in this example we consider an acyclic REN, where D_{11} is strictly lower triangular. The final network obtains a FIT of 85.9%, comparable but slightly worse than the result obtained in Chapter 5 for the REN with the complete output transformation. Note

that the offset-free formulation of the MPC allows to achieve zero steady state error despite the model plant mismatch.

For the REN model, the lipschitzianity of the function g associating the equilibrium $(x_\mathrm{s}, u_\mathrm{s})$ to the steady state output y_s has been verified by numerically checking that the associated Jacobian is nonsingular for all $y_\mathrm{s} \in \mathcal{Y}_\mathrm{t}$.

9.6.2 Design of the augmented observer

The state observer for both model state and disturbance is designed by augmenting the observer for the REN model proposed in Chapter 5, which guarantees a converging estimation of the REN state only, and does not cover the estimation of the disturbance. In this work, the small gain theorem is used to derive a condition for the convergence of the augmented observer, starting from convergence of the original observer, so that Assumptions 9.3 and 9.4 are fulfilled. The observer has the following equations

$$\hat{x}_{k+1} = A\hat{x}_k + B_1\hat{z}_k + B_2 u_k + b_x + L(y_{\mathrm{d},k} - \hat{y}_k) \tag{9.17a}$$
$$\hat{z}_k = \tanh(D_{11}\hat{z}_k + C_1\hat{x}_k + D_{12}u_k + b_v) \tag{9.17b}$$
$$\hat{d}_{k+1} = \hat{d}_k + L_\mathrm{d}(y_{\mathrm{d},k} - \hat{y}_k) \tag{9.17c}$$
$$\hat{y}_k = C_2\hat{x}_k + b_y + \hat{d}_k \tag{9.17d}$$

where $L \in \mathbb{R}^{5\times 1}$ and $L_\mathrm{d} \in \mathbb{R}$ are tunable gains. The first two equations (9.17a)-(9.17b) for the estimation of the model state have the same structure of (5.1a)-(5.1b), except for the presence of $\hat{d}$ in the definition of $\hat{y}$. In Theorem 5.1 a condition on the gain L is provided, under which it is shown that for the observer with $\hat{d} = 0$

$$\begin{aligned}\|x_{k+1} - \hat{x}_{k+1}\|_{P_\mathrm{o}} &= \|(A - LC_2)(x_k - \hat{x}_k) + B_1(z_k - \hat{z}_k)\|_{P_\mathrm{o}} \\ &\leq \alpha_\mathrm{o}\|x_k - \hat{x}_k\|_{P_\mathrm{o}}\end{aligned} \tag{9.18}$$

for a positive definite matrix P_o and $\alpha_\mathrm{o} \in (0, 1)$ (see Equation (5.12)). In particular, this condition is satisfied by the trivial open-loop observer with $L = 0$.

To study the estimation error of observer augmented with the disturbance, it is possible to consider the overall error as the interconnection of two subsystems: a subsystem describing the estimation error on the state $x - \hat{x}$, and one describing the estimation error on the disturbance $d - \hat{d}$. In this way it is possible to use the small gain theorem to derive a sufficient condition for the stability of the interconnection of the two systems. Consider first the system of $x - \hat{x}$, and assume that L satisfies the conditions of

Theorem 5.1

$$\begin{aligned}
&\|x_{k+1} - \hat{x}_{k+1}\|_{P_\mathrm{o}} \\
&\overset{(9.16)(9.17)}{=} \|(A - LC_2)(x_k - \hat{x}_k) + B_1(z_k - \hat{z}_k) - L(d_k - \hat{d}_k)\|_{P_\mathrm{o}} \\
&\leq \|(A - LC_2)(x_k - \hat{x}_k) + B_1(z_k - \hat{z}_k)\|_{P_\mathrm{o}} + \|L(d_k - \hat{d}_k)\|_{P_\mathrm{o}} \\
&\overset{(9.18)}{\leq} \alpha_\mathrm{o}\|x_k - \hat{x}_k\|_{P_\mathrm{o}} + \|P_\mathrm{o}^{1/2}L(d_k - \hat{d}_k)\|_2 \\
&\leq \alpha_\mathrm{o}\|x_k - \hat{x}_k\|_{P_\mathrm{o}} + \|P_\mathrm{o}^{1/2}L\|_2\|d_k - \hat{d}_k\|_2.
\end{aligned}$$

Consider now the evolution of $d - \hat{d}$

$$\begin{aligned}
&\|d_{k+1} - \hat{d}_{k+1}\|_2 \\
&\overset{(9.1\mathrm{b})(9.17)}{=} \|(\mathbf{I}_p - L_\mathrm{d})(d_k - \hat{d}_k) - L_\mathrm{d}C_2(x_k - \hat{x}_k) + w_k\|_2 \\
&\leq \|\mathbf{I}_p - L_\mathrm{d}\|_2\|d_k - \hat{d}_k\|_2 + \|L_\mathrm{d}C_2(x_k - \hat{x}_k)\|_2 + \|w_k\|_2 \\
&= \|\mathbf{I}_p - L_\mathrm{d}\|_2\|d_k - \hat{d}_k\|_2 + \|L_\mathrm{d}C_2P_\mathrm{o}^{-1/2}P_\mathrm{o}^{1/2}(x_k - \hat{x}_k)\|_2 + \|w_k\|_2 \\
&\leq \|\mathbf{I}_p - L_\mathrm{d}\|_2\|d_k - \hat{d}_k\|_2 + \|L_\mathrm{d}C_2P_\mathrm{o}^{-1/2}\|_2\|x_k - \hat{x}_k\|_{P_\mathrm{o}} + \|w_k\|_2.
\end{aligned}$$

It is now possible to apply the small gain theorem for Lyapunov functions [114, Theorem 3] to the interconnection of the subsystems with Lyapunov functions $\|x - \hat{x}\|_{P_\mathrm{o}}$ and $\|d - \hat{d}\|_2$, respectively, to obtain the following sufficient condition for the ISS of the complete system with respect to w:

$$(1 - \alpha_\mathrm{o})^{-1}(1 + \varepsilon)\|P_\mathrm{o}^{1/2}L\|_2(1 - \|\mathbf{I}_p - L_\mathrm{d}\|_2)^{-1}(1 + \varepsilon)\|L_\mathrm{d}C_2P_\mathrm{o}^{-1/2}\|_2 < 1$$

for some $\varepsilon > 0$. In case of single output systems, if L_d is selected in $(0, 1)$, the condition reduces to the following condition on the gain L:

$$(1 - \alpha_\mathrm{o})^{-1}(1 + \varepsilon)\|P_\mathrm{o}^{1/2}L\|_2(1 + \varepsilon)\|C_2P_\mathrm{o}^{-1/2}\|_2 < 1. \tag{9.19}$$

For the tuning of the observer for the simulations, $L_\mathrm{d} = 0.5$ is chosen. To select L, first the optimization (5.8) is solved, and then the resulting gain is multiplied with a sufficiently small constant so that the small gain condition (9.19) is satisfied. This procedure can be applied to augment the design of converging observers for more general nonlinear systems and obtain observers that meet Assumptions 9.3 and 9.4.

9.6.3 Simulation results

For the implementation of the MPC, the stage cost and the offset cost are set to

$$\begin{aligned}
\ell(y - y_\mathrm{s}, u - u_\mathrm{s}, \Delta u) &= \|y - y_\mathrm{s}\|_{Q_y}^2 + \|u - u_\mathrm{s}\|_{Q_u}^2 + \|\Delta u\|_R^2, \\
V_\mathrm{O}(y_\mathrm{s} - y_\mathrm{t}) &= \|y_\mathrm{s} - y_\mathrm{t}\|_T^2,
\end{aligned}$$

with

$$Q_y = 100, \quad Q_u = 1, \quad R = 100, \quad T = 10^6.$$

The prediction horizon is set to $N = 3$. In the proof of Theorem 4.3, it is shown that the REN model has a δISS-Lyapunov function in the form $V(x^{\mathrm{a}} - x^{\mathrm{b}}) = \|x^{\mathrm{a}} - x^{\mathrm{b}}\|_P^2$, where $P \in \mathbb{R}^{n \times n}$ depends on the weights of the network. Then, the terminal cost for the MPC is chosen as $V_{\mathrm{f}}(x - x_{\mathrm{s}}, y_{\mathrm{s}}) = s\|x - x_{\mathrm{s}}\|_P^2$, where the scalar parameters s is selected according to (8.7) considering $Q = C_2^\top Q_y C_2$, and the cost detectability function is $\Psi(x - x_{\mathrm{s}}, u - u_{\mathrm{s}}) = a_\ell \|x - x_{\mathrm{s}}\|_P^2$ where the scaling parameter a_ℓ is selected as proposed in Section 9.5. The nonlinear MPC problem is solved using CasADi with Ipopt optimizer [6].

The MPC is compared with the one proposed in Chapter 8, which can also cope with input rate constraints, but it is designed for regulation at a constant setpoint. In particular, the algorithm does not include an artificial reference and does not offer offset-free tracking capabilities. In the comparison we use an observer the same expression and gain L, with the exception of equation (9.17c), which is equivalent to set $L_{\mathrm{d}} = 0$. The MPC is tuned using the same positive semi-definite stage cost ℓ and terminal cost V_{f}, even if Chapter 8 only proves stability for positive definite stage costs. In this simulation it was not possible to use the prediction horizon $N = 3$, because it gave infeasibility in presence of changes of the reference. This is in accordance with the theory, since in Chapter 8 recursive feasibility is proved only for constant references, and the step-wise variations of the setpoints have been treated as reinitializations in the simulation. To maintain feasibility in presence of the first setpoints variations, the prediction horizon was enlarged to $N = 20$.

The results of the simulations are reported in Figure 9.2. The simulation with the MPC of Chapter 8 stops at 4000s, because the algorithm is designed under the assumption that the reference output respects the constraints. When this condition does not hold, the FHOCP results infeasible for any prediction horizon N. Instead, with the proposed algorithm feasibility is maintained also for the infeasible setpoint in the interval $[4000, 5000]s$, and the system reaches the closest feasible output. In this example no external disturbance is introduced in the simulation, but there are modeling errors in the REN model used by the MPC, that cause a static gain mismatch for the MPC of Chapter 8, where the estimation of the disturbance is not implemented. Instead, the proposed algorithm tracks feasible setpoints with zero error, and achieves similar transient performances of Chapter 8 with a shorter prediction horizon.

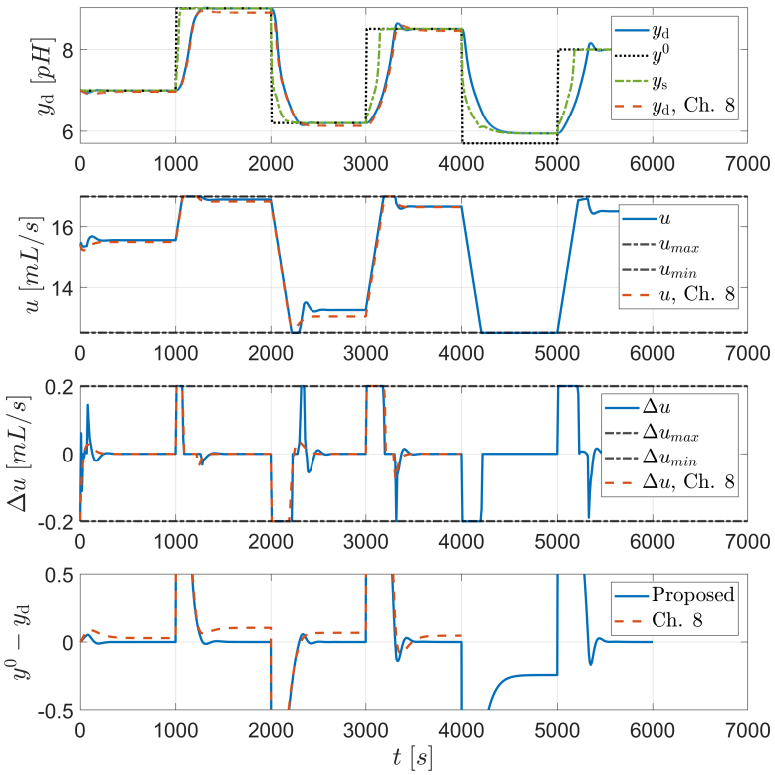

Figure 9.2: Closed-loop simulation. Top: output y_d for the proposed MPC (blue, solid line) and for the MPC from Chapter 8 (orange, dashed line), setpoint y^0 (black, dotted line), and auxiliary reference y_s (green, dashed-dotted line). Middle-top: input u for the proposed MPC (blue, solid line) and and for the MPC from Chapter 8 (orange, dashed line), constraints (black, dashed-dotted lines) . Middle-bottom: input rate Δu for the proposed MPC (blue, solid line) and for the MPC from Chapter 8 (orange, dashed line), constraints (black, dashed-dotted lines). Bottom: tracking error $y^0 - y_d$ for the proposed MPC (blue, solid line) and for the MPC from Chapter 8 (orange, dashed line).

9.7 Conclusions

This chapter deals with offset-free, output feedback, tracking MPC for δISS systems subject to input and input rate constraints. Specifically, the control scheme offers recursive feasibility and stability guarantees, by relying on a Lyapunov-based terminal weight on the system state, and on a terminal equality constraint on the system input. A cost detectability term can be included in the controller cost function to enable the use of positive semi-definite stage cost (e.g. in case of output weighting for black-box or high dimensional models). The use of artificial reference variables allows for an extended feasibility region. A state observer that estimates the system states and an output disturbance allows output feedback and offset-free tracking of asymptotically constant reference signals. The proposed approach can be applied to linear asymptotically stable systems [77] and to nonlinear ones, including systems modeled using RNNs, as shown in the illustrative example.

9.8 Proofs

9.8.1 Auxiliary lemmas

Lemma 9.3. *Consider system Σ_{u} subject to constraints* (9.9e)-(9.9k)*. Suppose that Assumptions from 9.2 to 9.10 hold. Consider a given setpoint y_{t}, and assume that for a given state x, and a given integrator state u, the optimal solution to the FHOCP is such that $x = x_{\mathrm{s}}^{\star}(x,u,y_{\mathrm{t}}) = g_{\mathrm{x}}(y_{\mathrm{s}}^{\star}(x,u,y_{\mathrm{t}}))$, $u = u_{\mathrm{s}}^{\star}(x,u,y_{\mathrm{t}}) = g_{\mathrm{u}}(y_{\mathrm{s}}^{\star}(x,u,y_{\mathrm{t}}))$. Then, $V_N(x,u,y_{\mathrm{t}}) = V_{\mathrm{O}}(y_{\mathrm{s}}^{\diamond} - y_{\mathrm{t}})$.*

Proof. The lemma is proved by contradiction. Assume that $V_{\mathrm{O}}(y_{\mathrm{s}}^{\star} - y_{\mathrm{t}}) > V_{\mathrm{O}}(y_{\mathrm{s}}^{\diamond} - y_{\mathrm{t}})$. Then, since $y_{\mathrm{s}}^{\diamond}$ is the unique minimizer of V_{O}, $y_{\mathrm{s}}^{\star} \neq y_{\mathrm{s}}^{\diamond}$. Consider $\beta \in [0,1]$, and define then $\hat{y}_{\mathrm{s}}$ as

$$\hat{y}_{\mathrm{s}} := \beta y_{\mathrm{s}}^{\star} + (1-\beta) y_{\mathrm{s}}^{\diamond}. \tag{9.20}$$

From the definition of set $\mathcal{Y}_{\mathrm{t}}$, it follows that $u_{\mathrm{s}}^{\star} \in \hat{\mathcal{U}}$. Therefore, there exists a $\hat{\beta} \in [0,1)$ such that, for $\hat{y}_{\mathrm{s}}$ given by a $\beta \in [\hat{\beta}, 1]$, the sequence of inputs $\boldsymbol{\Delta}\hat{\mathbf{u}} = \{\Delta\hat{u}_{i|k}\}_{i=0}^{N-1}$, defined by $\Delta\hat{u}_{0|k} := \hat{u}_{\mathrm{s},k} - u$, and and $\Delta\hat{u}_{i|k} := 0$ for $i = 1, ..., N-1$, and the auxiliary reference $\hat{y}_{\mathrm{s},k} = \hat{y}_{\mathrm{s}}$ constitute a feasible solution to the FHOCP. Denote by $\hat{x}_{i|k}$, $i = 0, ..., N$, the associate state trajectory. From the Lipschitz continuity of the functions g, g_{x} and g_{u}, and taking into account that $y_{\mathrm{s}}^{\star} - \hat{y}_{\mathrm{s}} = (1-\beta)(y_{\mathrm{s}}^{\star} - y_{\mathrm{s}}^{\diamond})$ and the optimality of the solution, the following holds

$$\begin{aligned}
V_{\mathrm{O}}(y_{\mathrm{s}}^{\star} - y_{\mathrm{t}}) &= V_N(x,u,y_{\mathrm{t}}) \leq J_N(x,u,y_{\mathrm{t}}; \boldsymbol{\Delta}\hat{\mathbf{u}}, \hat{y}_{\mathrm{s}}) \\
&\overset{(9.11a)}{\leq} \ell(x_{\mathrm{s}}^{\star} - \hat{x}_{\mathrm{s}}, u_{\mathrm{s}}^{\star} - \hat{u}_{\mathrm{s}}, \hat{u}_{\mathrm{s}} - u_{\mathrm{s}}^{\star}) + V_{\mathrm{f}}(f(x_{\mathrm{s}}^{\star}, \hat{u}_{\mathrm{s}}) - \hat{x}_{\mathrm{s}}, \hat{y}_{\mathrm{s}}) \\
&+ V_{\mathrm{O}}(\hat{y}_{\mathrm{s}} - y_{\mathrm{t}}) + c\|\chi_{\mathrm{s}}^{\star} - \hat{\chi}_{\mathrm{s}}\|_2^{\xi}
\end{aligned}$$

$$
\begin{aligned}
&\overset{(9.13)}{\leq} \ell(x_{\mathrm{s}}^\star - \hat{x}_{\mathrm{s}}, u_{\mathrm{s}}^\star - \hat{u}_{\mathrm{s}}, \hat{u}_{\mathrm{s}} - u_{\mathrm{s}}^\star) + V_{\mathrm{f}}(x_{\mathrm{s}}^\star - \hat{x}_{\mathrm{s}}, \hat{y}_{\mathrm{s}}) \\
&- \ell(x_{\mathrm{s}}^\star - \hat{x}_{\mathrm{s}}, 0, 0) + V_{\mathrm{O}}(\hat{y}_{\mathrm{s}} - y_{\mathrm{t}}) + c\|\chi_{\mathrm{s}}^\star - \hat{\chi}_{\mathrm{s}}\|_2^\xi \\
&\overset{(9.10)(9.12)}{\leq} \lambda_1\|u_{\mathrm{s}}^\star - \hat{u}_{\mathrm{s}}\|_2^{\eta_1} + \lambda_2\|u_{\mathrm{s}}^\star - \hat{u}_{\mathrm{s}}\|_2^{\eta_2} + b\|x_{\mathrm{s}}^\star - \hat{x}_{\mathrm{s}}\|_2^\sigma \\
&+ V_{\mathrm{O}}(\hat{y}_{\mathrm{s}} - y_{\mathrm{t}}) + c\|\chi_{\mathrm{s}}^\star - \hat{\chi}_{\mathrm{s}}\|_2^\xi \\
&\overset{\text{Ass.9.2}}{\leq} g_1 L_g^{\eta_1}\|y_{\mathrm{s}}^\star - \hat{y}_{\mathrm{s}}\|_2^{\eta_1} + g_2 L_g^{\eta_2}\|y_{\mathrm{s}}^\star - \hat{y}_{\mathrm{s}}\|_2^{\eta_2} \\
&+ bL_g\|y_{\mathrm{s}}^\star - \hat{y}_{\mathrm{s}}\|_2^\sigma + V_{\mathrm{O}}(\hat{y}_{\mathrm{s}} - y_{\mathrm{t}}) + cL_g^\xi\|y_{\mathrm{s}}^\star - \hat{y}_{\mathrm{s}}\|_2^\xi \\
&\overset{(9.20)}{=} g_1 L_g^{\eta_1}(1-\beta)^{\eta_1}\|y_{\mathrm{s}}^\star - y_{\mathrm{s}}^\diamond\|_2^{\eta_1} + g_2 L_g^{\eta_2}(1-\beta)^{\eta_2}\|y_{\mathrm{s}}^\star - y_{\mathrm{s}}^\diamond\|_2^{\eta_2} \\
&+ bL_g^\sigma(1-\beta)^\sigma\|y_{\mathrm{s}}^\star - y_{\mathrm{s}}^\diamond\|_2^\sigma + V_{\mathrm{O}}(\hat{y}_{\mathrm{s}} - y_{\mathrm{t}}) + cL_g^\xi(1-\beta)^\xi\|y_{\mathrm{s}}^\star - y_{\mathrm{s}}^\diamond\|_2^\xi.
\end{aligned}
$$

From the convexity of V_{O}, it follows that

$$
V_{\mathrm{O}}(\hat{y}_{\mathrm{s}} - y_{\mathrm{t}}) \leq \beta V_{\mathrm{O}}(y_{\mathrm{s}}^\star - y_{\mathrm{t}}) + (1-\beta)V_{\mathrm{O}}(y_{\mathrm{s}}^\diamond - y_{\mathrm{t}}).
$$

Therefore

$$
\begin{aligned}
V_{\mathrm{O}}(y_{\mathrm{s}}^\star - y_{\mathrm{t}}) \leq\ & g_1 L_g^{\eta_1}(1-\beta)^{\eta_1}\|y_{\mathrm{s}}^\star - y_{\mathrm{s}}^\diamond\|_2^{\eta_1} \\
&+ g_2 L_g^{\eta_2}(1-\beta)^{\eta_2}\|y_{\mathrm{s}}^\star - y_{\mathrm{s}}^\diamond\|_2^{\eta_2} + bL_g^\sigma(1-\beta)^\sigma\|y_{\mathrm{s}}^\star - y_{\mathrm{s}}^\diamond\|_2^\sigma \\
&+ \beta V_{\mathrm{O}}(y_{\mathrm{s}}^\star - y_{\mathrm{t}}) + (1-\beta)V_{\mathrm{O}}(y_{\mathrm{s}}^\diamond - y_{\mathrm{t}}) + cL_g^\xi(1-\beta)^\xi\|y_{\mathrm{s}}^\star - y_{\mathrm{s}}^\diamond\|_2^\xi,
\end{aligned}
$$

which leads to the following inequality

$$
\begin{aligned}
V_{\mathrm{O}}(y_{\mathrm{s}}^\star - y_{\mathrm{t}}) - V_{\mathrm{O}}(y_{\mathrm{s}}^\diamond - y_{\mathrm{t}}) \leq\ & g_1 L_g^{\eta_1}(1-\beta)^{\eta_1 - 1}\|y_{\mathrm{s}}^\star - y_{\mathrm{s}}^\diamond\|_2^{\eta_1} \\
&+ g_2 L_g^{\eta_2}(1-\beta)^{\eta_2 - 1}\|y_{\mathrm{s}}^\star - y_{\mathrm{s}}^\diamond\|_2^{\eta_2} \\
&+ bL_g^\sigma(1-\beta)^{\sigma-1}\|y_{\mathrm{s}}^\star - y_{\mathrm{s}}^\diamond\|_2^\sigma + cL_g^\xi(1-\beta)^{\xi-1}\|y_{\mathrm{s}}^\star - y_{\mathrm{s}}^\diamond\|_2^\xi.
\end{aligned}
$$

Since $\sigma, \eta_1, \eta_2, \xi > 1$, taking the limit of both sides of the inequality as β approaches 1 from the right, leads to

$$
V_{\mathrm{O}}(y_{\mathrm{s}}^\star - y_{\mathrm{t}}) - V_{\mathrm{O}}(y_{\mathrm{s}}^\diamond - y_{\mathrm{t}}) \leq 0
$$

which in turn leads to a contradiction and concludes the proof. □

Lemma 9.4. *Suppose that Assumptions from 9.1 to 9.10 hold. Then, there exists a $\mathcal{K}_\infty$-function α_{d} verifying*

$$
\|\hat{\chi} - \chi_{\mathrm{s}}^\star\|_2 \geq \alpha_{\mathrm{d}}(\|\hat{\chi} - \chi_{\mathrm{s}}^\diamond\|_2) \tag{9.21}
$$

for all $y_{\mathrm{t}} \in \mathcal{Y}_{\mathrm{t}}$ and all feasible $\hat{\chi} \in (\hat{\mathcal{X}} \times \mathcal{U})$, with $\chi_{\mathrm{s}}^\diamond = g(y_{\mathrm{s}}^\diamond)$.

Proof. First note that $\|\hat{\chi} - \chi_{\mathrm{s}}^\star\|_2 = 0 \iff \|\hat{\chi} - \chi_{\mathrm{s}}^\diamond\|_2 = 0$. In fact, $\|\hat{\chi} - \chi_{\mathrm{s}}^\star\|_2 = 0 \implies \|\hat{\chi} - \chi_{\mathrm{s}}^\diamond\|_2 = 0$ follows from Lemma 9.3, while $\|\hat{\chi} -$

$\chi_{\mathrm{s}}^{\diamond}\|_2 = 0 \implies \|\hat{\chi} - \chi_{\mathrm{s}}^{\star}\|_2 = 0$ follows by optimality. Then it also holds $\|\hat{\chi} - \chi_{\mathrm{s}}^{\diamond}\|_2 > 0 \iff \|\hat{\chi} - \chi_{\mathrm{s}}^{\star}\|_2 > 0$.

Moreover, since the set $\mathcal{U}$ is compact, in view of the δISS property of Σ, $\mathcal{Z}_{\mathrm{s}}$ is also compact. Then, there exists a $\mathcal{K}_\infty$ function α_{d} verifying

$$\|\hat{\chi} - \chi_{\mathrm{s}}^{\star}\|_2 \geq \alpha_{\mathrm{d}}(\|\hat{\chi} - \chi_{\mathrm{s}}^{\diamond}\|_2)$$

for all $y_{\mathrm{t}} \in \mathcal{Y}_{\mathrm{t}}$ and all feasible $\hat{\chi}$. □

Lemma 9.5. *Consider a discrete-time, nonlinear time invariant system Σ_{a}, with input u and state x^{a}, and a discrete-time, nonlinear time invariant system Σ_{b}, with input $v = x^{\mathrm{a}}$ and state x^{b}. Assume Σ_{a} is ISS w.r.t. u, and Σ_{b} is ISpS w.r.t. v. Then, the overall system Σ, with input u and state $\chi = [(x^{\mathrm{a}})^\top \ (x^{\mathrm{b}})^\top]^\top$ is ISpS w.r.t. u.*

Proof. For Σ_{a}, there exist functions $\beta_{\mathrm{a}} \in \mathcal{KL}$ and $\gamma_{\mathrm{a}} \in \mathcal{K}$, such that for any $k \in \mathbb{Z}_{\geq 0}$, any initial condition $x_0^{\mathrm{a}} \in \mathbb{R}^n$ and any input sequence $\mathbf{u}_{0,k} = \{u_0, u_1, ..., u_{k-1}\}$ with $u_h \in \mathbb{R}^m$ for $h = 0, ..., k-1$, it holds

$$\|x_k^{\mathrm{a}}\|_2 \leq \beta_{\mathrm{a}}(\|x_0^{\mathrm{a}}\|_2, k) + \gamma_{\mathrm{a}}\left(\|\mathbf{u}_{0,k}\|\right). \tag{9.22}$$

For Σ_{b}, there exist functions $\beta_{\mathrm{b}} \in \mathcal{KL}$ and $\gamma_{\mathrm{b}} \in \mathcal{K}$, and a constant $\varphi \geq 0$, such that for any $k \in \mathbb{Z}_{\geq 0}$, any initial condition $x_0^{\mathrm{b}} \in \mathbb{R}^n$ and any input sequence $\mathbf{v}_{0,k} = \{v_0, v_1, ..., v_{k-1}\}$ with $v_h \in \mathbb{R}^m$ for $h = 0, ..., k-1$, it holds

$$\|x_k^{\mathrm{b}}\|_2 \leq \beta_{\mathrm{b}}(\|x_0^{\mathrm{b}}\|_2, k) + \gamma_{\mathrm{b}}\left(\|\mathbf{v}_{0,k}\|\right) + \varphi = \beta_{\mathrm{b}}(\|x_0^{\mathrm{b}}\|_2, k) + \gamma_{\mathrm{b}}\left(\|\mathbf{x}_{0,k}^{\mathrm{a}}\|\right) + \varphi. \tag{9.23}$$

The proof is inspired by the proof of Proposition 4.7 in [7], and makes use of the weak triangle inequality (2.2). Define $\bar{k} := \lceil \frac{k}{2} \rceil$, where $\lceil \cdot \rceil$ denotes the ceiling function. Then

$$\begin{aligned}
\|x_k^{\mathrm{b}}\|_2 &\overset{(9.23)}{\leq} \beta_{\mathrm{b}}(\|x_{\bar{k}}^{\mathrm{b}}\|_2, k - \bar{k}) + \gamma_{\mathrm{b}}\left(\|\mathbf{x}_{\bar{k},k}^{\mathrm{a}}\|\right) + \varphi \\
&\overset{(9.23)}{\leq} \beta_{\mathrm{b}}\left(\beta_{\mathrm{b}}(\|x_0^{\mathrm{b}}\|_2, \bar{k}) + \gamma_{\mathrm{b}}\left(\|\mathbf{x}_{0,\bar{k}}^{\mathrm{a}}\|\right) + \varphi, k - \bar{k}\right) + \gamma_{\mathrm{b}}\left(\|\mathbf{x}_{\bar{k},k}^{\mathrm{a}}\|\right) + \varphi \\
&\leq \beta_{\mathrm{b}}\left(3\beta_{\mathrm{b}}(\|x_0^{\mathrm{b}}\|_2, \bar{k}), k - \bar{k}\right) + \beta_{\mathrm{b}}\left(3\gamma_2\left(\|\mathbf{x}_{0,\bar{k}}^{\mathrm{a}}\|\right), k - \bar{k}\right) \\
&\quad + \beta_{\mathrm{b}}\left(3\varphi, k - \bar{k}\right) + \gamma_{\mathrm{b}}\left(\|\mathbf{x}_{\bar{k},k}^{\mathrm{a}}\|\right) + \varphi \\
&\overset{(9.22)}{\leq} \beta_{\mathrm{b}}\left(3\beta_{\mathrm{b}}(\|x_0^{\mathrm{b}}\|_2, \bar{k}), k - \bar{k}\right) \\
&\quad + \beta_{\mathrm{b}}\left(3\gamma_{\mathrm{b}}\left(\beta_{\mathrm{a}}(\|x_0^{\mathrm{a}}\|_2, 0) + \gamma_{\mathrm{a}}\left(\|\mathbf{u}_{0,\bar{k}}\|\right)\right), k - \bar{k}\right) \\
&\quad + \beta_{\mathrm{b}}\left(3\varphi, k - \bar{k}\right) + \varphi + \gamma_{\mathrm{b}}\left(\beta_{\mathrm{a}}(\|x_0^{\mathrm{a}}\|_2, \bar{k}) + \gamma_{\mathrm{a}}\left(\|\mathbf{u}_{\bar{k},k}\|\right)\right) \\
&\leq \beta_{\mathrm{b}}\left(3\beta_{\mathrm{b}}(\|x_0^{\mathrm{b}}\|_2, \bar{k}), k - \bar{k}\right) + \beta_{\mathrm{b}}\left(3\gamma_{\mathrm{b}}\left(2\beta_{\mathrm{a}}(\|x_0^{\mathrm{a}}\|_2, 0)\right), k - \bar{k}\right) \\
&\quad + \beta_{\mathrm{b}}\left(3\gamma_{\mathrm{b}}\left(2\gamma_{\mathrm{a}}\left(\|\mathbf{u}_{0,\bar{k}}\|\right)\right), k - \bar{k}\right) + \beta_{\mathrm{b}}\left(3\varphi, k - \bar{k}\right) + \varphi \\
&\quad + \gamma_{\mathrm{b}}\left(2\beta_{\mathrm{a}}(\|x_0^{\mathrm{a}}\|_2, \bar{k})\right) + \gamma_{\mathrm{b}}\left(2\gamma_{\mathrm{a}}\left(\|\mathbf{u}_{\bar{k},k}\|\right)\right).
\end{aligned}$$

Then

$$\|x_k^{\mathrm{b}}\| \leq \hat{\beta}_{\mathrm{a}}(\|x_0^{\mathrm{a}}\|_2, k) + \hat{\beta}_{\mathrm{b}}(\|x_0^{\mathrm{b}}\|_2, k) + \hat{\gamma}\left(\|\mathbf{u}_{0,k}\|\right) + \hat{\varphi} \tag{9.24}$$

where

$$\begin{aligned}
\hat{\beta}_{\mathrm{a}}(r,k) &:= \beta_{\mathrm{b}}\left(3\gamma_{\mathrm{b}}\left(2\beta_{\mathrm{a}}(r,0)\right), k-\bar{k}\right) + \gamma_{\mathrm{b}}\left(2\beta_{\mathrm{a}}(r,\bar{k})\right) \\
\hat{\beta}_{\mathrm{b}}(r,k) &:= \beta_{\mathrm{b}}\left(3\beta_{\mathrm{b}}(r,\bar{k}), k-\bar{k}\right) \\
\hat{\gamma}(r) &:= \beta_{\mathrm{b}}\left(3\gamma_{\mathrm{b}}\left(2\gamma_{\mathrm{a}}\left(r\right)\right), 0\right) + \gamma_{\mathrm{b}}\left(2\gamma_{\mathrm{a}}\left(r\right)\right) \\
\hat{\varphi} &:= \beta_{\mathrm{b}}\left(3\varphi, 0\right) + \varphi.
\end{aligned}$$

Finally, ISpS of the complete system comes from the sum of (9.22) and (9.24). □

9.8.2 Proof of Theorem 9.1

The proof of Theorem 9.1 requires three steps. Recursive feasibility of the FHOCP is proved for any y_{t} in the first step. ISpS w.r.t. the disturbance w is proved for the closed-loop system Σ_{C} in the second step. Asymptotic convergence of the closed-loop system Σ_{C} is proved for asymptotically constant setpoint y^0 and output disturbance d in the last step.

Recursive Feasibility

Consider the optimal solution to the FHOCP at time step k, that is given by $\boldsymbol{\Delta}\mathbf{u}_k^\star = \{\Delta u_{i|k}\}_{i=0}^{N-1}$ and $y_{\mathrm{s},k}^\star$, and denote the corresponding optimal input and state trajectory by $u_{i|k}^\star$ and $x_{i|k}^\star$ for $i = 1, ..., N$, where $x_{0|k}^\star = \hat{x}_k$ and $u_{0|k}^\star = u_{k-1}$. Assuming that the FHOCP is feasible at time step k, recursive feasibility can be proven by considering as candidate solution at time step $k+1$:

- the feasible auxiliary reference $\tilde{y}_{\mathrm{s},k+1} = y_{\mathrm{s},k}^\star$
- the control sequence $\boldsymbol{\Delta}\tilde{\mathbf{u}}_{k+1} = \{\Delta\tilde{u}_{i|k+1}\}_{i=0}^{N-1}$, defined by $\Delta\tilde{u}_{i|k+1} := \Delta u_{i+1|k}^\star$ for $i = 0, ..., N-2$ and $\Delta\tilde{u}_{N-1|k+1} := 0$, which satisfies all the constraints in the FHOCP.

Input-to-State Practical Stability

Consider the overall closed-loop system Σ_{C}. Since Assumption 9.4 holds for any input sequence in $\mathcal{U}$, Σ_{C} can be reformulated as the series connection of the system that describes the observer estimation error Σ_{O}, and the closed loop system Σ_{n} composed of the system Σ, the MPC controller, and the discrete time integrator, where the observer estimation error e_{d} acts as an input. Since Assumption 9.4 ensures that Σ_{O} is ISS with respect to the

disturbance w, in order to conclude that the overall closed-loop system is ISpS with respect to the disturbance w, the proof first shows that Σ_{n} is ISpS with respect to the state estimation error e_{d}, and then relies on Lemma 9.5 to derive the stability properties of full system.

To prove that Σ_{n} is ISpS with respect to e_{d}, the following candidate ISpS Lyapunov function is considered, where $\hat{\chi}_k = [\hat{x}_k^\top \; u_{k-1}^\top]^\top$

$$\begin{aligned} W_k &= W(\hat{\chi}_k; \boldsymbol{\Delta}\mathbf{u}_k^\star, y_{\mathrm{s},k}^\star) \\ &:= J_N(\hat{x}_k, u_{k-1}, y_{\mathrm{t},\infty}; \boldsymbol{\Delta}\mathbf{u}_k^\star, y_{\mathrm{s},k}^\star) - V_{\mathrm{O}}(y_{\mathrm{s},\infty}^\diamond - y_{\mathrm{t},\infty}). \end{aligned}$$

The proof shows that W is an ISpS Lyapunov function, by deriving lower and upper bound to W, as well as to its decrease, consistently with Definition 2.15.

Lower Bound Consider the following lower bound

$$\begin{aligned} W_k \geq \ell(\hat{x}_k - x_{\mathrm{s},k}^\star, u_{k-1} - u_{\mathrm{s},k}^\star, \Delta u_{0|k}^\star) \\ + V_{\mathrm{O}}(y_{\mathrm{s},k}^\star - y_{\mathrm{t},\infty}) - V_{\mathrm{O}}(y_{\mathrm{s},\infty}^\diamond - y_{\mathrm{t},\infty}) + \Psi(\hat{x}_k - x_{\mathrm{s},k}^\star, u_{k-1} - u_{\mathrm{s},k}^\star). \end{aligned}$$

From Assumption 9.9 and Lipschitz continuity of g, it holds

$$\begin{aligned} W_k \geq \ell(\hat{x}_k - x_{\mathrm{s},k}^\star, u_{k-1} - u_{\mathrm{s},k}^\star, \Delta u_{0|k}^\star) \\ + \Psi(\hat{x}_k - x_{\mathrm{s},k}^\star, u_{k-1} - u_{\mathrm{s},k}^\star) + \alpha_{\mathrm{O}}(L_g^{-1}\|\chi_{\mathrm{s},k}^\star - \chi_{\mathrm{s},\infty}^\diamond\|_2). \end{aligned}$$

Then, there exists a $\mathcal{K}_\infty$ function $\hat{\alpha}_O$ defined as $\hat{\alpha}_O(r) := \alpha_{\mathrm{O}}(L_g^{-1}r)$ such that

$$\begin{aligned} W_k \geq \ell(\hat{x}_k - x_{\mathrm{s},k}^\star, u_{k-1} - u_{\mathrm{s},k}^\star, \Delta u_{0|k}^\star) \\ + \Psi(\hat{x}_k - x_{\mathrm{s},k}^\star, u_{k-1} - u_{\mathrm{s},k}^\star) + \hat{\alpha}_O(\|\chi_{\mathrm{s},k}^\star - \chi_{\mathrm{s},\infty}^\diamond\|_2). \end{aligned} \tag{9.25}$$

Note that Assumption 9.8 can be rearranged as

$$\begin{aligned} \ell(\hat{x}_k - x_{\mathrm{s},k}^\star, u_{k-1} - u_{\mathrm{s},k}^\star, \Delta u_{0|k}^\star) \\ + \Psi(\hat{x}_k - x_{\mathrm{s},k}^\star, u_{k-1} - u_{\mathrm{s},k}^\star) \geq \varepsilon_0 \mu(\|\hat{\chi}_k - \chi_{\mathrm{s},k}^\star\|_2). \end{aligned} \tag{9.26}$$

Combining (9.25) and (9.26), and using the weak triangle inequality (2.2), there exists a $\mathcal{K}_\infty$ function α_W so that

$$\begin{aligned} W_k &\geq \hat{\alpha}_O(\|\chi_{\mathrm{s},k}^\star - \chi_{\mathrm{s},\infty}^\diamond\|_2) + \varepsilon_0\mu(\|\chi_k - \chi_{\mathrm{s},k}^\star\|_2) \\ &\geq \alpha_W(2\|\chi_{\mathrm{s},k}^\star - \chi_{\mathrm{s},\infty}^\diamond\|_2) + \alpha_W(2\|\chi_k - \chi_{\mathrm{s},k}^\star\|_2) \\ &\geq \alpha_W(\|\chi_{\mathrm{s},k}^\star - \chi_{\mathrm{s},\infty}^\diamond\|_2 + \|\hat{\chi}_k - \chi_{\mathrm{s},k}^\star\|_2). \end{aligned}$$

Therefore, applying the triangle inequality, a lower bound for W_k is obtained:

$$W_k \geq \alpha_W(\|\hat{\chi}_k - \chi_{\mathrm{s},\infty}^\diamond\|_2). \tag{9.27}$$

Upper Bound For this part of the proof, we define $\chi_{\mathrm{s}}^{\diamond} = [(x_{\mathrm{s}}^{\diamond})^{\top}\ (u_{\mathrm{s}}^{\diamond})^{\top}] := g(y_{\mathrm{s}}^{\diamond})$.

The proof starts by adding and subtracting $V_{\mathrm{O}}(y_{\mathrm{s},k}^{\star} - y_{\mathrm{t},k})$ to W_k:

$$\begin{aligned} W_k = & \sum_{i=0}^{N-1} \ell(x_{i|k}^{\star} - x_{\mathrm{s},k}^{\star}, u_{i|k}^{\star} - u_{\mathrm{s},k}^{\star}, \Delta u_{i|k}^{\star}) \\ & + V_{\mathrm{f}}(x_{N|k}^{\star} - x_{\mathrm{s},k}^{\star}, y_{\mathrm{s},k}^{\star}) + V_{\mathrm{O}}(y_{\mathrm{s},k}^{\star} - y_{t_\infty}) + \Psi(\hat{x}_k - x_{\mathrm{s},k}^{\star}, u_{k-1} - u_{\mathrm{s},k}^{\star}) \\ & - V_{\mathrm{O}}(y_{\mathrm{s},\infty}^{\diamond} - y_{\mathrm{t},\infty}) + V_{\mathrm{O}}(y_{\mathrm{s},k}^{\star} - y_{\mathrm{t},k}) - V_{\mathrm{O}}(y_{\mathrm{s},k}^{\star} - y_{\mathrm{t},k}) \\ \overset{(9.8)}{=} & V_N(\hat{x}_k, u_{k-1}, y_{\mathrm{t},k}) + V_{\mathrm{O}}(y_{\mathrm{s},k}^{\star} - y_{\mathrm{t},\infty}) - V_{\mathrm{O}}(y_{\mathrm{s},k}^{\star} - y_{\mathrm{t},k}) \\ & - V_{\mathrm{O}}(y_{\mathrm{s},\infty}^{\diamond} - y_{\mathrm{t},\infty}). \end{aligned} \tag{9.28}$$

Consider now the case in which $u_{\mathrm{s},k}^{\diamond} - u_{k-1} \in \Delta\mathcal{U}$, i.e. the input steady-state reference $u_{\mathrm{s},k}^{\diamond}$ is reachable in one step from u_{k-1}. A locally feasible sequence $\boldsymbol{\Delta}\tilde{\mathbf{u}}_k = \{\Delta\tilde{u}_{i|k}\}_{i=0}^{N-1}$ can be defined by $\Delta\tilde{u}_{0|k} := u_{\mathrm{s},k}^{\diamond} - u_{k-1}$, and $\Delta\tilde{u}_{i|k} := 0$ for $i = 1, ..., N-1$, and the (locally) feasible auxiliary reference $\tilde{y}_{\mathrm{s},k} := y_{\mathrm{s},k}^{\diamond}$. Denote by $\tilde{x}_{i|k}$, $i = 0, ..., N$, the associated state trajectory. Then, using Assumption 9.10,

$$\begin{aligned} & V_N(\hat{x}_k, u_{k-1}, y_{\mathrm{t},k}) \leq J_N(\hat{x}_k, u_{k-1}, y_{\mathrm{t},k}; \boldsymbol{\Delta}\tilde{\mathbf{u}}_k, \tilde{y}_{\mathrm{s},k}) \\ & \quad = \ell(\hat{x}_k - x_{\mathrm{s},k}^{\diamond}, u_{k-1} - u_{\mathrm{s},k}^{\diamond}, \Delta\tilde{u}_{0|k}) \\ & \quad + \sum_{i=1}^{N-1} \ell(\tilde{x}_{i|k} - x_{\mathrm{s},k}^{\diamond}, 0, 0) + V_{\mathrm{f}}(\tilde{x}_{N|k} - x_{\mathrm{s},k}^{\diamond}, y_{\mathrm{s},k}^{\diamond}) \\ & \quad + V_{\mathrm{O}}(y_{\mathrm{s},k}^{\diamond} - y_{\mathrm{t},k}) + \Psi(\hat{x}_k - x_{\mathrm{s},k}^{\diamond}, u_{k-1} - u_{\mathrm{s},k}^{\diamond}) \\ & \quad \overset{(9.13)}{\leq} \ell(\hat{x}_k - x_{\mathrm{s},k}^{\diamond}, u_{k-1} - u_{\mathrm{s},k}^{\diamond}, \Delta\tilde{u}_{0|k}) + V_{\mathrm{f}}(\tilde{x}_{1|k} - x_{\mathrm{s},k}^{\diamond}, y_{\mathrm{s},k}^{\diamond}) \\ & \quad + V_{\mathrm{O}}(y_{\mathrm{s},k}^{\diamond} - y_{\mathrm{t},k}) + \Psi(\hat{x}_k - x_{\mathrm{s},k}^{\diamond}, u_{k-1} - u_{\mathrm{s},k}^{\diamond}) \\ & \quad \overset{(9.12)}{\leq} \ell(\hat{x}_k - x_{\mathrm{s},k}^{\diamond}, u_{k-1} - u_{\mathrm{s},k}^{\diamond}, u_{\mathrm{s},k}^{\diamond} - u_{k-1}) + b\|\tilde{x}_{1|k} - x_{\mathrm{s},k}^{\diamond}\|_2^{\sigma} \\ & \quad + V_{\mathrm{O}}(y_{\mathrm{s},k}^{\diamond} - y_{\mathrm{t},k}) + \Psi(\hat{x}_k - x_{\mathrm{s},k}^{\diamond}, u_{k-1} - u_{\mathrm{s},k}^{\diamond}) \\ & \quad \overset{\text{Ass.9.6}}{\leq} L_\ell\|\hat{x}_k - x_{\mathrm{s},k}^{\diamond}\|_2 + 2L_\ell\|u_{k-1} - u_{\mathrm{s},k}^{\diamond}\|_2 + b\|\tilde{x}_{1|k} - x_{\mathrm{s},k}^{\diamond}\|_2^{\sigma} \\ & \quad + V_{\mathrm{O}}(y_{\mathrm{s},k}^{\diamond} - y_{\mathrm{t},k}) + \Psi(\hat{x}_k - x_{\mathrm{s},k}^{\diamond}, u_{k-1} - u_{\mathrm{s},k}^{\diamond}). \end{aligned}$$

In view of the δISS property of the model, there exists a $\mathcal{KL}$ function β such that

$$\|\tilde{x}_{i|k} - x_{\mathrm{s},k}^{\diamond}\|_2 \leq \beta(\|\tilde{x}_{0|k} - x_{\mathrm{s},k}^{\diamond}\|_2, i) = \beta(\|\hat{x}_k - x_{\mathrm{s},k}^{\diamond}\|_2, i).$$

Then

$$\begin{aligned} V_N(\hat{x}_k, u_{k-1}, y_{\mathrm{t},k}) \leq\ & L_\ell \|\hat{x}_k - x^\diamond_{\mathrm{s},k}\|_2 + 2L_\ell \|u_{k-1} - u^\diamond_{\mathrm{s},k}\|_2 \\ & + b\beta(\|\hat{x}_k - x^\diamond_{\mathrm{s},k}\|_2, 1)^\sigma + V_{\mathrm{O}}(y^\diamond_{\mathrm{s},k} - y_{\mathrm{t},k}) \\ & + \Psi(\hat{x}_k - x^\diamond_{\mathrm{s},k}, u_{k-1} - u^\diamond_{\mathrm{s},k}). \end{aligned}$$

Therefore, there exist two $\mathcal{K}_\infty$ functions β_1 and β_2 such that

$$\begin{aligned} V_N(\hat{x}_k, u_{k-1}, y_{\mathrm{t},k}) \leq\ & \beta_1(\|\hat{x}_k - x^\diamond_{\mathrm{s},k}\|_2) + \beta_2(\|u_{k-1} - u^\diamond_{\mathrm{s},k}\|_2) \\ & + V_{\mathrm{O}}(y^\diamond_{\mathrm{s},k} - y_{\mathrm{t},k}) + \Psi(\hat{x}_k - x^\diamond_{\mathrm{s},k}, u_{k-1} - u^\diamond_{\mathrm{s},k}). \end{aligned}$$

Combining with the expression of W_k, and using the upper bound for Ψ

$$\begin{aligned} W_k &\overset{(9.28)(9.11a)}{\leq} \beta_1(\|\hat{x}_k - x^\diamond_{\mathrm{s},k}\|_2) + \beta_2(\|u_{k-1} - u^\diamond_{\mathrm{s},k}\|_2) \\ &+ |V_{\mathrm{O}}(y^\diamond_{\mathrm{s},k} - y_{\mathrm{t},k}) - V_{\mathrm{O}}(y^\diamond_{\mathrm{s},\infty} - y_{\mathrm{t},\infty})| \\ &+ |V_{\mathrm{O}}(y^\star_{\mathrm{s},k} - y_{\mathrm{t},\infty}) - V_{\mathrm{O}}(y^\star_{\mathrm{s},k} - y_{\mathrm{t},k})| + \gamma_0\mu(\|\hat{\chi}_k - \chi^\diamond_{\mathrm{s},k}\|_2) \\ &\overset{\text{Ass.9.6}}{\leq} \beta_1(\|\hat{x}_k - x^\diamond_{\mathrm{s},k}\|_2) + \beta_2(\|u_{k-1} - u^\diamond_{\mathrm{s},k}\|_2) + \gamma_0\mu(\|\hat{\chi}_k - \chi^\diamond_{\mathrm{s},k}\|_2) \\ &+ L_{V_{\mathrm{O}}}\|y^\diamond_{\mathrm{s},k} - y_{\mathrm{t},k} - y^\diamond_{\mathrm{s},\infty} + y_{\mathrm{t},\infty}\|_2 \\ &+ L_{V_{\mathrm{O}}}\|y^\star_{\mathrm{s},k} - y_{\mathrm{t},\infty} - y^\star_{\mathrm{s},k} + y_{\mathrm{t},k}\|_2 \\ &\leq \beta_1(\|\hat{x}_k - x^\diamond_{\mathrm{s},k}\|_2) + \beta_2(\|u_{k-1} - u^\diamond_{\mathrm{s},k}\|_2) + \gamma_0\mu(\|\hat{\chi}_k - \chi^\diamond_{\mathrm{s},k}\|_2) \\ &+ L_{V_{\mathrm{O}}}\|y^\diamond_{\mathrm{s},k} - y^\diamond_{\mathrm{s},\infty}\|_2 + 2L_{V_{\mathrm{O}}}\|y_{\mathrm{t},k} - y_{\mathrm{t},\infty}\|_2. \end{aligned}$$

Then, there exists a $\mathcal{K}_\infty$ function β_3 such that

$$\begin{aligned} W_k &\leq \beta_3(\|\hat{\chi}_k - \chi^\diamond_{\mathrm{s},k}\|_2) + L_{V_{\mathrm{O}}}\|y^\diamond_{\mathrm{s},k} - y^\diamond_{\mathrm{s},\infty}\|_2 + 2L_{V_{\mathrm{O}}}\|y_{\mathrm{t},k} - y_{\mathrm{t},\infty}\|_2 \\ &\leq \beta_3(\|\hat{\chi}_k + \chi^\diamond_{\mathrm{s},\infty} - \chi^\diamond_{\mathrm{s},\infty} - \chi^\diamond_{\mathrm{s},k}\|_2) \\ &+ L_{V_{\mathrm{O}}}\|y^\diamond_{\mathrm{s},k} - y^\diamond_{\mathrm{s},\infty}\|_2 + 2L_{V_{\mathrm{O}}}\|y_{\mathrm{t},k} - y_{\mathrm{t},\infty}\|_2. \end{aligned}$$

Hence, there exists a $\mathcal{K}_\infty$ function β_W defined by $\beta_W(r) := \beta_3(2r)$ such that

$$\begin{aligned} W_k &\leq \beta_W(\|\hat{\chi}_k - \chi^\diamond_{\mathrm{s},\infty}\|_2) + \beta_W(\|\chi^\diamond_{\mathrm{s},\infty} - \chi^\diamond_{\mathrm{s},k}\|_2) \\ &\quad + L_{V_{\mathrm{O}}}\|y^\diamond_{\mathrm{s},k} - y^\diamond_{\mathrm{s},\infty}\|_2 + 2L_{V_{\mathrm{O}}}\|y_{\mathrm{t},k} - y_{\mathrm{t},\infty}\|_2 \\ &= \beta_W(\|\hat{\chi}_k - \chi^\diamond_{\mathrm{s},\infty}\|_2) + \rho_{1_k} \end{aligned}$$

with

$$\rho_{1,k} := \beta_W(\|\chi^\diamond_{\mathrm{s},\infty} - \chi^\diamond_{\mathrm{s},k}\|_2) + L_{V_{\mathrm{O}}}\|y^\diamond_{\mathrm{s},k} - y^\diamond_{\mathrm{s},\infty}\|_2 + 2L_{V_{\mathrm{O}}}\|y_{\mathrm{t},k} - y_{\mathrm{t},\infty}\|_2. \quad (9.29)$$

Then, using Lipschitz continuity of the function g, there exists a $\mathcal{K}_\infty$ function $\tilde{\beta}_W$ such that

$$\rho_{1,k} \leq \tilde{\beta}_W(\|y^\diamond_{\mathrm{s},k} - y^\diamond_{\mathrm{s},\infty}\|_2) + 2L_{V_{\mathrm{O}}}\|y^0_k - y^0_\infty\|_2 + 2L_{V_{\mathrm{O}}}\|\hat{d}_\infty - \hat{d}_k\|_2.$$

In view of [221, Theorem 2.5], of the properties of V_{O} and of convexity of $\mathcal{Y}_{\mathrm{t}}$, there exists a $\mathcal{K}$ function ω such that

$$\|y^{\diamond}_{\mathrm{s},k} - y^{\diamond}_{\mathrm{s},\infty}\|_2 \leq \omega(\|y_{\mathrm{t},k} - y_{\mathrm{t},\infty}\|_2) = \omega(\|y^0_k - \hat{d}_k - (y^0_\infty - \hat{d}_\infty)\|_2). \quad (9.30)$$

Hence, by applying the weak triangle inequality, there exists a $\mathcal{K}$ function $\tilde{\omega}_1$ such that

$$\rho_{1,k} \leq \tilde{\omega}_1(\|y^0_k - y^0_\infty\|_2) + \tilde{\omega}_1(\|\hat{d}_k - \hat{d}_\infty\|_2) \leq \overline{\rho}_1$$

where

$$\overline{\rho}_1 := \tilde{\omega}_1(\mathcal{S}(\mathcal{Y}^0)) + \tilde{\omega}_1(\mathcal{S}(\hat{\mathcal{D}})). \quad (9.31)$$

Since all the sets involved in the definition of $\overline{\rho}_1$ are bounded, it holds $\overline{\rho}_1 < \infty$. To conclude

$$W_k \leq \beta_W(\|\hat{\chi}_k - \chi^{\diamond}_{\mathrm{s},\infty}\|_2) + \overline{\rho}_1. \quad (9.32)$$

Given this local upper bound derived under the assumption that $u^{\diamond}_{\mathrm{s},k} - u_{k-1} \in \Delta\mathcal{U}$, the existence of an upper bound valid also if $u^{\diamond}_{\mathrm{s},k} - u_{k-1} \notin \Delta\mathcal{U}$ can be derived from [149, Lemma 4] by showing that $W(\hat{x}, u, y_{\mathrm{t}}) < \infty$ for all $\hat{x} \in \hat{\mathcal{X}}$, $y^\star \in \mathcal{Y}^0$, $\hat{d} \in \hat{\mathcal{D}}$, and all feasible u. First, based on (9.28), $W_k \leq J_N(\hat{x}_k, u_{k-1}, y_{\mathrm{t},k}; \mathbf{\Delta u}_k, y_{\mathrm{s},k}) + V_{\mathrm{O}}(y^\star_{\mathrm{s},k} - y_{\mathrm{t},\infty}) - V_{\mathrm{O}}(y^\star_{\mathrm{s},k} - y_{\mathrm{t},k}) - V_{\mathrm{O}}(y^{\diamond}_{\mathrm{s},\infty} - y_{\mathrm{t},\infty})$ for all feasible $\mathbf{\Delta u}_k, y_{\mathrm{s},k}$. Then, boundedness of J_N and V_{O} follows from boundedness of their arguments and Assumption 9.6. Specifically, boundedness of $\hat{x}$ and $\hat{d}$ follows from Lemma 9.1; boundedness of y_{t} follows from boundedness of $\mathcal{Y}^0$ and boundedness of $\hat{\mathcal{D}}$; boundedness of y_{s} follows from boundedness of $\mathcal{Y}_{\mathrm{t}}$; boundedness of u follows from boundedness of $\mathcal{U}$.

Decrease For this part of the proof, we recall that $u_k = u_{k-1} + \mu_N(\hat{x}_k, u_{k-1}, y_{\mathrm{t},k})$, and that

$$\hat{x}_{k+1} = f(\hat{x}_k, u_k) + \delta x_{\mathrm{d},k}. \quad (9.33)$$

In the following, $\delta x_{\mathrm{d},k}$ is considered as an external disturbance. The candidate Lyapunov function at time $k+1$ is given by

$$\begin{aligned} W_{k+1} &= W(\hat{\chi}_{k+1}; \mathbf{\Delta u}^\star_{k+1}, y^\star_{\mathrm{s},k+1}) \\ &= J_N(\hat{x}_{k+1}, u_k, y_{\mathrm{t},\infty}; \mathbf{\Delta u}^\star_{k+1}, y^\star_{\mathrm{s},k+1}) - V_{\mathrm{O}}(y^{\diamond}_{\mathrm{s},\infty} - y_{\mathrm{t},\infty}) \end{aligned}$$

where $\mathbf{\Delta u}^\star_{k+1}$ and $y^\star_{\mathrm{s},k+1}$ are the optimal control sequence and optimal auxiliary reference computed by the MPC at step $k+1$, given the observer estimate $\hat{x}_{k+1}$.

Adding and subtracting $V_{\mathrm{O}}(y^\star_{\mathrm{s},k+1} - y_{\mathrm{t},k+1})$ leads to

$$\begin{aligned}
W_{k+1} = & \sum_{i=0}^{N-1} \ell(x_{i|k+1} - x^\star_{\mathrm{s},k+1}, u_{i|k+1} - u^\star_{\mathrm{s},k+1}, \boldsymbol{\Delta}\mathbf{u}^\star_{i|k+1}) \\
& + V_{\mathrm{f}}(x_{N|k+1} - x^\star_{\mathrm{s},k+1}, y^\star_{\mathrm{s},k+1}) + V_{\mathrm{O}}(y^\star_{\mathrm{s},k+1} - y_{\mathrm{t}_\infty}) \\
& + \Psi(\hat{x}_{k+1} - x^\star_{\mathrm{s},k+1}, u_k - u^\star_{\mathrm{s},k+1}) - V_{\mathrm{O}}(y^\diamond_{\mathrm{s},\infty} - y_{\mathrm{t},\infty}) \\
& + V_{\mathrm{O}}(y^\star_{\mathrm{s},k+1} - y_{\mathrm{t},k+1}) - V_{\mathrm{O}}(y^\star_{\mathrm{s},k+1} - y_{\mathrm{t},k+1}) \\
\overset{(9.8)}{\leq} & V_N(\hat{x}_{k+1}, u_k, y_{\mathrm{t},k+1}) - V_{\mathrm{O}}(y^\diamond_{\mathrm{s},\infty} - y_{\mathrm{t},\infty}) \\
& + |V_{\mathrm{O}}(y^\star_{\mathrm{s},k+1} - y_{\mathrm{t},\infty}) - V_{\mathrm{O}}(y^\star_{\mathrm{s},k+1} - y_{\mathrm{t},k+1})| \\
\overset{\text{Ass.9.6}}{\leq} & V_N(\hat{x}_{k+1}, u_k, y_{\mathrm{t},k+1}) - V_{\mathrm{O}}(y^\diamond_{\mathrm{s},\infty} - y_{\mathrm{t},\infty}) \\
& + L_{V_{\mathrm{O}}} \|y_{\mathrm{t},k+1} - y_{\mathrm{t},\infty}\|_2.
\end{aligned}$$

Consider now the feasible sequence $\boldsymbol{\Delta}\tilde{\mathbf{u}}_{k+1} = \{\Delta\tilde{u}_{i|k+1}\}_{i=0}^{N-1}$, defined in the proof of recursive feasibility, and the feasible auxiliary reference $\tilde{y}_{\mathrm{s},k+1} := y^\star_{\mathrm{s},k}$. Then

$$\begin{aligned}
V_N(\hat{x}_{k+1}, u_k, y_{\mathrm{t},k+1}) &\leq J_N(\hat{x}_{k+1}, u_k, y_{\mathrm{t},k+1}; \boldsymbol{\Delta}\tilde{\mathbf{u}}_{k+1}, \tilde{y}_{\mathrm{s},k+1}) \\
&= J_N(\hat{x}_{k+1}, u_k, y_{\mathrm{t},k+1}; \boldsymbol{\Delta}\tilde{\mathbf{u}}_{k+1}, y^\star_{\mathrm{s},k}).
\end{aligned}$$

Hence, denoting by $\tilde{x}_{i|k+1}$ and $\tilde{u}_{i|k+1}$ the state and input trajectories associated to $\boldsymbol{\Delta}\tilde{\mathbf{u}}_{k+1}$, we have that

$$\begin{aligned}
W_{k+1} \leq & \sum_{i=0}^{N-1} \ell(\tilde{x}_{i|k+1} - x^\star_{\mathrm{s},k}, \tilde{u}_{i|k+1} - u^\star_{\mathrm{s},k}, \Delta\tilde{u}_{i|k+1}) \\
& + V_{\mathrm{f}}(\tilde{x}_{N|k+1} - x^\star_{\mathrm{s},k}, y^\star_{\mathrm{s},k}) + V_{\mathrm{O}}(y^\star_{\mathrm{s},k} - y_{\mathrm{t},k+1}) \\
& + \Psi(\hat{x}_{k+1} - x^\star_{\mathrm{s},k}, u_k - u^\star_{\mathrm{s},k}) \\
& + L_{V_{\mathrm{O}}} \|y_{\mathrm{t},k+1} - y_{\mathrm{t},\infty}\|_2 - V_{\mathrm{O}}(y^\diamond_{\mathrm{s},\infty} - y_{\mathrm{t},\infty}).
\end{aligned}$$

Then

$$\begin{aligned}
& W_{k+1} - W_k \\
& \leq \Big(\sum_{i=0}^{N-1} \ell(\tilde{x}_{i|k+1} - x^\star_{\mathrm{s},k}, \tilde{u}_{i|k+1} - u^\star_{\mathrm{s},k}, \Delta\tilde{u}_{i|k+1}) + V_{\mathrm{f}}(\tilde{x}_{N|k+1} - x^\star_{\mathrm{s},k}, y^\star_{\mathrm{s},k}) \\
& \quad + V_{\mathrm{O}}(y^\star_{\mathrm{s},k} - y_{\mathrm{t},k+1}) + \Psi(\hat{x}_{k+1} - x^\star_{\mathrm{s},k}, u_k - u^\star_{\mathrm{s},k}) \\
& \quad + L_{V_{\mathrm{O}}} \|y_{\mathrm{t},k+1} - y_{\mathrm{t},\infty}\|_2 - V_{\mathrm{O}}(y^\diamond_{\mathrm{s},\infty} - y_{\mathrm{t},\infty}) \Big) \\
& \quad - \Big(\sum_{i=0}^{N-1} \ell(x^\star_{i|k} - x^\star_{\mathrm{s},k}, u^\star_{i|k} - u^\star_{\mathrm{s},k}, \Delta u^\star_{i|k}) + V_{\mathrm{f}}(x^\star_{N|k} - x^\star_{\mathrm{s},k}, y^\star_{\mathrm{s},k}) \\
& \quad + V_{\mathrm{O}}(y^\star_{\mathrm{s},k} - y_{\mathrm{t},\infty}) + \Psi(\hat{x}_k - x^\star_{\mathrm{s},k}, u_{k-1} - u^\star_{\mathrm{s},k}) - V_{\mathrm{O}}(y^\diamond_{\mathrm{s},\infty} - y_{\mathrm{t},\infty}) \Big)
\end{aligned}$$

$$
\begin{aligned}
&= \sum_{i=0}^{N-1} \ell(\tilde{x}_{i|k+1} - x^\star_{\mathrm{s},k}, \tilde{u}_{i|k+1} - u^\star_{\mathrm{s},k}, \Delta\tilde{u}_{i|k+1}) \\
&\quad - \sum_{i=0}^{N-1} \ell(x^\star_{i|k} - x^\star_{\mathrm{s},k}, u^\star_{i|k} - u^\star_{\mathrm{s},k}, \Delta u^\star_{i|k}) \\
&\quad + V_{\mathrm{f}}(\tilde{x}_{N|k+1} - x^\star_{\mathrm{s},k}, y^\star_{\mathrm{s},k}) - V_{\mathrm{f}}(x^\star_{N|k} - x^\star_{\mathrm{s},k}, y^\star_{\mathrm{s},k}) \\
&\quad + V_{\mathrm{O}}(y^\star_{\mathrm{s},k} - y_{\mathrm{t},k+1}) - V_{\mathrm{O}}(y^\star_{\mathrm{s},k} - y_{\mathrm{t},\infty}) \\
&\quad + \Psi(\hat{x}_{k+1} - x^\star_{\mathrm{s},k}, u_k - u^\star_{\mathrm{s},k}) - \Psi(\hat{x}_k - x^\star_{\mathrm{s},k}, u_{k-1} - u^\star_{\mathrm{s},k}) \\
&\quad + L_{V_{\mathrm{O}}} \|y_{\mathrm{t},k+1} - y_{\mathrm{t},\infty}\|_2 \\
&\overset{\text{Ass.9.6}}{\leq} \sum_{i=0}^{N-1} \ell(\tilde{x}_{i|k+1} - x^\star_{\mathrm{s},k}, \tilde{u}_{i|k+1} - u^\star_{\mathrm{s},k}, \Delta\tilde{u}_{i|k+1}) \\
&\quad - \sum_{i=0}^{N-1} \ell(x^\star_{i|k} - x^\star_{\mathrm{s},k}, u^\star_{i|k} - u^\star_{\mathrm{s},k}, \Delta u^\star_{i|k}) \\
&\quad + V_{\mathrm{f}}(\tilde{x}_{N|k+1} - x^\star_{\mathrm{s},k}, y^\star_{\mathrm{s},k}) - V_{\mathrm{f}}(x^\star_{N|k} - x^\star_{\mathrm{s},k}, y^\star_{\mathrm{s},k}) \\
&\quad + \Psi(\hat{x}_{k+1} - x^\star_{\mathrm{s},k}, u_k - u^\star_{\mathrm{s},k}) - \Psi(\hat{x}_k - x^\star_{\mathrm{s},k}, u_{k-1} - u^\star_{\mathrm{s},k}) \\
&\quad + 2L_{V_{\mathrm{O}}} \|y_{\mathrm{t},k+1} - y_{\mathrm{t},\infty}\|_2 \\
&= \sum_{i=0}^{N-2} \ell(\tilde{x}_{i|k+1} - x^\star_{\mathrm{s},k}, \tilde{u}_{i|k+1} - u^\star_{\mathrm{s},k}, \Delta\tilde{u}_{i|k+1}) \\
&\quad - \sum_{i=1}^{N-1} \ell(x^\star_{i|k} - x^\star_{\mathrm{s},k}, u^\star_{i|k} - u^\star_{\mathrm{s},k}, \Delta u^\star_{i|k}) \\
&\quad + V_{\mathrm{f}}(\tilde{x}_{N|k+1} - x^\star_{\mathrm{s},k}, y^\star_{\mathrm{s},k}) - V_{\mathrm{f}}(x^\star_{N|k} - x^\star_{\mathrm{s},k}, y^\star_{\mathrm{s},k}) \\
&\quad + \Psi(\hat{x}_{k+1} - x^\star_{\mathrm{s},k}, u_k - u^\star_{\mathrm{s},k}) - \Psi(\hat{x}_k - x^\star_{\mathrm{s},k}, u_k - u^\star_{\mathrm{s},k}) \\
&\quad + 2L_{V_{\mathrm{O}}} \|y_{\mathrm{t},k+1} - y_{\mathrm{t},\infty}\|_2 \\
&\quad + \ell(\tilde{x}_{N-1|k+1} - x^\star_{\mathrm{s},k}, \tilde{u}_{N-1|k+1} - u^\star_{\mathrm{s},k}, \Delta\tilde{u}_{N-1|k+1}) \\
&\quad - \ell(\hat{x}_k - x^\star_{\mathrm{s},k}, u_{k-1} - u^\star_{\mathrm{s},k}, \Delta u^\star_{0|k}).
\end{aligned}
$$

Define $\tilde{x}_{N+1|k}$ using the auxiliary control law $\Delta\tilde{u}_{N|k} = 0$, i.e. $\tilde{x}_{N+1|k} := f(x^\star_{N|k}, \tilde{u}_{N+1|k})$ where $\tilde{u}_{N+1|k} := \tilde{u}_{N|k}$. Then, by adding and subtracting $V_{\mathrm{f}}(\tilde{x}_{N+1|k} - x^\star_{\mathrm{s},k}, y^\star_{\mathrm{s},k})$ and $\ell(x^\star_{N|k} - x^\star_{\mathrm{s},k}, 0, 0)$, and recalling $\Delta\tilde{u}_{N-1|k+1} = 0$,

we have that

$$\begin{aligned}
&W_{k+1} - W_k \\
&\leq \sum_{i=1}^{N-1} |\ell(\tilde{x}_{i-1|k+1} - x^\star_{\mathrm{s},k}, \tilde{u}_{i-1|k} - u^\star_{\mathrm{s},k}, \Delta\tilde{u}_{i-1|k+1}) \\
&\quad - \ell(x^\star_{i|k} - x^\star_{\mathrm{s},k}, u^\star_{i|k} - u^\star_{\mathrm{s},k}, \Delta u^\star_{i|k})| \\
&\quad + |\ell(\tilde{x}_{N-1|k+1} - x^\star_{\mathrm{s},k}, 0, 0) - \ell(x^\star_{N|k} - x^\star_{\mathrm{s},k}, 0, 0)| \\
&\quad + |V_\mathrm{f}(\tilde{x}_{N|k+1} - x^\star_{\mathrm{s},k}, y^\star_{\mathrm{s},k}) - V_\mathrm{f}(\tilde{x}_{N+1|k} - x^\star_{\mathrm{s},k}, y^\star_{\mathrm{s},k}))| \\
&\quad + \Psi(\hat{x}_{k+1} - x^\star_{\mathrm{s},k}, u_k - u^\star_{\mathrm{s},k}) - \Psi(\hat{x}_k - x^\star_{\mathrm{s},k}, u_{k-1} - u^\star_{\mathrm{s},k}) \\
&\quad - \ell(\hat{x}_k - x^\star_{\mathrm{s},k}, u_{k-1} - u^\star_{\mathrm{s},k}, \Delta u^\star_{0|k}) + 2L_{V_\mathrm{O}}\|y_{\mathrm{t},k+1} - y_{\mathrm{t},\infty}\|_2 \\
&\quad + V_\mathrm{f}(\tilde{x}_{N+1|k} - x^\star_{\mathrm{s},k}, y^\star_{\mathrm{s},k}) - V_\mathrm{f}(x^\star_{N|k} - x^\star_{\mathrm{s},k}, y^\star_{\mathrm{s},k}) + \ell(x^\star_{N|k} - x^\star_{\mathrm{s},k}, 0, 0).
\end{aligned} \tag{9.34}$$

Due to Assumption 9.10

$$V_\mathrm{f}(\tilde{x}_{N+1|k} - x^\star_{\mathrm{s},k}, y^\star_{\mathrm{s},k}) - V_\mathrm{f}(x^\star_{N|k} - x^\star_{\mathrm{s},k}, y^\star_{\mathrm{s},k}) + \ell(x^\star_{N|k} - x^\star_{\mathrm{s},k}, 0, 0) \leq 0. \tag{9.35}$$

Due to the definition of $\boldsymbol{\Delta\tilde{\mathbf{u}}}_{k+1}$, Lipschitz continuity of ℓ, and δISS of the system Σ

$$\begin{aligned}
&\sum_{i=1}^{N-1} |\ell(\tilde{x}_{i-1|k+1} - x^\star_{\mathrm{s},k}, \tilde{u}_{i-1|k} - u^\star_{\mathrm{s},k}, \Delta\tilde{u}_{i-1|k+1}) \\
&\quad - \ell(x^\star_{i|k} - x^\star_{\mathrm{s},k}, u^\star_{i|k} - u^\star_{\mathrm{s},k}, \Delta u^\star_{i|k})| \\
&= \sum_{i=1}^{N-1} |\ell(\tilde{x}_{i-1|k+1} - x^\star_{\mathrm{s},k}, u^\star_{i|k} - u^\star_{\mathrm{s},k}, \Delta u^\star_{i|k}) \\
&\quad - \ell(x^\star_{i|k} - x^\star_{\mathrm{s},k}, u^\star_{i|k} - u^\star_{\mathrm{s},k}, \Delta u^\star_{i|k})| \\
&\overset{\text{Ass.9.6}}{\leq} \sum_{i=1}^{N-1} L_\ell\|\tilde{x}_{i-1|k+1} - x^\star_{i|k}\|_2 \overset{\text{Ass.9.1}}{\leq} \gamma_1(\|\delta x_\mathrm{d}\|_2)
\end{aligned} \tag{9.36}$$

with a $\mathcal{K}$-function γ_1.

Lipschitz continuity of ℓ, and δISS of the system Σ also imply that

$$\begin{aligned}
&|\ell(\tilde{x}_{N-1|k+1} - x^\star_{\mathrm{s},k}, 0, 0) - \ell(x^\star_{N|k} - x^\star_{\mathrm{s},k}, 0, 0)| \\
&\overset{\text{Ass.9.6}}{\leq} L_\ell\|\tilde{x}_{N-1|k+1} - x^\star_{N|k}\|_2 \overset{\text{Ass.9.1}}{\leq} \gamma_2(\|\delta x_\mathrm{d}\|_2)
\end{aligned} \tag{9.37}$$

with a $\mathcal{K}$-function γ_2.

Moreover, due to the Lipschitz continuity of V_f, and δISS of the system Σ

$$\begin{aligned}
&|V_\mathrm{f}(\tilde{x}_{N|k+1} - x^\star_{\mathrm{s},k}, y^\star_{\mathrm{s},k}) - V_\mathrm{f}(\tilde{x}_{N+1|k} - x^\star_{\mathrm{s},k}, y^\star_{\mathrm{s},k})| \\
&\overset{\text{Ass.9.6}}{\leq} L_{V_\mathrm{f}}\|\tilde{x}_{N|k+1} - \tilde{x}_{N+1|k}\|_2 \overset{\text{Ass.9.1}}{\leq} \gamma_3(\|\delta x_\mathrm{d}\|_2)
\end{aligned} \tag{9.38}$$

with a $\mathcal{K}$-function γ_3.

In view of Assumption 9.8, Lipschitzianity of Ψ, and using Lemma 9.4, it holds that

$$\begin{aligned}
&- \ell(\hat{x}_k - x^\star_{\mathrm{s},k}, u_{k-1} - u^\star_{\mathrm{s},k}, \Delta u^\star_{0|k}) \\
&+ \Psi(\hat{x}_{k+1} - x^\star_{\mathrm{s},k}, u_k - u^\star_{\mathrm{s},k}) - \Psi(\hat{x}_k - x^\star_{\mathrm{s},k}, u_{k-1} - u^\star_{\mathrm{s},k}) \\
&\overset{(9.33)}{=} -\ell(\hat{x}_k - x^\star_{\mathrm{s},k}, u_{k-1} - u^\star_{\mathrm{s},k}, \Delta u^\star_{0|k}) \\
&+ \Psi(f(\hat{x}_k, u_k) + \delta x_{\mathrm{d},k} - x^\star_{\mathrm{s},k}, u_k - u^\star_{\mathrm{s},k}) - \Psi(\hat{x}_k - x^\star_{\mathrm{s},k}, u_{k-1} - u^\star_{\mathrm{s},k}) \\
&+ \Psi(f(\hat{x}_k, u_k) - x^\star_{\mathrm{s},k}, u_k - u^\star_{\mathrm{s},k}) - \Psi(f(\hat{x}_k, u_k) - x^\star_{\mathrm{s},k}, u_k - u^\star_{\mathrm{s},k}) \\
&\overset{(9.11\mathrm{b})}{\leq} -\varepsilon_0 \mu(\|\hat{\chi}_k - \chi^\star_{\mathrm{s},k}\|_2) + \Psi(f(\hat{x}_k, u_k) + \delta x_{\mathrm{d},k} - x^\star_{\mathrm{s},k}, u_k - u^\star_{\mathrm{s},k}) \\
&- \Psi(f(\hat{x}_k, u_k) - x^\star_{\mathrm{s},k}, u_k - u^\star_{\mathrm{s},k}) \\
&\overset{(9.21),\ \mathrm{Ass.9.6}}{\leq} -\upsilon(\|\hat{\chi}_k - \chi^\diamond_{\mathrm{s},k}\|_2) + L_\Psi \|\delta x_{\mathrm{d},k}\|_2
\end{aligned} \tag{9.39}$$

with a $\mathcal{K}_\infty$-function υ. Furthermore

$$\begin{aligned}
\upsilon(0.5\|\hat{\chi}_k - \chi^\diamond_{\mathrm{s},\infty}\|_2) &\leq \upsilon(0.5\|\hat{\chi}_k - \chi^\diamond_{\mathrm{s},k}\|_2 + 0.5\|\chi^\diamond_{\mathrm{s},k} - \chi^\diamond_{\mathrm{s},\infty}\|_2) \\
&\leq \upsilon(\|\hat{\chi}_k - \chi^\diamond_{\mathrm{s},k}\|_2) + \upsilon(\|\chi^\diamond_{\mathrm{s},k} - \chi^\diamond_{\mathrm{s},\infty}\|_2).
\end{aligned}$$

Then there exists a $\mathcal{K}_\infty$-function Υ

$$\begin{aligned}
-\upsilon(\|\hat{\chi}_k - \chi^\diamond_{\mathrm{s},k}\|_2) &\leq -\upsilon(0.5\|\hat{\chi}_k - \chi^\diamond_{\mathrm{s},\infty}\|_2) + \upsilon(\|\chi^\diamond_{\mathrm{s},k} - \chi^\diamond_{\mathrm{s},\infty}\|_2) \\
&\leq -\Upsilon(\|\hat{\chi}_k - \chi^\diamond_{\mathrm{s},\infty}\|_2) + \upsilon(\|\chi^\diamond_{\mathrm{s},k} - \chi^\diamond_{\mathrm{s},\infty}\|_2).
\end{aligned} \tag{9.40}$$

Combining (9.34), (9.35), (9.36), (9.37), (9.38), (9.39), (9.40), we have that

$$\begin{aligned}
W_{k+1} - W_k \leq{}& \gamma_1(\|\delta x_{\mathrm{d},k}\|_2) + \gamma_2(\|\delta x_{\mathrm{d},k}\|_2) + \gamma_3(\|\delta x_{\mathrm{d},k}\|_2) + L_\Psi \|\delta x_{\mathrm{d},k}\|_2 \\
&+ \upsilon(\|\chi^\diamond_{\mathrm{s},k} - \chi^\diamond_{\mathrm{s},\infty}\|_2) + 2L_{V_\mathrm{O}} \|y_{\mathrm{t},k+1} - y_{\mathrm{t},\infty}\|_2 - \Upsilon(\|\hat{\chi}_k - \chi^\diamond_{\mathrm{s},\infty}\|_2).
\end{aligned}$$

Then, there exists a $\mathcal{K}$-function γ_4 such that

$$\begin{aligned}
W_{k+1} - W_k \leq{}& -\Upsilon(\|\hat{\chi}_k - \chi^\diamond_{\mathrm{s},\infty}\|_2) + \gamma_4(\|\delta x_{\mathrm{d},k}\|_2) \\
&+ \upsilon(\|\chi^\diamond_{\mathrm{s},k} - \chi^\diamond_{\mathrm{s},\infty}\|_2) + 2L_{V_\mathrm{O}} \|y_{\mathrm{t},k+1} - y_{\mathrm{t},\infty}\|_2.
\end{aligned}$$

Due to Assumption 9.3, there exists a $\mathcal{K}$-function γ such that

$$\begin{aligned}
W_{k+1} - W_k &\leq -\Upsilon(\|\hat{\chi}_k - \chi^\diamond_{\mathrm{s},\infty}\|_2) + \gamma(\|e_{\mathrm{d},k}\|_2) \\
&\quad + \upsilon(\|\chi^\diamond_{\mathrm{s},k} - \chi^\diamond_{\mathrm{s},\infty}\|_2) + 2L_{V_\mathrm{O}} \|y_{\mathrm{t},k+1} - y_{\mathrm{t},\infty}\|_2 \\
&= -\Upsilon(\|\hat{\chi}_k - \chi^\diamond_{\mathrm{s},\infty}\|_2) + \gamma(\|e_{\mathrm{d},k}\|_2) + \rho_{2,k}
\end{aligned}$$

with

$$\rho_{2,k} := \upsilon(\|\chi^\diamond_{\mathrm{s},k} - \chi^\diamond_{\mathrm{s},\infty}\|_2) + 2L_{V_\mathrm{O}} \|y_{\mathrm{t},k+1} - y_{\mathrm{t},\infty}\|_2. \tag{9.41}$$

Moreover, using Lipschitz continuity of the function g, there exists a $\mathcal{K}_\infty$-function $\tilde{\upsilon}$ such that

$$\rho_{2,k} \leq \tilde{\upsilon}(\|y^\diamond_{\mathrm{s},k} - y^\diamond_{\mathrm{s},\infty}\|_2) + 2L_{V_\mathrm{O}}\|y^0_{k+1} - y^0_\infty\|_2 + 2L_{V_\mathrm{O}}\|\hat{d}_\infty - \hat{d}_{k+1}\|_2.$$

Using (9.30) again and applying the weak triangle inequality, there exists a $\mathcal{K}$-functions $\tilde{\omega}_2$

$$\rho_{2,k} \leq \overline{\rho}_2 = \tilde{\omega}_2(\mathcal{S}(\mathcal{Y}^0)) + \tilde{\omega}_2(\mathcal{S}(\hat{\mathcal{D}})). \tag{9.42}$$

Since all the sets involved in the definition of $\overline{\rho}_2$ are bounded, it holds $\overline{\rho}_2 < \infty$. To conclude

$$W_{k+1} - W_k \leq -\Upsilon(\|\hat{\chi}_k - \chi^\diamond_{\mathrm{s},\infty}\|_2) + \gamma(\|e_{\mathrm{d},k}\|_2) + \overline{\rho}_2. \tag{9.43}$$

In view of (9.27), (9.32) and (9.43), it is possible to conclude that W_k is an ISpS Lyapunov function for the closed-loop system Σ_n. The ISpS property of the overall closed-loop system Σ_C with respect to the disturbance w follows from Assumption 9.4 and Lemma 9.5.

Remark 9.5. *Based on the ISpS-Lyapunov function constants, $\overline{\rho}_1$ and $\overline{\rho}_2$, it is possible to provide (a conservative) estimate of the ISpS constant φ, and characterize the transient behavior of the closed-loop system. Note that $\overline{\rho}_1$ and $\overline{\rho}_2$ depend only on the size of sets $\mathcal{Y}^0$ and $\hat{\mathcal{D}}$. Therefore, the transient behavior of the control loop can be improved by being more restrictive in the choice of available setpoints (thus reducing $\mathcal{S}(\mathcal{Y}^0)$), and, based on Assumption 9.4, by improving the observer initialization (thus reducing $\mathcal{S}(\hat{\mathcal{D}})$). In fact, according to Assumption 9.4, $\mathcal{S}(\hat{\mathcal{D}})$ decreases as $\mathcal{S}(\mathcal{W})$ decreases. Also note that, if the control scheme is used for disturbance rejection only, then $\mathcal{Y}^0 = \{y^0_\infty\}$, and $\mathcal{S}(\mathcal{Y}^0) = 0$. Additionally, in case of measurable disturbance d, $\hat{d}_k = d_k$ and $\mathcal{S}(\hat{\mathcal{D}}) = \mathcal{S}(\mathcal{D})$. Finally, as it will be detailed in the following Subsection, the ISpS-Lyapunov function can be used to prove asymptotic convergence in case of asymptotically constant setpoint y^0 and output disturbance d.*

Asymptotic Convergence

To prove asymptotic convergence, consider the term $\rho_{1,k}$ appearing in the upper bound for W, as defined in (9.29). Then, in view of Assumption 9.9, for $k \to \infty$, $y_{\mathrm{t},k} \to y_{\mathrm{t},\infty}$, $y^\diamond_{\mathrm{s},k} \to y^\diamond_{\mathrm{s},\infty}$ and therefore $x^\diamond_{\mathrm{s},k} \to x^\diamond_{\mathrm{s},\infty}$ and $u^\diamond_{\mathrm{s},k} \to u^\diamond_{\mathrm{s},\infty}$. Therefore $\rho_{1,k} \to 0$ for $k \to \infty$, and

$$W_k \leq \beta_W(\|\hat{\chi}_k - \chi^\diamond_{\mathrm{s},\infty}\|_2). \tag{9.44}$$

Similarly, consider the term $\rho_{2,k}$ appearing in the decrease of W, as defined in (9.41). Then, for $k \to \infty$, $\delta x_{\mathrm{d},k} \to 0$ in view of Assumptions 9.3 and 9.4, and both $y_{\mathrm{t},k}$ and $y_{\mathrm{t},k+1} \to y_{\mathrm{t},\infty}$. Moreover, in view of Assumption 9.9, for

$k \to \infty$, $y^\diamond_{\mathrm{s},k} \to y^\diamond_{\mathrm{s},\infty}$ and therefore $x^\diamond_{\mathrm{s},k} \to x^\diamond_{\mathrm{s},\infty}$ and $u^\diamond_{\mathrm{s},k} \to u^\diamond_{\mathrm{s},\infty}$. Therefore $\rho_{2,k} \to 0$ for $k \to \infty$, and

$$W_{k+1} - W_k \leq -\Upsilon(\|\hat{\chi}_k - \chi^\diamond_{\mathrm{s},\infty}\|_2). \tag{9.45}$$

Thus, asymptotic converge follows from (9.44) and (9.45), and from Assumption 9.4. In fact, for $k \to \infty$, Assumption 9.4 and $w_k \to 0$ guarantee that $\hat{x}_k \to x_k$ and $\hat{d}_k \to d_k$, while (9.44) and (9.45) guarantee that $\hat{\chi}_k \to \chi^\diamond_{\mathrm{s},\infty}$. Therefore, $x_k \to x^\diamond_{\mathrm{s},\infty}$, $u_k \to u^\diamond_{\mathrm{s},\infty}$ and $y_k \to y^\diamond_{\mathrm{s},\infty}$. If $y_{\mathrm{t},\infty} \in \mathcal{Y}_\mathrm{t}$, then $y^\diamond_{\mathrm{s},\infty} = y_{\mathrm{t},\infty}$, which implies $y_k \to y_{\mathrm{t},\infty}$. Since $y_k = y_{\mathrm{d},k} - d_k$ and $y_{\mathrm{t},k} = y^0_k - \hat{d}_k$, and recalling that $d_k \to d_\infty$ for $k \to \infty$, it can be concluded that $y_{\mathrm{d},k} \to y^0_\infty$. On the contrary, if $y_{\mathrm{t},\infty} \notin \mathcal{Y}_\mathrm{t}$, using again $y_k = y_{\mathrm{d},k} - d_k$, it holds $y_{\mathrm{d},k} \to y^\diamond_{\mathrm{s},\infty} + d_\infty$. □

9.8.3 Proof of Lemma 9.2

The existence of a suitable upper bound follows from (9.14) and $\|x - x_\mathrm{s}\| \leq \|\chi - \chi_\mathrm{s}\|$:

$$a_\ell V(x - x_\mathrm{s}) \overset{(9.14)}{\leq} a_\ell c \|x - x_\mathrm{s}\|_2^\xi \leq a_\ell c \|\chi - \chi_\mathrm{s}\|_2^\xi.$$

To prove the decrease property, start by upper bounding the decrease of the δISS-Lyapunov function V

$$\begin{aligned}
&a_\ell V(x_{k+1} - x_\mathrm{s}) - a_\ell V(x_k - x_\mathrm{s}) \\
&\overset{(9.3\mathrm{b})}{\leq} -a_\ell \alpha_3(\|x_k - x_\mathrm{s}\|_2) + a_\ell \gamma_1(\|u_k - u_\mathrm{s}\|_2) \\
&\overset{(9.7\mathrm{b})}{=} -a_\ell \alpha_3(\|x_k - x_\mathrm{s}\|_2) + a_\ell \gamma_1(\|u_{k-1} + \Delta u_k - u_\mathrm{s}\|_2) \\
&\leq -a_\ell \alpha_3(\|x_k - x_\mathrm{s}\|_2) + a_\ell \gamma_1(2\|u_{k-1} - u_\mathrm{s}\|_2) + a_\ell \gamma_1(2\|\Delta u_k\|_2).
\end{aligned}$$

Then, by adding and subtracting $\varepsilon_\ell \gamma_1(2\|u_{k-1} - u_\mathrm{s}\|_2)$, and using Assumption 9.11, we have that

$$\begin{aligned}
&a_\ell V(x_{k+1} - x_\mathrm{s}) - a_\ell V(x_k - x_\mathrm{s}) \\
&\leq -a_\ell \alpha_3(\|x_k - x_\mathrm{s}\|_2) - \varepsilon_\ell \gamma_1(2\|u_{k-1} - u_\mathrm{s}\|_2) \\
&+ (a_\ell + \varepsilon_\ell)\gamma_1(2\|u_{k-1} - u_\mathrm{s}\|_2) + a_\ell \gamma_1(2\|\Delta u_k\|_2) \\
&\overset{(9.15)}{\leq} -a_\ell \alpha_3(\|x_k - x_\mathrm{s}\|_2) - \varepsilon_\ell \gamma_1(2\|u_{k-1} - u_\mathrm{s}\|_2) \\
&+ \ell(x_k - x_\mathrm{s}, u_{k-1} - u_\mathrm{s}, \Delta u_k).
\end{aligned}$$

Therefore, there exists a constant ε_0 and a $\mathcal{K}_\infty$-function μ such that

$$\begin{aligned}
&a_\ell V(x_{k+1} - x_\mathrm{s}) - a_\ell V(x_k - x_\mathrm{s}) \\
&\leq -\varepsilon_0 \mu(\|\chi_k - \chi_\mathrm{s}\|_2) + \ell(x_k - x_\mathrm{s}, u_{k-1} - u_\mathrm{s}, \Delta u_k)
\end{aligned}$$

for any $x_k \in \mathbb{R}^n$, any $u_{k-1} \in \mathcal{U}$, any $\Delta u_k \in \Delta\mathcal{U}$ and any $(x_\mathrm{s}, u_\mathrm{s}) \in \mathcal{Z}_\mathrm{s}$. □

Part III

Data-driven MPC in the Koopman operator framework

Chapter 10

Introduction to the Koopman operator

This part of the thesis is devoted to the design of MPC algorithms using Koopman operator-based surrogate models. The Koopman operator was introduced in the 1930s by Koopman [136], and provides a powerful theoretical framework for data-driven analysis, prediction, and control of dynamical systems. In the last years, approaches related to Koopman's idea have received significant interest [36], and many Koopman-based data-driven methods for estimation and control of dynamical systems have been developed [181], see also the recent review [226]. One of the key features of Koopman-based surrogate models is the availability of bounds on the model estimation error. This property can be exploited to provide guarantees on the behavior of the MPC algorithm when applied to the real plant.

In this chapter, we introduce the Koopman operator and different data-driven methods for its approximation. Moreover, in Section 10.5, we present a brief review on the use of Koopman-based models in MPC.

10.1 Definition of the Koopman operator

The Koopman operator is a linear but infinite dimensional operator that encodes the behavior of the associated nonlinear autonomous dynamical system [171, 205]. In this thesis, we define the Koopman operator for discrete-time systems, even if the Koopman operator was first developed in the continuous-time framework. The main reason for this choice is that we want to exploit the Koopman operator theory to derive data-driven models of dynamical systems, and the system data are inherently in discrete-time. Moreover, discrete-time is the typical framework for MPC, that is the final goal for the use of these models in the thesis.

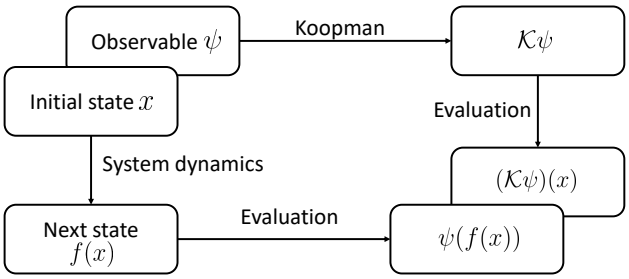

Figure 10.1: Schematic representation of the definition of the Koopman operator (10.2).

Consider an autonomous discrete-time system given by

$$x_{k+1} = f(x_k) \tag{10.1}$$

with a map $f : \Omega \to \mathbb{R}^n$, with $\Omega \subset \mathbb{R}^n$ a compact and non-empty set. For sake of simplicity, in this thesis we assume the set Ω to be positive invariant for the system (10.1), and we refer to [134] for the necessary technical modification needed to manage the case in which this property is not valid.

The Koopman operator $\mathcal{K} : \mathcal{C}_b(f(\Omega)) \to \mathcal{C}_b(\Omega)$ associated to system (10.1) is defined considering functions $\psi : \mathbb{R}^n \to \mathbb{R}$, called *observables*, by the identity

$$(\mathcal{K}\psi)(x) = \psi(f(x)) \qquad \forall x \in \Omega,\ \psi \in \mathcal{C}_b(f(\Omega)). \tag{10.2}$$

The idea behind (10.2) is illustrated in Figure 10.1. The Koopman operator propagates the observable function ψ, obtaining another function $\mathcal{K}\psi$. Evaluating this new function in the original state x is equivalent to compute the next state of the system, that is $f(x)$, and evaluating the observable in the next state. This means that the Koopman operator allows to compute the value of the observable functions in the next system state without using the system dynamics f.

10.2 Approximation of the Koopman operator for autonomous systems

The Koopman operator provides a nice theoretical framework for the derivation of alternative descriptions of dynamical systems. What is particularly of interest is the possibility of obtaining approximations of the Koopman operator for unknown systems using data [18]. The most popular method to do so is extended dynamic mode decomposition (EDMD), which is described in the next section. EDMD has been successfully applied in many fields, including climate prediction [9], molecular dynamics [247], power systems [251], turbulent flows [80], neuroscience [35], and deep learning [65].

10.2.1 Extended Dynamic Mode Decomposition

Extended Dynamic Mode Decomposition (EDMD) is a data-driven method to obtain a finite-dimensional approximation of the Koopman operator [242]. Consider a finite dictionary of observable functions $\{\psi_j \in \mathcal{C}_b(\mathbb{R}^n) : j \in [1 : M]\}$, and let $\mathbb{V} := \text{span}(\{\psi_j\}_{j\in[1:M]})$ be the M-dimensional space spanned by the chosen observables. With EDMD we obtain an estimation of $P_{\mathbb{V}}\mathcal{K}|_{\mathbb{V}}$, that is the compression of the Koopman operator restricted to the finite dimensional space $\mathbb{V}$. In particular, $\mathcal{K}|_{\mathbb{V}}$ denotes the restriction of the Koopman operator to the functions in $\mathbb{V}$, i.e. it represents how the Koopman operator acts on the functions in $\mathbb{V}$, while $P_{\mathbb{V}}$ denotes the projection onto $\mathbb{V}$. The projection operation is needed because it is not guaranteed that the result of the application of the Koopman operator to functions in a given subspace remains in the same subspace. In view of the linearity of the Koopman operator, the estimation of $P_{\mathbb{V}}\mathcal{K}|_{\mathbb{V}}$ is a matrix $\widehat{K} \in \mathbb{R}^{M\times M}$.

In EDMD, $\widehat{K}$ is obtain as the solution of a linear regression problem. We assume to have a dataset $\mathcal{D} := \{(x_i, x_i^+)\}_{i=1}^d$ containing couples of state and subsequent state, where the subscript i is the index of the data item and $x_i^+ = f(x_i)$ for all $i \in [1 : d]$. Note that it is not required that the data come from the same trajectory. Let

$$\Psi = (\psi_1, \dots, \psi_M)^\top \tag{10.3}$$

be the stacked vector of observables, with $\Psi : \mathbb{R}^n \to \mathbb{R}^M$. Then, we can create the following matrices of lifted data

$$\Psi_X := [\Psi(x_1) \ \dots \ \Psi(x_d)], \quad \Psi_Y := [\Psi(x_1^+) \ \dots \ \Psi(x_d^+)]. \tag{10.4}$$

The approximation $\widehat{K}$ of $P_{\mathbb{V}}\mathcal{K}|_{\mathbb{V}}$ is then given by the solution of the linear regression problem

$$\widehat{K} = \underset{K\in\mathbb{R}^{M\times M}}{\arg\min} \|K\Psi_X - \Psi_Y\|_F,$$

which can be explicitly computed by

$$\widehat{K} = (\Psi_X\Psi_X^\top)^{-1}\Psi_X\Psi_Y^\top.$$

It is now possible to write the data-driven model, which can be given either in the lifted space, i.e. the space of observable, or in the original state space.

The model in the lifted space is given by

$$z_0 = \Psi(x_0) \tag{10.5a}$$

$$z_{k+1} = \widehat{K}z_k \tag{10.5b}$$

and describes the evolution of the vector of observable functions $z \in \mathbb{R}^M$. To obtain the value of the original system state x from the value of the lifted state z we need the projection operation

$$x_k = P_\Omega z_k.$$

There are different possible methods to perform the projection. In the simplest case the coordinate functions are included in the observables, i.e. we have that $\psi_i(x) = x_{(i)} = e_i^\top x$ for $i \in [1 : n]$, where e_i denotes the i-th unit vector of $\mathbb{R}^n$. Then, the projection simply consists in taking the first n components of the lifted state z, i.e.

$$x_k = \begin{bmatrix} \mathbf{I}_n & \mathbf{0}_{n\times(M-n)} \end{bmatrix} z_k.$$

When the coordinate functions are not included in the observables, it is possible to identify a linear projection matrix $C \in \mathbb{R}^{n\times M}$ such that $x = Cz$ from data. In order to do so, consider the data matrix

$$X := [x_1 \ \dots \ x_d]. \tag{10.6}$$

Then, C is the solution of the linear regression problem

$$C = \underset{C\in\mathbb{R}^{n\times M}}{\arg\min} \|C\Psi_X - X\|_F, \tag{10.7}$$

whose solution can be obtained in closed-form. More advanced projection methods have been developed in [235], but are outside of the scope of the thesis.

With the model in the lifted space we can perform multi-step predictions using the linear model (10.5b), where the only step that involves a nonlinear function is the lifting of the initial state (10.5a). However, this method often has poor performances for predictions over a long horizons. This is due to the fact that it is not guaranteed that the predicted next lifted state z^+ can be written as $\Psi(\tilde{x}^+)$ for some $\tilde{x}^+ \in \mathbb{R}^n$. This causes an error that accumulates in multi-step predictions, causing a degradation of performances. This issue can be solved by writing the model in the original state space. To do so, a reprojection operation is performed at each prediction step, obtaining a model

$$x_{k+1} = P_\Omega \widehat{K} \Psi(x_k).$$

This model is nonlinear, since the state is lifted at each step, but it provides better performances for long prediction horizons, as pointed out in [168] and [180, Remark 20].

In [138], it is shown that EDMD converges to the Koopman operator in the infinite data limit and for an infinite number of observables. However, only a finite number of data are available for identification, and a finite number of observables is used to derive the EDMD model. Hence, it is interesting and useful to derive finite-data error bounds for EDMD models. The first results about finite data error bounds can be found in [170, 255]. Then, the probabilistic error bounds were further extended to stochastic systems using both i.i.d. and ergodic sampling in [180], also for systems with inputs.

10.2.2 Choice of the observables

When deriving an EDMD-based model, the choice of the observables dictionary is critical for the performances. Hence, many observable selection methods have been developed in the literature [168, 18].

First, it is a good practice to include the constant observable in the dictionary. Typically, the index 0 is assigned to the constant observable, i.e. $\psi_0(x) \equiv 1$. Then, the simplest method to design the other observables is to use functions belonging to standard classes, such as monomials or radial basis functions (RBF). This choice is straightforward, but it does not always provide the best prediction accuracy.

When there is some information about physics of the system, an effective choice is the use of physics informed observables. In this category we include, e.g., observables given by functions that are likely to appear in the state equations and observables that encode information about the symmetries of the system. An example is the use of trigonometric lifting functions for state variables related to angles. The effectiveness of physics informed observables has been shown in [24] for the derivation of surrogate models of non-holonomic robots, where the model obtained with a small dictionary of physics informed observables achieves a higher prediction accuracy than the model based on a large dictionary of monomials.

A different successful approach consists in the use of data-driven methods. A widely spread technique is the use of NNs [252] and deep learning methods. In this category we find, e.g., the use of autoencoder structures to learn simultaneously the lifting and projecting function and the matrix approximation of the Koopman operator [158, 9]. In [45], the authors present an hybrid method that combines the use of NNs for learning lifting functions and a physics-informed loss to ensure consistency in the projection step. Another data-driven method for the choice of observables is use of kernel functions, that will be described in details in Section 10.4.

10.3 Koopman operator for systems with input

While the theoretical framework of the Koopman operator for autonomous systems is well understood, its extension to systems with input is still object of research [193, 181]. In particular, various approaches have been proposed to generalize EDMD to actuated systems, which provide models with different degrees of complexity and approximation capabilities.

In the next sections, we describe different methods to obtain Koopman-based surrogate models for the discrete-time system

$$x_{k+1} = f(x_k, u_k) \tag{10.8}$$

with state $x \in \Omega \subseteq \mathbb{R}^n$ and input $u \in \mathcal{U} \subseteq \mathbb{R}^m$. System (10.8) can be inherently defined in discrete-time, or it can be derived from the discretization of

a continuous-time system fed with a piecewise constant input.

10.3.1 Extended Dynamic Mode Decomposition with control

Extended Dynamic Mode Decomposition with control (EDMDc) is the simplest method to generalize EDMD to actuated systems, and it provides a linear surrogate model in the lifted space. Dynamic mode decomposition with control was first introduced in [192], and was connected to the Koopman framework in [193].

In EDMDc, the approximated Koopman model is given by

$$\begin{aligned} z_0 &= \Psi(x_0) \\ z_{k+1} &= Az_k + Bu_k \\ x_k &= Cx_k \end{aligned}$$

where $A \in \mathbb{R}^{M\times M}$, $B \in \mathbb{R}^{M\times m}$ and $C \in \mathbb{R}^{n\times M}$. Similarly to the matrix $\widehat{K}$ in EDMD for autonomous systems, the model matrices A, B, C can be identified from data by means of a linear regression problem. In this case, the dataset is given by $\mathcal{D} := \{(x_i, u_i, x_i^+)\}_{i=1}^d$, with $x_i^+ = f(x_i, u_i)$. Defining

$$U := [u_1 \ \dots \ u_d],$$

and Ψ_X and Ψ_Y as in (10.4), matrices A, B are obtained by solving

$$(A, B) = \arg\min_{A,B} \|\Psi_Y - A\Psi_X - BU\|_F,$$

while C is obtained as in the autonomous case by solving (10.7).

Even if the basic formulation of EDMDc uses state data, this method can also be implemented when measurement of the system state are not available. In this case it is possible to use sequences of past input and output values in place of the state, see, e.g., [137, Section 7.1] and [116].

EDMDc is simple to implement and the linearity of the model is attractive from a computational point of view. However, in [108] it is shown that EDMDc may be insufficient to describe the overall system dynamics, even when the inputs enters linearly in the state dynamics. To improve the description capabilities of Koopman-based models it is possible to use more complex methods, such as bilinear EDMD [34].

10.3.2 Bilinear EDMD

Bilinear EDMD is a method for the extension of EDMD to control-affine systems that was firstly proposed in [243], and provides a model that is bilinear in the lifted space. Consider the discrete-time control-affine system

$$x_{k+1} = f(x_k, u_k) = g_0(x_k) + G(x_k)u_k \tag{10.9}$$

where $x \in \Omega \subset \mathbb{R}^n$ is the state, $u \in \mathcal{U} \subset \mathbb{R}^m$ is the input, and $G(x) = [g_1(x) \ \dots \ g_m(x)]^\top$.

Remark 10.1. *Continuous-time control-affine systems are a very wide class of systems, and control affinity is assumed by many nonlinear control techniques, such as feedback linearization and sliding mode control [125]. Consider a continuous-time control-affine system of the form*

$$\dot{x}(t) = \tilde{f}(x(t), u(t)) = \tilde{g}_0(x(t)) + \tilde{G}(x(t))u(t),$$

a sampling time $T_\mathrm{s} > 0$, and a piecewise constant input $u(t) \equiv u_k$ for $t \in [kT_\mathrm{s}, (k+1)T_\mathrm{s})$. Then, the corresponding discrete-time sampled-data system with zero-order hold is given by

$$x_{k+1} = x_k + \int_{kT_\mathrm{s}}^{(k+1)T_\mathrm{s}} \tilde{g}_0(x(\tau))\,\mathrm{d}\tau + \int_{kT_\mathrm{s}}^{(k+1)T_\mathrm{s}} \tilde{G}(x(\tau))u_k\,\mathrm{d}\tau$$

where $x_k := x(kT_\mathrm{s})$ and $x(\tau) = x(\tau; x_k, u_k)$. As pointed out, e.g., in [178] and [22, Remark 4.1], this discrete-time system is approximately control-affine, with an error term that scales with T_s^2.

Hereafter, we consider bilinear EDMD as proposed in [187]. This method exploits the property that the Koopman operator approximately preserves control affinity. In particular, system (10.9) can be seen as the linear combination of the autonomous systems $g_0, g_1, \dots, g_m$ weighted by the input components $u_{(i)}$. Hence, given a fixed control value $u \in \mathcal{U}$, an approximation of the Koopman operator $\widehat{K}_u \in \mathbb{R}^{M\times M}$ is given by a linear combination of matrices $\widehat{K}_i \in \mathbb{R}^{M\times M}$ for $i \in [0:m]$, where M denotes the number of observables. Let $u_0 = 0$ and consider the inputs $u_i \in \mathcal{U}$, $i \in [1:m]$ providing a base of the input space $\mathbb{R}^m$. Moreover, consider the coefficients λ_i solving the linear equations

$$\sum_{i=1}^{m} \lambda_i u_i = u.$$

If u_i are the unit vectors of $\mathbb{R}^m$, then $\lambda_i = u_{(i)}$. Then, $\widehat{K}_u$ is constructed by

$$\widehat{K}_u = \widehat{K}_0 + \sum_{i=1}^{m} \lambda_i \cdot \left(\widehat{K}_i - \widehat{K}_0\right). \tag{10.10}$$

The Koopman matrices $\widehat{K}_i$, $i \in [0:m]$, corresponding to the inputs u_i can be identified from data. To do so, we can consider $m+1$ distinct datasets $\mathcal{D}_i := \{(x_{ij}, x_{ij}^+)\}_{j=1}^{d_i}$ for $i = [0:m]$. The data in $\mathcal{D}_i$ are obtained applying the constant input u_i, i.e. $x_{ij}^+ = f(x_{ij}, u_i)$. Each matrix $\widehat{K}_i$ is obtained as in the autonomous system case using the data in $\mathcal{D}_i$.

Then, the model reads

$$\begin{aligned} z_0 &= \Psi(x_0) \\ z_{k+1} &= \widehat{K}_{u_k} z_k \\ x_k &= P_\Omega z_k, \end{aligned}$$

and is bilinear in the lifted space. It is also possible to consider a model in the original state space by adding a projection at each time step, obtaining

$$x_{k+1} = P_\Omega \widehat{K}_{u_k} \Psi(x_k).$$

If we consider a system with an equilibrium in the origin, i.e. with $f(0,0) = 0$, and a dictionary of observables $\Psi = (\psi_0, \psi_1, \dots, \psi_M)^\top$ with $\psi_0(x) \equiv 1$, it is possible to enforce a certain structure in the Koopman matrices to ensure that the equilibrium is preserved in the data-driven surrogate model. This is done in SafEDMD proposed in [228], where the Koopman matrices are structured as

$$\widehat{K}_0 = \begin{bmatrix} 1 & 0 \\ 0 & A \end{bmatrix}, \qquad \widehat{K}_i = \begin{bmatrix} 1 & 0 \\ b_i & B_i \end{bmatrix} \tag{10.11}$$

with $\widehat{K}_i \in \mathbb{R}^{(M+1)\times(M+1)}$ for all $i \in [0:m]$ and $A, B_i \in \mathbb{R}^{M\times M}$ and $b_i \in \mathbb{R}^M$.

The advantages in the use of bilinear EDMD in comparison to EDMDc are the better approximation capabilities [34], and the availability of finite data error bounds on the approximation error, that have been derived in [180, 207].

10.3.3 LPV formulation

In [108] it is shown that EDMDc and bilinear EDMD are insufficient to fully capture the dynamic of a general actuated nonlinear system

$$x_{k+1} = f(x_k, u_k).$$

Therefore, the authors propose a linear parameter-varying (LPV) approach, where the matrix B of the linear model in the lifted space depends on the state and input of the system. This approach is able to represent a wide class of nonlinear systems, but the surrogate model has a complex structure, that is less attractive when the model is used for control purposes.

10.4 Kernel EDMD

Kernel extended dynamic mode decomposition (kEDMD) is a technique for the approximation of the Koopman operator based on the use of kernel functions, that was proposed for the first time in [128, 129]. One of the

advantages of this method is that it does not require the selection of observable functions, since the dictionary consists of the canonical features of an a priori chosen kernel function centered at the data points. In particular, we follow the procedure proposed in [134], that allows to derive finite-data error bounds exploiting the properties of the reproducing kernel Hilbert space (RKHS) induced by the considered kernel functions.

Kernel EDMD has been recently extended to systems with input in [22], where finite-data error bounds are derived also for this more complex framework. The identification algorithm of kEDMD allows to use data samples with arbitrary input values. This is an advantage compared to bilinear EDMD for actuated systems, where the use of different datasets obtained with constant values of the input is required for the identification. An alternative data-driven kernel-based Koopman method for control-affine systems that shares the advantage of flexible state-control sampling was proposed in [19], using an additional kernel function to express the dependency on the control input. Therein, however, no error bounds were provided.

10.4.1 Reproducing kernel Hilbert spaces

A function $\mathsf{k} : \mathbb{R}^n \times \mathbb{R}^n \to \mathbb{R}$ is a symmetric and strictly positive definite kernel function if, for every set $X = \{x_1, \dots, x_p\} \subset \mathbb{R}^n$ of pairwise distinct elements, the *kernel matrix* $K_X := (\mathsf{k}(x_i, x_j))_{i,j=1}^p$ is positive definite. Then, for $z \in \mathbb{R}^n$, it is possible to define the *canonical features* Φ_z of k as

$$\Phi_z(x) := \mathsf{k}(z, x), \quad x \in \mathbb{R}^n. \tag{10.12}$$

By completion, the kernel k induces an Hilbert space $\mathbb{H}$ of functions with inner product $\langle \cdot, \cdot \rangle_{\mathbb{H}}$, see [239]. In addition, the elements $f \in \mathbb{H}$ fulfill the reproducing property, i.e.

$$f(x) = \langle f, \Phi_x \rangle \qquad \forall\, x \in \mathbb{R}^n,$$

showing that point evaluation is well defined in $\mathbb{H}$. $\mathbb{H}$ is called *reproducing kernel Hilbert space* (RKHS).

In the following, we use piecewise-polynomial and compactly-supported kernel functions based on the Wendland radial basis functions (RBF) $\Phi_{n,k}^{\mathrm{RBF}} : \mathbb{R}^n \to \mathbb{R}$ with smoothness degree $k \in \mathbb{N}$, where $\Phi_{n,k}^{\mathrm{RBF}}(x) := \phi_{n,k}(\|x\|_2)$. The RKHS induced by the Wendland kernels coincides with fractional Sobolev spaces with equivalent norms [239], a key property, which also holds for Matérn kernels; see [70]. The induced (Wendland) kernel is given by

$$\mathsf{k}(x, y) = \phi_{n,k}(\|x - y\|_2) \qquad \text{for } x, y \in \mathbb{R}^n,$$

where functions $\phi_{n,k}$ depend on the space dimension n and on the smoothness degree k, and can be found in [239, Table 9.1]. For $k = 1$, the Wendland

RBF is defined by

$$\phi_{n,1}(r) := \begin{cases} \frac{1}{20}(1-r)^4(4r+1) & r < 1 \\ 0 & \text{otherwise} \end{cases}$$

for $n \in \{2, 3\}$, and by

$$\phi_{n,1}(r) := \begin{cases} \frac{1}{30}(1-r)^5(5r+1) & r < 1 \\ 0 & \text{otherwise} \end{cases}$$

for $n \in \{4, 5\}$, and is such that $\phi_{n,1} \in \mathcal{C}^2([0, \infty), \mathbb{R})$.

10.4.2 Kernel EDMD for autonomous systems

Consider the autonomous discrete time system (10.1), and a set of $d \in \mathbb{N}$ pairwise distinct data points

$$X = \{x_1, \ldots, x_d\} \subset \Omega,$$

and assume that the images of the data points through the discrete time dynamics (10.1) are known, i.e. we have the set $\{f(x_1), \ldots, f(x_d)\}$. Then, using (10.12), it is possible to define the features as $\{\Phi_{x_1}, \ldots, \Phi_{x_d}\}$, and the d-dimensional subspace of features as $\mathbb{V} := \operatorname{span}\{\Phi_{x_1}, \ldots, \Phi_{x_d}\} \subset \mathbb{H}$. Moreover, we can define P_X as the orthogonal projection onto $\mathbb{V}$, i.e., for $f \in \mathbb{H}$, $P_X f$ solves the regression problem

$$\min_{g \in \mathbb{V}} \|g - f\|_{\mathbb{H}}^2.$$

By the reproducing property, $P_X f$ interpolates f at X. The objective of kernel EDMD is to use the data points in X and their images to obtain the matrix approximant $\widehat{K}$ of $P_X \mathcal{K}|_{\mathbb{V}}$. As derived in [134, Equation (3.7)], the solution of this problem is given by

$$\widehat{K} = K_X^{-1} K_{F(X)} K_X^{-1} \in \mathbb{R}^{d \times d}, \tag{10.13}$$

where $K_{F(X)} = (\mathsf{k}(x_i, F(x_j)))_{i,j=1}^d$ and K_X is the kernel matrix of the set X. Then, for an observable function $\psi \in \mathbb{H} \subset C_b(F(\Omega))$, the surrogate dynamics are given by

$$\psi(x^+) \approx \psi^+(x) = \sum_{i=1}^{d} (\widehat{K} \psi_X)_{(i)} \Phi_{x_i}(x), \tag{10.14}$$

where $\psi_X = (\psi(x_1), \ldots, \psi(x_d))^\top$, and ψ^+ is the propagation through the approximation of the Koopman operator of the observable ψ.

In [134, Theorem 5.2] it is shown that the quality of the kEDMD approximator of the Koopman operator depends on the fill distance of the dataset X, defined as

$$h_X := \sup_{x\in\Omega} \min_{x_i\in X} \|x - x_i\|_2.$$

In particular, the following uniform error bound holds.

Theorem 10.1 (Error bounds, [134])**.** *Let $\mathbb{H}$ be the RKHS on Ω generated by the Wendland kernels with smoothness degree $k \in \mathbb{N}$. Let the right-hand side $f \in \mathcal{C}_b^{\lceil \sigma_{n,k} \rceil}(\Omega; \mathbb{R}^n)$ of system (10.1), with $\sigma_{n,k} := \frac{n+1}{2} + k$. Then, there exist constants $C, h_0 > 0$ such that the bound on the full approximation error*

$$\|\mathcal{K} - \widehat{K}\|_{\mathbb{H}\to\mathcal{C}_b(\Omega,\mathbb{R}^n)} \leq C h_X^{k+1/2} \tag{10.15}$$

holds for all sets $X := \{x_i : i \in [1 : d]\} \subset \Omega$, $d \in \mathbb{N}$, of pairwise-distinct data points with fill distance h_X, $h_X \leq h_0$.

We note that, for a large number of data points in X, the computation of the approximation of the Koopman operator (10.13) can be numerically unstable due to bad conditioning of the kernel matrix K_X. To alleviate this, one may include regularization by replacing K_X^{-1} with $(K_X + \lambda I)^{-1}$ with regularization parameter $\lambda > 0$. Error bounds in the spirit of Theorem 10.1 for this regularized surrogate were proven in [22, Theorem 2.4].

10.4.3 Kernel EDMD for systems with input

In this section, we consider the extension of kEDMD for discrete-time control-affine systems in the form of (10.9), with Lipschitz continuous maps $g_0 : \Omega \to \mathbb{R}^n$ and $G : \Omega \to \mathbb{R}^{n\times m}$, as proposed in [22]. We denote the Lipschitz constants of g_0 and G respectively by L_{g_0} and L_G. For the relation to continuous-time systems, we refer the interested reader to [22, Rem. 4.2] and [227], where it is shown that the uniform and proportional error bounds presented below are preserved for fixed ε and sufficiently small time step $\Delta t > 0$ if only the continuous-time system is control affine. Moreover, incorporating minor modifications analogously to [228] leads to a bilinear data-driven surrogate model as shown in [227]. This method allows to use flexible data sampling, and is not restricted to the use of datasets obtained with constant values of the input as the bilinear EDMD method described in Section 10.3.2. In particular, we consider a dataset composed by data points in the form (x, u, x^+), with $x^+ = f(x, u)$. The key idea of the kEDMD identification algorithm is to use the procedure described in the previous section for autonomous systems to obtain data-driven approximations of the functions g_0 and G. However, differently from the autonomous system case, the data points do not directly contain the information about the functions $g_i(x)$, $i \in [0 : m]$. Hence, in [22], a two steps algorithm for

the kEDMD model identification is proposed. In Step 1, the available data points are used to reconstruct an approximation

$$H_i = [\tilde{g}_0(x_i) \mid \tilde{G}(x_i)] \in \mathbb{R}^{n\times(m+1)}$$

of the matrix $[g_0(x_i) \mid G(x_i)]$ in some virtual observation points (or cluster points) $x_i \in X$. This step is based on a clustering algorithm, where for each virtual observation point x_i we use d_i data points contained in $\mathcal{B}_{r_X}(x_i)$ to derive H_i. In the following, $r_X \geq 0$ is called *cluster radius*, and its value is related to the prediction accuracy of the surrogate model. We point out that the points x_i are called *virtual* because no sample is required in them. In Step 2, the interpolation coefficients are computed analogously to the autonomous case by using the approximation values H_i from Step 1.

The algorithm is based on the following data requirements assumption.

Assumption 10.1 (Data requirements)**.** *Let the set of virtual observation points*

$$X := \{x_1, \dots, x_d\} \subset \Omega$$

the cluster radius $r_X \geq 0$ and the bounded input set $\mathcal{U} \subset \mathbb{R}^m$ be given. Then, for each $i \in [1:d]$, assume to have $d_i \geq m+1$ data triplets $(x_{ij}, u_{ij}, x_{ij}^+)$, $j \in [1:d_i]$, with pairwise distinct u_{ij}, where $x_{ij}^+ = f(x_{ij}, u_{ij})$, $x_{ij} \in \mathcal{B}_{r_X}(x_i) \cap \Omega$, $u_{ij} \in \mathcal{U}$ and

$$\operatorname{rank}([u_{i1} \mid \dots \mid u_{id_i}]) = m. \tag{10.16}$$

The kEDMD identification procedure is reported in Algorithm 10.1.

If we choose the coordinate functions as observables, i.e. $\psi_i(x) = x^\top e_i$ for $i \in [1:n]$, we obtain a state space surrogate model in the form

$$x_{k+1} = f^\varepsilon(x_k, u_k) = g_0^\varepsilon(x_k) + G^\varepsilon(x_k)u_k. \tag{10.18}$$

The superscript ε refers to the error bounds, that are reported in the following theorem and depend on the fill distance of the virtual observation points h_X and on the cluster radius r_X.

Theorem 10.2 (Error bounds for kEDMD, Theorem 4.3 in [22])**.** *Assume that the data respects Assumption 10.1, and consider the kEDMD model* (10.18) *built by Algorithm 10.1. Then, there exist $C, h_0 > 0$ such that for any set $X \subset \Omega$ with $h_X < h_0$, the error between the real system f and the kEDMD model f^ε satisfies*

$$\|f(x,u) - f^\varepsilon(x,u)\|_\infty \leq CD(x)(1 + \|u\|_1) =: \varepsilon \tag{10.19}$$

for all $(x,u) \in \Omega \times \mathcal{U}$, where

$$D(x) := h_X^{k-1/2} \operatorname{dist}(x, X) \max_{p,q} \|H_{(pq)}\|_{\mathbb{H}}$$
$$+ \sqrt{2 \max_{i\in[1:d]} d_i} \left(\max_{v:\|v\|_\infty \leq 1} v^\top K_X^{-1} v \right)^{1/2} \max_{i\in[1:d]} \|U_i^\dagger\|_2 (L_{g_0} + L_G \overline{u}) \Phi_{n,k}^{1/2}(0) r_X$$

with $H := [g_0 \;\; G]$ and $\overline{u} := \max_{u\in\mathcal{U}} \|u\|_\infty$.

Algorithm 10.1 kEDMD for control-affine systems

Input: Virtual observation points X and data triplets $(x_{ij}, u_{ij}, x_{ij}^+)$ respecting Assumption 10.1.

Step 1 (Clustering):
For each $i \in [1:d]$:

- Set
$$U_i := \left[\begin{array}{c|c|c} 1 & \dots & 1 \\ u_{i1} & \dots & u_{id_i} \end{array}\right]$$
- Set
$$H_i := \arg\min_{H_i} \left\| [x_{i1}^+ \mid \dots \mid x_{id_i}^+] - H_i U_i \right\|_F.$$

Step 2 (Interpolation):
The propagation step of an observable ψ is

$$\psi(f(x,u)) \approx \psi^+(x) := \sum_{i=1}^{d} \Big[\big(\widehat{K}_0 + \sum_{j=1}^{m} u_{(j)} \widehat{K}_j\big) \psi_{\mathcal{X}} \Big]_{(i)} \Phi_{x_i}(x) \tag{10.17}$$

with $\widehat{K}_j = K_X^{-1} K_{\tilde{g}_j(X)} K_X^{-1}$, where K_X is the kernel matrix of the set X and

$$(K_{\tilde{g}_j(X)})_{(kl)} = \mathsf{k}(x_k, \tilde{g}_j(x_l)) = \mathsf{k}(x_k, (H_l)_{(*,j+1)})$$

for all $k, l \in [1:d]$ and $j \in [0:m]$.

10.5 Koopman operator for MPC

Koopman operator-based surrogate models have been successfully employed in MPC in a variety of different applications. Many works focus on the use of EDMDc-based surrogate models, that are computationally attractive for their linearity in the lifted space. In fact, if the cost is quadratic and the constraints are polytopic in the lifted space, the MPC optimization problem can be formulated as a quadratic program (QP) that can be solved in a more efficient way than the nonlinear program that is typically obtained from nonlinear MPC. One of the first papers to propose EDMDc-based MPC is [137], and the scheme was extended to robust linear tube-based MPC in [256]. In [116], recursive feasibility and ISS are proved for a linear MPC algorithm in the lifted space, based on a multi-step Koopman predictior that improves prediction accuracy compared with the standard single-step predictor.

The use of more complex classes of Koopman based-surrogate models in MPC is less computationally attractive, because it requires the solution of

a nonlinear optimization program. However, the better prediction accuracy make it a preferable choice in some application [34], and the availability of bounds of the modeling error provides an appealing theoretical framework to derive guarantees on the closed-loop stability. In [177], a bilinear continuous-time surrogate model is used in a Lyapunov-based predictive controller with guaranteed closed-loop stability. This work, however, does not consider the prediction error due to uncertainties. The model uncertainties are considered in [246] and [21], where the error bounds of the EDMD surrogate models are exploited to prove PAS of the closed-loop with MPC applied to the original system, respectively with and without terminal conditions.

To reduce the computational effort of MPC based on a bilinear EDMD model, some authors propose to approximate at each step the bilinear model in a linear one by fixing the value of the state in the bilinear term [34, 120]. This method allows to exploit the highest prediction accuracy of bilinear EDMD, while reducing the computational cost of the solution of the optimization problem to the solution of a QP.

EDMD-based MPC has been employed in a variety of applications, including soft actuators [236], control of vehicles [47], power grid transient stabilization [139], nonlinear chemical process systems [176], power systems [257], and control of non-holonomic robots [203].

Chapter 11

Offset-free MPC for EDMD models

EDMD models have been successfully applied in MPC in a variety of applications. Moreover, thanks to the availability of bounds on the approximation error, PAS of EDMD-based MPC with and without terminal conditions was proven respectively in [246] and [21]. In particular, it is shown that the system state converges asymptotically to a neighborhood of the origin, whose size depends on the quality of the model used in the predictions, and the closed-loop presents a non-zero asymptotic error. As already discussed in the thesis in Section 3.5 and Chapters 7 and 9, a possible remedy is offset-free MPC, which is able to guarantee zero steady-state error in presence of model-plant mismatch. In [222], linear offset-free MPC has been used in combination with EDMDc surrogate models, showing promising results. A similar method is employed in [42], where EDMDc-based offset-free MPC shows an improvement of performance in the control of a soft manipulator with respect to a standard EDMDc-based MPC.

In this chapter, we propose a nonlinear offset-free control algorithm for bilinear EDMD surrogates. Unlike the general case studied in offset-free MPC, we consider the state of the system to be measurable. Hence, an observer is designed to estimate the disturbance state only. Two different formulations of the MPC are proposed. In the simpler first case, the target equilibrium of the system under control is considered fully known. In the second case, only partial information about the desired set-point is available. Then, a reference calculator is included in the algorithm to compute the state and input references for the MPC based on the estimation of the disturbance state. The control algorithm is tested in two simulation examples. The first is the van-der-Pol oscillator, where the information about the equilibrium is known. The second is the four-tanks process, where only an approximated value of the equilibrium of the system is available.

The content of this chapter has been developed during the visiting period

at TU Ilmenau, and is published in:

- [208] **Schimperna, I.**, Bold, L. and Worthmann, K. (2025). *Offset-free Nonlinear MPC with Koopman-based Surrogate Models.* IFAC-PapersOnLine, 59(19), 466-471. Presented at the 13th IFAC Symposium on Nonlinear Control Systems.

11.1 Problem formulation

Consider a discrete-time control-affine system under control

$$x_{k+1} = f(x_k, u_k) = g_0(x_k) + G(x_k)u_k \tag{11.1}$$

with state $x \in \mathbb{R}^n$ and input $u \in \mathcal{U}$, where $\mathcal{U} \subset \mathbb{R}^m$ is a compact and convex set containing the origin in its interior. The dynamics of system (11.1) is assumed unknown, and a data-driven surrogate model is used for MPC design. In particular, the objective is to design an offset-free MPC algorithm based on an offline-learned data-driven surrogate model of the system (11.1), denoted by

$$x_{k+1} = \hat{f}(x_k, u_k),$$

obtained using bilinear EDMD. The surrogate model is obtained as described in Section 10.3.2, and is given by

$$x_{k+1} = P_\Omega \widehat{K}_{u_k} \Psi(x_k), \tag{11.2}$$

where $\widehat{K}_u$ is defined in (10.10). For sake of simplicity, we consider an observables dictionary $\Psi = (\psi_0 \ \psi_1 \ \dots \ \psi_M)^\top \in \mathbb{R}^{M+1}$ including the constant observable and the coordinate functions, so that $\psi_0(x) \equiv 1$ and $\psi_i(x) = x_{(i)}$ for $i \in [1 : n]$. In this way, the projection P_Ω reduces to a matrix multiplication, and the model becomes

$$x_{k+1} = \begin{bmatrix} \mathbf{0}_{n\times 1} & \mathbf{I}_n & \mathbf{0}_{n\times(M-n)} \end{bmatrix} \widehat{K}_{u_k} \Psi(x_k).$$

11.2 Offset-free MPC

In this section, we present the offset-free MPC algorithm. Therein, the model is augmented by a disturbance term, which is estimated online by an observer and used, together with the model, in the optimization step of the MPC scheme. A specific observer structure is proposed for EDMD surrogate models, where the state is measurable and only the estimation of the disturbance term is required. The offset-free MPC algorithm can handle both the following two distinct cases:

(ke) *Known Equilibrium*: full information about the system equilibrium is available.

(ue) *Unknown equilibrium*: only partial knowledge about the equilibrium is available.

In the following, we will first present the offset-free MPC algorithm for the known equilibrium case (ke), and then we will introduce the modifications that are needed to manage the case (ue).

11.2.1 Case of known system equilibrium

The objective of the MPC is to track without offset a constant reference, that is an equilibrium of the real system. In some cases the physics of the system allows us to know the full information about the equilibrium $(\bar{x}, \bar{u})$ of system (11.1), that we want to track. In the following, it is assumed that $\bar{u}$ is in the interior of $\mathcal{U}$. The control objective for the closed-loop system is

$$\lim_{k\to\infty} x_k = \bar{x}, \qquad \lim_{k\to\infty} u_k = \bar{u}.$$

In offset-free MPC, the model used in the optimal control problem is augmented with a term $\hat{d} \in \mathbb{R}^n$ to compensate for the presence of modeling errors. In particular, this term is added to the state equation of the model, and is estimated by an observer with the following equations

$$\begin{aligned} \tilde{x}_k &= \hat{f}(\hat{x}_{k-1}, u_{k-1}) + \hat{d}_{k-1}, \\ \hat{x}_k &= x_k, \\ \hat{d}_k &= \hat{d}_{k-1} + (\hat{x}_k - \tilde{x}_k). \end{aligned} \tag{11.3}$$

The observer includes a state $\hat{x} \in \mathbb{R}^n$ that is used to keep in memory the previous value of the state of the system, but is not used by the MPC, and a term $\tilde{x} \in \mathbb{R}^n$ that is the one-step prediction of model corrected by $\hat{d}$ starting from the previous value of the system state. The output of the observer is $\hat{d}$, that is used to update the MPC prediction model. If the system state is unmeasurable, a state and disturbance observer can be employed, as shown, e.g., in [173].

The MPC is designed based on the augmented model with stage cost function $\ell(x, u) : \mathbb{R}^n \times \mathbb{R}^m \to \mathbb{R}_{\geq 0}$. At time step k, the MPC algorithm solves the following finite horizon optimal control problem

$$\begin{aligned} \min_{\mathbf{u}} \ & \sum_{i=0}^{N-1} \ell(x_{i|k} - \bar{x}, u_{i|k} - \bar{u}) \\ \text{s.t. } & x_{0|k} = x_k \\ & x_{i+1|k} = \hat{f}(x_{i|k}, u_{i|k}) + \hat{d}_k \\ & u_{i|k} \in \mathcal{U} \qquad \text{for all } i \in [0 : N-1], \end{aligned} \tag{11.4}$$

given the measured initial value x_k, where $\mathbf{u} := \{u_{0|k}, \dots, u_{N-1|k}\}$. Note that the disturbance estimation from the observer is added to the state equations in the MPC optimal control problem (11.4), and it is kept constant along the horizon. The MPC control determines the control value u_k, that is given by

$$u_k = \mu^{\text{MPC}}(x_k, \hat{d}_k) = u^\star_{0|k},$$

where $u^\star_{0|k}$ is the first element of the optimal input sequence.

Remark 11.1. *Our MPC formulation does not consider a terminal cost or a terminal constraint. Hence, a sufficiently long prediction horizon should be used to guarantee recursive feasibility and stability of the MPC closed-loop, see Section 3.2.2.*

Remark 11.2. *In the description of offset-free MPC we have considered a system model in the form of* (11.2)*, where a projection operation is performed at each prediction step. The projection step improves the quality of the predictions, in particular with long prediction horizon, see, e.g., [168] and [180, Remark 20]. However, it is also possible to implement the offset-free MPC in the lifted space, without including a projection operation at each prediction step. In this case the disturbance state has the dimension of the lifted space, i.e.* $\hat{d} \in \mathbb{R}^{M+1}$*, and the prediction model used in the MPC algorithm has the form*

$$\begin{aligned} z_{0|k} &= \Psi(x_k), \\ z_{i+1|k} &= \widehat{K}_{u_{i|k}} z_{i|k} + \hat{d}_k, \quad i \in [0 : N-1]. \end{aligned}$$

The observer has the same structure of (11.3)*, but is designed in the lifted space.*

11.2.2 Case of unknown system equilibrium

In some systems only partial information about the equilibrium is available. An example is when we only know the values of a subset of the states at the equilibrium. The controlled output is y_{c} that is a function of the state

$$y_{\text{c}} = r(x)$$

and y^0 is the desired setpoint for y_{c}. The control objective for the closed-loop is to reach an equilibrium such that

$$\lim_{k\to\infty} y_{\text{c},k} = y^0.$$

To derive the full information about the equilibrium to be used in the MPC cost function, a reference calculator is introduced in the algorithm. The

reference calculator solves the following optimization problem

$$\begin{aligned} \min_{x,u} \quad & \ell_{\mathrm{r}}(x,u) && \text{(11.5a)} \\ \text{s.t.} \quad & x = \hat{f}(x,u) + \hat{d} && \text{(11.5b)} \\ & r(x) = y^0 && \text{(11.5c)} \\ & u \in \mathcal{U}, && \text{(11.5d)} \end{aligned}$$

where $\ell_{\mathrm{r}} : \mathbb{R}^n \times \mathbb{R}^m \to \mathbb{R}_{\geq 0}$ is a steady state cost function. It is assumed that (11.5) is feasible and that its (unique) solution is denoted by $(\bar{x}, \bar{u})$ and represents the reference to be used by the MPC. If (11.5b)-(11.5c) have a unique solution, then it is not needed to implement the reference calculation as an optimization problem, but it is sufficient to compute the unique solution of the system of equations. The MPC references are updated at every time step depending on the current value of $\hat{d}$. All the other parts of the algorithm are implemented as described in the previous subsection. The complete algorithm is summarized in Algorithm 11.1.

Algorithm 11.1 Offset-free MPC

Input: Horizon $N \in \mathbb{N}$, stage cost $\ell : \mathbb{R}^n \times \mathbb{R}^m \to \mathbb{R}_{\geq 0}$, data-driven model $\hat{f}$, input constraints $\mathcal{U}$, steady state cost function $\ell_{\mathrm{r}} : \mathbb{R}^n \times \mathbb{R}^m \to \mathbb{R}_{\geq 0}$, controlled output function r, controlled output set point y^0.

Initialization: Set $k = 0$ and $\hat{d}_0 = 0$.

(1) Measure current state x_k.

(2) Solve (11.5) to obtain the MPC reference $(\bar{x}, \bar{u})$.

(3) Solve the optimal control problem (11.4) to obtain the optimal control sequence $\mathbf{u}^\star = \{u^\star_{0|k}, \ldots, u^\star_{N-1|k}\}$.

(4) Set the feedback law $\mu^{\mathrm{MPC}}(x_k, \hat{d}_k) = u^\star_{0|k}$ and shift $k = k + 1$.

(5) Update the disturbance $\hat{d}_k$ with equation (11.3) and go to (1).

Now, we recall the theoretical results available in the literature for offset-free MPC, which also apply with EDMD-based surrogate models. First, define the modeling error as

$$w_k := f(x_k, u_k) - \hat{f}(x_k, u_k).$$

Then, the following theorem follows from Theorems 14 and 15 in [185].

Theorem 11.1. *Assume that w is bounded and asymptotically constant, i.e. there exists $\bar{w}$ such that*

$$\lim_{k \to \infty} w_k = \bar{w}.$$

Then $\lim_{k\to\infty} x_k - \tilde{x}_k = 0$ *and* $\lim_{k\to\infty} \hat{d}_k = \bar{w}$*, where* $\tilde{x}$ *is defined in* (11.3)*. Moreover, if the closed-loop system reaches an equilibrium with input* u_∞ *and state* x_∞*, then* $r(x_\infty) = y^0$*.*

Remark 11.3. *The theorem is formulated in considering the system equilibrium unknown. The case with the known system equilibrium can be seen as a particular case.*

Remark 11.4. *The error bounds of the EDMD model has been exploited in [21] to prove practical asymptotic stability of EDMD-based MPC. Practical asymptotic stability means that the tracking error reaches a neighborhood of the origin, but in general it does not go to zero in view of the presence of modeling errors. The proposed offset-free MPC algorithm overcomes this issue, allowing the system to asymptotically reach the reference with zero error.*

11.3 Illustrative examples

11.3.1 Van-der-Pol oscillator

As first example, we consider the nonlinear control-affine van-der-Pol oscillator

$$\begin{aligned} \dot{x}_1(t) &= x_2(t) \\ \dot{x}_2(t) &= \nu(1 - x_1(t))^2 x_2(t) - x_1(t) + u(t) \end{aligned} \tag{11.6}$$

with parameter $\nu = 0.1$. We consider the discretization of the ODE (11.6) obtained with the classic Runge-Kutta method of fourth order and step size $T_\mathrm{s} = 0.05$. This results in a discrete-time system

$$x_{k+1} = f(x_k, u_k) \tag{11.7}$$

which serves as ground truth. We point out that the system (11.7) is not control affine as assumed in (11.1), but the offset-free MPC is still able to exactly stabilize it, as shown in the following. For the approximation of the Koopman operator we use bilinear EDMD as described in Section 10.3.2. $d = 1000$ data points are sampled on the set $\Omega = [-2, 2]^2$ for each of the datasets $\mathcal{D}_i$, $i \in \{0, 1\}$ required for the derivation of the bilinear EDMD model. We have used a large number of data points to ensure a high prediction accuracy of the model, but similar results are obtained considering $d = 100$. The dictionary of observables is chosen to be $\{\psi(x) = x_1^p x_2^q : \ p, q \in [0:3] \text{ and } p + q \leq 3\}$, so it contains all monomial functions of the state variables up to degree 3. Other possible choices for the observable functions have been discussed in Section 10.2.2.

The objective of MPC is to reach the equilibrium point in the origin of the system, that is $(\bar{x}, \bar{u}) = (0, 0)$. In this example, the value of the

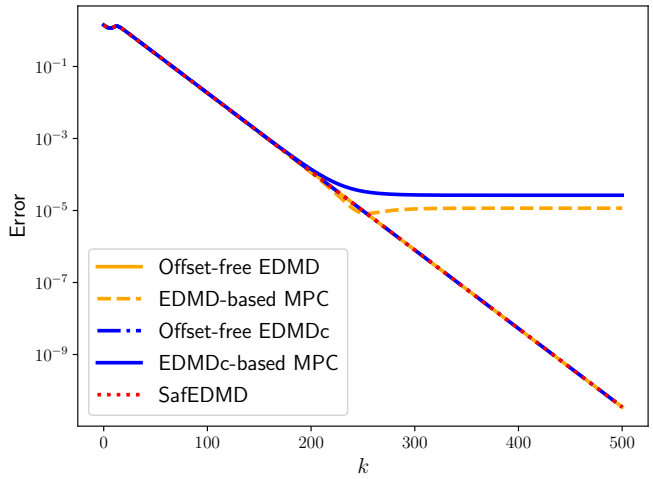

Figure 11.1: Norm $\|x_k\|_2$ of the closed-loop solution of the van-der-Pol oscillator (11.7) for bilinear EDMD-based and EDMDc-based MPC and offset-free MPC, and for SafEDMD-based MPC.

equilibrium can be easily deduced from the physical meaning of the state and input variables. The MPC stage cost function is chosen to be the quadratic function $\ell(x,u) = \|x\|_Q^2 + \|u\|_R^2$ with weighting matrices $Q = \mathbf{I}_2$ and $R = 10^{-2}$, subject to $-2 \leq u \leq 2$. For our simulations, the horizon $N = 50$ is set. In Figure 11.1 the errors in closed-loop simulations with initial state $x^0 = (1.0, 1.0)^\top$ are reported. The bilinear EDMD-based offset-free MPC and a standard bilinear EDMD-based MPC are compared to (offset-free) EDMDc-based MPC. In addition, we also report the results for a SafEDMD-based MPC algorithm. It can be seen that standard MPC can only provide practical asymptotic stability (see [21]), and the error stagnates at a value close to 10^{-5}, which also occurs in the EDMDc-based MPC case with a slightly larger offset. Instead, offset-free MPC, for both bilinear EDMD- and EDMDc-based algorithms, provides exponential convergence towards the origin, and the closed-loop behavior of the two algorithms is almost the same. The same precision is reached by using SafEDMD-based MPC without using the offset-free technique. This is due to the structure of the Koopman matrices in (10.11), which preserves the equilibrium of the system.

11.3.2 Four-tanks system

As a second example, we consider the four-tanks system [4] described in Section 6.4.1. We consider a sampling time of $T_s = 25s$. As in the previous example, the classic Runge-Kutta method of fourth order is used to numerically solve the integrals. For this system only an approximation $(\tilde{x}, \tilde{u})$ of the equilibrium is available, and is given by $\tilde{x} = (0.65, 0.66, 0.65, 0.66)^\top m$ and

$\tilde{u} = (1.63, 2.0)^\top m^3/h$. The objective of the control is to drive the controlled output $r(x) = (x_1, x_2)^\top$ to the value $y^0 = (\tilde{x}_1, \tilde{x}_2)$ for input constraints $\mathcal{U} = [0, 3.26]m^3/h \times [0, 4]m^3/h$. First, we carry out some simulations assuming that the full equilibrium information is available. These simulations are denoted with "known equilibrium" (ke) in the following. To do so, the real value of the system equilibrium $(\bar{x}, \bar{u})$ associated to y^0 is calculated using the system equations, which leads to $\bar{x} = (0.65, 0.66, 0.6417, 0.6882)^\top m$ and $\bar{u} = (1.666, 1.974)^\top m^3/h$. Note that this is in general not possible in a realistic setting, where only data from the system are available. For the derivation of the model, the states and inputs are shifted so that the equilibrium $(\bar{x}, \bar{u})$ corresponds to the origin, and the inputs are scaled using their maximum value, so that each component of the shifted and scaled input lies in the set $[-2, 2]$. As observables, we used monomials up to degree 2, resulting in $M = 14$ functions, and we considered $d = 1000$ data points for each approximation of the Koopman operator. The state data are randomly sampled with a uniform distribution in the set $\Omega = [0.2, 1.36]^2 \times [0.2, 1.30]^2$. Then some simulations are performed without using the information about the real value of the system equilibrium and are denoted by "unknown equilibrium" (ue). In this case, the model is obtained by shifting the states and inputs so that the approximated equilibrium $(\tilde{x}, \tilde{u})$ corresponds to the origin. In both the known equilibrium case and the unknown equilibrium case, the offset-free MPC is compared with a standard bilinear EDMD-based MPC. For all closed-loop simulations, the initial state of the system is $x^0 = (1.0, 1.0, 1.0, 1.0)^\top$. The cost of the MPC is $\ell(x, u) = \|x - \bar{x}\|_Q^2 + \|u - \bar{u}\|_R^2$, where $Q = \mathbf{I}_4$, $R = 10^{-4}\mathbf{I}_2$, and the prediction horizon is set to $N = 50$. In the offset-free MPC in the unknown equilibrium case, the reference calculator solves (11.5b)-(11.5c) using Newton's method at every time step to compute the reference $(\bar{x}, \bar{u})$ for the MPC. In the simulation with standard MPC and unknown equilibrium, the approximated equilibrium $(\tilde{x}, \tilde{u})$ is used in the MPC cost instead of $(\bar{x}, \bar{u})$.

Figure 11.2 shows the comparison of the tracking error of the controlled output of standard MPC and offset-free MPC based on bilinear EDMD and EDMDc for the scenario of a known equilibrium. As for the van-der-Pol oscillator, the errors of both MPC algorithms stagnate, whereas offset-free MPC leads to higher precision. In this example, the difference between bilinear EDMD and EDMDc becomes very obvious. Not only is the offset for EDMDc clearly higher when using MPC, but also the decay of the error is noticeably slower with offset-free MPC. In Figure 11.3, the norm of the tracking error for bilinear EDMD-based MPC and offset-free MPC is pictured for the two cases of a known and an unknown equilibrium. The error is larger when the real value of the equilibrium is unknown, and an approximation is used in the MPC implementation. Steady-state error is instead not present in the simulations with the offset-free MPC, both in the

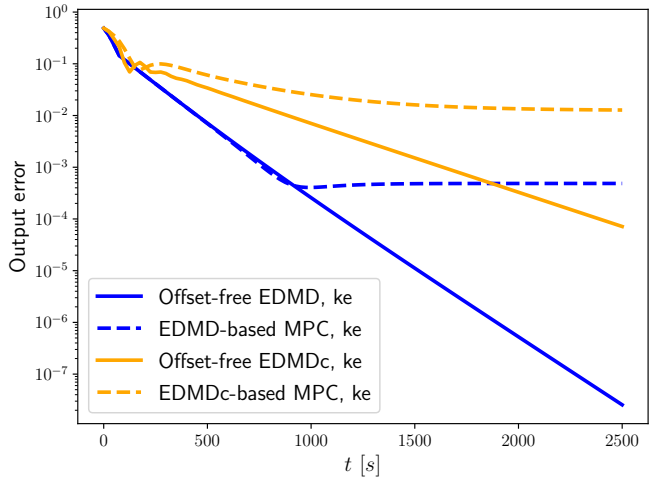

Figure 11.2: Output error $\|r(x) - y^0\|_2$ the four-tanks system for EDMD-based MPC and offset-free MPC comparing EDMDc and the bilinear approach for a known equilibrium.

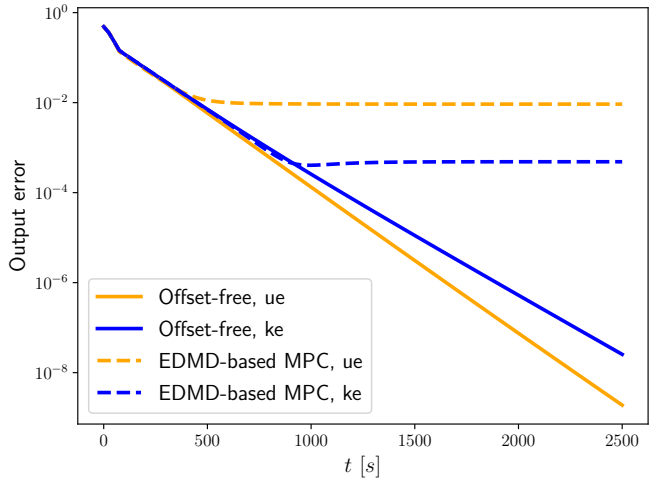

Figure 11.3: $\|r(x) - y^0\|_2$ of the four-tanks system for EDMD-based MPC and offset-free MPC, in the cases with unknown equilibrium (ue) and known equilibrium (ke).

known and unknown equilibrium cases.

11.4 Conclusions

In this chapter we proposed an offset-free algorithm for the control of systems modeled using EDMD. The observer is designed to estimate a disturbance term that is used to modify the prediction model of the MPC. To handle the case when the full information about the equilibrium is unknown, a reference calculator can be included in the closed-loop to provide the state and input references for the MPC. The effectiveness of the proposed approach is illustrated with two simulation examples, in which the offset-free MPC provides better performance compared to the standard EDMD-based MPC.

Chapter 12

Asymptotic Stability of kernel EDMD-based MPC in presence of approximation errors

In this chapter, we derive conditions under which data-driven MPC guarantees asymptotic stability in presence of approximation errors in the surrogate model. In fact, approximation errors are always present in data-driven models, and are related to the choice of the model class used for approximation and to the finite amount of data available for the identification. While the asymptotic stabilization of a steady-state equilibrium can be guaranteed in the nominal case, i.e. when the model used in the optimization step coincides with the system under control, in presence of modeling errors typically only PAS can be achieved. PAS means that the tracking error decreases until a certain threshold, and then stagnates to a value different from zero. The stagnation value can typically be related proportionally to the underlying approximation error.

Hence, the first contribution of the chapter is a general framework for stability analysis of MPC with data-driven surrogate models subject to approximation errors. In particular, we show that if the error of the surrogate can be bounded in a *proportional* way, the MPC algorithm designed using the data-driven surrogate model asymptotically stabilizes the system. With proportional we mean that the error vanishes at the desired set point, and its magnitude is bounded by a quantity that depends on the size of the state and input. We show that proportional error bounds imply the preservation of cost controllability for the data-driven model provided a sufficiently high approximation accuracy. Then, invoking this controllability property, we rigorously show asymptotic stability of the origin w.r.t. the MPC closed-loop using the surrogate model in the prediction and optimization step if

the prediction horizon is sufficiently long, where the origin serves as a prototypical controlled steady state.

The second part of the chapter is devoted to the verification of the assumptions for the class of kEDMD surrogate models. To this end, we consider the learning framework proposed in [22], suitably modified to ensure that the model is consistent with the system dynamics in the origin. We derive proportional and uniform error bounds without requiring invariance assumptions on finite dictionaries, and under non-restrictive data requirements.

The content of this chapter has been developed during the visiting period at TU Ilmenau, and has been submitted to:

- [216] **Schimperna, I.**, Worthmann, K., Schaller, M., Bold, L. and Magni L. (2025). *Data-driven Model Predictive Control: Asymptotic Stability despite Approximation Errors exemplified in the Koopman framework.* Submitted, available at `https://arxiv.org/abs/2505.05951`.

The preliminary version of this work, that considers a less general learning framework and where only PAS is proven (instead of asymptotic stability), is published in:

- [23] Bold, L., Schaller, M., **Schimperna, I.**, and Worthmann, K. (2025). *Kernel EDMD for data-driven nonlinear Koopman MPC with stability guarantees.* IFAC-PapersOnLine, 59(19), 478-483. Presented at the 13th IFAC Symposium on Nonlinear Control Systems.

12.1 Data-driven MPC formulation

Consider a discrete-time nonlinear control system given by

$$x_{k+1} = f(x_k, u_k) \tag{12.1}$$

with state $x \in \mathbb{R}^n$ and input $u \in \mathcal{U}$, where $\mathcal{U} \subseteq \mathbb{R}^m$ is a convex and compact set containing the origin in its interior, i.e., $\mathbf{0}_m \in \text{int}(\mathcal{U})$. The system dynamics f is assumed to be continuous and locally Lipschitz continuous in its first argument, i.e., for each compact set $K \subset \mathbb{R}^n$ there is a Lipschitz constant $L_f = L_f(K)$ such that, for all $x, y \in K$

$$\|f(x,u) - f(y,u)\|_2 \leq L_f \|x - y\|_2, \qquad \forall\, u \in \mathcal{U}. \tag{12.2}$$

Let the origin be a controlled equilibrium of the system (12.1) for the control input $u = 0$, i.e. $f(0,0) = 0$. The objective is to control the system to the origin using an MPC controller, while taking the input constraints $u \in \mathcal{U}$

into account.[1] However, since the system dynamics (12.1) is assumed to be unknown, the MPC design is based on a data-driven surrogate model

$$x_{k+1} = f^\varepsilon(x_k, u_k), \tag{12.3}$$

with $\varepsilon \in (0, \bar{\varepsilon}]$, $\bar{\varepsilon} \in (0, \infty)$. The superscript ε refers to the approximation accuracy and, throughout the chapter, will be used to refer to all the parameters related to the surrogate dynamics (12.3). Typically, the approximation error depends on the available data (quantity, distribution, etc.). To be more precise, we consider models accompanied by *proportional* error bounds, where proportional means that the error is zero at the origin and grows, at most, proportionally in the size of state and input. This property is formalized in the following assumption.

Assumption 12.1 (Error bounds on a set Ω)**.** *Consider a set $\Omega \subseteq \mathbb{R}^n$ containing the origin $\mathbf{0}_n$ in its interior. Let f^ε defined by* (12.3) *be a surrogate model for the control system* (12.1)*. For every $\varepsilon \in (0, \bar{\varepsilon}]$, let the surrogate model satisfy*

1. *proportional error bound*

$$\|f(x,u) - f^\varepsilon(x,u)\|_2 \leq c_x^\varepsilon \|x\|_2 + c_u^\varepsilon \|u\|_2 \tag{12.4}$$

2. *uniform error bound*

$$\|f(x,u) - f^\varepsilon(x,u)\|_2 \leq \eta^\varepsilon \tag{12.5}$$

for all $x \in \Omega$, $u \in \mathcal{U}$ such that the parameters c_x^ε, c_u^ε, and η^ε satisfy $\lim_{\varepsilon \to 0^+} \max\{c_x^\varepsilon, c_u^\varepsilon, \eta^\varepsilon\} = 0$.

The proportional error bound (12.4) of Assumption 12.1 requires that the surrogate model is exact at the origin, which is a reasonable assumption since the control objective is to stabilize the equilibrium located at the origin. While a proportional error bound is highly beneficial close to the origin, it may become rather conservative if the distance to the desired set point, i.e., the equilibrium located at the origin, grows. Then, using the uniform bound (12.5) on the approximation error may result in tighter bounds.

In addition to Assumption 12.1, we require uniform Lipschitz continuity of the surrogate model in the approximation accuracy ε to derive asymptotic stability of the origin w.r.t. the MPC closed loop.

Assumption 12.2 (Lipschitz continuity of surrogate model)**.** *Consider a set $\Omega \subseteq \mathbb{R}^n$ containing the origin $\mathbf{0}_n$ in its interior. Let the surrogate dynamics* (12.3) *be locally Lipschitz continuous in the first argument on the*

[1] The upcoming analysis can be directly applied to the regulation of arbitrary controlled equilibrium by considering the shifted dynamics.

set Ω uniformly in $u \in \mathcal{U}$ and $\varepsilon \in (0, \bar{\varepsilon}]$, i.e., for every compact set $K \subseteq \Omega$ there exists $\bar{L} = \bar{L}(K)$ such that, for every $\varepsilon \in (0, \bar{\varepsilon}]$, there is a Lipschitz constant L_{f^ε} with $L_{f^\varepsilon} \leq \bar{L}$ satisfying

$$\|f^\varepsilon(x,u) - f^\varepsilon(y,u)\|_2 \leq L_{f^\varepsilon}\|x-y\|_2$$

for all $x, y \in K$ and $u \in \mathcal{U}$.

In Section 12.3, we verify Assumptions 12.1 and 12.2 for data-driven surrogate models (12.3) generated by kernel EDMD using the Koopman operator theory under a suitable smoothness assumption on the system under control on bounded sets Ω.

In the following MPC algorithm, we use the quadratic stage costs

$$\ell(x,u) = \|x\|_Q^2 + \|u\|_R^2 = x^\top Q x + u^\top R u \tag{12.6}$$

with symmetric and positive-definite weighting matrices $Q \in \mathbb{R}^{n\times n}$ and $R \in \mathbb{R}^{m\times m}$. Moreover, we require the following notion of admissibility.

Definition 12.1 (Admissible control sequences)**.** *A control sequence $\mathbf{u} = \{u_k\}_{k=0}^{N-1} \subset \mathcal{U}$ of length $N \in \mathbb{N} \cup \{+\infty\}$ is said to be admissible. The set of admissible control sequences is denoted by $\mathcal{U}_N$.*

Admissibility according to Definition 12.1 does not depend on the system dynamics meaning that the definition is the same for the original dynamics (12.1) and the surrogate model (12.3).

The proposed data-driven MPC scheme is summarized in Algorithm 12.1.

The (optimal) value function $V_N^\varepsilon : \mathbb{R}^n \to \mathbb{R}_{\geq 0}$ for the MPC algorithm associated to the optimal control problem (12.7) is defined by

$$V_N^\varepsilon(\hat{x}) := \inf_{\mathbf{u}\in\mathcal{U}_N} J_N^\varepsilon(\hat{x}, \mathbf{u})$$

with $J_N^\varepsilon(\hat{x}, \mathbf{u}) := \sum_{i=0}^{N-1} \ell(x^\varepsilon(i; \hat{x}, \mathbf{u}), u_i)$ and $x^\varepsilon(i; \hat{x}, \mathbf{u})$ defined in (12.7). Analogously, we define the *nominal* cost $J_N(\hat{x}, \mathbf{u}) := \sum_{i=0}^{N-1} \ell(x(i; \hat{x}, \mathbf{u}), u_i)$, where $x(i; \hat{x}, \mathbf{u})$, $i \in [0 : N-1]$ is obtained by propagating the original system dynamics (12.1) starting from $x(0; \hat{x}, \mathbf{u}) = \hat{x}$. Finally, we define the *nominal* optimal value function by

$$V_N(\hat{x}) := \inf_{\mathbf{u}\in\mathcal{U}_N} J_N(\hat{x}, \mathbf{u}).$$

12.2 Asymptotic stability of MPC

In this section, we prove asymptotic stability of the origin for the MPC closed-loop dynamics defined in Algorithm 12.1. Since no terminal ingredients are used in the MPC formulation, we rely on cost controllability in

Algorithm 12.1 Data-driven MPC

Input: Horizon $N \in \mathbb{N}$, surrogate f^ε, input constraints $\mathcal{U}$, stage cost ℓ.

Initialization: Set $k = 0$.

(1) Measure current state x_k and set $\hat{x} = x_k$.

(2) Let $\mathbf{u} := \{u_i\}_{i=0}^{N-1}$ and solve the optimal control problem

$$\begin{aligned} \min_{\mathbf{u} \in \mathcal{U}_N} \quad & \sum_{i=0}^{N-1} \ell(x^\varepsilon(i; \hat{x}, \mathbf{u}), u_i) \\ \text{s.t.} \quad & x^\varepsilon(0; \hat{x}, \mathbf{u}) = \hat{x} \\ & x^\varepsilon(i+1; \hat{x}, \mathbf{u}) = f^\varepsilon(x^\varepsilon(i; \hat{x}, \mathbf{u}), u_i) \text{ for } i \in [0 : N-1], \end{aligned} \tag{12.7}$$

to obtain the optimal control sequence $\mathbf{u}^\star = \{u_i^\star\}_{i=0}^{N-1}$.

(3) Apply the MPC feedback law $\mu_N^\varepsilon(\hat{x}) = u_0^\star$ at the plant to generate the closed-loop

$$x_{k+1} = f(x_k, \mu_N^\varepsilon(x_k)),$$

shift $k = k + 1$, and go to Step (1).

combination with a sufficiently long prediction horizon N (see Section 3.2.2), to ensure a relaxed Lyapunov inequality

$$V_N(f(\hat{x}, \mu_N(\hat{x}))) \leq V_N(\hat{x}) - \alpha_N \ell(\hat{x}, \mu_N(\hat{x}))$$

with $\alpha_N \in (0, 1]$, where μ_N denots the MPC control law using the original dynamics f in the optimization step (2), see [51, 245] and also [133] for an extension to detectable stage costs. Then, asymptotic stability of the MPC closed-loop can be concluded using relaxed dynamic programming [91]. $\alpha_N \in (0, 1]$ is called suboptimality degree (performance index) since the MPC closed-loop costs on the infinite horizon are bounded by $V_\infty(\hat{x})/\alpha_N$, e.g., a factor two for $\alpha_N = 0.5$. The computation of the suboptimality degree α_N using cost controllability was originally proposed in [86, 233] as well as further elaborated in [88, 92], see also [244] for a unifying comparison. In particular, we follow the recent formulation of cost controllability proposed in [51, Assumption 1].

Definition 12.2 (Cost controllability on a set S)**.** *Consider a set $S \subseteq \mathbb{R}^n$ containing the origin $\mathbf{0}_n$ in its interior. The system* (12.1) *with stage cost* (12.6) *is* cost controllable *on the set S if there exists a monotonically increasing and bounded sequence $(B_N)_{N \in \mathbb{N}} = (B_N(S))_{N \in \mathbb{N}}$ such that for every $\hat{x} \in S$ there exists a control sequence $\mathbf{u} = \mathbf{u}(\hat{x}) \in \mathcal{U}_\infty$ that renders the*

set S invariant and satisfies the growth bound[2]

$$V_N(\hat{x}) \leq J_N(\hat{x}, \mathbf{u}) \leq B_N \ell^\star(\hat{x}) \tag{12.8}$$

for all $N \in \mathbb{N}$ with $\ell^\star(\hat{x}) := \min_{u \in \mathcal{U}} \ell(\hat{x}, u) = \|\hat{x}\|_Q^2$.

Cost controllability links controllability to the performance measure ℓ and, thus, ensures that the the system can be controlled to the origin sufficiently fast.

Next, we derive asymptotic stability of the origin for the MPC closed-loop relying on the surrogate (12.3) in the optimization step. To this end, we first show in Proposition 12.1 that the growth condition (12.8) is essentially preserved if only the approximation is sufficiently accurate, i.e., if the error bound of Assumption 12.1 are sufficiently small. Then, we conclude asymptotic stability in Theorem 12.1 and, finally, even prove cost controllability in Corollary 12.1.

Proposition 12.1. *Suppose that system* (12.1) *is cost controllable on a set S. Further, let $\bar{N} \in \mathbb{N}$ be given and the Assumptions 12.1 and 12.2 hold on a set Ω satisfying $S \oplus \mathcal{B}_{r(\bar{N})\eta^\varepsilon}(0) \subseteq \Omega$ with $r(\bar{N}) := \sum_{i=0}^{\bar{N}-1} \bar{L}^i$ for all $\varepsilon \in (0, \bar{\varepsilon}]$. Then, for the surrogate model* (12.3)*, the growth bound* (12.8) *is satisfied on S for all $N \in [1 : \bar{N}]$ uniformly in ε, i.e., there exists a monotonically increasing sequence $(B_N^\varepsilon)_{N \in [1:\bar{N}]}$ parametrized in ε such that, for each pair $(\hat{x}, N) \in S \times [1 : \bar{N}]$, there exists $\mathbf{u} = \mathbf{u}(\hat{x}) \in \mathcal{U}_N$ satisfying*

$$V_N^\varepsilon(\hat{x}) \leq J_N^\varepsilon(\hat{x}, \mathbf{u}) \leq B_N^\varepsilon \cdot \ell^\star(\hat{x}). \tag{12.9}$$

Moreover, $\lim_{\varepsilon \to 0^+} B_N^\varepsilon = B_N$ for all $N \in [1 : \bar{N}]$.

The statement holds also upon switching the roles of f and f^ε, i.e. if the cost controllability condition (12.8) *holds for the surrogate model f^ε, then the growth bound* (12.9) *holds for the original system f for all $N \in [1 : \bar{N}]$.*

Proof. The proof is reported in Section 12.6.1.

Proposition 12.1 shows that the growth bound (12.8) characterizing cost controllability of the system (12.1) is preserved for the surrogate model (12.3) up to a maximal horizon length $\bar{N}$. The restriction to an arbitrary, but fixed maximal horizon is necessary to apply the proposed proof technique in view of the condition $S \oplus \mathcal{B}_{r(\bar{N})\eta^\varepsilon}(0) \subseteq \Omega$ for all $\varepsilon \in (0, \bar{\varepsilon}]$. Otherwise, one has either to enlarge the set Ω on which Assumptions 12.1 and (12.2) hold or reduce $\bar{\varepsilon}$.

Note that, differently from cost controllability as stated in Definition 12.2, the sequence $(B_N^\varepsilon)_{N \in [1:\bar{N}]}$ derived in Proposition 12.1 is finite. In particular, if $\max\{c_x^\varepsilon, c_u^\varepsilon\} > 0$, the terms B_N^ε defined in (12.18) grow unboundedly for

[2]The first inequality directly follows from the definition of the value function and is only stated to link (12.8) to cost controllability as stated in [92].

$N \to \infty$. However, a finite sequence is sufficient to infer asymptotic stability of the origin w.r.t. the MPC closed-loop resulting from Algorithm 12.1 for sufficiently small ε (and, thus, sufficiently small c_x^ε and c_u^ε in Assumption 12.1). The existence of a bounded sequence $(\tilde{B}_N^\varepsilon)_{N\in\mathbb{N}}$ of infinite length satisfying the characteristic growth bound (12.8) of cost controllability for the data-driven surrogate model will then be proved in Corollary 12.1 leveraging the then established asymptotic stability.

The results of Proposition 12.1 are similar to [21, Proposition 9], but a tighter bound on the difference between B_N and B_N^ε is provided and it is clarified that for a given $\varepsilon > 0$, the sequence $(B_N^\varepsilon)_{N\in[1:\bar{N}]}$ can only be derived up to some horizon $\bar{N}$. Moreover, it is shown that the statement is symmetric and holds switching the role of the system and the surrogate model. This property, which was not studied in [21], can be particularly useful in practical applications, in which the real dynamics is unknown and cost controllability can only be checked on the surrogate model.

In the following theorem, we derive the first main result of this chapter. In essence, we show that, if the nominal MPC controller asymptotically stabilizes the origin, the data-driven MPC controller also ensures asymptotic stability of the origin w.r.t. the resulting closed-loop dynamics.

Theorem 12.1. *Let the assumptions of Proposition 12.1 hold with an optimization horizon $N = \bar{N}$ such that $\alpha_N \in (0, 1]$ holds, where α_N is given by*[3]

$$\alpha_N := 1 - \frac{(B_2 - 1)(B_N - 1)\prod_{i=3}^{N}(B_i - 1)}{\prod_{i=2}^{N} B_i - (B_2 - 1)\prod_{i=3}^{N}(B_i - 1)}. \tag{12.10}$$

Then, there exists $\varepsilon_0 \in (0, \bar{\varepsilon}]$ such that the MPC controller of Algorithm 12.1 ensures asymptotic stability of the origin on each sublevel set $V_N^{-\varepsilon}(c) := \{x \in \mathbb{R}^n \mid V_N^\varepsilon(x) \leq c\}$ satisfying the set inclusion $V_N^{-\varepsilon}(c) \subseteq S$ for $\varepsilon \in (0, \varepsilon_0)$.

Proof. The proof is reported in Section 12.6.2.

Based on Theorem 12.1 we can now even prove cost controllability of the surrogate model, i.e., existence of a bounded sequence $(B_k^\varepsilon)_{k\in\mathbb{N}}$ satisfying the growth bound (12.8) on the sub-level set $V_N^{-\varepsilon}(c)$ for which we were able to conclude asymptotic stability in Theorem 12.1.

Corollary 12.1 (Cost controllability of the surrogate model)**.** *Let the assumptions of Theorem 12.1 hold. Then there exists a monotonically increasing and bounded sequence $(B_k^\varepsilon)_{k\in\mathbb{N}}$ such that cost controllability holds for the surrogate model, i.e. for all pairs $(\hat{x}, N) \in V_N^{-\varepsilon}(c) \times \mathbb{N}$, there exists $\mathbf{u} \in \mathcal{U}_N$ satisfying*

$$V_N^\varepsilon(\hat{x}) \leq J_N^\varepsilon(\hat{x}, \mathbf{u}) \leq \tilde{B}_N^\varepsilon \ell^\star(\hat{x}).$$

[3]The condition $\alpha_N \in (0, 1]$ is always satisfied for sufficiently large N according to [92] if the system (12.1) is cost controllable with a bounded sequence $(B_N)_{N\in\mathbb{N}_0}$.

Proof. The proof is reported in Section 12.6.3.

Corollary 12.1 shows that cost controllability is inherited by the data-driven surrogate model (12.3) provided that Assumptions 12.1 and 12.2 hold. This result extends Proposition 12.1, in which the growth bound is only shown for finitely many optimization horizons N, $N \in [1 : \bar{N}]$.

Remark 12.1. *We point out that the sets Ω and S are not employed in the MPC algorithm meaning that we have not yet incorporated state constraints. Rather, we assume cost controllability of the original system* (12.1) *on a set S and, then, require Assumptions 12.1 and 12.2 on a (sufficiently large) set Ω, such that $S \oplus r(\bar{N})\eta^{\varepsilon} \subseteq \Omega$, in which we have to collect data to generate the surrogate model* (12.3)*. Clearly, a larger set S (and, thus, also a larger set Ω) allows for a larger sublevel set, which corresponds to the (guaranteed) domain of attraction. The incorporation of state constraints is left for future research and requires additional care to ensure recursive feasibility. This might, e.g., be done based on the techniques proposed in [20] or using the recently introduced concept of a constraint horizon [64], where only a finite number of predicted state are forced to obey the imposed state constraints. Moreover, we incorporated state constraints in a data-driven MPC with stabilizing terminal conditions in our recent work [217], where the constraints were tightened based on the Lipschitz constant $\bar{L}$ of the surrogate model. Then, combining both ideas using Assumptions 12.1 and 12.2 may resolve problems with so-far missing state constraints.*

Finally, we emphasize the symmetry in the derived results meaning that verifying cost controllability of the surrogate model (12.3) for sufficiently small accuracy parameter ε would suffice to conclude cost controllability of the original system and, thus, also to ensure asymptotic stability of the MPC closed loop based on the surrogate model, but applied to the original system (12.1).

12.3 Application to kernel EDMD surrogate models

In this section, we show how the assumptions used to derive asymptotic stability of the MPC closed-loop in Section 12.2 can be met using Koopman-based surrogate models. To this end, we leverage kEDMD, for which pointwise error bounds on the approximation errors are available, see Theorem 10.2. However, the error bound of Theorem 10.2 is proportional only for a cluster radius $r_X = 0$, which corresponds to zero approximation error in Step 1 of the identification algorithm. In fact, if $r_X = 0$ and we have a cluster point in the origin, i.e. $x_1 = 0$, the bound (10.19) becomes

$$\|f(x,u) - f^{\varepsilon}(x,u)\|_{\infty} \leq \tilde{C} h_X^{k-1/2} \operatorname{dist}(x, X) \leq \tilde{C} h_X^{k-1/2} \|x\|_2$$

where $\tilde{C} := C(1+\max_{u\in\mathcal{U}} \|u\|_1)\cdot\max_{p,q} \|H_{(pq)}\|_{\mathbb{H}}$. To achieve a proportional error bound also for $r_X > 0$, in the following we modify Step 1 of the kEDMD identification algorithm.

12.3.1 Modified kEDMD identification algorithm

Consider the control-affine discrete-time system under control

$$x_{k+1} = f(x_k, u_k) = g_0(x_k) + G(x_k)u_k \tag{12.11}$$

with locally Lipschitz-continuous maps $g_0 : \Omega \to \mathbb{R}^n$ and $G : \Omega \to \mathbb{R}^{n\times m}$ with Lipschitz constants L_{g_0}, L_G on Ω and control input u restricted to a compact set $\mathcal{U} \subset \mathbb{R}^m$ containing the origin in its interior. We denote by $g_i : \Omega \to \mathbb{R}^n$ the i-th column of the matrix-valued map G. Moreover, $g_0(0) = 0$ is assumed, so that the origin is an equilibrium of the system (12.11) with $u = 0$.

We consider similar data requirements of the standard kEDMD, but in addition we require the presence of a virtual observation point in the origin.

Assumption 12.3 (Data requirements)**.** *Let*

$$X = \{x_1, \dots, x_d\} \subset \Omega$$

with $x_1 = 0$ and a cluster radius $r_X \geq 0$ be given. Then, for each $i \in [1:d]$, let[4] *$d_i \geq m + (1 - \delta_{1i})$ and data triplets $(x_{ij}, u_{ij}, x_{ij}^+)$, $j \in [1:d_i]$, with pairwise distinct u_{ij} be given such that $x_{ij} \in \mathcal{B}_{r_X}(x_i) \cap \Omega$, $x_{ij}^+ = f(x_{ij}, u_{ij})$, and $\operatorname{rank}(U_i) = m + 1$ for all $i \in [1:d]$, where*

$$U_i := \begin{bmatrix} 1 & \dots & 1 \\ u_{i1} & \dots & u_{id_i} \end{bmatrix} \in \mathbb{R}^{(m+1)\times d_i}$$

Assumption 12.3 requires $D := \sum_{i=1}^d d_i$ data triplets.

Step 1 (Clustering): Approximation of the values $g_0(x_i)$ and $G(x_i)$ at the virtual observation points x_i, $i \in [1:d]$. The data triplets $(x_{ij}, u_{ij}, x_{ij}^+)$, $j \in [1:d_i]$, are used to compute an approximation

$$H_i = [\tilde{g}_0(x_i) \mid \tilde{G}(x_i)] \in \mathbb{R}^{n\times(m+1)}$$

of the matrix $[g_0(x_i) \mid G(x_i)]$ for each $x_i \in X$ by solving the linear regression problem

$$H_i = \operatorname*{arg\,min}_{H_i} \left\| [x_{i1}^+ \mid \dots \mid x_{id_i}^+] - H_i U_i \right\|_F.$$

The solution may be expressed by the pseudoinverse $U_i^\dagger$, which, for every virtual observation point x_i, is well defined in view of Assumption 12.3.

[4] δ_{1i} is the Kronecker-δ, i.e., $\delta_{11} = 1$ and $\delta_{1i} = 0$ for $i \in [2:d]$.

Later, we will become interested in a uniform bound on $\max_{i\in[1:d]} \sqrt{d_i}\|U_i^\dagger\|$. On the one hand, this may be achieved by generating (sufficiently) exciting control values u_{ij}, $j \in [1 : d_i]$, following the guidelines derived in [218] leveraging, among others, subspace-angle conditions, to ensure data efficiency ($d_i = m + (1 - \delta_{1i})$). On the other hand, one may also use randomly chosen input values in combination with a slightly larger d_i, see [22, Remark 4.6].

To derive *proportional* error bounds for the surrogate model, we directly incorporate our knowledge for the data point $x_1 = 0$, that is, $g_0(x_1) = 0$. Hence, we set $\tilde{g}_0(x_1) = 0$ while $\tilde{G}(x_1)$ is obtained by solving the reduced regression problem

$$\tilde{G}(x_1) = \operatorname*{arg\,min}_{G_1} \left\| [x_{11}^+ \mid \ldots \mid x_{1d_1}^+] - G_1[u_{11} \mid \cdots \mid u_{1d_1}] \right\|_F$$

resembling the approach presented, e.g., in [234, Section III.B].

Step 2 (Interpolation): The interpolation coefficients are computed analogously to Section 10.4.3, which leads to the following propagation step of an observable ψ:

$$\psi(f(x,u)) \approx \psi_\varepsilon^+(x) := \sum_{i=1}^{d} \Big[\big(\widehat{K}_0 + \sum_{j=1}^{m} u_j \widehat{K}_j\big)\psi_X \Big]_{(i)} \Phi_{x_i}(x) \tag{12.12}$$

with $\widehat{K}_j = K_X^{-1} K_{\tilde{g}_j(X)} K_X^{-1}$, where

$$(K_{\tilde{g}_j(X)})_{(kl)} = \mathsf{k}(x_k, \tilde{g}_j(x_l)) = \mathsf{k}(x_k, (H_l)_{(*,j+1)})$$

for all $k, l \in [1 : d]$ and $j \in [0 : m]$, and $\tilde{g}_j$ denotes the j-th column of $\tilde{G}$. Then, we directly construct the state-space surrogate of system (12.11), i.e.,

$$x_{k+1} = f^\varepsilon(x_k, u_k) = \begin{bmatrix} (\psi_1)_\varepsilon^+(x_k, u_k) \\ \vdots \\ (\psi_n)_\varepsilon^+(x_k, u_k) \end{bmatrix} = g_0^\varepsilon(x_k) + G^\varepsilon(x_k)u_k, \tag{12.13}$$

using the approximants (12.12) of the Koopman operator with observables $\psi_\ell(x) = x_{(\ell)}$ for $\ell \in [1 : n]$, that is,

$$\begin{aligned} g_0^\varepsilon(x)_{(\ell)} &:= \sum_{i=1}^{d} (\widehat{K}_0(x_{(\ell)})_X)_{(i)} \Phi_{x_i}(x), \\ (G^\varepsilon(x))_{(\ell j)} &:= \sum_{i=1}^{d} (\widehat{K}_j(x_{(\ell)})_X)_{(i)} \Phi_{x_i}(x), \end{aligned}$$

for $\ell \in [1 : n]$ and $(\ell, j) \in [1 : n] \times [1 : m]$, respectively. The i-th column of G^ε will also be denoted by g_i^ε.

12.3.2 Error bounds for kEDMD

In the following, we verify Assumptions 12.1 and 12.2 for the proposed Koopman surrogate model (12.13) of the control-affine dynamics (12.11). To this end, we derive the inequalities (12.4) and (12.5) and establish (uniform) Lipschitz continuity on the bounded set Ω. The bounds depend on the fill distance h_X and on the cluster radius r_X, and can be made arbitrarily tight by appropriately decreasing these two parameters of the proposed data-driven approximant.

The uniform error bound derived in the next theorem extends Theorem A.1 of the extended arXiv version[5] of [22] to control systems by adapting the arguments used in the proof of [22, Theorem 4.3].

Theorem 12.2 (Uniform approximation error)**.** *Let $k \geq 1$ be the smoothness degree of the Wendland kernel function. Further, let the dynamics* (12.11) *satisfy $f \in \mathcal{C}_b^{\lceil \sigma_{n,k} \rceil}(\Omega; \mathbb{R}^n)$ with $\sigma_{n,k} := \frac{n+1}{2} + k$. Suppose that the data satisfies Assumption 12.3 with fill distance h_X and cluster radius r_X satisfying $h_X \leq h_0$ and $r_X < h_X/2$, respectively. Then, there exist constants $C_1, C_2, h_0 > 0$ such that the error bound*

$$\|f(x,u) - f^\varepsilon(x,u)\|_\infty \leq C_1 h_X^{k+1/2} + C_2 c \|K_X^{-1}\|_2 r_X \tag{12.14}$$

holds for all $(x,u) \in \Omega \times \mathcal{U}$, where c is defined by

$$c := \max_{i \in [1:d]} \sqrt{d_i} \|U_i^\dagger\|_2 \cdot \Phi_{n,k}^{\mathrm{RBF}}(0)^{1/2} \left(\max_{v \in \mathbb{R}^d : \|v\|_\infty \leq 1} v^\top K_X^{-1} v \right)^{1/2}.$$

Proof. The proof is reported in Section 12.6.4.

As can be seen in Theorem 12.2, the approximation quality depends on the fill distance h_X of the grid X of cluster points and on the cluster radius $r_X \geq 0$. In particular, by choosing the cluster radius r_X such that the two terms are *balanced*, we may ensure the uniform upper bound $\eta^\varepsilon := 2C_1 h_0^{k+1/2}$ such that (12.5) holds. The choice of the virtual observation points not only influences the first term of the error bound via the fill distance, but also $\|K_X^{-1}\|_2$ and c in the second term. Depending on the choice of X, the cluster radius r_X has to be chosen sufficiently small to compensate for $C_2 c \|K_X^{-1}\|_2$.

In the following lemma we verify Assumption 12.2 for the kEDMD surrogate model, i.e. we show that the surrogate model is Lipschitz in the first argument, uniformly in u and ε.

Lemma 12.1 (Lipschitz continuity of surrogate f^ε)**.** *Let the assumptions of Theorem 12.2. Then, there exist constants $h_0, \bar{L} > 0$ such that, if the fill distance h_X and the cluster radius r_X satisfy $h_X \leq h_0$ and $r_X \leq h_X/2$, the*

[5] See the arXiv preprint `https://arxiv.org/abs/2412.02811`.

surrogate f^ε defined by (12.13) *is Lipschitz continuous in x uniformly in u with Lipschitz constant $L_{f^\varepsilon} \leq \bar{L}$, i.e.*

$$\|f^\varepsilon(x,u) - f^\varepsilon(y,u)\|_2 \leq L_{f^\varepsilon}\|x-y\|_2 \tag{12.15}$$

holds for all $x, y \in \Omega$ and $u \in \mathcal{U}$.

Proof. The proof is reported in Section 12.6.5.

The continuity in Lemma 12.1 is uniform in the approximation bound $\varepsilon > 0$. This is in contrast to finite-element dictionaries, see [207], where the derivative of the functions increases for decreasing mesh size.

The uniform error estimate in Theorem 12.2 still contains a constant offset in the upper bound, which results from Step 1 of the approximation scheme. Given an exact approximation of g_0 and G at the grid points in X, i.e., $r_X = 0$, the error bound (12.14) is proportional in the distance to the grid points. In the following, we show how one can obtain a proportional error bound even if $r_X > 0$ holds. To this end, we leverage the fact that we used the knowledge of the drift dynamics in the origin, that is, we enforced $g_0^\varepsilon(0) = 0$ in the first step of the algorithm, so that the model exactly describes the system in the origin. This is done in the following proposition.

Proposition 12.2 (Proportional error bound)**.** *Let the assumptions of Theorem 12.2 hold. Then, there exist constants h_0, r_0 such that, if the fill distance h_X and the cluster radius r_X satisfy $h_X \leq h_0$ and $r_X \leq r_0$, we have the proportional error bound*

$$\|f(x,u) - f^\varepsilon(x,u)\|_2 \leq c_x^\varepsilon\|x\|_2 + c_u^\varepsilon\|u\|_2,$$

for all $x \in \Omega$, $u \in \mathcal{U}$, where $c_u^\varepsilon := C_1 h_X^{k-1/2}\operatorname{dist}(x,X) + C_2 c\|K_X^{-1}\|_2 r_X$, and

$$c_x^\varepsilon := C_{J_{g_0}} h_X^{k-1/2} + m \max_{i=[1:m],u\in\mathcal{U}} C_{J_{g_i}}|u_{(i)}| h_X^{k-1/2} + n\sum_{i=0}^{m} c_{Xi},$$

where c_{Xi} are defined in (12.24) *and depend linearly on the cluster radius r_X.*

Proof. The proof is reported in Section 12.6.6.

Remark 12.2. *For the kEDMD surrogate, the coefficients in the proportional error bounds c_x^ε and c_u^ε are functions of the fill distance h_X and of the cluster radius r_X, and can be rewritten as*

$$c_x^\varepsilon = c_x^h h_X^{k-1/2} + c_x^r r_X$$
$$c_u^\varepsilon = c_u^h h_X^{k+1/2} + c_u^r r_X$$

for suitable $c_x^h, c_x^r, c_u^h, c_u^r$. The terms c_x^r and c_u^r have a dependence on $\|K_X^{-1}\|_2$, which is related to the location and number d of virtual observation points. For increasing d, the minimal eigenvalue of the kernel matrix K_X may decrease, and consequently $\|K_X^{-1}\|_2$ may increase. Hence, to satisfy given bounds for c_x^ε and c_u^ε, one should first select the location of the virtual observation points (that is related to the fill distance h_X) to obtain sufficiently small terms $c_x^h h_X^{k-1/2}$ and $c_u^h h_X^{k+1/2}$. Given the location of the virtual observation points, $\|K_X^{-1}\|_2$ is fixed. Then, in a second step, it is possible to select the cluster radius r_X sufficiently small to satisfy the required bounds for the terms $c_x^r r_X$ and $c_u^r r_X$.

The proportional error bound derived in Proposition 12.2 may be more conservative than the bounds of Theorem 12.2 further away from the origin, but converges to zero for $(x, u) \to (0, 0)$, which is a key property to rigorously show asymptotic stability of the MPC, as shown in Theorem 12.1 and summarized in the following theorem.

Theorem 12.3. *Let Assumption 12.3 on the data hold and consider the data-driven MPC scheme summarized in Algorithm 12.1 using the kEDMD surrogate model* (12.13) *of the control-affine dynamics* (12.11) *in the prediction and optimization step. Let $N \in \mathbb{N}$ be such that α_N defined in* (12.10) *is in* $(0, 1]$ *and assume that the system is cost controllable on a set $S \subseteq \Omega \ominus \mathcal{B}_{r(N)\eta^\varepsilon}$, see Definition 12.2, with $\mathbf{u} \in \mathcal{U}_N$. Then, if the fill distance h_X and the cluster radius r_X are sufficiently small, Algorithm 12.1 asymptotically stabilizes the system* (12.11).

Proof. We have verified (12.4) and (12.5) of Assumption 12.1, and Assumption 12.2 for the kEDMD surrogate of the control-affine dynamics (12.11) in Proposition 12.2, Theorem 12.2, and Lemma 12.1, respectively. Hence, all assumptions of Theorem 12.1 hold in view of the imposed cost controllability and the assertion can be inferred. □

12.4 Illustrative examples

In this section, we illustrate the asymptotic stability of the origin w.r.t. the MPC closed loop using the kEDMD surrogate in the prediction and optimization step by conducting numerical simulations. In the following, we denote by *physics-informed kEDMD* (**PI-kEDMD**) the models obtained with the modified Step 1 for the encoding of the equilibrium as described in Section 12.3.1, and with **kEDMD** the models obtained according to [22] without modifying Step 1 (see Algorithm 10.1).

12.4.1 Discretized Van-der-Pol oscillator

The first example is the forward Euler discretization of the nonlinear van-der-Pol oscillator (11.6). The Euler discretization yields the discrete-time

control-affine system

$$\begin{aligned} x_1^+ &= x_1 + T_\mathrm{s} x_2 \\ x_2^+ &= x_2 + T_\mathrm{s}(\nu(1-x_1)^2 x_2 - x_1 + u) \end{aligned}$$

with parameters $T_\mathrm{s} = 0.05$, $\nu = 0.1$, and control constraints $\mathcal{U} = [-2, 2]$ on the domain $\Omega = [-2, 2]^2$. The kEDMD surrogate (12.13) is constructed using Wendland kernels with smoothness degree $k = 1$, see Section 10.4.1 for details. The cluster points are chosen according to a Padua grid. The set of Padua points of order p in the domain $[-1, 1] \times [-1, 1]$ is defined as

$$\{(\mu_j, \eta_k), 0 \leq j \leq p, 1 \leq k \leq \lfloor \frac{p}{2} \rfloor + 1 + \delta_j\}$$

where $\delta_j = 1$ if p and j are both odd and $\delta_j = 0$ otherwise. Then, the pair (μ_j, η_k) is defined by

$$\mu_j := \cos\left(\frac{j\pi}{p}\right), \quad \eta_k := \begin{cases} \cos\left(\frac{(2k-2)\pi}{p+1}\right) & j \text{ odd}, \\ \cos\left(\frac{(2k-1)\pi}{p+1}\right) & j \text{ even}. \end{cases}$$

Moreover, we add a cluster point in the origin to the Padua grid, according to Assumption 12.3. The Padua grid is properly scaled to cover the domain Ω. Padua grids of order $p \in \{25, 50\}$ are considered, resulting in $d \in \{352, 1327\}$ state-space sample points. In comparison to a uniform grid, the use of a Padua grid allows to have a more uniform error through the domain, and lower condition numbers in the model matrices. In fact, Padua points minimize, analogously to Chebychev nodes in one dimension, the Lebesgue constant and, thus, the condition number and are, thus, preferable. The use of a uniform grid with a large number of data points may lead to numerical problems in the solution of the optimal control problem.

For each cluster point $x_i \in X$, $d_i = 25$ random control values $u_{ij} \in \mathcal{U}$ are chosen, yielding the data points $(x_{ij}, u_{ij}, x_{ij}^+)$. Herein, x_{ij} and u_{ij} are drawn according to our data requirements with $r_X = \frac{\sqrt{2}}{d}$ to specify the neighborhood of x_i. For the derivation of the PI-kEDMD model Step 1 of the algorithm is modified for the cluster point $x_1 = 0$ by setting $\tilde{g}_0(x_1) = 0$, while in the kEDMD model Step 1 is performed in the same way for all cluster points. The MPC cost function is chosen as in (12.6) with matrices $Q = \mathbf{I}_2$ and $R = 10^{-4}$. The following closed-loop simulations emanate from the initial state $x_0 = [0.5 \;\; 0.5]^\top$, and consider a prediction horizon $N \in \{10, 30\}$ in MPC. The comparison of the closed loop error with different number of clusters and different prediction horizons is reported in Figure 12.1.

In the simulations with the kEDMD model, we observe practical asymptotic stability only: the error stagnates at a positive constant value. The tracking accuracy increases with the number of cluster points. This is expected, as a large number of cluster points is related to lower modeling

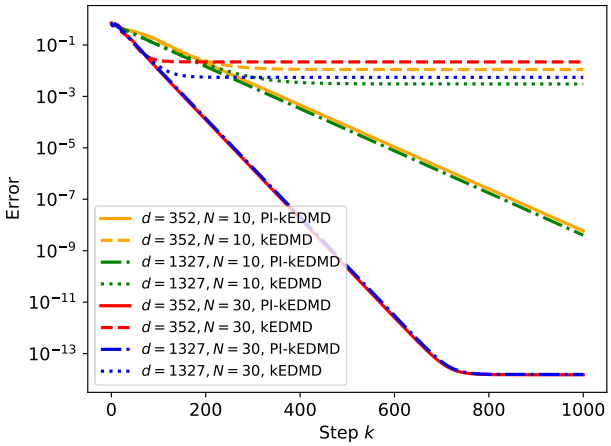

Figure 12.1: Van der Pol: Error $\|x_k\|_2$ for the kEDMD-based MPC closed loop with different horizons and number of clusters.

errors. On the other hand, the PI-kEDMD models allow to reach a lower error, with a decrease up to the solver tolerance at around 10^{-14}, in accordance to the shown asymptotic stability property of the MPC closed loop. We also notice that a fast decrease to the origin is obtained with the prolonged prediction horizon $N = 30$ – a property related to the degree of suboptimality α_N. Finally, in Figure 12.2, we report the trajectories of the same simulations in the phase space. We can see that, while the asymptotic behavior is strongly related to the accuracy of the model in the origin, the transient behavior is mainly influenced by the prediction horizon and the number of cluster points.

12.4.2 Four-tanks process

As a second example, we consider the four-tank system described in Section 6.4.1, with a sampling time $T_s = 10s$. In particular, the discrete-time version of (6.20) obtained with the forward Euler method is considered as ground truth. The controlled state for this system is the equilibrium given by $\bar{x} = [0.65,\ 0.66,\ 0.6417,\ 0.6882]^\top m$ and $\bar{u} = [1.666,\ 1.974]^\top m^3/h$. To derive the kEDMD surrogate model, the state and inputs are shifted around the origin. The state domain, where we sample, is $\Omega = [0.2\ m, 1.36\ m]^2 \times [0.2\ m, 1.30\ m]^2$, while the input is constrained by the set $\mathcal{U} = [0\ m^3/h, 3.26\ m^3/h] \times [0\ m^3/h, 4\ m^3/h]$. The cluster centers are chosen in a uniform grid in Ω. Moreover, an additional cluster center is added at the equilibrium. We consider datasets with $d \in \{626, 1297, 2402\}$ cluster centers, that correspond to $\sqrt[4]{d-1} \in \{5, 6, 7\}$. We decided to stick to a uniform grid, because the explicit construction of a grid minimizing the Lebesgue

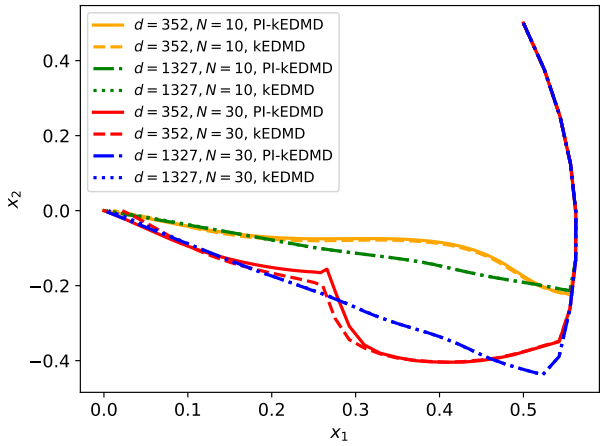

Figure 12.2: Van der Pol: trajectories of the kEDMD-based MPC closed loop with different horizons and number of clusters.

constant in dimensions higher than two is more involved and we did not run into numerical issues. Possible approaches to reduce the condition number of the model matrices are the use of the cartesian product of Padua grids or of more sophisticated approaches as outlined, e.g., in [115]. The cluster radius is $r_X = 2/d$ for all the models, and 25 data points $(x_{ij}, u_{ij}, x_{ij}^+)$ are are considered in each cluster. For the closed-loop simulations, we consider an initial state $x_0 = [1.0,\ 1.0,\ 1.0,\ 1.0]^\top m$, MPC cost matrices $Q = \mathbf{I}_4$ and $R = 10^{-4}\mathbf{I}_2$, and a prediction horizon $N = 10$.

The errors of the closed loop simulations are reported in Figure 12.3. As in the previous example, we can see that the error reaches a higher accuracy with the PI-kEDMD model, and the accuracy increases with a larger number of cluster points. The number of cluster points also influences how quickly the error decreases, which occurs more slowly for $d = 626$. In this example, the closed loop behavior remains the same if the prediction horizon is increased to $N = 20$, see Figure 12.4.

12.5 Conclusions

In this chapter, we have proposed a framework to rigorously show asymptotic stability of an equilibrium w.r.t. the MPC closed, where data-driven surrogate models are used in the optimization step, assuming cost controllability of the original system. The key ingredients are three properties of the data-driven surrogate: First, a uniform Lipschitz continuity w.r.t. the approximation accuracy (see Assumption 12.2). Second and third, uniform and foremost proportional finite-data error bounds (see Assumption 12.1).

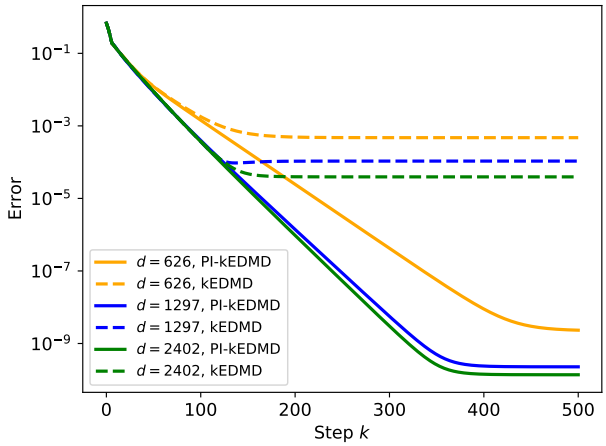

Figure 12.3: Four-tank: Error $\|x_k - \bar{x}\|_2$ for the kEDMD-based MPC closed loop with horizon $N = 10$.

Then, cost controllability is preserved and the desired asymptotic stability can be inferred despite the use of the data-driven surrogate for the prediction and optimization in MPC. Then, we rigorously verified all assumptions for a data-driven kEDMD surrogate models using Koopman operator theory resulting in finite-data error bounds. Finally, the theoretical results are verified by numerical simulations for two representative examples.

Note that the proposed method requires the exact knowledge of the system equilibrium to be implemented. When this information is not available, it is possible to rely to offset-free MPC algorithms, as described in Chapter 11. Moreover, the stability analysis can be extended to consider the presence of state constraints, disturbances and time-varying reference signals, which are not taken into account in this paper and require additional treatment as outlined in Remark 12.1. In addition, also an extension towards input-output data based would be of interest.

12.6 Proofs

12.6.1 Proof of Proposition 12.1

For given $\bar{N} \in \mathbb{N}$, let $\hat{x} \in S$ and $\mathbf{u} \in \mathcal{U}_{\bar{N}}$ satisfy the growth bound (12.8), and denote $x_k := x(k; \hat{x}, \mathbf{u})$ and $x_k^\varepsilon := x^\varepsilon(k; \hat{x}, \mathbf{u})$.

First, we show $x_k^\varepsilon \in \Omega$, $k \in [1 : N]$. Note that cost controllability yields $x_k \in S$, $k \in [1 : \bar{N}]$. We show $\|x_k^\varepsilon - x_k\| \leq r(k)\eta^\varepsilon = \sum_{i=0}^{k-1} L_{f^\varepsilon}^i \eta^\varepsilon$ by induction. For $k = 1$, we exploit (12.5) to derive

$$\|x_1^\varepsilon - x_1\| = \|f(\hat{x}, u_0) - f^\varepsilon(\hat{x}, u_0)\| \leq \eta^\varepsilon.$$

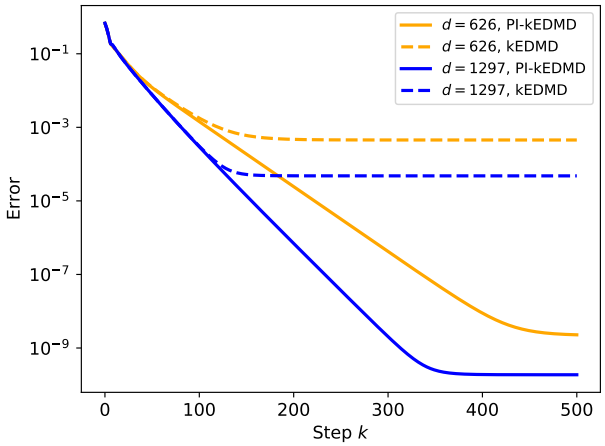

Figure 12.4: Four-tank: Error $\|x_k - \bar{x}\|_2$ for the kEDMD-based MPC closed loop with horizon $N = 20$.

Now, we assume that the assertion holds for k, and we prove it for $k+1$. We have

$$\begin{aligned}\|x^\varepsilon_{k+1} - x_{k+1}\| &= \|f(x_k,u_k) - f^\varepsilon(x^\varepsilon_k,u_k) + f^\varepsilon(x_k,u_k) - f^\varepsilon(x_k,u_k)\| \\ &\le \|f(x_k,u_k) - f^\varepsilon(x_k,u_k)\| + \|f^\varepsilon(x_k,u_k) - f^\varepsilon(x^\varepsilon_k,u_k)\| \\ &\le \eta^\varepsilon + L_{f^\varepsilon}\|x^\varepsilon_k - x_k\| \\ &\le \eta^\varepsilon + L_{f^\varepsilon}\sum_{i=0}^{k-1} L^i_{f^\varepsilon}\eta^\varepsilon = \sum_{i=0}^{k} L^i_{f^\varepsilon}\eta^\varepsilon.\end{aligned}$$

Hence, we have $x^\varepsilon_k \in S \oplus \mathcal{B}_{r(k)\eta^\varepsilon}(0) \subseteq S \oplus \mathcal{B}_{r(\bar{N})\eta^\varepsilon}(0) \subseteq \Omega$ for all $k \in [0:\bar{N}]$, so that Assumptions 12.1 and 12.2 hold.

Now, we study the difference between $J_N(\hat{x},\mathbf{u})$ and $J^\varepsilon_N(\hat{x},\mathbf{u})$. Let $\bar{\lambda} := \lambda_{\max}(Q)$ and $\underline{\lambda} := \min\{\lambda_{\min}(Q),\lambda_{\min}(R)\}$. Then, we have

$$\begin{aligned}\ell(x^\varepsilon_k,u_k) - \ell(x_k,u_k) &\overset{(12.6)}{=} \|x^\varepsilon_k - x_k + x_k\|^2_Q + \|u_k\|^2_R - \|x_k\|^2_Q + \|u_k\|^2_R \\ &\le \bar{\lambda}\|x^\varepsilon_k - x_k\|_2^2 + 2\bar{\lambda}\|x^\varepsilon_k - x_k\|_2\|x_k\|_2.\end{aligned}$$

Then, using the shorthand notation $e_k := \|x^\varepsilon_k - x_k\|_2$ for the error, summing up this inequality over $k \in [0:N-1]$ yields (as $e_k = 0$ for $k = 0$)

$$J^\varepsilon_N(\hat{x},\mathbf{u}) \le J_N(\hat{x},\mathbf{u}) + \bar{\lambda}\Big(\sum\nolimits_{k=1}^{N-1} e_k^2 + 2e_k\|x_k\|_2\Big).$$

Hence, we next derive bounds on e_k^2 and $e_k\|x_k\|_2$. To this end, the error $e_{k+1} := \|x^\varepsilon_{k+1} - x_{k+1}\|_2$ at time $k+1$ is estimated using the triangle inequality

by

$$\begin{aligned}
e_{k+1} &= \|f^\varepsilon(x_k^\varepsilon, u_k) - f(x_k^\varepsilon, u_k) + f(x_k^\varepsilon, u_k) - f(x_k, u_k)\|_2 \\
&\overset{(12.4),(12.2)}{\leq} c_x\|x_k^\varepsilon\|_2 + c_u\|u_k\|_2 + L_f\|x_k^\varepsilon - x_k\|_2 \\
&= c_x\|x_k^\varepsilon - x_k + x_k\|_2 + c_u\|u_k\|_2 + L_f\|x_k^\varepsilon - x_k\|_2 \\
&\leq c_x\|x_k\|_2 + c_u\|u_k\|_2 + (L_f + c_x)e_k \\
&\leq \bar{c}(\|x_k\|_2 + \|u_k\|_2) + (L_f + c_x)e_k \qquad (12.16) \\
&\leq \bar{c}\sum_{i=0}^{k}(L_f + c_x)^{k-i}(\|x_i\|_2 + \|u_i\|_2). \qquad (12.17)
\end{aligned}$$

with $\bar{c} := \max\{c_x, c_u\}$. Let $d := L_f + c_x$. Using inequality (12.16) and the fact that $(a+b)^2 \leq 2a^2 + 2b^2$, we get

$$\begin{aligned}
e_k^2 &\leq 4\bar{c}^2(\|x_{k-1}\|_2^2 + \|u_{k-1}\|_2^2) + 2d^2e_{k-1}^2 \\
&\overset{(12.6)}{\leq} 4\bar{c}^2\underline{\lambda}^{-1}\cdot\ell(x_{k-1}, u_{k-1}) + 2d^2e_{k-1}^2 \\
&\leq 4\bar{c}^2\underline{\lambda}^{-1}\cdot\sum_{i=0}^{k-1}(2d^2)^{k-1-i}\ell(x_i, u_i) \\
&= 4\bar{c}^2\underline{\lambda}^{-1}\cdot\sum_{j=1}^{k}(2d^2)^{j-1}\ell(x_{k-j}, u_{k-j}).
\end{aligned}$$

Analogously, leveraging inequality (12.17) and the fact that $2\|a\|_2\|b\|_2 \leq \|a\|_2^2 + \|b\|_2^2$ yields

$$\begin{aligned}
e_k\|x_k\|_2 &\leq \bar{c}\sum_{i=0}^{k-1} d^{k-1-i}\Big(\overbrace{\|x_i\|_2\|x_k\|_2 + \|u_i\|_2\|x_k\|_2}^{\leq\frac{1}{2}(\|x_i\|_2^2+\|u_i\|_2^2+2\|x_k\|_2^2)}\Big) \\
&\overset{(12.6)}{\leq} \frac{\bar{c}}{2\underline{\lambda}}\sum_{i=0}^{k-1} d^{k-i-1}\Big(\ell(x_i, u_i) + 2\ell^\star(x_k)\Big) \\
&= \frac{\bar{c}}{2\underline{\lambda}}\sum_{j=1}^{k} d^{j-1}\Big(\ell(x_{k-j}, u_{k-j}) + 2\ell^\star(x_k)\Big).
\end{aligned}$$

We begin with studying the term $\sum_{k=1}^{N-1} e_k^2$. Then, applying the derived inequality for e_k^2 yields

$$\sum_{k=1}^{N-1} e_k^2 \leq \frac{4\bar{c}^2}{\underline{\lambda}}\sum_{k=1}^{N-1}\sum_{j=1}^{k}(2d^2)^{j-1}\ell(x_{k-j}, u_{k-j}).$$

Then, noting that the summation $\sum_{k=1}^{N-1}\sum_{j=1}^{k}$ is equivalent to $\sum_{1\leq j\leq k\leq N-1} =$

$\sum_{j=1}^{N-1}\sum_{k=j}^{N-1}$ and invoking the assumed cost controllability (12.8) leads to

$$\begin{aligned}\sum_{k=1}^{N-1} e_k^2 &\leq \frac{4\bar{c}^2}{\underline{\lambda}} \sum_{j=1}^{N-1} \Big[(2d^2)^{j-1} \underbrace{\sum_{k=j}^{N-1} \ell(x_{k-j}, u_{k-j})}_{=\sum_{r=0}^{N-j-1}\ell(x_r,u_r)} \Big] \\ &\leq \bar{c}^2 \underbrace{\frac{4}{\underline{\lambda}} \sum\nolimits_{j=1}^{N-1} (2d^2)^{j-1} B_{N-j}}_{=:c_N} \ell^\star(\hat{x}).\end{aligned}$$

We proceed similarly for the term $\sum_{k=1}^{N-1} e_k \|x_k\|_2$:

$$\begin{aligned}\sum_{k=1}^{N-1} e_k\|x_k\|_2 &\leq \frac{\bar{c}}{2\underline{\lambda}} \sum_{k=1}^{N-1}\sum_{j=1}^{k} d^{j-1}\Big(\ell(x_{k-j},u_{k-j}) + 2\ell^\star(x_k)\Big) \\ &= \frac{\bar{c}}{2\underline{\lambda}} \sum_{j=1}^{N-1} d^{j-1}\Bigg(\underbrace{\sum_{r=0}^{N-j-1} \ell(x_r,u_r)}_{\overset{(12.8)}{\leq} B_{N-j}\ell^\star(\hat{x})} + 2 \underbrace{\sum_{k=j}^{N-1} \ell^\star(x_j)}_{=(N-j)\ell^\star(x_j)} \Bigg) \\ &\leq \underbrace{\bar{c}\,\frac{1}{2\underline{\lambda}}\Bigg(\sum_{j=1}^{N-1} d^{j-1} B_{N-j} + 2B_N \max_{j\in[1:N-1]} d^{j-1}\cdot(N-j)\Bigg)}_{=:\bar{c}_N} \ell^\star(\hat{x}),\end{aligned}$$

with $d = L_f + c_x$ and $\bar{c} = \max\{c_x, c_u\}$.

Combining the previous estimates leads to

$$J_N^\varepsilon(\hat{x},\mathbf{u}) \leq \big(B_N + \bar{c}^2 c_N + \bar{c}\bar{c}_N\big)\,\ell^\star(\hat{x}) =: B_N^\varepsilon \ell^\star(\hat{x}), \tag{12.18}$$

where, for each $N \in [1:\bar{N}]$, $B_N^\varepsilon \to B_N$ for $\bar{c} := \max\{c_x^\varepsilon, c_u^\varepsilon\} \to 0$ as claimed.

Finally, note that the proof is only based on the bounds on the difference between x_k and x_k^ε. Hence, the same reasoning can be applied to derive a bound on $J_N(\hat{x},\mathbf{u})$ starting from $J_N^\varepsilon(\hat{x},\mathbf{u})$. □

12.6.2 Proof of Theorem 12.1

First, we show a relaxed Lyapunov inequality

$$V_N^\varepsilon(f^\varepsilon(x,\mu_N^\varepsilon(x))) \leq V_N^\varepsilon(x) - \alpha_N^\varepsilon \ell(x,\mu_N^\varepsilon(x)). \tag{12.19}$$

for the surrogate system f^ε, following the proof of [21, Theorem 10]. First, we infer a lower bound on the optimal value function by

$$V_N^\varepsilon(\hat{x}) = \inf_{\mathbf{u}\in\mathcal{U}_N} J_N^\varepsilon(\hat{x},\mathbf{u}) \geq \inf_{u\in\mathcal{U}} \ell(\hat{x},u) = \|\hat{x}\|_Q^2 \geq \lambda_{min}(Q)\|\hat{x}\|_2^2.$$

Second, we derive an upper bound on the value function V_N^ε on the set S directly follows from the imposed (and essentially preserved) growth bound (12.9). Then, the suboptimality index α_N^ε of the surrogate model (12.3) is defined analogously to Formula (12.10) using the sequence $(B_i^\varepsilon)_{i=2}^N$ instead. Since $B_i^\varepsilon \to B_i$ converges monotonically for $\varepsilon \to 0$ in view of Proposition 12.1, we have that $\alpha_N^\varepsilon \in (0, \alpha_N)$ for all $\varepsilon \in (0, \varepsilon_0)$ for some sufficiently small $\varepsilon_0 \in (0, \bar{\varepsilon}]$. This ensures the relaxed Lyapunov inequality (12.19) with Lyapunov function V_N^ε, $\varepsilon \in (0, \bar{\varepsilon}]$ by applying [92, Theorem 5.4] and [51, Theorem 1] on $V_N^{-\varepsilon}(c)$ provided c is chosen sufficiently small such that $V_N^{-\varepsilon}(c) \subseteq S$. Hence, we established the value function $V_N^\varepsilon(\hat{x})$ as a Lyapunov function for the closed-loop of the surrogate dynamics f^ε.

In the following, we derive novel bounds to show that V_N^ε is a Lyapunov function also for the system dynamics f. We have that

$$\begin{aligned} V_N^\varepsilon(f(\hat{x}, \mu_N^\varepsilon(\hat{x}))) &= V_N^\varepsilon(f(\hat{x}, \mu_N^\varepsilon(\hat{x}))) + V_N^\varepsilon(f^\varepsilon(\hat{x}, \mu_N^\varepsilon(\hat{x}))) - V_N^\varepsilon(f^\varepsilon(\hat{x}, \mu_N^\varepsilon(\hat{x}))) \\ &\overset{(12.19)}{\leq} V_N^\varepsilon(\hat{x}) - \alpha_N^\varepsilon \ell(\hat{x}, \mu_N^\varepsilon(\hat{x})) + V_N^\varepsilon(f(\hat{x}, \mu_N^\varepsilon(\hat{x}))) - V_N^\varepsilon(f^\varepsilon(\hat{x}, \mu_N^\varepsilon(\hat{x}))). \end{aligned} \tag{12.20}$$

Next, we exploit the proportional bounds of Assumption 12.1 to derive a bound for $V_N^\varepsilon(f(\hat{x}, \mu_N^\varepsilon(\hat{x}))) - V_N^\varepsilon(f^\varepsilon(\hat{x}, \mu_N^\varepsilon(\hat{x})))$. To this end, we recall that $f^\varepsilon(\hat{x}, \mu_N^\varepsilon(\hat{x})) = x^\varepsilon(1; \hat{x}, \mathbf{u}^\star)$, where $\mathbf{u}^\star$ is the optimal solution of (12.7) with initial state $\hat{x}$, and we denote the real successor state of the system by $x^+ := f(\hat{x}, \mu_N^\varepsilon(\hat{x}))$. $\tilde{\mathbf{u}} = (\tilde{u}_i)_{i=0}^{N-1}$ represents the solution of MPC optimization problem initialized with $\tilde{x}^+ := x^\varepsilon(1; \hat{x}, \mathbf{u}^\star)$.[6] Then, for the optimality of MPC, we have that

$$\begin{aligned} &\underbrace{V_N^\varepsilon(f(\hat{x}, \mu_N^\varepsilon(\hat{x})))}_{= V_N^\varepsilon(x^+) \leq J_N^\varepsilon(x^+, \tilde{\mathbf{u}})} - V_N^\varepsilon(f^\varepsilon(\hat{x}, \mu_N^\varepsilon(\hat{x}))) \\ &\leq \sum_{i=0}^{N-1} \Big(\ell(x^\varepsilon(i; x^+, \tilde{\mathbf{u}}), \tilde{u}_i) - \ell(x^\varepsilon(i; \tilde{x}^+, \tilde{\mathbf{u}}), \tilde{u}_i) \Big). \end{aligned} \tag{12.21}$$

Consider now the i-th term of this summation

$$\begin{aligned} & \ell(x^\varepsilon(i; x^+, \tilde{\mathbf{u}}), \tilde{u}_i) - \ell(x^\varepsilon(i; \tilde{x}^+, \tilde{\mathbf{u}}), \tilde{u}_i) \\ \overset{(12.6)}{=} \; & \|x^\varepsilon(i; x^+, \tilde{\mathbf{u}})\|_Q^2 - \|x^\varepsilon(i; \tilde{x}^+, \tilde{\mathbf{u}})\|_Q^2 \\ \leq \; & \|Q\|_2 \|x^\varepsilon(i; x^+, \tilde{\mathbf{u}}) - x^\varepsilon(i; \tilde{x}^+, \tilde{\mathbf{u}})\|_2 \cdot \underbrace{\|x^\varepsilon(i; x^+, \tilde{\mathbf{u}}) + x^\varepsilon(i; \tilde{x}^+, \tilde{\mathbf{u}})\|_2}_{= \|x^\varepsilon(i; x^+, \tilde{\mathbf{u}}) - x^\varepsilon(i; \tilde{x}^+, \tilde{\mathbf{u}}) + 2x^\varepsilon(i; \tilde{x}^+, \tilde{\mathbf{u}})\|_2} \\ \leq \; & 2\|Q\|_2 \|x^\varepsilon(i; \tilde{x}^+, \tilde{\mathbf{u}})\|_2 \|x^\varepsilon(i; \tilde{x}^+, \tilde{\mathbf{u}}) - x^\varepsilon(i; x^+, \tilde{\mathbf{u}})\|_2 \\ & + \|Q\|_2 \|x^\varepsilon(i; \tilde{x}^+, \tilde{\mathbf{u}}) - x^\varepsilon(i; x^+, \tilde{\mathbf{u}})\|_2^2, \end{aligned} \tag{12.22}$$

[6] Note that $\tilde{\mathbf{u}}$ is never computed in practice, but is needed to define $V_N^\varepsilon(f^\varepsilon(\hat{x}, \mu_N^\varepsilon(\hat{x})))$ in the relaxed Lyapunov inequality (12.19), which we are going to leverage in the remainder of the proof.

where we have used the inequality

$$\|a\|_M^2 - \|b\|_M^2 = (a+b)^\top M(a-b) \leq \|M\|_2 \|a-b\|_2 \|a+b\|_2.$$

In the following, we derive upper bounds for the two terms appearing in (12.22), that are $\|x^\varepsilon(i;\tilde{x}^+,\tilde{\mathbf{u}}) - x^\varepsilon(i;x^+,\tilde{\mathbf{u}})\|_2$ and $\|x^\varepsilon(i;\tilde{x}^+,\tilde{\mathbf{u}})\|_2$.

First, we consider the term $\|x^\varepsilon(i;\tilde{x}^+,\tilde{\mathbf{u}}) - x^\varepsilon(i;x^+,\tilde{\mathbf{u}})\|_2$. For $i=0$, we use the proportional error bound (12.4) of Assumption 12.1 to derive that

$$\begin{aligned} & \|x^\varepsilon(0;\tilde{x}^+,\tilde{\mathbf{u}}) - x^\varepsilon(0;x^+,\tilde{\mathbf{u}})\|_2 = \|\tilde{x}^+ - x^+\|_2 \\ = \; & \|f^\varepsilon(\hat{x},\mu_N^\varepsilon(\hat{x})) - f(\hat{x},\mu_N^\varepsilon(\hat{x}))\|_2 \overset{(12.4)}{\leq} c_x^\varepsilon \|\hat{x}\|_2 + c_u^\varepsilon \|\mu_N^\varepsilon(\hat{x})\|_2. \end{aligned}$$

Using Lipschitz continuity of the surrogate model (12.3) given by f^ε with Lipschitz constant L_{f^ε} due to Assumption 12.2, we obtain for $i \geq 1$

$$\begin{aligned} \|x^\varepsilon(i;\tilde{x}^+,\tilde{\mathbf{u}}) - x^\varepsilon(i;x^+,\tilde{\mathbf{u}})\|_2 &\leq L_{f^\varepsilon}^i \|x^\varepsilon(0;\tilde{x}^+,\tilde{\mathbf{u}}) - x^\varepsilon(0;x^+,\tilde{\mathbf{u}})\|_2 \\ &\leq L_{f^\varepsilon}^i (c_x^\varepsilon \|\hat{x}\|_2 + c_u^\varepsilon \|\mu_N^\varepsilon(\hat{x})\|_2). \end{aligned}$$

Second, we consider the term $\|x^\varepsilon(i;\tilde{x}^+,\tilde{\mathbf{u}})\|_2$. For the growth bound of f^ε derived in Proposition 12.1 and for the relaxed Lyapunov inequality (12.19), we have that

$$\begin{aligned} V_N^\varepsilon(f^\varepsilon(\hat{x},\mu_N^\varepsilon(\hat{x}))) &= \sum_{i=0}^{N-1} \ell(x^\varepsilon(i;\tilde{x}^+,\tilde{\mathbf{u}}),\tilde{u}_i) \\ &\overset{(12.19)}{\leq} V_N^\varepsilon(\hat{x}) \overset{(12.9)}{\leq} B_N^\varepsilon \ell^\star(\hat{x}) = B_N^\varepsilon \|\hat{x}\|_Q^2. \end{aligned}$$

Since, for each $i \in [0:N-1]$, we have the inequality

$$\ell(x^\varepsilon(i;\tilde{x}^+,\tilde{\mathbf{u}}),\tilde{u}_i) \geq \|x^\varepsilon(i;\tilde{x}^+,\tilde{\mathbf{u}})\|_Q^2,$$

we also have

$$\|x^\varepsilon(i;\tilde{x}^+,\tilde{\mathbf{u}})\|_Q^2 \leq B_N^\varepsilon \|\hat{x}\|_Q^2.$$

By exploiting standard inequalities of weighted squared norms and taking the square root, we have that

$$\|x^\varepsilon(i;\tilde{x}^+,\tilde{\mathbf{u}})\|_2 \leq \sqrt{B_N^\varepsilon \frac{\lambda_{max}(Q)}{\lambda_{min}(Q)}} \|\hat{x}\|_2.$$

Then, substituting this inequalities in (12.22), we obtain

$$\begin{aligned}
& \ell(x^\varepsilon(i;x^+,\tilde{\mathbf{u}}),\tilde{u}_i) - \ell(x^\varepsilon(i;\tilde{x}^+,\tilde{\mathbf{u}}),\tilde{u}_i) \\
\leq\ & 2\|Q\|_2\sqrt{B_N^\varepsilon \frac{\lambda_{max}(Q)}{\lambda_{min}(Q)}}\|\hat{x}\|_2 L_{f^\varepsilon}^i(c_x^\varepsilon\|\hat{x}\|_2 + c_u^\varepsilon\|\mu_N^\varepsilon(\hat{x})\|_2) \\
& + \|Q\|_2 L_{f^\varepsilon}^{2i}(c_x^\varepsilon\|\hat{x}\|_2 + c_u^\varepsilon\|\mu_N^\varepsilon(\hat{x})\|_2)^2 \\
\leq\ & 2\|Q\|_2\sqrt{B_N^\varepsilon \frac{\lambda_{max}(Q)}{\lambda_{min}(Q)}} L_{f^\varepsilon}^i(c_x^\varepsilon\|\hat{x}\|_2^2 + \underbrace{c_u^\varepsilon\|\hat{x}\|_2\|\mu_N^\varepsilon(\hat{x})\|_2}_{\leq \frac{1}{2}c_u^\varepsilon(\|\hat{x}\|_2^2 + \|\mu_N^\varepsilon(\hat{x})\|_2^2)}) \\
& + 2\|Q\|_2 L_{f^\varepsilon}^{2i}\Big((c_x^\varepsilon)^2\|\hat{x}\|_2^2 + (c_u^\varepsilon)^2\|\mu_N^\varepsilon(\hat{x})\|_2^2\Big).
\end{aligned}$$

Substituting this back in (12.21) and (12.20), we obtain that

$$V_N^\varepsilon(f(\hat{x},\mu_N^\varepsilon(\hat{x}))) \leq V_N^\varepsilon(\hat{x}) - \alpha_N^\varepsilon \ell(\hat{x},\mu_N^\varepsilon(\hat{x})) + C_x\|\hat{x}\|_2^2 + C_u\|\mu_N^\varepsilon(\hat{x})\|_2^2,$$

where

$$C_x := 2\|Q\|_2 \sum_{i=0}^{N-1}\left(\sqrt{B_N^\varepsilon \frac{\lambda_{max}(Q)}{\lambda_{min}(Q)}} L_{f^\varepsilon}^i(c_x^\varepsilon + \frac{1}{2}c_u^\varepsilon) + (L_{f^\varepsilon}^i c_x^\varepsilon)^2\right),$$

and

$$C_u := 2\|Q\|_2 \sum_{i=0}^{N-1}\left(\sqrt{B_N^\varepsilon \frac{\lambda_{max}(Q)}{\lambda_{min}(Q)}} L_{f^\varepsilon}^i \frac{1}{2}c_u^\varepsilon + (L_{f^\varepsilon}^i c_u^\varepsilon)^2\right).$$

C_x and C_u can be made arbitrarily small with a sufficiently small proportionality constants c_x^ε and c_u^ε. Then there exists a sufficiently small ε_0 (potentially further tightened in comparison to our first choice resulting from the computation of the lower bound $\alpha_N^{\varepsilon_0}$ on the suboptimality index) such that $\bar{c}_x$, $\bar{c}_u$ are sufficiently small to ensure the inequality

$$-\alpha_N^\varepsilon \ell(\hat{x},\mu_N^\varepsilon(\hat{x})) + C_x\|\hat{x}\|_2^2 + C_u\|\mu_N^\varepsilon(\hat{x})\|_2^2 \leq -\bar{\alpha}\|\hat{x}\|_2^2$$

for some $\bar{\alpha} \in (0, \alpha_N^{\varepsilon_0})$ and for all $\varepsilon \in (0, \varepsilon_0)$. This completes the proof and, thus, shows asymptotic stability of the MPC closed loop based on the surrogate model (12.3). □

12.6.3 Proof of Corollary 12.1

The proof resembles the proof of Proposition 6 in [174]. In the proof of Theorem 12.1, in (12.19), we showed that there exists a sufficiently small ε such that

$$V_N^\varepsilon(f^\varepsilon(x,\mu_N^\varepsilon(x))) \leq V_N^\varepsilon(x) - \alpha_N^\varepsilon \ell(x,\mu_N^\varepsilon(x))$$

holds for all $x \in V_N^{-\varepsilon}(c)$. Then, denoting by $\mathbf{u}_{\mathrm{MPC}}$ the input sequence obtained applying the MPC control law μ_N^ε to the surrogate f^ε, we can relate the infinite-horizon optimal cost to α_N^ε

$$\begin{aligned} V_\infty^\varepsilon(\hat{x}) \le J_\infty^\varepsilon(\hat{x}, \mathbf{u}_{\mathrm{MPC}}) &\le \sum_{i=0}^{\infty} \ell(x^\varepsilon(i;\hat{x},\mathbf{u}_{\mathrm{MPC}}), \mu_N^\varepsilon(x^\varepsilon(i;\hat{x},\mathbf{u}_{\mathrm{MPC}}))) \\ &\le (\alpha_N^\varepsilon)^{-1} \sum_{i=0}^{\infty} \Big(V_N^\varepsilon(x^\varepsilon(i;\hat{x},\mathbf{u}_{\mathrm{MPC}})) \\ &\quad - V_N^\varepsilon(f^\varepsilon(x^\varepsilon(i;\hat{x},\mathbf{u}_{\mathrm{MPC}}), \mu_N^\varepsilon(x^\varepsilon(i;\hat{x},\mathbf{u}_{\mathrm{MPC}})))\Big) \\ &\le (\alpha_N^\varepsilon)^{-1} V_N^\varepsilon(\hat{x}) \le (\alpha^\varepsilon)^{-1} B_N^\varepsilon \ell^\star(\hat{x}). \end{aligned}$$

Since $V_N^\varepsilon(\hat{x}) \le V_{N+1}^\varepsilon(\hat{x}) \le V_\infty^\varepsilon(\hat{x})$ for all $N \in \mathbb{N}$, it follows that

$$V_N^\varepsilon(\hat{x}) \le (\alpha_N^\varepsilon)^{-1} B_N^\varepsilon \ell^\star(\hat{x}).$$

Hence, the growth bounds holds with $B_k^\varepsilon := B_N^\varepsilon / \alpha_N^\varepsilon$ for $k > N$, which shows the assertion. □

12.6.4 Proof of Theorem 12.2

In a first step, completely analogous to [22, Proof of Theorem 4.3], we obtain

$$|H_{(pq)}(x_i) - (H_i)_{(pq)}| \le \sqrt{2d_i}(L_{g_0} + L_G\overline{u})\|U_i^\dagger\|_2 \cdot r_X$$

for $i \in [1:d]$, where $H : \mathbb{R}^n \to \mathbb{R}^{n\times(m+1)}$ is defined by $H(x) = [g_0(x) \,|\, G(x)]$ and $\overline{u} := \max\{\|u\|_\infty : u \in \mathcal{U}\}$. Due to uniform continuity of the kernel k on $\overline{\Omega} \times \overline{\Omega}$,[7] we get the estimate

$$\|K_{\tilde{g}_j(X)} - K_{g_j(X)}\|_2 \le c_{\mathsf{k}}[L_{g_0} + L_G\overline{u}] \max\{\sqrt{2d_i}\|U_i^\dagger\|_2 \mid i \in [1:d]\} r_X \tag{12.23}$$

for a constant $c_{\mathsf{k}} \ge 0$ depending on the continuity modulus of the kernel k. Consequently, (12.23) implies

$$\begin{aligned} \|\widehat{K}_j - K_X^{-1} K_{g_j(X)} K_X^{-1}\|_2 &= \|K_X^{-1}(K_{\tilde{g}_j(X)} - K_{g_j(X)})K_X^{-1}\|_2 \\ &\le \|K_X^{-1}\|_2^2 \|K_{\tilde{g}_j(X)} - K_{g_j(X)}\|_2 \\ &\le \tilde{c}\|K_{\mathcal{X}}^{-1}\|^2 \max_{i\in[1:d]} \sqrt{d_i}\|U_i^\dagger\| \cdot r_X \end{aligned}$$

with $\tilde{c} = \sqrt{2}c_{\mathsf{k}} \cdot (L_{g_0} + L_G\overline{u})$.

Next, we prove the assertion or, to be more precise, we show inequality (12.14) with $h_X^{k-1/2}\,\mathrm{dist}(x, X)$ instead of $h_X^{k+1/2}$, which will turn out to be

[7] With $\overline{\Omega}$ we denote the closure of the set Ω.

beneficial in the proof of Proposition 12.2. Using [239, Theorem 11.17] with multiindex $|\alpha| = 1$ together with [22, Theorem 3.7], we get the proportional bound

$$|(K_X^{-1} K_{g_j(X)} K_X^{-1} \varphi_X)^\top \mathbf{k}_X(x) - \varphi \circ g_j(x)| \leq \hat{c} h_X^{k-1/2} \|\varphi\|_{\mathbb{H}} \operatorname{dist}(x, X)$$

with $\hat{c} \geq 0$ for all $\varphi \in \mathbb{H}$ and $\mathbf{k}_X := (\Phi_{x_1}, \dots, \Phi_{x_d})^\top$. Thus, by the triangle inequality, we obtain a bound on the full error:

$$|(\widehat{K}_j \varphi_X)^\top \mathbf{k}_X(x) - \varphi \circ g_j(x)| \leq \left(\hat{c} h_X^{k-1/2} \operatorname{dist}(x, X) + \tilde{c} c \|K_X^{-1}\| r_X \right) \|\varphi\|_{\mathbb{H}}.$$

Last, choosing the coordinate functions as observables, we have that the observable function φ is linear. Thus,

$$\varphi(x^+) = \varphi(g_0(x) + G(x)u) = \varphi(g_0(x)) + \sum_{j=1}^{m} \varphi(g_j(x)) u_i$$

and hence, we get (12.14) with $C_1 = \hat{c} \max_{i \in [1:n]} \|x_i\|_{\mathbb{H}}$ and $C_2 = \tilde{c} \max_{i \in [1:n]} \|x_i\|_{\mathbb{H}}$, where x_i, $i \in [1:n]$ denotes the i-th coordinate map. □

12.6.5 Proof of Lemma 12.1

In the proof, the notation J_f is used to denote the Jacobian of the function f, and $J_{f,x}$ is used to denote the Jacobian of f w.r.t. its argument x.

Let $x, y \in \Omega$ and $u \in \mathcal{U}$ be given. Then, it holds by using Taylor's theorem

$$f^\varepsilon(x, u) = f^\varepsilon(y, u) + (x - y)^\top J_{f^\varepsilon, x}(\xi, u)$$

for some $\xi \in \{\tilde{\xi} \in \mathbb{R}^n \mid \tilde{\xi} = (t-1)x + ty,\ t \in [0, 1]\}$. Hence, we may estimate

$$\begin{aligned} \|f^\varepsilon(x, u) - f^\varepsilon(y, u)\|_2 &\leq \|x - y\|_2 \|J_{f^\varepsilon, x}(\xi, u) - J_{f,x}(\xi, u) + J_{f,x}(\xi, u)\|_2 \\ &\leq \|x - y\|_2 (\|J_{f^\varepsilon, x}(\xi, u) - J_{f,x}(\xi, u)\|_2 + \|J_{f,x}(\xi, u)\|_2). \end{aligned}$$

In the following, let $\hat{g}_i$ for $i \in [0:m]$ be the approximation of g_i obtained with $r_X = 0$, i.e. without errors in Step 1 of the identification algorithm. To compute a bound for $\|J_{f^\varepsilon, x}(\xi, u) - J_{f,x}(\xi, u)\|_2$, we first leverage the control-affine structure and, then, apply [239, Theorem 11.17] with multiindex $|\alpha| = 1$ to obtain

$$\begin{aligned} \|J_{f^\varepsilon, x}(z, u) - J_{f,x}(z, u)\|_2 &\leq \|J_{g_0^\varepsilon}(z) - J_{g_0}(z) + J_{\hat{g}_0}(z) - J_{\hat{g}_0}(z)\|_2 \\ &\quad + \sum_{i=1}^{m} \|(J_{g_i^\varepsilon}(z) - J_{g_i}(z) + J_{\hat{g}_i}(z) - J_{\hat{g}_i}(z)) u_{(i)}\|_2 \\ &\leq \left[C_{J_{g_0}} + \max_{u \in \mathcal{U}} \sum_{i=1}^{m} C_{J_{g_i}} |u_{(i)}| \right] h_X^{k-1/2} \\ &\quad + \|J_{\hat{g}_0}(z) - J_{g_0^\varepsilon}(z)\|_2 + \sum_{i=1}^{m} \|(J_{\hat{g}_i}(z) - J_{g_i^\varepsilon}(z)) u_{(i)}\|_2, \end{aligned}$$

where $C_{J_{g_i}}$, $i \in [0:m]$, are constants independent of h_X and r_X. Analogously to the proof of [22, Theorem 4.3], letting $u_0 = 1$, we can estimate for $i \in [0:m]$ and $j \in [1:n]$

$$\begin{aligned}
&\|(\nabla \hat{g}_{ij}(z) - \nabla g_{ij}^{\varepsilon}(z))u_i\|_2 \\
&\leq \max_{u\in\mathcal{U}} |u_i| L_{J_{g_i}} \sqrt{2 \max_{k\in[1:d]} d_k} \left(\max_{\ell\in[1:d]} \|U_\ell^\dagger\|_2 \right) \|K_X^{-1}\mathbf{k}_X(z)\|_2 \|K_X^{-1}\|_2 r_X \\
&\leq \max_{u\in\mathcal{U}} |u_i| L_{J_{g_i}} \sqrt{2 \max_{k\in[1:d]} d_k} \left(\max_{\ell\in[1:d]} \|U_\ell^\dagger\|_2 \right) \Phi_{n,k}^{\mathrm{RBF}}(0) \\
&\cdot \max_{v:\|v\|_\infty\leq 1} v^\top K_X^{-1} v \|K_X^{-1}\|_2 r_X =: c_{Xi},
\end{aligned} \tag{12.24}$$

where $\mathbf{k}_X(z) = (\mathsf{k}(x_1,z),\dots,\mathsf{k}(x_d,z))^\top$ and $L_{J_{g_i}}$ are the Lipschitz constants of the matrix-valued functions J_{g_i}. Since the function f is continuously differentiable w.r.t. its first argument on the compact set Ω, we have $\|J_{f,x}(\xi,u)\|_2 \leq \widetilde{C} \in (0,\infty)$. Overall, we have verified inequality (12.15) with Lipschitz constant L_{f^ε} given by

$$\widetilde{C} + C_{J_{g_0}} h_X^{k-1/2} + m \max_{i=[1:m],u\in\mathcal{U}} C_{J_{g_i}} |u_i| h_X^{k-1/2} + n \sum_{i=0}^{m} c_{Xi}.$$

Hence, suitably adjusting the cluster radius r_X depending on the virtual observation points and, thus, $\|K_X^{-1}\|_2$, shows the statement. □

12.6.6 Proof of Proposition 12.2

To prove the statement, we first show that the difference $\|J_{f^\varepsilon}(x,u) - J_f(x,u)\|_2$ between the differentials of f and f^ε is bounded. From the proof of Lemma 12.1 we obtain the bound

$$\|J_{f^\varepsilon,x}(x,u) - J_{f,x}(x,u)\|_2 \leq \underbrace{C_{J_{g_0}} h_X^{k-1/2} + m \max_{i=[1:m],u\in\mathbb{U}} C_{J_{g_i}} |u_i| h_X^{k-1/2} + n \sum_{i=0}^{m} c_{Xi}}_{=:c_x^\varepsilon}.$$

To compute a bound for $\|J_{f^\varepsilon,u}(x,u) - J_{f,u}(x,u)\|_2$, we exploit the error bounds of Theorem 12.2, to obtain

$$\begin{aligned}
\|J_{f^\varepsilon,u}(x,u) - J_{f,u}(x,u)\|_2 &= \|G^\varepsilon(x) - G(x)\|_2 \\
&\leq C_1 h_X^{k-1/2} \operatorname{dist}(x,X) + C_2 c \|K_X^{-1}\|_2 r_X =: c_u^\varepsilon.
\end{aligned}$$

Now, let $e(x,u) := f^\varepsilon(x,u) - f(x,u)$. In view of the modified learning algorithm, there is no approximation error in the origin, i.e. $e(0,0) = 0$. We

now study $e(x,u)$ using Taylor's theorem. There exists $t \in [0,1]$ such that, denoting $z = tx$ and $v = tu$,

$$\begin{aligned}\|e(x,u)\|_2 &= \|\underbrace{e(0,0)}_{=0} + J_{e,x}(z,v)x + J_{e,u}(z,v)u\|_2 \\ &\leq \|J_{f^\varepsilon,x}(z,v) - J_{f,x}(z,v)\|_2\|x\|_2 + \|J_{f^\varepsilon,u}(z,v) - J_{f,u}(z,v)\|_2\|u\|_2 \\ &\leq c_x^\varepsilon\|x\|_2 + c_u^\varepsilon\|u\|_2,\end{aligned}$$

which proves the statement. □

Part IV

Applications

Chapter 13

Velocity form MPC for current control in Synchronous Reluctance motors

In recent years, Synchronous Reluctance motor (SynchRel) drives have gained attention in academia and industry as an alternative to induction motors and Permanent Magnet Synchronous Motors (PMSM). SynchRel motors are a cheap solution since no rotor windings and no rare-Earth materials are required. Hence, this chapter is devoted to the design of an MPC algorithm for the control of currents in a SynchRel motor. Differently from the majority of the control schemes available in the literature, our design considers the stability issue of MPC. In particular, we propose an equality terminal constraint formulation of velocity form MPC, and we introduce an artificial reference in the optimization to enlarge the feasibility region and improve the closed-loop performances. This algorithm is simple to implement, does not require the introduction of a state observer, and guarantees zero tracking error in presence of the model approximations. The proposed equality constraint formulation of the velocity form MPC does not require terminal inequality constraints. This is an advantage compared to the method proposed in [15], where the terminal region may require a large number of inequalities constraints to be described, resulting in a significant increase of the computational complexity for the solution of the optimization problem. The MPC is inserted in a cascade scheme that involves also an external loop for the control of the motor speed. The velocity form MPC is based on a linear approximation of the SynchRel electrical dynamics in the (d, q) reference frame [182], that does not require a precise knowledge of the inductance values of the motor. Finally, the effectiveness of the proposed algorithm is compared in simulation to a current control based on Proportional-Integral (PI) regu-

lators and decoupling and to a classic MPC, also considering uncertainties in the inductances models, showing better performances both in the nominal and in the perturbed case.

The work reported in this chapter was carried out in collaboration with SPIN Applicazioni Magnetiche Srl, and is published in:

- [214] **Schimperna, I.**, Rubino, A. and Magni, L. (2025). *Velocity Form MPC for Current Control in Synchronous Reluctance Motors*. IEEE Transactions on Control Systems Technology, 33(6), 2463-2469.

13.1 Introduction to the control of electric motors

Two main concepts that are often used for the control of SynchRel motors are Direct Torque Control (DTC) [144] and Field-Oriented Control (FOC) [166, 17, 250]. DTC is known for its robustness and fast dynamics [26], but can lead to high current distortions and torque ripples [43]. FOC is able to improve the efficiency of the system [119] and the torque response [195], but requires precise values of the system parameters to be implemented.

When a speed sensor is available, a common approach to implement the motor control is to apply a cascade scheme, where an inner closed-loop controls the motor currents, that have a fast dynamics, and an external closed-loop controls the speed and provides the references for the current control. The most common implementation of the cascade schema employs PI regulators for both the control loops. When a rotational transducer is not available, position estimation algorithms can be applied to obtain the speed value [94].

An alternative to classical approaches for the control of electric motors is the use of MPC, that can be employed in a cascade schema to substitute the PI in one or both the two control loops [152, 2], or can be used as a unique controller for both the speed and the currents [175, 40]. The advantages of the use of MPC in electrical drives and power electronics are the possibility to be applied to a variety of systems, and the fact that constraints, nonlinearities and multivariable systems can be easily considered [52]. Moreover, MPC is based on a model of the system under control, that is typically available in these applications. There are two possible ways to implement MPC for transistor-based systems: Finite Control Set MPC (FCS-MPC) and Continuous Control Set MPC (CCS-MPC). In FSC-MPC, the transistor states are directly regarded as control variables, without the need of an additional modulation stage [78, 202, 140]. Instead, in CCS-MPC, a continuous optimization problem is considered and the determination of switching sequences is delegated to an external modulator [78, 254]. CCS-MPC is typical more computational demanding, but recent works have shown that with the current technologies and optimization algorithms it is possible to solve the MPC optimization problem in real time even in the high sampling

frequencies required by the motor drives. For instance, in [48], an explicit MPC algorithm [12] is employed to solve the quadratic programming problem associated to the MPC for the current control of a PMSM. The worst case solution time is assessed, and the proposed approach is experimentally validated. In [254], instead, the MPC optimization problem related to the current control in SynchRel motors is solved online on embedded hardware, and meets the sampling times required by the application.

The stability and feasibility issues are often neglected when MPC is applied for the control of electric motors, and the few works considering these problems are focused on FCS-MPC. The stability issue is considered in [93] in the control of induction motors, where the FCS-MPC objective function is reformulated using the Lyapunov function time derivative as objective function, and introducing some stability constraints in the optimization. In [1], closed-loop practical stability of horizon-one quadratic FCS-MPC for linear power converters is obtained by designing the terminal cost and terminal set for the MPC on the base of the discrete time Riccati equation.

The use of velocity form MPC for the control of electric motors is not a novelty. For instance, velocity form MPC is applied to SynchRel motors in [72] for the regulation of the currents at constant set-points. Since no input and state constraints are considered, the solution of the MPC is a linear state feedback control law that can be computed explicitly. In [40], the velocity form MPC is considered for the control of speed and currents in a PMSM. However, none of the cited works provides a formal analysis of the stability of the closed-loop system.

13.2 Stabilizing MPC in velocity form

13.2.1 Incremental model

Consider a discrete-time linear model in the form

$$x_{k+1} = Ax_k + Bu_k \tag{13.1a}$$

$$y_k = Cx_k \tag{13.1b}$$

where $x \in \mathbb{R}^n$, $u \in \mathbb{R}^m$, $y \in \mathbb{R}^p$ and the subscript k denotes the discrete time instant. The objective of the control is to steer the output of the system to a desired reference y_{ref}, also in presence of model uncertainties. The following standard assumption on the model is required to introduce the integral action.

Assumption 13.1. *The pair (A, B) is controllable, $m \geq p$, and the input-output system does not have invariant zeros in 1, i.e.*

$$\operatorname{rank}\left(\begin{bmatrix} \mathbf{I}_n - A & -B \\ -C & 0 \end{bmatrix}\right) = n + p.$$

To derive the velocity formulation, the model is firstly enlarged with an integral action on the tracking error

$$x_{k+1} = Ax_k + Bu_k \tag{13.2a}$$
$$v_{k+1} = v_k + e_{k+1} \tag{13.2b}$$

where $e_k := y_k - y_{\text{ref}}$. The enlarged system (13.2) is not directly used in the MPC design. Instead, an incremental system is considered, with states that are the variations of the states of (13.2), and the input variation as controlled input. In particular, the incremental system has state $\xi := [\delta x^\top \ e^\top]^\top \in \mathbb{R}^{n+p}$ and input $\delta u \in \mathbb{R}^m$, where $\delta x_k := x_k - x_{k-1}$ and $\delta u_k := u_k - u_{k-1}$. The dynamics of δx can be derived as follows

$$\begin{aligned}\delta x_{k+1} &= x_{k+1} - x_k = Ax_k + Bu_k - (Ax_{k-1} + Bu_{k-1}) \\ &= A(x_k - x_{k-1}) + B(u_k - u_{k-1}) = A\delta x_k + B\delta u_k.\end{aligned}$$

The dynamics of e is derived in the following way

$$\begin{aligned}e_{k+1} &= v_{k+1} - v_k = v_k + y_{k+1} - y_{\text{ref}} - v_k \\ &= Cx_{k+1} - y_{\text{ref}} = C(\delta x_{k+1} + x_k) - y_{\text{ref}} \\ &= C(A\delta x_k + B\delta u_k) + Cx_k - y_{\text{ref}} \\ &= CA\delta x_k + CB\delta u_k + (y_k - y_{\text{ref}}) \\ &= CA\delta x_k + e_k + CB\delta u_k.\end{aligned}$$

Combining the previous computations, the following dynamics is obtained

$$\begin{bmatrix}\delta x_{k+1} \\ e_{k+1}\end{bmatrix} = \underbrace{\begin{bmatrix}A & 0 \\ CA & \mathbf{I}_m\end{bmatrix}}_{\bar{A}} \begin{bmatrix}\delta x_k \\ e_k\end{bmatrix} + \underbrace{\begin{bmatrix}B \\ CB\end{bmatrix}}_{\bar{B}} \delta u_k \tag{13.3}$$

to be used as model for the MPC.

13.2.2 MPC formulation

The objective of the MPC is to steer the incremental variables δx and δu and the error e to zero, independently on the value of the reference y_{ref}, while respecting the input constraints given by the compact set $\mathcal{U} \subset \mathbb{R}^m$. This is an advantage with respect to other MPC formulations, because it is not required to use the model, which may be inaccurate, to compute the equilibrium correspondent to the reference.

Stability of the closed-loop system with the MPC control law is obtained using a terminal equality constraint. This strategy is simple to implement and does not require the use of possibly computationally expensive algorithms for the offline computation of the terminal set. However, the introduction of the terminal constraint can lead to problems of infeasibility and a

decrease of performances. In particular, feasibility can be achieved only for values of the initial state ξ that are sufficiently close to zero, and the solution of the optimization is strongly influenced by the terminal constraint and may not reflect the objective required by the cost. To solve these issues, it is possible to introduce an artificial reference $\bar{y}$ in the optimization problem [150]. The artificial reference is an additional variable of the optimization problem, and its deviation from the real reference y_{ref} is penalized in the cost.

The velocity form MPC with equality terminal constraint and artificial reference solves the following optimal control problem

$$\min_{\bar{y},\delta u_{\cdot|k}} \sum_{i=0}^{N-1} \left(\left\|\xi_{i|k}\right\|_Q^2 + \left\|\delta u_{i|k}\right\|_R^2 \right) + \left\|\bar{y} - y_{\text{ref}}\right\|_S^2 \tag{13.4a}$$

$$\text{s.t. } \xi_{0|k} = \begin{bmatrix} \delta x_k \\ y_k - \bar{y} \end{bmatrix} \tag{13.4b}$$

$$\xi_{i+1|k} = \bar{A}\xi_{i|k} + \bar{B}\delta u_{i|k} \quad i = 0, ..., N-1 \tag{13.4c}$$

$$u_{i|k} = u_{k-1} + \sum_{j=0}^{i} \delta u_{j|k} \in \mathcal{U} \quad i = 0, ..., N-1 \tag{13.4d}$$

$$\xi_{N|k} = 0 \tag{13.4e}$$

where the cost matrices $Q = Q^\top \succ 0$, $R = R^\top \succ 0$ and $S = S^\top \succ 0$ are design choices. Note that the artificial reference $\bar{y}$ is used in (13.4b) to initialize the prediction error. Initializing the error as the difference with respect to the artificial reference allows the error with respect to the real reference (i.e. $y - y_{\text{ref}}$) to be different from zero at the end of the horizon. In this way feasibility is guaranteed also in presence of sudden variations of y_{ref}. Denoting the optimal input increment sequence by $\delta u^\star_{0|k}, ..., \delta u^\star_{N-1|k}$, the control law is obtained according to the receding horizon principle as

$$u_k = u_{k-1} + \mu^{\text{MPC}}(\delta x_k, u_{k-1}, y_k, y_{\text{ref}}) = u_{k-1} + \delta u^\star_{0|k}. \tag{13.5}$$

Note that state constraints are not considered in the MPC formulation because they are not present in the SynchRel motor application, but they can be easily included in the algorithm.

13.2.3 Stability result

The equality terminal constraint formulation of the velocity form MPC allows to prove stability of the closed-loop system. Moreover, the introduction of the artificial reference guarantees recursive feasibility also when y_{ref} varies or is outside of the set of the set-points that can be reached while respecting the input constraints. All these results can be derived along the lines of

Symbol	Description	Unit
I_d, I_q	Stator currents	[A]
V_d, V_q	Stator voltages	[V]
R_s	Stator winding resistance	[Ω]
L_d, L_q	Inductances	[H]
ω	Mechanical speed of the rotor	[rad/s]
ω_e	Electric speed of the rotor	[rad/s]
T	Torque produced by the motor	[Nm]
T_L	Load torque	[Nm]
n_p	Number of pole pairs	-
k_w	Friction coefficient	$\left[\frac{\mathrm{Nm}\cdot\mathrm{s}^2}{\mathrm{rad}^2}\right]$
J	Motor inertia	$[\mathrm{kg}\cdot\mathrm{m}^2]$

Table 13.1: Parameters of the SynchRel motor model.

[151, Theorem 2]. In order to do so, the set of admissible equilibria is first defined as

$$\begin{aligned}\mathcal{Y} := \{y \in \mathbb{R}^p : \exists (x,u) \in \mathbb{R}^n \times \mathcal{U} \\ \text{such that } y = Cx,\ x = Ax + Bu\}.\end{aligned}$$

Theorem 13.1 ([151])**.** *Let Assumption 13.1 hold and the prediction horizon satisfy $N \geq n + p$. Then, if a feasible solution to* (13.4) *exists at time $k = 0$, the resulting MPC controller is recursively feasible and asymptotically steers the system* (13.1) *to the admissible set-point $\hat{y}$, where*

$$\hat{y} := \arg\min_{y \in \mathcal{Y}} \|y - y_\mathrm{ref}\|_S^2 .$$

13.3 Reluctance synchronous motors control

The mathematical model of the SynchRel motor can be divided into the electric subsystem and the mechanical subsystem. In Table 13.1 the descriptions of the physical quantities involved in the motor model are reported. The electrical subsystem of the SynchRel motor can be described, using the Clarke-Park transformation, with respect to the (d, q) reference frame [182], that is rotating synchronously with the rotor, with the following equations

$$\begin{aligned}\dot{I}_\mathrm{d}(t) =& \frac{-R_\mathrm{s}}{L_\mathrm{d}(I_\mathrm{d}(t), I_\mathrm{q}(t))} I_\mathrm{d}(t) + \frac{1}{L_\mathrm{d}(I_\mathrm{d}(t), I_\mathrm{q}(t))} V_\mathrm{d}(t) \\ &+ \omega_\mathrm{e}(t) \frac{L_\mathrm{q}(I_\mathrm{d}(t), I_\mathrm{q}(t))}{L_\mathrm{d}(I_\mathrm{d}(t), I_\mathrm{q}(t))} I_\mathrm{q}(t)\end{aligned} \tag{13.6a}$$

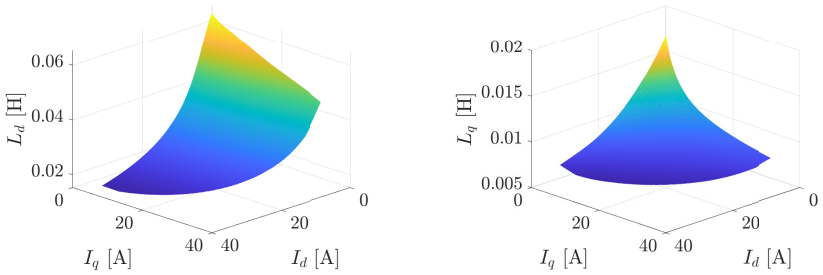

Figure 13.1: Inductances L_d (left) and L_q (right) as functions of I_d and I_q.

$$\begin{aligned}\dot{I}_\mathrm{q}(t) =& \frac{-R_\mathrm{s}}{L_\mathrm{q}(I_\mathrm{d}(t), I_\mathrm{q}(t))} I_\mathrm{q}(t) + \frac{1}{L_\mathrm{q}(I_\mathrm{d}(t), I_\mathrm{q}(t))} V_\mathrm{q}(t) \\ & - \omega_\mathrm{e}(t) \frac{L_\mathrm{d}(I_\mathrm{d}(t), I_\mathrm{q}(t))}{L_\mathrm{q}(I_\mathrm{d}(t), I_\mathrm{q}(t))} I_\mathrm{d}(t)\end{aligned} \tag{13.6b}$$

where $\omega_\mathrm{e}(t) = n_\mathrm{p} \cdot \omega(t)$. The subscripts d and q indicate the quantities on the two axes. $V = [V_\mathrm{d}\ V_\mathrm{q}]^\top$ is the control variable, that can be forced by means of an inverter. The electric state $I = [I_\mathrm{d}\ I_\mathrm{q}]^\top$ is considered measurable. The output of the electric dynamics is the torque produced by the motor, that is a nonlinear function of the currents

$$T(t) = \frac{3}{2} n_\mathrm{p} (L_\mathrm{d}(I_\mathrm{d}(t), I_\mathrm{q}(t)) - L_\mathrm{q}(I_\mathrm{d}(t), I_\mathrm{q}(t))) I_\mathrm{d}(t) I_\mathrm{q}(t). \tag{13.7}$$

Given the torque T, the mechanical dynamics of the motor can be described by

$$\dot{\omega}(t) = \frac{1}{J}(T(t) - T_\mathrm{L}(t) - k_\mathrm{w}\omega(t)|\omega(t)|) \tag{13.8}$$

where T_L is an external time variant load torque, whose value is in general unknown and unmeasurable. In Equations (13.6) and (13.7) the inductances L_d and L_q are nonlinear functions of the currents I_d and I_q. The values assumed by the inductances at a given value of current can be estimated using the Finite-Element Method (FEM). In particular, in the simulations, two 2-dimensional Look-Up Tables (LUT) obtained from FEM data are used to relate the values of L_d and L_q with the values of I_d and I_q. The plots of the inductances as functions of I_d and I_q for the considered motor are reported in Figure 13.1.

13.3.1 Cascade control scheme

The objective of the motor control is to track a speed reference ω_ref by acting on the stator voltages V_d and V_q, and to reject the unmeasurable disturbance given by the load torque T_L. In Figure 13.2 the scheme of the

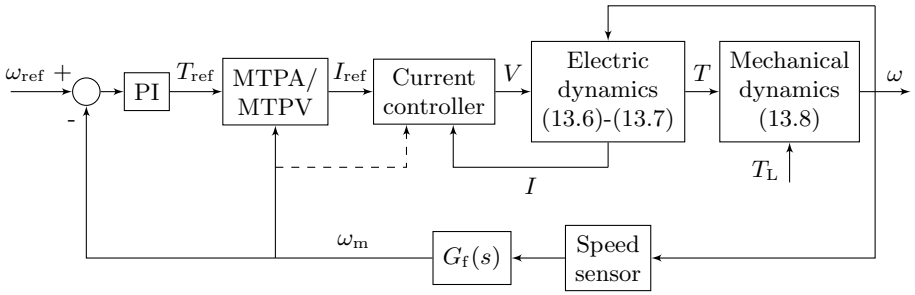

Figure 13.2: Block diagram of the general schema of the motor control.

motor control is reported. Since the motor dynamics is composed by two main parts with different time constants, a cascade control scheme is typically applied. In particular, an internal control loop is closed around the electric dynamics (13.6), that is faster, while an external control loop considers the mechanical dynamics (13.8). This technique allows to exploit the redundancy of the control action in order to minimize the power consumption. In fact, two control variables V_{d} and V_{q} are available to control a single output ω. Hence, it is possible to select, between the different combinations of the control variables that give ω_{ref} as output, the more energy efficient one. This is done by means of the MTPA/MTPV (Maximum Torque Per Ampere/Maximum Torque Per Volt) block, as it is better explained later.

To obtain a measurement of the motor speed, a speed sensor is included in the schema. The sensor can introduce measurement noise and a nonlinearity, for example due to the quantization error. To mitigate these effects, that act mainly in high frequency, a low-pass filter $G_{\text{f}}(s)$ is typically introduced after the sensor. The motor currents are assumed measurable by the inverter. The control variables V_{d} and V_{q} are saturated at a value that depend on the external voltages supplied to the inverter V_{DC}. In particular

$$V_{\text{d}}, V_{\text{q}} \in \left[-\frac{V_{\text{DC}}}{\sqrt{3}}, \frac{V_{\text{DC}}}{\sqrt{3}} \right]. \tag{13.9}$$

The external speed controller is composed by two blocks. The first block is a PI, whose output is interpreted as a torque reference T_{ref}. The second block, denoted by MTPA/MTPV, provides the optimal current reference $I_{\text{ref}} = [I_{\text{d,ref}} \; I_{\text{q,ref}}]^\top$ given the torque reference T_{ref} and the measured and filtered speed ω_{m}. In particular I_{ref} is the couple of currents that provides the torque T_{ref} at the current speed of the motor using the minimum amount of power and respecting the machine constraints. The MTPA/MTPV block is typically implemented using a LUT, that can be derived from the FEM data.

13.3.2 Current control with velocity form MPC

To implement the velocity form MPC, a discrete-time linear approximation of the electric dynamics (13.6) in a working point is considered. The working point is defined by the nominal values of the speed $\bar{\omega}$ and of the load torque $\bar{T}_\mathrm{L}$. By considering the equilibrium of (13.8), it is possible to derive the steady state motor torque $\bar{T}$ in the working point as $\bar{T} = \bar{T}_\mathrm{L} + k_\mathrm{w}\bar{\omega}|\bar{\omega}|$. Then, the desired values of steady state currents $\bar{I}_\mathrm{d}$ and $\bar{I}_\mathrm{q}$ can be derived as the output of the MTPA/MTPV block with inputs $\bar{T}$ and $\bar{\omega}$. Finally, the values of the inductances in the working point $\bar{L}_\mathrm{d}$ and $\bar{L}_\mathrm{q}$ can be obtained from $\bar{I}_\mathrm{d}$ and $\bar{I}_\mathrm{q}$ using the FEM data, as $\bar{L}_\mathrm{d} = L_\mathrm{d}(\bar{I}_\mathrm{d}, \bar{I}_\mathrm{q})$ and $\bar{L}_\mathrm{q} = L_\mathrm{q}(\bar{I}_\mathrm{d}, \bar{I}_\mathrm{q})$.

Then, the continuous time linear approximation of the electric dynamics is

$$\begin{bmatrix} \dot{I}_\mathrm{d}(t) \\ \dot{I}_\mathrm{q}(t) \end{bmatrix} = \begin{bmatrix} -\frac{R_\mathrm{s}}{\bar{L}_\mathrm{d}} & \bar{\omega}_\mathrm{e}\frac{\bar{L}_\mathrm{q}}{\bar{L}_\mathrm{d}} \\ -\bar{\omega}_\mathrm{e}\frac{\bar{L}_\mathrm{d}}{\bar{L}_\mathrm{q}} & -\frac{R_\mathrm{s}}{\bar{L}_\mathrm{q}} \end{bmatrix} \begin{bmatrix} I_\mathrm{d}(t) \\ I_\mathrm{q}(t) \end{bmatrix} + \begin{bmatrix} \frac{1}{\bar{L}_\mathrm{d}} & 0 \\ 0 & \frac{1}{\bar{L}_\mathrm{q}} \end{bmatrix} \begin{bmatrix} V_\mathrm{d}(t) \\ V_\mathrm{q}(t) \end{bmatrix} \tag{13.10}$$

where $\bar{\omega}_\mathrm{e} = n_\mathrm{p} \cdot \bar{\omega}$. Note that a single working point is considered in order to derive the linear approximation. The same approximated model is used in the MPC also when the working point varies, and the zero tracking error property is maintained despite the model mismatch thanks to the velocity formulation of the MPC. To derive a discrete time model to be used in the MPC, (13.10) is discretized with a sampling time T_s using a zero-order hold method, obtaining a discrete time linear model in the form

$$x_{k+1} = Ax_k + Bu_k \tag{13.11}$$

where

$$x_k = \begin{bmatrix} I_\mathrm{d}(kT_\mathrm{s}) \\ I_\mathrm{q}(kT_\mathrm{s}) \end{bmatrix}, \quad u_k = \begin{bmatrix} V_\mathrm{d}(kT_\mathrm{s}) \\ V_\mathrm{q}(kT_\mathrm{s}) \end{bmatrix}$$

with $k \in \mathbb{Z}_{\geq 0}$. Since the objective is to control with zero offset the current on both axes, in the output transformation (13.1b) $C = \mathbf{I}_2$ is considered. The model obtained in this way satisfies Assumption 13.1 on controllability. Then, the velocity form MPC is implemented as described in Section 13.2, considering (13.9) as input constraint set.

13.4 Implementation and simulation results

In Table 13.2 the numerical values of the parameters considered in the simulation, carried out on the true continuous-time system, are reported. An encoder is employed as speed sensor, that introduces a measurement error due to the quantization in the measurement of the rotor angle. To mitigate this effect a low-pass filter with transfer function

$$G_\mathrm{f}(s) = \frac{1}{1 + 0.002s}$$

Parameter	**Symbol**	**Value**	**Unit**
Stator resistance	R_{s}	0.62	$[\Omega]$
Pole pairs	n_{p}	3	-
Friction coefficient	k_{w}	5×10^{-6}	$\left[\frac{\mathrm{Nm \cdot s^2}}{\mathrm{rad^2}}\right]$
Motor inertia	J	8.4×10^{-3}	$[\mathrm{kg \cdot m^2}]$
Inverter sampling frequence	$\frac{1}{T_{\mathrm{s}}}$	8000	[Hz]
Nominal speed	$\bar{\omega}$	2500	[rpm]
Nominal load torque	$\bar{T}_{\mathrm{L}}$	10	[Nm]
DC supply voltage	V_{DC}	650	[V]

Table 13.2: Numerical values of the parameters for the motor simulator.

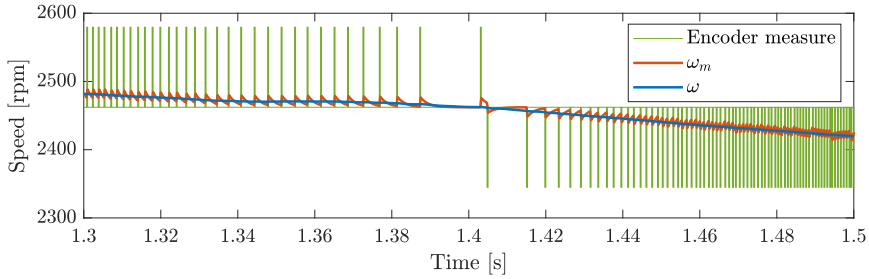

Figure 13.3: Comparison between the motor speed ω (blue), the the encoder measure (green) and the filtered measure ω_{m} (orange).

is introduced on the measured speed. The bandwidth of the filter is chosen to alleviate the effect of the oscillations on the measured speed, but not too narrow in order to avoid large delays that could compromise the stability of the closed-loop. In Figure 13.3 an example of the encoder measure compared with the actual angular velocity of the motor ω and the filtered measure ω_{m} is reported. The presence of the filter significantly improves the quality of the measure used to implement the control, but some oscillations are still present on the filtered measure ω_{m}.

For the simulations, a time variant speed reference and a time variant load torque profile, reported in Figure 13.4, of the duration of 106 s are used. The reference speed profile varies between 1870 rpm = 196 rad/s and 2645 rpm = 277 rad/s, while the load torque varies between -35.9 Nm and 28.5 Nm. This duty cycle comes from a traction automotive application, and is selected in order to excite the motor in different working points for the currents.

The PI for the speed closed-loop is tuned on the base of a linearization of the mechanical dynamic (13.8) around the desired working point, taking into account the delay effect introduced by the filter $G_{\mathrm{f}}(s)$. The selected propor-

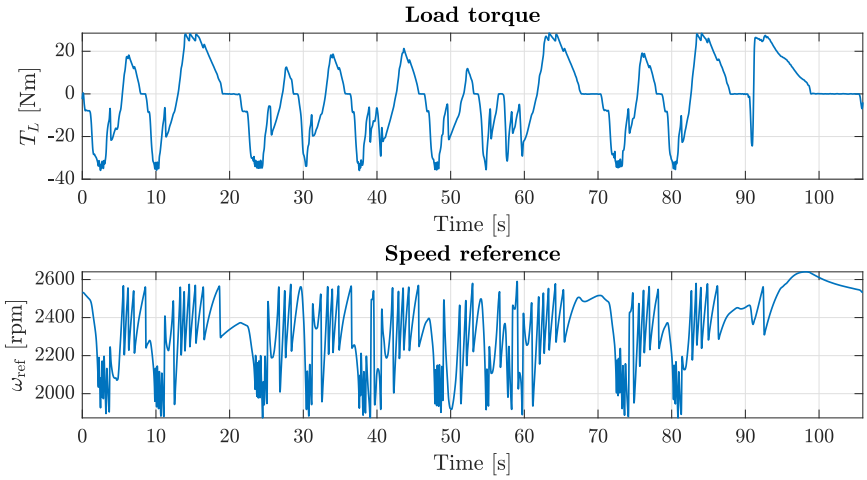

Figure 13.4: Load torque and speed reference profiles considered in the simulations.

tional and integral constants are respectively $K_{\text{P}} = 1$ and $K_{\text{I}} = 20$. The cost matrices for the velocity form MPC are set to $Q = \text{diag}(0.1, 0.1, 10, 5)$, $R = 0.1\mathbf{I}_2$ and $S = \text{diag}(100, 10)$, while the prediction horizon is $N = n + p = 4$, that is the minimum value that guarantees the properties of Theorem 13.1. Note that the error of the current on the d axis is penalized more than the one on the q axis because the variation of the current on the d axis is in general slower, since $L_{\text{d}} > L_{\text{q}}$.

The velocity form MPC algorithm is compared with a schema with PI controllers and decoupling, that is the most commonly used in the industry, and with a classic MPC. All the simulations are implemented in Matlab/Simulink environment on a standard laptop, and the MPC optimization is solved using Matlab *quadprog* function. This setup does not allow to analyze the real time feasibility of the optimization problem, since in the considered application the controller is typically implemented on a micro controller. Nevertheless, recent works [254, 48] have shown that MPC algorithms for electric motors with a similar complexity to the one proposed in this chapter can be successfully implemented in real time.

13.4.1 Current control with PI and decoupling

A PI control with decoupling is considered as first baseline controller for the inner closed-loop. The electric dynamics (13.6) is firstly decoupled by considering new auxiliary control variables

$$\tilde{V}_{\text{d}}(t) = V_{\text{d}}(t) + \omega_{\text{e}}(t) L_{\text{q}}(I_{\text{d}}(t), I_{\text{q}}(t)) I_{\text{q}}(t) \tag{13.12a}$$

$$\tilde{V}_{\text{q}}(t) = V_{\text{q}}(t) - \omega_{\text{e}}(t) L_{\text{d}}(I_{\text{d}}(t), I_{\text{q}}(t)) I_{\text{d}}(t). \tag{13.12b}$$

Then, considering the values of the inductances in the working point, the following linear approximation of the decoupled electric dynamics is obtained

$$\dot{I}_{\mathrm{d}}(t) = -\frac{R_{\mathrm{s}}}{\bar{L}_{\mathrm{d}}} I_{\mathrm{d}}(t) + \frac{1}{\bar{L}_{\mathrm{d}}} \tilde{V}_{\mathrm{d}}(t) \tag{13.13a}$$

$$\dot{I}_{\mathrm{q}}(t) = -\frac{R_{\mathrm{s}}}{\bar{L}_{\mathrm{q}}} I_{\mathrm{q}}(t) + \frac{1}{\bar{L}_{\mathrm{q}}} \tilde{V}_{\mathrm{q}}(t). \tag{13.13b}$$

In this way the MIMO system is approximated as a collection of two SISO independent subsystems, and a PI controller for each subsystem can be tuned using standard techniques. In particular, the zeros of the two PIs are selected to cancel the poles of the SISO approximation of the decoupled system (13.13). Then, the two gains are selected to have a bandwidth of about 500 rad/s for the two closed-loops. The gains of the PI for the d axis are $K_{\mathrm{P}} = 24$ and $K_{\mathrm{I}} = 300$, while for the q axis are $K_{\mathrm{P}} = 4.8$ and $K_{\mathrm{I}} = 300$. The outputs of the two PIs are $\tilde{V}_{\mathrm{d}}$ and $\tilde{V}_{\mathrm{q}}$, and the original control variables V_{d} and V_{q} can be retrieved from (13.12). Note that to apply (13.12) the values of the speed ω and of the inductances $L_{\mathrm{d}}(I_{\mathrm{d}}, I_{\mathrm{q}})$ and $L_{\mathrm{q}}(I_{\mathrm{d}}, I_{\mathrm{q}})$ must be known.

13.4.2 Current control with classic MPC

As a second baseline controller, a classic MPC for regulation is considered. The classic MPC considers the same linear discrete time model (13.11) of the velocity form MPC, and uses a quadratic stage cost that penalizes the difference of the state and input with respect to their references x_{ref} and u_{ref}, that are the equilibrium state and input correspondent to the output y_{ref}. In particular $x_{\mathrm{ref}} = y_{\mathrm{ref}}$ and $u_{\mathrm{ref}} = B^{-1}(\mathbf{I}_2 - A)x_{\mathrm{ref}}$. The optimization problem of the MPC is the following

$$\begin{aligned}
&\min_{u_{\cdot|k}} \sum_{i=0}^{N-1} \left(\left\| x_{i|k} - x_{\mathrm{ref}} \right\|_{\tilde{Q}}^2 + \left\| u_{i|k} - u_{\mathrm{ref}} \right\|_{\tilde{R}}^2 \right) + \left\| x_{N|k} - x_{\mathrm{ref}} \right\|_{\tilde{S}}^2 \\
&\text{s.t. } x_{0|k} = x_k \\
&\quad x_{i+1|k} = A x_{i|k} + B u_{i|k} \quad i = 0, ..., N-1 \\
&\quad u_{i|k} \in \mathcal{U} \quad i = 0, ..., N-1
\end{aligned}$$

where $\tilde{Q}$, $\tilde{R}$ and $\tilde{S}$ are design choice, and in the implementation are set to $\tilde{Q} = 10^4 \mathbf{I}_2$, $\tilde{R} = \mathbf{I}_2$, while $\tilde{S}$ is selected as the solution of the discrete time Riccati equation. The prediction horizon is selected to be the same of the velocity form MPC, i.e. $N = 4$. Then, denoting with $u^\star_{0|k}, ..., u^\star_{N-1|k}$ the solution of the optimization, the MPC control law is $u_k = u^\star_{0|k}$. Note that, as typical for this application, this formulation of MPC does not guarantee closed-loop stability. The introduction of a terminal inequality constraint

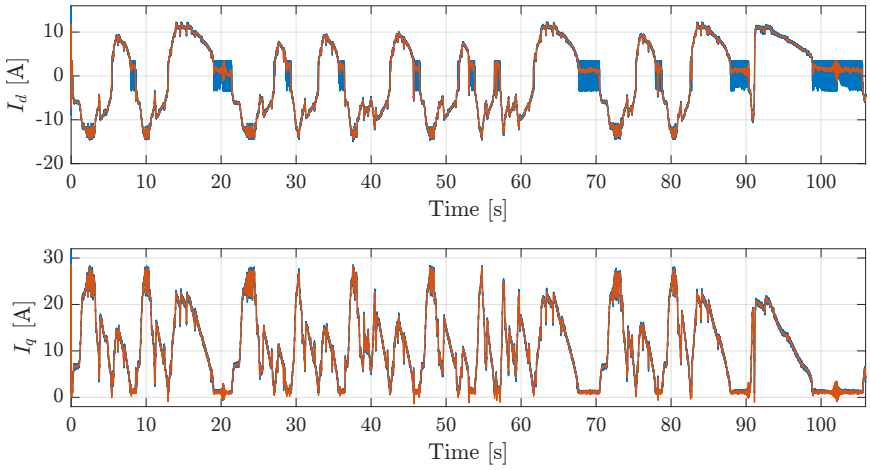

Figure 13.5: Currents with the velocity form MPC control: reference (blue) and actual values (orange).

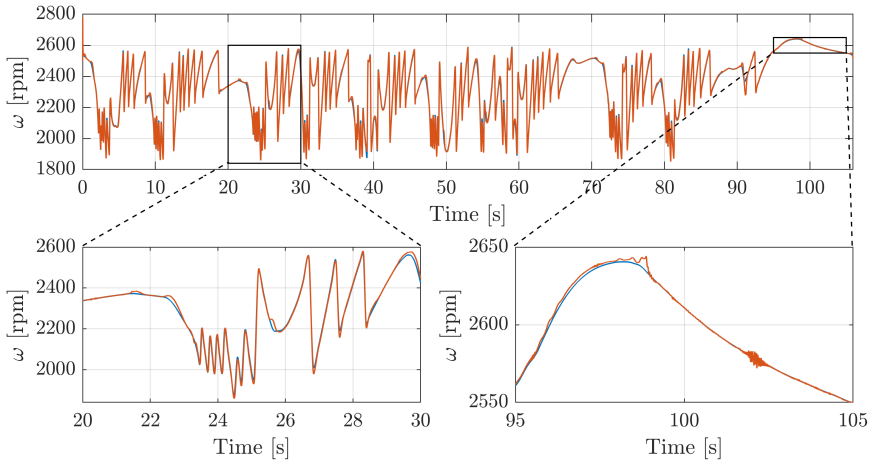

Figure 13.6: Speed with the velocity form MPC control: reference (blue) and actual value (orange).

to guarantee stability is not straightforward since the MPC references may change at each sampling instant.

13.4.3 Simulations on the nominal system

In Figures 13.5-13.10 the currents and speed of the closed-loop simulations with the three controllers are reported. In the current profiles of all the simulations there are regions where the current references have large oscillations, in particular on the d axis. This is due to the interpolation of the values in the MTPA/MTPV LUT, that in those regions are less dense. Small oscillations on the current references are also present independently

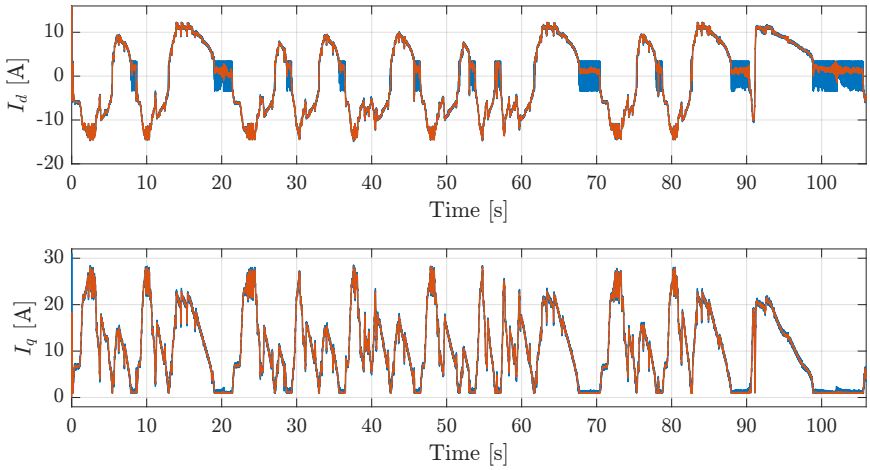

Figure 13.7: Currents with the PI and decoupling control: reference (blue) and actual values (orange).

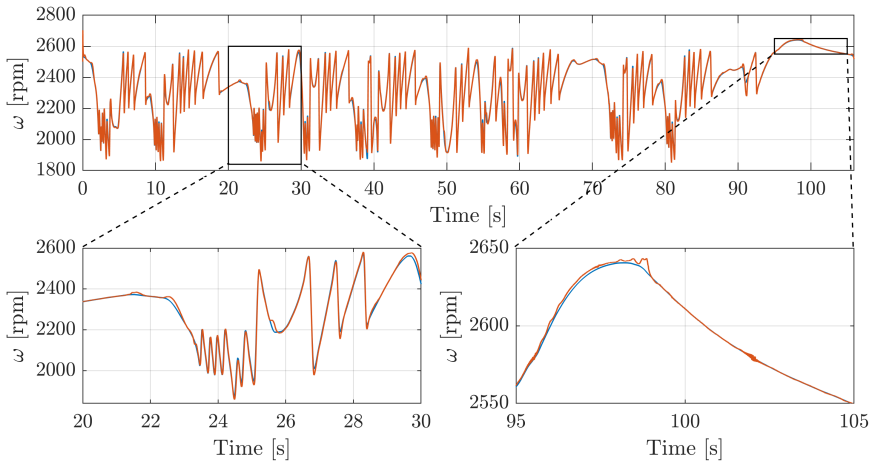

Figure 13.8: Speed with the PI and decoupling control: reference (blue) and actual value (orange).

on the working point because of the oscillations on the filtered speed measure ω_{m}. Both the velocity form MPC and the PI with decoupling are able to control the motor in a satisfactory way, giving comparable closed-loop performances. Instead, the classic MPC is not able to correctly follow the current reference on the q axis, and the tracking error on the current causes a degradation of the speed profile. This is due to the approximation errors in the model used by the MPC, that are not compensated by the presence of an integral action as in the velocity form MPC. Moreover, the simulations show that the introduction of the artificial reference is a key element for the implementation of the velocity form MPC with the terminal equality con-

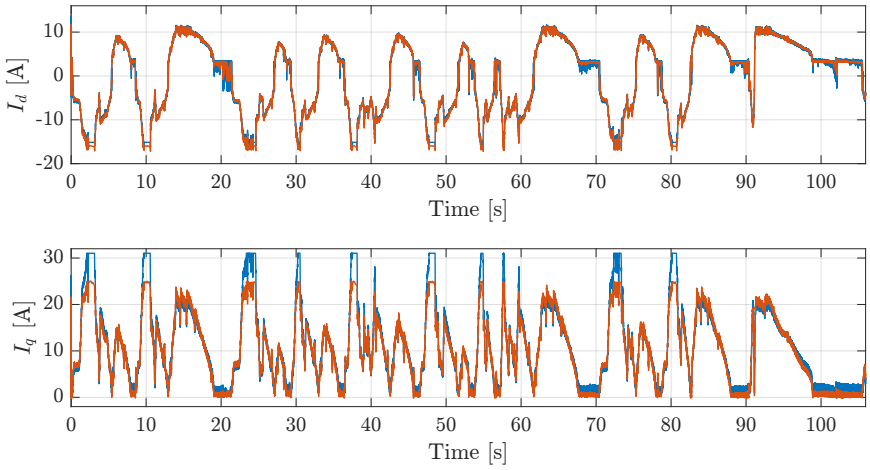

Figure 13.9: Currents with the classic MPC control: reference (blue) and actual values (orange).

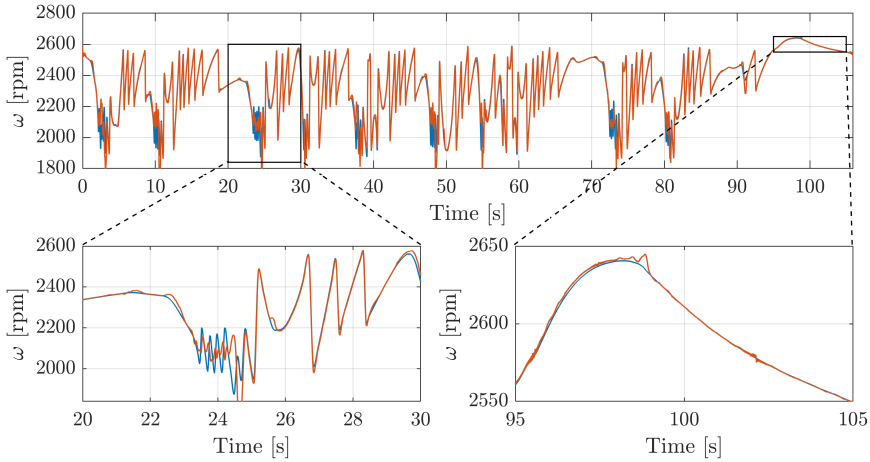

Figure 13.10: Speed with the classic MPC control: reference (blue) and actual value (orange).

straint. If the artificial reference is not included, the optimization problem results infeasible. Note that the velocity form MPC is based on constant values of L_d and L_q, and does not require the use of the LUT describing the relation between the currents and the inductances. On the contrary, the decoupling in the PI control scheme assumes the knowledge of the relation between the inductances and the currents. If only constant values are used, as for the MPC, the closed-loop has a strong oscillatory behavior, and the simulation, reported in Figure 13.11, encounters an error after about 1.4 s. This is an important difference because the derivation of the LUT can be time consuming since it requires a FEM model of the motor or specific

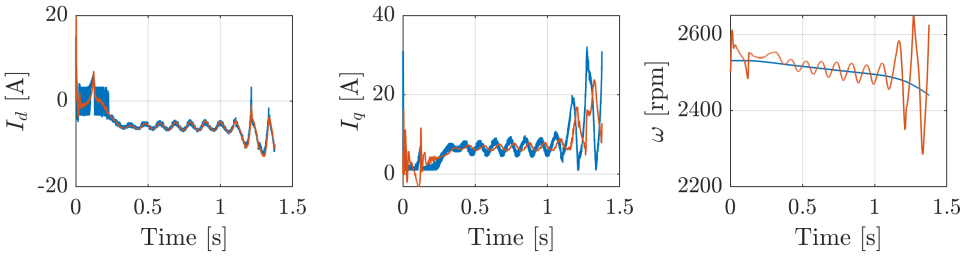

Figure 13.11: Currents and speed with PI and decoupling control, using constant inductance values to compute the decoupling terms: references (blue) and actual values (orange). The simulation encounters an error after about 1.4 s.

experiments on the physical machine. Moreover, both FEM and physical experiments are affected by uncertainties. Hence, in the next subsection, the performances of the velocity form MPC and of the PI control are tested in presence of uncertainties in the inductances values.

13.4.4 Simulations in presence of model uncertainties

To test the robustness of the proposed control approaches to errors in the inductances values, some additional simulations are carried out using perturbed versions of the inductances LUT in the motor simulator. Firstly, some measurements of the inductances have been performed on the physical motor at different values of I_d and I_q, and the measured values $L_\mathrm{d,m}$ and $L_\mathrm{q,m}$ have been compared with the nominal values obtained from the FEM model $L_\mathrm{d,n}$ and $L_\mathrm{q,n}$. In this way the following uncertainty ranges have been derived

$$0.88 \leq \frac{L_\mathrm{d,m}}{L_\mathrm{d,n}} \leq 1.26, \quad 0.72 \leq \frac{L_\mathrm{q,m}}{L_\mathrm{q,n}} \leq 1.53. \tag{13.14}$$

Note that since $L_\mathrm{q} < L_\mathrm{d}$ it is expected that the uncertainty on L_q is in proportion larger than the uncertainty on L_d. To derive the perturbed LUTs it was considered that the error on the inductance may be different in different current regions, but the inductances that correspond to close values of currents are similar. Hence, some matrices of random coefficients in the ranges (13.14) with a dimension that is much smaller than the dimension of the inductances LUT have been extracted. Then, the random matrices have been linearly interpolated to obtain matrices of the same dimension of the LUT, to be multiplied element by element with the nominal LUT to obtain the perturbed LUT. Using this procedure, 7 different sets of perturbed LUT have been derived. The simulations have been preformed using the nominal LUT in for the controller, and the perturbed LUT in the motor simulation model.

The results of the simulation with one of the perturbed LUT are in

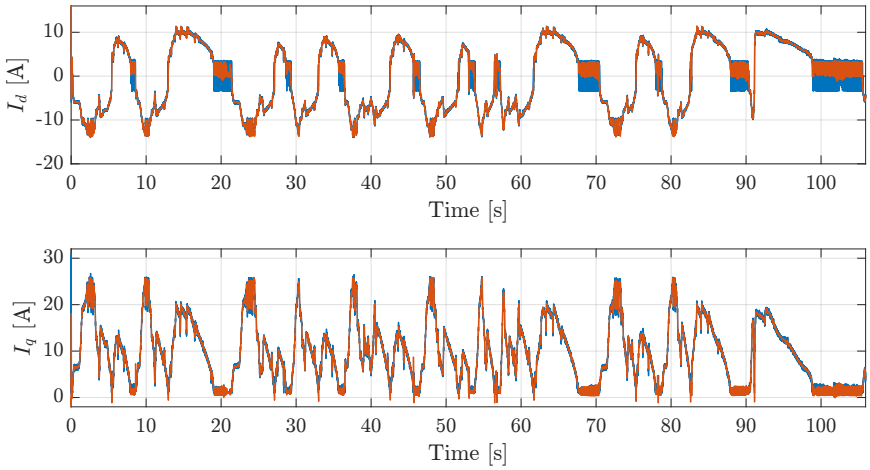

Figure 13.12: Currents with the PI and decoupling control, and the perturbed LUT in the simulation model: reference (blue) and actual values (orange).

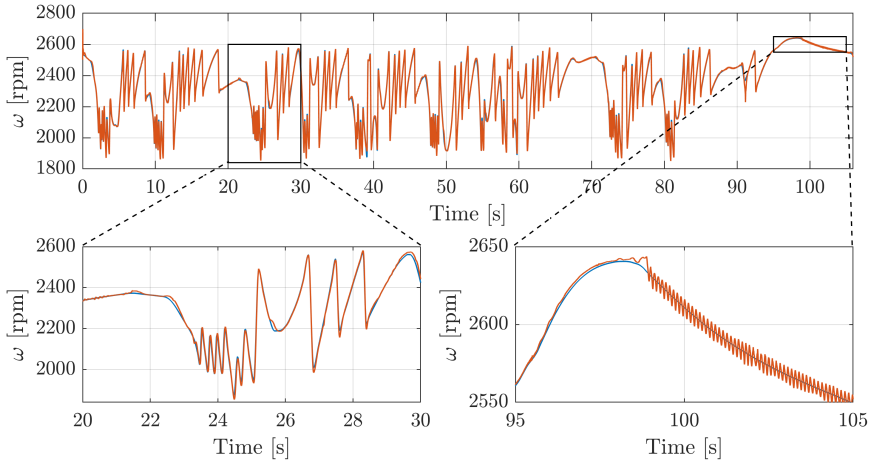

Figure 13.13: Speed with the PI and decoupling control, and the perturbed LUT in the simulation model: reference (blue) and actual value (orange).

Figures 13.12-13.15. The performances with the velocity form MPC are comparable with the simulation with the nominal model of the motor. This is expected, because only one value of inductance is used in the MPC algorithm, and the algorithm is already designed to cope with modeling errors. Instead, in the simulation with the PI, there is a degradation of performances with respect to the simulation with the nominal model of the motor. In particular, in some time intervals some undesired oscillations appear on the speed profile (see Figure 13.13).

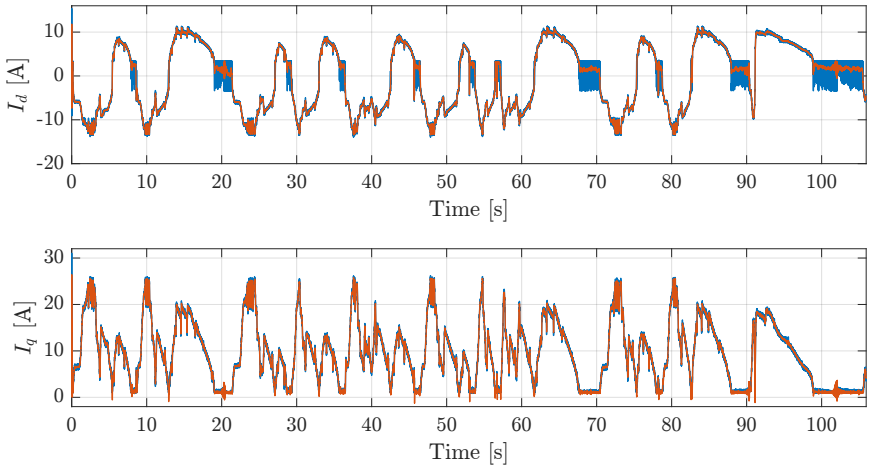

Figure 13.14: Currents with the velocity form MPC, and the perturbed LUT in the simulation model: reference (blue) and actual values (orange).

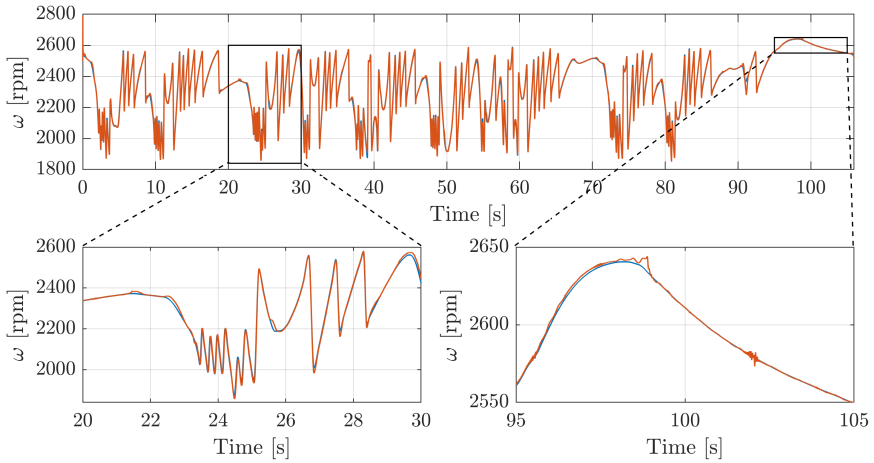

Figure 13.15: Speed with the velocity form MPC, and the perturbed LUT in the simulation model: reference (blue) and actual value (orange).

13.5 Conclusions

In this chapter, the use of velocity form MPC for the control of currents in SynchRel motors is proposed. The velocity form MPC is designed to guarantee closed-loop stability and zero-error regulation, and consists in a quadratic programming optimization problem that can be solved in efficient way. The introduction of an artificial reference in the MPC is fundamental to guarantee feasibility and better performances in presence of the terminal equality constraint. The velocity form MPC algorithm requires the knowledge of a single value of inductance for the implementation. This is a significant improvement with respect to the standard PI control with decoupling, where

the use of accurate values of the inductances is fundamental to maintain an acceptable closed-loop behavior. Moreover, the velocity form MPC shows better performances in presence of model uncertainties with respect to the PI and decoupling control, and can explicitly manage the voltage saturation constraints.

Chapter 14

Conclusions

In this thesis, we studied how to provide theoretical guarantees on stability, robustness and performances in nonlinear MPC using data-driven models, with a particular focus on the presence of modeling errors. This was achieved considering two families of models: RNNs and Koopman operator-based models.

RNNs were used to model open-loop δISS systems. Since the system under control was assumed to be δISS, we have considered RNN models satisfying the same stability property. The δISS property of the model was exploited in the design of the ingredients of the MPC algorithm. In particular, we showed how to design observers for this class of systems and how a δISS-Lyapunov function of the model can be employed to synthesize stabilizing terminal ingredients for the MPC and constraint tightening for robust satisfaction of output constraint. In this framework, we have also shown how it is possible to manage hard constraints on the input variation and how to prove stability in presence of positive semi-definite stage costs. On the performance point of view, we showed how to implement offset-free MPC to achieve zero-error regulation in presence of modeling error and disturbances, and how to employ an artificial reference to enlarge the feasibility region of the optimization problem. The MPC algorithms were designed for different RNN architecture. Along the chapters, we highlighted that the general design ideas can be applied to all the RNN classes, provided that the δISS property is guaranteed, and even to δISS systems that are not described by RNNs. Instead, the specific expression of the MPC ingredients (such as the terminal cost or the observer structure) have to be adapted depending on the particular equations of the model.

For Koopman operator-based models, we focused on the problem of convergence of MPC to the desired equilibrium. Our main result is that it is possible to guarantee asymptotic stability of data-driven MPC provided that there exist sufficiently tight proportional and uniform error bounds on the modeling error. Moreover, we showed how these requirement can be

satisfied using kernel EDMD to approximate the Koopman operator. When proportional error bounds cannot be guaranteed or when the full description of the reference equilibrium is unknown, an alternative to ensure that the closed-loop reaches asymptotically the setpoint is the use of offset-free MPC, that was presented in Chapter 11 using different model classes in the Koopman framework.

Finally, in the application to the current control of SynchRel motors, we showed a possible way to implement a stabilizing MPC that guarantees offset-free tracking in a real world application, obtaining an improvement of performances with respect to standard control strategies in presence of uncertainties in the motor model.

The results of this thesis allows to combine powerful learning-based methods with MPC in a safe way. In particular, the derived theoretical results take explicitly into account the presence of uncertainties in the data-driven models. This is an improvement with respect to many results in the literature, that are often based on heuristics or are derived only in the nominal case, i.e. assuming that the data-driven model exactly describes the plant. The theoretical results are validated in simulation on popular benchmark processes, showing the effectiveness of the proposed approaches.

14.1 Future research directions

The results of this thesis open many possible future research directions and extensions.

Uncertainty estimation for RNN models The robust MPC algorithms proposed for RNN models rely on the assumption that the uncertainty is bounded. However, we did not provide a rigorous method to assess the uncertainty bounds, that have been estimated from testing data in the simulation examples. If the bounds are underestimated, there is the risk of loss of feasibility and of constraint violations, while an overestimation of the uncertainty leads to a high conservatism of the algorithm. The availability of bounds on the modeling errors could also allow to extend the stability analysis carried out in Chapter 12 to RNN models.

Stochastic MPC The boundedness of uncertainty assumed by the robust MPC algorithms proposed in the thesis is not always easy to guarantee in a real world setting. Moreover, most of the deterministic approaches to robust MPC suffer of conservatism, in particular in the nonlinear framework. A possible method to reduce the conservatism while maintaining (probabilistic) guarantees on the constraint satisfaction is the use of stochastic MPC algorithms.

Extension to multi-layer RNN All the RNN-based MPC algorithms presented in the thesis rely on shallow RNNs, i.e. RNNs composed by a single layer. However, it has been shown that for complex systems the use of multi-layer RNNs (also known as *deep RNNs*) can provide a higher prediction accuracy. The results of Section 2.4 and of [28, 30] show that if each layer of a deep RNN is δISS, then the overall model is δISS. This property could be exploited to design MPC algorithms for deep RNN models similarly to how it was done in the thesis for shallow RNNs.

Enlargement of the class of systems for RNN-based MPC In the thesis, we have always considered systems that are open-loop δISS to be modeled with RNNs. While this choice guarantees a degree of safety, since it ensures that the state initialization vanishes and that similar input sequences lead to similar output predictions, it also reduces the class of systems to which the control algorithms can be applied. Hence, the study of RNN-based MPC for systems that are not open-loop δISS would expand the applicability of the methodology to many more systems.

Koopman-based MPC with terminal ingredients In Chapter 12 we have derived conditions on the modeling error that guarantee asymptotic stability of data-driven MPC without terminal ingredients. Similar results can also be obtained for MPC with terminal ingredients, in the presence of proportional and uniform error bounds and of a properly designed quadratically upper bounded terminal cost [217].

Other Koopman-based MPC extensions The results in Part III of the thesis are focused on the stability properties of Koopman-based MPC algorithms, but do not consider the presence of state constraints. The availability of tight error bounds in error bounds in EDMD models could also allow to design robust MPC algorithms, see the preliminary results in [217]. Moreover, an interesting open research point is the derivation of error bounds for kernel EDMD for stochastic systems, see the recent results in [98] for autonomous stochastic dynamics, that could be applied in the design of stochastic MPC algorithms. Finally, the use of input/output data for the derivation of Koopman-based models would broaden the applicability of Koopman MPC to the wide class of systems with unmeasurable states.

Application to real world systems The proposed data-driven MPC algorithms have been successfully tested in simulation on different benchmark examples. However, the thesis lacks of experiments on real world applications, that would further confirm the effectiveness of the proposed approaches.

Bibliography

[1] Ricardo P Aguilera and Daniel E Quevedo. "Predictive control of power converters: Designs with guaranteed performance". In: *IEEE Transactions on Industrial Informatics* 11.1 (2014), pp. 53–63.

[2] Abdelsalam A Ahmed, Byung Kwon Koh, and Young Il Lee. "A comparison of finite control set and continuous control set model predictive control schemes for speed control of induction motors". In: *IEEE Transactions on Industrial Informatics* 14.4 (2017), pp. 1334–1346.

[3] Douglas A Allan, James Rawlings, and Andrew R Teel. "Nonlinear detectability and incremental input/output-to-state stability". In: *SIAM Journal on Control and Optimization* 59.4 (2021), pp. 3017–3039.

[4] Ignacio Alvarado et al. "A comparative analysis of distributed MPC techniques applied to the HD-MPC four-tank benchmark". In: *Journal of Process Control* 21.5 (2011), pp. 800–815.

[5] Donald G Anderson. "Iterative procedures for nonlinear integral equations". In: *Journal of the ACM (JACM)* 12.4 (1965), pp. 547–560.

[6] Joel A E Andersson et al. "CasADi – A software framework for nonlinear optimization and optimal control". In: *Mathematical Programming Computation* 11.1 (2019), pp. 1–36.

[7] David Angeli. "A Lyapunov approach to incremental stability properties". In: *IEEE Transactions on Automatic Control* 47.3 (2002), pp. 410–421.

[8] Luca Bugliari Armenio et al. "Model predictive control design for dynamical systems learned by echo state networks". In: *IEEE Control Systems Letters* 3.4 (2019), pp. 1044–1049.

[9] Omri Azencot et al. "Forecasting sequential data using consistent Koopman autoencoders". In: *International Conference on Machine Learning*. PMLR. 2020, pp. 475–485.

[10] Shaojie Bai, J Zico Kolter, and Vladlen Koltun. "Deep equilibrium models". In: *Advances in Neural Information Processing Systems* 32 (2019).

[11] Florian Bayer, Mathias Bürger, and Frank Allgöwer. "Discrete-time incremental ISS: A framework for robust NMPC". In: *2013 European Control Conference (ECC)*. IEEE. 2013, pp. 2068–2073.

[12] Alberto Bemporad et al. "The explicit linear quadratic regulator for constrained systems". In: *Automatica* 38.1 (2002), pp. 3–20.

[13] Julian Berberich et al. "Data-driven model predictive control with stability and robustness guarantees". In: *IEEE Transactions on Automatic Control* 66.4 (2020), pp. 1702–1717.

[14] Pauline Bernard, Vincent Andrieu, and Daniele Astolfi. "Observer design for continuous-time dynamical systems". In: *Annual Reviews in Control* 53 (2022), pp. 224–248.

[15] Giulio Betti, Marcello Farina, and Riccardo Scattolini. "A robust MPC algorithm for offset-free tracking of constant reference signals". In: *IEEE Transactions on Automatic Control* 58.9 (2013), 2394—2400.

[16] Giulio Betti, Marcello Farina, and Riccardo Scattolini. "An MPC algorithm for offset-free tracking of constant reference signals". In: *2012 IEEE 51st IEEE conference on decision and control (CDC)*. IEEE. 2012, pp. 5182–5187.

[17] Robert E Betz et al. "Control of synchronous reluctance machines". In: *IEEE Transactions on Industry Applications* 29.6 (1993), pp. 1110–1122.

[18] Petar Bevanda, Stefan Sosnowski, and Sandra Hirche. "Koopman operator dynamical models: Learning, analysis and control". In: *Annual Reviews in Control* 52 (2021), pp. 197–212.

[19] Petar Bevanda et al. "Nonparametric Control Koopman Operators". In: *arXiv preprint arXiv.2405.07312* (2025).

[20] Andrea Boccia, Lars Grüne, and Karl Worthmann. "Stability and feasibility of state constrained MPC without stabilizing terminal constraints". In: *Systems & control letters* 72 (2014), 14–21.

[21] Lea Bold et al. "Data-Driven MPC With Stability Guarantees Using Extended Dynamic Mode Decomposition". In: *IEEE Transactions on Automatic Control* 70.1 (2025), pp. 534–541.

[22] Lea Bold et al. "Kernel-based Koopman approximants for control: Flexible sampling, error analysis, and stability". In: *SIAM Journal on Control and Optimization* 63.6 (2025), pp. 4044–4071.

[23] Lea Bold et al. “Kernel EDMD for data-driven nonlinear Koopman MPC with stability guarantees”. In: *IFAC-PapersOnLine* 59.19 (2025), pp. 478–483.

[24] Lea Bold et al. “On Koopman-based surrogate models for non-holonomic robots”. In: *IFAC-PapersOnLine* 58.21 (2024), pp. 55–60.

[25] Max Bolderman et al. “Physics-guided neural networks for feedforward control with input-to-state-stability guarantees”. In: *Control Engineering Practice* 145 (2024), p. 105851.

[26] Silverio Bolognani, Luca Peretti, and Mauro Zigliotto. “Online MTPA control strategy for DTC synchronous-reluctance-motor drives”. In: *IEEE Transactions on Power Electronics* 26.1 (2010), pp. 20–28.

[27] Fabio Bonassi. “Reconciling deep learning and control theory: recurrent neural networks for model-based control design”. PhD thesis. Politecnico di Milano, 2023.

[28] Fabio Bonassi, Marcello Farina, and Riccardo Scattolini. “On the stability properties of gated recurrent units neural networks”. In: *Systems & Control Letters* 157 (2021), p. 105049.

[29] Fabio Bonassi, Marcello Farina, and Riccardo Scattolini. “Stability of discrete-time feed-forward neural networks in NARX configuration”. In: *IFAC-PapersOnLine* 54.7 (2021), pp. 547–552.

[30] Fabio Bonassi et al. “Deep long-short term memory networks: Stability properties and experimental validation”. In: *2023 European Control Conference (ECC)*. IEEE. 2023, pp. 1–6.

[31] Fabio Bonassi et al. “LSTM neural networks: Input to state stability and probabilistic safety verification”. In: *Learning for Dynamics and Control*. PMLR. 2020, pp. 85–94.

[32] Fabio Bonassi et al. “Nonlinear MPC design for incrementally ISS systems with application to GRU networks”. In: *Automatica* 159 (2024), p. 111381.

[33] Fabio Bonassi et al. “On Recurrent Neural Networks for learning-based control: Recent results and ideas for future developments”. In: *Journal of Process Control* 114 (2022), pp. 92–104.

[34] Daniel Bruder, Xun Fu, and Ram Vasudevan. “Advantages of bilinear Koopman realizations for the modeling and control of systems with unknown dynamics”. In: *IEEE Robotics and Automation Letters* 6.3 (2021), pp. 4369–4376.

[35] Bingni W Brunton et al. “Extracting spatial–temporal coherent patterns in large-scale neural recordings using dynamic mode decomposition”. In: *Journal of neuroscience methods* 258 (2016), pp. 1–15.

[36] Steven L. Brunton et al. “Modern Koopman Theory for Dynamical Systems”. In: *SIAM Review* 64.2 (2022), 229 – 340.

[37] Chaohong Cai and Guanrong Chen. “Synchronization of complex dynamical networks by the incremental ISS approach”. In: *Physica A: Statistical Mechanics and its Applications* 371.2 (2006), pp. 754–766.

[38] Chaohong Cai and Andrew R Teel. “Input–output-to-state stability for discrete-time systems”. In: *Automatica* 44.2 (2008), pp. 326–336.

[39] Marco C Campi, Andrea Lecchini, and Sergio M Savaresi. “Virtual reference feedback tuning: a direct method for the design of feedback controllers”. In: *Automatica* 38.8 (2002), pp. 1337–1346.

[40] Shan Chai, Liuping Wang, and Eric Rogers. “Model predictive control of a permanent magnet synchronous motor with experimental validation”. In: *Control Eng. Pract.* 21.11 (2013), pp. 1584–1593.

[41] Hong Chen and Frank Allgöwer. “A quasi-infinite horizon nonlinear model predictive control scheme with guaranteed stability”. In: *Automatica* 34.4 (1998), 1205–1217.

[42] Jie Chen, Yu Dang, and Jianda Han. “Offset-free model predictive control of a soft manipulator using the Koopman operator”. In: *Mechatronics* 86 (2022), p. 102871.

[43] Abdesselam Chikhi, Mohamed Djarallah, and Khaled Chikhi. “A comparative study of field-oriented control and direct-torque control of induction motors using an adaptive flux observer”. In: *Serbian Journal of Electrical Engineering* 7.1 (2010), pp. 41–55.

[44] Kyunghyun Cho et al. “Learning phrase representations using RNN encoder-decoder for statistical machine translation”. In: 2014.

[45] Jiwoo Choi and Jong-Han Kim. “LiftProj: Physics-Informed Koopman Lifting and Projection for Nonlinear Optimal Control via First-Order Optimization”. In: *IEEE Control Systems Letters* (2025).

[46] Junyoung Chung et al. “Empirical evaluation of gated recurrent neural networks on sequence modeling”. In: *arXiv preprint arXiv:1412.3555* (2014).

[47] Vít Cibulka et al. “Model predictive control of a vehicle using Koopman operator”. In: *IFAC-PapersOnLine* 53.2 (2020), pp. 4228–4233.

[48] Gionata Cimini et al. “Embedded model predictive control with certified real-time optimization for synchronous motors”. In: *IEEE Transactions on Control Systems Technology* 29.2 (2020), pp. 893–900.

[49] Pablo SG Cisneros and Herbert Werner. “A velocity algorithm for nonlinear model predictive control”. In: *IEEE Transactions on Control Systems Technology* 29.3 (2020), pp. 1310–1315.

[50] David A Copp and Joao P Hespanha. "Simultaneous nonlinear model predictive control and state estimation". In: *Automatica* 77 (2017), pp. 143–154.

[51] Jean-Michel Coron, Lars Grüne, and Karl Worthmann. "Model predictive control, cost controllability, and homogeneity". In: *SIAM Journal on Control and Optimization* 58.5 (2020), pp. 2979–2996.

[52] Patricio Cortés et al. "Predictive control in power electronics and drives". In: *IEEE Transactions on industrial electronics* 55.12 (2008), pp. 4312–4324.

[53] Enrico Creaco, Giacomo Galuppini, and Alberto Campisano. "Unsteady flow modelling of hydraulic and electrical RTC of PATs for hydropower generation and service pressure regulation in WDN". In: *Urban Water Journal* 19.3 (2022), pp. 233–243.

[54] Salvatore Cuomo et al. "Scientific machine learning through physics–informed neural networks: Where we are and what's next". In: *Journal of Scientific Computing* 92.3 (2022), p. 88.

[55] George Cybenko. "Approximation by superpositions of a sigmoidal function". In: *Mathematics of control, signals and systems* 2.4 (1989), pp. 303–314.

[56] Li Dai et al. "Robust tracking model predictive control with quadratic robustness constraint for mobile robots with incremental input constraints". In: *IEEE Transactions on Industrial Electronics* 68.10 (2020), pp. 9789–9799.

[57] William D'Amico, Alessio La Bella, and Marcello Farina. "An Incremental Input-to-State Stability Condition for a Class of Recurrent Neural Networks". In: *IEEE Transactions on Automatic Control* 99 (2023), pp. 1–16.

[58] William D'Amico, Marcello Farina, and Giulio Panzani. "Recurrent neural network controllers learned using virtual reference feedback tuning with application to an electronic throttle body". In: *2022 European Control Conference (ECC)*. IEEE. 2022, pp. 2137–2142.

[59] Arka Daw et al. "Physics-guided architecture (PGA) of neural networks for quantifying uncertainty in lake temperature modeling". In: *Proceedings of the 2020 siam international conference on data mining*. SIAM. 2020, pp. 532–540.

[60] Stefano De Carli et al. "Infinity-norm-based Input-to-State-Stable Long Short-Term Memory networks: a thermal systems perspective". In: *arXiv preprint arXiv:2503.11553* (2025).

[61] Giuseppe De Nicolao, Lalo Magni, and Riccardo Scattolini. "Stabilizing predictive control of nonlinear ARX models". In: *Automatica* 33.9 (1997), pp. 1691–1697.

[62] Claudio De Persis and Pietro Tesi. "Formulas for data-driven control: Stabilization, optimality, and robustness". In: *IEEE Transactions on Automatic Control* 65.3 (2019), pp. 909–924.

[63] Shankar A Deka et al. "Global asymptotic stability and stabilization of long short-term memory neural networks with constant weights and biases". In: *Journal of Optimization Theory and Applications* 181 (2019), pp. 231–243.

[64] Allan Andre Do Nascimento et al. "Constraint Horizon in Model Predictive Control". In: *IEEE Control Systems Letters* (2025).

[65] Akshunna S Dogra and William Redman. "Optimizing neural networks via Koopman operator theory". In: *Advances in Neural Information Processing Systems* 33 (2020), pp. 2087–2097.

[66] Ján Drgoňa et al. "Physics-constrained deep learning of multi-zone building thermal dynamics". In: *Energy and Buildings* 243 (2021), p. 110992.

[67] Ross Drummond, Pablo Baldivieso, and Giorgio Valmorbida. "Mapping back and forth between model predictive control and neural networks". In: *6th Annual Learning for Dynamics & Control Conference*. PMLR. 2024, pp. 1228–1240.

[68] Matthew Ellis, Helen Durand, and Panagiotis D Christofides. "A tutorial review of economic model predictive control methods". In: *Journal of Process Control* 24.8 (2014), pp. 1156–1178.

[69] Marcello Farina et al. "An approach to output-feedback MPC of stochastic linear discrete-time systems". In: *Automatica* 55 (2015), pp. 140–149.

[70] Gregory E Fasshauer and Qi Ye. "Reproducing kernels of generalized Sobolev spaces via a Green function approach with distributional operators". In: *Numerische Mathematik* 119 (2011), pp. 585–611.

[71] Timm Faulwasser et al. "Behavioral theory for stochastic systems? A data-driven journey from Willems to Wiener and back again". In: *Annual Reviews in Control* 55 (2023), pp. 92–117.

[72] Andrea Favato et al. "A model predictive control for synchronous motor drive with integral action". In: *IECON 2018-44th Annual Conference of the IEEE Industrial Electronics Society*. IEEE. 2018, pp. 325–330.

[73] Marco Forgione and Dario Piga. "Continuous-time system identification with neural networks: Model structures and fitting criteria". In: *European Journal of Control* 59 (2021), pp. 69–81.

[74] Marco Forgione and Dario Piga. "Model structures and fitting criteria for system identification with neural networks". In: *2020 IEEE 14th International Conference on Application of Information and Communication Technologies (AICT)*. IEEE. 2020, pp. 1–6.

[75] Giacomo Galuppini, Enrico F Creaco, and Lalo Magni. "Multinode Real-Time Control of Pressure in Water Distribution Networks via Model Predictive Control". In: *IEEE Transactions on Control Systems Technology* 31.5 (2023), pp. 2201–2216.

[76] Giacomo Galuppini, Lalo Magni, and Antonio Ferramosca. "Nonlinear MPC for tracking piecewise-constant reference signals: the positive semidefinite stage cost case". In: *IFAC-PapersOnLine* 56.1 (2023), pp. 210–215.

[77] Giacomo Galuppini, Irene Schimperna, and Lalo Magni. "Offset-free Output Feedback Tracking MPC for δISS Nonlinear Systems Subject to Input and Input Rate Constraints". In: *IEEE Transactions on Automatic Control* (2025).

[78] Tobias Geyer. *Model predictive control of high power converters and industrial drives*. John Wiley & Sons, 2016.

[79] Mattia Giaccagli, Daniele Astolfi, and Vincent Andrieu. "Further results on incremental input-to-state stability based on contraction-metric analysis". In: *2023 62nd IEEE Conference on Decision and Control (CDC)*. IEEE. 2023, pp. 1925–1930.

[80] Dimitrios Giannakis et al. "Koopman analysis of the long-term evolution in a turbulent convection cell". In: *Journal of Fluid Mechanics* 847 (2018), pp. 735–767.

[81] Elmer G Gilbert and Kok Tin Tan. "Linear systems with output constraints: The theory and application of maximal output admissible sets". In: *1991 American Control Conference*. IEEE. 1991, pp. 351–359.

[82] Laura Boca de Giuli, Alessio La Bella, and Riccardo Scattolini. "Physics-informed neural network modeling and predictive control of district heating systems". In: *IEEE Transactions on Control Systems Technology* 32.4 (2024), pp. 1182–1195.

[83] Laura Boca de Giuli et al. "Modeling and predictive control of networked systems via physics-informed neural networks". In: *2024 IEEE 63rd Conference on Decision and Control (CDC)*. IEEE. 2024, pp. 3005–3010.

[84] Ian Goodfellow, Yoshua Bengio, and Aaron Courville. *Deep Learning*. `http://www.deeplearningbook.org`. MIT Press, 2016.

[85] Alex Graves. "Generating Sequences With Recurrent Neural Networks". In: *arXiv preprint arXiv:1308.0850* (2013).

[86] Gene Grimm et al. “Model predictive control: for want of a local control Lyapunov function, all is not lost”. In: *IEEE Transactions on Automatic Control* 50.5 (2005), pp. 546–558.

[87] Gene Grimm et al. “Nominally robust model predictive control with state constraints”. In: *IEEE Transactions on Automatic Control* 52.10 (2007), pp. 1856–1870.

[88] Lars Grüne. “Analysis and design of unconstrained nonlinear MPC schemes for finite and infinite dimensional systems”. In: *SIAM Journal on Control and Optimization* 48.2 (2009), pp. 1206–1228.

[89] Lars Grüne and Roberto Guglielmi. “Turnpike properties and strict dissipativity for discrete time linear quadratic optimal control problems”. In: *SIAM Journal on Control and Optimization* 56.2 (2018), pp. 1282–1302.

[90] Lars Grüne and Christopher M Kellett. “ISS-Lyapunov functions for discontinuous discrete-time systems”. In: *IEEE Transactions on Automatic Control* 59.11 (2014), pp. 3098–3103.

[91] Lars Grune and Anders Rantzer. “On the infinite horizon performance of receding horizon controllers”. In: *IEEE Transactions on Automatic Control* 53.9 (2008), pp. 2100–2111.

[92] Lars Grüne et al. “Analysis of unconstrained nonlinear MPC schemes with time varying control horizon”. In: *SIAM Journal on Control and Optimization* 48.8 (2010), pp. 4938–4962.

[93] Ozan Gulbudak, Mustafa Gokdag, and Hasan Komurcugil. “Model predictive control strategy for induction motor drive using Lyapunov stability objective”. In: *IEEE Transactions on Industrial Electronics* 69.12 (2022), pp. 12119–12128.

[94] Jung-Ik Ha, Seog-Joo Kang, and Seung-Ki Sul. “Position-controlled synchronous reluctance motor without rotational transducer”. In: *IEEE transactions on Industry Applications* 35.6 (1999), pp. 1393–1398.

[95] Raymond C. Hall and Dale E. Seborg. “Modelling and Self-Tuning Control of a Multivariable pH Neutralization Process Part I: Modelling and Multiloop Control”. In: *1989 American Control Conference*. 1989, pp. 1822–1827.

[96] Tor Akel N. Heirung et al. “Stochastic model predictive control — how does it work?” In: *Computers & Chemical Engineering* 114 (2018), pp. 158–170.

[97] Michael A. Henson and Dale E. Seborg. “Adaptive nonlinear control of a pH neutralization process”. In: *IEEE Transactions on Control Systems Technology* 2.3 (1994), pp. 169–182.

[98] Maximiliano Hertel et al. “Koopman for stochastic dynamics: error bounds for kernel extended dynamic mode decomposition”. In: *arXiv preprint arXiv:2512.20247* (2025).

[99] Michael Hertneck et al. “Learning an approximate model predictive controller with guarantees”. In: *IEEE Control Systems Letters* 2.3 (2018), pp. 543–548.

[100] Lukas Hewing, Juraj Kabzan, and Melanie N Zeilinger. “Cautious model predictive control using gaussian process regression”. In: *IEEE Transactions on Control Systems Technology* 28.6 (2019), pp. 2736–2743.

[101] Lukas Hewing, Kim P Wabersich, and Melanie N Zeilinger. “Recursively feasible stochastic model predictive control using indirect feedback”. In: *Automatica* 119 (2020), p. 109095.

[102] Hakan Hjalmarsson et al. “Iterative feedback tuning: theory and applications”. In: *IEEE control systems magazine* 18.4 (1998), pp. 26–41.

[103] Sepp Hochreiter and Jürgen Schmidhuber. “Long Short-Term Memory”. In: *Neural Computation* 9.8 (1997), pp. 1735–1780.

[104] Matthias Höger and Lars Grüne. “On the relation between detectability and strict dissipativity for nonlinear discrete time systems”. In: *IEEE Control Systems Letters* 3.2 (2019), pp. 458–462.

[105] Kurt Hornik, Maxwell Stinchcombe, and Halbert White. “Multilayer feedforward networks are universal approximators”. In: *Neural networks* 2.5 (1989), pp. 359–366.

[106] Zhong-Sheng Hou and Zhuo Wang. “From model-based control to data-driven control: Survey, classification and perspective”. In: *Information Sciences* 235 (2013), pp. 3–35.

[107] Kenneth J Hunt et al. “Neural networks for control systems—a survey”. In: *Automatica* 28.6 (1992), pp. 1083–1112.

[108] Lucian Cristian Iacob, Roland Tóth, and Maarten Schoukens. “Koopman form of nonlinear systems with inputs”. In: *Automatica* 162 (2024), p. 111525.

[109] Z P Jiang, Andrew R Teel, and Laurent Praly. “Small-gain theorem for ISS systems and applications”. In: *Mathematics of Control, Signals and Systems* 7 (1994), pp. 95–120.

[110] Zhong-Ping Jiang. “A combined backstepping and small-gain approach to adaptive output feedback control”. In: *Automatica* 35.6 (1999), pp. 1131–1139.

[111] Zhong-Ping Jiang and Tengfei Liu. “Small-gain theory for stability and control of dynamical networks: A survey”. In: *Annual Reviews in Control* 46 (2018), pp. 58–79.

[112] Zhong-Ping Jiang, Iven MY Mareels, and Yuan Wang. “A Lyapunov formulation of the nonlinear small-gain theorem for interconnected ISS systems”. In: *Automatica* 32.8 (1996), pp. 1211–1215.

[113] Zhong-Ping Jiang and Yuan Wang. “A converse Lyapunov theorem for discrete-time systems with disturbances”. In: *Systems & control letters* 45.1 (2002), pp. 49–58.

[114] Zhong-Ping Jiang and Yuan Wang. “Input-to-state stability for discrete-time nonlinear systems”. In: *Automatica* 37.6 (2001), pp. 857–869.

[115] Albert Jiménez-Ramos, Abel Gargallo-Peiró, and Xevi Roca. “Approximating Optimal Points of a Lebesgue Constant Proxy for Interpolation in the Simplex”. In: *SIAM Journal on Scientific Computing* 47.2 (2025), A889–A915.

[116] Thomas de Jong et al. “Koopman Data-Driven Predictive Control with Robust Stability and Recursive Feasibility Guarantees”. In: *2024 IEEE 63rd Conference on Decision and Control (CDC)*. 2024, pp. 140–145.

[117] Marvin Jung et al. “Model Predictive Control when utilizing LSTM as dynamic models”. In: *Engineering Applications of Artificial Intelligence* 123 (2023), p. 106226.

[118] Neelay Junnarkar et al. “Synthesis of stabilizing recurrent equilibrium network controllers”. In: *2022 IEEE 61st Conference on Decision and Control (CDC)*. IEEE. 2022, pp. 7449–7454.

[119] Marten J Kamper, FS Van der Merwe, and S Williamson. “Direct finite element design optimisation of the cageless reluctance synchronous machine”. In: *IEEE Transactions on Energy Conversion* 11.3 (1996), pp. 547–555.

[120] Masaki Kanai and Masaki Yamakita. “Linear model predictive control with lifted bilinear models by Koopman-based approach”. In: *SICE Journal of Control, Measurement, and System Integration* 15.2 (2022), pp. 162–171.

[121] Anuj Karpatne et al. “Theory-Guided Data Science: A New Paradigm for Scientific Discovery from Data”. In: *IEEE Transactions on Knowledge and Data Engineering* 29.10 (2017), pp. 2318–2331.

[122] Christoph Kawan, Andrii Mironchenko, and Majid Zamani. “A Lyapunov-based ISS small-gain theorem for infinite networks of nonlinear systems”. In: *IEEE Transactions on Automatic Control* 68.3 (2022), pp. 1447–1462.

[123] S Sathiya Keerthi and Elmer G Gilbert. "Optimal infinite-horizon feedback laws for a general class of constrained discrete-time systems: Stability and moving-horizon approximations". In: *Journal of optimization theory and applications* 57 (1988), pp. 265–293.

[124] Christopher M Kellett. "A compendium of comparison function results". In: *Mathematics of Control, Signals, and Systems* 26 (2014), pp. 339–374.

[125] Hassan K Khalil and Jessy W Grizzle. *Nonlinear systems*. Vol. 3. Prentice hall Upper Saddle River, NJ, 2002.

[126] Hassan K Khalil and Laurent Praly. "High-gain observers in nonlinear feedback control". In: *International Journal of Robust and Nonlinear Control* 24.6 (2014), pp. 993–1015.

[127] Diederik P Kingma and Jimmy Ba. "Adam: A method for stochastic optimization". In: *arXiv preprint arXiv:1412.6980* (2014).

[128] Stefan Klus, Feliks Nüske, and Boumediene Hamzi. "Kernel-based approximation of the Koopman generator and Schrödinger operator". In: *Entropy* 22.7 (2020), p. 722.

[129] Stefan Klus, Ingmar Schuster, and Krikamol Muandet. "Eigendecompositions of transfer operators in reproducing kernel Hilbert spaces". In: *Journal of Nonlinear Science* 30 (2020), pp. 283–315.

[130] Johannes Köhler, Frank Allgöwer, and Matthias A Müller. "A simple framework for nonlinear robust output-feedback MPC". In: *2019 18th European Control Conference (ECC)*. IEEE. 2019, pp. 793–798.

[131] Johannes Köhler, Matthias A. Müller, and Frank Allgöwer. "A nonlinear tracking model predictive control scheme for dynamic target signals". In: *Automatica* 118 (2020), p. 109030.

[132] Johannes Köhler, Matthias A Müller, and Frank Allgöwer. "A novel constraint tightening approach for nonlinear robust model predictive control". In: *2018 Annual American control conference (ACC)*. IEEE. 2018, pp. 728–734.

[133] Johannes Köhler, Melanie N. Zeilinger, and Lars Grune. "Stability and performance analysis of NMPC: Detectable stage costs and general terminal costs". In: *IEEE Transactions on Automatic Control* (2023).

[134] Frederik Köhne et al. "L^∞-error Bounds for Approximations of the Koopman Operator by Kernel Extended Dynamic Mode Decomposition". In: *SIAM Journal on Applied Dynamical Systems* 24.1 (2025), pp. 501–529.

[135] Torsten Koller et al. “Learning-based model predictive control for safe exploration”. In: *2018 IEEE conference on decision and control (CDC)*. IEEE. 2018, pp. 6059–6066.

[136] Bernard O Koopman. “Hamiltonian systems and transformation in Hilbert space”. In: *Proceedings of the National Academy of Sciences* 17.5 (1931), pp. 315–318.

[137] Milan Korda and Igor Mezić. “Linear predictors for nonlinear dynamical systems: Koopman operator meets model predictive control”. In: *Automatica* 93 (2018), pp. 149–160.

[138] Milan Korda and Igor Mezić. “On convergence of extended dynamic mode decomposition to the Koopman operator”. In: *Journal of Nonlinear Science* 28 (2018), pp. 687–710.

[139] Milan Korda, Yoshihiko Susuki, and Igor Mezić. “Power grid transient stabilization using Koopman model predictive control”. In: *IFAC-PapersOnLine* 51.28 (2018), pp. 297–302.

[140] Samir Kouro et al. “Model predictive control: MPC’s role in the evolution of power electronics”. In: *IEEE Industrial Electronics Magazine* 9.4 (2015), pp. 8–21.

[141] Pablo Krupa, Daniel Limon, and Teodoro Alamo. “Harmonic based model predictive control for set-point tracking”. In: *IEEE Transactions on Automatic Control* 67.1 (2020), pp. 48–62.

[142] Pablo Krupa et al. “Model predictive control for tracking using artificial references: Fundamentals, recent results and practical implementation”. In: *2024 IEEE 63rd Conference on Decision and Control (CDC)*. IEEE. 2024, pp. 2977–2991.

[143] Alessio La Bella et al. “Regional stability conditions for recurrent neural network-based control systems”. In: *Automatica* 174 (2025), p. 112127.

[144] Rolf Lagerquist, Ion Boldea, and Timothy JE Miller. “Sensorless-control of the synchronous reluctance motor”. In: *IEEE Transactions on Industry Applications* 30.3 (1994), pp. 673–682.

[145] Wilbur Langson et al. “Robust model predictive control using tubes”. In: *Automatica* 40.1 (2004), 125–133.

[146] Maciej Ławryńczuk and Krzysztof Zarzycki. “LSTM and GRU type recurrent neural networks in model predictive control: A Review”. In: *Neurocomputing* (2025), p. 129712.

[147] Werner Leonhard. *Control of electrical drives*. Springer Science & Business Media, 2001.

[148] Frank L Lewis, Draguna Vrabie, and Kyriakos G Vamvoudakis. "Reinforcement learning and feedback control: Using natural decision methods to design optimal adaptive controllers". In: *IEEE Control Systems Magazine* 32.6 (2012), pp. 76–105.

[149] Daniel Limon et al. "Input-to-state stability: a unifying framework for robust model predictive control". In: *Nonlinear Model Predictive Control: Towards New Challenging Applications* (2009), pp. 1–26.

[150] Daniel Limón et al. "MPC for tracking piecewise constant references for constrained linear systems". In: *Automatica* 44.9 (2008), pp. 2382–2387.

[151] Daniel Limon et al. "Nonlinear MPC for tracking piece-wise constant reference signals". In: *IEEE Transactions on Automatic Control* 63.11 (2018), 3735–3750.

[152] Tian-Hua Liu, Hade Saputra Haslim, and Shao-Kai Tseng. "Predictive controller design for a high-frequency injection sensorless synchronous reluctance drive system". In: *IET Electric Power Applications* 11.5 (2017), pp. 902–910.

[153] Lennart Ljung. "System identification". In: *Signal analysis and prediction*. Springer, 1998, pp. 163–173.

[154] Jorge Lo Presti, Lalo Magni, and Chiara Toffanin. "Ship manoeuvering modelling with a physics-oriented neural network-based approach". In: *IFAC-PapersOnLine* 56.2 (2023), pp. 3471–3476.

[155] Winfried Lohmiller and Jean-Jacques E Slotine. "On contraction analysis for non-linear systems". In: *Automatica* 34.6 (1998), pp. 683–696.

[156] Sara Luciani et al. "Model predictive control for comfort optimization in assisted and driverless vehicles". In: *Advances in Mechanical Engineering* 12.11 (2020), p. 1687814020974532.

[157] David Luenberger. "An introduction to observers". In: *IEEE Transactions on automatic control* 16.6 (1971), pp. 596–602.

[158] Bethany Lusch, J Nathan Kutz, and Steven L Brunton. "Deep learning for universal linear embeddings of nonlinear dynamics". In: *Nature communications* 9.1 (2018), p. 4950.

[159] Urban Maeder, Francesco Borrelli, and Manfred Morari. "Linear offset-free model predictive control". In: *Automatica* 45.10 (2009), pp. 2214–2222.

[160] Lalo Magni and Rodolphe Sepulchre. "Stability margins of nonlinear receding-horizon control via inverse optimality". In: *Systems & Control Letters* 32.4 (1997), pp. 241–245.

[161] Lalo Magni et al. “A stabilizing model-based predictive control algorithm for nonlinear systems”. In: *Automatica* 37.9 (2001), pp. 1351–1362.

[162] Antonio Marino, Claudio Pacchierotti, and Paolo Robuffo Giordano. “Input state stability of gated graph neural networks”. In: *IEEE Transactions on Control of Network Systems* 11.4 (2024), pp. 2052–2063.

[163] Ivan Markovsky and Florian Dörfler. “Behavioral systems theory in data-driven analysis, signal processing, and control”. In: *Annual Reviews in Control* 52 (2021), pp. 42–64.

[164] Daniel Limón Marruedo, Teodoro Alamo, and Eduardo F Camacho. “Input-to-state stable MPC for constrained discrete-time nonlinear systems with bounded additive uncertainties”. In: *Proceedings of the 41st IEEE Conference on Decision and Control, 2002.* Vol. 4. IEEE. 2002, pp. 4619–4624.

[165] Daniele Masti and Alberto Bemporad. “Learning nonlinear state–space models using autoencoders”. In: *Automatica* 129 (2021), p. 109666.

[166] Takayoshi Matsuo and Thomas A Lipo. “Field oriented control of synchronous reluctance machine”. In: *Proceedings of IEEE Power Electronics Specialist Conference-PESC’93.* IEEE. 1993, pp. 425–431.

[167] Per Mattsson et al. “On the equivalence of direct and indirect data-driven predictive control approaches”. In: *IEEE Control Systems Letters* 8 (2024), pp. 796–801.

[168] Alexandre Mauroy and Jorge Goncalves. “Koopman-based lifting techniques for nonlinear systems identification”. In: *IEEE Transactions on Automatic Control* 65.6 (2019), pp. 2550–2565.

[169] David Q Mayne et al. “Constrained model predictive control: Stability and optimality”. In: *Automatica* 36.6 (2000), pp. 789–814.

[170] Igor Mezić. “On numerical approximations of the Koopman operator”. In: *Mathematics* 10.7 (2022), p. 1180.

[171] Igor Mezić. “Spectral properties of dynamical systems, model reduction and decompositions”. In: *Nonlinear Dynamics* 41 (2005), pp. 309–325.

[172] John Miller and Moritz Hardt. “Stable recurrent models”. In: *arXiv preprint arXiv:1805.10369* (2018).

[173] Manfred Morari and Urban Maeder. “Nonlinear offset-free model predictive control”. In: *Automatica* 48.9 (2012), pp. 2059–2067. ISSN: 0005-1098.

[174] Matthias A Müller and Karl Worthmann. “Quadratic costs do not always work in MPC”. In: *Automatica* 82 (2017), pp. 269–277.

[175] Zbynek Mynar, Libor Vesely, and Pavel Vaclavek. "PMSM model predictive control with field-weakening implementation". In: *IEEE Transactions on Industrial Electronics* 63.8 (2016), pp. 5156–5166.

[176] Abhinav Narasingam and Joseph Sang-Il Kwon. "Koopman Lyapunov-based model predictive control of nonlinear chemical process systems". In: *AIChE Journal* 65.11 (2019), e16743.

[177] Abhinav Narasingam, Sang Hwan Son, and Joseph Sang-Il Kwon. "Data-driven feedback stabilisation of nonlinear systems: Koopman-based model predictive control". In: *International Journal of Control* 96.3 (2023), pp. 770–781.

[178] Dragan Nesic and Andrew R Teel. "A framework for stabilization of nonlinear sampled-data systems based on their approximate discrete-time models". In: *IEEE Transactions on automatic control* 49.7 (2004), pp. 1103–1122.

[179] Vesna Nevistić and James A Primbs. "Receding horizon quadratic optimal control: Performance bounds for a finite horizon strategy". In: *1997 European Control Conference (ECC)*. IEEE. 1997, pp. 3584–3589.

[180] Feliks Nüske et al. "Finite-data error bounds for Koopman-based prediction and control". In: *Journal of Nonlinear Science* 33.1 (2023), p. 14.

[181] Samuel E Otto and Clarence W Rowley. "Koopman operators for estimation and control of dynamical systems". In: *Annual Review of Control, Robotics, and Autonomous Systems* 4.1 (2021), pp. 59–87.

[182] Colm J O'Rourke et al. "A geometric interpretation of reference frames and transformations: dq0, Clarke, and Park". In: *IEEE Transactions on Energy Conversion* 34.4 (2019), pp. 2070–2083.

[183] Gabriele Pannocchia. "Offset-free tracking MPC: A tutorial review and comparison of different formulations". In: *2015 European control conference (ECC)*. IEEE. 2015, pp. 527–532.

[184] Gabriele Pannocchia and Alberto Bemporad. "Combined design of disturbance model and observer for offset-free model predictive control". In: *IEEE Transactions on Automatic Control* 52.6 (2007), pp. 1048–1053.

[185] Gabriele Pannocchia, Marco Gabiccini, and Alessio Artoni. "Offset-free MPC explained: novelties, subtleties, and applications". In: *IFAC-PapersOnLine* 48.23 (2015), pp. 342–351.

[186] Gabriele Pannocchia and James B Rawlings. "Disturbance models for offset-free model-predictive control". In: *AIChE Journal* 49.2 (2003), pp. 426–437.

[187] Sebastian Peitz, Samuel E Otto, and Clarence W Rowley. "Data-driven model predictive control using interpolated Koopman generators". In: *SIAM Journal on Applied Dynamical Systems* 19.3 (2020), pp. 2162–2193.

[188] Maik Pfefferkorn and Rolf Findeisen. "Probabilistically Input-to-State Stable Stochastic Model Predictive Control". In: *2024 IEEE 63rd Conference on Decision and Control (CDC)*. 2024, pp. 1807–1813.

[189] Stephen Piche et al. "Nonlinear model predictive control using neural networks". In: *IEEE Control Systems Magazine* 20.3 (2000), pp. 53–62.

[190] Dario Piga et al. "Performance-oriented model learning for data-driven MPC design". In: *IEEE control systems letters* 3.3 (2019), pp. 577–582.

[191] Gilberto Pin et al. "Robust model predictive control of nonlinear systems with bounded and state-dependent uncertainties". In: *IEEE Transactions on automatic control* 54.7 (2009), pp. 1681–1687.

[192] Joshua L Proctor, Steven L Brunton, and J Nathan Kutz. "Dynamic mode decomposition with control". In: *SIAM Journal on Applied Dynamical Systems* 15.1 (2016), pp. 142–161.

[193] Joshua L Proctor, Steven L Brunton, and J Nathan Kutz. "Generalizing Koopman theory to allow for inputs and control". In: *SIAM Journal on Applied Dynamical Systems* 17.1 (2018), pp. 909–930.

[194] Davide Martino Raimondo et al. "Min-max model predictive control of nonlinear systems: A unifying overview on stability". In: *European Journal of Control* 15.1 (2009), pp. 5–21.

[195] EM Rashad, TS Radwan, and MA Rahman. "A maximum torque per ampere vector control strategy for synchronous reluctance motors considering saturation and iron losses". In: *Conference Record of the 2004 IEEE Industry Applications Conference, 2004. 39th IAS Annual Meeting.* Vol. 4. IEEE. 2004, pp. 2411–2417.

[196] James B Rawlings, David Angeli, and Cuyler N Bates. "Fundamentals of economic model predictive control". In: *2012 IEEE 51st IEEE conference on decision and control (CDC)*. IEEE. 2012, pp. 3851–3861.

[197] James B Rawlings, David Q Mayne, and Moritz M Diehl. *Model Predictive Control: Theory, Computation, and Design*. Santa Barbara, California: Nob Hill Publishing, 2019.

[198] Marcus Reble and Frank Allgöwer. "Unconstrained model predictive control and suboptimality estimates for nonlinear continuous-time systems". In: *Automatica* 48 (2012), 1812–1817.

[199] Yi Ming Ren et al. “A tutorial review of neural network modeling approaches for model predictive control”. In: *Computers & Chemical Engineering* 165 (2022), p. 107956.

[200] Max Revay, Ruigang Wang, and Ian R Manchester. “Lipschitz bounded equilibrium networks”. In: *arXiv preprint arXiv:2010.01732* (2020).

[201] Max Revay, Ruigang Wang, and Ian R Manchester. “Recurrent equilibrium networks: Flexible dynamic models with guaranteed stability and robustness”. In: *IEEE Transactions on Automatic Control* (2023).

[202] Jose Rodriguez et al. “State of the art of finite control set model predictive control in power electronics”. In: *IEEE Transactions on Industrial Informatics* 9.2 (2012), pp. 1003–1016.

[203] Mario Rosenfelder et al. “Data-driven predictive control of nonholonomic robots based on a bilinear Koopman realization: Data does not replace geometry”. In: *Robotics and Autonomous Systems* (2025), p. 105156.

[204] Bas J. P. Roset et al. “On robustness of constrained discrete-time systems to state measurement errors”. In: *Automatica* 44.4 (2008), pp. 1161–1165.

[205] Clarence W Rowley et al. “Spectral analysis of nonlinear flows”. In: *Journal of fluid mechanics* 641 (2009), pp. 115–127.

[206] David E Rumelhart, Geoffrey E Hinton, Ronald J Williams, et al. *Learning internal representations by error propagation*. 1985.

[207] Manuel Schaller et al. “Towards reliable data-based optimal and predictive control using extended DMD”. In: *IFAC-PapersOnLine* 56.1 (2023), pp. 169–174.

[208] Irene Schimperna, Lea Bold, and Karl Worthmann. “Offset-free Nonlinear MPC with Koopman-based Surrogate Models”. In: *IFAC-PapersOnLine* 59.19 (2025), pp. 466–471.

[209] Irene Schimperna, Giacomo Galuppini, and Lalo Magni. “Recurrent Neural Network Based MPC for Systems With Input and Incremental Input Constraints”. In: *IEEE Control Systems Letters* 8 (2024), pp. 814–819.

[210] Irene Schimperna and Lalo Magni. “On Incremental Input-to-State Stability of interconnected discrete-time systems”. In: *Automatica* 179 (2025), p. 112406.

[211] Irene Schimperna and Lalo Magni. “Recurrent equilibrium network models for nonlinear model predictive control”. In: *IFAC-PapersOnLine* 58.18 (2024), pp. 226–231.

[212] Irene Schimperna and Lalo Magni. "Robust constrained nonlinear Model Predictive Control with Gated Recurrent Unit model". In: *Automatica* 161 (2024), p. 111472.

[213] Irene Schimperna and Lalo Magni. "Robust offset-free constrained Model Predictive Control with Long Short-Term Memory Networks". In: *IEEE Transactions on Automatic Control* 69.12 (2024), pp. 8172–8187.

[214] Irene Schimperna, Alberto Rubino, and Lalo Magni. "Velocity Form MPC for Current Control in Synchronous Reluctance Motors". In: *IEEE Transactions on Control Systems Technology* 33.6 (2025), pp. 2463–2469.

[215] Irene Schimperna, Chiara Toffanin, and Lalo Magni. "On offset-free Model Predictive Control with Long Short-Term Memory Networks". In: *IFAC-PapersOnLine* 56.1 (2023), pp. 156–161.

[216] Irene Schimperna et al. "Data-driven model predictive control: Asymptotic stability despite approximation errors exemplified in the Koopman framework". In: *arXiv preprint arXiv:2505.05951* (2025). Submitted.

[217] Irene Schimperna et al. "Stability of data-driven Koopman MPC with terminal conditions". In: *arXiv preprint arXiv:2511.21248* (2025).

[218] Philipp Schmitz et al. "On excitation of control-affine systems and its use for data-driven Koopman approximants". In: *arXiv preprint arXiv:2511.03734* (2025).

[219] Pierre OM Scokaert, James B Rawlings, and Edward S Meadows. "Discrete-time stability with perturbations: application to model predictive control". In: *Automatica* 33.3 (1997), pp. 463–470. ISSN: 0005-1098.

[220] Katrine Seel et al. "Neural network-based model predictive control with input-to-state stability". In: *2021 American Control Conference (ACC)*. IEEE. 2021, pp. 3556–3563.

[221] Ilya Shvartsman. "On stability of minimizers in convex programming". In: *Nonlinear Analysis: Theory, Methods & Applications* 75.3 (2012), pp. 1563–1571.

[222] Sang Hwan Son, Abhinav Narasingam, and Joseph Sang-Il Kwon. "Development of offset-free Koopman Lyapunov-based model predictive control and mathematical analysis for zero steady-state offset condition considering influence of Lyapunov constraints on equilibrium point". In: *Journal of Process Control* 118 (2022), pp. 26–36.

[223] Sarah K Spurgeon. "Sliding mode observers: a survey". In: *International journal of systems science* 39.8 (2008), pp. 751–764.

[224] Dušan M Stipanović et al. “Stability of gated recurrent unit neural networks: Convex combination formulation approach”. In: *Journal of Optimization Theory and Applications* 188.1 (2021), pp. 291–306.

[225] Dušan M Stipanović et al. “Some Local Stability Properties of an Autonomous Long Short-Term Memory Neural Network Model”. In: *2018 IEEE International Symposium on Circuits and Systems (ISCAS)*. 2018, pp. 1–5.

[226] Robin Strässer et al. “An overview of Koopman-based control: From error bounds to closed-loop guarantees”. In: *Annual Reviews in Control* 61 (2026), p. 101035.

[227] Robin Strässer et al. “Kernel-based error bounds of bilinear Koopman surrogate models for nonlinear data-driven control”. In: *arXiv preprint arXiv:2503.13407* (2025).

[228] Robin Strässer et al. “SafEDMD: A certified learning architecture tailored to data-driven control of nonlinear dynamical systems”. In: *Automatica* 185 (2026), p. 112732.

[229] Christian Szegedy et al. “Intriguing properties of neural networks”. In: *International Conference on Learning Representations (ICLR)*. arXiv preprint arXiv:1312.6199. 2013.

[230] Enrico Terzi et al. “Learning model predictive control with long short-term memory networks”. In: *International Journal of Robust and Nonlinear Control* 31.18 (2021), pp. 8877–8896.

[231] Duc N Tran, Björn S Rüffer, and Christopher M Kellett. “Convergence properties for discrete-time nonlinear systems”. In: *IEEE Transactions on Automatic Control* 64.8 (2018), pp. 3415–3422.

[232] Duc N Tran, Björn S Rüffer, and Christopher M Kellett. “Incremental stability properties for discrete-time systems”. In: *2016 IEEE 55th Conference on Decision and Control (CDC)*. IEEE. 2016, pp. 477–482.

[233] S Emre Tuna, Michael J Messina, and Andrew R Teel. “Shorter horizons for model predictive control”. In: *2006 American Control Conference*. IEEE. 2006.

[234] Jonas Umlauft, Lukas Pöhler, and Sandra Hirche. “An uncertainty-based control Lyapunov approach for control-affine systems modeled by Gaussian process”. In: *IEEE Control Systems Letters* 2.3 (2018), pp. 483–488.

[235] Pieter Van Goor et al. “Reprojection methods for Koopman-based modelling and prediction”. In: *2023 62nd IEEE Conference on Decision and Control (CDC)*. IEEE. 2023, pp. 315–321.

[236] Jiajin Wang et al. “An improved Koopman-MPC framework for data-driven modeling and control of soft actuators”. In: *IEEE Robotics and Automation Letters* 8.2 (2022), pp. 616–623.

[237] Liuping Wang. “A Tutorial on Model Predictive Control: Using a Linear Velocity-Form Model”. In: *Developments in Chemical Engineering and Mineral Processing* 12.5-6 (2004), pp. 573–614.

[238] Greg Welch, Gary Bishop, et al. “An introduction to the Kalman filter”. In: *Chapel Hill, NC, USA* (1995).

[239] Holger Wendland. *Scattered data approximation*. Vol. 17. Cambridge university press, 2004.

[240] Jared Willard et al. “Integrating scientific knowledge with machine learning for engineering and environmental systems”. In: *ACM Computing Surveys* 55.4 (2022), pp. 1–37.

[241] Jan C Willems et al. “A note on persistency of excitation”. In: *Systems & Control Letters* 54.4 (2005), pp. 325–329.

[242] Matthew O Williams, Ioannis G Kevrekidis, and Clarence W Rowley. “A data–driven approximation of the Koopman operator: Extending dynamic mode decomposition”. In: *Journal of Nonlinear Science* 25 (2015), pp. 1307–1346.

[243] Matthew O Williams et al. “Extending data-driven Koopman analysis to actuated systems”. In: *IFAC-PapersOnLine* 49.18 (2016), pp. 704–709.

[244] Karl Worthmann. “Estimates on the prediction horizon length in MPC”. In: *Proc. 20th Int. Symp. on Mathematical Theory of Networks and Systems (MTNS), Melbourne, Australia*. `https://epub.uni-bayreuth.de/id/eprint/5657/1/worthmann_mtns_2012.pdf`. 2012.

[245] Karl Worthmann. “Stability analysis of unconstrained receding horizon control schemes”. `https://epub.uni-bayreuth.de/id/eprint/273/`. PhD thesis. University of Bayreuth, 2011.

[246] Karl Worthmann et al. “Data-driven MPC with terminal conditions in the Koopman framework”. In: *2024 IEEE 63rd Conference on Decision and Control (CDC)*. 2024, pp. 146–151.

[247] Hao Wu et al. “Variational Koopman models: Slow collective variables and molecular kinetics from short off-equilibrium simulations”. In: *The Journal of chemical physics* 146.15 (2017).

[248] Zhe Wu, David Rincon, and Panagiotis D Christofides. “Process structure-based recurrent neural network modeling for model predictive control of nonlinear processes”. In: *Journal of Process Control* 89 (2020), pp. 74–84.

[249] Zhe Wu et al. “Machine learning-based predictive control of nonlinear processes. Part I: theory”. In: *AIChE Journal* 65.11 (2019), e16729.

[250] Longya Xu et al. “Vector control of a synchronous reluctance motor including saturation and iron loss”. In: *IEEE transactions on industry applications* 27.5 (1991), pp. 977–985.

[251] Yijun Xu et al. “A data-driven koopman approach for power system nonlinear dynamic observability analysis”. In: *IEEE Transactions on Power Systems* 39.2 (2023), pp. 4090–4104.

[252] Enoch Yeung, Soumya Kundu, and Nathan Hodas. “Learning deep neural network representations for Koopman operators of nonlinear dynamical systems”. In: *2019 American Control Conference (ACC)*. IEEE. 2019, pp. 4832–4839.

[253] Shuyou Yu et al. “Inherent robustness properties of quasi-infinite horizon MPC”. In: *IFAC Proceedings Volumes* 44.1 (2011), pp. 179–184.

[254] Andrea Zanelli et al. “Continuous control set nonlinear model predictive control of reluctance synchronous machines”. In: *IEEE Transactions on Control Systems Technology* 30.1 (2021), pp. 130–141.

[255] Christophe Zhang and Enrique Zuazua. “A quantitative analysis of Koopman operator methods for system identification and predictions”. In: *Comptes Rendus. Mécanique* 351.S1 (2023), pp. 1–31.

[256] Xinglong Zhang et al. “Robust tube-based model predictive control with Koopman operators”. In: *Automatica* 137 (2022), p. 110114.

[257] Tianqiao Zhao, Meng Yue, and Jianhui Wang. “Deep-learning-based Koopman modeling for online control synthesis of nonlinear power system transient dynamics”. In: *IEEE Transactions on Industrial Informatics* 19.10 (2023), pp. 10444–10453.